

University of Dundee

DOCTOR OF PHILOSOPHY

Migration Stimulating Factor, the search for inhibitors.

Florence, Margaret Mary

Award date:
2013

Awarding institution:
University of Dundee

[Link to publication](#)

General rights

Copyright and moral rights for the publications made accessible in the public portal are retained by the authors and/or other copyright owners and it is a condition of accessing publications that users recognise and abide by the legal requirements associated with these rights.

- Users may download and print one copy of any publication from the public portal for the purpose of private study or research.
- You may not further distribute the material or use it for any profit-making activity or commercial gain
- You may freely distribute the URL identifying the publication in the public portal

Take down policy

If you believe that this document breaches copyright please contact us providing details, and we will remove access to the work immediately and investigate your claim.

Download date: 17. Feb. 2017

DOCTOR OF PHILOSOPHY

Migration Stimulating Factor, The Search for Inhibitors.

Margaret Mary Florence

May 2013

University of Dundee

Conditions for Use and Duplication

Copyright of this work belongs to the author unless otherwise identified in the body of the thesis. It is permitted to use and duplicate this work only for personal and non-commercial research, study or criticism/review. You must obtain prior written consent from the author for any other use. Any quotation from this thesis must be acknowledged using the normal academic conventions. It is not permitted to supply the whole or part of this thesis to any other person or to post the same on any website or other online location without the prior written consent of the author. Contact the Discovery team (discovery@dundee.ac.uk) with any queries about the use or acknowledgement of this work.



**MIGRATION STIMULATING FACTOR,
THE SEARCH FOR INHIBITORS.**

Margaret M. Florence

**MIGRATION STIMULATING FACTOR,
THE SEARCH FOR INHIBITORS**

Margaret M. Florence

Thesis submitted for the degree of Doctor of Philosophy

in Dentistry

to the College of Medicine, Dentistry and Nursing.

University of Dundee.

Unit of Cell and Molecular Biology,

Dundee Dental Hospital and School,

University of Dundee.

May 2013

TABLE OF CONTENTS

Table of Contents	IV
List of Tables	XII
List of Figures	XVI
Acknowledgments	XXII
Declaration	XXIII
Certificate	XXIV
Dedication	XXV
List of Abbreviations	XXVI
Abstract	XXXIV

Chapter one: LITERATURE REVIEW

1.1	The Hallmarks of Cancer.....	1
1.2	An introduction to Migration Stimulating Factor.....	3
1.3	MSF and Cancer Progression.....	9
1.4	The Epithelial- Mesenchymal Transition in Cancer Progression	
	Introduction.....	13
1.4i	The Process of EMT.....	15
1.4ii	The Molecular Mechanisms Involved in EMT.....	21
1.4iii	The Controversy of EMT.....	24
1.4iv	The Additional Consequences of EMT.....	27
1.4v	Therapies Targeting EMT.....	28
1.5	Angiogenesis and Anti-Angiogenic Therapy	
	Introduction.....	30
1.5i	Tumour Angiogenesis.....	36
1.5ii	Tumour Vasculature.....	43
1.5iii	The First Generation of Anti- Angiogenic Agents.....	45
1.5iv	Toxicity of Anti-Angiogenic Therapy.....	56
1.5v	Anti-angiogenic Resistance.....	61

1.5vi	The Next Generation of Anti-Angiogenic Agents - New Targets.....	63
1.5vii	Normalisation of Tumour Vasculature.....	73
1.5viii	Future Perspectives.....	75
1.6	Project Aims.....	77

Chapter two: MATERIALS AND METHODS

2.1	Cell Culture.....	81
2.1.i	Cell lines and Culture Conditions.....	81
2.1.ii	Cell Culture Maintenance Protocols.....	81
2.1.iii	Conditioned Medium Collection and Storage Conditions.....	82
2.2	3D Type I Collagen Gel Migration Bioassay.....	85
2.2.i	Extraction of Type I Collagen.....	85
2.2.ii	3D Collagen Gel Migration Bioassay.....	85
2.2.iii	Assessment of the 3D Type I Collagen Gel Migration Bioassay.....	86
2.3	Cell Proliferation and Viability Bioassays.....	86
2.3.i	Growth Curve: An Assessment of Cell Proliferation and Viability.....	86
2.3.ii	Trypan Blue Exclusion- Assessment of Cell Viability.....	87
2.3.iii	MTT Assay- Assessment of Cell Viability.....	88
2.4	Endothelial Sprouting Assays.....	89
2.4.i	2D Post-confluent Sprouting Assay.....	89
2.4.ii	3D Spontaneous Sprouting Assay.....	89
2.5	Antibodies.....	91
2.5.i	Antibodies Raised Against Peptides in the MSF Primary Sequence, Produced In House.....	91
2.5.ii	Purification of Mouse Monoclonal IgG Antibodies from Hybridoma Conditioned Medium, using Protein G Chromatography.....	91
2.6	Recombinant Proteins	92
2.6.i	Recombinant Proteins produced In House.....	92
2.6.ii	Recombinant Protein Production.....	92
2.7	Procedures to Fracationate Conditioned Medium.....	95
2.7.i	Ammonium Sulphate Precipitation.....	95

2.7.ii	Size Exclusion Chromatography (SEC).....	95
2.7.iii	Ion Exchange Chromatography.....	96
2.7.iv	SDS- PAGE Electrophoresis.....	97
2.7.v	Gel Elution of Protein Bands.....	98
2.8	Immunoblot (Western Blot) - Indirect Method.....	98
2.9	Immunoprecipitation of MSF.....	99
2.10	Mass Spectroscopy.....	99
2.11	Quantification of Proteins.....	100
2.11.i	Colourimetric Indirect ELISA	100
2.11.ii	Colourimetric Sandwich ELISA.....	100
2.12	Immunolocalisation Methods.....	101
2.12.i	Cell Pellet Preparation.....	101
2.12.ii	Immunostaining Protocol.....	102
2.12.iii	Optimum Conditions for Immunostaining Reagents.....	103

Chapter three

Results: ASSESSMENT OF THE BIOACTIVITY OF CONDITIONED MEDIUM

3.1	Aims.....	104
3.2	Background	104
3.3	The Motogenic Activity of Recombinant MSF.....	106
3.4	The Testing of Fibroblast Cell Lines CM for Bioactivity in the 3D Collagen Gel Fibroblast Migration Assay.....	109
3.5	The Testing of Endothelial Cell Lines CM for Bioactivity in the 3D Collagen Gel Fibroblast Migration Assay.....	112
3.5.i	Bioactivity of Conditioned Medium from Endothelial Cells Grown on a 2D Surface.....	114
3.5.ii	Bioactivity of Conditioned Medium from Endothelial Cells Grown within a 3D Collagen Matrix.....	118
3.6	The Testing of Epithelial Cell Lines CM for Bioactivity in the 3D Collagen Gel Fibroblast Migration Assay.....	123
3.6.i	The Testing of an Epithelial Cell Line for Bioactivity in the 3D Collagen Gel Fibroblast Migration Assay.....	124
3.7	Discussion.....	127

Chapter four**Results:****THE IDENTIFICATION OF MSF-I PRODUCED BY KERATINOCYTES.**

4.1	Aims.....	133
4.2	Background.....	133
4.3	The Superdex Fractionation of HaCaT Conditioned Medium.....	135
4.4	The Bioactivity of Size- Exclusion Fractionated HaCaT Conditioned Medium.....	136
4.5	The Identification of MSF Expression by HaCaT Keratinocytes.....	141
4.5.i	Western Blot Identification of MSF.....	141
4.5.ii	Colourimetric Sandwich ELISA for Total MSF.....	141
4.5.iii	Immunolocalisation of MSF in HaCaT Keratinocytes.....	142
4.5.iv	The Characterisation of HaCaT Endogenous Motogenic Bioactivity.....	144
4.5.v	The Identification of MSF Expression in HaCaT Size Exclusion Fractionated Conditioned Medium.....	145
4.6	The Isolation and Identification of MSF-I.....	148
4.6.i	The Ion Exchange Fractionation of HaCaT Conditioned Medium.....	149
4.6.ii	The SDS Electrophoresis Separation of HaCaT Anion Exchange Unbound Fractions.....	149
4.6.iii	The Identification of MSF-I by Peptide Mass Fingerprinting.....	150
4.7	The Verification of NGAL as the HaCaT MSF-I.....	154
4.7.i	Western Blot Identification of NGAL in Un-Fractionated HaCaT CM.....	155
4.7.ii	Colourimetric Indirect ELISA for NGAL in Un- Fractionated HaCaT CM.....	155
4.7.iii	Immunolocalisation of NGAL in HaCaT Series.....	157
4.7.iv	The MSF Inhibitory Activity of NGAL.....	159
4.7.v	The Effect of NGAL on Fibroblast Morphology, Viability and Proliferation.....	162
4.7.vi	The MSF- Inhibitory Activity of NGAL can be Temporally Separated from MSF.....	163
4.7.vii	The MSF-Inhibitory activity of NGAL is Iron Independent.....	164

4.8	Discussion.....	168
-----	-----------------	-----

Chapter five

Results: THE EXPRESSION OF MSF AND NGAL IN RELATION TO TUMOUR PROGRESSION.

5.1	Aims.....	184
5.2	Background.....	184
5.3	The Identification of MSF Expression in the HaCaT Series Cell Lines.....	186
5.3.i	Western Blot Identification of MSF.....	186
5.3.ii	Colourimetric Sandwich Elisa For Total MSF.....	186
5.3.iii	Immunolocalisation of MSF in HaCaT Series Keratinocytes.....	187
5.4	The Identification of NGAL Expression in the HaCaT Series Cell Lines.....	192
5.4.i	Western Blot Identification of NGAL.....	192
5.4.ii	Colourimetric Indirect ELISA for NGAL.....	193
5.4.iii	Immunolocalisation of NGAL in HaCaT Series.....	195
5.5	Discussion.....	199

Chapter six

Results: THE EXPRESSION OF PRO- AND ANTI- MOTOGENIC BIOACTIVITY BY THE HACAT RAS-CLONES.

6.1	Aims.....	204
6.2	Background	204
6.3	The Assessment of the Bioactivity of HaCaT Series Conditioned Medium.....	205
6.3i	The Motogenic Activity of HaCaT Series Conditioned Medium.....	205
6.3ii	The MSF-Inhibitory Activity of HaCaT Series Conditioned Medium.....	206
6.3iii	The Motogenic Activity of Recombinant MSF in the presence of HaCaT Series Conditioned Medium.....	207
6.4	The Characterisation of HaCaT Series Endogenous Motogenic Bioactivity.....	208
6.5	The Superdex Fractionation of HaCaT Series Conditioned Medium.....	219
6.6	The Assessment of the Bioactivity of SEC Fractionated	

HaCaT Series Conditioned Medium.....	223
6.6i The Motogenic Activity of Size- Exclusion Fractionated HaCaT Series Conditioned Medium.....	223
6.6ii The MSF-Inhibitory Activity of Size- Exclusion Fractionated HaCaT Series Conditioned Medium.....	223
6.6iii The Motogenic Activity of Recombinant MSF in the Presence of HaCaT Series Size- Exclusion Fractionated Conditioned Medium.....	224
6.7 The Identification of NGAL in the HaCaT Series Size- Exclusion Fractionated Conditioned Medium.....	228
6.8 The Identification of MSF in the HaCaT Series Size-Exclusion Fractionated Conditioned Medium.....	230
6.9 The SDS Polyacrylamide Gel Electrophoresis of HaCaT Series Conditioned Medium.....	236
6.10 The Assessment of the Bioactivity of SDS Electrophoresis Fractionated HaCaT Series Conditioned Medium.....	236
6.10i The Motogenic Activity of SDS Electrophoresis Fractionated HaCaT Series Conditioned Medium.....	236
6.10ii The MSF- Inhibitory Activity of SDS Electrophoresis Fractionated HaCaT Series Conditioned Medium.....	237
6.10iii The Motogenic Activity of Recombinant MSF in the presence of HaCaT Series SDS Electrophoresis Fractionated Conditioned Medium.....	237
6.11 Discussion.....	244

Chapter seven

Results: THE IDENTIFICATION OF MSF-I PRODUCED BY ENDOTHELIAL CELLS

7.1 Aims.....	251
7.2 Background.....	251
7.3 The Identification of NGAL Expression in Endothelial Cell Lines.....	252
7.3.i Western Blot Identification of NGAL	252
7.3.ii Immunolocalisation of NGAL in Endothelial Cell Lines	254
7.4 The Identification of MSF Expression in Endothelial Cell Lines.....	256
7.4.i Western Blot Identification of MSF.....	256

7.4.ii	Immunolocalisation of MSF in Endothelial Cell Lines.....	257
7.5	The Characterisation of Endothelial Endogenous Motogenic Bioactivity.....	259
7.5i	The Motogenic Activity of Size- Exclusion Fractionated ENDO 742 Conditioned Medium.....	260
7.5ii	The Effect of MSF-Inhibitors on the ENDO742 Motogenic SEC Fractionated Conditioned Medium.....	261
7.5iii	The Motogenic Activity of SDS PAGE Fractionated ENDO 742 Conditioned Medium.....	266
7.5iv	The Effect of MSF-Inhibitors on the ENDO742 Motogenic SDS PAGE Fractionated Conditioned Medium.....	266
7.6	The Characterisation of Endothelial MSF-Inhibitory Bioactivity.....	269
7.6i	The MSF-Inhibitory Activity of Size- Exclusion Fractionated ENDO 742 Conditioned Medium.....	270
7.6ii	The Motogenic Activity of Recombinant MSF in the presence of ENDO 742 Size- Exclusion Fractionated Conditioned Medium.....	272
7.6iii	The MSF- Inhibitory Activity of SDS PAGE Fractionated ENDO 742 Conditioned Medium.....	274
7.6 iv	The Motogenic Activity of Recombinant MSF in the presence of ENDO 742 SDS PAGE Fractionated Conditioned Medium.....	276
7.7	The Effect of MSF on Endothelial Morphology.....	278
7.7i	The Induction of Endothelial Sprouting Phenotype by rhMSF.....	278
7.7ii	The Effect of MSF Inhibitor, PEPQ 1.1 Antibody, on Spontaneous Endothelial Sprouts.....	283
7.7iii	The Effect of MSF Inhibitor, NGAL, on Spontaneous Endothelial Sprouts.....	285
7.7iv	The Effect of MSF Inhibitor, NGAL, on Post- Confluent Endothelial Sprouts.....	287
7.7v	The Effect of NGAL on Endothelial Proliferation and Viability.....	289
7.8	Discussion.....	292

Chapter eight: <u>CONCLUDING DISCUSSION</u>	303
Chapter nine: <u>FUTURE WORK</u>	321
Chapter ten: <u>REFERENCES</u>	325
Chapter eleven: <u>APPENDICES</u>	
2.1a The preparation methods of cell culture reagents.....	357
2.1b Supplier details for the cell culture reagents.....	359

LIST OF TABLES

Chapter one: LITERATURE REVIEW

Table 1.1: The hallmarks of cancer	2
Table 1.2: The bioactivities of MSF	7
Table 1.3: A list of the seminal papers which have increased the understanding of EMT and the cancer progression.....	16
Table 1.4: The process of epithelial to mesenchymal transition.....	20
Table 1.5: A list of epithelial and mesenchymal markers.....	23
Table 1.6: Evidence of epithelial- mesenchymal transition taking place during human cancer progression.....	25
Table 1.7a: A list of conditions regularly described as having a faulty angiogenic switch.....	31
Table 1.7b: A list of diseases which could be treated with anti-angiogenic therapy.....	31
Table 1.8: A list of the seminal papers which have increased our understanding of angiogenesis and the therapeutic potential of anti-angiogenic therapies.....	32
Table 1.9: The key steps in angiogenesis.....	39
Table 1.10: Regulators of angiogenesis.....	40
Table 1.11: Key pro-angiogenic growth factors.....	41
Table 1.12: The differences between normal and tumour vasculature.....	44
Table 1.13: The classification of tumour vasculature.....	45
Table 1.14: Anti-VEGF agents. FDA approved Bevacizumab Treatments.....	55
Table 1.15: A list of common side effects associated with anti-angiogenic therapy.	59
Table 1.16: A list of the next generation of anti-angiogenic agents and their research status.....	70

Chapter two: METHODS AND MATERIALS

Table 2.1: The optimum culture conditions for cell lines.....	83
Table 2.2: In house prepared MSF specific antibodies; information regarding type, function and purification technique.....	91
Table 2.3. Details of in- house prepared recombinant proteins.....	92

Table 2.4: Recipe for SDS- polyacrylamide gel preparation.....	97
Table 2.5: The operational concentrations of antibodies for performing immunoblotting.....	99
Table 2.6: The operational conditions for performing the Indirect ELISA.....	100
Table 2.7: The operational conditions for performing the Sandwich ELISA.....	101
Table 2.8: The operational conditions for performing Immunostaining.....	103

Chapter three

Results: ASSESSMENT OF THE BIOACTIVITY OF CONDITIONED MEDIUM

Table 3.1: List of cultured cell lines of which conditioned medium was collected under serum free conditions and used for testing for the presence of MSF- inhibitory activity in the 3D collagen gel fibroblast migration assay.....	123
Table 3.2: List of endothelial cell lines, whose conditioned medium was tested for the presence of motogenic and MSF-I activity.....	129

Chapter four

Results:

THE IDENTIFICATION OF MSF-I PRODUCED BY KERATINOCYTES.

Table 4.1: The OD readings and calculated concentration of NGAL in HaCaT conditioned medium, as measured in the Indirect ELISA assay using a specific anti-NGAL antibody (polyclonal antibody, AF1757).....	156
Table 4.2: The effect of the iron chelator deferoxamine mesylate (DFOM) on fibroblast viability and proliferation.....	167
Table 4.3: Summary of experimental data providing evidence of that cultured HaCaT keratinocytes express MSF.....	174
Table 4.4: Summary of experimental data providing evidence of that cultured HaCaT keratinocytes express NGAL.....	175
Table 4.5: The verification of NGAL as an inhibitor of MSF motogenic bioactivity.....	176
Table 4.6: The role of NGAL in malignant disease.....	177

Chapter five**Results: THE EXPRESSION OF MSF AND NGAL IN RELATION TO TUMOUR PROGRESSION.**

Table 5.1: Immunolocalisation of MSF in human fibroblasts and keratinocytes.....	191
Table 5.2. The average cell counts per 90mm dish for the HaCaT series keratinocytes.....	195
Table 5.3: The concentration of NGAL in HaCaT series conditioned medium, as measured by the colorimetric indirect ELISA for NGAL.....	195
Table 5.4: Immunolocalisation of NGAL in human fibroblasts and keratinocytes.....	198

Chapter six**Results: THE EXPRESSION OF PRO- AND ANTI- MOTOGENIC BIOACTIVITY BY THE HACAT-RAS CLONES.**

Table 6.1: The characterisation of HaCaT Series endogenous motogenic bioactivity.....	216
Table 6.2: Result Summary 1. The bioactivity of HaCaT Series CM.....	217
Table 6.3.: Result Summary 2. The bioactivity of HaCaT Series CM.....	218
Table 6.4: The estimated molecular weight of the Size Exclusion Chromatography fractions.....	220
Table 6.5: Result Summary. The bioactivity of fractionated HaCaT Series conditioned medium.....	243

Chapter seven**Results:****THE IDENTIFICATION OF MSF-I PRODUCED BY ENDOTHELIAL CELLS**

Table 7.1: The effects of rhMSF on endothelial morphology.....	281
Table 7.2: The effects of rhMSF on endothelial morphology.....	282
Table 7.3: The effect of MSF inhibitor PEPQ1.1 on the number of spontaneous endothelial sprouts present in a Type I collagen gel.....	285
Table 7.4: The effect of NGAL on endothelial viability and proliferation.....	290-1
Table 7.5: Summary of experimental data providing evidence that cultured ENDO 742 endothelial cells displaying both the cobblestone	

and sprouting phenotype express MSF.....	300
Table 7.6: Result Summary. The bioactivity of fractionated ENDO 742 conditioned medium.....	301
Table 7.7: A comparison of MSF-Inhibitory bioactivity present detected in the fractionated conditioned medium of endothelial cells exhibiting either the cobblestone or sprouting phenotype.....	302

Chapter eight: CONCLUDING DISCUSSION

Table 8.1: Summary of project aims and results.....	312
---	-----

LIST OF FIGURES

Chapter one: LITERATURE REVIEW

- Figure 1.1: A comparison of the modular structures of fibronectin and MSF.....8
 Figure 1.2: The protein sequence of MSF.....8

Chapter three

Results: ASSESSMENT OF THE BIOACTIVITY OF CONDITIONED MEDIUM

- Figure 3.1: The motogenic activity of recombinant MSF.....108
 Figure 3.2: The effect of MSF- neutralising antibody, PEPQ1.1, on
 the motogenic bioactivity of recombinant MSF.....108
 Figure 3.3: The comparison of the bioactivity present in the
 conditioned medium collected from adult and foetal fibroblast
 cell lines, with and without the addition of rhMSF.....111
 Figure 3.4: The comparison of the bioactivity present in the
 conditioned medium collected from the bovine aortic endothelial
 cell line, BAEC, displaying either a cobblestone or sprouting
 phenotype, when grown on a 2D surface.....116
 Figure 3.5: The comparison of the bioactivity present in the
 conditioned medium collected from the transformed human
 mammary microvascular cell line, Endo 742, displaying
 either a cobblestone or sprouting phenotype, when grown
 on a 2D surface.....117
 Figure 3.6: The bioactivity of conditioned medium collected from
 a blank collagen gel.....120
 Figure 3.7: The comparison of the bioactivity present in the
 conditioned medium collected from the bovine endothelial
 cell line, BAEC, displaying either a cobblestone or
 sprouting phenotype, when grown on or within a
 3D collagen matrix, respectively.....121
 Figure 3.8: The comparison of the bioactivity present in the
 conditioned medium collected from the transformed human
 mammary microvascular cell line, Endo 742, displaying
 either a cobblestone or sprouting phenotype, when grown

on or within a 3D collagen matrix, respectively.....	122
Figure 3.9: The bioactivity of HaCaT keratinocyte conditioned medium in the fibroblast migration assay.....	126

Chapter four

Results:

THE IDENTIFICATION OF MSF-I PRODUCED BY KERATINOCYTES.

Figure 4.1: The fractionation of HaCaT keratinocyte conditioned medium by size-exclusion chromatography.....	137
Figure 4.2: The motogenic activity of Superdex 75 fractionated conditioned medium from HaCaT keratinocytes.....	138
Figure 4.3: The MSF-Inhibitory activity of Superdex 75 fractionated conditioned medium from HaCaT keratinocytes.....	139
Figure 4.3: The motogenic activity of exogenous rhMSF in the presence of Superdex 75 fractionated conditioned medium from HaCaT keratinocytes.....	140
Figure 4.4: The standard curve of colorimetric sandwich Elisa for total MSF.....	142
Figure 4.5: Immunolocalisation of MSF in human fibroblasts and keratinocytes.....	144
Figure 4.6: The effect of the MSF-Inhibitor, function neutralising antibody PEPQ 1.1, on the endogenous motogenic bioactivity of HaCaT fractionated conditioned medium.....	147
Figure 4.7: The motogenic activity of HaCaT SEC fractionated conditioned medium before and after immunoprecipitation with MSF-specific identification antibody RpVSI.....	148
Figure 4.8: The purification of MSF-I active SEC fractions by anion- exchange chromatography.....	152
Figure 4.9: The bioactivity of anion-exchange, ANX, purified MSF-I bioactive HaCaT SEC fractions.....	152
Figure 4.10: The MSF-Inhibitory activity of gel elutions from the SDS electrophoresis fractionation of ANX purified MSF-I bioactive HaCaT SEC fractions.....	153
Figure 4.11: A.The purification of MSF-I by SDS electrophoresis B.The identification of NGAL in HaCaT un-fractionated	

conditioned medium by immunoblotting.....	154
Figure 4.12: The standard curve of NGAL indirect ELISA.....	156
Figure 4.13: Immunolocalisation of NGAL in human fibroblasts and keratinocytes.....	158
Figure 4.14: The MSF-Inhibitory activity of NGAL purified from MMP-9/NGAL complex.....	161
Figure 4.15 The MSF-Inhibitory activity of NGAL purified from a eukaryotic and prokaryotic source.....	162
Figure 4.16: The effect of NGAL on fibroblast viability and proliferation.....	165
Figure 4.17: The effect of a NGAL pre-incubation on MSF bioactivity in the 3D collagen gel fibroblast migration assay.....	166
Figure 4.18: The effect of the iron chelator deferoxamine mesylate (DFOM) on the MSF inhibitory activity of NGAL.....	167
Figure 4.19: A systematic representation of the protocol employed for the isolation and subsequent identification of the protein responsible for the MSF inhibitory activity of total HaCaT conditioned medium- NGAL.....	173

Chapter five

Results: THE EXPRESSION OF MSF AND NGAL IN RELATION TO TUMOUR PROGRESSION.

Figure 5.1: Immunolocalisation of MSF in human fibroblasts and keratinocytes.....	190
Figure 5.2. The identification of NGAL in HaCaT series conditioned medium by immunoblotting.....	193
Figure 5.3: The standard curve of colorimetric indirect ELISA for NGAL.....	194
Figure 5.4: Immunolocalisation of NGAL in human fibroblasts and keratinocytes.....	197

Chapter six

Results: THE EXPRESSION OF PRO- AND ANTI- MOTOGENIC BIOACTIVITY BY THE HACAT-RAS CLONES.

Figure 6.1: The motogenic activity of conditioned medium from HaCaT Series cells, comparison with rhMSF.....	211
---	-----

Figure 6.2: The MSF-inhibitory activity of conditioned medium from HaCaT Series cells, comparison with rhNGAL.....	212
Figure 6.3. The motogenic activity of exogenous rhMSF in the presence of conditioned medium.....	213
Figure 6.4: The effect of NGAL on the endogenous motogenic bioactivity of HaCaT Series CM, comparison with rhMSF.....	214
Figure 6.5: The effect of MSF-neutralising antibody, PEPQ1.1, on the endogenous motogenic bioactivity of HaCaT Series conditioned medium comparison with rhMSF.....	215
Figure 6.6. The fractionation of HaCaT Series conditioned medium by Size-Exclusion Chromatography.....	221
Figure 6.7. The fractionation of HaCaT Series conditioned medium by Size-Exclusion Chromatography.....	222
Figure 6.8: The motogenic activity of Superdex 75 fractionated conditioned medium from HaCaT Series cells, comparison with rhMSF.....	226
Figure 6.9: The MSF-inhibitory activity of Superdex 75 fractionated conditioned medium from HaCaT Series cells, comparison with rhNGAL.....	227
Figure 6.10. The motogenic activity of exogenous rhMSF in the presence of Superdex 75 fractionated conditioned medium.....	228
Figure 6.11. The NGAL Indirect ELISA analysis of Superdex 75 fractionated conditioned medium.....	230
Figure 6.12: The motogenic activity of the HaCaT Series SEC fractionated conditioned medium before and after immunoprecipitation with MSF-specific identification antibody RpVSI.....	234
Figure 6.13: The effect of MSF-Inhibitors, NGAL and function neutralising antibody PEPQ1.1, on the endogenous motogenic bioactivity of HaCaT series fractionated conditioned medium post immunoprecipitation....	235
Figure 6.14: The motogenic activity of the gel elutions from the SDS Electrophoresis fractionation of HaCaT Series conditioned medium, comparison with rhMSF.....	240
Figure 6.15: The MSF-inhibitory activity of gel elutions from the SDS Electrophoresis fractionation of HaCaT Series conditioned medium, comparison with rhNGAL.....	241
Figure 6.16. The motogenic activity of exogenous rhMSF in the presence of gel elutions from the SDS Electrophoresis	

fractionation of HaCaT Series conditioned medium.....	242
---	-----

Chapter seven

Results:

THE IDENTIFICATION OF MSF-I PRODUCED BY ENDOTHELIAL CELLS

Figure 7.1: A. The separation of endothelial conditioned medium by SDS PAGE.....	254
B. The identification of NGAL in endothelial cell lines by immunoblotting.....	254
Figure 7.2: Immunolocalisation of NGAL in endothelial cells.....	255
Figure 7.3: The identification of MSF in endothelial cell lines by immunoblotting.....	256
Figure 7.4: Immunolocalisation of MSF in endothelial cells.....	258
Figure 7.5: The motogenic activity of Superdex 75 fractionated conditioned medium from ENDO 742 cells. Comparison with rhMSF.....	263
Figure 7.6: The motogenic bioactivity of Superdex 75 fractionated ENDO 742 conditioned medium. Comparison with rhMSF.....	264
Figure 7.7: The effect of MSF-Inhibitors, NGAL and function neutralising antibody PEPQ1.1, on the endogenous motogenic bioactivity of Superdex 75 fractionated ENDO 742 conditioned medium.....	265
Figure 7.8: The motogenic activity of the gel elutions from the SDS electrophoresis fractionation of ENDO 742 conditioned medium. Comparison with rhMSF.....	267
Figure 7.9: The effect of MSF-Inhibitors, NGAL and function neutralising antibody PEPQ1.1, on the endogenous motogenic bioactivity of the gel elutions from the SDS electrophoresis fractionation of ENDO 742 conditioned medium.....	268
Figure 7.10 : The MSF-inhibitory activity of Superdex 75 fractionated conditioned medium from ENDO 742 cells. Comparison with rhNGAL.....	271
Figure 7.11. The motogenic activity of exogenous rhMSF in the presence of Superdex 75 fractionated ENDO 742 conditioned medium.....	273
Figure 7.12: The MSF-inhibitory activity of gel elutions from the SDS PAGE fractionation of ENDO 742 conditioned medium. Comparison with rhNGAL.....	275
Figure 7.13. The motogenic activity of exogenous rhMSF in the presence	

of gel elutions from the SDS PAGE fractionation of ENDO 742 conditioned medium.....	277
Figure 7.14: The effect of MSF on endothelial morphology.....	280
Figure 7.15. The effect of MSF-Inhibitor PEPQ1.1 antibody on endothelial cells exhibiting the spontaneous sprouting phenotype.....	284
Figure 7.16: The effect of MSF-Inhibitor, NGAL on endothelial cells exhibiting the spontaneous sprouting phenotype.....	287

ACKNOWLEDGEMENTS

I would firstly, like to express my gratitude to Prof William Saunders, Prof Seth Schor and Dr Ana Schor for enabling me to undertake my project within the Unit of Cell and Molecular Biology at the Dental School. I specifically thank Dr Ana Schor, who was originally my supervisor, and wish her a long and happy retirement. I thank Dr Dorothy Crouch, Prof Peter Mossey and Prof David Ricketts for all their time and assistance during this process.

I owe my sincerest gratitude to Dr Sarah Jones for her continued supervision and guidance. I truly appreciate how generous she has been with her time, especially in the final stages of my project. I cannot express how grateful and indebted I am for all her support.

I would also like to thank all the members of the Unit of Cell and Molecular Biology, especially Dr Ian Ellis, Mrs Jacqueline Cox and Mrs Anne Anderson whose expertise, training and advice have been invaluable.

I am completely indebted to my partner, Gary, for his love, patience and understanding without which I would be lost. His absolute love and belief in me has made all this possible.

I thank my sister Helen and the kids, Faye and Stefan, for their love, understanding and support. I apologise to all my friends and family for being posted absent and I am truly grateful for all their boundless love, encouragement and tolerance.

Finally, a big cheer to all my gym bunnies for their laughter, pearls of wisdom and inspiration.

DECLARATION

I declare that I am the author of this thesis and that I have consulted all the references cited. The work of which this thesis is a record has been done by myself and not previously been accepted for a higher degree. This work has been carried out in Unit of Cell and Molecular Biology, University of Dundee Dental School, under the supervision of Dr Sarah J. Jones and Dr Dorothy H. Crouch.

Signed.....

Date.....

Margaret M. Florence

CERTIFICATE

I hereby certify that Margaret M. Florence has fulfilled the conditions of ordinance 39 of the University of Dundee and is qualified to submit thesis for the degree of Doctor of Philosophy.

Signed

Date.....

Dr Sarah J. Jones
Lecturer
Unit of Cell and Molecular Biology
Dundee Dental School
University of Dundee

Signed.....

Date.....

Dr Dorothy H. Crouch
Senior Lecturer
Unit of Cell and Molecular Biology
Dundee Dental School
University of Dundee

DEDICATION

To, the two most important men in my life.

My Dad, whose unconditional love I will always treasure.

And my drummer boy Gary, who is my world.

Words cannot express my love and devotion.

LIST OF ABBREVIATIONS

>	greater than
≥	greater than or equal to
<	less than
≤	less than or equal to
%	Percentage
2D	Two Dimensional
3D	Three Dimensional
α-SMA	Alpha Smooth Muscle Actin
Ab	Antibody
ABC	Avidin Biotin Complex
aFGF	Acidic Fibroblast Growth Factor
Akt	Protein kinase B
ALK1	Activin receptor-Like Kinase-1
Ang	Angiopoietin
BAD	Bcl-2 associated death promoter
BAEC	Bovine Aortic Endothelial Cell
Bcl2	B-cell lymphoma 2
Bcl-XL	B-cell lymphoma extra large
BFA	Brefeldin A
bFGF	Basic Fibroblast Growth Factor
bHLH	Basic Helix-Loop-Helix
bp	base pair
BSA	Bovine Serum Albumin
CAF	Carcinoma Activated Fibroblasts
CDI	Cartilage Derived Inhibitor

Cell-BD	RGD- mediated binding to integrins
cFn	Cellular Fibronectin
CM	Conditioned Medium
Conc	Concentration
CMM	Cutaneous Malignant Melanoma
CO₂	Carbon dioxide
CRC	Colorectal Carcinoma
CSC	Cancer Stem Cells
CSF-1	Macrophage colony-stimulating factor-1
CXCL	Chemokine (C-X-C motif) ligand
CXCR	Chemokine (C-X-C motif) receptor
DAAP	Double Anti-angiogenic Protein
DCS	Donor Calf Serum
DEAE	Diethylaminoethyl Cellulose
DFOM	Deferoxamine Mesylate
Dll4	Delta-like ligand 4
DMSO	Dimethyl Sulphoxide
DNA	Deoxyribonucleic Acid
DPX	Distyrene, Plasticizer, Xylene mountant
DTT	Dithiothreitol
°C	degree Celsius
ECM	Extracellular Matrix
EDA	Extra domain A
EDB	Extra domain B
EGF	Endothelial Growth Factor

EGFR	Endothelial Growth Factor Receptor
EGTA	Ethylene Glycol Tetraacetic Acid
ELISA	Enzyme-Linked Immunosorbent Assay
EMT	Epithelial to Mesenchymal Transition
EPC	Endothelial Cell Progenitors
ER	Endoplasmic Reticulum
ET	EGTA Trypsin
FDA	Federal Drug Agency (USA)
FGF	Fibroblast Growth Factor
F-msa	Fractions displaying migration stimulating activity
Fn	Fibronectin
Fib	Fibrin
Fib2	COOH-terminal fibrin binding site
FSF	Foreskin foetal fibroblasts
GBD	Gelatin Binding Domain
G-CSF	Granulocyte Colony-Stimulating Factor
Gel-BD	Binding to gelatin/collagen
HA	Hyaluronic Acid
HAEC	Human Aortic Endothelial Cells
HBBS	Hanks Balance Salt Solution
HCC	Human Hepatocellular Carcinoma
hCG	Human Chorionic Gonadotropin
HCl	Hydrochloric Acid
Hep1/Fib1	NH ₂ -terminal low-affinity binding to heparin and fibrin
Hep	Heparin
Hep2	High affinity heparin binding

HGF	Hepatocyte Growth Factor
HIF	Hypoxic Inducible Factor
HMEC	Human Mammary Tumour Progression Model
HNL	Human Neutrophil Lipocalin
HOEC	Human Omentum microvascular Endothelial Cells
HOX	Homeobox gene
HPV	Human Papillomavirus
HRE	Hypoxia Response Element
HRP	Horse radish Peroxidase
H₂SO₄	Sulphuric Acid
HUVEC	Human Umbilical Vein Endothelial Cells
IGD	Isoleucine-glycine-aspartic acid
IGF	Insulin-like Growth Factor
IGFR	Insulin-like Growth Factor Receptor
IgG	Immunoglobulin
IHC	Immunohistochemistry
IL-8	Interleukin-8
IP	Immunoprecipitation
IPTG	Isopropyl- β -D-thiogalactopyranoside
JNK	Jun N-terminal Kinase
kDa	Kilo Dalton
LPS	Lipopolysaccharides
MAb	Monoclonal Antibody
MCG	Methyl Cellulose Gel
MEM	Minimum Essential Medium Eagle
MET	Mesenchymal to Epithelial Transition

ml	millilitre
MMP	Matrix Metalloproteinase
mRNA	Messenger Ribonucleic Acid
miRNA	Micro Messenger Ribonucleic Acid
MSF	Migration Stimulating Factor
MSF-I	Migration Stimulating Factor Inhibitor
MTT	3-(4,5-Dimethylthiazol-2-yl)-2,5-diphenyltetrazolium bromide
m/v	mass/ volume
MW	Molecular Weight
µg/ml	micro gram per millilitre
µl	microlitre
NaCl	Sodium Chloride
NaHCO₃	Sodium Hydrogen Carbonate
ng/ml	nano gram per millilitre
NGAL	Neutrophil Gelatinase Associated Lipocalin
NGALR	Neutrophil Gelatinase Associated Lipocalin Receptor
NGS	Normal Goat Serum
nm	Nanometres
NSS	Normal Swine Serum
NSLC	Non-small Cell Lung Carcinoma
OD	Optical Density
p53	Tumour Suppressor Gene
PBS	Phosphate Buffered Saline
PBS-T	Phosphate Buffered Saline Tween 20
PD-ECGF	Platelet-Derived Endothelial Cell Growth Factor
PDGF	Platelet Derived Growth Factor

PDGFR	Platelet Derived Growth Factor Receptor
pg/ml	pico gram per millilitre
PHD	Prolyl 4-Hydroxylase Domain
PIGF	Placental Growth Factor
PIGFR	Placental Growth Factor Receptor
PI3K	Phosphoinositol-3-kinase
PLC	Phospholipase C
PKC	Protein Kinase C
PTC	Papillary Thyroid Carcinoma
PTEN	Phosphatase and tensin homolog
PVDF	Polyvinylidene Fluoride
Ras	small GTPase of the Ras homolog family
RGD	Arginine-Glycine-Aspartic Acid
Rp	Rabbit Polyclonal
rh	Recombinant Human
rhMSF	Human Recombinant Migration Stimulating Factor
rhNGAL	Human Recombinant Neutrophil Gelatinase Associated Lipocalin
RNA	Ribonucleic Acid
ROS	Reactive Oxygen Species
rpm	Revolutions per minute
RT	Room Temperature
RTK	Receptor Tyrosine Kinase
RTKI	Receptor Tyrosine Kinase Inhibitor
RT-PCR	Real Time Polymerase Chain Reaction
SCC	Squamous Cell Carcinoma
SD	Standard Deviation

SDF-1α	Stromal cell Derived Factor 1 α
SDS	Sodium Dodecyl Sulphate
SDS PAGE	Sodium Dodecyl Sulphate Polyacrylamide Gel Electrophoresis
SEC	Size Exclusion Chromatography
SF	Scatter Factor
SF	Serum Free
SF MEM	Serum Free Minimum Essential Medium Eagle
SV-40	Simian Virus 40
S-1-P	Sphingosine-1-Phosphate
TAF	Tumour Angiogenesis Factor
TAF	Tumour Associated Fibroblast
TAM	Tumour Associate Macrophages
TBS	Tris Buffer Saline
TBST	Tris Buffer Saline Tween 20
TGF	Transforming Growth Factor
TGS	Tris Glycine SDS
TIMP	Tissue Inhibitor of Metalloproteinase
TMB	Tetramethylbenzidine
TNFα	Tumour Necrosis Factor - α
TPI	Triosephosphate Isomerase
Tris	Trisaminomethane
Tris- HCl	Trisaminomethane Hydrochloride
TSP	Thrombospondin
UTR	Untranslated Region
UV	Ultraviolet
V	Volts

VHL	von Hippel-Lindau
VPF	Vascular Permeability Factor
v/v	volume/ volume
VEGF	Vascular Endothelial Growth Factor
VEGFR	Vascular Endothelial Growth Factor Receptor
WT	Wild Type
w/v	weight/ volume

ABSTRACT**MIGRATION STIMULATING FACTOR, THE SEARCH FOR INHIBITORS**

The oncofetal protein Migration Stimulating Factor (MSF) is a truncated isoform of human fibronectin which exhibits numerous bioactivities that are pertinent to cancer progression. The MSF protein (70kDa) has potent motogenic activity, with only femtomolar concentrations required to produce half-maximal. The proteolytic degradation of MSF generates the functionally equivalent 43kDa Gel-BD domain and 21kDa IGD peptide. The screening of conditioned medium (CM) for bioactivity revealed two sources of MSF-inhibitory (MSF-I) activity; the spontaneously immortalised human keratinocyte cell line (HaCaT) and endothelial cells (ENDO 742) specifically when exhibiting a cobblestone phenotype.

The CM from the HaCaT keratinocyte line was fractionated by both molecular weight and ionic charge, followed by sequence analysis which identified the inhibitor as Neutrophil Gelatinase Associated Lipocalin (NGAL). Both recombinant and cell-produced NGAL neutralise the motogenic activity of MSF. This novel bioactivity for NGAL is not dependent on its iron transportation capability or direct binding to MSF. HaCaT cells also secrete MSF; the bioactivity of which is masked by the co-expression of NGAL.

The relative expression levels of the pro- and anti-motogenic factors, MSF and NGAL, were assessed using an *in vitro* model for human skin carcinogenesis, the HaCaT *-ras* clones. The shift in tumorigenic potential from benign to metastatic was characterised by a decrease in NGAL and an increase in MSF expression, indicating their potential role in tumour progression.

The protein responsible for the MSF inhibitory activity is cell- type specific; NGAL is not expressed by endothelial cells *in vitro*. MSF stimulates the generation of sprouting endothelial cells from a cobblestone monolayer and acts a survival factor for spontaneously sprouting cells within a 3D matrix. NGAL does not selectively target sprouting phenotype of endothelial cells, but induces apoptosis in all endothelial cells. Fractionation of endothelial CM revealed that both sprouting and cobblestone cells express bioactive MSF and a MSF-I. Endothelial MSF-I was located in fractions of MW 70kDa, 40kDa and ≤ 25 kDa; further investigation is required to identify the protein responsible.

Chapter 1: Literature Review

1.1 THE HALLMARKS OF CANCER

The progressive transformation of normal cells into highly malignant derivatives is considered to be a multistep process. Evidence was gained from the analysis of human cancers, which revealed that the lesions could represent intermediate steps in a process through which cells evolve progressively from normalcy via a series of malignant states into invasive cancers; with each step the cell acquires a specific growth advantage (Foulds, 1954, Nowell, 1976). Furthermore, several types of pre-malignant lesions, such as dysplasia and hyperplasia, have been detected prior to the emergence of fully malignant invasive tumours (Yokota, 2000). Transgenic models of tumourigenesis have also frequently conferred that a series of rate limiting steps is involved in cancer progression (Bergers *et al.*, 1998). These discoveries have formed the basis of the clinical and pathological methods for cancer staging.

The final stage of cancer progression is the formation of secondary tumours at a distant site, a process termed metastasis. It is these distant metastases that are responsible for the majority of cancer-related deaths (Yokota, 2000). 80% of all first relapses of breast cancer patients are due to secondary tumours alone or concurrent with loco-regional area (Citron *et al.*, 2003). The five year survival rate of ductal carcinoma *in situ* post-surgery is 95% compared to only 15% for stage IV breast cancer (that is with systemic metastases) despite the administration of every available therapeutic treatment (Bastid, 2012). Undeniably, the most important clinical prognostic factor is the presence of distant metastases. Therefore, research efforts have focused on how a cancer cell accomplishes this journey to invade and ultimately colonise.

Neoplastic disease is considerably diverse, with over a hundred human cancers identified. Yet, in 2000, Hanahan and Weinberg proposed that this vast catalogue of cancer cell genotypes is achieved by the acquisition of six essential alterations in cell physiology. That is, as a normal cell progressively evolves to a neoplastic state, they acquire a succession of these hallmark capabilities. The six hallmarks of cancer are: self-sufficiency in proliferative signals, insensitivity to growth suppressors, resistance to programmed cell death (apoptosis), a limitless replicative potential, induction of angiogenesis and activation of invasion and metastasis (Table 1.2). Hanahan and Weinberg have subsequently added two new emerging hallmarks; the capability to deregulate cellular metabolism and to resist immune defence mechanisms (2011).

Table 1.1: The Hallmarks of Cancer. Originally proposed in 2000 by Hanahan and Weinberg. (Hanahan and Weinberg, 2000, 2011).

Hallmarks of Cancer	Potential Mechanisms
Sustaining proliferative signalling	<ul style="list-style-type: none"> • Autocrine proliferative stimulation • Cancer cell stimulation of cells in tumour-associated stroma, which respond by expressing various growth factors. • Elevated level of receptor proteins, resulting in cells becoming hyper-responsive to a limited source of growth factor • Structural changes in receptor molecules facilitate ligand-independent stimulation. • Constitutive activation of signalling pathways downstream of receptors. • Defective negative feedback mechanisms.
Resisting cell death	<ul style="list-style-type: none"> • Loss of TP53 tumour suppressor function. • Increased expression of anti-apoptotic regulators (Bcl-2, Bcl-xL). • Increased expression of survival factors (Igf1/2). • Down-regulation of pro-apoptotic factors (Bax, Bim, Puma). • Adaptation of autophagic program. • Release of pro-tumoural factors by necrotic cell death of cancer cells.
Evading growth suppressors	<ul style="list-style-type: none"> • Inactivation of tumour suppressor genes (RB and TP53). • Loss of contact mediated growth suppression (NF2 gene/ Merlin, LKB1).
Activating invasion and metastasis	<ul style="list-style-type: none"> • Down-regulation or mutational inactivation of the cell to cell adhesion molecule, E-cadherin. • Expression of epithelial –mesenchymal transition (EMT) inducing transcription factors (Snail, Slug, Twist, Zeb1/2). • Cancer cell activation of stromal cells to promote local invasion. • Tissue-specific colonisation programs.
Enabling replicative immortality	<ul style="list-style-type: none"> • Maintenance of telomeric DNA. • Transient telomere deficiency.
Inducing angiogenesis	<ul style="list-style-type: none"> • Activation of angiogenic switch. • Imbalance of angiogenesis inducers (VEGF-A, FGF) and inhibitors (TSP-1). • Oncogene (<i>Ras</i>, <i>Myc</i>) upregulation of angiogenic factors expression. • Pro- angiogenic contribution by the innate immune system (macrophages, neutrophils, mast cells, myeloid progenitors).

1.2 AN INTRODUCTION TO MIGRATION STIMULATING FACTOR

Migration Stimulating Factor (MSF) was the first truncated isoform of human fibronectin to be described (Schor *et al.*, 2003). Discovery was led by experimental *in vitro* observations of the disparity in migratory potential between adult and foetal fibroblasts (Schor *et al.*, 1985). Isolated from foetal skin fibroblast conditioned medium, MSF was shown to be responsible for the foetal cell's ability to migrate into a 3D matrix of native type I collagen gel by a substantially greater extent than their healthy adult counterparts (Schor *et al.*, 1988, Grey *et al.*, 1989). However, although the adult fibroblasts do not express MSF themselves, they react to its presence when exposed to foetal fibroblast conditioned medium, with increased motogenic activity equivalent to that of foetal cells. The responsiveness of adult fibroblasts to MSF is integral to the sensitive 3D collagen gel migration bioassay, which has become pivotal in assessing MSF expression by numerous cell lines *in vitro* and its subsequent purification from bioactive conditioned medium (Schor *et al.*, 1988 and 1989).

MSF was cloned from a foetal fibroblast cDNA library and shown to be a product of variant alternative splicing (Schor *et al.*, 2001, 2003). The 2.1Kb MSF message is generated from the fibronectin gene by read-through of intron 12, which separates exon III-1a and III-1b, followed by premature intra-intronic cleavage and polyadenylation. Consequently, due to this post-transcriptional foreshortening, the MSF message is identical to the 5' end of fibronectin, up to and including exon III-1a, followed by a 30bp intron-derived in frame coding sequence and a 165bp 3'UTR. Therefore, the 70kDa MSF protein is identical to the N- terminus of fibronectin and terminates in a MSF-unique (intron coded) 10 amino acid sequence, which is not present in any full length fibronectin. (EMBL accession number AJ535086-NCBI/Pub Med) (Schor *et al.*, 2003, Kay *et al.*, 2005, Jones *et al.*, 2007).

In addition to the 2.1Kb MSF transcript, subsequent studies using Northern Blot analysis with an MSF-specific probe identified an additional 5.9Kb MSF mRNA. Unlike the 2.1Kb MSF mRNA which is specific to foetal fibroblasts, the 5.9Kb version is present in all cultured fibroblasts. Both MSF mRNA species share an identical coding region, however they differ in the length of the remaining intron- derived 3' – untranslated region (UTR) and their ability to be transported from the nucleus. MSF expression therefore appears to be regulated by a multistep process; initially a 5.9Kb mRNA is transcribed and sequestered within the nucleus, cleavage of its 3'UTR

produces a truncated 2.1Kb version which is permitted export to the cytoplasm and subsequently translated. Control of this cleavage event is perhaps a potential novel mechanism for the therapeutic control of gene expression. Transforming Growth Factor beta 1 (TGFβ1) has been shown to increase 3'UTR cleavage of the 5.9Kb mRNA and has been suggested as a mechanism for increasing MSF expression during tumour progression. Adult fibroblasts transfected with constructs expressing dominant-negative p53 mutants exhibited altered MSF mRNA and protein secretion, implying that tumour promoting factors may induce MSF as part of their oncogenic repertoire. (Kay *et al.*, 2005). Due to the presence of an AU rich instability element in the 3'UTR MSF has an extremely short half-life (Schor *et al.*, 2003).

Approximately 20 distinct full length isoforms of human fibronectin have been identified (molecular mass approximately 250kDa) (Kornblihtt, 1996). These full length forms are generated by alternative splicing of the fibronectin primary gene transcript resulting in either the retention or deletion of the type III exons EDA and EDB; in addition to further splicing in the down-stream IIICS region (Hynes 1990). MSF is a truncated isoform of fibronectin and was the first to be described in humans. Zebrafish also produce a truncated form of fibronectin; Fn2, a C terminus 70kDa isoform which terminates in a unique 20 amino acid sequence (Zhao *et al.*, 2001). Other truncated fibronectin isoforms have been detected in goldfish, trout, mice and humans (Liu *et al.*, 2003).

Fibronectin (Fn) is a modular extracellular matrix glycoprotein (Type I, Type II and Type III) consisting of various proteolysis-resistant functional domains, named on the basis of their binding affinities for other matrix macromolecules (fibrin, collagen and proteoglycans) and members of the integrin family. Cell adhesion is often described as the principle function of fibronectin but the ability of its domains to form different structures results in fibronectin having numerous cryptic activities, including the mediation of cellular interactions within the ECM with important roles in cell migration, growth and differentiation (Hynes, 1990). Obviously, MSF shares a similar modular structure to the fibronectin N-terminus (Figure 1.1).

A potent motogenic factor, MSF has the ability to stimulate the migration of fibroblast, epithelial and endothelial cells. The motogenic bioactivity of MSF is mediated by the IGD amino acid motif (iso-gly-asp) bioactive sequence located within its gelatin binding domain (GBD) (Schor *et al.*, 1996) (Figure 1.2). GBD is a highly conserved feature of the fibronectin type I module; MSF contains four such motifs in Fn1 modules 3, 5, 7 and 9. Antibody neutralisation experiments have shown that MSF-stimulated

migration is completely inhibited by an anti-GBD monoclonal antibody whilst unaffected by antibodies raised to other FN functional domains. *In vitro* mutagenesis experiments revealed that only Fn1 modules 7 and 9 are bioactive in serum free conditions, whilst modules 3 and 5 require presence of serum or vitronectin to be motogenic. The IGD sequences appear to act in a manner which induces Focal Adhesion Kinase (FAK) phosphorylation (Schor *et al.*, 1993, 1994, 1996, 2003. Ellis *et al.*, 2010).

The development of a recombinant MSF protein has progressed the understanding of the motogenic activity of MSF. The recombinant protein, which is identical to MSF purified from foetal fibroblast conditioned medium, possesses half maximal activity at femomolar concentrations with activity characterised by a bell shaped dose response curve. Similarly its activity is neutralised by anti-GBD antibodies (Schor *et al.*, 2003). Recombinant MSF and GBD experiments led to the discovery that the fibroblast motogenic response is strictly matrix dependent, being only manifest by cells that are adherent to native but not denatured type I collagen (Schor, 2001). It has been suggested that the matrix dependence of MSF may provide a means of controlling cellular responsive to MSF during pathological processes characterised by matrix remodelling i.e cancer.

Consequently, MSF and GBD are considered to be functionally equivalent. That is, two independent mechanisms create a factor whose end point is to produce the same motogenic activity. MSF is the genetically produced truncated isoform of fibronectin, whilst GBD is generated by the proteolytic degradation of matrix fibronectin. The obvious advantage of a genetically generated MSF is having the controlled production of a single bioactive factor without the necessity of proteolysis producing a mixture of Fn fragments that express a complex array of cryptic bioactivities, some of which maybe actually be inhibitory (Schor *et al.*, 2003). Described “neo-activities” attributed to proteolysis generated Fn fragments include inhibition of cell proliferation (Muir and Manthorpe, 1992), adipocyte differentiation (Fukai *et al.*, 1993) and stimulation of monocyte migration (Clark *et al.*, 1988).

Furthermore to its motogenic bioactivity, MSF also possesses the ability to stimulate matrix remodelling via proteolytic activity and hyaluronic acid biosynthesis, and angiogenesis (Schor *et al.*, 1988, 1989, 1990. Kay *et al.*, 2005. Ellis *et al.*, 1992. Houard *et al.*, 2005). Yet, all of MSF’s bioactivities appear to have a causal link to its motogenic activity (Table 1.2).

Concentrations of MSF which induce cell migration also produce a parallel stimulation in the synthesis of high molecular weight hyaluronic acid (HA) (Ellis *et al.*, 1992). The response of adult fibroblasts to MSF appears to be mediated by HA synthesis. Co-incubating MSF with Streptococcal hyaluronidase prevented the stimulation of adult fibroblasts to migrate. In addition, the application of HA to adult fibroblast stimulates their migration (Schor *et al.*, 1989). Foetal fibroblasts, which have a greater migratory potential, have been shown to produce significantly more HA than their adult counterparts; both hyaluronidase and MSF function- neutralising antibodies have the ability to diminish their migration activity (Chen *et al.*, 1989, Aljorani, 2012).

Site-directed mutagenesis determined that the zinc-binding motif, HEEGH, located in module I-8, is responsible for MSF's fibronectin proteinase activity. The substitution of the two histidine residues of HEEGH for phenylalanine resulted in the complete loss of both motogenic and proteinase bioactivity. Approximately 65% of MSF's motogenic activity has been shown to be dependent on its proteinase activity, via either extracellular matrix digestion or by the processing of cell surface molecules. The invasive potential of several adenocarcinoma cell lines appears to relate to their MSF expression levels (Houard *et al.*, 2005). Perhaps by modulating the matrix composition MSF is creating a permissive microenvironment which promotes cells to adopt a more invasive phenotype, subsequently promoting cancer progression (Schor *et al.*, 2003).

Both *in vivo* and *in vitro* assays have shown the ability of MSF to elicit an angiogenic response. In the chick yolk sac assay an application of MSF induced blood vessel formation within a 24 hour period; acting in a bell-shaped dose response over a broad concentration range, 0.5-500ng/MCG (unpublished data, Schor and Schor, 2010).

Collagenous graft matrices containing MSF subcutaneously implanted into rats and pigs induce endothelial cell and fibroblast infiltration into the graft matrix, which subsequently leads to the establishment of a significantly greater number of blood vessels when compared to the controls (Schor and Schor, 2010).

In a reflection of the *in vivo* situation, cultured endothelial cells have the ability to adopt different phenotypes. The resting or cobblestone phenotype is characterised by a homogenous monolayer of contact-inhibited polygonal cells considered to be morphologically similar to the endothelial lining of the blood vessel wall *in vivo*. The second phenotype appears in post-confluent cultures, when the resting cells undergo a transition into a distinctive elongated fibroblastoid morphology and begin to grow underneath the intact cobblestone monolayer, eventually forming an interactive network; described as displaying a sprouting phenotype they reflect endothelial cells *in*

vivo undergoing an angiogenic response (Folkmann and Haundenschild 1979 and 1980, Makarski 1982, Schor *et al.*, 1983). MSF has been shown to induce endothelial activation *in vitro*; homogenous cobblestone endothelial cells are stimulated to adopt the sprouting phenotype (Schor and Schor, 2010). Unlike MSF stimulation of fibroblast migration, which only requires the two IGD motifs present in Fn type I modules 1-7 and 1-9, endothelial migration requires all four IGD motifs (1-3, 1-5, 1-7, 1-9) to be bioactive (Schor and Schor, 2010).

The expression pattern and effective bioactivities of MSF, *in vitro* and *in vivo*, all of which are pertinent to cancer progression and wound healing, led to its description as a potent soluble oncofetal regulatory molecule. Using both the 3D collagen gel migration bioassay and immunohistochemistry with MSF specific antibodies (raised against its unique c-terminal decapeptide) it has been shown that during foetal development MSF is expressed by keratinocytes, fibroblasts and vascular endothelial cells but is generally not expressed in the equivalent healthy adult cells. However, it is transiently re-expressed during acute wound healing and persistently re-expressed by both tumour and stromal cells in various common human cancers, including breast, lung, colorectal, oral, prostate and oesophageal. (Unpublished data. Schor *et al.*, 2003, 2005, Jones *et al.*, 2007).

Table 1.2: The Bioactivities of MSF. The numerous actions of MSF target a variety of cell types and the resulting effects are relevant to the progression of cancer (Schor *et al.*, 1988, 1989, 1990, 1996, 2003; Kay *et al.*, 2005, Ellis *et al.*, 1992, Houard *et al.*, 2005).

BIOACTIVITY	TARGET	EFFECT
Endothelial cell activation	Endothelial cells	Angiogenesis.
Hyaluronic acid synthesis	Fibroblasts	Matrix remodelling. Cellular migration
Motogenesis	Fibroblasts Endothelial cells Epithelial cells	Cellular migration Invasion. Metastasis
Proteolysis	Fibroblasts Extracellular Matrix	Matrix remodelling. Processing of cell surface molecules.

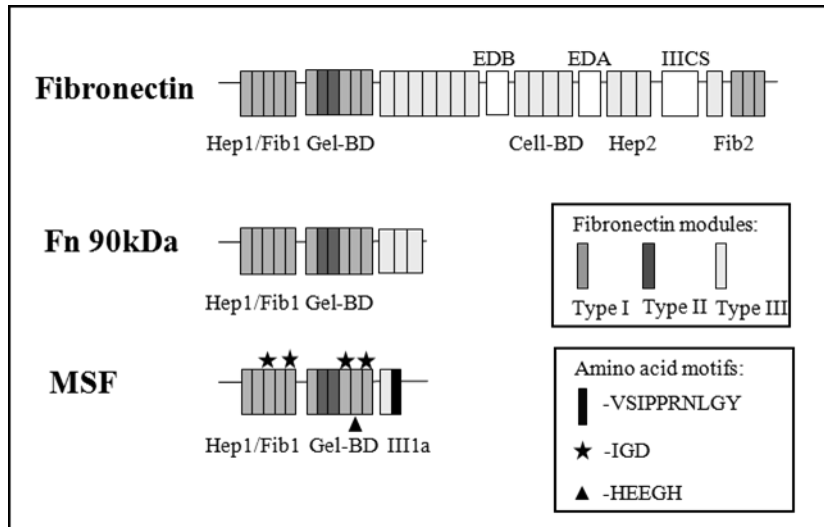


Figure 1.1: A comparison of the modular structures of fibronectin and MSF.

Consisting of the functional domains: Hep-1/Fib1 (NH₂-terminal low-affinity binding to heparin and fibrin), Gel-BD (binding to gelatin/collagen), Cell-BD (RGD-mediated binding to integrins), Hep-2 (high affinity heparin binding), Fib2 (COOH-terminal fibrin binding site). Each functional domain is composed of three possible homology modules (types I, type II and type III). Alternative splicing of the fibronectin primary gene transcript at the sites EDA, EDB and IIICS produce various “full-length” isoforms of fibronectin. MSF contains two domains also present in the N-terminus of fibronectin and the first part of the third domain; the truncation takes place in the first type III repeat. Image courtesy of Dr S. Jones (Schor and Schor, 2001; Ellis *et al.*, 2010)

MSF

MLRGP GPGLLLLLAVQCLGTAVPSTGASKSKRQAQQMVQPQSPVAVSQSKPGCYDNGKHY
 QINQQWERTYLGNALVCTCYGGSRGFNCESKPEAEETCFDKYTGNTYRVGDTYERPKDS
 MIWDCTCIGAGRGRISCTIANRCHEGGQSYK**IGD**TWRRPHETGGYMLECVCLGNGKGEW
 TCKPIAEKCFDHAAGTSYVVGETWEKPYQGWMMVDCTCLGEGSGRITCTSRNRCNDQDT
 RTSYR**IGD**TWRKKDNRGNLLQCICTGNRGEWK CERHTSVQTTSSGSGPFTDVRAAVYQ
 PQPHQP PPYPGHCVTD SGVVYSVGMQWLKTQGNKQMLCTCLGNGVSCQETAVTQTYGGN
 SNGEPCVLPFTYNGRTFYSC TTEGRQDGHLCSTTSNYEQDQKYSFCTDHTVTLVQTRGG
 NSNGALCHFPFLYNNHNYTDCTSEGRDNMKWCGTTQNYDADQKFGFCPMAAHEEICTT
 NEGVMYR**IGD**QWDKQHDMGHMMRCTCVGNRGEWTCIAYSQLRDQCI VDDITYNVNDF
 HKR**HEEGH**MLNCTCFGQGRGRWKCDPVDQCQDSETGTFYQ**IGD**SWEKYVHGVRVYQCYCY
 GRGIGEWHCQPLQTYPSSSGPVEVFITETPSQPNSHPIQWNAPQPSHISKYILRWRPVS
 IPPRNLGY

Figure 1.2: The protein sequence of MSF. The IGD and HEEGH amino acid motifs are highlighted. The protein sequence was confirmed by mass spectrometry. Image courtesy of Dr S. Jones (Schor and Schor, 2001; Ellis *et al.*, 2010)

1.3 MSF AND CANCER PROGRESSION

MSF is present in more than 80% of common human tumours. Its diverse functionality has led to the postulation that MSF is a driver of cancer progression (Table 1.2) (Schor and Schor, 2010). As previously discussed, MSF exhibits number of potent bioactivities, including the stimulation of cell migration/ invasion, matrix remodelling and angiogenesis, which are all pertinent to cancer evolution (Kay *et al.*, 2005, Hu *et al.* 2009, Schor and Schor 2010) (Table 1.1). The importance of MSF in cancer progression is made all the more relevant when paralleling its bioactivities with Hanahan and Weinberg's description of the essential alterations in cell physiology required for cancer development (Hanahan and Weinberg, 2000 and 2011).

Recent research has shown how MSF contributes to achieving these hallmarks of cancer; thereby, rendering MSF as a potential novel tumour biomarker and prognostic indicator (Schor and Schor, 2010). Detectable quantities of serum MSF have been measured in more than 90% of breast cancer patients, compared to only 10-15% of the healthy age matched controls (Picardo *et al.*, 1991). Evidence suggests that this systemic expression of MSF may continue, even after resection of the primary tumour and without reoccurrence of the disease; implying that the level of serum MSF does not relate to tumour burden (Aljorani *et al.*, 2011). *In situ* hybridisation experiments, using a MSF specific antisense riboprobe, detected weak MSF expression in a small percentage of ductal epithelial cells and interlobular fibroblasts in normal tissue whilst in the breast tumours strong expression was detected in carcinoma cells, stromal fibroblasts and some blood vessels. Initial *ex vivo* observations have suggested a poorer prognosis associated with an elevated MSF expression in breast tumours. As in breast cancer, MSF is over-expressed in both epithelial and stromal cells of malignant salivary gland tumours (Aljorani *et al.*, 2011).

Cell migration and invasion into tissue matrices is essential for cancer cell metastasis. MSF is a potent stimulator of cell migration/ invasion; responsible for the increased migratory activity of fetal fibroblasts, as compared to their adult counterparts (Schor *et al.*, 1988, Grey *et al.*, 1989). The generation of an hTERT-immortalised fibroblast cell line overexpressing MSF conferred a greater migratory potential than the vector-alone control fibroblasts. However, the overexpression of MSF also resulted in a change of phenotype to that of a cancer-associated fibroblast. The MSF fibroblasts were characterised by myofibroblast differentiation with the expression of markers including

smooth muscle-specific proteins and two small GTPase proteins, Rac1 and Cdc42. In addition, they appeared to be functioning as a chemo-attractant stimulating cancer cell migration. Finally, MSF overexpression led to the increased production of TGF β , which is upregulated in most tumours and acknowledged to play a vital role in cancer progression (Carito *et al.*, 2012).

The effect of MSF on invasiveness was also examined by upregulating MSF in the human bronchial-alveolar carcinoma cell line, A549 (Deng *et al.*, 2013). The migration and invasion of A549 cells increased substantially after MSF upregulation, although the proliferation rate remained unchanged. As there was no detected increase in MMP-2 and MMP-9 expression, it was suggested that MSF may promote cell migration and invasion by enhancing amoeboid invasion, in the absence of proteolytic ECM breakdown (Deng *et al.*, 2013).

A further study investigating the effect a tobacco carcinogen, benzo(a)pyrene, had on A549 cell gene expression levels, revealed the induction of changes in expression levels of numerous genes related to the epithelial to mesenchymal transition (EMT) process (Yoshino *et al.*, 2007). EMT is considered an essential process in tumour progression. Of these EMT related genes, MSF was the most up regulated; suggesting that MSF may influence the transformation of tumour cells and may also promote EMT in lung epithelium (Yoshino *et al.*, 2007). A subsequent examination of MSF expression in non-small cell lung cancer (NSLC) discovered that MSF was overexpressed in both tumour cells and a variety of tumour-associated stromal cells including fibroblasts, microvascular endothelial cells and macrophage dust cells. Indicating that MSF is over expressed during tumour occurrence and progression, and maybe a potential biomarker of NSLC (Deng *et al.*, 2013)

Critical to a role for MSF in cancer progression is considered to be its ability to create a more permissive tumour microenvironment by remodelling via its proteolytic bioactivity and synthesis of HA (Schor *et al.*, 2003). However, MSF has also been shown to metabolically remodel the tumour microenvironment by reprogramming cancer-associated fibroblasts toward glycolytic metabolism which results in the generation of a catabolic tumour microenvironment that actively “fuels” anabolic tumour growth (Carito *et al.*, 2012). MSF overexpressing fibroblasts activate the inflammation-associated transcription factor NF κ B, which controls the autophagic process, resulting in the generation of elevated L-lactate production and a decrease in mitochondrial activity, thereby directing a shift toward glycolytic metabolism. Glycolytic fibroblasts are thought to increase tumour growth by providing high-energy

nutrients (L-lactate) to epithelial cancer cells; MSF overexpressing fibroblasts increased tumour growth by up to four fold (Carito *et al.*, 2012).

Another, consequence of MSF overexpression was the activation of the Akt pathway, which may protect the cells against apoptosis due to the transcription of pro-survival genes. It was suggested that Akt activation by MSF in stromal fibroblasts may lead to activation of protein synthesis, as a compensatory mechanism to prevent apoptotic cell death in cells undergoing constitutive autophagy/ mitophagy (Carito *et al.*, 2012).

Tumour-associated macrophages (TAMs), have recently become recognised as having a crucial role in the development of a tumour microenvironment; directly affecting neoplastic cell growth, stimulating angiogenesis and extracellular remodelling (Solinas *et al.*, 2010). MSF has been shown to be expressed by TAMs *in vitro*; being associated with the M2 polarisation of macrophages thereby contributing to the macrophage – mediated promotion of cancer cell invasion and metastasis. Experiments performed using MSF-containing supernatants of tumour-conditioned macrophages showed that due to its Gel-BD, MSF had a strong chemotactic activity for monocytes and tumour cells; suggesting an autocrine regulatory loop for leukocyte recruitment in addition to paracrine effects on the tumour cells (Solinas *et al.*, 2010).

The induction of angiogenesis is a key step in cancer progression (Folkman, 1971). The establishment of tumour vasculature is essential to enable tumour growth and metastasis (Mauriz and Gonzalez-Gallego, 2008). As discussed, MSF is known to induce an angiogenic response in both *in vitro* and *in vivo* models. Exposure of endothelial cells *in vitro* to MSF results in endothelial activation as manifested by the adoption of a sprouting cell phenotype. Whilst *in vivo* rat and pig models and the chick yolk sac assay have shown MSF elicit the induction of an angiogenic response, over a broad concentration range (unpublished data, Schor *et al.*, 1983, Schor and Schor, 2010).

The subsequent discovery that endothelial cells present within tumours express MSF implied a role of MSF in tumour-related angiogenesis (Schor *et al.*, 2003, Kay *et al.*, 2005). Experiments performed by Hu *et al* (2009) have revealed that the *in vivo* bio-distribution of a labelled anti-MSF antibody (1D2 monoclonal antibody) was selectively concentrated in tumour blood vessels in a mouse model of xenograft oesophageal carcinoma and the inhibition of MSF bioactivity resulted in a 70% reduction in tumour growth. Thus, implying MSF could be a target for anti-angiogenic treatment of oesophageal cancer (Hu *et al.*, 2009).

MSF has been described as a pleiotropic effector, capable of eliciting multiple responses from various target cell types (Schor and Schor, 2010). A critical functional role of this

oncofetal protein appears to be as a driver of cancer progression. MSF bioactivities are consistent with Hanahan and Weinberg's hallmarks of cancer progression; the ability to activate migration/ invasion of both stromal and tumour cells, the creation of a permissive tumour microenvironment, the induction of angiogenesis and the deregulation of cell metabolism. Additional evidence is the significant association between elevated MSF expression and poor survival in patients with breast and oral cancer (Schor and Schor, 2010).

A mechanism of control of MSF bioactivities is therefore essential. It is already known that MSF expression is controlled by an mRNA cleavage event within the nucleus, but it is not known whether there is a mechanism to regulate the bioactivity of the actual MSF protein. Only femtomolar concentrations of MSF are required to produce half-maximal motogenic activity, plus there is the potential of a prolonged cellular response due to MSF degradation releasing active IGD domains (Ellis *et al.*, 2010). Therefore, considering the consequences of unrestricted MSF bioactivity, the co-secretion of a functional inhibitor appears plausible. It is the aim of this project to identify potential MSF inhibitors and to determine their role in the regulation of MSF bioactivity. Special emphasis is made to MSF's association to cancer progression and its pro-angiogenic activity; investigating the possible anti-angiogenic activity of potential MSF inhibitors, as targeting MSF in tumours may have a therapeutic potential.

Therefore, the subsequent literature review will discuss two of hallmarks of cancer which correlate to the bioactivities of MSF; firstly, how cancer cells acquire migratory and invasive capabilities through the process of epithelial-mesenchymal transition and secondly, the process of tumour angiogenesis. In addition, since it is the aim of this project to identify potential MSF inhibitors special emphasis is made to the development of anti- angiogenic therapies.

Chapter 1: Literature Review

THE EPITHELIAL- MESENCHYMAL TRANSITION IN CANCER PROGRESSION

1.4 Introduction.

The term metastasis was first coined in 1829 by Jean Claude Reclaire and is now defined as “the transfer of disease from one organ or part to another not directly connected to it” (Dorland, 1965). Tumour metastasis is itself a multistage process during which malignant cells disseminate from the primary tumour to distant organs. Metastasis is the primary clinical challenge as it is unpredictable in onset and it exponentially increases the clinical impact on the host; resulting in ineffective treatment and poor patient prognosis. The majority of cancer patients die from their disease as a result of metastasis (Talmadge and Fidler, 2010, Thiery *et al.*, 2009, Bastid, 2012). Research was focused on how epithelial-derived cancers accomplish the complex process of metastasis and similarities to the developmental programs of cell migration and invasion were observed (Table 1.3). During embryonic development, epithelial cells are considered to be highly plastic, possessing the ability to switch back and forth between an epithelial and mesenchymal phenotype via the processes of epithelial-mesenchymal transition (EMT) and the reverse, mesenchymal-epithelial transition (MET). These processes play crucial roles in the formation of the body plan and in the differentiation of multiple tissues and organs (Thiery *et al.*, 2009). In the adult, EMT is also essential in both physiological and pathological processes such as wound healing and organ fibrosis, respectively (Zeisberg and Neilson, 2013).

In metastatic dissemination, the essential first step is local invasion. Due to similarities with embryonic morphogenesis, EMT and epithelial plasticity were hypothesised to contribute to tumour progression (Thiery, 2002). Thereby, implying that during tumorigenesis, embryonic developmental pathways are reactivated inappropriately, enabling epithelial cancer cells to acquire the abilities to invade, to resist apoptosis and to disseminate; attributes that facilitate metastatic spread (Micalizzi *et al.*, 2010).

Numerous *in vitro* experiments and xenografted and transgenic models have demonstrated that epithelial carcinoma cells can acquire a mesenchymal phenotype; confirming that induction of EMT confers tumour cells with invasive and metastatic abilities. This multifaceted EMT program can be activated transiently or consistently,

and to differing extents by carcinoma cells during the course of invasion and metastasis. Certain tumour cells will retain many epithelial traits while acquiring some mesenchymal ones; others will shed all traces of their epithelial origin and become fully mesenchymal (Kalluri and Weinberg, 2013).

However, a contradiction to this hypothesis was raised when an examination of secondary metastatic colonies revealed that the majority of cells resembled, at the histopathological level, the primary tumour from which they originated rather than the mesenchymal phenotype attributed to a metastasising carcinoma cells (Tarin *et al.*, 2005, Bastid, 2012). This prompted the suggestion that during secondary tumour formation the metastasising cancer cells have the ability resume an epithelial phenotype via a reversal the EMT process; the mesenchyme to epithelial transition (MET) (Zeisberg *et al.*, 2005). Subsequently, the new microenvironment of the metastatic colony was proposed to provoke the disseminated cells to undergo MET due to an absence of the heterotypic signals they experienced in the primary tumour which were responsible for inducing EMT in the first place (Thiery, 2002, Bissell *et al.*, 2002). This therefore proposes that both EMT and MET are pivotal for cancer progression. EMT as the mechanism to allow tumour cells to invade and spread to distant sites and MET to enable the subsequent colonisation process (Kalluri and Weinberg, 2013).

The type of invasiveness involving EMT has been termed “mesenchymal”. In addition, two other distinct modes of invasion have been identified and implicated in cancer cell invasion (Friedl and Wolf, 2008, 2010). “Collective invasion/ migration” is a vital cellular process especially during mammary gland branching morphogenesis, intestinal epithelial differentiation and wound healing (Micalizzi *et al.*, 2010). Squamous cell carcinomas adopt collective invasion; nodules of cancer cells have been observed advancing en masse into adjacent tissues. Since these cancers are rarely metastatic this type of invasion appears to lack the functional properties to facilitate metastasis (Hanahan and Weinberg 2011). “Amoeboid invasion” involves individual cells gaining morphological plasticity and rather than forming a migratory path themselves, they take advantage of existing spaces in the ECM and slip through (Madsen and Sahai, 2010, Sabeh *et al.*, 2009).

The process of EMT has been classified into three different subtypes according to functional consequences and biological context (Zeisberg and Neilson, 2009). Type I EMT occurs during implantation, embryogenesis and organ development. Type II EMT is usually associated with an inflammatory response and occurs during wound healing, tissue regeneration and organ fibrosis. Type III is the oncogenic EMT which provides a

mechanism for tumour cells to leave the primary tumour and invade into the local tissue and blood vessels, thereby increasing their metastatic potential. The three classes of EMT represent distinct biological processes, however they appear to share a common set of genetic and biochemical components that appear to facilitate these outwardly diverse phenotypic programs (Kalluri and Weinberg, 2009).

1.4i The Process of EMT

Epithelial cells have many distinguishing features including apical- basal polarity and close connection to neighbouring cells established by adherens junctions, desmosomes and tight junctions. Layers of epithelial cells communicate via gap junctional complexes and are separated from adjacent tissues by a basal lamina. These features convey the ability to function as barriers or absorption surfaces. In contrast, mesenchymal or stromal cells are loosely organised in the 3D extracellular matrix and form connective tissues adjacent to epithelia (Thiery *et al.*, 2009). During development a highly coordinated and specific series of events define the transition between epithelial cells and mesenchymal cells. Yet, during oncogenic EMT this series of steps is less clear and is specific to individual cancer pathologies. However, overall the basic steps are similar (Table 1.4).

Firstly, epithelial connections to neighbouring cells disintegrate with the loss of epithelial cell surface proteins such as E-cadherin and the gain of mesenchymal markers, like N-cadherin. The tight junctions between the epithelial cells are dissolved thereby losing apical-basal polarity; this allows the interaction of apical and basolateral membrane components and the acquisition of a front-rear polarisation. Adherens and gap junctions disassemble. The activation of proteolytic enzymes, such as matrix metalloproteinases, degrade the underlying basement membrane and cell-matrix adhesion is altered. Remodelling of the cytoskeleton occurs with the peripheral actin cytoskeleton replaced by stress fibers and vimentin replacing cytokeratin intermediate filaments. The cell changes from a polygonal/ epithelial shape to a spindly/ fibroblastic morphology. Finally, devoid of any cell-cell contacts the cell disengages from the primary tumour, acquiring the ability to invade and move into the surrounding ECM. Subsequently, the cell can enter the circulation with the potential to reach new metastatic sites (Iwatsuki *et al.*, 2010, Micalizzi *et al.*, 2010, Hanahan and Weinberg 2011).

Table 1.3: A list of the seminal papers which have increased the understanding of EMT and the cancer progression.

Date	Author(s)	Paper Title	Journal	Contents
1968	E.D. Hay	Organisation and fine structure of epithelium and mesenchyme in the developing chick embryo.	Epithelial-mesenchymal Interactions. Williams & Wilkins, 31-55.	Defined the process of EMT and MET using the chick primitive streak as a model. Proposed that epithelial cells can undergo phenotypic changes that reflect their transformation to mesenchymal cells.
1982	G. Greenburg, E.D. Hay.	Epithelia suspended in collagen gels can lose polarity and express characteristics of migrating mesenchymal cells.	Journal of Cell Biology, 95 (1), 333-339.	The first characterisation of the EMT process. Revealed the profound effect environmental conditions have on epithelial phenotype, cell shape and apical-basal polarity.
1985	M. Stoker, M. Perryman.	An epithelial scatter factor released by embryo fibroblasts.	Journal of Cell Science, 77, 209-223.	Described the induction of EMT in MDCK cells when exposed to medium conditioned by human embryo fibroblasts. The presence of a scattering factor appeared to initiate separation and mobilisation of the epithelial cells.
1987	M. Stoker, E. Gherardi, M. Perryman, J. Gray.	Scatter factor is a fibroblast-derived modulator of epithelial cell mobility.	Nature, 327, 239-242.	Described Scatter Factor as a paracrine effector of epithelial-mesenchymal interaction. Released by embryonic fibroblasts with the ability to cause disruption of epithelial cell to cell junctions, increase local cell motility and scattering of contiguous sheets of cells. Proposed an involvement with epithelial migration during embryogenesis and wound healing.
1999	R. Maestro, A.P. Dei Tos, Y. Hamamori, S. Krasnokutsky, V. Sartoreeli, L. Kedes, C. Doglioni, D.H. Beach, G. J. Hannon.	Twist is a potential oncogene that inhibits apoptosis.	Genes & Development, 13, 2207-2217.	cDNA functional screen identified two related bHLH family members, Twist and Dermo 1, which could counteract the proapoptotic effects of myc oncogene. Twist shown to inhibit oncogene and p53-mediated apoptosis. Proposed Twist had numerous roles in the formation of rhabdomyosarcomas, arresting terminal differentiation, inhibiting apoptosis and interfering with the p53 tumour-suppressor pathway.
2000	A. Cano, M.A. Perez-Moreno, I. Rodrigo, A. Locascio, M.J. Blancos,	The transcription factor Snail controls epithelial-mesenchymal transitions by repressing E-cadherin expression.	Nature Cell Biology, 2, 76-83.	Snail shown to be a strong repressor of transcription of the E-Cadherin gene. Snail expression by epithelial cells results in fibroblastoid phenotypic and acquirement of tumorigenic and invasive properties. Snail suggested as a marker of malignancy since the Snail protein is present in invasive mouse and human carcinoma cell lines and tumours which have

	M.G del Barrios, F. Portillo, M. Angela Nietos			lost E-Cadherin expression. Described how the same molecules trigger epithelial-mesenchymal transitions during both embryonic development and tumour progression.
2000	E. Batlle, E. Sancho, C. Franci, D. Dominguez, M. Monfar, J. Baulida, A. Garcia de Herreros.	The transcription factor Snail is a repressor of E-Cadherin gene expression in epithelial tumour cells.	Nature Cell Biology, 2, 84-89.	Expressed by fibroblasts and some E-cadherin- negative epithelial tumour cell lines, the transcription factor Snail was shown to repress transcription of E-cadherin by binding to three E-boxes present in the human E-cadherin promoter. Expression of the E-cadherin gene can be restored by the inhibition of Snail function.
2002	J.P. Thiery	Epithelial- mesenchymal transitions in tumour progression.	Nature Reviews Cancer, 2 (6), 442-454.	First comprehensive review of epithelial-mesenchymal transitions and the role in progression of carcinoma towards dedifferentiated and more malignant states.
2002	A. Inoue, M.G. Seidel, W.Wu, S. Kamizono, A.A. Feraando, <i>et al.</i>	Slug, a highly conserved zinc finger transcriptional repressor, protects hematopoietic progenitor cells from radiation-induced apoptosis <i>in vivo</i> .	Cancer Cell, 2 (4), 279-288.	The zinc finger transcriptional repressor, Slug, was shown to act as an antiapoptotic factor by promoting the survival of hematopoietic progenitors which have undergone DNA damage. Implicated Slug in a novel survival pathway.
2004	J. Yang, S.A. Mani, J.L. Donaher, S. Ramaswamy,	Twist, a master regulator of morphogenesis, plays an essential role in tumour metastasis.	Cell, 117, 927-939.	Using a murine breast tumour model, the transcription factor Twist, a master regulator of embryonic morphogenesis, was shown to contribute to metastasis by promoting an epithelial- mesenchymal transition. High levels of Twist expression in human breast cancer correlated with highly invasive lobular carcinoma which is associated with loss of E-cadherin expression.
2004	M. Kajita, K.N. McClinic, P.A. Wade.	Aberrant expression of the transcription factors Snail and Slug alters the response to genotoxic stress.	Molecular and Cellular Biology, 24 (17), 7559-7566.	Investigated the effects of aberrant expression of Snail and Slug transcriptional repressors in human cancer cells; which resulted in changes in cell morphology, loss of cell-cell contacts and acquirement of invasive growth properties. Snail and Slug implicated as promoters of tumorigenesis by an increased resistance to apoptosis.
2005	D. Tarin.	The fallacy of epithelial mesenchymal transition in neoplasia.	Cancer Research, 65 (14), 5996-6000.	Investigated the validity of the proposal that EMT is active during embryonic development, wound healing, carcinogenesis and tumour metastasis. Concluding that <i>in vivo</i> there was no conclusive proof of a conversion of epithelial cells into mesenchymal cell lineages.
2005	W-S. Wu, S. Heinrichs,	Slug antagonises p53-mediated apoptosis of hematopoietic progenitors	Cell, 123 (4), 641-653.	Showed that upon irradiation, the transcriptional repressor, Slug is transcriptionally induced by the tumour suppressor p53. This results in the

	D.Xu, S.P. Garrison, G.P. Zambetti, J.M. Adams, A.T. Look.	by repressing puma.		damaged cell being protected from apoptosis by directly repressing p53-mediated transcription of <i>puma</i> , a key BH3-only antagonist of the antiapoptotic Bcl-2 proteins.
2006	K.L. Knutson, H. Lu, B. Stone, J.M. Reiman, M.D. Behrens,	Immunoediting of Cancers may lead to epithelial to mesenchymal transition.	Journal of Immunology, 177 (3), 1526-1533.	Revealed that immunoedited tumour cells undergo EMT characterised by an up-regulation of invasion factors and increased invasive potential. The immunoedited tumour cells are able evade immune surveillance.
2006	C.L. Chaffer, J.P. Brennan, J.L. Slavin, T. Blick, E.W. Thompson, E.D. Williams.	Mesenchymal-to- epithelial transition facilitates bladder cancer metastasis: role of fibroblast growth factor receptor-2.	Cancer Research, 66 (23), 11271-11278.	The bladder carcinoma TSU-Pr1 (T24) progression series of cell lines which display increasing metastatic potential was used to investigate role played by mesenchymal to epithelial transition metastasis (MET). Overexpression of fibroblast growth factor receptors shown to reverse MET.
2006	S. Spaderna, O. Schmalhofer, F.Hlubek, G. Berx, A. Eger, S. Merkel, A. Jung, T. Kirchner, T. Brabletz.	A transient, EMT-linked loss of basement membranes indicates metastasis and poor survival in colorectal cancer.	Gastroenterology, 131 (3), 830-840.	Investigated the clinical relevance of basement membrane (BM) turnover in the progression of malignant colorectal cancer; discovering a transient loss of the BM at the invasive front of the tumour which correlates with increased distant metastasis and decreased patient survival. The invasion-associated loss of BM appears to be due to a reduction in synthesis associated with EMT. The zinc-finger enhancer protein 1 (ZEB1) identified as the crucial transcriptional repressor of BM components in colorectal cancer.
2007	H. Peinado, D. Olmeda, A.Cano.	Snail, ZEB and bHLH factors in tumour progression: an alliance against the epithelial phenotype?	Nature Reviews Cancer, 7 (6), 415-428.	A review of the involvement of transcription factors Snail, ZEB and basic helix-loop-helix (bHLH) in the repression of E-cadherin and the induction of EMT.
2008	A.J. Trimboli, K. Fukino, A. de Bruin., G. Wei, L. Shen, <i>et al.</i>	Direct evidence for epithelial-mesenchymal transitions in breast cancer.	Cancer Research, 68 (3), 937-945.	Oncogene-driven mouse mammary tumour models and cell-fate mapping strategies provide direct evidence of EMT occurring <i>in vivo</i> in breast cancer. Although rare, the incidence of EMT in invasive human breast carcinomas is associated with an amplification of <i>MYC</i> .
2008	S.A. Mani, W. Guo, M-J. Liao,	The epithelial-mesenchymal transition generates cells with properties of stem cells.	Cell, 133, 704-715.	Described a direct connection between EMT and the gain of epithelial stem cell properties. The induction of EMT in immortalised human mammary epithelial cells resulted in the acquirement of mesenchymal

	E. N. Eaton, A. Ayyanan, <i>et al.</i>			characteristics and the expression of stem cell markers.
2008	S. Ansieau, J. Bastid, A. Doreau, A-P. Morel, B.P. Bouchet, C. Thomas, F. Fauvet, I. Puisieux, C. Doglioni, <i>et al.</i>	Induction of EMT by Twist proteins as a collateral effect of tumour-promoting inactivation of premature senescence.	Cancer Cell, 14, 79-89.	The major regulators of embryogenesis, Twist1 and Twist2, shown to be overexpressed in a large variety of human cancers. The Twist proteins are described as the early drivers of tumorigenesis as they completely revoked oncogene-induced senescence by inhibiting the key regulators of the p53 and Rb-dependent pathways. Describe complete EMT requiring collaboration between the Twist proteins and activated motogenic oncoproteins, such as Ras or ErbB2.
2008	A-P. Morel, M. Lievre, C. Thomas, G. Hinkal, S. Ansieau, A. Puisieux.	Generation of breast cancer stem cells through epithelial-mesenchymal transition.	PLoS ONE, 3 (8), e2888.	A human mammary tumour progression model (HMEC) demonstrated that cells possessing both stem and tumorigenic characteristics of “cancer stem cells” can be generated from non-tumorigenic mammary epithelial cells via the activation of the Ras/MAPK pathway. The process is accelerated by EMT induction.
2008	M-H. Yang, M-Z Wu, S-H. Chiou, P-M. Chen, S-Y. Chang, C-J. Liu, S-C. Teng, K-J. Wu.	Direct regulation of Twist by HIF-1 α promotes metastasis.	Nature Cell Biology, 10 (3), 295-305.	Show that hypoxia or over-expression of hypoxia-inducible factor-1 α (HIF-1 α) promotes EMT and metastasis. Twist expression is regulated by HIF-1 α through direct binding to the hypoxia-response element (HRE) in the Twist proximal promoter. EMT and metastatic phenotypes can be reversed in HIF-1 α overexpressing or hypoxic cells by the siRNA – mediated repression of Twist.
2009	J. P. Thiery, H. Acloque, R.Y.J. Huang, M. A. Nieto.	Epithelial-mesenchymal transitions in development and disease.	Cell, 139, 871-890.	Comprehensive review of EMT involvement in embryonic development, tissue homeostasis, wound healing, fibrosis and cancer progression. Special focus on EMT and tumour progression and the impact on drug resistance.
2009	M. Santisteban, J.M. Remain, M.K. Asiedu, M.D. Behrens, A. Nassar, <i>et al.</i>	Immune-induced epithelial to mesenchymal transition <i>in vivo</i> generates breast cancer stem cells.	Cancer Research, 69 (70), 2887-2895.	Described how in breast cancer EMT can be induced by CD8 T cells with the resulting tumours displaying characteristics of breast cancer stem cells. Questions the hierarchal cancer stem cell hypothesis.
2011	C-J. Chang, C-H. Chao,	p53 regulates epithelial-mesenchymal transition and stem cell properties	Nature Cell Biology, 13 (3), 317-323.	Reveal a role for p53 in regulating EMT-MET and differentiation plasticity. By directly binding to the microRNA miR-200c promoter p53

	W. Xia, J-Y. Yang, C-W Li, W-H. Yu, S. K. Rehman, J.L. Hsu, H-H. Lee, M. Liu, <i>et al.</i>	through modulating miRNAs.		transcriptional activates the miR-200c. In mammary epithelial cells the loss of p53 expression results in a decrease in miR-200c expression with an activation of the EMT process and an increase in the number of mammary stem cells. This is exhibited by an increase in expression of EMT and stem cell phenotype markers and subsequent development of a group of high grade breast tumours.
2012	A. Bonnomet, L. Syne, A. Brysse, E. Feyereisen, E.W. Thompson, A. Noel, J-M. Foidart, P. Birembaut, M. Polette, C. Gilles.	A dynamic <i>in vivo</i> model of epithelial-to –mesenchymal transitions in circulating tumour cells and metastases of breast cancer.	Oncogene, 31, 3741-3753.	Describe the transient and reversible nature of EMT <i>in vivo</i> that accompany metastatic spread. In primary tumours EMT affords the tumour cells a greater ability to intravasate and generates circulating tumour cells. Post extravasation in the secondary organ(s) MET occurs to facilitate metastatic growth. Developed an animal model with transplantable human breast tumour cells which showed the spontaneous nature of EMT and allowed the metastatic process to be followed. The dynamic expression of vimentin, a marker of EMT, was assessed throughout, along with the expression of epithelial (E-cadherin, ZO-3, JAM-A) and mesenchymal (Snail, Slug, fibroblast-specific protein-1) specific molecules.

Table1.4: The process of epithelial to mesenchymal transition.

<ol style="list-style-type: none"> 1. Loss of Apical-Basal Polarity. The dissolution of tight junctions, allow apical and basal membrane proteins intermix Disassembly of adherens and gap junctions. 2. Loss of Epithelial Cell to Cell Connections. Epithelial specific integrins and cell surface proteins, such as E-cadherin, are switched to mesenchymal specific integrins and N-cadherin. 3. Remodelling of Cytoskeleton. Stress fibres replace the peripheral actin cytoskeleton and accumulate at cell protrusions. Vimentin replaces cytokeratin intermediate filaments. 4. Degradation of Basement Membrane. 5. Cell Invasion.
--

1.4ii The Molecular Mechanisms Involved in EMT.

Four fundamental regulatory networks are thought to drive EMT in cancer cells. EMT is thought to be initiated when the balance of these networks is disturbed and the subsequent level of EMT achieved is defined by how far the balance is tipped in one direction or the other (DeCraene and Berx, 2013). The regulatory networks are so closely interconnected that an alteration of one network will result in knock-on effects on the others. The most extensively studied network is that built around the nuclear transcription factors Snail, Zeb and Twist families. The three other networks are the expression of small non-coding RNAs, differential splicing and translational and post-translational control (which affect protein stabilisation and localisation) (DeCraene and Berx, 2013). Many of the factors were first identified by developmental genetics and relate to migratory processes during embryogenesis.

The loss of E-cadherin expression is a fundamental event in EMT and is a marker for poor prognosis in various human cancers (colorectal, breast and gastric) (Table 1.5). E-cadherin is a calcium dependent transmembrane glycoprotein expressed by the majority of epithelial tissues. It exerts a role as repressor of tumour progression by forming tight junctions connecting adjacent epithelial cells and therefore is a key suppressor of cell motility, invasion and metastatic dissemination (Peinado *et al.*, 2004).

Normally, E-Cadherin is regulated at both mRNA and protein levels by several processes including translational or transcriptional events, protein degradation and altered subcellular distribution (Yang and Weinberg, 2008). Many human cancers are characterised by the functional loss of E-cadherin due to the expression of a defective protein, this may be the consequence of a gene mutation, abnormal post-translational modification (phosphorylation or glycosylation) or increased proteolysis (Tiwari *et al.*, 2012). At the transcriptional level E-cadherin gene expression can be silenced due to promoter hypermethylation. E-cadherin was one of the first genes with promoter hypermethylation identified at very high frequencies in human cancer (van Roy and Berx, 2008, Tiwari *et al.*, 2012).

E-cadherin regulation also occurs by transcriptional repression. Transcriptional repressors of E-cadherin such as zinc finger proteins (Zeb1, Zeb2), basic helix-loop-helix protein (Twist) and the snail family of zinc finger proteins (Snail, Slug) are all associated with EMT (Iwatsuki *et al.*, 2010). These transcription factors can be classified into two groups; those which bind to and repress the activity of the E-cadherin promoter (Snail, Zeb, E47, KLF8) and those which repress E-cadherin transcription

directly (Twist, Goosecoid, E2.2, FoxC2) (Yang and Weinberg, 2008, Thiery *et al.*, 2009). Various signal pathways such as TGF β , Wnt cascade, and PI3K/AKT axis are connected with these transcriptional repressors of E-Cadherin (Iwatsuki *et al.*, 2010). The level of EMT achieved by the cancer cells is primarily dependent on the potency of EMT-inducing transcription factors which are the triggering cellular reprogramming. The power of these factors relies not only on direct repression of E-cadherin but also on the simultaneous repression of several other factors which facilitate the general dedifferentiation programme (De Craene and Berx, 2013). Snail1 and Zeb1 can determine the loss of cell polarity since the three protein complexes are involved in maintaining the apical-basal polarity in epithelial cells (Par, Crumbs and Scribble) can each be regulated by the Snail1 and Zeb1 (Thiery *et al.*, 2009). Snail and Zeb also induce the expression of matrix metalloproteinases which degrade the basement membrane, thereby assisting invasion. Conversely, MMP3 promotes EMT by increasing the cellular levels of reactive oxygen species, which in turn induces Snail1 expression (Radisky *et al.*, 2005).

MicroRNAs (miRNAs) are small non-coding RNA molecules that suppress gene expression by interacting with the 3' untranslated regions (3'UTRs) of target mRNAs and have been linked to EMT and cancer. The miR-200 family and miR-205 have the ability to inhibit the E-cadherin transcriptional repressors, Zeb1 and Zeb2. Conversely, Zeb1 and Zeb2 repress the expression of the miR-200 gene cluster (Burk *et al.*, 2008). It has recently been revealed that p53 activates miR-200c through direct binding to its promoter. The loss of p53 in mammary epithelial cells correlates with a decreased expression of miR-200c and an increase in EMT markers with the subsequent development of a cohort of high grade breast tumours (Chang *et al.*, 2011). In metastatic breast cancer miR-10b is overexpressed due to up-regulation by Twist and is associated with invasiveness and metastatic potential (Ma *et al.*, 2007).

It is well acknowledged that TGF β prompts numerous responses in cancer progression including angiogenesis, immune suppression and anti-apoptosis (Derynck *et al.*, 2001). TGF β , the ubiquitously expressed cytokine, is also an important inducer of EMT. During development TGF β is required for heart development and palatogenesis (Micalizzi *et al.*, 2010). *In vitro* experiments have shown that exposure to TGF β results in dramatic consequences; loss of apical-basal polarity, down-regulation of cell-cell adhesions and expression of mesenchymal markers such as vimentin (Micalizzi *et al.*, 2010). Studies have revealed that TGF β induces EMT programs via numerous signal pathways, including Smad 2 and Smad 3, integrin, Notch and Wnt (Iwatsuki *et al.*,

2010). TGF β has been implicated in the loss of cell polarity during EMT by adopting two approaches. The more established pathway is by the induction of Snail and Zeb expression. However, TGF β can also initiate the downregulation of Par3 expression and the Par6-mediated degradation of RhoA resulting in the local alteration of actin cytoskeleton (Theiry *et al.*, 2009).

Many developmental studies have presented evidence that in the embryo, neighbouring cells are involved in triggering the expression of EMT-inducing transcription factors in cells destined to pass through EMT (Micalizzi *et al.*, 2010). There is also increasing evidence that tumour-associated stromal cells appear to be inducing cancer cells to undergo EMT. EMT occurring in carcinomas *in vivo*, is often located at the invasive margins of the tumour, implying that these cancer cells are subjected to a specific microenvironmental stimuli which is distinct from those exposed to cancer cells located in the core of the tumour (Hlubeck *et al.*, 2007, Hanahan and Weinberg, 2011). While cancer cells that have disseminated from the primary tumour to metastatic sites no longer experience these tumour associated –stromal originated EMT-inducing signals and thus the absence of signals may cause the carcinoma cells to revert via MET to their non-invasive epithelial phenotype. This would explain why many new tumour colonies exhibit histopathology similar to the primary tumour (Hugo *et al.*, 2007).

Table1.5: A list of epithelial and mesenchymal markers.

Epithelial Markers	Mesenchymal Markers
E-cadherin	α -SMA
Cadherin-16	B-catenin
Cadherin-6B	CyclinD1
VE-cadherin	Fibroblast specific protein -1
Claudin 1	(FSP-1)
Connexin 43	Fibronectin
Crumbs3	Forkhead box C2
Cytokeratin	Goosecoid
Entactin	N-cadherin
Dig1	Snail1
HNF-1 β	Snail2
Integrin α 3	SIP1
Laminins α 3, α 5, α 6	Syndecan-1
miR200 family	Twist
Mucin-1	Vitronectin
Nephrin	Vimentin
Occludins	Zeb1
PTEN	
Zona occludens-1	

1.4iii The Controversy of EMT

The clinical relevance of EMT during human cancer progression has been contentious. Although *in vitro* studies are numerous and well documented, there has been a distinct lack of direct and conclusive evidence of complete EMT in clinical samples (DeCraene and Berx, 2013). The importance of EMT has been difficult to prove since the changes are often transient and occur in a small population of cancer cells. Developmental EMT is characterised by sequential step-wise process under the tight control of morphogenic signals. However, oncogenic EMT is particularly difficult to predict due to the genetic instability of the tumour cells coupled with the abnormal local tumour environment (Micalizzi *et al.*, 2010).

It is especially challenging, *in vivo* to make the morphologic distinction between carcinoma cells undergoing EMT and neighbouring stromal cells, since they will appear as mesenchymal-like cells (Bastid, 2012). However, the advancement of *in vivo* imaging has helped gain evidence of EMT in cancer progression (Wyckoff *et al.*, 2007). In 2007, Prall described cords or small aggregates of tumour cells extending and detaching from the primary tumour mass into the local stroma. This process of tumour budding is commonly observed and the tumour cells have been shown to have down-regulated E-Cadherin (Iwatsuki *et al.*, 2010). Xenograft experiments and genetically modified mouse cancer models have supported these clinical observations.

Assessing the gain or loss of markers is also considered to be subjective since many cancers, due to presence of genetically unstable cells, express both epithelial and mesenchymal markers (Talmadge and Fidler, 2010). Yet, there are numerous recorded examples of carcinoma cells at the invasive front of tumours expressing an EMT profile (Table 1.6). In colon carcinoma, EMT has been observed in single migratory cells at the invasive front; cells lose E-cadherin expression, the Wnt pathway is deregulated and there is a selective loss of the basement membrane (Brabletz *et al.*, 2001). In addition the expression of EMT inducers, including the transcription factors Snail 1 and 2 have been shown to significantly correlate with poor prognosis and disease relapse in breast, colorectal and ovarian cancer (Thiery *et al.*, 2009). Many EMT markers are now used to predict patient prognosis (Iwatsuki *et al.*, 2010) (Table 1.5).

Table 1.6: Evidence of epithelial- mesenchymal transition taking place during human cancer progression.

Cancer Type	Evidence of EMT	Reference
Cervical Carcinoma	<ul style="list-style-type: none"> • Compared to primary tumours, lymph node micrometastases of cervical cancer display an increased expression of EMT-related genes. • SNAIL 1 expression correlates with EMT and invasiveness. • The invasive front of cervical tumours characterised by Vimentin expression and loss of E-cadherin. 	Hagemann <i>et al.</i> , 2007. Lee <i>et al.</i> , 2008 Hsu <i>et al.</i> , 2007
Colorectal carcinoma (CRC)	<ul style="list-style-type: none"> • Snail 2 expression shown to be an independent prognostic parameter for poor survival. • Invasive front of CRC characterised by selective loss of basement membrane and deregulation of Wnt pathway. • The epithelial and stromal signalling pathway profiles are more similar to each other in CRC than in the normal colon. 	Shioiri <i>et al.</i> , 2006. Brabletz <i>et al.</i> , 2001. Sheehan <i>et al.</i> , 2008
Cutaneous malignant melanoma (CMM)	<ul style="list-style-type: none"> • A subset of EMT genes associated with cell adhesion, cell motility, migration and ECM interaction are differentially expressed in CMM with metastasis as compared to samples without metastasis. 	Alonso <i>et al.</i> , 2007.
Breast Carcinoma	<ul style="list-style-type: none"> • Histological grade of breast tumours have been related to expression profiles of EMT. • EMT-signalling pathways of TGFβ and Wnt shown to regulate EMT programs. TGFβ signalling induces EMT and metastasis of breast cancer cells to bone via Smad4. • Homeobox gene HOXB7 which induces EMT in MCF10A cells is overexpressed in primary and metastatic breast cancer tissues and cell lines. 	Teschendorff <i>et al.</i> , 2007. Deckers <i>et al.</i> , 2006. Wu <i>et al.</i> , 2006.
Head and neck carcinoma	<ul style="list-style-type: none"> • EMT-related genes identified in high risk squamous cell carcinoma 	Chung <i>et al.</i> , 2004, Chung <i>et al.</i> , 2006
Hepatocellular carcinoma (HCC)	<ul style="list-style-type: none"> • Snail1 and Zeb2 expression, induced by TGFβ, increases invasion of HCC cells due to an upregulation of metalloproteinase expression. • The sensitivity of HCC cell lines to EGFR-targeted therapies (erlotinib, 	Miyoshi <i>et al.</i> , 2004 Fuchs <i>et al.</i> , 2008.

	<p>gefitinib, cetuximab) has been associated to EMT.</p> <ul style="list-style-type: none"> • Snail1 and Twist overexpression in HCC samples correlated with a worse prognosis. 	Yang <i>et al.</i> , 2009
Ovarian Carcinoma	<ul style="list-style-type: none"> • Snail1 expression correlates with lower survival rate. 	Blechschmidt <i>et al.</i> , 2008.
Pancreatic Carcinoma	<ul style="list-style-type: none"> • EMT in pancreatic carcinoma cells can be induced by TGFβ and EGF family member HB-EGF. • Snail1 and Snail 2 expression reported in 78% and 50% of pancreatic carcinoma tissues, respectively. 	Bardeesy <i>et al.</i> , 2006, Jungert <i>et al.</i> , 2007. Hotz <i>et al.</i> , 2007.
Papillary Thyroid Carcinoma (PTC)	<ul style="list-style-type: none"> • The invasive front of PTC tumours shown to have an expression profile consistent with EMT; characterised by limited expression of genes related to cell adhesion while over expression of integrin and TGFβ pathway components, including Snail 1 and 2 genes. 	Vasko <i>et al.</i> , 2007, Hardy <i>et al.</i> , 2007
Prostate Carcinoma	<ul style="list-style-type: none"> • Zeb1 expression correlates to a high Gleason score in prostate carcinoma tissues. • The EMT process to switch from E to N-cadherin was shown to be an independent prognostic factor for treatment failure, metastasis, reoccurrence and overall survival. 	Graham <i>et al.</i> , 2008. Gravadal <i>et al.</i> , 2007.
Uterine Carcinoma	<ul style="list-style-type: none"> • Zeb1 expression correlated with EMT and invasive potential. 	Spoelstra <i>et al.</i> , 2006.

1.4iv The Additional Consequences of EMT

EMT induction in cancer cells has also been linked to an acquisition of various additional capabilities that are also highly relevant to cancer progression. The nature and strength of the EMT induction apparently determines the magnitude of these cancer progression associated capabilities (Tiwari *et al* 2012).

When a cancer cell disengages from the tumour mass and enters the circulation, the lack of cellular adhesion can induce a type of apoptosis called anoikis. However, cancer cells that have undergone EMT appear to have acquired resistance to cell death. TGF β has been implicated in enabling cancer cell survival by activating the E-cadherin repressors Snail and Twist which are known to confer resistance to cell death (Thiery *et al.*, 2009). Several weeks exposure of breast tumour derived NMuMG cells to TGF β has been shown to generate cells which display a sustained EMT and have the ability to escape apoptosis (Gal *et al.*, 2008). Furthermore, in neuroblastomas Twist antagonises Myc-mediated pro-apoptosis (Puisieux *et al.*, 2006).

E-cadherin repressors also seem to protect the EMT-induced carcinoma cells from undergoing oncogene induced premature senescence. Twist 1 and 2 confer resistance to senescence induced by oncogenes by inhibiting p16/ink4 and p21/cip (Ansieau *et al.*, 2008). It has also been reported that Zeb1 protects mouse embryonic fibroblasts from senescence (Liu *et al.*, 2008). These findings would therefore suggest that the process of EMT not only yields cancer cells possessing an invasive and metastatic phenotype but also ensures their survival by suppressing two safeguard mechanisms against cancer progression: premature senescence and apoptosis (Thiery *et al.*, 2009).

EMT also appears to allow carcinoma cells to evade the immune defence mechanism. Cells undergoing EMT gain the expression of a number of cytokines and secreted factors that inhibit immune responses (Tiwari *et al.*, 2012). By undergoing EMT, Neu-driven tumours appear to elude immune surveillance (Knutson *et al.*, 2006). EMT inducer, Snail 1 expression is associated with the activation of immunosuppressive cytokines, regulatory T cells, cytotoxic T lymphocytes resistance and the generation of impaired dendritic cells (Kudo-Saito *et al.*, 2009, Thiery *et al.*, 2009). Interestingly, immunosuppressive agents used to reduce host rejection after organ transplantation, such as cyclosporine, also induce epithelial de-differentiation. These agents induce the production of TGF β which serves to stimulate and maintain partial EMT (Tiwari *et al.*, 2012).

Carcinoma cells undergoing EMT have been reported to develop a resistance to chemotherapy. Conversely, anticancer agents and radiotherapy can actually induce EMT by creating a “stress” environment within the tumour, characterised by hypoxia. Continual exposure of colon and ovarian carcinoma cell lines to oxaliplatin and paclitaxel, respectively, lead to the development of resistance whilst the cells exhibit a mesenchymal phenotype and express several EMT markers (Yang *et al.*, 2006, Kajiyama *et al.*, 2007). Having undergone EMT the cell lines MCF7 and MDA-MB-434 are reported to have elevated Twist expression and resistance to Paclitaxel (Cheng *et al.*, 2007).

EMT is considered to be accountable for the relapses that befall patients who had initially presented with tumours highly sensitive to treatment. EMT derived multi- drug resistance permits rapid progression of the tumour (Iwatsuki *et al.*, 2010). However, the restoration of chemotherapeutic sensitivity has been shown by the forced expression of miR-200C, a negative regulator of EMT (Cochrane *et al.*, 2009). Multidrug resistance in breast cancer cells can be partially reversed by depletion of Twist (Li *et al.*, 2009). Cancer stem cells (CSC) have been recently identified in breast, colon and pancreatic cancer. This minority population of cancer cells have the ability to self-renew and give rise to differentiated tumour cells. Evidence suggests that cells that undergo EMT acquire stem cell-like properties (Morel *et al.*, 2008). HMLE cells, an immortalised human mammary epithelial cells induced to undergo EMT by ectopic expression of Twist or Snail have been shown to have up-regulated mesenchymal markers (N-cadherin, vimentin, fibronectin) as well as exhibiting many characteristics of CSC; a CD44^{high}/CD24^{low} phenotype, the ability to self-renewal and the capacity to form mammospheres (Mani *et al.*, 2008, Iwatsuki *et al.*, 2010). The human mammary tumour progression model (HMEC) has been used to demonstrate that activation of the Ras/MAPK pathway can generate CSC from non-tumorigenic mammary epithelial cells; a process which is accelerated by EMT induction. These findings imply that EMT may play a role in cancer stem cell development.

1.4v Therapies Targeting EMT.

A consequence of reducing EMT could be the decrease in the occurrence of anticancer drug resistance and subsequent improved efficacy to conventional chemotherapy. The development of anti-EMT targeted therapy is problematic as the inducers of the EMT process are transcription factors and thus difficult to target. The new techniques of RNA

interference and microRNA have been adopted. The silencing of Snail by shRNA reversed EMT and reduced tumour growth, *in vivo* (Olmeda *et al.*, 2007). As discussed previously, miR-200C has been shown to reverse EMT instigated chemotherapy resistance (Cochrane *et al.*, 2009). However, further development is required in order to increase reagent stability, improve efficiency of cell targeting and intracellular delivery. In addition, agents originally developed as inhibitors to cell proliferation and/or angiogenesis, such as small-molecule inhibitors or antibodies directed against EGFR, IGFR, PDGFR, cMET and TGF β R, may prove to also interfere with the EMT process (Chu *et al.*, 2008).

Chapter 1: Literature Review

ANGIOGENESIS AND ANTI-ANGIOGENIC THERAPY

1.5 Introduction

During embryogenesis the first system to develop and reach a functional state is the cardiovascular system (Chung and Ferrara, 2011), highlighting the essential role the vasculature has in embryonic development. Vasculature development is controlled by genetic and epigenetic mechanisms, molecular cues and cell behaviour both temporally and spatially (Adams and Alitalo, 2007). A functional vasculature is fundamental for tissue growth; ensuring a continuous and consistent supply of the essentials for life, oxygen and nutrients, whilst removing harmful bi-products. It is also crucial in the maintenance of homeostasis, transport of endocrine hormones and the immune response.

Although, the vasculature was initially described in the 17th century, only the last 40 years has seen an intensification of interest by researchers. Numerous experimental procedures, *in vivo* and *in vitro*, have been specifically developed to increase our understanding of how blood vessels are formed from endothelial and mural cells.

Copious publications have provided valuable insights into the key mechanisms and molecular factors which control blood vessel growth; a process which is termed angiogenesis (in adults). It is now appreciated that the strict regulation of angiogenesis is due to dynamic balance between pro-angiogenic and anti-angiogenic factors. A consequence of an imbalance in expression of these factors is either uncontrolled or inadequate angiogenesis.

Deficiencies in the process of angiogenesis are associated with an ever growing list of disorders (over 70 at present); often described as a “disease common denominator”. The most reported illnesses for which angiogenesis is aberrantly switched on is cancer, ocular and inflammatory disorders, but many additional conditions are affected such as obesity, asthma, diabetes, cirrhosis, multiple sclerosis, endometriosis, AIDS and autoimmune disease (Mauriz and Ganzolez-Gallego, 2008). Conditions characterised by insufficient angiogenesis include ischaemic heart disease, preeclampsia, stroke and non-healing wounds (Carmeliet, 2005). (Table 1.7a). It is predicted that worldwide over

500 million people would benefit from angiogenic therapeutic strategies (Carmeliet and Jain, 2011, Herbert and Stainer, 2011) (Table 1.7b).

A seminal publication in 1971, by Judah Folkman linked the progression of cancer to the ability of a tumour to express pro-angiogenic factors which stimulated the formation of its own vasculature. The establishment of an efficient blood supply is essential for tumour growth and subsequent expansion via metastatic spread through the circulation to other sites. A tumour's acquisition of an angiogenic phenotype occurs early in development and is a rate-limiting step of tumour progression (Hanahan *et al.*, 1996). Subsequently, Folkman proposed that the inhibition of tumour blood vessel formation would be an effective and but selective way to treat cancer (Folkman, 1971). Although, Folkman was initially derided for his theory anti-angiogenic therapy has now become a hotbed of research bringing together scientists, oncologists, chemists and the pharmaceutical industry (Table 1.8).

Table 1.7a: A list of conditions regularly described as having a faulty angiogenic switch.

Excessive Angiogenesis	Insufficient Angiogenesis
Age-related macular regeneration	Chronic non-healing wounds
Cancer	Coronary artery disease
Diabetic blindness	Preeclampsia
Psoriasis	Stroke
Rheumatoid arthritis	

Table 1.7b: A list of diseases which could be treated with anti-angiogenic therapy.

Disease
Cancer
Atherosclerotic plaques
Benign prostatic hypertrophy
Crohn's Disease
Diabetic retinopathy
Endometriosis
Psoriasis
Rheumatoid arthritis
Uterine fibroids

Table 1.8: A list of the seminal papers which have increased our understanding of angiogenesis and the therapeutic potential of anti-angiogenic therapies.

Date	Author(s)	Paper Title	Journal	Contents
1907	E. Goldman.	The growth of malignant disease in man and the lower animals with special reference to the vascular system.	Lancet, ii, 1236-1240.	First description of tumour vasculature.
1932	E.R. Clark, E.L. Clark	Observations on living blood vessels as seen in a transparent chamber inserted into the rabbit ear.	American Journal of Anatomy, 49, 441-447	Placed glass chambers in the rabbit ear in order to draw the branching patterns of blood vessels that entered the wound. Their work established the field of vascular biology.
1939	A.G. Ide, N.H. Baker, S.L. Warren	Vascularisation of the Brown Pearce rabbit epithelioma transplant as seen in the transparent ear chamber.	American Journal of Roentgenology, 42, 891-899	Observed that tumour growth was accompanied by infiltration of newly formed blood vessels in a rabbit tumour model.
1945	G.H. Algire, H.W.Chalkey, F.Y. Legallais, H.D. Park	Vascular reactions of normal and malignant tumours <i>in vivo</i> . Vascular reactions of mice to wounds and to normal and neoplastic transplants.	Journal of National Cancer Institute, 6, 73-85	Description of blood vessels migrating towards tumours in wound chambers. First demonstration that tumours actively attract new blood vessels.
1971	J. Folkman.	Tumour angiogenesis: therapeutic implications.	New England Journal of Medicine, 285, 1182-1186.	Seminal hypothesis on the relevance of tumour angiogenesis. Introduced the concept of using angiogenesis inhibitors for treatment of cancer.
1971	J. Folkman, E. Merler, C. Abernathy, G. Williams.	Isolation of a tumour factor responsible for angiogenesis.	Journal of Experimental Medicine, 133 (2), 275-288.	Isolation of a soluble factor from human and animal tumours, Tumour angiogenesis factor (TAF), which induced growth of new capillaries.
1972	M.A.Gimbrone, S Leapman, R.S. Cotran, J. Folkmann.	Tumour dormancy <i>in vivo</i> by prevention of neovascularisation.	Journal of Experimental Medicine, 136 (2), 261-276.	Observation that malignant growth of solid tumours requires neovascularisation. Suggestion that blockade of tumour induced angiogenesis could control neoplastic growth.
1973	J. Folkman, M. Hochberg.	Self-regulation of growth in three dimensions.	Journal of Experimental Medicine, 138 (4), 745-753.	Exponential growth of solid tumours beyond 1-2mm requires angiogenesis.
1974	M.A.Gimbrone, R.S. Cotran,	Tumour growth and neovascularization: an experimental	Journal of the National Cancer Institute, 52 (2),	Description of a new model for the characterisation of mediators of neovascularisation.

	S.B. Leapman, J. Folkman.	model using the rabbit cornea.	413-427.	
1975	H. Brem, J. Folkman.	Inhibition of tumour angiogenesis mediated by cartilage.	Journal of Experimental Medicine, 141 (2), 427-439.	Description of first angiogenesis inhibitor. Soluble factor from rabbit neonatal scapular cartilage shown to inhibit tumour angiogenesis.
1979	J. Folkman, C.C. Haudenschild, B.R. Zetter	Long-term culture of capillary endothelial cells.	Proceedings of National Academy of Sciences, USA, 76 (10), 5217-5221.	Method for long term culture of pure capillary endothelial cells, enabling in vivo angiogenesis studies.
1984	Y. Shing, J. Folkman, R. Sullivan, C. Butterfield, J. Murray, M. Klagsburn	Heparin affinity: purification of a tumour-derived capillary endothelial cell growth factor.	Science, 223 (4642), 1296-1299.	Procedure for the purification of capillary endothelial cell growth factor(s).
1987	A. Orlidge, P.A. D'Amore.	Inhibition of capillary endothelial cells by pericytes and smooth muscle cells.	Journal of Cell Biology, 105 (3), 1455-1462.	The development of co-culture models, showed the inhibitory effects on pericytes and smooth muscle cells on capillary endothelial cell proliferation. Role of cell-cell interactions in modulating growth.
1989	D.W. Leung, G. Cachianes, W.J. Kuang, D.V. Goeddel, N. Ferrara.	Vascular endothelial growth factor (VEGF) is a secreted angiogenic mitogen.	Science, 246 (4935), 1306-1309.	Description of VEGF as a stimulator of angiogenesis.
1989	J. Plouet, J. Schilling, D. Gospodarowicz.	Isolation and characterization of a newly identified endothelial cell mitogen produced by AtT-20 cells.	EMBO Journal, 8 (12), 3801-3806.	Description of Vasculotrophin, subsequently shown to be identical to VEGF.
1989	C.W. White, H.M. Sondheimer, E.C. Crouch, H. Wilson, L.L. Fan.	Treatment of pulmonary hemangiomas with recombinant interferon alfa-2a.	New England Journal of Medicine, 320 (18), 1197-1200	First clinical "proof of concept" of antiangiogenic therapy for tumours.
1989	J. Folkman, K. Watson, D. Ingber,	Induction of angiogenesis during the transition from hyperplasia to neoplasia.	Nature, 339, 58-61.	Description of the induction of angiogenesis as an important step in carcinogenesis.

	D. Hanahan.			
1990	D. Ingber, T. Fujita, S. Kishimoto, K. Sudo, T. Kanamaru, H. Brem, J. Folkman.	Synthetic analogues of fumagillin that inhibits angiogenesis and suppresses tumour growth.	Nature, 348, 555-557.	Fumagillin analogue, TNP-470, was the first angiogenic inhibitor to be tested clinically.
1993	K.J. Kim, B. Li, J.Winer, M. Armanini, N.Gillett, H.S.Phillips, N Ferra.	Inhibition of vascular endothelial growth factor-induced angiogenesis suppresses tumour growth in vivo.	Nature, 362 (6423), 841-844.	Description of a VEGF specific monoclonal antibody which inhibited tumour growth by decreasing vessel density. The blocking of VEGF induced angiogenesis suggested as a therapeutic target.
1994	M.S. O'Reilly, L. Holmgren, Y. Shing, C. Chen, R.A. Rosenthal, M. Moses, W.S. Lane, Y. Cao, E.H. Sage, J. Folkman.	Angiostatin: a novel angiogenesis inhibitor that mediates the suppression of metastases by a Lewis lung carcinoma.	Cell, 79, 315-328.	Angiostatin, released by the primary mouse tumour, shown to be responsible for the inhibition of metastases.
1997	M.S. O'Reilly, T. Boehm, Y. Shing, N. Fukai, G. Vasios, W.S. Lane, E. Flynn, J. Folkman	Endostatin: An endogenous inhibitor of angiogenesis and tumour growth.	Cell, 88 (2), 277-285	Endostatin, a fragment of collagen XVIII, identified as an angiogenic inhibitor. Suggested the theme of protein fragments as angiogenesis inhibitors and demonstrated dormancy therapy.
2000	T. Brower C.E. Butterfield, B.M Kruling, B. Shi,	Antiangiogenic scheduling of chemotherapy improves efficacy against experimental drug-resistant cancer.	Cancer Research, 60 (7), 1878-1886	Description of Metronomic Therapy; combination therapy of chemotherapy and specific angiogenic inhibitors for improved treatment.

	B. Marshall, M.S. O'Reilly, J. Folkman.			
2004	N. Ferrera, K.J.Hillian, H-P. Gerber, W.Novotny.	Discovery and development of Bevacizumab, an anti-VEGF antibody for treating cancer.	Nature Reviews, 3 (5), 391-400.	Bevacizumab (Avastin), a humanized anti-VEGF monoclonal antibody, the first USA FDA approved antiangiogenic drug. First line therapy for metastatic colorectal cancer.

1.5i Tumour Angiogenesis

New blood vessels can be formed either spontaneously via vasculogenesis or from pre-existing vasculature by the process of angiogenesis or intussusception. Blood vessel formation can also be classified according to whether the vessels are formed during embryogenesis, (vasculogenesis), during a physiological process (regulated / normal angiogenesis) or during a disease process (pathological or dysregulated angiogenesis) (Herbert and Stainer, 2011, Claesson-Welsh, 2012).

Embryonic vasculogenesis refers to the formation of primitive vessels within both the embryo and its amniotic membranes. Newly formed angioblasts aggregate into a primitive vascular plexus which then undergoes a complex remodelling process resulting in the formation of a functional vasculature (Chung and Ferrara, 2011).

Intussusception is when a pre-existing vessels splits creating two vessels (Burri *et al.*, 2004).

Normal angiogenesis is a strictly controlled event. In the adult, most pre-existing vasculature is considered to be in a quiescent state with angiogenesis only normally occurring during the female reproductive cycle, bone morphogenesis and wound healing and repair (Carmeliet, 2003). However, the endothelial cells still retain the ability to respond to an angiogenic stimulus, such as an injury or hypoxia (Carmeliet, 2005). It is the retained responsiveness of endothelial cells which is hijacked during pathological angiogenesis.

The process of angiogenesis consists of a highly coordinated series of linked, sequential steps. Endothelial cells undergo an ordered series of events, which include activation, proliferation, migration, alignment, tube formation, branching and anastomosis (Mauriz and Gonzalez- Gallego, 2008) (Table 1.9). Under normal physiological conditions angiogenesis is controlled by the balance in production of pro- angiogenic and anti-angiogenic factors; at present over 30 have been identified (Table 1.10). Pathological angiogenesis shares many processes with physiological angiogenesis, however the major difference is that pathological angiogenesis does not reach resolution upon establishment of vascular perfusion. The angiogenic cascade is persistent and unresolved, driven by the pathological condition (Chung & Ferrara, 2010).

As Folkman described, pathological angiogenesis occurs in tumours whereby an avascular tumour converts to an angiogenic phenotype (Hanahan & Folkman, 1996). This has been termed as the “angiogenic switch” and represents a distinct step in the

multistep pathogenesis of cancer (Hanahan *et al.*, 1996, Hanahan and Weinberg 2000). Tumour angiogenesis is fuelled by the relentless uncontrolled production of angiogenic stimulators, in excess of inhibitors, which tips the balance in favour of hyperactive vessel growth (DeBock *et al.*, 2011). The establishment of tumour vasculature is essential to enable tumour growth and metastasis (Mauriz and Gonzalez- Gallego, 2008).

The trigger for tumour angiogenesis appears to be tumour size (Folkman, 1973, 1990). Similar to what occurs during embryogenesis; the tumour grows to a size beyond which the passive diffusion of oxygen, nutrients, and metabolic waste is ineffectual. The hypoxic environment created within the tumour appears to, in addition to oncogenic events (glucose deprivation, oxidative and mechanical stress), be responsible for promoting angiogenesis (Dayan *et al.*, 2008, Longo *et al.*, 2002). The heterodimeric transcription factors, hypoxic inducible factors (HIFs) initiate the process by inducing the expression of pro-angiogenic mediators, especially VEGF-A. HIFs are composed of two subunits, α and β . It is the α subunit which is regulated by oxygen levels, which under normal conditions are present at low levels due to regulation by the tumour suppressor von Hippel-Lindau (VHL) (Longo *et al.*, 2002, Chung & Ferrara, 2011). Mutations in VHL have been described in renal cell carcinoma, increasing the stability of HIF-1 α and thereby promoting angiogenesis (Pugh & Ratcliffe, 2003). It would appear that the pro-angiogenic phenotype of a tumour is due to a combination of oncogene activation and loss of tumour suppressor function, preceding the activation of growth factor signalling (Liao & Johnson, 2007). It is these mutations which enable angiogenesis to give the tumour a selective development advantage.

Vascular endothelial growth factor A (VEGFA) overexpression appears to be crucial in most tumour angiogenesis. Many tumour cells overexpress VEGFA and its major receptor, VEGFR-2, is highly expressed by endothelial cells engaged in tumour angiogenesis (Kerbel, 2008). VEGFA levels are also enhanced by secretion by tumour stromal cells such as fibroblasts, monocytes and platelets (Kut *et al.*, 2007). VEGFA is the prototypic member of a gene family that also includes VEGFB, VEGFC, VEGFD and placenta growth factor (PlGF) (Ferrara, 2004). Numerous effects have been attributed to VEGF signalling including endothelial migration, proliferation, survival and gene expression. It affects vascular permeability by inducing pores and fenestrations in the endothelium. VEGF is also responsible for the recruitment of bone-marrow derived progenitor endothelial cells and can induce their differentiation; the differentiation of haemopoietic lineages and dendritic cells can be influenced by VEGF

(McMahon, 2000). FGF, PDGF and PIGF have also been implicated in angiogenesis. (Table 1.11).

Tumour angiogenesis is perpetuated by the recruitment of other cell types to add to the relentless production of pro-angiogenic factors. Tumour associated fibroblasts (TAFs) secrete proangiogenic factors such as VEGF and FGF and aid in the recruitment of bone-marrow derived endothelial progenitors by release of stromal-cell-derived factor-1 α (SDF-1 α) (Chung & Ferrara, 2011, Orimo *et al.*, 2005). The recruitment of mature myeloid cells, such as neutrophils, has been reported in various cancers including gastric, colon and bronchioalveolar carcinoma and correlates with a poor prognosis (Tazzyman, 2009). They are attracted to the tumour by the production of G-CSF and CXCL chemokines (CXCL8 and CXCL6), which bind to and activate their CXCR1 and CXCR2 receptors. Neutrophils are responsible for the majority of MMPs present within the tumour (Coussens *et al.*, 2000). The MMPs mediate the release of proangiogenic factors from the surrounding ECM (Pahler *et al.*, 2008).

As in physiological angiogenesis, immune cells are recruited due to release of tumour derived chemoattractants (PIGF, VEGF, CSF-1) including monocytes, dendritic cells and lymphocytes. The extent of macrophage infiltration into a tumour has been shown to correlate with increased vascular density and poor prognosis (Bingle *et al.*, 2002). Macrophage recruitment appears to amplify angiogenesis due to cooperation with tumour cells in mediating HIF-1 α transcription of proangiogenic factors VEGF-A, bFGF, and CXCL8 (Chung and Ferrara, 2011).

Table 1.9: The key steps in angiogenesis.

1. Production of pro-angiogenic factors, by either injured tissues or tumour, diffuse into nearby tissues. VEGF is the most common of at least 6 pro-angiogenic proteins (PDGF, bFGF).
2. Specific receptors on endothelial cells of pre-existing vessels bind the pro-angiogenic factors stimulating an intracellular signalling process.
3. Intracellular signalling activates the endothelial cells into the production of new molecules and enzymes.
4. Degradative enzymes, such as MMPs, dissolve tiny holes in the blood vessel's basement membrane.
5. Endothelial cell proliferation.
6. Directional migration of the endothelial cells towards the injured tissue or tumour. Adhesion molecules, integrins ($\alpha\text{v}\beta\text{3}$, $\alpha\text{v}\beta\text{5}$) serve as grappling hooks to help pull the sprouting new blood vessel sprout forward
7. ECM remodelling by MMPs. Tissue in front of the sprouting vessel tip is dissolved to accommodate the extending vessels whilst tissue is remolded around it.
8. Tube formation. Sprouting endothelial cells roll up to form the characteristic blood vessel tube structure.
9. Loop formation. Blood vessel tubes connect to form blood vessel loops that are capable of circulating blood.
10. Vascular stabilisation and maturation. Vessels are covered by pericytes which provide perivascular support.
11. Blood flow begins.

Table 1.10: Regulators of Angiogenesis

Angiogenic Stimulators	Angiogenic Inhibitors
Angiogenin	Angioarrestin
Angiopoietin-1 (Ang-1)	Angiostatin (plasminogen fragment)
Del-1	Angiopoietin-2 (Ang-2)
Epidermal growth factor	Antiangiogenic antithrombin III
Endothelial growth factor (EGF)	Cartilage-derived inhibitor (CDI)
Fibroblast Growth Factors: acidic (aFGF) and basic (bFGF)	CD59 complement fragment
Follistatin	Endostatin (collagen XVIII fragment)
Granulocyte colony-stimulating factor (G-CSF)	Fibronectin fragment
Hepatocyte growth factor (HGF)/ Scatter factor (SF)	Gro-beta
Interleukin-8 (IL-8/ CXCL8)	heparinases
Leptin	Heparin hexasaccharide fragment
Midkine	Human chorionic gonadotropin (hCG)
Placental growth factor (PIGF)	Interferon alpha/ beta/ gamma
Platelet-derived endothelial cell growth factor (PD-ECGF)	Interleukin-12
Platelet- derived growth factor-BB (PDGF-BB)	Kringle 5 (plasminogen fragment)
Pleiotrophin	Metalloproteinase inhibitors (TIMPS)
Progranulin	2- Methoxyestradiol
Proliferin	Placental ribonuclease inhibitor
Transforming growth factor- alpha (TGF- α)	Plasminogen activator inhibitor
Transforming growth factor- beta (TGF- β)	Platelet factor-4
Tumour necrosis factor- alpha (TNF- α)	Prolactin 16kD fragment
Vascular endothelial growth factor Family (VEGFA/B/C/D)/ Vascular permeability factor (VPF)	Proliferin- related protein (PRP)
	Retinoids
	Tetrahydrocortisol-S
	Thrombospondin-1 (TSP-1)
	Tissue inhibitor of metalloproteinase (TIMP) 1, 2, 3
	Transforming growth factor –beta (TGF- β)
	Vasculostatin
	Vasostatin (calreticulin fragment)

Table 1.11: Key pro-angiogenic growth factors

Factor	Ligands	Receptors	Signalling Pathways	Effects
Vascular Endothelial Growth Factor (VEGF)/ Vascular Permeability Factor (VPF)	5 structurally related: VEGFA, VEGFB, VEGFC, VEGFD and Placental growth factor (PIGF)	3 related receptor tyrosine kinases composed of a extracellular domain with seven Ig-like folds and a short kinase insert: VEGFR1- binds VEGFA, VEGFB, PIGF - expressed in monocytes, macrophages VEGFR2- binds VEGFA, VEGFC, VEGFD - expressed vasculature endothelial cells VEGFR3- binds VEGFC, VEGFD - expressed lymphatic endothelial cells VEGF co-receptors: Heparin sulphate proteoglycans/ heparin Neuropilins Integrins	Ras- mitogen activated protein kinase (MAPK), Phosphoinositol-3-kinase (PI3K), Phospholipase C (PLC), Rho-GTPase	Endothelial migration, proliferation, survival and gene expression, vascular permeability, ECM degradation. Normal expression: Embryonic development, wound healing, female reproductive cycle, after exercise.
Fibroblast Growth Factor (FGF)	FGF family comprises 22 proteins (FGF1-23).	4 receptor tyrosine kinases composed of three extracellular	Ras- mitogen activated protein kinase (MAPK),	Endothelial cell proliferation, migration

	7 sub families based on sequence comparisons.	Ig-like loops, a transmembrane domain and a split tyrosine kinase domain FGF co- receptors: Heparin sulphate proteoglycans/ heparin Neuropilins	Extracellular Signal-regulated kinase (ERKs), Src, p38 MAPKs, Phospholipase-C-Gamma (PLC-gamma), Protein Kinase-C (PKC-C), Jun N-terminal kinase (JNK).	and production of proteases. Normal expression: Wound healing, especially tissue remodelling. Embryonic development.
Platelet- derived Growth Factor (PDGF)	5 dimeric isoforms, assembled from polypeptide chains denoted A, B, C and D: PDGF-AA, PDGF-BB, PDGF-AB, PDGF-CC, PDGF-DD (only A and B forms secreted as active forms)	2 structurally highly related receptor tyrosine kinases, with 5 extracellular Ig-like loops and a split tyrosine kinase domain. Both expressed on mesenchymal cells PDGFRa PDGFRb PDGF co-receptors: Heparin sulphate proteoglycans/ heparin Integrins	Ras- mitogen activated protein kinase (MAPK), Phospholipase-C-Gamma (PLC-gamma), Protein Kinase-C (PKC-C), Phosphoinositol-3-kinase (PI3K),	Pericyte coverage of endothelial cells- vessel maturation. Interstitial pressure regulation. Normal expression: Wound healing, regulates interstitial pressure.

1.5ii Tumour Vasculature

Tumours are similar to normal tissues in regards to requiring a proficient blood supply to deliver oxygen and nutrients, whilst removing harmful bi-products. Early researchers, pre-1960, presumed that a tumour simply received its blood supply from the dilation of neighbouring pre-existing vessels. Subsequently, it was discovered that a tumour requires development of its own vasculature if it is to grow beyond 1-2mm in size (Folkman, 1973).

Normal vasculature is characterised by a distinct hierarchical organisation (arteries, capillaries and veins) which ensures tissues are efficiently perfused with a continual flow of blood (Herbert and Stainer, 2011). The endothelial cells form an uninterrupted lining of the vessels, with tight junctions between individual cells. Endothelial cells also deposit a basement membrane composed of fibronectin, collagen IV, laminins and heparan sulphate proteoglycans (Sottile, 2004). Specialised mesenchymal cells, pericytes, surround and support the vessels. Thus, vessel permeability is highly regulated creating a healthy tissue environment. However, in tumours the uncontrolled and persistent release of pro-angiogenic factors results in an imbalance, with the angiogenic switch turned in favour of hyperactive vessel growth. Consequently tumour vasculature is abnormal in both structure and function (Wu and Li, 2008, Claesson-Welsh, 2012) (Table 1.12).

Tumour vessels are routinely described as mal-shaped, irregular and disorganised with a tortuous architecture. The normal organisation does not exist, although attempts have been made to classify the vessels (Eberhard *et al.*, 2000, Hanahan and Weinberg, 2000) (Table 1.13). The vessels are highly dysfunctional, exhibiting spatiotemporal heterogeneity. The irregular shape of endothelial cells results in a loss of the normal vessel lining; tumour endothelial cells will stack on top of each other causing protrusions which obstruct blood flow through the vessel (DeBock *et al.*, 2011).

Connections between endothelial cells are often loose due to wider junctions and lack of perivascular support owing to coverage by fewer and abnormal pericytes (Mauriz and Gonzalez-Gallego, 2008). Gaps also form in the endothelium where the endothelial cells have either died or migrated away. This results in poor inconsistent blood flow and a leaky endothelium.

Many of the abnormalities including tortuosity, fragility, lack of pericytes and propensity for bleeding and exudation are attributed to an abundant expression of VEGFA (Nagy *et al.*, 2007). A consequence of a leaky endothelium and poor

inconsistent blood flow is a rise in interstitial pressure (Claesson-Welsh, 2012). A unique, feature of tumour vasculature is the de-differentiation program of tumour cells called vasculogenic mimicry; whereby the tumour cells actually line the blood vessels instead of endothelial cells (Hendrix *et al.*, 2003).

Tumour angiogenesis is frequently described as non-productive due the resultant vasculature being dysfunctional. The lack of adequate perfusion of the tumour creates an adverse hypoxic and acidic environment which promotes a pro-malignant programming of the tumour cells, leading to disease progression (Rapisarda and Melillo, 2009, Lunt *et al.*, 2009, DeBock *et al.*, 2011). This also affects the efficiency of how anti-tumoural chemo-therapeutics can be administered. Metastasis is aided by the leaky vessels; allowing tumour cells to escape into the blood stream and subsequent distribution throughout the body where they can seed forming secondary tumours. Therefore, the tumour vasculature promotes tumour invasiveness, dissemination and overall malignancy (DeBock *et al.*, 2011).

Table 1.12: The differences between normal and tumour vasculature.



<u>Normal Vasculature</u>	<u>Tumour Vasculature</u>
	
<ul style="list-style-type: none"> • Well organised • Defined arterioles and venules • Non-dilated • Non- permeable • Mature and coated with pericytes. • Low interstitial pressure • Complete basement membrane • Normal rate of blood flow. 	<ul style="list-style-type: none"> • Disorganised • Undefined vessels • Unevenly distributed • Tortuous routes • Obstructed and/ or restricted flow • Dilated • Highly permeable • Premature and lack pericytes • Lack basement membrane

Table 1.13: The classification of tumour vasculature.

Name	Features
Capillaries	Similar to normal capillaries.
Feeder Arteries (FA)	Greatly enlarged, tortuous pericyte coated vessels that supply the complex of tumour blood vessels.
Draining Veins (DV)	Enlarged and tortuous vessels that drain blood away from tumour.
Mother Vessel (MV)	Greatly enlarged, tortuous, thin walled, immature in regards to pericyte coating, hyperpermeable.
Glomeruloid Microvascular Proliferations (GMP)	Tangles of tiny vessels immersed in a complex mixture of irregularly ordered pericytes and extensive multilayered basement membrane.
Vascular Malformations (MV)	Large vessels with irregular coating of pericytes.

1.5iii The First Generation of Anti- Angiogenic Agents

It has been over 40 years since Folkman first published the theory of stopping tumour growth and metastasis by a therapy aimed at interfering with tumour angiogenesis. Anti-angiogenic therapy has since been described as having the potential to become the “fourth modality for cancer treatment”, joining surgery, chemotherapy and radiotherapy (Abdollahi *et al.*, 2005). Over 60 anti-angiogenic agents have been evaluated in the clinical trial process. In 2004 the first FDA approval was given to a drug solely developed as an angiogenesis inhibitor; Bevacizumab (Avastin, Genentech) for the treatment of advanced colorectal cancer. The process of the discovery and development of any new drug is a long, costly, complicated process. Success is preceded by many failures.

In order to develop anti-angiogenic treatments specific assays were required to identify and characterise potential agents. After purification, preliminary evaluation of an angi-suppressive effect is performed using *in vitro* assays of cultured endothelial cells on a gelatinised surface; testing the pharmacodynamics effects of the agent on endothelial growth, proliferation, migration, invasiveness and tube formation. Human capillary endothelial cells are considered to be more representative of tumour endothelia than cells extracted from the larger blood vessels (Folkman *et al.*, 1979, Longo *et al.*, 2002). The next stage is to define the agents’ pharmacokinetic parameters, for example mode of administration and dosing strategy. Numerous *in vivo* angiogenesis assays allow the

direct effect of the agent to be tested. Matrigel assays are the simplest, where the agent's response to specific angiogenic stimuli can be quantified histologically. Chick chorioallantoic membrane (CAM) is a semi-quantitative assay whereby tumours are implanted onto the CAM and the agent is assessed by its ability to inhibit the growth of capillaries (Auerbach *et al.*, 1974). Corneal neovascularisation assay permits the direct visualisation of the agents' effect on both new vessels and pre-existing vasculature in cornea of experimental animals. Orthotopically transplanted human tumours in nude mice is routinely the model of choice, as not only can the agents effect on inhibiting neovascularisation on tumour growth be measured but the systemic impact can be monitored via serum and urine testing (Longo *et al.*, 2002).

After vigorous testing, an application is then made to undertake human clinical trials. The three phases of trials are designed to provide the highest level of confidence in the validity of the results. The initial Phase I human testing, is performed on a small group of healthy volunteers upon which the drugs' safety and dosing range is evaluated: pharmacokinetics factors assessed include absorption, metabolism and elimination of the agent whilst pharmacodynamic tests screen for side effects. Phase II evaluates the effectiveness of the agent in a small group of patients (100-500) with the disease / condition under study; optimising dosage and treatment schedules, assessing short-term effects and the drugs' mechanism of action. Phase III is the longest and most expensive, often involving multi-centre, global contributors. A large group of patients (1000-5000) are tested in order to generate statistically significant data about safety, efficacy and the overall benefit/risk relationship of the agent. Patients are randomly assigned to either receive the test drug or standard treatment. Finally, the FDA reviews all the data collected, determining if the agent has any clinical benefit and whether to approve it for treatment. The whole process from initial discovery to FDA approval can take up to 15 years and cost millions (Longo *et al.*, 2002, DiMasi *et al.*, 2003).

Compared to conventional therapy, anti-angiogenic treatments were considered to have many advantages. Homogenous and diploid the endothelial cells were seen as genetically stable uniform target, where spontaneous mutations were thought to rarely occur (Rak and Kerbel, 1996). Unlike the heterogenetic tumour cells which displayed high genetic instability and mutation rates; characteristics which promote the selection subpopulations with acquired resistance to anti- tumoural drugs. By nature of their active proliferation and migratory activity the tumour endothelial cells could be selectively targeted, as opposed to the quiescent normal endothelia (Longo *et al.*, 2002). Also, endothelial cells are easily accessible via the blood; allowing systemic

administration of drugs thereby avoiding the difficulties of low penetration experienced with anti-tumoral drugs in solid tumours. In addition, a tumour's vasculature will support the growth of numerous and various different populations of tumour cells, by targeting the vasculature it would subsequently affect the survival of many tumour cells (Mauriz *et al.*, 2005, Mauriz-Gonzalez-Gallego, 2008). Finally, some anti-angiogenic drugs also have synergistic effects when combined with cytotoxic drugs and radiation therapy (Kakeji and Teicher, 1997).

There are many ways in which anti-angiogenic agents can be classified and at present there is not a universally agreed approach. For ease of discussion the first generation of anti-angiogenic agents, which were developed to specifically target the tumour vasculature endothelium, will be reviewed first. Tumour endothelial inhibitors fall into three categories; firstly those which target the endothelial cells directly by stopping proliferation, secondly those which block the ability of endothelial cells to migrate through inhibiting MMPs and adhesion molecules and finally those which inhibit the angiogenic signalling cascade by interfering with either angiogenic factors or their receptors. In a subsequent section, the next generation of anti-angiogenic treatments will be discussed.

Blocking the Endothelial Cells Directly.

According to the angiogenic switch hypothesis, tumours secrete both stimulators and inhibitors of angiogenesis and it is the altered balance of production which results in an excess of stimulators compared to inhibitors. Hence, tumours express an angiogenic phenotype. Two of the most researched endogenous angiogenic inhibitors were discovered in Folkman's laboratory by his colleague Michael O'Reilly: angiostatin (1994) and endostatin (1997). Other endogenous inhibitors include angiogenin (Fett *et al.*, 1985), thrombospondin-1 (Nicosia and Tuszynski, 1994), interferons (Dinney *et al.*, 1998), platelet factor-4 (Nicosia *et al.*, 1994) and 16kDa prolactin (Hanahan and Folkman, 1996).

Originally isolated from tumour bearing mice, Angiostatin is a 38kDa amino-terminal fragment of plasminogen which is produced in the tumour stroma (O'Reilly, 1997). Angiostatin inhibits endothelial proliferation by down-regulating the protein level of cyclin-dependent kinase 5 (cdk5), a cdk absent in quiescent cells but induced by pro-angiogenic factors. It can also act by upregulating of the mRNA level of FasL and reducing the level of c-Flip which activates the extrinsic apoptotic pathway (Mauriz and Gonzalez-Gallego, 2008). Other effects include inhibiting endothelial cell migration,

tube formation and vessel network formation and primary metastasis in mouse models (Miriam *et al.*, 2004). Elevated angiostatin levels have been observed in the serum, urine and ascites fluid of cancer patients (Cao *et al.*, 2000, Yokoyama *et al.*, 2000). Endostatin was isolated from a hemangi endothelioma cell line and is a naturally occurring 20kDa C terminal fragment derived from type XVIII collagen. It is a member of multiplexin family which are characterised by multiple triple-helix domains and interruptions (Abdollahi *et al.*, 2005). Of the endogenous angiogenesis inhibitors, Endostatin has the broadest anti-cancer spectrum; targeting angiogenesis regulatory gene on more than 12% of the human genome (Folkman, 2006). It interferes with endothelial proliferation by numerous mechanisms; reducing mRNA level of several proliferative genes including MAPK1, MAPK2 or c-myc, disturbing the survival/death balance by inhibiting the anti-apoptotic signal induced by the P13K/PKB pathway and alternatively activating pro-apoptotic pathways through induction of caspase-9 by reducing the level of anti-apoptotic proteins Bcl-2, Bcl-XL and Bad (Mauriz and Gonzalez-Gallego, 2008).

Using recombinant proteins, the efficacy of angiostatin and endostatin has been demonstrated in many animal model studies, on a wide selection of solid tumour types (O'Reilly *et al.*, 1997). However, this has not translated to clinical trials. A notable feature of the Endostatin Phase I trials was the complete absence of drug-related toxic effects, but unfortunately there was limited efficacy in humans compared to the mice models; there was a 50 fold difference in proliferation rates between tumour tissue and normal endothelium in mice whilst human studies indicated only a 10 fold difference (Rubin, 1998). Although requiring prolonged administration, a similar result was gained using Angiostatin (Dell'Eva *et al.*, 2002). Lack of acquired resistance was also a feature of mouse models studies (Boehm *et al.*, 1997). However, problems with purity, stability, storage and handling plus the lack of critical folding of the recombinant protein(s) appeared to be responsible for the lack of clinical success (Marshall 2002). However, Chinese researchers developed a novel recombinant form of endostatin, Endostar, expressed and purified in *E.Coli* with an additional nine amino-acid sequence added to the N- terminal which forms a six-histidine tag (Ling *et al.*, 2007). In 2005, the Chinese FDA approved Endostar for treatment of Non-small-cell lung cancer (NSCLC); further trials in lung, breast, pancreas and colorectal cancer are being undertaken (cancertherapychina.com). The use of gene therapy also has the potential to produce the either/both angiostatin and endostatin, at high concentrations for a prolonged period in a specific area (Dell'Eva *et al.*, 2002).

The inhibition of endothelial cell proliferation was the first experimental strategy for the screening of new anti-angiogenic drugs. The first angiogenic inhibitor to be clinically tested was Fumagillin (although initially described as antimicrobial agent). Isolated from the mould *Aspergillus fumigatus* Fresenius it has a potent endothelial cytostatic activity by inhibiting the enzymatic activity of methionine aminopeptidase-2 (MetAP-2) (Lien *et al.*, 2004). Unfortunately severe side effects impeded progress but in collaboration with Takeda Chem Industries, Folkman developed fumagillin analogues as a novel class of anti-proliferative agents (Folkman, 1990). TNP-470 was reported to be fifty times more potent than fumagillin and was the first MetAP-2 inhibitor to enter clinical trials. TNP-470 inhibits angiogenesis due to endothelial cell cycle arrest late in G1 phase, it may also induce p53 pathway, thereby stimulating the production of cyclin-dependent kinase inhibitor p21 (Mauriz *et al.*, 2007). Although, initially promising results in early Phase I/II studies, with tumour growth slowed in patients with metastatic cancer, the clinical testing was terminated due to dose-limiting toxicities and a poor clinical pharmacokinetic profile. The small size of the TNP-470 molecules was considered to be a reason for the neurotoxic effects. New analogues with a better toxicity profile, PP1-2458 (Praecis Pharma/ Glaxo Smith Kline), are now in Phase I trials (Bernier *et al.*, 2005, Cooper *et al.*, 2006, Lefkore *et al.*, 2007).

Blocking Endothelial Cell Migration.

MMP enzymes are one of the first products manufactured by growing endothelial cells. MMPs are a family of zinc-dependent neutral endopeptidases that proteolytically degrade various components of the ECM (Hidalgo *et al.*, 2001). The family is subdivided according to their primary structure and substrate specificity; collagenases, gelatinases, matrilysins, membrane type MMP and stromelysins. The numerous MMPs exhibit several roles which enhance angiogenesis including releasing angiogenic factors bound to ECM, generating pro-migratory ECM component fragments, pericyte detachment of angiogenic vessels and the cleavage of endothelial cell-cell adhesions promoting endothelial cell migration (Rundhaug, 2005). MMPs are also essential in allowing tumour cells to gain access to the circulation via basement membrane breakdown thereby facilitating metastasis. Numerous studies have reported increased expression of MMPs in tumours. For example MMP-1 is overexpressed in breast, colorectal, gastric, ovarian and oesophageal cancers whilst MMP-2 is overexpressed in

melanoma and sarcoma metastatic models (Mauriz and Gonzalez-Gallego, 2008, Hofmann *et al.*, 2000).

TIMPs are endogenous MMP inhibitors which have anti-angiogenic activities. TIMPs 1-4 have been shown to inhibit VEGF- induced endothelial migration as well as cell proliferation and tube formation (Jiang *et al.*, 2002). Numerous synthetic MMP inhibitors have been developed; showing promising anti- angiogenic activity *in vitro* and *in vivo* pre-clinical models but so far having limited success in clinical trials (BMS-275291, Marimastat, Tanomastat). The inhibitors are able to target numerous MMPs which may explain the reported adverse side effects. (Li *et al.*, 2010) more specific inhibitors are in development; pre-clinical trials include monoclonal antibodies to MT1-MMP and recombinant PEX domain to inhibit proMMP2 activation (Galvez *et al.*, 2001, Pfeifer *et al.*, 2000).

Endothelial cell migration is also dependent on integrins; cell adhesion molecules which allow endothelial cells to adhere to ECM proteins, such as vitronectin (Auerbach, 1994). Integrins are cell surface glycoproteins that are formed by α and β subunits. Angiogenic endothelial cells express different integrins compared to quiescent cells. $\alpha v \beta 3$ and $\alpha v \beta 5$ integrins are upregulated on the surface of activated endothelial cells. The fibronectin receptor $\alpha 5 \beta 1$ integrin is also selectively expressed (Erdreich-Epstein *et al.*, 2000, Kim *et al.*, 2000, Dunehoo *et al.*, 2006). In various animal models, antagonists of $\alpha v \beta 3$ such as the LM609 antibody have caused a decrease in angiogenesis and induced tumour regression. They appear to trigger apoptosis within the activated vessels (Brooks *et al.*, 1994). Vitaxin (Applied Molecular Evolution), a humanised version of LM609, also appears to induce apoptosis in newly generated endothelial cells and has undergone a promising Phase I study (Gutheil *et al.*, 2000).

Blocking the Angiogenic Signalling Cascade.

Numerous proteins and molecules have been classified as being stimulators of angiogenesis but none have proven as essential as the VEGF family. The VEGF family (originally identified as vascular permeability factor (VPF)) consists of five structurally related ligands VEGFA, VEGFB, VEGFC, VEGFD and Placental growth factor (PlGF); which functionally differ in their ECM binding capacity (Ferrara, 1989). Secreted as a cysteine knot glycoprotein, VEGF is transcriptionally activated in epithelial, mesenchymal and tumour cells in response to hypoxia (Nieves *et al.*, 2009). VEGF isoforms bind to principally two main receptor kinases (RTKs); VEGFR1 (Flt-1) and VEGFR2 (Flk-1) located on neighbouring endothelial cells. The VEGF receptors

display a similar organisation of an extracellular ligand binding domain, a juxtamembrane domain, a split tyrosine kinase domain and a C-terminal tail (Claesson-Welsh, 2012). The activation of VEGF receptors by VEGF-specific binding leads to homo-or hetero dimerisation of the receptor proteins thereby initiating a number of signalling pathways including Ras-mitogen activated protein kinase (MAPK), phosphoinositol-3-kinase (PI3K) and phospholipase C (PLC) gamma which promote endothelial migration, proliferation, permeability, ECM degradation, survival and gene expression. (Table 1.11).

VEGFA is often described as the master regulator of angiogenesis. Although not considered as a cancer biomarker, it is the most frequently expressed pro-angiogenic factor in the tumour microenvironment (Claesson-Welsh, 2012). Elevated expression levels of VEGF receptors are also common in tumour vasculature; a rat glioma model of tumour angiogenesis has been reported to have increased numbers of VEGFR1 and VEGFR2 (Plate *et al.*, 1993). VEGF deletion and neutralisation studies in tumorigenic mice suggested that VEGF signalling was not required in the adult (Gerber *et al.*, 1999, Kuo *et al.*, 2001); apart from during wound healing responses, female reproductive cycle and following exercise (Maharaj and D'Amore, 2007). Thus targeting of VEGF and/or its receptors became a prime objective, as it was thought such treatments would spare healthy tissues from non-specific damage. Strategies to inhibit the VEGF signalling cascade are monoclonal antibodies against the VEGF protein or its receptors, VEGFR tyrosine kinase inhibitors (TKRIs), VEGF-R targeted ribozymes and VEGF decoy receptors.

Monoclonal antibodies have the potential to modulate signalling pathways by either interacting with the growth factor thereby stopping binding to its receptor or directly with receptors themselves to prevent ligand binding. Initially, lack of suitable production methods hampered progress but the development of large-scale bioreactors helped to improve both the quality and quantity of the recombinant antibodies. Another advancement was the humanisation of antibodies as previously antibodies were usually of murine origin. The insertion of human sequences to the antibody resulted in a longer-life and less immunogenicity.

In 1993 Kim *et al.*, showed that a neutralising antibody against mouse VEGF (A.4.6.1) inhibited tumour growth and angiogenesis in mouse models. The positive results obtained led to the development of a humanised version of this antibody, bevacizumab (Avastin, Genetech), which is considered to be one of the most successful compounds within the anti-angiogenic therapy field. The monoclonal antibody has the ability to

neutralise biologically active forms of VEGF which interact with VEGFR1 and VEGFR2 thereby repressing endothelial cell mitogenic activity and vascular permeability (Brekken *et al.*, 2000). In 2004, bevacizumab was the first Food and Drug Administration (FDA) and European Medicines Agency (EMA) approved anti-angiogenic treatment for cancer and subsequently experienced numerous successes in clinical trials in combination with chemotherapy (Hurwitz, 2004). Bevacizumab combined with specific chemotherapeutic agents was shown to improve patient survival time and have been FDA approved for the treatment of metastatic colorectal cancer, non-small cell lung cancer, metastatic breast cancer, renal cell carcinoma and glioblastoma multiforme (Kesisis *et al.*, 2007, Norden *et al.*, 2008, Ferrara, 2010). (Table 1.14).

DC101, a rat anti-mouse Flk-1 monoclonal antibody against the extracellular domain of VEGFR2 blocked tumour growth in a variety of xenograft models, as well as hepatic metastasis derived from colon cancer (Bruns *et al.*, 2000). A fully humanised version, ramucirumab (IMC-1121B, ImClone Systems) was developed, which has been shown in preclinical and animal models, to inhibit VEGF-induced VEGFR2 activation thereby inhibiting VEGF-stimulated cellular migration and proliferation. Ramucirumab is currently being investigated in multiple clinical trials involving a variety of tumour types (Spratlin, 2011). Tanibumab (TTAC-0001, PharmAbcine) another anti-VEGFR2 monoclonal antibody is undergoing preclinical assessment (Lee, 2011). Inhibition of VEGFR2 is a promising anti-angiogenic target since VEGFR2 expression has been shown to be up-regulated several fold in tumour vascular endothelial cells (Plate *et al.*, 1994, Spratlin, 2011).

Over time, the tumour environment varies considerably leading to fluctuations in the levels of angiogenic factors thereby making drug dosing and optimum neutralisation of VEGF difficult. However, researchers believed the number of VEGF receptors in tumour endothelial cells was relatively low making them more easily saturable, as less antagonist molecules would be required in order to block all the receptors (Mauriz and Gonzalez- Gallego, 2008). Receptor tyrosine kinase inhibitors (RTKIs) block the intracellular activation of growth factor receptor signalling by competitive inhibition of ATP binding to the tyrosine domain and are smaller molecules compared to the large antibodies used to target growth factors. They are considered adept to suppress tumour growth as monotherapy because of an ability to inhibit multiple targets; VEGFR, PDGFR, EGFR, cKit, MAPK and other kinase pathways. The most advanced broad

spectrum tyrosine kinase inhibitors are Sunitinib (Sutent, Pfizer), Sorafenib (Nexavar, Bayer) and Pazopanib (Votrient, GSK).

Sunitinib (sunitinib malate, SU11248, Sutent, Pfizer) is an orally bioavailable, oxindole, multi-targeted tyrosine kinase inhibitor of numerous receptors including VEGFR1-3, PDGFR α and β (Mauriz and Gonzalez- Gallego, 2008). Sunitinib was approved first for the treatment of metastatic or unresectable gastro-intestinal tumours in 2006. In 2009, NICE guidance led it to be the first line drug treatment for patients with advanced / metastatic renal cell carcinoma and in 2011 it was approved by the FDA for treatment of advanced refractory pancreatic neuroendocrine tumours. Currently, numerous Sunitinib trials are in progress for various cancers with and without the addition of chemotherapeutic agents (National Cancer Institute).

The originality of Sorafenib (Nexavar/ Bayer) is its ability to simultaneously target the Raf/Mek/Erk pathways by inhibiting Raf kinase, PDGFR, VEGFR-2 and VEGFR-3 and c-Kit (Flaherty, 2007). In 2006 it was FDA and EU approved for the treatment of advanced refractory clear-cell renal- cell carcinoma, having been shown to increase progression free survival by approximately 3 months. Pazopanib (GW786034, GSK) is an orally available, inhibitor of VEGFR-1, VEGFR-2, VEGFR-3, PDGFR and c-kit (Mauriz and Gonzalez- Gallego, 2008).

Another method of targeting receptor tyrosine kinases is the use of decoy receptors. Also described as a VEGF trap, the decoy receptors bind to VEGF thereby preventing it from binding to the native cell receptors therefore stopping any signalling cascade (Holash *et al.*, 2002). The most established VEGF Trap is known as Aflibercept or Zaltrap (Regeneron Pharmaceuticals/ Sanofi-Aventis); a fully human soluble VEGF receptor fusion protein with the ability to bind to VEGF-A, VEGF-B and PlGF more tightly than native receptors and any anti-angiogenic monoclonal antibody therapies (Konner and Dupont, 2004). Aflibercept is a recombinant protein comprised of portions of the extracellular domain of human VEGFR-1 and VEGFR-2 fused to the constant region (Fc) of human IgG1. It is currently awaiting results of a regulatory review having undergone a Phase III trial for the treatment of refractory, metastatic colorectal cancer (Konner and Dupont, 2004). In 2011 Aflibercept was approved by the United States FDA as an anti-angiogenic treatment for wet macular degeneration (Stewart *et al.*, 2012).

Compared to the other anti-angiogenic drugs, ribozyme drugs use an entirely different mechanism to elicit an anti-angiogenic response. Instead of obstructing the activity of the target protein, ribozyme drugs actually destroy the mRNA therefore stopping the

target protein from being synthesised in the first place. A ribozyme is a catalytic RNA molecule which has the capability to cut other RNA molecules into fragments, thereby preventing translation into protein. Angiozyme (RPI.4610) (Ribozyme pharmaceuticals) was developed to recognise the conserved region of human, mouse and rat VEGFR-1 mRNA; one of the most important VEGF receptors. Angiozyme treatment has been shown in mouse models to have anti-angiogenic, anti-tumour and anti-metastatic activity (Weng and Usman, 2001). Phase I and II trials have been conducted as a mono-therapy and in conjunction with chemotherapy (Bergsland, 2004).

Table 1.14: Anti-VEGF Agents. FDA approved Bevacizumab (Genentech,Avastin) Treatments (Additional data from National Cancer Institute). Bevacizumab treatment combined with standard chemotherapeutic agents.

Cancer type	Chemotherapeutic Agent	FDA Approval	Trial Number	Median Progression Free Survival (months)	Side- effects
Colorectal cancer (metastatic)	5' fluorouracil/ irinotecan	2004	-----	3-4	GIT perforation, impaired wound healing, hypertension, fatigue, thrombosis, diarrhoea, infection, headaches.
Non-small cell lung cancer (advanced, recurrent, metastatic)	paclitaxel/ carboplatin	2006	E4599	2	Neutropenia, fatigue, hypertension, infection, thrombosis/embolism, hypernatremia, proteinuria, GIT perforation
Breast Cancer (metastatic)	paclitaxel/ docetaxel	2008 Revoked 2011	Study 7/ E2100	No evidence for extended life or quality of life.	Sensory neuropathy, hypertension, fatigue, infection, vomiting, diarrhoea, bone pain, headache, proteinuria, cerebrovascular ischemia
Glioblastoma multiforme (recurrent)	+/- Irinotecan	2009	AVF3708g/ NCI 06-C-0064E	3.9 - 4.2	Infection, fatigue, headaches, hypertension, epistaxis, diarrhoea
Renal Cell Carcinoma (metastatic)	Interferon α	2009	B017705	5	Hypertension, haemorrhage, thrombosis, proteinuria.

1.5iv Toxicity of Anti-angiogenic Therapy

It was maybe a naive of the first researchers to underestimate the systemic effects anti-angiogenic therapy would have. Initially, they believed that targeting angiogenesis would result in a selective and specific attack on the tumour vasculature since normal blood vessels were considered to be in a quiescent state. Normal angiogenesis was reported to only occur during the reproductive cycle, pregnancy and in response to injury during wound healing (Chung and Ferrara, 2011). In addition, first generation anti-angiogenic drugs were supposedly developed to inhibit only one pathway. However, the side effects reported in experimental models and clinical trials reinforce angiogenesis as a multifactorial process which is, through its diverse signalling pathways, associated with numerous processes including the regulation of blood pressure, coagulation cascade and immune system (Mauriz and Gonzalez-Gallego, 2008). The role angiogenic factors have in vessel maintenance was also misjudged; VEGF functions in established vessels to promote endothelial cell survival and induce capillary fenestrations (Inai *et al.*, 2004). In the adult, VEGFR2 phosphorylation occurs in many tissues suggesting that even in a supposed quiescent vasculature VEGF signalling is still required (Maharaj *et al.*, 2006).

Determining optimal dosing of anti-angiogenic drugs at biologically active levels has also been problematic. Initially the concept of “the more the better” was applied, with many drugs administered at fixed doses irrespective of body weight (Mauriz and Gonzalez-Gallego, 2008). In addition, treatment strategies often involve anti-angiogenic therapy in conjunction with traditional chemo- or radiotherapy, which have toxicity issues of their own. The reported toxicity of anti-angiogenic therapy, from both experimental models and clinical trials and an increased understanding of angiogenic signalling (VEGF especially) has subsequently led to a more cautious approach and reassessment of long-term treatment. Pregnant women and children are considered unsuitable for anti-VEGF treatment due to its numerous roles during development (Mitchell and Bryan, 2010).

Reported side effects frequently include hypertension, proteinuria, thrombosis, impaired wound healing, bowel and nasal perforations and leuokencephaolpathy (Table 1.15). Although rarely life threatening and clinically manageable, their occurrence may require either an altered dosing strategy, a treatment “holiday” or in severe cases a cessation of therapy. In general, the clinical benefits of anti-angiogenic therapy are considered to out-weigh the adverse side effects (Mitchell and Bryan, 2010).

The most common side effect, experienced by 16-35% of all patients, is hypertension. Anti-hypertensive drugs are effective in resolving the problem; the majority of patients on bevacizumab therapy will require anti-hypertensive medication in order to achieve a normal blood pressure (Ranpura *et al.*, 2010). The anti-VEGF therapies appear to affect the renin-angiotensin system and subsequently aldosterone release; which regulate pressure via electrolyte (Na/ K) and blood volume balance and through modulation of nitric oxide regulated arterial smooth muscle relaxation and vasodilation (Mitchell and Bryan, 2010). A reduction in angiotensin receptor activity has been reported during VEGF inhibition (Sane *et al.*, 2004). Complications with kidney function, including proteinuria, thrombotic microangiopathy and renal microangiopathic haemolytic anaemia are also considered to be a consequence VEGF inhibition. VEGF has a direct effect on kidney function; VEGF signalling is required for repair of glomerular vessels and control glomerular permeability (Eremina *et al.*, 2007, Zhu *et al.*, 2007).

Reversible posterior leukoencephalopathy (RPLS), an oedema of posterior areas of the cerebral hemispheres, is also associated with anti-VEGF therapy. The specific cause is not known but an increase in vascular permeability of the blood-brain barrier is a possibility (Shord *et al.*, 2009). The discovery that VEGF receptors are not singularly specific to endothelial cells has called into question the belief that anti-angiogenic therapy would exclusively target tumour vasculature. Expression of VEGF receptors have been reported in numerous non-endothelial cells including chondrocytes, keratinocytes, retinal neurons, dental odontoblasts, and skeletal myocytes (Mitchell and Bryan, 2010).

In general, cancer patients have an increased risk of thrombotic events because the tumour itself promotes blood coagulation due to cytokine release and fibrinolytic activity. However, the inability of endothelial repair to occur normally during anti-angiogenic therapy augments healing deficiencies and blood clotting problems. If unrepaired damage to the endothelium results in the exposure of the basement membrane, the subsequent release of tissue factor activates the coagulation cascade which promotes thrombogenic activity (Zangari *et al.*, 2009). Complications can result in deep vein thrombosis and pulmonary embolism.

Healing and tissue regeneration deficiencies are a direct result of angiogenic inhibition causing numerous complications including disturbed wound closure, bruising, mucocutaneous bleeding, haemorrhages, bowel and nasal septum perforations (Mitchell and Bryan, 2010). Anti-angiogenic therapy is often stopped prior to and post-surgery.

Between 3.4-13% of colorectal cancer patients receiving bevacizumab treatment have experienced post-surgery wound healing problems (Scappaticci *et al*, 2005).

Table1.15: A list of common side effects associated with anti-angiogenic therapy.

Many of these side effects can be correlated to the role of VEGF.

Side Effect	Clinical Manifestation	Cause(s)
Hypertension	High blood pressure.	<ul style="list-style-type: none"> • Interference with renin-angiotensin-aldosterone system which regulates blood pressure through alterations in electrolyte and fluid balance (Khakoo <i>et al.</i> 2008). • Modulation of nitric oxide regulated arterial smooth muscle relaxation and vasodilation (Hood <i>et al.</i> 1998)
Kidney dysfunction	Proteinuria. Swelling. Thrombotic microangiopathy. Renal microangiopathic haemolytic anaemia.	<ul style="list-style-type: none"> • Interference with kidney filtration processes due to alteration in the integrity of glomerular vascular endothelium. • Impaired repair to damaged glomerular vessels. • Modulation of glomerular permeability (Zhu <i>et al.</i> 2007).
Thrombotic events	Deep vein thrombosis. Pulmonary embolism. Mesenteric venous thrombosis. Axillary venous thrombosis.	<ul style="list-style-type: none"> • Impaired endothelial repair and regeneration. • Exposure of sub-endothelial collagen, due to endothelial damage, stimulates the release of tissue factor which activates the coagulation cascade. (Zangari <i>et al</i> 2009). • Tumour cells promote thrombotic events through procoagulation activity, fibrinolytic activity and cytokine release (Mitchell and Bryan 2010).
Impaired wound healing	Wound closure failure (especially after surgery). Bruising. Mucocutaneous bleeding. Haemorrhages. Bowel perforation. Nasal spectrum perforation.	<ul style="list-style-type: none"> • Disruption of normal angiogenic process which is essential for normal wound healing and tissue regeneration (Hapani <i>et al.</i> 2009, Shord <i>et al.</i> 2009).
Hypothyroidism	Fatigue Hair loss	<ul style="list-style-type: none"> • Reduced vascularity of the thyroid (Faivre <i>et al</i> 2006) • Autoimmune hypothyroidism (Mauriz and Gonzalez-Gallego 2008).

	Anaemia Personality changes Depression	
Reversible Posterior Leukoencephalopathy (RPLS)	Oedema in the white matter of posterior regions of the cerebral hemispheres.	<ul style="list-style-type: none"> Exact mechanism unknown. Possibly due to increased vascular permeability of the blood- brain barrier (Shord <i>et al</i> 2009, Maharaj <i>et al</i> 2008).
Epidermal Toxicity	Hair loss Hair depigmentation Acral erythema	<ul style="list-style-type: none"> Epidermal cell apoptosis (Mauriz and Gonzalez-Gallego 2008).

1.5v Anti-angiogenic Resistance

Anti-angiogenic therapy does increase progression free survival but unfortunately fails to produce an enduring clinical response in patients. Transient disease stabilisation, with possible tumour regression, is often followed by tumour revascularisation and subsequent tumour resurgence, frequently at an accelerated pace. Generally patient survival is minimally increased. Many tumours appear capable of developing a complete resistance to the anti-angiogenic drugs (Mitchell, 2010).

Several mechanisms have been ascribed to explain the refractoriness to anti-angiogenic treatment. Frequent explanations are attributed to the heterogeneity and plasticity of cancer cells whilst first generation anti-angiogenic therapeutics have a limited capacity as they were developed to target a specific angiogenic factor or pathway. During tumour progression cancer cells can undergo a number of mutations and chromosomal arrangements which may result in the emergence of a tumour clone which either increases expression of the same or other pro-angiogenic factor(s) thereby making the anti-angiogenic treatment ineffective. Tumours are proficient in their ability to activate alternative pro-angiogenic signalling pathways (Ferrara, 2010). In mice VEGF inhibition reportedly upregulates VEGF, PlGF, ANG-1 and FGF (Casanovas *et al.*, 2005). Colorectal and renal cancer patients undergoing anti-VEGF therapy have shown increased expression in VEGF and PlGF (Mitchell and Bryan, 2010). Infiltrating fibroblasts, immune cells (macrophages), and stem cells (bone-marrow-derived cells) will also contribute to the release of alternative compensatory pro-angiogenic factors. Endothelial cells were considered an ideal therapeutic target as they were thought to be genomically stable and therefore would not develop a resistance to anti-angiogenic therapy (Carmeliet *et al.*, 2005, Wu & Li, 2008). However, many differences have now been described between endothelial cells from normal tissues and those associated with tumours. *In vitro*, tumour endothelial cells have an altered morphology and fail to senesce, exhibiting cytogenetic abnormalities. Aneuploidy is shown to increase with long term culture (Hida *et al.*, 2008). Normal endothelial cells do not express epidermal growth factor receptors (EGFR), however in cancers that express EGF such as prostate, EGFR are found on tumour endothelial cells (Yazici *et al.*, 2005). The tumour microenvironment may indeed promote the endothelial cells genetic instability, de-differentiation and even cell fusion with tumour cells (Mitchell and Bryan, 2010).

Also, angiogenesis is not the only mechanism that can be adopted to create blood vessels. Vasculogenesis and vascular mimicry have been described in tumours. Bone marrow derived endothelial cell progenitors (EPCs) can be recruited by the tumour to form endothelial cells and subsequently form an endothelium (Nolan *et al.*, 2007). In addition EPCs can secrete numerous pro-angiogenic factors (VEGF, ANG-1, ANG-2, SDF-1); thereby circumventing single target anti-angiogenic drugs and aiding blood vessel formation (Wu and Li, 2008, Mitchell and Bryan, 2010). Vascular mimicry, whereby tumour cells imitate endothelial cells and form vessels, will be completely unaffected by anti-angiogenic therapies that specifically target endothelial cells (Zhang *et al.*, 2007). Once again, the failure of treatment appears to be the limitations of a single anti-angiogenic agent (for example anti-VEGF) to inhibit the numerous possible, often over-lapping mechanisms by which the vasculature can be formed.

The aim of anti-angiogenic therapy is the regression of tumour vasculature which in itself can contribute to the development of resistance. Successful inhibition of tumour angiogenesis, limiting the already restricted blood supply in the tumour will enhance the hypoxic tumour microenvironment. Such an adverse environment promotes malignant progression of tumour cells and survival of pro-angiogenic inflammatory cells (Carmeliet, 2005, Rapisarda and Melillo, 2009, Weis and Cheresh, 2011). Hypoxia inducible factor-1 alpha (HIF-1 α) is known to advance the genetic instability of tumour cells, either by binding to hypoxia responsive elements or displacing the Myc oncoprotein transcription factor, with the resultant up regulation of genes associated with cell survival and disease progression (To *et al.*, 2005). Furthermore, a regressed tumour vasculature will result in the inadequate delivery of the anti-angiogenic drugs to the tumour cells thus exacerbating its ineffectiveness.

A reaction by many tumour types to anti-angiogenic therapy has been an increase in tumour cell invasiveness (Ebos *et al.*, 2009, Paez-Ribes *et al.*, 2009). A cessation of anti-angiogenic therapy or drug holiday appears to exacerbate the problem. The exact explanation is not known but increased matrix metalloproteinase activity has been described in glioblastoma tumours (Bergers and Hanahan, 2008). Once again, the hostile tumour environment enhanced by anti-angiogenic therapy induced vessel regression appears to promote metastasis. Numerous studies have reported that hypoxia fosters tumour metastasis in several tumour types through numerous mechanisms; in breast cancer, hypoxia potentiates Notch signalling leading to decreased E-cadherin expression whilst the up-regulation of HIF-1 α affects the expression levels of E-cadherin, vimentin and MMP-2 in prostate cancer and hepatocyte growth factor in

pancreatic cancer (Chen *et al.*, 2010, Luo *et al.*, 2006, Kitajima *et al.*, 2008). In addition, metastasis can also occur via the lymphatic system; lymphatic vessel growth will not necessarily be blocked by anti-angiogenic therapy.

1.5vi The Next Generation of Anti-angiogenic Agents- New Targets

The inherent or acquired resistance to anti-angiogenic therapy highlights the need for targeting additional angiogenesis pathways to fully explore the potential of anti-angiogenic therapy. There is a necessity to develop strategies that delay, minimise or even avoid resistance. Our increased knowledge of the tumour microenvironment and the involvement of cells other than tumour endothelial cells in the angiogenic process, have seen the emergence of new targets (Table 1.16). It is also evident that for prolonged efficacy, anti-angiogenic treatment plans will no longer solely focus on one target but be a combined therapy where different targets are treated together or subsequently. Furthermore, any future treatment strategy will probably still include the inhibition of the master regulator of angiogenesis VEGF, whether directly or indirectly.

Alternative Angiogenic Pathways

The regulation of VEGF by HIF-1 α is essential in both physiological and pathological angiogenesis. HIF-1 α I as a therapeutic target is appealing as it also regulates the transcription of genes involved in cell proliferation and survival, glucose metabolism, pH regulation and apoptosis (Patiar and Harris, 2006). In normal oxygen conditions HIF-1 α binds to the tumour suppressor VHL protein, which facilitates its proteosomal degradation. However, in hypoxic conditions HIF-1 α is post-translationally modified and remains stable, binding to hypoxia- response elements (HREs) and activating numerous hypoxia response genes, which includes VEGF. Cell survival factors are also upregulated, thereby protecting tumour cells from hypoxia- induced cell death (Longo *et al.*, 2002). The ability of tumour cells to adapt to a hypoxic environment is considered to be partly responsible for the development of resistance to anti-angiogenic therapy (Weis and Cheresh, 2011).

Until recently, no agent had been developed which directly inhibited HIF-1 α . In previous studies, agents inhibited the HIF-1 α pathway by disrupting HIF-1 α /DNA or co-activator binding, HIF-1 α translation or inhibit the stabilising prolyl hydroxylase enzymes (prolyl 4-hydroxylase domain (PHD) proteins). Inhibition of PHD2 by staurosporine or TRAIL in glioblastomas resulted in restricting the ability of tumour

cells to adjust to hypoxic conditions and control cell survival (Mitchell and Bryan, 2010). However, EZN-2968 (Santaris Pharma), a HIF-1 α RNA antagonist (hybridises with HIF-1 α mRNA under both normal and hypoxic conditions) blocks HIF-1 α expression. *In vitro* and *in vivo* pre-clinical studies have shown its ability to limit tumour growth; tumour regression in mice prostate cancer xenografts, blocking endothelial tube formation by HUVEC cells (Greenberger *et al.*, 2008). Phase I trial of EZN-2968 is in process with patients suffering with advanced solid tumours and lymphomas (Mitchell and Bryan, 2010) (Table 1.16).

The hepatocyte growth factor (HGF) /c-MET tyrosine kinase signalling pathway plays a significant role during development and in tumourigenesis (You and McDonald, 2008). Normally HGF is secreted by fibroblasts and smooth muscle cells and promotes mitosis, cell motility and cell survival of epithelial and endothelial cells. In cancer, where it can be secreted by tumour cells, it can also promote cell proliferation, invasion, metastasis and angiogenesis (Teicher, 2011). In the vasculature c-Met activation through paracrine HGF, regulates tumour angiogenesis mainly by induction of proliferation, migration and survival of endothelial cells resulting in vascular tubulogenesis and branching morphogenesis (Shojaei *et al.*, 2010). HGF also promotes angiogenesis through up regulation of VEGF and also down regulating the potent anti-angiogenic factor thrombospondin-1 (TSP-1) (Lee and Kim, 2009). HGF/c-Met signalling increases VEGF levels in the tumour and VEGFR2 on endothelial cells. c-Met activation also effects the tumour cells directly via the signalling pathways PIK3/Akt, Src, STAT3 and Ras/mek; promoting proliferation, survival and increasing invasive phenotype. Expression of both c-Met and HGF can be induced by HIF-1 α (Shojaei *et al.*, 2010). Activation of HGF/ c-Met pathway is a poor prognostic factor in many cancers. In tumours the c-Met receptor can be constitutively phosphorylated, its gene mutated or amplified (Grepin and Pages, 2010). The inhibition of HGF/c-Met pathway produces enhanced VEGF/VEGFR axis-mediated inhibition of angiogenesis and can also overcome the increased response to tumour hypoxia induced by anti-angiogenic therapy. In pre-clinical mouse models, HGF expression levels were found to be higher in Sunitinib resistant tumours; however combined treatment with a selective c-Met inhibitor had an additive effect in inhibiting tumour growth (Shojaei *et al.*, 2010). Monoclonal antibodies to HGF and c-Met, small molecule kinase inhibitors and decoy receptors have been developed and currently being assessed in clinical trials for treatment of a variety of cancer types; either as a monotherapy or in combination with chemotherapeutic agents (Teicher, 2011) (Table 1.16).

The Notch pathway is an evolutionary conserved signalling system which appears to provide critical regulatory information to endothelial (and smooth muscle cells) downstream of the initiating signal induced by VEGF. It regulates cell fate specification, tissue patterning and morphogenesis by modulating cell differentiation, proliferation, apoptosis and survival (Kuhnert *et al.*, 2011). Recently, Notch and its endothelium specific ligand Dll4 (delta-like 4) have emerged as a critical regulator of developmental and tumour angiogenesis. Acting downstream of VEGF stimulation, it limits the effects of VEGF on the vasculature by means of a negative feedback loop. Dll4-Notch signalling decreases angiogenesis by suppressing endothelial tip cell formation. Functioning by a different mechanism to standard anti-angiogenic therapies; the blockade of Dll4-Notch signalling in tumours results in excessive, non-productive angiogenesis and subsequent inhibitory effect on tumour growth (Dufraigne *et al.*, 2008). In preclinical models, Dll4 blockade using neutralising anti-Dll4 antibodies resulted in growth inhibition of both VEGF –sensitive and resistant tumours. Efficient as a monotherapy, the anti-tumour effects are significantly enhanced when combined with anti-VEGF therapy (Bevacizumab). Phase I trials have begun testing the effect of two different monoclonal antibodies, OMP-21M18 and REGN42. Gamma-secretase inhibitors also block Notch signalling; gamma-secretase releases the Notch intracellular domain permitting translocation to the nucleus where it regulates Notch target gene transcription. In addition a Notch decoy has shown to restrain the growth of tumour vasculature in the mouse mammary Mm5MT model (Dufraigne *et al.*, 2008). However, preclinical studies have raised safety issues concerning the adverse effect on normal organ homeostasis, especially liver complications and the need to selectively target Notch1 only as blocking Notch 2 causes severe intestinal toxicity (Kuhnert *et al.*, 2011, Teicher, 2011) (Table 1.16).

Targeting Mural and Stromal Cells

Normal vasculature undergoes a process of stabilisation via the local release of PDGF, VEGF and Ang-1 (Carmeliet, 2005). Released by endothelial cells, PDGF attracts pericytes to embed in the newly formed vessel. Pericytes are mural cells which differentiate from pools of c-Kit+Sca-1+ VEGF-1+ perivascular progenitor cells which are mobilised from the bone marrow in response to PDGF-BB (Song *et al.*, 2005). They have an important role in maintaining capillary structural integrity, mediating endothelial cell survival and blood flow regulation (Fakhrejehani and Toi, 2012). PDGF is structurally related to VEGF, consisting of 5 dimeric isoforms occurring as covalently

linked homo- or hetero-dimers which bind to two structurally related tyrosine kinases, denoted PDGFR α and PDGFR β (Fredriksson *et al.*, 2004). In the adult PDGF contributes to wound healing and regulates interstitial pressure (Ostman and Heldin, 2007).

Tumour vasculature is characterised by a lack of pericyte coverage which resulting in poor vascular functionality, affecting perfusion and vessel permeability (Fakhrejehani and Toi, 2012, Claesson-Welsh, 2012). When PDGF is overexpressed in tumour vessels, pericyte coverage improves, resulting in increased vessel stability and subsequently increased tumour growth (Ostman, 2004). PDGF overexpression has also been linked to atherosclerosis and fibrotic conditions. Gene rearrangements, mutations and amplification of PDGFR or PDGF family members have been associated with gastrointestinal stromal tumours, a rare form of cancer (Ostman and Heldin, 2007). However, when pericytes are targeted using kinase inhibitors and PDGFR β signalling is inhibited the tumour vessels recruit fewer pericytes and dilate; endothelial cell apoptosis is also increased. The simultaneous targeting of endothelial cells and pericytes, with RTKIs inhibiting VEGFRs and PDGFR β has been shown to increase the anti-angiogenic effect, even in late stage solid tumours (Bergers *et al.*, 2003). PDGFR β inhibitors also appear to destabilise the larger vessels covered by smooth muscle cells, which supply bulk flow to tumours, rendering them more susceptible to endothelial cell specific inhibitors (Carmeliet, 2005).

The angiopoietin pathway is also implicated in vessel maturation. Opposing roles have been attributed to Ang-1 and Ang-2; both bind to tyrosine kinase TIE2 receptor. Ang-1 maintains vessel integrity by recruiting and stabilising pericytes. Ang-2, normally expressed during wound healing and vascular remodelling, triggers loss of pericytes allowing endothelial cells to be exposed to pro-angiogenic factors thereby antagonising the stabilisation action of Ang-1. Endothelial destabilisation is initiated by Ang-2 binding to TIE-2 receptor, which in the presence of VEGF induces an angiogenic response. The pathway is considered to have an important role in brain, breast, hepatocellular and lung carcinomas (Longo *et al.*, 2002). A clinical trial with the peptibody, AMG-386 (Amgen), which prevents both Ang-1 and Ang-2 binding to TIE-2 receptor, has shown a similar response to VEGF inhibition (Herbst *et al.*, 2009, Mita *et al.*, 2010). Numerous Phase II trials combining treatment with chemotherapeutics are now be progress (Teicher, 2011) (Table 1.16).

The tumour stroma is also an active contributor to tumour progression. Carcinoma-activated fibroblasts (CAFs) have been attributed to promoting angiogenesis (Guo *et al.*, 2008). CAFs, like pericytes, are recruited to the tumour by PDGF signalling where they proliferate and increase the angiogenic stimulus by releasing VEGF and PIGF (Ostman, 2004). PDGF-BB antagonists have been shown to inhibit angiogenesis. In addition, interstitial fluid pressure was lowered thus improving drug delivery via the tumour vasculature. The exact mechanism is unknown but PDGF is thought to stimulate CAFs to contract the interstitial matrix via microfibrillar networks, thereby constricting the tumour vessels (Carmeliet, 2005).

Targeting Haematopoietic Cells

A feature of many tumours is an inflammatory infiltrate. The release of numerous cytokines and chemokines by the tumour attracts dendritic cells, haematopoietic progenitors, macrophages, mast cells and T Cells (Coussens and Werb, 2002).

Stimulating angiogenesis is one of the many malignancy promoting roles attributed to these cells; including mitogenic and survival factor release, DNA damage, ECM remodelling, host defence evasion (Takakura *et al.*, 2000). They are also considered as contributors to the development of tumour anti-angiogenic resistance.

Mast cells, platelets, tie-2 expressing monocytes (TEM) and tumour associated macrophages (TAMS) are all known to be another source of pro-angiogenic factors. Indeed TAMS specifically accumulate in hypoxic areas of the tumour and producing VEGF, VEGF-C and VEGF-D. Whilst bone marrow derived haematopoietic cells (recruited to tumours in response to VEGF and PIGF and are retained by SDF-1 α) can either stimulate tumour vessels growth by releasing pro-angiogenic factors (VEGF, PIGF and Ang-2) or act as haemangioblasts, producing both haematopoietic and endothelial progenitors that can form new blood vessels (Mitchell and Bryan 2010). Maybe by co-targeting VEGF, PIGF and SDF-1 the migration of these cells will be blocked and thereby reduce angiogenesis, growth and possible metastasis (Carmeliet, 2005).

Bone marrow derived cells are also recruited to tumours through the interaction of HIF-1-dependent CXCL12 and CXCR4. Many divergent pathways are stimulated by the binding of the CXCL12 ligand to the CXCR4 receptor resulting in angiogenesis as well as tumour progression, metastasis and survival (Teicher and Fricker 2010). CXCR4 neutralising antibodies and the CXCR4 antagonist Plerixafor have been reported to prevent mobilisation of bone marrow derived cells and development of tumour growth,

subsequently stopping tumour regrowth (Kioi *et al.*, 2010). Clinical trials are underway for non-Hodgkins lymphoma and acute myeloid leukemia as the CXCL12/CXCR4 pathway is responsible for retaining these cancer cells in the bone marrow (Table 1.16). Termed the macrophage index, a positive correlation between the levels of TAMs and tumour angiogenesis have been described for many human cancers (breast, prostate, cervical, endometrial, liver, bladder, kidney, brain, oral and melanoma) (Singh *et al.*, 2009). Stimulated by the hypoxic tumour environment TAMs upregulate their production of CXCL8 (interleukin-8), an endothelial cell mitogen and angiogenesis promoter. CXCL8 binds to CXCR2 chemokine receptor. Neutrophils can also mediate CXCL8-induced angiogenesis in cancer. Overexpression of CXCL8 correlates with tumour stage as well as disease progression and recurrence. Malignant colonic epithelial cells overexpress CXCL8, therefore CXCR2 maybe a valid target for anti-angiogenic therapy in colorectal cancer (Teicher, 2011). In process are numerous preclinical studies using CXCR2 targeted antagonist antibodies and dual CXCR1/CXCR2 small molecule inhibitors, it remains to be seen whether they will progress to clinical trials (Singh *et al.*, 2009) (Table 1.16).

Targeting Neoplastic Cells

The conventional anti- cancer treatments of chemotherapy and radiation can also have a direct and indirect effect on tumour vasculature. Normally the high compressive mechanical stresses found within tumours compress the vasculature. However, by killing the tumour cells with cytotoxic therapy this pressure is removed. This improves blood flow thereby increasing drug delivery, which can ultimately produce tumour regression. In addition the death of tumour cells, which are largely responsible for constant supply of pro-angiogenic and pro-tumorigenic factors, helps to restore the angiogenic balance (Carmeliet, 2005).

Cytotoxic agents when administered at low and frequent doses have been shown to suppress angiogenesis; due to the high proliferative rate of tumour endothelial cells. Termed Metronomic Therapy, the continuous low-dose of chemotherapy appears to enhance the anti-angiogenic and pro-apoptotic effects of some agents in both tumour cells and endothelial cells, for example cyclophosphamide (Hanahan *et al.*, 2000, Browder *et al.*, 2000, Klement *et al.*, 2000). The tumour endothelial cells are killed by much lower doses of chemotherapy than the tumour cells, therefore reducing the adverse effects to healthy tissue found with conventional dosage (Hanahan *et al* 2000).

The combining of metronomic therapy with selective anti-angiogenic inhibitors has also shown improved efficacy (Scharorsky *et al.*, 2009). Klement's study using a mouse model, combined metronomic doses of the chemotherapeutic vinblastine and the anti-angiogenic drug DC101 (anti-VEGF). Treatment only with either drug briefly slowed tumour growth followed by resurgence. Whereas combining the two drugs resulted in complete tumour regression, with no recurrence reported after 6 months. The anti-angiogenic agent TNP-470 in combination with cytotoxic cyclophosphamide eliminated most drug-resistant Lewis lung carcinomas. (Browder *et al.*, 2000). Numerous pre-clinical studies have been reported and clinical trials are underway. One of the first Phase I trials involved treating children suffering from recurrent and progressive cancers; the combined oral anti-angiogenic chemotherapy showed a prolonged and persistent disease-free status (Kieran *et al.*, 2005). Yet, obstacles have arisen due to the lack of specific markers to allow the correct selection of patients for treatment and their subsequent monitoring to determine whether the treatment is having an anti-angiogenic effect (Longo *et al.*, 2002).

Table 1.16: A list of the next generation of anti-angiogenic agents and their research status.

Target	Angiogenic Mechanism	Therapeutic Agent	Research Status	Company
Placental Growth Factor (PlGF)	Ligand for VEGFR1. Vascular remodelling factor leading to normalisation of tumour vasculature (Hedlund <i>et al.</i> , 2009, Cao <i>et al.</i> , 2009) Direct effect on some malignant cells, increasing proliferation and migration (Chen <i>et al.</i> , 2009).	TB-403, humanised monoclonal antibody to PlGF (Nielsen and Sengelov, 2012, Martinsson, 2011)	Phase I	Roche/Thrombogenesis and BioInvent International.
Angiopoietins 1 and 2 (ang1 and ang2)	Ligand for Tie-2 receptor Opposing roles of ang1 and ang2, thought to control vascular remodelling and maturation. (Teicher, 2011).	AMG-386 peptibody, prevents interaction of ang1 and ang 2 with Tie-2 receptor. (Herbst <i>et al.</i> , 2009, Mita <i>et al.</i> , 2010, Karlan, 2012)	Phase II, in combination with chemotherapy agent Paclitaxel. Ovarian cancer.	Amgen
CXCL12/ CXCR4	Binding of CXCL12 to receptor CXCR4 promotes mobilisation of haematopoietic stem cells. (Teicher, 2010)	Plerixafor, CXCR4 antagonist (DiPersio <i>et al.</i> , 2009)	Phase III. In combination with GCSF. Non-Hodgkins Lymphoma.	Genzyme
		Plerixafor, CXCR4 antagonist (Nervi <i>et al.</i> , 2009)	Preclinical studies. Acute myeloid leukemia.	
		Plerixafor, CXCR4 antagonist. (Uy <i>et al.</i> , 2011)	Phase I/II. Acute Myeloid Leukemia.	
		AMD3100, small molecule inhibitor of CXCL12/ CXCR4 interaction (Kioi <i>et al.</i> , 2010).	Preclinical studies. Glioblastoma.	
CXCR2	Interleukin-8 receptor, which	SCH-479833 and SCH-	Preclinical studies.	Schering-Plough

	is an endothelial cell mitogen stimulating angiogenesis. (Singh <i>et al.</i> , 2009).	527123, small molecule CXCR4 antagonists. (Singh <i>et al.</i> , 2009).	Melanoma	
Notch Pathway	Regulates cell fate specification, tissue patterning and morphogenesis by modulating cell differentiation, proliferation, apoptosis and survival (Kuhnert <i>et al.</i> , 2011).	RG-4733, gamma secretase inhibitor which inhibits Notch signalling. (Teicher, 2011).	Phase II	Roche/ Abbott
		REGN-421, human monoclonal antibody against Notch ligand Delta-like ligand-4 (Dll4) (Thompson <i>et al.</i> , 2011).	Phase I. Solid malignancies.	Sanofi-Aventis/ Regeneron
		OMP-21M18, human monoclonal antibody against Notch ligand Delta-like ligand-4 (Dll4) (Yan <i>et al.</i> , 2011).	Phase I. Advanced solid malignancies.	OncoMed Pharmaceuticals
Transforming Growth Factor Pathway	Activin receptor-like kinase-1 (ALK1), a Type I cell surface receptor, regulates vessel growth, stability and maintenance of a functional vasculature (Mitchell <i>et al.</i> , 2010).	ACE-041, soluble ALK1 receptor which binds to members of TGF β super family (BMP-9, BMP-10) and prevents signalling via ALK1. (Mitchell <i>et al.</i> , 2010).	Phase I. Advanced solid tumours.	Acceleron Pharma
		PF-03446962, human monoclonal antibody against ALK1. (Mitchell <i>et al.</i> , 2010).	Phase I. Advanced solid tumours.	Pfizer
Hypoxia inducible factor -1 alpha (HIF-1 α)	A key transcription regulator of numerous genes important for cellular adaptation of hypoxic conditions. Has a	EZN-2968, synthetic antisense oligodeoxynucleotide targeting HIF-1 α , hybridises with HIF-1 α mRNA and blocks protein	Phase I. Advanced solid tumours and lymphomas.	Enzon Pharma / Santaris Pharma

	critical role in angiogenesis, survival, metastasis, drug resistance and glucose metabolism (Patiar and Harris, 2006)	expression (Greenberger <i>et al.</i> , 2008).		
Sphingosine-1-phosphate (S-1-P)	Bioactive lipid molecule which stimulates endothelial cell migration, proliferation and survival (Xie <i>et al.</i> , 2009).	Sonepcizumab, human monoclonal antibody against S-1-P (Gordon <i>et al.</i> , 2010, Sabbadini, 2011).	Phase I Advanced solid malignancies	Merck/ Serono/ Lpath
Hepatocyte Growth Factor (HGF)/ c-Met tyrosine kinase signalling pathway	Induces VEGF expression as well as downregulating Thrombospondin 1 (TSP-1), thereby stimulating endothelial cell proliferation, migration (Lee and Kim, 2009).	MetMab, monovalent antagonist antibody to receptor Met (Belalcazar <i>et al.</i> , 2012).	Phase II. In combination with Tarceva. Lung cancer.	Genentech/Roche
		SCH900105, anti-HGF monoclonal antibody (Patnaik <i>et al.</i> , 2010).	Phase I. Single agent and in combination with Erlotinib. Advanced solid tumours.	Schering-Plough/ Aveo (Merck)
		TAK-701, anti-HGF monoclonal antibody (Jones <i>et al.</i> , 2010).	Phase I. Advanced malignancies	Takeda/ Galaxy
		NK4, a competitive HGF antagonist and cMet receptor (Kubota, 2009).	Preclinical studies: lung cancer.	KringlePharma

1.5vii Normalisation of Tumour Vasculature

Tumours are characterised by a self-perpetuating cycle of non-productive angiogenesis resulting in the formation of dysfunctional and abnormal blood vessels. The irregular vasculature enhances tumour tissue swelling, obstructs anti-tumour immune defence (by commandeering inflammatory cells) and makes chemoradiotherapy ineffective whilst simultaneously promoting tumour invasiveness and metastasis. The expectation of anti-angiogenic therapy was that by inhibiting tumour angiogenesis the existing tumour vasculature would regress and new blood vessel growth would be prevented, resulting in the tumour starving due to the inadequate supply of oxygen and nutrients.

Unfortunately, success has been limited to the treatment of glioblastomas and renal cell carcinomas with the majority of solid tumours only showing a transient benefit, often followed by (aggressive) disease progression. However, for many solid tumours (breast, lung and colorectal) anti-angiogenic treatment (targeting VEGF) has a far greater clinical benefit when administered in combination with conventional chemotherapy. Logic would suggest that the regression (pruning) of tumour vessels caused by anti-angiogenic therapy would actually impede vascular delivery of chemotoxic drugs. But, by restricting the unregulated flow of pro-angiogenic factors in the tumour, the vasculature is actually normalised improving perfusion and therefore drug delivery. The temporary benefit of anti-angiogenic treatment appears to be due in part to the normalisation of tumour vasculature thereby fostering a less hypoxic, malignancy promoting tumour environment. A consequence of prolonged anti-angiogenic treatment would therefore be an exacerbation of the aberrant tumour environment thereby fuelling tumour invasiveness and metastasis (Ebos *et al.*, 2009, Paez-Ribes *et al.*, 2009).

This discovery has led to the concept of a novel anti-cancer treatment, whereby anti-angiogenic agents are used to restore the angiogenic balance found in normal tissues, by inducing vessel normalisation. Tumour vessel normalisation strategies offer an opportunity to convert a malignant invasive, metastatic cancer into a more benign, encapsulated, metabolically less aggressive, poorly invasive tumour which will respond better to conventional anti-cancer chemoradiation therapy (DeBock *et al.*, 2011). Vessel normalisation may also have potential uses in the treatment of inflammatory and ischaemic diseases.

The most common target of anti-angiogenic therapy is VEGF. Neutralisation of VEGF by blocking either VEGF directly or its signalling pathways induces vessel normalisation, for example as reported in rectal cancer patients (Jain, 2005, Willett *et*

al., 2004). Immature vessels are pruned, while remaining vessels are stabilised (matured) by increasing their pericyte coverage. The process is mediated via induction of ANG-1 and PDGFR β signalling (Winkler *et al.*, 2004, Greenberg *et al.*, 2008). Consequently, tumour vessel permeability and interstitial pressure decreases whilst tumour perfusion and oxygenation improves; restoring the hydrostatic pressure gradient across the vessel wall. Administered drugs are reported to penetrate deeper into the tumour and in the majority of studies chemo-radiotherapy efficacy is enhanced (Franco *et al.*, 2006, Winkler *et al.*, 2004).

In order, to gain success in the use of anti-angiogenic agents to normalise tumour vasculature, lessons must be learnt from the outcomes of anti-angiogenic therapy. The flexibility of tumour cells to adapt and find alternative pathways must be recognised. But, as important is the discovery that by blocking one specific pro-angiogenic factor the upregulation of others occurs, thereby perpetuating the pro-malignancy agenda of the tumour.

It has been reported (in models, mice and patients) that a consequence of blocking VEGF is an upregulation of another member of VEGF family, placental growth factor. Therefore, a successful normalisation of tumour vasculature may require a treatment strategy which neutralises both factors. Anti-PlGF treatment has been shown to induce vessel normalisation in hepatocellular models and tumours (Van der Veire *et al.*, 2010, Alpini *et al.*, 2010).

Members of the angiopoietin family are also known to regulate vessel normalisation. The normalisation activity of anti-VEGF relies on upregulating Ang-1 expression. Ang-1 promotes pericyte coverage and establishment of tight endothelial intercellular junctions by binding its Tie2 receptor. However, Ang-2 whose expression is controlled by HIF-1 α , induces opposing effects; inhibiting Ang-1, reducing pericyte recruitment and vessel maturation. Plasma levels of Ang-2 correlate with poor patient prognosis, whilst loss of Ang-2 has been shown to reduce early stage tumour growth (Helfrich *et al.*, 2009). A consequence of anti-VEGF therapy is an upregulation of Ang-2.

Combined targeting of both factors with a double anti-angiogenic protein, DAAP, has been shown to improve anti-cancer efficacy (Koh *et al.*, 2010).

In addition, Notch, an endothelial cell receptor for Dll4 is emerging as a potential target to facilitate vessel quiescence. Notch/Dll4 signalling controls vessel branching by suppressing the formation of endothelial tip cells. Overexpression of Dll4 by tumour cells reduces vessel density, while enhancing lumen size and perfusion, overall improving oxygenation (Li *et al.*, 2007). Dll4 expression in patient tumour biopsies of

bladder cancer correlates with vessel maturation (Patel et al., 2006). When endothelial cells are stimulated with Dll4, a quiescent phenotype is induced and a down-regulation of VEGFR2 results in a reduced response to VEGF (Phng and Gerhardt, 2009).

1.5viii Future Perspectives

Judah Folkman, envisaged that angiogenic inhibitors would be the magic bullets that would eradicate cancer. Overall anti-angiogenic therapy has improved survival time but can certainly not be described as a cure.

During the development of new anti-angiogenic drugs it has become obvious that the models used in pre-clinical research need to be more relevant to human tumourigenesis. Mouse models are currently used and although they have been crucial in the development of many cancer-targeted drugs, they do not appear to be suitable for anti-angiogenic therapies. In relation to angiogenesis many disparities with the human disease exist. Firstly, habitually cancer in humans arises slowly, sometimes over a period of years, however in mice the disease is acute. Secondly, angiogenesis is induced in the mice models thereby making it more susceptible to anti-angiogenic therapy. In addition, human tumours grow in a highly vascularised tissue environment where tumour growth is not solely dependent on angiogenesis but also vessel co-option, thus increasing resistance to anti-angiogenic drugs (Claesson-Welsh, 2012). In addition, findings from mice are based on the primary tumour irrespective of any metastatic spread. Studies are curtailed due to ethical concerns for the animals. In humans however, it is secondary tumours which present with the worst clinical outcome. Future treatment with anti-angiogenic drugs requires a flexible approach; mirroring the dynamic plasticity of the tumours response to treatment. We now know that inhibition of a single target usually results in the upregulation of additional angiogenic factors for example PlGF is up regulated after anti-VEGF therapy and VEGF after anti-VEGFR2 or anti-EGFR. New treatment strategies need to combine treatment of agents which have complementary targets. By targeting various angiogenic molecules and/ or endothelial cells and/or other pro-angiogenic cell types (fibroblasts, macrophages, neutrophils) there is a reduced chance the tumour will develop resistance and evade treatment. Unfortunately, a side effect of combined therapy will probably be increased toxicity.

Combination therapy of anti-angiogenic and conventional chemotherapy has been more successful than exclusively focusing on angiogenesis inhibition. However, prolonged anti-angiogenic therapy reduces uptake of chemotherapeutics by the tumour cells. As discussed previously, angiogenesis inhibition appears to initially normalise the tumour vasculature improving circulation and therefore drug delivery.

Evidently, there appears to be a “window of treatment” for optimum tumour vasculature normalisation. Another, advantage of using anti-angiogenics for vasculature normalisation is that lower doses will be required, therefore milder side effects. The aim of the treatment is to return the balance of pro and anti- angiogenic factors; the use of anti-angiogenics to maintain a constant level of tumour- stimulated angiogenesis rather than the characterised hyperstimulation of tumour angiogenesis that subsequently leads to increased tumourigenesis.

In order, for success in this approach of anti-angiogenic therapy it will require the development of non-invasive markers of vessel maturation concurrently with improved imaging techniques. The ability to “stage” an individual’s tumours vasculature and microenvironment will lead to a more personalised approach to treatment. Such personalised medicine requires improved patient screening; at present screening is limited not only by a shortage of validated biomarkers but also expense. Advances in the characterisation of tumour vasculature will possibly lead to new treatment targets and markers of disease stage. In addition, clinical trials of these treatments need biomarkers to allow for the selection of responders within the patient cohorts (Claesson-Welsh, 2012).

1.6 PROJECT AIMS

Chapter 3: ASSESSMENT OF THE BIOACTIVITY OF CONDITIONED MEDIUM

Aims	Principal Assays
1. Primary screen of total CM collected from various cell lines for the presence of motogenic activity.	<ul style="list-style-type: none"> • 3D collagen gel fibroblast migration assay
2. Primary screen of total CM collected from various cell lines for the presence of MSF-inhibitory bioactivity.	<ul style="list-style-type: none"> • 3D collagen gel fibroblast migration assay

Chapter 4: THE IDENTIFICATION OF MSF-I PRODUCED BY KERATINOCYTES.

Aims	Principal Assays
1. To isolate the factor responsible for MSF-inhibitory activity detected in HaCaT CM.	<ul style="list-style-type: none"> • Size exclusion chromatography (Superdex) of HaCaT total CM. * • Ion exchange chromatography (ANX) of SEC fractions MW 16-27kDa.* • SDS Electrophoresis of ANX unbound fraction. *
2. To identify the factor responsible for MSF-inhibitory activity detected in HaCaT CM.	<ul style="list-style-type: none"> • Sequence analysis (tryptic digest, mass spectrometry) of SDS electrophoresis elution of MW 20-25kDa. • Immunolocalisation of NGAL (Anti-NGAL antibody, AF1757). • Immunoblot for NGAL (Anti-NGAL antibody, MAB1757). • Colorimetric Indirect ELISA for NGAL (Anti-NGAL antibody, AF1757)
3. To verify the ability of NGAL to inhibit the motogenic bioactivity of MSF.	<p>NGAL from three sources tested for MSF-I activity:</p> <ul style="list-style-type: none"> • NGAL isolated from NGAL/MMP-9 Complex (Calbiochem), 20-25kDa Gel elution 3. * • Eukaryotic NGAL (R&D Systems). * • Prokaryotic NGAL (In-house Prep). *
4. To characterise the nature the MSF-inhibitory activity of NGAL.	<ul style="list-style-type: none"> • NGAL from three sources tested for MSF-I activity.*

	<ul style="list-style-type: none"> • Effect of iron chelator, DFOM, on NGAL ability to inhibit rhMSF. * • NGAL pre-incubation 3D Type I collagen gel fibroblast migration experiments.
5. To verify MSF as the factor responsible for the motogenic bioactivity detected in fractionated HaCaT CM.	<ul style="list-style-type: none"> • Immunoblot for MSF (Anti-MSF antibody, RpVSI). • Immunolocalisation of MSF (Anti-MSF antibody, Rp2/98pFA2pFn1). • IGD Function Neutralisation of Motogenic Activity (Pep Q 1.1 antibody). * • Immunoprecipitation for MSF (Protein G coupled to RpVSI antibody).* • NGAL inhibition of motogenic activity. *

*bioactivity confirmed by testing in the 3D collagen gel fibroblast migration assay.

Chapter 5: THE EXPRESSION OF MSF AND NGAL IN RELATION TO TUMOUR PROGRESSION.

Aims	Principal Assays
1. To establish whether MSF was expressed by the other cell lines of the HaCaT series (BEN, MAL and MET), which displayed an increasing tumorigenic potential.	<ul style="list-style-type: none"> • Immunoblot for MSF (Anti-MSF antibody, RpVSI). • Immunolocalisation of MSF (Anti-MSF antibody, Rp2/98pFA2pFn1).
2. To establish whether NGAL was expressed by the other cell lines of the HaCaT series (BEN, MAL and MET), which displayed an increasing tumorigenic potential.	<ul style="list-style-type: none"> • Immunoblot for NGAL (Anti-NGAL antibody, MAB1757). • Immunolocalisation of NGAL (Anti-NGAL antibody, AF1757). • Colorimetric Indirect ELISA for NGAL (Anti-NGAL antibody, AF1757).
3. To determine whether NGAL and MSF expression levels could be related to tumorigenic potential.	<ul style="list-style-type: none"> • Assays as above.

Chapter 6: THE EXPRESSION OF PRO- AND ANTI- MOTOGENIC BIOACTIVITY BY THE HACAT-RAS CLONES.

Aims	Principal Assay
1. To ascertain bioactivity of total CM of the HaCaT series cell lines.	<ul style="list-style-type: none"> ● 3D collagen gel fibroblast migration assay
2. To ascertain whether the fractionated CM of the HaCaT series cell lines exhibited motogenic activity.	<ul style="list-style-type: none"> ● Size exclusion chromatography (Superdex) of HaCaT series total CM.* ● SDS Electrophoresis of HaCaT series total CM.*
3. To ascertain whether MSF was responsible for the motogenic activity of HaCaT series CM.	<ul style="list-style-type: none"> ● Immunoprecipitation for MSF (Protein G coupled to RpVSI antibody).* ● IGD Function Neutralisation of Motogenic Activity (Pep Q 1.1 antibody). * ● NGAL inhibition of motogenic activity.*
4. To ascertain whether the fractionated CM of the HaCaT series cell lines exhibited MSF-inhibitory activity.	<ul style="list-style-type: none"> ● Size exclusion chromatography (Superdex) of HaCaT series total CM.* ● SDS Electrophoresis of HaCaT series total CM.*
5. To ascertain whether NGAL was responsible for the MSF-I inhibitory activity of HaCaT series CM.	<ul style="list-style-type: none"> ● Colorimetric Indirect ELISA for NGAL (Anti-NGAL antibody, AF1757). ● Immunoblot for NGAL (Anti NGAL antibody, MAB1757).

Chapter 7: THE IDENTIFICATION OF MSF-I PRODUCED BY ENDOTHELIAL CELLS

Aims	Principal Assay
1. To determine whether endothelial cells express NGAL.	<ul style="list-style-type: none"> ● Immunoblot for NGAL (Anti-NGAL antibody, MAB1757). ● Immunolocalisation of NGAL (Anti-NGAL antibody, AF1757).
2. To determine whether endothelial cells express MSF.	<ul style="list-style-type: none"> ● Immunolocalisation of MSF (Anti-MSF antibody, Rp2/98pFA2pFn1).
3. To characterise the bioactivity of endothelial cells expressing a sprouting phenotype.	<ul style="list-style-type: none"> ● Size exclusion chromatography (Superdex).* ● SDS Electrophoresis.*
4. To characterise the bioactivity of endothelial cells expressing a cobblestone phenotype.	<ul style="list-style-type: none"> ● Size exclusion chromatography (Superdex).* ● SDS Electrophoresis.*
5. To determine whether MSF was responsible for the motogenic activity detected in fractionated endothelial CM.	<ul style="list-style-type: none"> ● IGD Function Neutralisation of Motogenic Activity (Pep Q 1.1 antibody). * ● NGAL inhibition of motogenic activity.*
6. To determine what effect MSF had on endothelial morphology.	<ul style="list-style-type: none"> ● 2D Post-confluent endothelial sprouting assay.
7. To determine the effect IGD Function Neutralisation, PEPQ 1.1 antibody had on endothelial morphology.	<ul style="list-style-type: none"> ● 3D Spontaneous endothelial sprouting assay.
8. To determine the effect MSF inhibitor, NGAL had on endothelial morphology.	<ul style="list-style-type: none"> ● 2D Post-confluent endothelial sprouting assay. ● 3D Spontaneous endothelial sprouting assay. ● Endothelial proliferation and viability assay.

*bioactivity confirmed by testing in the 3D collagen gel fibroblast migration assay.

Chapter 2:**METHODS AND MATERIALS****2.1 CELL CULTURE****2.1.i Cell lines and Culture Conditions.**

Unless stated otherwise, all cell lines were grown at 37°C in a humidified atmosphere containing 5% CO₂, 95% air. Stock cultures were maintained in the following, in-house prepared, growth medium - Eagle's minimal essential medium (MEM), supplemented with 15% (v/v) heat-inactivated donor calf serum (DCS), 1mM sodium pyruvate, 2mM glutamine, non-essential amino acids (81.4mg/ml), 100units/ml penicillin and streptomycin. This medium will be referred to as 15% DCS MEM, or in the absence of serum SF-MEM. Medium on stock cultures was routinely changed every 2-3 days.

All tissue culture plastic dishes (90, 60 and 35mm) and multi-well plates were purchased from the Nunc range.

See Table 2.1 for specific cell culture requirements for the cell lines used.

2.1.ii Cell Culture Maintenance Protocols.**Subculture of Adherent Cell Lines.**

Upon reaching appropriate confluence the cultures were washed twice with Hanks' balanced Salt solution to remove serum proteins. Cells were then brought into suspension by using the protease 0.05% (v/v) trypsin in EGTA (ethylene glycol tetraacetic acid) for 5 minutes at 37°C. Once the cells had rounded up and begun to detach, an equal volume of growth medium containing 15% (v/v) DCS was added, to neutralise the trypsin. The dish was washed over numerous times to ensure all cells had been retrieved. After collecting the cells by centrifugation, for 5 minutes at 900rpm, they were re-suspended in growth medium and plated onto an appropriate number of tissue culture dishes.

Cryopreservation of Cell Lines.

In order to preserve the cell lines and maintain a good viable stock, cultures were frozen at various passages. Following, the trypsinisation and centrifugation step of the subculturing protocol, a cell pellet was obtained, which was re-suspended in 22% (v/v) DCS and 5% (v/v) DMSO in MEM and stored in cryovials at -80°C.

Resuscitation of Frozen Cell Lines.

Upon removal from -80°C freezer, cryovials were placed in a 37°C waterbath (half-submerged). When only a small amount of ice remained, the cells were added drop-wise into pre-warmed 15% DCS (v/v) MEM. After a 2 hour incubation at 37°C, 5% CO₂ cell attachment was assessed microscopically. When the majority of cells had attached, growth medium was changed. Cultures were thawed quickly and diluted in medium to minimise the toxic effects of the cryoprotectant, DMSO, which can induce differentiation in some cell lines.

2.1.iii Conditioned Medium Collection and Storage Conditions

To obtain conditioned medium (CM), confluent cultures in 90mm dishes were rinsed with 5ml of Hanks' balanced salt solution, followed by 2x rinses with SF-MEM and incubated for 1 hour at 37°C. This medium was discarded and dishes rinsed again with SF-MEM. Cells were then incubated in fresh SF-MEM, 5-7ml per 90mm dish, for 24-48 hours. Upon collection, the CM was spun for 5 minutes at 900g, to remove any cell debris, and the supernatant stored at -20°C. CM was collected in batches of a minimum of 50-100ml. These were concentrated by Amicon filtration (2-10 fold), using a 3,000 kDa cut-off filter. Later, batches of conditioned medium were pre-dialysed before Amicon concentration to remove any salts that may also be concentrated. Dialysis was performed overnight against distilled water, which was changed twice. Concentrated samples were aliquoted and frozen at -20°C.

Table 2.1. The optimum culture conditions for cell lines.

Name	Cell Type	Source	Culture Media	Subculture Ratio	Culture Surface	Experimental Passage
FFD4	Human fetal fibroblast.	Explant culture, Ninewells Hospital, University of Dundee (Schor <i>et al.</i> , 1985, 1988)	15% DCS MEM	1 to 4	Plastic	12-18
F110 a	Human fetal fibroblast.	Explant culture, Dr. I. Ellis, University of Manchester (Schor <i>et al.</i> , 1985, 1988)	15% DCS MEM	1 to 4	Plastic	12-17
FSF44	Human foreskin fibroblast. Obtained from one year old healthy donor.	Explant culture, Dr I. Ellis, University of Manchester (Schor <i>et al.</i> , 1985, 1988)	15% DCS MEM	1 to 4/5	Plastic	15-22
DFSF1	Human adult foreskin fibroblast.	Explant culture, University of Dundee (Schor <i>et al.</i> , 1985, 1988).	15% DCS MEM	1 to 4	Plastic	12-17
ENDO 742	Transformed human microvascular endothelial cells, derived from normal breast tissue.	Gifted by Dr Micheal O'Hare, 2001 (O'Hare <i>et al.</i> , 2001)	15% DCS MEM, 50µg/ml Ascorbic acid	1 to 4	0.1% (w/v) gelatin coated plastic	---
HUVEC 1666	Human umbilical vein endothelial cells	Cell Applications Inc. Cat No : 200-05n Lot No: 1666	15% DCS MEM, 50µg/ml Ascorbic acid	1 to 3	0.1% (w/v) gelatin coated plastic	5-10
HOEC	Human omentum microvascular endothelial cells		15% DCS MEM, 50µg/ml Ascorbic acid	1 to 3	0.1% (w/v) gelatin coated plastic	18-22
HAEC	Human aortic endothelial cells	Life Technologies Ltd. Cat No: C-006-SC	15% DCS MEM, 50µg/ml Ascorbic acid	1 to 3	0.1% (w/v) gelatin coated plastic	12-16
HUVEC	Human umbilical vein endothelial cells	Dr Shane Foo, CRT. Originally purchased from Promo Cell: HUVEC-c, cryopreserved, cat no:C-12200	15% DCS MEM, 50µg/ml Ascorbic acid	1 to 3	0.1% (w/v) gelatin coated plastic	18-24
BAEC Clones 2 & 3	Bovine aortic endothelial cells.	In house preparation. Schor <i>et al.</i> , 1983	15% DCS MEM, 50µg/ml Ascorbic acid	1 to 3	0.1% (w/v) gelatin coated plastic	15-22

BAEC 2-2 U7	Bovine aortic endothelial cells.	In house preparation (Schor <i>et al.</i> , 1983). Bovine aorta No 2 cultures started June 2003.	15% DCS MEM, 50µg/ml Ascorbic acid	1 to 3	0.1% (w/v) gelatin coated plastic	15-25
HACAT	Spontaneously immortalised human trunk skin keratinocytes.	Gifted by Dr. Norbett Fusenig (Boukmap <i>et al.</i> , 1988).	15% DCS MEM	1 to 5	Plastic	45-55
BEN	HACAT derived, forms benign tumours <i>in vivo</i> .	Gifted by Dr. Norbett Fusenig (Boukamp <i>et al.</i> , 1990, 1997. Mueller <i>et al.</i> , 2001).	15% DCS MEM	1 to 5	Plastic	9-20
MAL	HACAT derived, forms malignant tumours <i>in vivo</i> .	Gifted by Dr. Norbett Fusenig (Boukamp <i>et al.</i> , 1990, 1997. Mueller <i>et al.</i> , 2001).	15% DCS MEM	1 to 5	Plastic	13-20
MET	HACAT derived, forms metastatic tumours <i>in vivo</i> .	Gifted by Dr. Norbett Fusenig (Boukamp <i>et al.</i> , 1990, 1997. Mueller <i>et al.</i> , 2001).	15% DCS MEM	1 to 5	Plastic	10-21
HEK, 102-05a	Normal human adult skin keratinocytes.	ECACC No: 06091505, Sigma –Aldrich (Fuchs 1990)	Keratinocyte growth medium kit (ECACC No: 06091505)	1 to 3	Plastic	3-5
Mv.1.Lu	Foetal Aleutian Mink lung epithelial.	ECaCC No: 88050503, LGC Promochem (Motegi 2008)	15% DCS MEM	1 to 4/5	Plastic	15-25

2.2 3D TYPE I COLLAGEN GEL MIGRATION BIOASSAY

2.2.i Extraction of Type I Collagen

Type I collagen was prepared from the tendons of rat tails. Tails from freshly killed rats were obtained from the animal house, Ninewells Hospital and stored, protected at -20°C until required.

Per each batch of collagen, ten tails were thawed and “sterilised” by placing in 70% (v/v) ethanol for approximately 30 minutes. In a laminar flow cabinet, the tendons were removed by using forceps to snap the tail in half and the tendon was then pulled out from the inside. The tendons were dissolved in 500ml 3% (v/v) acetic acid and mixed overnight at 4°C, to extract the collagen. The extract was then centrifuged at 3000rpm, at 4°C for 150 minutes. The extracted collagen was then redissolved in sterile 20% (w/v) NaCl, and spun overnight at 4°C, followed by a repeat centrifugation.

The following day, the extracted collagen was then decanted off and placed into pre-sterilised cellulose membrane dialysis tubing (Sigma-Aldrich) and dialysed against distilled water for 24 hours (the water was changed 5 times). The dialysate was then re-centrifuged as before and diluted to 2mg/ml. (Schor, 1980).

2.2.ii 3D Collagen Gel Migration Bioassay

The type I collagen, 2mg/ml, extracted from rat tail tendons was used to make 2ml collagen gels. In order for the collagen gel to set properly, gels were made in 10ml batches of 5 x 2ml per 35mm plastic tissue culture dishes (8.5ml Type I collagen, 0.5ml Sodium Bicarbonate, 1ml 10x Eagle Minimum Essential Medium), as described by Schor 1980.

Once the 2ml collagen gels, in the 35mm dishes, had set they were overlaid with 1ml of either serum-free MEM (SF-MEM) containing no further additives (baseline control) or the material to be tested (e.g. rhMSF, conditioned medium) at 4x the final concentration required. All controls and unknowns were tested on duplicate gels. Confluent stock cultures of fibroblasts (FSF44) were trypsinised, pelleted by centrifugation, resuspended in growth medium containing 4% (v/v) donor calf serum at $2-3 \times 10^5$ cells/ml and 1ml aliquots were added to the overlaid gels. Considering the 2ml volume of gel, 1ml

medium overlay (with or without test materials) and 1ml cell inoculum, this procedure gives a final concentration of 1% (v/v) serum (1% DCS-MEM) in both control and test cultures.

The assay cultures were incubated for 4 days at 37°C, 5% CO₂. The percentage of fibroblasts found within the 3D gel matrix was determined by counting the number of cells on the collagen surface and within the collagen matrix in 10 randomly selected fields, using a Leitz Labovert microscope. (Schor 1994, 1999).

2.2.iii Assessment of the 3D Collagen Gel Migration Bioassay

After 4 day incubation, the media was carefully removed from the cell culture on collagen gels so as not to disturb the gel. 1ml of neutral buffered formalin was added to fix the cells. The gels were then stored at 4°C, until they were counted.

Each gel was examined using phase contrast optics with a Lietz Labovert microscope fitted with s SY2 photographic graticule defining an area of 0.9 x 0.65cm, using the 20x objective. The numbers of cells on and below the gel surface, within the area defined by the area of the graticule were counted at 10 randomly selected areas. A cell was defined as having migrated into the gel when the cells on the surface could no longer be seen. These data were then used to calculate the mean and standard deviation of the total cell number per field and the percentage of cells within the collagen gel.

2.3 CELL PROLIFERATION AND VIABILITY BIOASSAYS

2.3.i Growth Curve: An Assessment of Cell Proliferation and Viability

Numerous variations of a standard growth curve were carried out in order to:

1. Evaluate the morphology and growth characteristics of a cell line i.e. lag time, population doubling time and saturation density.
2. To assess the effect of test substances, at various concentrations, (e.g. recombinant proteins, conditioned media, serum) on a cell lines' morphology, viability and proliferation when compared to a control.
3. To assess the effect of plating density on cell morphology, viability and proliferation.

Variations to the standard protocol were also determined by the cell line used because:

1. Cell lines vary in the time taken to attach to the surface of a dish, for example Mink Lung Cells (Mv.1.Lu) attach within 2 hours, while the tumour cell lines can take over 6 hours. This will therefore determine when the first baseline/ attachment count is taken.
2. Cell lines have different growth rates. This will therefore determine the time course and seeding/ plating density of the experiment.
3. Some cell lines' viability and morphology can also be affected by the seeding density, for example the BAEC endothelial cell line.

The standard method, adapted from J.P. Mather and P.E. Roberts, 1998.

Following the subculturing protocol, a cell suspension was obtained from stock cultures. A cell count of this suspension was obtained by using a Coulter Counter Z1 Series (Beckman Coulter). This count was then used to determine the appropriate dilution of the cell suspension in order to have the correct amount of medium and cells to achieve the desired seeding density. The diluted cell suspension was then plated out onto the appropriate number of dishes and incubated at 37°C, 5% CO₂ until the cells had attached. After which, the first baseline count was taken (x2 dishes). The media on the remaining dishes was then replaced with either control media or that containing the test substance(s). Morphology, cell viability and numbers (duplicates counted) were then assessed every 24/48 hour incubation, for the duration of the experiment. Cell morphology was assessed microscopically. Cell viability was determined by Trypan blue exclusion. Cell numbers were counted using the Coulter Counter. Media on the dishes was replaced every 2-3 days for the duration of the experiment.

2.3.ii Trypan Blue Exclusion- Assessment of Cell Viability

Trypan blue is a vital stain that is used to estimate the proportion of viable cells in a population. The reactivity is based on the fact that the chromophore is negatively charged and does not react with a cell unless the membrane is damaged. Live (viable) cells do not take up the dye and dead (non-viable) cells do.

A cell suspension was prepared using the previously described subculturing protocol. 0.5ml of Hanks' balanced Salt solution was added to cell suspension, followed by 0.5ml 0.4% (v/v) trypan blue solution (Sigma-Aldrich). The cell suspension was gently agitated with a fine tip pasttete and then left for 5 minutes (no longer than 15 minutes is recommended). After which, 200µl of the suspension was removed and placed on a clean slide or dish. Ten randomly selected fields were selected and examined using

phase contrast optics with a Lietz Labovert microscope fitted with sSY2 photographic graticule defining an area of 0.9 x 0.65cm, using the 20x objective. Per field, the total number of cells were counted in addition to the number of viable and non-viable cells. The percentage of viable cells was calculated as follows, cell viability, % = (total viable cells/ total number of cells) x 100 (Louis and Siegel, 2011).

2.3.iii MTT Assay- Assessment of Cell Viability

MTT assays were carried out to determine the effect that various factors have on cellular growth. The standard assay protocol used was adapted from Mossaman 1983 and Wilson 2000.

Cells used for the assay were passaged either 1 to 2 or 1 to 3, dependent on cell line, the day before the MTT assay was set up. On the subsequent day, cells were plated at the appropriate density on a 96 well plate in FCS-MEM (FCS concentration varied with experiment but was usually 10% (v/v) FCS) and were incubated at 37°C, 5% CO₂ until cells attached (for Mv.1.Lu 2 hour attachment time). One plate was set up for each time point.

Plate t = 0 was assessed for the first baseline count. Media was removed; cells were washed twice with SF-MEM and then incubated for 3 hours with a final concentration of 1mg/ml filtered sterilised MTT in a total volume 100µl (at 37°C, 5% CO₂). During the incubation period the yellow MTT (3-(4, 5-Dimethylthiazol-2-yl)-2, 5-diphenyltetrazolium bromide) is reduced to purple formazan in the mitochondria of any living cells attached to the plate. The MTT was then removed and 100µl of DMSO (dimethyl sulfoxide) was added to dissolve the formazan, creating a coloured solution (20 minutes on a shaker). The resulting coloured solution was assessed by reading the plate spectrophotometrically on the Flurostar Optima plate reader (BMG LABTECH) at 550nm, reference filter 620nm.

The remaining plates were changed to test conditions and incubated until required and then developed as stated for t =0.

2.4 ENDOTHELIAL SPROUTING ASSAYS

2.4.i 2D Post-Confluent Sprouting Assay

Numerous variations of this assay were performed however the foundation of the assay was to plate endothelial cells on a 2D surface followed by growth in a high serum concentration, 15-20% DCS MEM, until confluence was attained.

Confluent stock cultures of endothelial cells were trypsinised, pelleted by centrifugation and resuspended in 15% DCS MEM. The cells were then plated onto a variety of 2D surfaces on 35mm dishes; these included a coating of 0.1% (w/v) gelatin, native collagen, the upper surface of a type I collagen gel and the surface of the plastic dish. The cells were then cultured until confluence at 37°C, 5% CO₂; the medium changed every 2-3 days, as required.

Once the endothelial cultures reached confluence and formed a uniform cobblestone monolayer the overlying medium was changed to test conditions. The cells were overlaid with 2ml of medium containing a low serum concentration (0-5% DCS) with or without the material to be tested. All controls and unknowns were tested in triplicate cultures. Over the course of the experiment the overlays were changed every 2-3 days. Post-confluence observational data was obtained microscopically over the time-course of the experiment. A variety of observations were made, focusing specifically on the emergence of endothelial cells exhibiting the sprouting phenotype. Typically these observations would include type of endothelial morphology exhibited, number of fields of view containing sprouting cells, 40 point counts (number of points were sprouting cells present), number of sprouts present as either single cells or integrated with other sprouts to form sprout associations. Irrespective of the method used, data was collected from ten fields of view per dish.

The time course of the experiment would be determined by comparing observations of the test material to the control cultures and ultimately by the condition (health) of the endothelial cultures.

2.4.ii 3D Spontaneous Sprouting Assays

This assay was based on the ability of endothelial cells to spontaneously exhibit a homologous sprouting phenotype when plated within a type I collagen gel.

Confluent stock cultures of endothelial cells were trypsinised, followed by collection in 2-5mls 15% DCS MEM. A cell count of this suspension was obtained by using a Coulter Counter Z1 Series (Beckman Coulter). The plating density of the endothelial cells was 6.5×10^5 per ml of type I collagen gel. To ensure the gels to set properly they were made in batches of 10ml gels which therefore required a total of 6.5×10^6 cells. The correct volume of the cell suspension was removed and pelleted by centrifugation. Meanwhile the components of the type I collagen gel were combined together; 8.5ml Type I collagen, 0.5ml Sodium Bicarbonate, 1ml 10x Eagle Minimum Essential Medium, as described by Schor 1980. The cell pellet was resuspended in this mixture and aliquoted at the appropriate volumes; 2ml per 35mm plastic tissue culture dish, 0.5ml per well of a 24 well tissue culture plate. The gels were left to set for at least 30 minutes, followed by over-laying with 20% DCS MEM; 2ml per 35mm dish, 0.5ml per well of 24 well plate.

After a 2-3day incubation period at 37°C, 5% CO₂ observations of the status of the cells were made microscopically. Only healthy cultures displaying a typical sprout morphology, with single sprouts and small associations (groups of 2- 5 sprouts), were selected for testing. Without disturbing the collagen gel the overlying medium was removed and changed to the test conditions. Typically, the test factors were diluted with a low serum concentration of MEM, to give a final serum concentration of 1-5% DCS. Each control and test overlay were performed in triplicate.

Observations were made over the time-course of the experiment, typically after each 24-48 hour incubation period. The analysis of the effect the test material had on the endothelial sprouts consisted of performing a 40point count in ten fields per gel, with the total number of sprouts counted calculated for each variable. The time course of the experiment was determined by the effect(s) seen, as compared to the control cultures, and the health and quality of the endothelial cells.

2.5 ANTIBODIES

2.5.i. Antibodies Raised Against Peptides in the MSF Primary Sequence, Produced In House

Table 2.2: In house prepared MSF specific antibodies; information regarding type, function and purification technique.

Antibody	Antigen	Type	Purification technique	Function	Methods employed
RP2 RpVSI	MSF-unique carboxyl-terminal decapeptide VSIPPRNLGY	Rabbit polyclonal	POROS A, affinity chromatography	Identification of total MSF	IHC, ELISA, IP
Pep Q 1.1 Pep Q 3.2 Pep Q 5.1 Pep Q 5.2	21-mer peptide containing the IGDQ sequence in module 1-7 TNEGVMYRIG DQWDKQHDM GH	Mouse monoclonal	Protein G chromatography	IGD function neutralising antibody,	Bioassays, ELISA, capture antibody

2.5.ii. Purification of Mouse Monoclonal IgG Antibodies from Hybridoma Conditioned Medium, using Protein G Chromatography.

Typically, a volume of 300-500ml of hybridoma conditioned media was collected under serum free conditions (Hybridoma SF media, Gibco Invitrogen), which was spun at 900rpm for 5 minutes to remove any cellular matter. Followed by, dialysis with 20mM Sodium Phosphate pH 7.0 at 4°C (buffer changed after first hour and then dialysis continued overnight) Centrifugation was repeated to remove any particulates before chromatography, 10,000-20,000g for 10 minutes.

The sample was applied slowly, 1-2ml/minute, to a pre-equilibrated HiTrap Protein G Sepharose (GE Biosystems) 0.2µm filtered 20mM Sodium Phosphate pH7.0. The column was then washed to remove any unbound material. Elution buffer, 0.1M Glycine pH 2.7, that had been filtered (0.2µm) was then applied to the column; the low pH resulting in the antibody being eluted. However, this low pH is not suitable for antibody storage so the pH was raised by the addition of 1M Tris-HCl pH8.0 (50µl/ml) to each of the antibody containing fractions. Purified antibody was immediately transferred to non-stick eppendorfs, for storage at -20°C. Before storage, the column

was washed with 5 column volumes of 0.2µm filtered 20% (v/v) ethanol to prevent microbial growth.

Using a spectrophotometer, the antibody concentration was estimated by absorbance at 280nm using the following calculation: Antibody concentration= (OD 280nm x10 x dilution factor) / 14. The blank (reference) was 1ml of elution buffer and 50µl 1M Tris-HCl pH8.0.

When the antibodies were required for bioassays post-purification dialysis was performed; the antibody was dialysed 4hours (dialysis buffer changed after first 2 hours) at room temperature with MEM without phenol red.

2.6 RECOMBINANT PROTEINS

2.6.i Recombinant Proteins produced In House.

Table 2.3. Details of in- house prepared recombinant proteins.

Recombinant protein	Source of cDNA	Expression host and vector	Purification method	Storage
MSF aa+ isoform		BL21 pLysS (host) bacteria (Promega) using the pRSET vector (Invitrogen Ltd., Paisley, UK)	Affinity purification utilising the His ₆ tags on nickel charged 1ml Hi-Trap HP chelating columns	Dialysed against PBS. -20°C.
NGAL, lipocalin	the full length gene for NGAL was amplified from cDNA image clone ID 5421124 (Geneservice Ltd., Cambridge, UK),	BL21 pLysS bacteria using the pRSET vector (Invitrogen Ltd., Paisley, UK)	Affinity purification utilising the His ₆ tags on nickel charged 1ml Hi-Trap HP chelating columns	Dialysed against Binding buffer. -20°C

2.6.ii Recombinant Protein Production

Preparation and Selection of Bacterial Colonies

Escherichia coli strain BL21 (DE3) was used for the expression of the recombinant proteins. Stocks of the bacterial hosts harbouring the recombinant proteins were stored at -80°C. DE3 pLysS transformed with the relevant plasmid were grown overnight in

liquid culture at 37°C under carbenicillin selection (50µg/ml) in 10ml of LB broth, shaking at 275rpm in an orbital incubator.

These cultures were then streaked onto carbenicillin, LB-agar plates, which were then incubated overnight at 37°C. The following day the plates were inspected and an isolated single colony was selected using a pipette tip and placed in a 10ml aliquot of LB media containing 1% (w/v) glucose and 50µg/ml carbenicillin. Followed by, incubation overnight at 37°C with constant shaking at 275rpm.

Protein Production By *E.Coli*.

Successful 10ml cultures were added to 500ml of LB broth, 1% (w/v) glucose and grown at 37°C under carbenicillin selection (50µg/ml) in conical flasks. When the culture reached an OD_{600nm} of between 0.4-0.6, the optimum for protein production, isopropyl-β-D-thiogalactopyranoside (IPTG) was added to give a final concentration of 1mM. IPTG induces gene expression. The culture was left mixing for 2 hours at 37°C, after which the media was split into 50ml aliquots and spun for 10 minutes, at 3000rpm. The supernatant was then carefully removed and discarded. The pellets were stored at -20°C until required.

Extraction of Bacterial Recombinant Insoluble Protein

For each bacterial pellet, collected from 50ml culture, 2.5ml of Bug Buster (Invitrogen) and 1µl/ml benzonase was added and thoroughly resuspended by vortexing, followed by vigorous shaking for 20 minutes at room temperature. The Bug Buster gently disrupts the cell wall of the *E.coli* and liberates the soluble proteins without denaturing them, whilst the benzonase, an endonuclease, is added to reduce the viscosity of the extract caused by the liberation of chromosomal DNA.

The lysate was then split between four centrifuge tubes and spun at 20,000rpm for 15 minutes. The supernatant, which will contain the soluble proteins, was decanted and stored at -20°C. Each of the four pellets, containing the insoluble proteins was resuspended in 5ml of Bug Buster containing 10mg/ml lysozyme; to enhance extraction efficiency. 20 minutes of vigorous shaking at room temperature, followed. 30ml of 1:10 diluted Bug Buster was added to each tube and then spun at 20,000rpm for 20 minutes. The supernatant was discarded and the pellet resuspended again in the diluted Bug Buster followed by centrifugation.

Discarding the supernatant, 2.5ml of 500mM CAPS pH11.0, 0.5% (w/v) n-laurylsarcosine and 10mM DTT was added to each pellet and left to dissolve for a maximum of one hour, at room temperature. The solubilised protein solution was then spun, 20,000rpm for 10 minutes, and then dialysed at 4°C as follows; initially for 4 hours and then overnight in 20mM Tris-HCl pH 8.5, 0.1mM DTT, followed by 4 hours in 20mM Tris-HCl pH 8.5.

Purification of Solubilised Recombinant Protein

The solubilised recombinant proteins were purified by virtue of their His₆ tags on nickel charged 1ml Hi-Trap HP chelating columns (GE Healthcare, Amersham, Buckinghamshire, UK).

The HiTrap Chelating Hp column was charged with nickel ions by washing the column with 0.1M nickel chloride. The solubilised protein sample is spun, 20,000rpm for 10 minutes, to remove any particulate before being loaded onto the column followed by the binding buffer; 50mM sodium phosphate, 300mM NaCl, 10mM imidazole. The histidine –tagged proteins which bind to the column were eluted by the increased concentration of imidazole in the elution buffer; 50mM sodium phosphate, 300mM NaCl, 500mM imidazole. The collected fractions were stored at 4°C.

Recombinant Protein Identification and Protein Estimation.

Identification of the positive fractions, containing the recombinant protein, was by SDS- PAGE Electrophoresis. Each fraction was loaded onto a 12% resolving, 4.5% stacking acrylamide gel, under reducing conditions alongside known molecular weight markers (Biorad Broad Range). Protein bands were visualised by Coomassie blue staining. Fractions containing the recombinant protein were pooled together and then dialysed at room temperature for 4 hours against either PBS for recombinant MSF isoforms or the Hi- Trap Binding buffer for recombinant lipocalin. Protein concentration was estimated, after dialysis, by comparing the sample against known standards, BSA or GBD, on a 12% resolving, 4.5% stacking acrylamide gel, under reducing conditions. All recombinant proteins were stored at -20°C in non-stick eppendorfs.

2.7 PROCEDURES TO FRACTIONATE CONDITIONED MEDIUM

2.7.i Ammonium Sulphate Precipitation

Proteins were precipitated from conditioned medium (CM) by the stepwise addition of solid ammonium sulphate. To obtain the first fraction (0-10% saturation), solid ammonium sulphate (0.056g/ml) was slowly added to neat CM; the sample was then vigorously agitated on Vortex mixer and left to form a precipitate at 4°C for a minimum of 2 hours. After centrifugation at 1000g for 5 minutes, the supernatant was aspirated and kept for the next step. The pellet was resuspended in 20mM Tris.HCl pH 7.4 containing 0.1M NaCl. The following fractions were then obtained by adding the indicated amount of solid ammonium sulphate to the supernatant and repeating the above procedure in a stepwise fashion: 10-20% saturation (0.057g/ml); 20-30% saturation (0.059g/ml); 30-50% saturation (0.127g/ml); 50-80% saturation (0.214g/ml); final supernatant >80% saturation (Jakoby, 1971).

All of the fractions were subsequently assessed for biological activity in the collagen gel fibroblast migration assay. Each fraction was dialysed at 4°C for 24 hours against PBS. The dialysed fractions were sterile filtered by 0.2µm Millipore filtration before use in the migration assay.

2.7.ii Size Exclusion Chromatography (SEC)

This is a separation process based on gel filtration, whereby a sample is passed through a column that is packed with a porous resin. The exclusion range of the resin, i.e. the range of pore sizes, determines the size of molecules that can be separated. Larger molecules, because they cannot enter the pores, flow more rapidly around the resin beads and emerge earlier from the column. Smaller molecules, because they can penetrate the pores, travel a longer path through a larger buffer volume and emerge later. Typically the excluded volume (i.e. the column volume experienced by larger molecules) is about 35% of the resin volume, while the total volume experienced by the small molecules is nearly equal to the total resin volume.

Conditioned medium (CM), routinely 10x concentrated, was fractionated by SEC initially using Superose 12 HR 10/30 (GE Healthcare) fractionation range 1-300kDa. This method was subsequently scaled-up using a Superdex 75 HiLoad 26/60 (GE Healthcare), fractionation range 3-70kDa, to provide sufficient material for down-

stream analyses. The Superdex column was pre-equilibrated with three column volumes of running buffer, 20mM HEPES, 150mM Sodium chloride, pH 7.4. Prior to sample loading, the column was calibrated with known molecular mass markers; including BSA (66kDa), ovalbumin (45kDa) and chymotrypsinogen (25kDa) (GE Healthcare). Prior to separation, the concentrated CM was spun at 13,000rpm for 5 minutes to remove any debris. 4ml aliquots of the concentrated CM was applied to the column and allowed to enter the resin bed. Additional buffer was applied to the column and the emerging fractions were collected. Multiple runs were completed to provide sufficient material for downstream analyses, 100 x 3ml fractions were collected from each run (2 ml/min). Aliquots of the resultant fractions were tested for bioactivity in the 3D collagen gel assay. Fractions containing biological activity, of either MSF or MSF-I, were pooled from each run and stored at -80°C.

2.7.iii Ion Exchange Chromatography

During ion exchange chromatography a sample is passed through a charged column. Charged groups on the surface of a protein interact with oppositely charged groups immobilised on the ion exchange support. When the net overall charge of the protein is zero, the protein is at its isoelectric point (pI). When a protein is in a buffer with a pH higher than its pI, the protein will have a negative net charge and will bind to a positively charged support or anion exchange medium. When the buffer has a pH below the protein pI it will have a positive net charge and bind to a negatively charged support or cation exchange medium. Changing the pH of the binding buffer will allow for elution of the bound protein. (Current protocols in Protein Science 1990. Supp.8.4, John Wiley & Sons, Inc.).

After SEC, fractions containing MSFI activity were pooled, dialysed against 20mM Tris-HCl pH 7.5 and then pumped at 1ml/minute onto an ANX column (Hi Trap FF 1ml, GE Healthcare) pre-equilibrated with the dialysis buffer. Material unbound to the ANX column was collected and bound material eluted as a single peak by washing the column with 20mM Tris-HCl pH 7.5 1M NaCl. Aliquots (200-1000µl) of the bound and unbound fractions were tested for bioactivity in the 3D collagen gel assay, in the presence of 100pg/ml rhMSF. Unbound material (containing MSFI bioactivity) was then stored at -20°C and subsequently concentrated by freeze drying, after dialysis against distilled water. Freeze dried samples were stored frozen at -80°C.

2.7.iv SDS- PAGE Electrophoresis

Polyacrylamide gel electrophoresis is used to separate “fractions/samples” according to their physical properties as they are forced through a gel by an electrical current. PAGE was used both as an analytical tool to provide information on the molecular mass, purity or presence of a protein and as a preparative tool to obtain a pure protein sample. SDS-PAGE separates proteins primarily according to size because the SDS-coated proteins have a uniform charge: mass ratio. Protein molecular weight was estimated by running standard proteins of known molecular weights in a separate lane of the same gel (Biorad broad range markers). Since we knew the protein we were looking for had a small molecular mass a high percentage acrylamide gel was used; routinely a 12% resolving gel and 4.5% stacking gel, under reducing conditions.

Samples were redissolved in Laemmli loading buffer (BioRad Laboratories Ltd., Hemel Hempstead, Hertfordshire UK) containing 5% (v/v) 2-mercaptoethanol and heated for 5 minutes at 80°C prior to loading onto the gel. Electrophoresis was performed in a Tris/glycine/SDS buffered cooled tank at 30mA, 150V (Biorad Mini-Protean Electrophoresis Apparatus, LKB Macro Drive 1 power supply). Protein bands were visualised using Gel code Blue Staining reagent (Perbio). (Method adapted from Laemmli, 1970).

Table 2.4: Recipe for SDS- Polyacrylamide gel preparation.

Reagent	RESOLVING GEL 12% Acrylamide	STACKING GEL 4.5% Acrylamide
1M Tris pH 8.7 (Sigma-Aldrich)	3.76ml	-----
1M Tris pH6.9 (Sigma- Aldrich)	-----	625µl
30% (v/v) Acrylamide/ Bis (BioRad)	4.0ml	750µl
Distilled Water	2.14ml	3.525ml
10% (w/v) sodium dodecyl sulphate (Sigma-Aldrich)	100µl	100µl
10% (w/v) ammonium persulphate (Biorad)	50µl	50µl
TEMED (Sigma-Aldrich)	5µl	10µl

2.7.v Gel Elution of Protein Bands

In order to remove any potential contaminants, SDS-PAGE gels that were to be used for gel elution of protein bands were pre-run for 1 hour at 150V. After which, the running buffer was replaced and then the samples were then loaded. After SDS PAGE, gel lanes were cut into 0.5cm slices and each slice placed into individual 1.5ml tubes containing 1ml of elution buffer (100mM ammonium bicarbonate, 1mM SDS). Elution was performed overnight, at room temperature, by mixing end on end. After elution, samples were stored at -20°C and 4µl aliquots were subsequently tested for MSF and MSFI bioactivity in the 3D collagen gel assay (Kurien and Scofield, 2012).

2.8 IMMUNOBLOT (WESTERN BLOT) - INDIRECT METHOD

After electrophoresis the separated proteins were transferred onto a secondary matrix of nitrocellulose membrane by electroelution; 15V for 42 minutes, using a BioRad semi-dry blotting apparatus and the conducting buffer 48mM Tris, 39mM glycine, 1.3mM SDS, 20% (v/v) methanol (Towbin, 1979). Buffers used during development of the blots were based on TBS (20mM Tris-HCl, 137mM sodium chloride pH 7.6). To prevent any non-specific binding, the membrane was blocked using 1% (w/v) low fat skimmed milk powder, 0.05% (v/v) Tween 20, in TBS for 10-30 minutes at room temperature. The primary antibody, diluted in blocking buffer, was incubated overnight at room temperature.

The following day, the blot was washed, 3 x 20 minutes, in TBST (TBS, 0.05% (v/v) Tween 20). A horseradish peroxidase labelled secondary antibody that is directed against the primary antibody, diluted in blocking buffer, was incubated with the blot at room temperature for 1 hour. Finally, blots were washed 3 x 20 minutes in TBST and 1x 5 minutes in TBS. Using the Genome Gel analysis system, bands were then detected by chemiluminescence using the substrate SuperSignal West Dura (Perbio). (Method adapted from Towbin *et al.*, 1979).

Table 2.5: The operational concentrations of antibodies for performing immunoblotting.

Antigen	Primary Antibody	Secondary Antibody
NGAL	Anti-NGAL MAB1757 (R&D Systems) 2µg/ml	Rabbit anti-rat HRP (DAKO) 1:10,000 dilution
Total MSF	Rp VSI (In house prep) 1:10,000 dilution	Goat anti- rabbit HRP (Pierce) 1:10,000 dilution

2.9 IMMUNOPRECIPTATION OF MSF

MSF was immunoprecipitated from CM using the MSF-specific rabbit polyclonal antibody (RpVSI) and the Seize Classic Immunoprecipitation Kit (Perbio). Following SEC, fractions containing migration stimulating activity (F-msa) were pooled and concentrated 100 fold by freeze drying. After resuspension and dialysis against PBS, 100µg of POROS A purified RpVSI antibody was added to a 1ml aliquot of F-msa. Samples were mixed gently overnight at 4°C and on the following day 400µl of washed and equilibrated immobilised Protein G was added. The samples were then mixed for 3 hours at 4°C. The immobilised complex was washed and eluted from the beads according to the kit instructions. The elution was repeated 5x, eluted fractions were tested for MSF bioactivity in the fibroblast migration assay.

2.10 MASS SPECTROSCOPY

Protein mass fingerprint data was obtained by MALDI-Tof-Tof (MS/MS) analysis performed at the University of Dundee ‘Fingerprints’ Proteomics Facility, using an Applied Biosystems 4700 Proteomic Analyser.

2.11 QUANTIFICATION OF PROTEINS

2.11.i Colorimetric Indirect ELISA

Polystyrene 96-well microplates (Costar, Insight Biotechnology Limited, Wembley, UK) were coated overnight, at room temperature in a humidified chamber, with the appropriate standards (serial dilutions in carbonate buffer pH 9.6, 100µl per well) and samples to be tested. After washing with 200µl PBS per well, non-specific binding sites were blocked by incubation with 200µl/well 1% (w/v) BSA PBST (PBS with 0.05% (v/v) Tween 20) for one hour at room temperature with gentle agitation. The plate was then washed, 200µl per well, with PBS, twice with PBST and again with PBS. Primary antibody, diluted in 1% (w/v) BSA-PBS-T was then added to each well and the plate incubated for 1 hour at room temperature. The four step washing procedure was then repeated. The secondary antibody, a HRP conjugate, diluted in 1% (w/v) BSA- PBS-T was then added and the plate incubated for 1 hour at room temperature, followed by the washing procedure. Tetramethylbenzidine (TMB, DAKO), the substrate for HRP, was then added (50µl per well) and the plates were incubated for 10 minutes with gentle orbital shaking. The reaction was stopped with 50µl 2M H₂SO₄, and OD 450nm (reference 570nm) measured by plate reader (Flurostar Optima, BMG LABTECH and MRX DYNEX, DYNEX Technologies Limited, Worthing, West Sussex UK). (Weller 1954).

Table 2.6: The operational conditions for performing the Indirect ELISA.

ANTIGEN	STANDARDS	PRIMARY ANTIBODY	SECONDARY ANTIBODY
NGAL	200-1.56ng/ml NGAL (In house prep)	Goat anti-NGAL 1µg/ml (AF1757, R&D Systems)	Rabbit anti-goat HRP (DAKO) 1:1000 dilution

2.11.ii Colorimetric Sandwich ELISA

Polystyrene 96-well microplates (Costar, Insight Biotechnology Limited, Wembley, UK) were coated overnight at room temperature in a humidified chamber with the capture antibody, 100µl per well diluted in coating buffer (carbonate buffer, pH 9.6,

Pierce) On the following day, the plate was washed with PBS and blocked for 1 hour in 1% (w/v) BSA-PBS-T (blocking buffer, 200µl per well) with gentle agitation. The plate was then washed with PBS, twice with PBST (PBS with 0.05% (v/v) Tween 20, Pierce) and again with PBS. Using the appropriate standards, a standard curve was prepared in serial twofold dilutions in blocking buffer. Test samples and standards were added 100µl per well and incubated for 90 minutes at ambient temperature. The plate was then washed, as described previously. The sandwich antibody, was then diluted in 1% (w/v) BSA-PBS-T, 100µl added per well and the plate incubated for 90 minutes at ambient temperature. The plate was then washed, as described previously. The detection antibody, a HRP conjugate, was then added 100µl to each well and incubated for 90 minutes at room temperature, followed by the washing procedure. The substrate for HRP (tetramethylbenzidine, DAKO) was then added and the plates were incubated for 10 minutes with gentle orbital shaking. The reaction was stopped with 2M H₂SO₄, and OD 450nm measured by plate reader (Fluorstar Optima, BMG LABTECH or MRX DYNEX, DYNEX Technologies Limited, Worthing, West Sussex UK). (Palomaki, 1992)

Table 2.7: The operational conditions for performing the Sandwich ELISA.

ANTIGEN	STANDARDS	CAPTURE ANTIBODY	SANDWICH ANTIBODY	DETECTION ANTIBODY
MSF (total)	200-1.56ng/ml Recombinant MSF	MAB Pep Q 5.1 10µg/ml	RpVSI (protein A purified rabbit polyclonal serum 1:1000 dilution (~2µg/ml)	Goat anti-rabbit HRP conjugate (Pierce) 1:1000 dilution

2.12 IMMUNOLOCALISATION METHODS

2.12.i Cell Pellet Preparation

Cell lines used for immunohistochemical staining were prepared by two methods; either plated onto a plastic surface, namely chamber slides or 24 well plates (Nunc) or plated within and/or on a 3D collagen type I matrix.

Cells were plated onto the plastic surfaces at densities of 5-9 x 10³ cells/cm² and incubated for 1-3 days under standard conditions, until reaching approximately 70-80% confluency. After which, media was removed and cells fixed with 2% (v/v) formalin in

PBS for 30 minutes at room temperature, followed by permeabilisation with 100% (v/v) methanol (VWR) for 10 minutes at -20°C.

For collagen gel cell pellets; 1x 90mm confluent dish of cells were trypsinised, as described previously, to obtain a cell suspension which was spun, for 5 minutes at 900rpm. The cell pellet was gently resuspended in 100µl of 15% (v/v) DCS MEM which was then added to 2ml of collagen gel solution (1.7ml Type I Collagen (preparation previously described), 100µl 7.5% (v/v) solution sodium bicarbonate, 200µl 10X MEM). After, the collagen gel had set, around 5-10 minutes, growth media was added and the collagen pellet was incubated at 37°C, 5% CO₂ for 3-4 days.

To obtain cells on the surface of the pellet, a cell suspension in 15% (v/v) DCS MEM was added to a set 2ml collagen gel. A 1-2 hour incubation followed to allow cells to attach to the gel surface. After which the growth media was replenished followed by appropriate incubation time.

All cell pellets were fixed overnight at 4°C in 10mls neutral buffered formalin (VWR), followed by paraffin wax embedding (Dr. David Kellock, Department of Surgery and Molecular Oncology, Ninewells Hospital, Dundee). Depending on the degree of gel contraction, each pellet was split 1-2 or 3 and then individually embedded. Each paraffin block was cut into 3µm sections and baked for 30 minutes at 60°C to dissolve the wax. Before commencing staining sections were deparaffinised with xylene (VWR).

2.12.ii Immunostaining Protocol

Sections were firstly, rehydrated through decreasing concentrations of ethanol.

Endogenous peroxidase activity was blocked by immersion in 3% (v/v) hydrogen peroxide in PBS for 20 minutes and non-specific binding was blocked by incubating in 20% (v/v) normal serum in PBS (same species as secondary antibody) for 30 minutes. Sections were ringed using an immuno pen (Dako pen, Dako, Denmark) to minimise the volume of reagents required. To reduce non-specific background staining sections were pre-treated with Avidin/ Biotin blocking step (Avidin/Biotin Blocking Kit, Vector Labs, Peterborough, UK).

Following optimisation the appropriate dilution of primary antibody was made using 20% (v/v) normal serum in PBS and incubated overnight in a humidified chamber at 4°C, followed by 1 hour at room temperature. Controls were incubated with normal serum IgG from the same species as the primary antibody was raised in. Secondary antibody incubation was for 1 hour at room temperature in a humidified chamber, with

an appropriate dilution made in 20% (v/v) normal serum PBS. Staining was visualised using the avidin-biotinylated enzyme complex (Vectastain ABC Kit, Standard Elite, Vector Labs, Peterborough, UK) and incubation with DAB (3', 3'-diaminobenzidine), a substrate for the enzyme (Sigma, Dorset, UK). Slides were counterstained with haematoxylin and blueing agent. Followed by dehydration through a series of increasing concentrations of ethanol and cleared in two changes of xylene (this step omitted for plastic slides and plates) before being coverslipped with mounting medium, aqueous mount (Sigma, Dorset, UK) for plastics and for glass, DPX (BDH, VWR, Leicestershire, UK).

2.12.iii Optimum Conditions for Immunostaining Reagents

Table 2.8: The operational conditions for performing Immunostaining.

Antigen	Primary Antibody	Serum Block	Secondary Antibody	Negative Control
Total MSF	Rp2/98pFA2 pFn1, Rabbit Polyclonal Cells on Plastic 2.5 - 5µg/ml Cells on/in collagen: 33µg/ml	20% (v/v) Normal Goat Serum (NGS) in PBS (Vector, S-1000)	Biotinylated Goat Anti-Rabbit IgG (H+L) (Vector, BA9200) 6µl/ml in 20% (v/v) NGS in PBS	Normal Rabbit IgG preabsorbed to Fibronectin (Dako Cytomation, X0936)
NGAL	Anti-Human Lipocalin- 2/NGAL Polyclonal Goat IgG (R&D AF1757) Cells on Plastic: 0.1 – 0.5µg/ml Cells on/in collagen: 2µg/ml	20% (v/v) Normal Swine Serum (NSS) with PBS (Vector, S-4000)	Polyclonal Swine Anti-Goat, Mouse, Rabbit IgG/ Biotinylated (DakoCytomation E0453) 1:150 dilution in 20% (v/v) NSS in PBS	Normal Goat IgG (R&D, AB-108-C)

Chapter 3: Results

THE ASSESSMENT OF THE BIOACTIVITY OF CONDITIONED MEDIUM

3.1 AIMS

To collect conditioned medium from various cultured cell lines, followed by the analysis of bioactivity in the 3D collagen gel migration assay. The primary objective was to test conditioned medium for the ability to inhibit the motogenic activity of rhMSF. The conditioned medium collected and subsequently tested was a complex mixture of multifarious proteins and this screening phase will only give a rudimentary indication of its constituents and their bioactivity. This screening procedure was the first step in a process to identify inhibitor(s) to Migration Stimulating Factor.

3.2 BACKGROUND

The numerous bioactivities attributed to MSF (motogenesis, matrix remodelling, hyaluron biosynthesis and angiogenesis), all appear to have a causal link to its motogenic activity. Therefore, the sensitive *in vitro* bioassay for assessing the motogenic bioactivity of MSF, the 3D collagen gel fibroblast migration assay, was selected as being fundamental to the identification of potential MSF-I activity. The preliminary search focused on assessing the ability of conditioned medium, from numerous cultured cell lines, to inhibit the MSF stimulated migration of adult fibroblasts in a 3D Type I collagen gel.

The 3D collagen gel fibroblast migration assay was developed as a means to explore the activity of cultured cells within a physiologically relevant 3D macromolecular matrix. Collagens are triple helical proteins that occur in the extracellular matrix (ECM); comprising a family of over 30 collagens and collagen-related proteins. Type I collagen, a fibrous, structural protein consisting of D-periodic fibrils forms the major component and is the primary determinant of tensile strength of the ECM. Commonly used as a thin layer on tissue-culture surfaces, Type I collagen enhances the attachment and proliferation of a variety of cells including endothelial, epithelial, fibroblasts and hepatocytes. *In vitro*, collagen fibrillogenesis is a spontaneous self-assembly process with the Type I collagen fibrils forming a 3D supermolecular gel. However, *in vivo* the

process is not so simple with cellular mechanisms controlling the self-assembly process with the inclusion of fibronectin, integrins and collagen V (Kadler *et al.*, 2008). As described in Chapter 2, Material & Methods, collagen I was extracted from rat tail tendons by incubating in a dilute acid solution (3% v/v acetic acid) and then reconstituted into fibrils by neutralisation, forming a homogenous 3D gel (Schor *et al.*, 1990).

A collagen substratum is regarded as an appropriate biological scaffold to study diverse aspects of cell behaviour *in vitro*, including positioning and migration, cell growth and differentiation and matrix contraction (Schor *et al.*, 1982, Allen *et al.*, 1984). The fibre distribution and biophysical architecture is considered the closest resemblance to interstitial soft tissues, dermis and the network-like stroma of the lymph node cortex, promoting a more *in vivo*-like cellular morphology and function (Friedl and Brocker, 2000). In 3D collagen gel experiments, fibroblasts retain their tissue phenotype including polarised morphology and *in vivo* like positioning (Doane and Birk, 1991). The sensitivity and consistent reproducibility of the 3D collagen gel fibroblast migration assay, in displaying the motogenic activity of MSF has been attributed to the retained responsiveness of the adult fibroblasts. The inability of adult fibroblasts to produce MSF whilst still remaining responsive to it provides a perfect internal control. That is, any effect on fibroblast behaviour is completely in response to the experimental conditions and the subsequent introduction of bioactive test materials. In each separate experiment the baseline migration of the fibroblasts was always measured; that is the level of fibroblast migration when test overlay is serum-free MEM (SF-MEM) containing no further additives (final concentration of 1% (v/v) serum). Details of how the 3D collagen gel fibroblast migration assay was assessed can be found in Chapter 2. Initially, MSF was purified from foetal fibroblast conditioned medium (CM) but the subsequent development and purification of a recombinant form further increased efficiency and reproducibility of the migration assay. The motogenic activity of recombinant MSF (rhMSF) is indistinguishable from foetal fibroblast CM; characterised by a bell-shaped dose-response curve with half maximal activity at femtomolar concentrations which can be neutralised by anti-fibronectin Gel-BD antibodies (Schor *et al.*, 2003). During the course of this project a number of batches of recombinant MSF were produced and used. The consistency of quality and performance of the rhMSF was assured through a vigorous testing process including the assessment of motogenic activity of each batch by a dose response collagen gel fibroblast migration assay; a range of rhMSF (1 to 10,000pg/ml) was tested, in duplicate. A rhMSF concentration of

100pg/ml was selected for testing the inhibitory activity of the conditioned medium, as it reliably increased fibroblast migration 2 to 3 fold, above the baseline level.

Complications may arise when analysing the effects of the test CM on fibroblast migration due to the bell shaped dose- response bioactivity of MSF. MSF's motogenic activity increases steadily with increasing concentration, peaking at a maximum (500pg/ml) followed by a mirror-image decrease in activity towards the baseline level as the concentration increases further. It was therefore necessary to ensure any inhibitory activity detected was not merely an effect of additional MSF, present within the test CM, shifting the bell-shaped response of MSF into the inhibitory territory of bioactivity. Consequently the CM was tested with and without the addition of rhMSF in order to assess the presence of any residual motogenic activity in the CM.

In order for potential MSF-I activity to be assessed, a strict protocol and criteria was established for the collection of CM. Conditioned medium was only collected from cultured cell lines under serum free conditions; when the confluent cells were displaying a typical, normal morphology (Chapter 2). For cell lines which had the ability to exhibit multiple phenotypes, namely endothelial cells, separate collections of CM were made in order to determine any phenotypic dependent effects on bioactivity. The effect of different storage conditions (duration/ temperature) and CM concentration techniques were also assessed in order to determine optimum collection conditions.

3.3 THE MOTOGENIC ACTIVITY OF RECOMBINANT MSF

During the course of this project a number of batches of prokaryotically expressed rhMSF were prepared. The protein concentration of each batch was estimated, by comparison to known concentrations of GBD on a 12% resolving, 4.5% stacking acrylamide gel under reducing conditions (Chapter 2). Subsequently, the motogenic activity was assessed in the 3D collagen gel fibroblast migration assay. The rhMSF was tested at a range of concentrations from 1pg/ml to 10ng/ml in either duplicate or triplicate gels. The number of fibroblasts which had migrated into the gel, over a four day incubation period, was counted in ten separate fields of view per gel. The number of fibroblasts migrated under test conditions was expressed as a percentage of the SF MEM control baseline migration with the criteria for motogenic activity determined by the ability to stimulate fibroblast migration by a minimum of 50% (Figure 3.1).

In order to prove that the motogenic activity was indeed due to rhMSF stimulating the fibroblasts, the migration assays were repeated with the addition of an MSF function neutralising antibody, PEPQ 1.1. This mouse monoclonal antibody raised against a 21-mer peptide containing the IGDQ sequence in module 1-7 of MSF (and fibronectin), TNEGVMYRIGDQWDKQHDMGH, has been shown to neutralise MSF activity. Furthermore, when tested alone the PEPQ1.1 antibody has no effect on baseline fibroblast migration. (Schor *et al.*, 2003). Addition of the PEPQ 1.1 antibody (50ng/ml) was able to reduce MSF stimulated motogenic activity back to SF MEM baseline levels. (Figure 3.2).

A batch of rhMSF was considered suitable for use if it met the following requirements:

1. A molecular weight of approximately 77kDa.
2. The ability to stimulate the migration of adult fibroblasts in the 3D collagen gel fibroblast migration assay with the motogenic activity being characterised by a bell-shaped dose- response curve.
3. The ability of 100pg/ml rhMSF to stimulate fibroblast motogenic activity by 2-3 times more than the SF MEM baseline levels.
4. The rhMSF stimulated motogenic activity was neutralised by the addition of PEPQ 1.1 antibody.

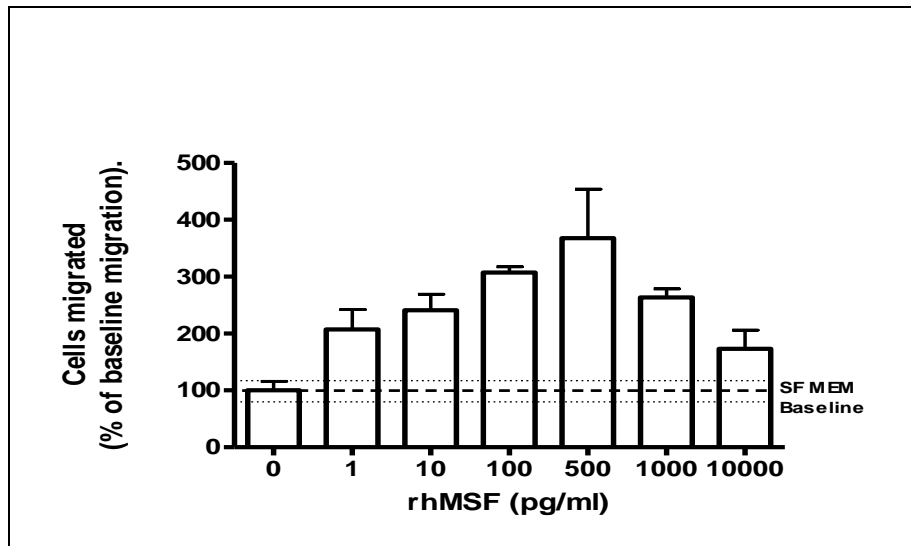


Figure 3.1: The motogenic activity of recombinant MSF.

Recombinant MSF was tested at a range of concentrations in the 3D collagen gel fibroblast migration assay. The number of cells migrated is expressed as a percentage of the SF MEM control baseline migration i.e SF MEM baseline = 100 +/- 16.07%, as represented by the hatched and dotted lines (mean and SD respectively). This was equivalent to 2.8 +/- 0.45 migrated cells. 100pg/ml rhMSF only equals 8.6 +/- 0.28 migrated cells. This is a representative experiment of the results achieved when testing the batches of rhMSF.

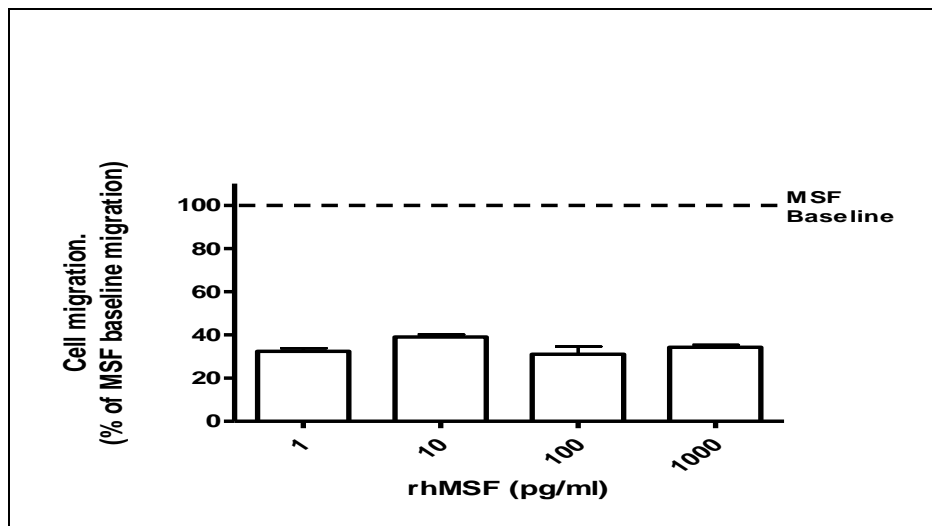


Figure 3.2: The effect of MSF- neutralising antibody, PEPQ1.1, on the motogenic bioactivity of recombinant MSF.

A range of concentrations of rhMSF was tested in the 3D collagen gel fibroblast migration assay in the presence of the PEPQ1.1 antibody (50ng/ml). The number of cells migrated is expressed as a percentage of the rhMSF only baseline migration, at each individual concentration, i.e 100pg/ml rhMSF = 100%, as represented by the hatched line. A representative experiment is shown.

3.4 THE TESTING OF FIBROBLAST CELL LINES FOR BIOACTIVITY IN THE 3D COLLAGEN GEL FIBROBLAST MIGRATION ASSAY

As previously discussed, the Schor group discovered a difference in the motogenic potential between adult and foetal fibroblast cell lines, with the expression of MSF subsequently identified as responsible for this difference (Schor *et al.*, 1988, Grey *et al.*, 1989). In order, to confirm this finding CM was collected (Chapter 2) from two foetal and two adult fibroblast cell lines (in house cell preparations) and then tested at a range of dilutions ($\frac{1}{4}$ to $\frac{1}{40,000}$) with and without the presence of 100pg/ml rhMSF. The foetal lines selected were FFD4 and F110a, whilst the adult lines were FSF44 and DFSF1 (Table 3.1).

In order to assess the results, criteria were set to determine stimulatory and inhibitory activity. Firstly, the CM was tested by itself without the addition of rhMSF, in order to determine the presence of any endogenous motogenic activity. The benchmark for motogenic activity was set as the ability to increase the number of fibroblasts migrated into the collagen gel by a minimum of 50% as compared to the negative control, the SF MEM baseline. This limit was set in comparison to rhMSF which reproducibly increased fibroblast migration by at least two fold when used at a final concentration of 100pg/ml.

Next, the criterion for the inhibition of MSF (MSF- inhibitory activity) was determined by the ability of the CM upon addition of 100pg/ml rhMSF to reduce fibroblast migration by at least 50% as compared to the positive control, the MSF baseline. For example, this would mean that the migration level for 100pg/ml rhMSF would be reduced down to SF MEM baseline levels. Furthermore, the possibility that endogenous stimulatory activity within the CM may conceal the activity of any MSF-inhibitor(s) present in the CM required exclusion. Therefore, instead of determining an alteration in migration by comparison to the positive and negative controls, the CM when tested alone, at each individual dilution, is considered the baseline migration. That is, MSF-inhibitory activity was defined, upon addition of 100pg/ml rhMSF, as the inability to increase CM baseline migration by a minimum of 50%.

Equivalent results were achieved for both foetal lines and the adult lines shared a strong similarity too. As expected, when tested alone, the foetal CM displayed a strong motogenic dose-responsive bioactivity; very similar to the dose response curve of rhMSF (Figure 3.1, Figure 3.3b). Foetal CM displayed stimulatory activity in dilutions $\frac{1}{10}$ to $\frac{1}{1000}$, with activity peaking with approximately a threefold increase, compared

to the SF MEM baseline, at the 1/100 dilution point. The adult fibroblast CM displayed no bioactivity, with migration levels comparable to the SF MEM baseline (Figure 3.3a). When 100pg/ml rhMSF was added to the adult CM, migration increased on average by 2.7 fold. Irrespective of whether the migration levels were compared to the rhMSF baseline or the CM only baseline, all dilution points displayed no MSF inhibitory activity (Figure 3.3 c and e). However, the foetal CM initially appeared to be displaying an inhibitory effect when compared to the MSF baseline level (Figure 3.3f) although a different picture emerged when endogenous stimulatory activity was taken into account. The comparison to CM only migration levels showed that the addition of MSF appeared to have no effect on the dilution points 1/4 to 1/1000. Whilst the addition of rhMSF increased migration on average by 1.9 fold at dilution points 1/5000 to 1/40,000. As discussed, the ability of foetal fibroblast CM to stimulate cell migration was shown to be due to the expression of foetal MSF (Schor *et al.*, 1988, Grey *et al.*, 1989). Plus, as seen from the dose response curve of rhMSF the motogenic activity declines at the higher concentrations of 1ng/ml and above. Therefore it seems that the combination of foetal MSF present in the lowest dilutions, where the MSF concentrations are highest, and the additional rhMSF have resulted in decreased migration as the total MSF concentration reached levels where motogenic activity is no longer detected. Whilst at the highest dilutions of foetal CM, where endogenous MSF concentrations will be considerably lower, the addition of rhMSF results in increased migration.

In conclusion, these results corroborate previous findings that there is a difference in the motogenic activity of foetal and adult fibroblast conditioned media. They also show that no endogenous MSF- inhibitory activity was detected in either adult or foetal fibroblast CM. Regarding the suitability of the 3D collagen gel fibroblast migration assay as a means of screening CM for MSF inhibitory activity the results confirm that the FSF44 fibroblasts used in the assay are ideal; since they respond to the presence of rhMSF and express no endogenous motogenic or MSF inhibitory bioactivity which may have caused complications with the interpretation of results.

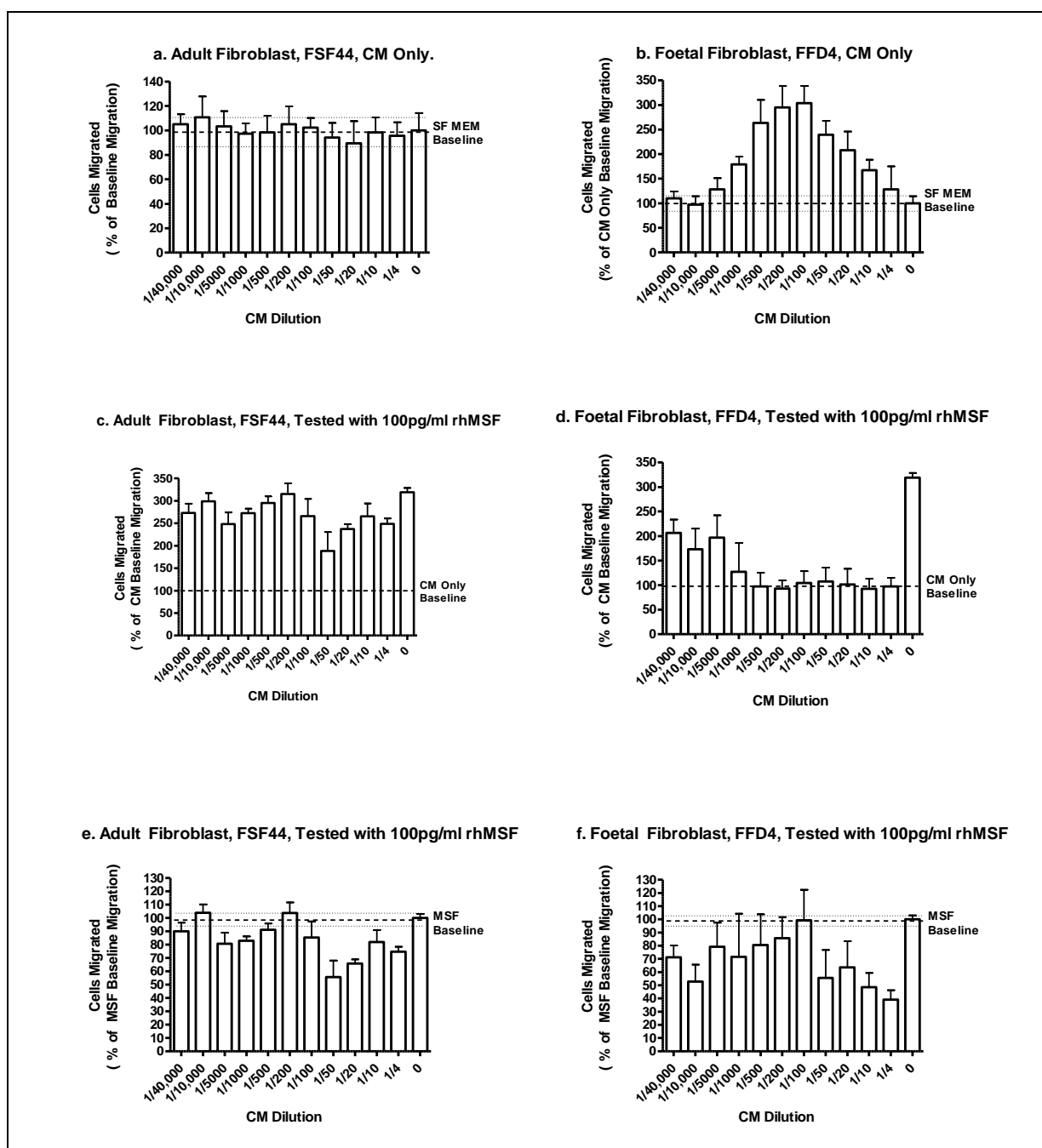


Figure 3.3: The comparison of the bioactivity present in the conditioned medium collected from adult and foetal fibroblast cell lines, with and without the addition of rhMSF.

Conditioned medium (CM) from the adult and foetal fibroblasts, FSF44 and FFD4

respectively, was tested on its own and in the presence of 100pg/ml rhMSF, at a range of dilutions from 1 in 4 to 1/40,000 in the fibroblast migration assay. The number of cells migrated is expressed as either:

Graphs a and b: the percentage of the SF MEM control baseline migration i.e. SF MEM baseline = 100+/- 14.23, as represented by hatched and dotted lines (mean and standard deviation respectively). Equivalent to 2.6 +/- 0.37 migrated cells.

Graphs c and d: the percentage of CM only baseline migration at each individual dilution point i.e. 1/4 dilution CM only = 100%, as represented by the hatched line.

Graphs e and f: Percentage of the 100pg/ml rhMSF control baseline migration i.e. MSF baseline = 100+/- 3.01, as represented by hatched and dotted lines (mean and standard deviation respectively). Equivalent to 8.3 +/- 0.25 migrated cells.

The results show a representative experiment.

3.5 THE TESTING OF ENDOTHELIAL CELL LINES FOR BIOACTIVITY IN THE 3D COLLAGEN GEL FIBROBLAST MIGRATION ASSAY

Endothelial cells form the inner lining of blood vessels, the endothelium. They are essential in maintaining vessel wall integrity and blood circulation, functioning as a semi-permeable anticoagulant barrier. Endothelial cells are also considered to be dynamic multifunctional cells performing a variety of metabolic and synthetic functions; which are pivotal in both angiogenesis and vasculogenesis (Coultas *et al.*, 2005, Sumpio *et al.*, 2002).

In vivo, endothelial cells are capable of adopting two distinctive and reversible phenotypes. The endothelial cells lining blood vessel walls form a contact- inhibited polygonal cobblestone-like uniform monolayer and are often described as displaying a “resting” phenotype. Whilst during angiogenesis the “resting” cells adopt an elongated fibroblastoid phenotype migrating into the surrounding connective tissue where they self-associate into solid cords of elongated “sprouting” cells. Eventually after further transformations these cords form new patent vessels (Folkmann and Haundenschild 1979 and 1980, Makarski 1982, Schor *et al.*, 1983).

Endothelial cells *in vitro* retain the ability to undergo this reversible phenotypic conversion. The different phenotypes are considered to be *in vitro* counterparts to the resting and angiogenic cells observed *in vivo*. Endothelial cells plated on to a 2D substratum (e.g. gelatin-coated culture dishes) will proliferate to confluence, forming a contact-inhibited cobblestone monolayer, morphologically similar to the endothelium lining of the blood vessel wall. The second phenotype appears in post-confluent cultures, when the resting cells undergo a transition into a distinctive elongated sprouting morphology and begin to grow underneath the intact cobblestone monolayer, eventually forming an interactive network. These sprouting cells often appear vacuolated and visualisation of individual cells becomes difficult due to the interconnected network of loops and rings. Both cell phenotypes are considered endothelial in origin since they stain positive for Factor VIII (Schor *et al.*, 1983). The sprouting phenotype can also be induced by culturing endothelial cells within a 3D matrix (e.g Type I collagen gel matrix) (Canfield *et al.*, 1986). The cells spontaneously and uniformly adopt an elongated morphology, subsequently forming sprouting networks. It is assumed that the loss of apical- basal polarity, which cells forming a cobblestone monolayer experience, induces the sprouting phenotype. Cells grown within a 3D environment or those growing underneath a monolayer lack a free apical

surface and can therefore form interactions over their entire cell surface (Schor *et al.*, 1983).

The ability to culture homogenous populations of either endothelial phenotype enables the investigation of possible differences in protein expression. Differential synthesis of various matrix macromolecules including laminin, thrombospondin, type I collagen and heparan sulphate proteoglycan have already been described (Canfield *et al.*, 1986, 1990, 1992, and 1995. Cotta- Pereira *et al.*, 1980). These differences are reputed to contribute to the angiogenic process.

MSF has been shown to induce angiogenesis *in vivo* and *in vitro*. Subcutaneous implants of collagenous graft matrices containing MSF, induce angiogenesis in rat and pig models, plus MSF applied to chicken yolk-sac membranes provoke a significant angiogenic response (Schor 2010, unpublished observations). Also, *in vitro* under serum free culture conditions an application of rhMSF to an endothelial cobblestone monolayer will induce a greater number of sprouting cells compared to a serum free only control (Schor 2010). It was therefore of interest to explore the possibility that the two endothelial phenotypes may differentially express MSF or differ in their synthesis of an inhibitor to MSF.

Numerous endothelial cell lines, of both bovine and human origin, were initially selected to be screened (HUVEC, HOEC, HAEC, BAEC, Endo 742) (Table 3.1). Obviously, the cell lines had to possess the ability to clearly display both phenotypes but also ease of culture and life- span were taken into consideration. The first line chosen was an in house preparation of bovine aortic endothelial cells (BAEC) which form typical cobblestone and sprouting phenotypes but have a limited passage capacity, undergoing senescence on average after 16-19 passages (Schor *et al.*, 1983, Motegi 2008). The second endothelial cell line was Endo 742; a transformed human mammary microvascular line, gifted by Dr Micheal O'Hare (O'Hare *et al.*, 2001). Although the Endo 742 does not form a typical cobblestone monolayer as seen in BAEC cultures, there is a distinct morphological difference between confluent and post-confluent cultures. The major advantage of the Endo 742 line is the ease of culture, fast doubling time and unlimited proliferative potential, essential when collection of large volumes of conditioned media is required. The other human cell lines were not selected as they were less robust, grew slowly and were frequently adversely affected when switching to a new batch of donor calf serum.

3.5i Bioactivity of Conditioned Medium From Endothelial Cells Grown On a 2D Surface.

The selected endothelial cell lines, BAEC 2-2 U7 and Endo 742, were grown on a 2D surface of 0.1% (w/v) gelatin coated plastic cell cultures dishes. In order to assess the difference between the two phenotypes expressed by the endothelial cells conditioned medium was collected (under serum free conditions) when the cells were either displaying a cobblestone monolayer when confluent (cobblestone CM) or from post-confluent cultures where sprouting cells were present underneath the monolayer (sprouting CM). Therefore, the “sprouting” conditioned medium was actually from a heterogeneous population of both resting and sprouting phenotypes. Since the confluent density of Endo 742 cells was less than BAEC 2-2 U7 the range of dilutions tested were limited accordingly. (Endo 742: 4.8×10^6 cells per 90mm equivalent to 9.6×10^6 cells per ml of CM collected. BAEC 2-2 U7: 5.9×10^6 cells per 90mm is equivalent to 11.8×10^6 cells per ml of CM.) For ease of discussion the cell line BAEC 2-2 U7 will from now be referred to as BAEC.

Immediately, an obvious difference emerged between the two endothelial phenotypes. For both BAEC and ENDO 742, the cobblestone CM displayed no motogenic bioactivity over a range of dilutions; cell migration was similar to the SF baseline (Figure 3.4a and 3.5a). However, the sprouting CM exhibited a potent motogenic activity. For BAEC CM, migration was stimulated by a range of sprouting CM dilutions, $\frac{1}{4}$ to $\frac{1}{1000}$; when compared to the baseline, maximal activity of an average of 86.4% was present in $\frac{1}{4}$ to $\frac{1}{10}$ dilutions (Figure 3.4b). Endo 742 sprout CM appeared to possess greater motogenic activity with an average of 119.5% increase in migration for dilutions $\frac{1}{4}$ to $\frac{1}{40}$ (Figure 3.5b).

When 100pg/ml rhMSF was added to the BAEC cobblestone medium, the migration level was comparable to the CM only baseline level; that is the motogenic activity of MSF was inhibited (Figure 3.4c). A similar effect was observed for ENDO 742 CM; however the higher dilutions ($\frac{1}{200}$ to $\frac{1}{4000}$) showed a 50% increase in migration compared to CM only baseline levels but the high standard deviations reflect poor experimental reproducibility (Figure 3.4d). By comparing the amount of migration achieved to the MSF baseline level, the inhibitory effect was still obvious (Figure 3.4e and 3.5e). The conclusion being that endothelial cobblestone CM contains MSF inhibitory activity.

Endothelial sprouting CM appears to have a more complex effect on the activity of MSF. Applying the set criteria for the presence of MSF-inhibitory activity, as a reduction of migration of at least 50% when compared to the MSF control baseline levels (100pg/ml rhMSF only) one would conclude that no inhibitory activity was present in either BAEC or ENDO742 sprouting CM (Figure 3.4f and 3.5f). However, this assessment does not take into account the endogenous motogenic activity present in the sprouting CM; comparing to the CM only baseline level, a different picture emerges. Those dilutions of both BAEC and ENDO 742 CM which displayed motogenic activity when tested alone possessed the ability to inhibit MSF. Conversely, the non- motogenic dilutions responded to the addition of rhMSF with migration increasing 50% above the CM only baseline level (Figure 3.4d and 3.5d). Unfortunately, reduced experimental reproducibility was reflected by high standard deviations. An explanation for this could be that the CM was collected from a mixed population of both sprouting and cobblestone cells making standardisation of CM collection conditions problematic. Analysis of these results seems to imply that the motogenic activity observed in the endothelial sprouting CM is due to the expression of MSF. The highest potency of endogenous motogenic activity of the sprouting CM was measured in the lowest dilution points which would obviously contain a higher concentration of the motogen compared to the higher dilutions, which consequently showed no motogenic activity. When rhMSF was added to these low dilution points the effect was a reduction in migration, whilst addition to the higher CM dilutions stimulated migration. As previously described, MSF is characterised by a bell shaped dose response activity (Figure 3.1). Presuming endothelial MSF is bioactive in these low dilutions the subsequent addition of rhMSF would result in the total MSF present at a level which actually resulted in MSF having an inhibitory effect on migration (above 500pg/ml). Whilst addition of rhMSF to the higher dilutions, where endothelial MSF was too dilute to be bioactive, would increase the total MSF concentration to levels where migration is stimulated (1-500pg/ml).

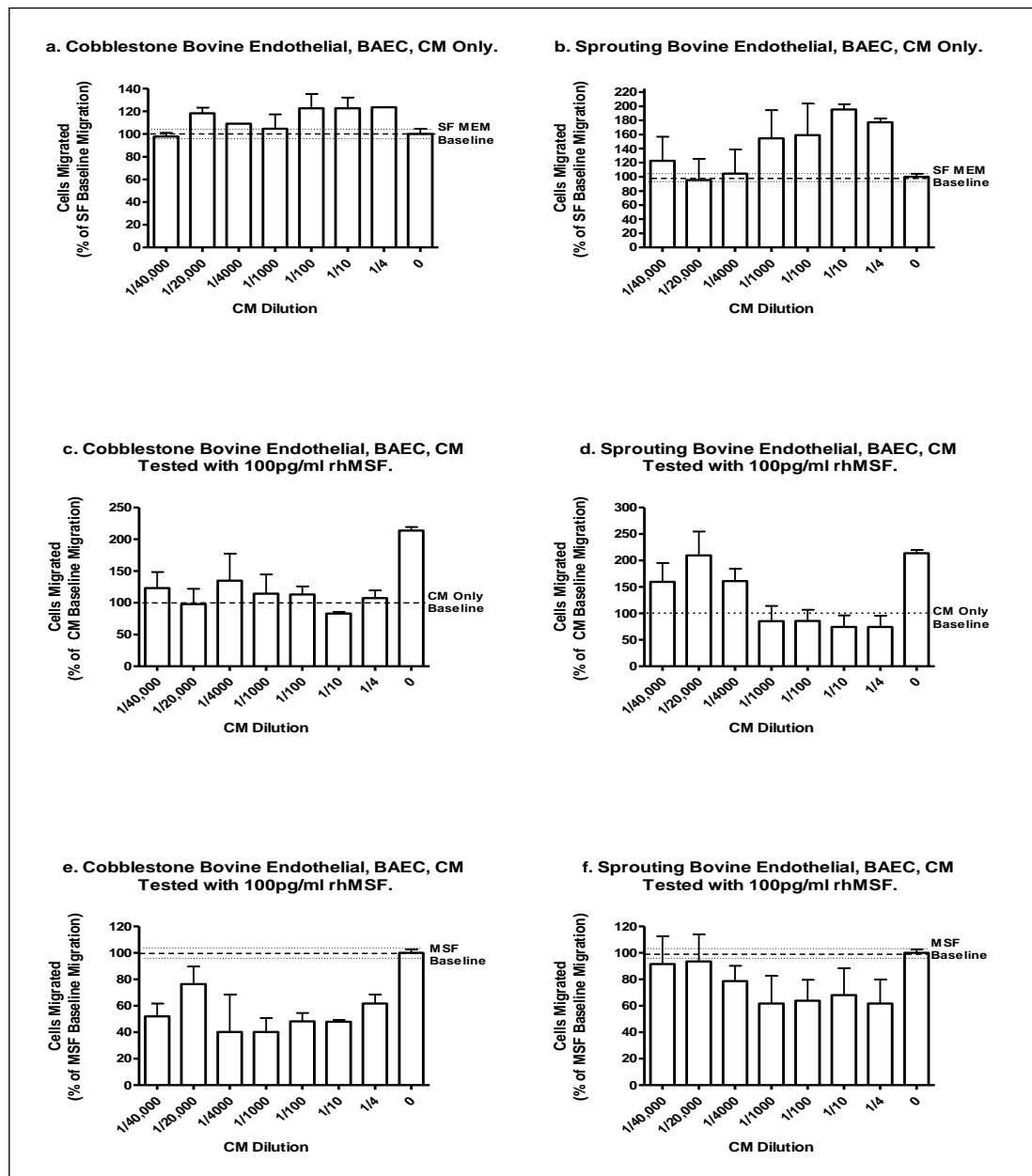


Figure 3.4: The comparison of the bioactivity present in the conditioned medium collected from the bovine aortic endothelial cell line, BAEC, displaying either a cobblestone or sprouting phenotype, when grown on a 2D surface. The CM for each phenotype was tested on its own and in the presence of 100pg/ml rhMSF, at a range of dilutions from 1 in 4 to 1/40,000 in the fibroblast migration assay. The number of cells migrated is expressed as either: Graphs a and b: a percentage of the SF MEM control baseline migration i.e. SF MEM baseline = 100 ± 4.55 , as represented by hatched and dotted lines (mean and standard deviation respectively). Equivalent to 2.2 ± 0.10 migrated cells. Graphs c and d: a percentage of CM only baseline migration at each individual dilution point i.e. $\frac{1}{4}$ dilution CM only = 100%, as represented by the hatched line. Graphs e and f: a percentage of the 100pg/ml rhMSF control baseline migration i.e. MSF baseline = 100 ± 2.77 , as represented by hatched and dotted lines (mean and standard deviation respectively). Equivalent to 4.7 ± 0.13 migrated cells. The results show a representative experiment.

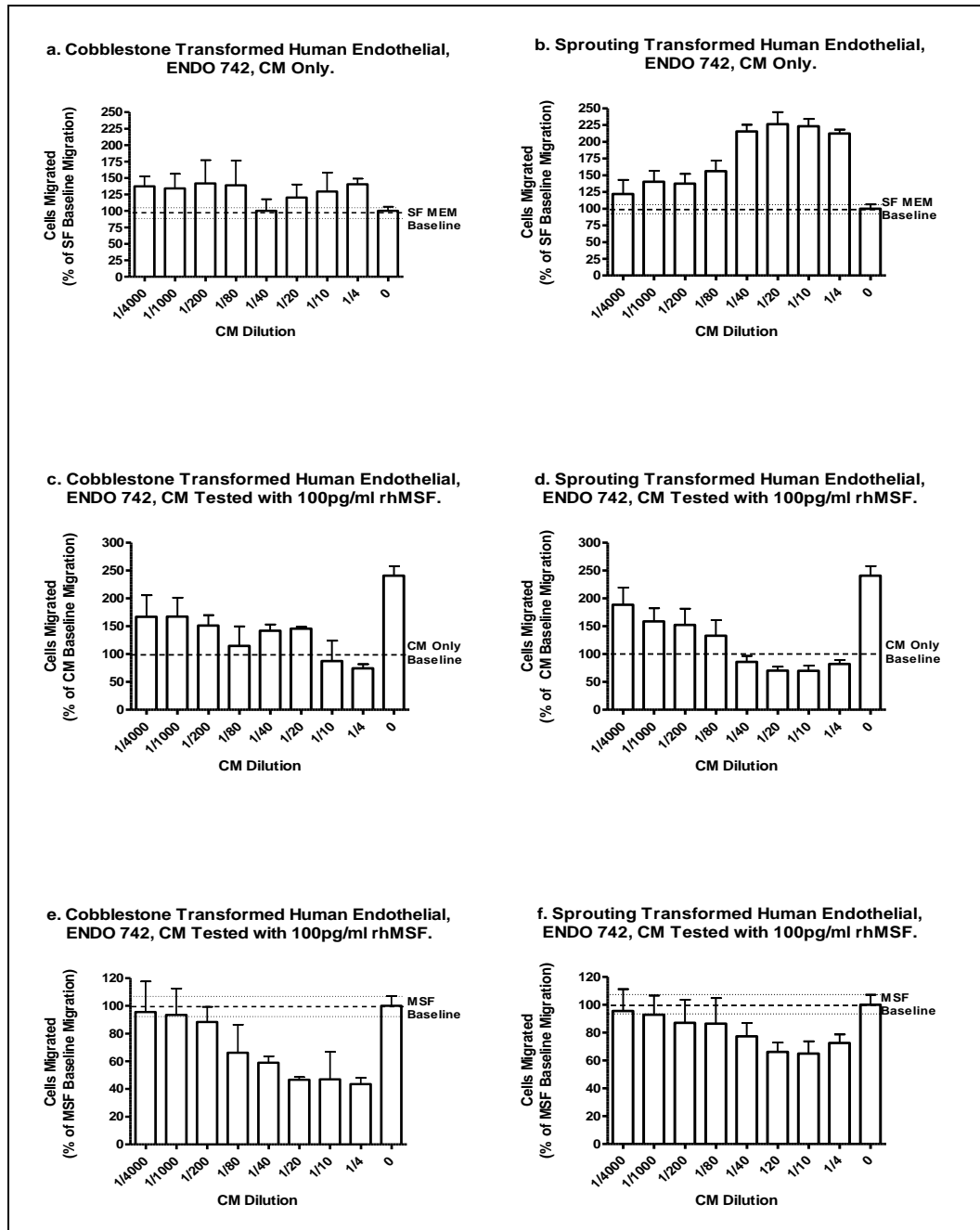


Figure 3.5: The comparison of the bioactivity present in the conditioned medium collected from the transformed human mammary microvascular cell line, Endo 742, displaying either a cobblestone or sprouting phenotype, when grown on a 2D surface. The CM for each phenotype was tested on its own and in the presence of 100pg/ml rhMSF, at a range of dilutions from 1 in 4 to 1/4000 in the fibroblast migration assay. The number of cells migrated is expressed as either: Graphs a and b: a percentage of the SF MEM control baseline migration i.e. SF MEM baseline = 100 \pm 6.56, as represented by hatched and dotted lines (mean and standard deviation respectively). Equivalent to 3.2 \pm 0.21 migrated cells. Graphs c and d: a percentage of CM only baseline migration at each individual dilution point i.e. ¼ dilution CM only = 100%, as represented by the hatched line. Graphs e and f: a percentage of the 100pg/ml rhMSF control baseline migration i.e. MSF baseline = 100 \pm 7.14, as represented by hatched and dotted lines (mean and standard deviation respectively). Equivalent to 7.7 \pm 0.55 migrated cells. The results show a representative experiment.

3.5ii Bioactivity of Conditioned Medium from Endothelial Cells Grown Within a 3D Collagen Matrix.

As described, when performing experiments using sprouting CM from endothelial cells cultured on a 2D surface, inconsistencies in bioactivity were observed between different batches of CM. Although, for ease of description, the CM was described as sprouting it was actually from a mixed population of the endothelial phenotypes (sprouts beneath a cobblestone monolayer). Therefore, in order to ensure a homogenous population of source cells, CM was collected from endothelial cells cultured within a 3D type I collagen gel, where the cells spontaneously adopt the sprouting phenotype. As controls, CM was collected from endothelial cells plated on the surface of a collagen gel, where the cells formed a cobblestone monolayer and from a blank collagen gel (no cells). To collect a large volume of CM, the type I collagen gels were plated on a 90mm cell culture dish and to reduce any effect of the gel itself the same volume of gel, 15ml, was used for both the blank, as well as the sprouting and cobblestone phenotypes. For the sprouting CM, the endothelial cells were dispersed with 5ml of collagen gel (6.5×10^5 cells per ml) which was sandwiched between two 5ml collagen gels; thereby eliminating the possibility of the cells migrating to the surface of the gel and forming a monolayer. The cobblestone CM was collected from endothelial cells that had been plated directly on the surface of a 15ml collagen gel in 5ml of medium (5×10^4 cells per ml). The endothelial cells were allowed to attach and form a cobblestone monolayer after which the CM was collected. 5ml of SF MEM was added to each 90mm dish, with the CM collected after 2-3 day incubation.

As expected, the SF media cultured on a blank type I collagen gel had no effect on cell migration when tested in the migration assay. The migration level for the blank gel CM when tested alone, at all dilution points, was similar to the SF baseline whilst the addition of 100pg/ml rhMSF increased migration to the MSF baseline level (Figure 3.6 a-c). Consequently, in conclusion, any bioactivity measured from the sprout or cobblestone CM was considered to be solely due to factors expressed by the endothelial cells.

Once again, the bioactivity of the CM from both BAEC and ENDO742 shared a similarity and was phenotype dependent. Cobblestone CM from both cell lines displayed no motogenic activity when tested alone unlike the sprouting CM, which stimulated fibroblast migration in a similar manner to MSF. In addition, by ruling out

the effect of the endogenous motogenic activity present in the sprouting CM genuine MSF-I activity appeared to be present in the cobblestone CM.

Cobblestone CM from both cell lines appeared to have no bioactivity when tested alone, with migration levels similar to the SF MEM control (Figure 3.7a and 3.8a). However, upon addition of 100pg/ml rhMSF it became clear that the cobblestone CM possessed the ability to inhibit MSF motogenic activity with maximum MSF-I activity achieved in the mid- range of dilutions tested (1/500-1000) (Figure 3.7c/e and 3.8c/e). The level of MSF-I activity seemed comparable to that measured previously in CM collected from an endothelial cobblestone monolayer cultured on a 2D surface.

The motogenic activity of sprouting CM (BAEC and ENDO742) displayed a bell-shaped dose response activity; maximal activity in dilutions 1/500- 1/100, whilst reducing at the lower and higher dilution points. As the same number of both BAEC and ENDO742 cells were plated within the collagen gel it would appear the motogenic activity of their CM appears to be comparable, peaking at 189.4 +/- 6.81% and 181.0 +/- 20.00% respectively. Although, the motogenic activity was present at a higher level over the range of dilution points tested in the BAEC compared; an average of 139.5 +/- 57.23% compared to 111.9 +/- 48.9% over all dilution points, respectively (Figure 3.7b and 3.8b).

As seen with the previous experiment (sprouting CM collected from 2D surface), the endogenous motogenic activity of the sprouting CM has to be considered when interpreting the effect of adding 100pg/ml rhMSF, because if the set criteria of MSF inhibitory activity (the reduction of migration of at least 50% when compared to MSF control baseline level) was applied it would appear that no inhibition occurred (Figure 3.7f and 3.8f). However, comparison to the CM-only baseline shows that addition of rhMSF to the dilutions with the maximal motogenic activity results in a decrease in fibroblast migration (ENDO742 dilution points 1/50 and 1/500, BAEC dilution points 1/50-1/5000) (Figure 3.7d and 3.8d). Again, this would imply that the factor expressed by the sprouting endothelial cells, which stimulates fibroblast migration, is endothelial expressed MSF.

In conclusion, these results suggest that the bioactivity of endothelial cells is phenotype dependent and not matrix dependent. That is, sprouting cells whether formed on a 2D matrix or within a 3D matrix express a motogenic factor that stimulates fibroblasts to migrate in a manner similar to rhMSF. Whilst endothelial cells displaying the “resting” cobblestone phenotype express an MSF-inhibitory factor. Also, this endothelial phenotype-dependent bioactivity appears to be common to both primary and

transformed cell lines (and different species). A limited analysis of the other endothelial cell lines endorses this conclusion (Table 3.2).

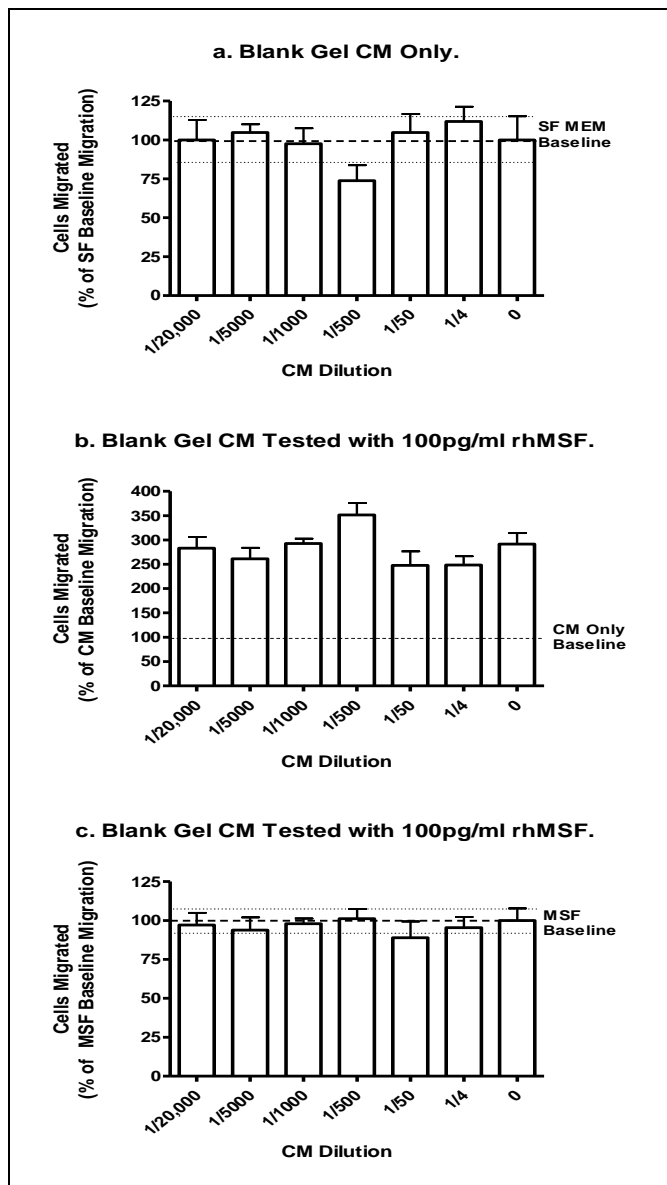


Figure 3.6: The bioactivity of conditioned medium collected from a blank collagen

gel. A blank type I collagen gel was cultured in SF MEM under the same conditions as for standard CM collection. The media was then collected and tested in the fibroblast migration assay on its own and in the presence of 100pg/ml rhMSF, at a range of dilutions from 1 in 4 to 1/20,000. The number of cells migrated is expressed as either:

Graph a: a percentage of the SF MEM control baseline migration i.e. SF MEM baseline = 100+/- 15.23, as represented by hatched and dotted lines (mean and standard deviation respectively). Equivalent to 2.1 +/- 0.32 migrated cells.

Graph b: a percentage of CM only baseline migration at each individual dilution point i.e. 1/4 dilution CM only = 100%, as represented by the hatched line.

Graphs c: a percentage of the 100pg/ml rhMSF control baseline migration i.e. MSF baseline = 100+/- 7.84, as represented by hatched and dotted lines (mean and standard deviation respectively). Equivalent to 6.1 +/- 0.48 migrated cells. The results show a representative experiment.

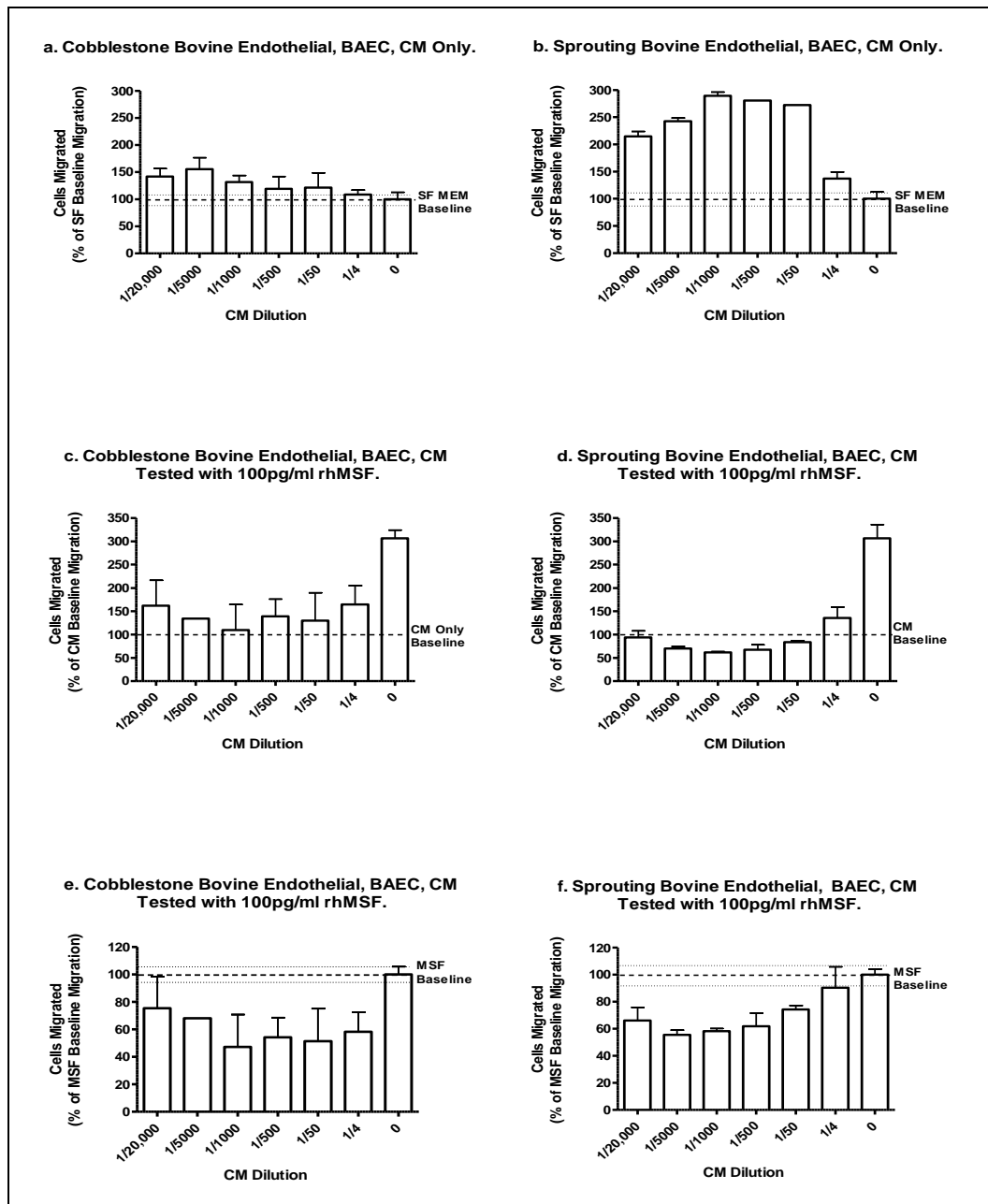


Figure 3.7: The comparison of the bioactivity present in the conditioned medium collected from the bovine endothelial cell line, BAEC, displaying either a cobblestone or sprouting phenotype, when grown on or within a 3D collagen matrix, respectively. The CM for each phenotype was tested on its own and in the presence of 100pg/ml rhMSF, at a range of dilutions from 1 in 4 to 1/20,000 in the fibroblast migration assay. The number of cells migrated is expressed as either: Graphs a and b: a percentage of the SF MEM control baseline migration i.e. SF MEM baseline = 100 ± 12.77 , as represented by hatched and dotted lines (mean and standard deviation respectively). Equivalent to 2.35 ± 0.30 migrated cells. Graphs c and d: a percentage of CM only baseline migration at each individual dilution point i.e. $\frac{1}{4}$ dilution CM only = 100%, as represented by the hatched line. Graphs e and f: a percentage of the 100pg/ml rhMSF control baseline migration i.e. MSF baseline = 100 ± 5.69 , as represented by hatched and dotted lines (mean and standard deviation respectively). Equivalent to 7.2 ± 0.41 migrated cells. The results show a representative experiment.

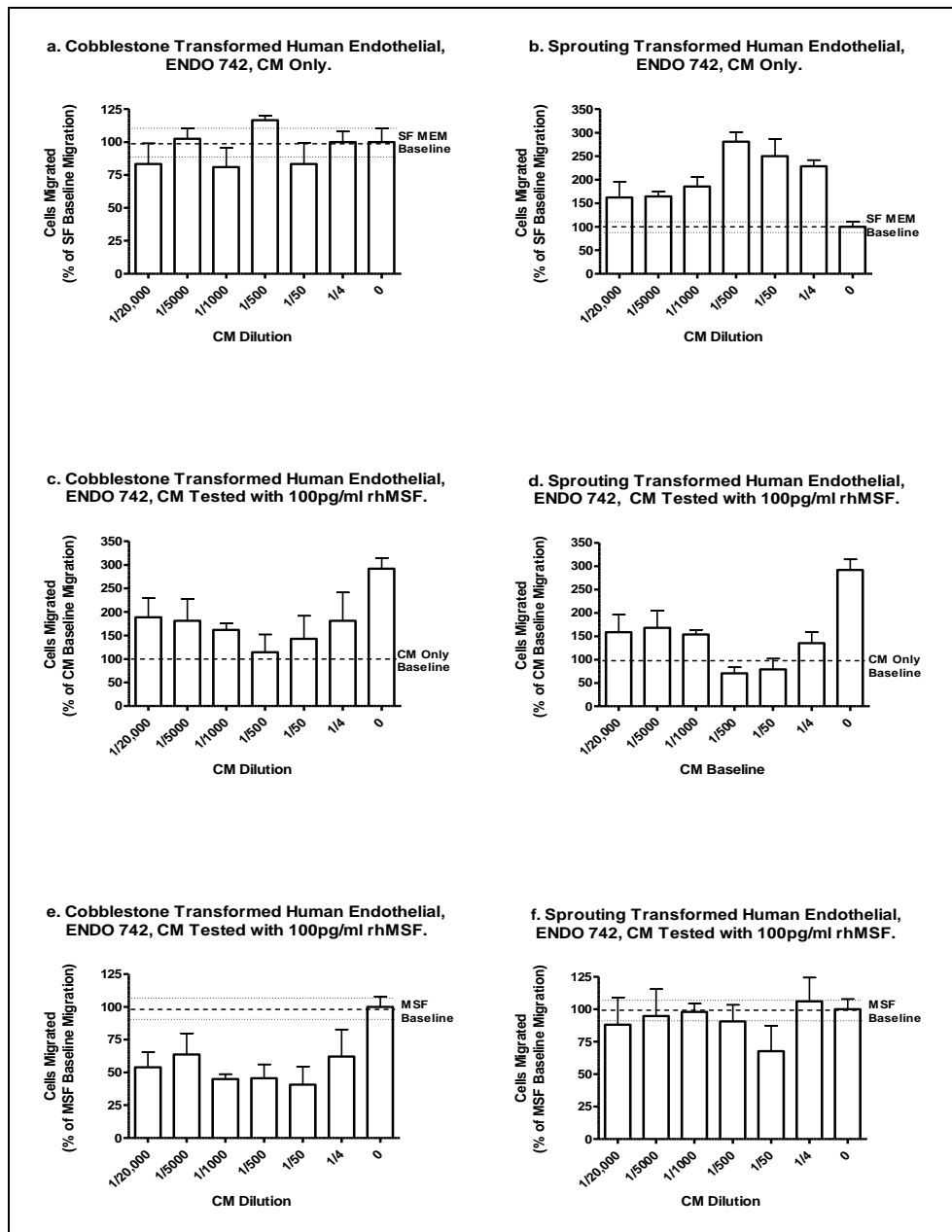


Figure 3.8: The comparison of the bioactivity present in the conditioned medium collected from the transformed human mammary microvascular cell line, Endo 742, displaying either a cobblestone or sprouting phenotype, when grown on or within a 3D collagen matrix, respectively. The CM for each phenotype was tested on its own and in the presence of 100pg/ml rhMSF, at a range of dilutions from 1 in 4 to 1/20,000 in the fibroblast migration assay. The number of cells migrated is expressed as either: Graphs a and b: a percentage of the SF MEM control baseline migration i.e. SF MEM baseline = 100 ± 10.48 , as represented by hatched and dotted lines (mean and standard deviation respectively). Equivalent to 2.1 ± 0.22 migrated cells. Graphs c and d: a percentage of CM only baseline migration at each individual dilution point i.e. $1/4$ dilution CM only = 100%, as represented by the hatched line. Graphs e and f: a percentage of the 100pg/ml rhMSF control baseline migration i.e. MSF baseline = 100 ± 7.84 , as represented by hatched and dotted lines (mean and standard deviation respectively). Equivalent to 6.1 ± 0.48 migrated cells. The results show a representative experiment.

Table 3.2: List of endothelial cell lines, whose conditioned medium (CM) was tested for the presence of motogenic and MSF-I activity.

The CM, collected under serum free conditions, was collected from the endothelial cells plated on a 2D surface when either expressing a cobblestone or sprouting phenotype.

The collected CM was tested at a range of dilutions in the fibroblast migration assay to determine the presence of motogenic and MSF-inhibitory activity.

Cell Line	Cell Type	<u>Cobblestone CM</u> dilutions displaying		<u>Sprouting CM</u> dilutions displaying	
		Motogenic activity	MSF-I activity	Motogenic activity	MSF-I activity
BAEC Clone 2	Bovine aortic endothelial cells	none	neat - 1/1000	1/20-1/40	1/20 – 1/40
BAEC Clone 3	Bovine aortic endothelial cells	none	neat – 1/1000	1/20 – 1/40	1/20 – 1/40
BAEC 2-2 U7	Bovine aortic endothelial cells	none	1/4 - 1/40, 000	1/4 - 1/1000	1/4 - 1/1000
Endo 742	Transformed human microvascular endothelial cells	none	1/4 - 1/80	1/4 - 1/40	1/4 - 1/40
HAEC	Human aortic endothelial cells	none	neat – 1/25	1/10 – 1/20	1/10 – 1/20
HOEC	Bovine omentum endothelial cells	none	neat - 1/25	not tested	not tested
HUVEC	Human umbilical vein endothelial cells	none	neat – 1/25	1/10- 1/20	1/10 -1/40

3.6 THE TESTING OF EPITHELIAL CELL LINES FOR BIOACTIVITY IN THE 3D COLLAGEN GEL FIBROBLAST MIGRATION ASSAY.

Keratinocytes are found in the epidermal layer of the skin. They are principally responsible for structure of the outer layer of stratified epithelium. This layer is fundamental to the primary function of skin; to act as the first line of defence forming a barrier against various forms of environmental damage (U.V. radiation, water loss, heat, pathogens etc.) Keratinocyte differentiation and keratinisation are essential to performing this role (Proksch *et al.*, 2008, Brenner and Hearing 2008).

Keratinocytes also are vital in the process of wound healing and the concurrent immune response. Depending on how the skin barrier is breached, they have the ability to

express specific proinflammatory mediators or cytokines in response to the injury; thus facilitating the coordinated response of various cell types including melanocytes, Langerhans cells, lymphocytes and fibroblasts (Myers *et al.*, 2007).

Previously, the Schor group tested conditioned medium from a primary keratinocyte culture and the preliminary experiments showed the presence of potential MSF inhibitory activity. Difficulties however arose because the primary keratinocytes were extremely challenging to culture, making the condition medium collection at the volumes required impracticable. It was hoped the use of the spontaneously transformed epithelial cell line, HaCaT would resolve this issue as they are undemanding cell line. (Table 3.1).

Petra Boukamp's group developed the first permanent epithelial cell line from normal adult human skin, after a prolonged cultivation at a reduced calcium concentration and elevated temperature (Boukamp *et al.*, 1988). Despite being immortal, HaCaT cells are considered to be similar to normal keratinocytes. They are non-tumorigenic and form an organised and differentiated epidermal tissue when transplanted into nude mice, with the keratin expression being very similar to normal keratinocyte transplants. Due to this preserved differentiation capacity, even after prolonged passages; they are extensively used as a substitute for normal keratinocytes (Schoop *et al.*, 1999).

3.6i The Testing of an Epithelial Cell Line for Bioactivity in the 3D Collagen Gel Fibroblast Migration Assay.

Testing the HaCaT CM in the 3D collagen gel migration showed that it exhibited no endogenous motogenic activity but did possess the ability to inhibit the motogenic function of rhMSF. The level of fibroblast migration of HaCaT CM tested alone was equivalent, at each dilution point (1/4 to 1/40,000), to the SF MEM baseline control; that is a migration rate of 2.3 +/- 0.21 fibroblasts per gel (Figure 3.9a). Normally, the addition of 100pg/ml rhMSF would increase migration by 2-3 fold, however the presence of HaCaT CM completely eliminated this activity. HaCaT CM diluted 1/4 to 1/1000 completely inhibited the effect of MSF has on fibroblast migration (Figure 3.9b and c).

The presence of an MSF inhibitor in the HaCaT CM was obvious; whether comparing the migration levels to the CM only baseline or to the rhMSF positive control baseline. Also, the higher dilutions beyond 1/1000 revealed that the inhibitor activity could be diminished as the concentration of HaCaT CM was reduced. The rhMSF motogenic

activity was restored to expected levels when tested with HaCaT CM dilutions above 1/40,000 (Figure 3.9b and c). In addition, the lack of any endogenous motogenic activity in the HaCaT CM made the interpretation of the results straightforward, as compared to previous experiments with the other cell lines tested.

From the observation of normal fibroblast morphology during the assay and the similarity to the SF MEM baseline migration we eliminated the presence of any “toxic” effect present in the HaCaT CM. The results were also established to be consistently reproducible. Various batches of HaCaT CM were tested, either freshly collected or stored at -20°C, in order to remove any possible effect of storage or the freeze thaw cycle in activating factors present within the HaCaT. Another researcher, Dr I Ellis, also performed a duplicate experiment achieving the same results, therefore increasing confidence in attributing the effect of the HaCaT CM on the motogenic activity of MSF to the presence of an MSF inhibitor (MSFI).

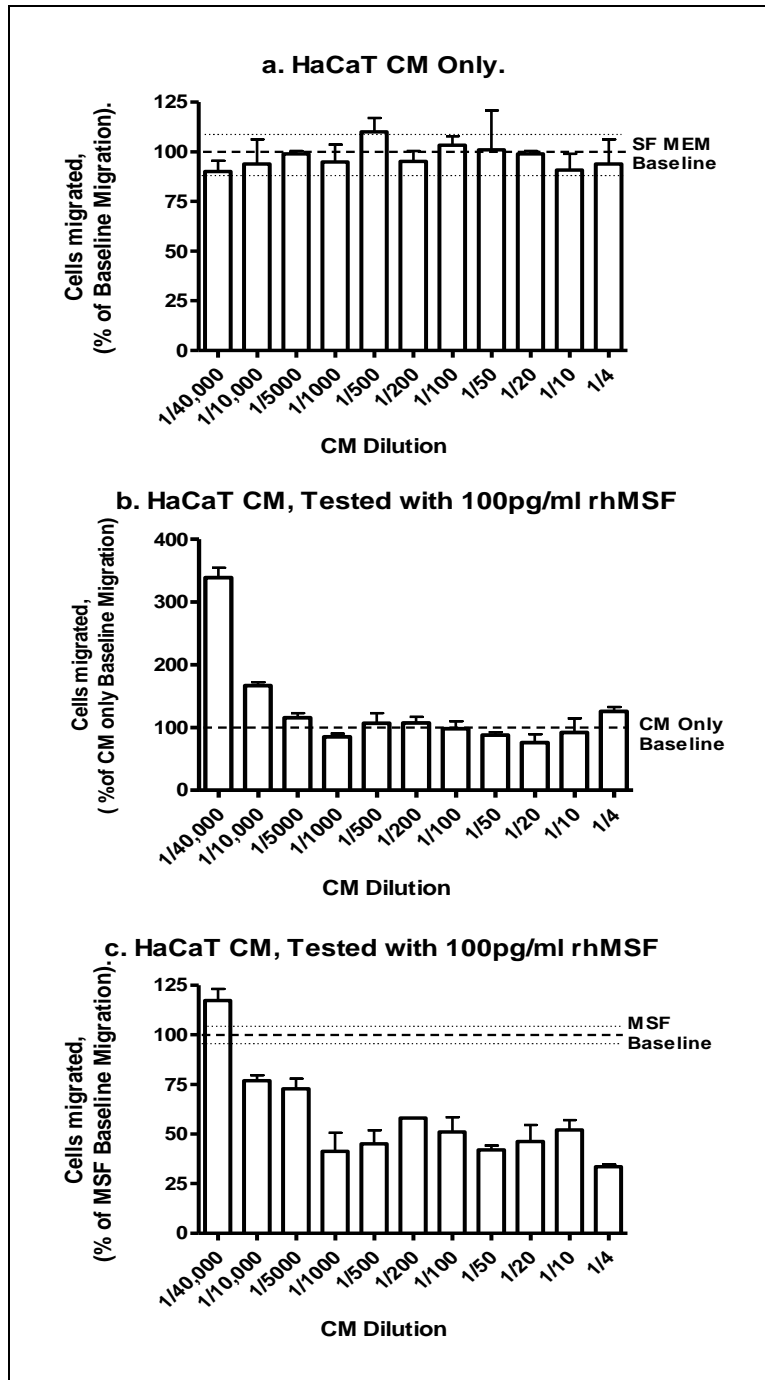


Figure 3.9: The bioactivity of HaCaT keratinocyte conditioned medium in the fibroblast migration assay. The CM was tested on its own and in the presence of 100pg/ml rhMSF, at a range of dilutions from 1 in 4 to 1/40,000. The number of cells migrated is expressed as either: Graph a: a percentage of the SF MEM control baseline migration i.e. SF MEM baseline = 100 \pm 9.13, as represented by hatched and dotted lines (mean and standard deviation respectively). Equivalent to 2.3 \pm 0.21 migrated cells. Graph b: a percentage of CM only baseline migration at each individual dilution point i.e. 1/4 dilution CM only = 100%, as represented by the hatched line. Graph c: a percentage of the 100pg/ml rhMSF control baseline migration i.e. MSF baseline = 100 \pm 4.59, as represented by hatched and dotted lines (mean and standard deviation respectively). Equivalent to 6.1 \pm 0.28 migrated cells. The results show a representative experiment.

3.7 DISCUSSION

The first phase of this project was to screen for potential MSF inhibitors by testing the conditioned medium, collected from various cell lines, in the 3D collagen gel fibroblast migration assay. Through these experiments many observations can be drawn.

Firstly, the selection of the 3D collagen gel fibroblast migration assay as a MSF-I screening tool was advocated. Substantiating previous findings, that the adult fibroblasts (FSF44) used in the assay do not express either MSF or any MSF-I, but respond reproducibly to the motogenic activity of rhMSF (Schor *et al.*, 2003).

Therefore, the effect on fibroblast migration can be attributed only to the specific experimental conditions and the relationship between rhMSF and the test CM.

Secondly, two sources of MSF-I activity were identified. MSF-I activity was detected within the CM collected from two different cell types, endothelial and keratinocyte. In addition, the expression of the endothelial MSF-I appears to be phenotype dependent; bioactive in “resting” cobblestone CM but not detected in sprouting CM. Whilst, sprouting endothelial cells appear to be producing a motogen that has a similar activity to rhMSF.

No presumptions could be made that MSF-I present in the keratinocyte and cobblestone endothelial CM is the same factor. Therefore, the next stage was to isolate and identify the MSF-I from each source. Since, the culture and collection of HaCaT CM was more efficient this avenue was pursued first, thereby developing a protocol that could subsequently be applied to the endothelial CM. In addition, conditioned medium is a complex mixture and the results achieved from this MSF-I screening process can only be seen as a crude indication of its constituents; the fractionation and purification of the CM is therefore the essential next stage in achieving the identification of MSF inhibitor(s).

The situation with the endothelial cells was further complicated by what emerged to be a phenotype dependence of MSF-I expression and by the presence of an endogenous motogenic activity, caused by endothelial MSF-like motogen. The next stage was to determine, the identity of the MSF inhibitor and the motogen and to subsequently understand the relationship between the two.

In addition, the HaCaT keratinocyte cell line has been further developed by the Fusenig/Boukmap group into an *in vitro* model used to study human skin carcinogenesis.

HaCaT-*ras* clones, each displaying a shift in tumourigenic potential, have been established as the cell lines BEN, MAL and MET representing respectively the benign,

malignant and metastatic stages of carcinogenesis (Fusenig and Boukamp 1998). It would therefore be interesting to determine whether the presence and bioactivity of keratinocyte MSF-I can be related to tumorigenic potential.

Table 3.1: List of cultured cell lines of which conditioned medium was collected under serum free conditions and used for testing for the presence of MSF- inhibitory activity in the 3D collagen gel fibroblast migration assay.

Details include cell type, source and reference.

Name	Cell Type	Source	Reference
FFD4	Human fetal fibroblast.	Explant culture, Ninewells Hospital, University of Dundee	Unpublished
F110 a	Human fetal fibroblast.	Explant culture, Dr. I. Ellis, University of Manchester.	R.G.Ham. Dermal fibroblasts. In <i>Methods in Cell Physiology</i> , Vol 21 (ed. C. Harris, B.F. Trump & G.Stoner) New York, Academic Press, 255-276.
FSF44	Human foreskin fibroblast. Obtained from one year old healthy donor.	Explant culture, Dr I. Ellis, University of Manchester	R.G.Ham. Dermal fibroblasts. In <i>Methods in Cell Physiology</i> , Vol 21 (ed. C. Harris, B.F. Trump & G.Stoner) New York, Academic Press, 255-276. S.L.Schor. Cell proliferation and migration on collagen substrata in vitro. <i>Journal of Cell Science</i> . 1980, 4,159-175. S.L. Schor <i>et al.</i> Foetal and cancer patient fibroblasts produce an autocrine migration-stimulating factor not made by normal adult cells. <i>Journal of Cell Science</i> , 1988, 90, 391-399. S.L.Schor <i>et al.</i> Substratum- dependent stimulation of fibroblast migration by the gelatine binding domain of fibronectin. <i>Journal of Cell Science</i> , 1996, 109, 2581-2590. S.L.Schor <i>et al.</i> MSF: A genetically truncated oncofoetal fibronectin isoform expressed by carcinoma and tumour-associated stromal cells. <i>Cancer Research</i> , 2003, 63 (24), 8827-8836. S.L.Schor <i>et al.</i> A novel sandwich assay for quantifying chemo-regulated cell migration within a 3Dmatrices: wound healing cytokines exhibit distinct motogenic activities compared to transmembrane assay. <i>Cell Motility Cytoskeleton</i> , 2006, 63, 287-300.

			<p>C.J.Millard <i>et al.</i> The role of the fibronectin IGD motif in stimulating fibroblast migration. <i>Journal of Biological Chemistry</i>, 2007, 282 (49), 35530-35535.</p> <p>S.J.Jones <i>et al.</i> Co-expression by keratinocytes of migration stimulating factor (MSF) and a functional inhibitor of its activity (MSF-I). <i>Experimental Cell Research</i>, 2007, 313, 4145-4157.</p> <p>K.Motegi. Differential involvement of TGFβ-1 in mediating the motogenic effects of TSP-1 on endothelial cells, fibroblasts and oral tumours. <i>Experimental Cell Research</i> 2008, 314, 2323-2333.</p>
DFSF1	Human adult foreskin fibroblast.	Explant culture, University of Dundee	R.G.Ham. Dermal fibroblasts. In <i>Methods in Cell Physiology</i> , Vol 21 (ed. C. Harris, B.F. Trump & G.Stoner) New York, Academic Press, 255-276.
ENDO 742	Transformed human microvascular endothelial cells	Dr Micheal O'Hare	<p>M. J. O'Hare, J. Bond, C.Clarke, Y. Takeuchi, A. J. Atherton, C. Berry, j. Moody, A.R.J. Silver, D.C. Davies, A.E. Alsop, A.M. Neville, P.S. Jat, Conditional Immortalisation of Freshly Isolated Human Mammary Fibroblasts and Endothelial Cells. <i>Proceedings of National Academy of Science, USA</i> , 2001, 98, 646-65.</p> <p>K.Motegi. Differential involvement of TGFβ-1 in mediating the motogenic effects of TSP-1 on endothelial cells, fibroblasts and oral tumours. <i>Experimental Cell Research</i>, 2008, 314, 2323-2333.</p>
HUVEC 1666	Human umbilical vein endothelial cells	Cell Applications Inc. Cat No : 200-05n Lot No: 1666	<p>J.Wojta, M Gallicchio, <i>et al.</i> Interleukin-4 Stimulates expression of urokinase- type-plasminogen activator in cultured human foreskin microvascular endothelial cells. <i>Blood</i> 1993, 81 (12), 3285-3292.</p> <p>B. Furie, B.C.Furie. <i>The Molecular Basis of Blood coagulation.</i> Cell, 1988, 53 (4), 505-518.</p>
HOEC	Human omentum microvascular endothelial cells		N.Chung-Welch <i>et al.</i> Two-stage isolation procedure for obtaining homogenous population of microvascular endothelial and mesothelial cells from human omentum. <i>Microvascular Research</i> , 1997, 54, 121-134.
HAEC	Human aortic endothelial cells	Life Technologies Ltd.	Unpublished

		Cat No: C-006-SC	
HUVEC	Human umbilical vein endothelial cells	Dr Shane Foo, CRT. Originally purchased from Promo Cell: HUVEC-c, cryopreserved, cat no:C-12200	K.Motegi. Differential involvement of TGF β -1 in mediating the motogenic effects of TSP-1 on endothelial cells, fibroblasts and oral tumours. <i>Experimental Cell Research</i> , 2008, 314, 2323-2333.
BAEC Clones 2 & 3	Bovine aortic endothelial cells	In house preparation.	A.M. Schor, S.L.Schor, T.D.Allen Effects of Culture Conditions on the Proliferation, Morphology and Migration of Bovine Aortic Endothelial Cells. <i>Journal of Cell Science</i> , 1983, 62, 267-285. A.B.Sutton <i>et al.</i> The response of endothelial cells to TGF- β 1 is dependent upon cell shape, proliferative state and the nature of the substratum. <i>Journal of Cell Science</i> , 1991, 99, 777-787.
BAEC 2-2 U7	Bovine aortic endothelial cells	In house preparation. Bovine aorta No:2. cultures started June2003	A.M. Schor, S.L.Schor, T.D.Allen Effects of Culture Conditions on the Proliferation, Morphology and Migration of Bovine Aortic Endothelial Cells. <i>Journal of Cell Science</i> , 1983, 62, 267-285. A.B.Sutton <i>et al.</i> The response of endothelial cells to TGF- β 1 is dependent upon cell shape, proliferative state and the nature of the substratum. <i>Journal of Cell Science</i> , 1991, 99, 777-787. K.Motegi. Differential involvement of TGF β -1 in mediating the motogenic effects of TSP-1 on endothelial cells, fibroblasts and oral tumours. <i>Experimental Cell Research</i> , 2008, 314, 2323-2333.
HACAT	Spontaneously immortalised human trunk skin	Dr. Norbett Fusenig	P. Boukamp, R.T. Petrussevska, D. Breitkreutz, J. Hornung, A. Markham, N.E. Fusenig, Normal Keratinization in a Spontaneously Immortalized Aneuploid Human Keratinocyte Cell Line. <i>Journal of Cell Biology</i> , 1988, 106, 761-771. M.M. Mueller, W. Peter, M. Mappes, <i>et.al.</i> , Tumour Progression of Skin Carcinoma

	keratinocytes		cells in Vivo promoted by Clonal selection, Mutagenesis, and Autocrine Growth Regulation by Granulocyte Colony-stimulating factor and Granulocyte- macrophage Colony Stimulating factor. American Journal of Pathology, 2001, 159, 1567-1579.
--	---------------	--	---

Chapter 4: Results

THE IDENTIFICATION OF MSF-I PRODUCED BY KERATINOCYTES.

4.1 AIMS

The initial screening of the conditioned medium of the spontaneously immortalised human keratinocyte cell line, HaCaT, showed it possessed the ability to consistently inhibit the bioactivity of rhMSF in the 3D collagen gel fibroblast migration. The next phase was therefore to isolate and identify the factor(s) responsible for this MSF inhibitory activity from the complex mixture of proteins present within the HaCaT conditioned media. Furthermore, although no motogenic bioactivity was detected when the total HaCaT conditioned medium was tested the process of fractionation may potentially disrupt protein interactions resulting in the appearance of previously masked bioactivities. Therefore, the fractionated HaCaT conditioned medium, was analysed in the 3D collagen gel fibroblast migration assay for the presence of both motogenic and MSF inhibitory activity.

Please note that the SEC and Ion Exchange fractionation of the HaCaT CM was performed by Dr S.J. Jones, whilst subsequent handling and analysis of the bioactivity of fractions was carried out by M.M. Florence. In order to validate results Dr. I.R. Ellis and M.M. Florence concurrently performed the 3D collagen gel fibroblast migration assays.

4.2 BACKGROUND

The HaCaT human keratinocyte cell line is a spontaneously immortalised cell line derived from histologically normal adult body skin. Named after its development from prolonged cultivation at a reduced calcium concentration and elevated temperature (Boukamp *et al.*, 1988). It is unique, as the first clonal origin, permanent epithelial cell line from adult human skin which exhibits practically normal differentiation. However, despite displaying transformed phenotype *in vitro*, HaCaT keratinocytes are non-tumorigenic and non invasive *in vivo* (Boukamp *et al.*, 1997, Fusenig and Boukamp 1998).

It has been discovered that, unlike rodent tissue, human cells are rather resistant to transformation; a difference that has been ascribed to the higher stability of the human genome (Sager *et al.*, 1983, Dipalo 1983). Previous attempts to immortalise human cells using DNA viruses (simian virus 40, adenovirus types 5 and 12, human papilloma virus types 16, 18 and 31) resulted in cells exhibiting altered growth properties and a significant reduction of normal keratinisation with a partial re-expression of foetal characteristics (Boukamp *et al.*, 1997).

Although the exact mechanism of spontaneous immortalisation remains elusive, evidence does suggest that numerous genetic alterations are required including the inactivation of senescence genes or activation of immortalising genes. These genetic changes are visible as chromosomal alterations. The immortalisation of HaCaT cells is thought to be a consequence of UV type mutations in both alleles of the p53 tumour suppressor gene similar to those found in a high percentage of skin carcinomas and premalignant lesions (Lehmann *et al.*, 1993, Brash *et al.*, 1991). They also show a loss of chromosomes 3p, 4p and 9p; the location of senescence genes. Yet in spite of these genetic alterations HaCaT cells still retain a stable chromosome content and remain non-tumorigenic throughout 320 passages (Boukamp *et al.*, 1997).

Cell immortalisation is considered to be a foremost step in the transformation process of human cells and is typically associated by a loss or reduction in a cell's differentiation potential. However, HaCaT keratinocytes retain their differentiation capacity, possessing the ability to form a practically normal epidermal architecture when transplanted onto subcutaneous tissue of athymic mice and when grown in an organotypic co-culture system (Boukamp *et al.*, 1988, Ryle *et al.*, 1989, Schoop *et al.*, 1996). The organised epithelium formed, typically expresses most differentiation-specific keratins (1 and 10) and markers (involucrin and flaggarin) and ultrastructurally closely resembles the epidermis including the formation of a basement membrane (Boukamp *et al.*, 1988, Breitkreutz *et al.*, 1998, Schoop *et al.*, 1999).

Due to the similarity to normal human keratinocytes in their growth and differentiation potential the HaCaT cell line is a regularly used model system to study keratinocyte biology and transformation. Including examining epithelial –mesenchymal interactions and the effect matrix components and paracrine acting differentiation factors have on tissue organisation and keratinisation *in vitro* (Schoop *et al.*, 1996). HaCaT keratinocytes are also one of the most frequently used cell lines in three dimensional culture and artificial skin models; aiding in the study of epidermal gene expression, epidermal-dermal interactions and wound healing. These models are also increasingly

been adopted as an *in vitro* pharmacotoxicological test (Gay *et al.*, 1992). Furthermore, HaCaT cells can be stably transfected with candidate genes, enabling the investigation into oncogenes and other factors in the process of malignant conversion of human epithelial cells (Schoop *et al.*, 1999).

Ever since Boukamp *et al.*, (1988) established the HaCaT cell line, they have become a valuable tool in the study of human epithelial cells. In comparison to other epithelial lines, there are numerous advantages in using the HaCaT cells including their independence of donor variation and availability in unlimited quantities. Also, since they are not virally transformed, they do not contain any viral sequences which could cause genetic instability, thus maintaining their non-tumourigenic phenotype for extended culture passages (Boukamp *et al.*, 1997). Finally, because of their genetic and phenotypic characteristics HaCaT keratinocytes are considered analogous to cells present at the very early stage of skin carcinogenesis and have become the foundation of a multistage skin carcinogenesis model system (Fusenig *et al.*, 1998, Mueller *et al.*, 2001).

4.3 THE SUPERDEX FRACTIONATION OF HACAT CONDITIONED MEDIUM

The MSF inhibiting activity of conditioned medium (CM) collected from cultured HaCaT keratinocytes can be detected up to CM dilutions of 1:1000. This activity was attributed to the presence of a putative inhibitor of MSF, referred to as MSF-I. In order to isolate and ultimately identify this MSF-I, the HaCaT CM was fractionated by molecular weight using size exclusion chromatography (SEC).

Initial SEC experiments were performed using the Superose 12HR 10/30 column (GE Healthcare) and subsequently with the Superdex 75 HiLoad 26/60 (GE Healthcare) column, which has a fractionation range of 3-70kDa. Multiple runs using ten times concentrated CM was performed in order to provide sufficient material for downstream analyses. Per run, 4mls of ten times concentrated CM was loaded onto the column, as described previously in Materials & Methods, Chapter 2. For each individual run 100 x 3ml fractions were collected (2ml/min) and numbered 1 to 100; the corresponding fractions from the duplicate runs were then pooled together. Subsequently the fractions were pooled into groups of three; Groups 1 to 33. For each cell line Groups 9-18 (fractions 30-59), which span the two main absorbance peaks with a molecular weight

range of approximately >70kDa to 20kDa, were tested for bioactivity in the 3D collagen gel fibroblast migration assay (Figure 4.1).

4.4 THE BIOACTIVITY OF SIZE- EXCLUSION FRACTIONATED HACAT CONDITIONED MEDIUM.

As previously described for HaCaT total CM, the SEC fractionated HaCaT CM was tested alone and in the presence of 100pg/ml rhMSF in the 3D collagen gel fibroblast migration assay. Fraction groups 9-18 were tested at a final dilution of 1/20 (all dilutions made with SF MEM). A criterion was set in order to determine each fraction's bioactivity. For a fraction to be considered motogenic, when tested alone, it must have stimulated fibroblast migration by a minimum of 50% as compared to the SF MEM control baseline levels. While the existence of MSF-inhibitory bioactivity was established as a fraction's ability to reduce fibroblast migration by at least 50% upon addition of 100pg/ml rhMSF, as compared to MSF baseline. Another method of analysis took into account the existence of any motogenic activity present in the fractions which may mask the effect of any MSF-inhibitors present. The baseline was set as the level of migration achieved for each fraction group when tested alone and MSF- inhibition determined as the failure to increase migration by 50% above this level upon addition of 100pg/ml rhMSF.

Total HaCaT CM displayed only MSF-I bioactivity, however upon fractionation motogenic activity was also detected within the HaCaT CM. When tested alone it was clearly apparent that motogenic activity was present in the high molecular weight fraction groups 11 and 12, equivalent to 63-84kDa. Reproduced in four separate experiments, fraction groups 11 and 12 on average stimulated migration by 2-3 fold, as compared to the SF MEM control baseline migration. The remaining fraction groups displayed migration levels comparable to the SF MEM control (Figure 4.2).

While testing the fraction groups in the presence of rhMSF, distinct MSF- inhibitory activity was observed in the lower molecular weight fractions (Figure 4.3) Equivalent to 16-27kDa, fraction groups 15-17 inhibited the activity of 100pg/ml rhMSF by 57.0 +/- 9.08% (in an average of six experiments). A borderline MSF-I activity was also detected in Fraction groups 11 and 12 (3/6 experiments) (Figure 4.4). As motogenic activity had also been detected in this area, plus the molecular weight corresponded to that of MSF it was hypothesised that HaCaT expressed MSF must be responsible for

this bioactivity. Therefore, this inhibitory activity was actually due to the nature of MSF's bell shaped dose response bioactivity; the addition of "excess" rhMSF causing a shift in the bell-shaped response resulting in an inhibition of migration as compared to the rhMSF control baseline.

These results from fractionated CM indicate that the HaCaT keratinocytes are expressing two opposing factors; one which stimulates migration in a manner similar to MSF and another which possesses the ability to inhibit the motogenic activity of MSF. Since, the only bioactivity detected in the total HaCaT CM was MSF inhibition one could propose that the endogenous motogenic activity discovered is normally rendered inactive by the co-secretion of an inhibitor. The next stage therefore, was to identify the factors responsible for this bioactivity.

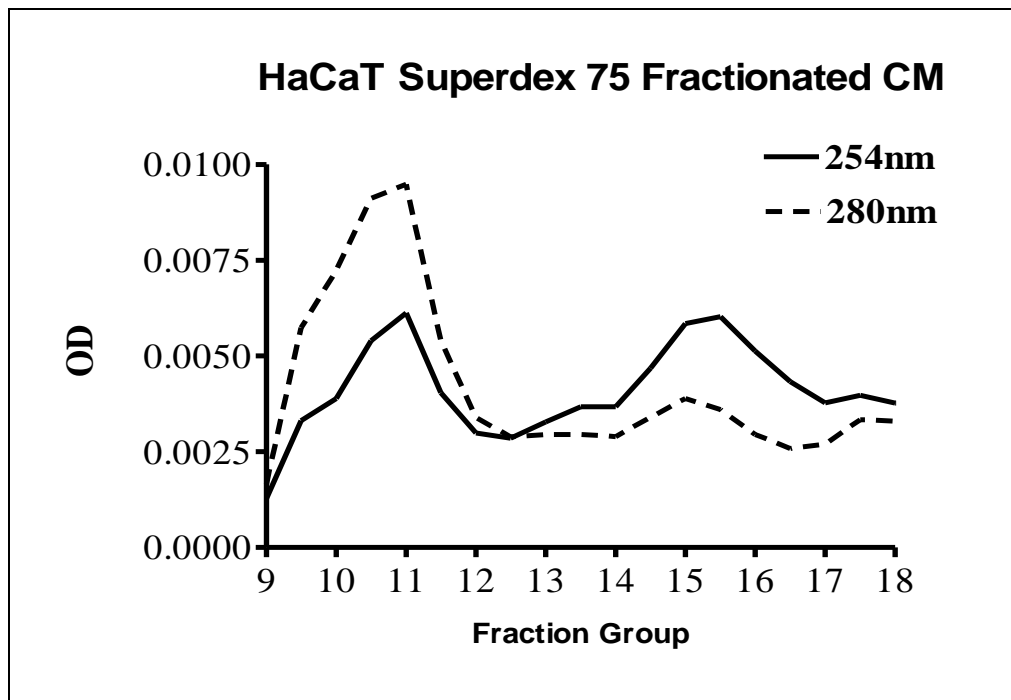


Figure 4.1: The fractionation of HaCaT keratinocyte conditioned medium by Size-Exclusion Chromatography. 4ml of 10x concentrated conditioned medium (CM) from HaCaT keratinocytes was applied to a Superdex 75 HiLoad 26/60 column (performed by Dr. S Jones). The eluant was monitored for absorbance at 254nm and 280nm. 100 x 3ml fractions were collected (2ml/min). The collected fractions were pooled together into groups of three. Fraction groups 9 to 18, equivalent to the main absorbance peak, were assayed for biological activity in the 3D collagen fibroblast migration assay.

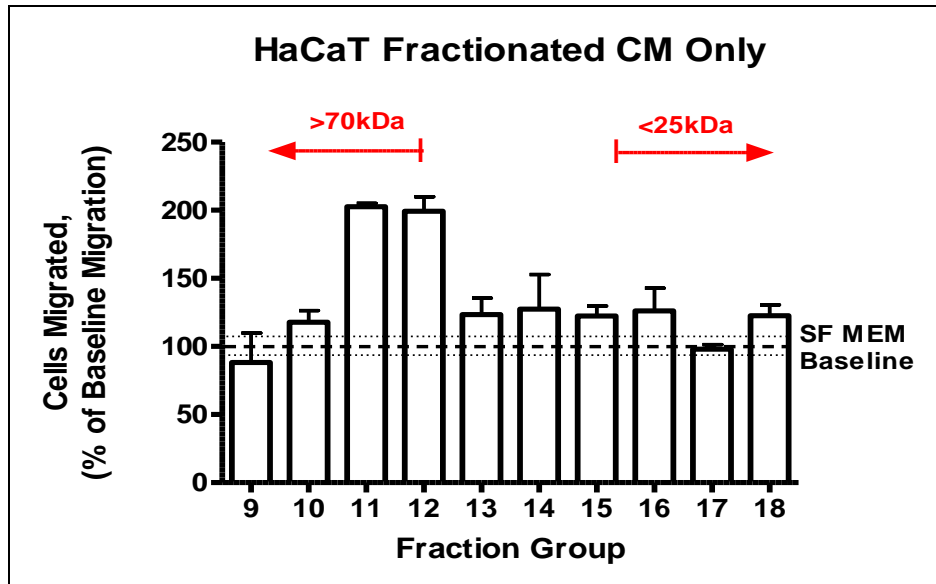


Figure 4.2: The motogenic activity of Superdex 75 fractionated conditioned medium from HaCaT keratinocytes. The fractionated conditioned medium (CM), fraction groups 9-18, from the HaCaT cell line was tested alone (final dilution 1/20), in the 3D collagen gel fibroblast migration assay. The number of cells migrated is expressed as a percentage of the SF MEM control baseline i.e. SF MEM Baseline = 100 +/- 8.6% as represented by the hatched and dotted lines (mean and SD respectively). This is equivalent to 2.2 +/- 0.66 migrated cells. The results represent an average of four experiments (one of the four experiments was performed by Dr.I.Ellis).

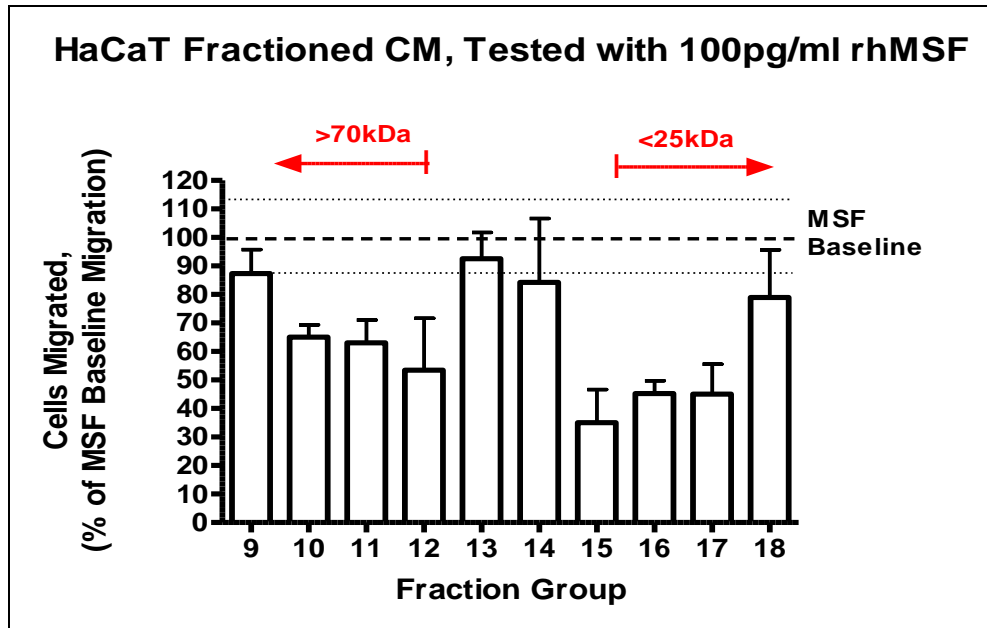


Figure 4.3: The MSF-Inhibitory activity of Superdex 75 fractionated conditioned medium from HaCaT keratinocytes. The fractionated conditioned medium (CM), fraction groups 9-18, from HaCaT cell line was tested in the 3D collagen gel fibroblast migration assay (final dilution 1/20), in the presence of 100pg/ml rhMSF. The number of cells migrated is expressed as a percentage of the 100pg/ml rhMSF control baseline migration i.e. MSF Baseline = 100 +/- 13.86%, as represented by the hatched and dotted lines (mean and SD respectively). This is equivalent to 5.7 +/- 0.79 migrated cells. The results represent an average of 6 experiments (one of the six experiments was performed by Dr.I.Ellis).

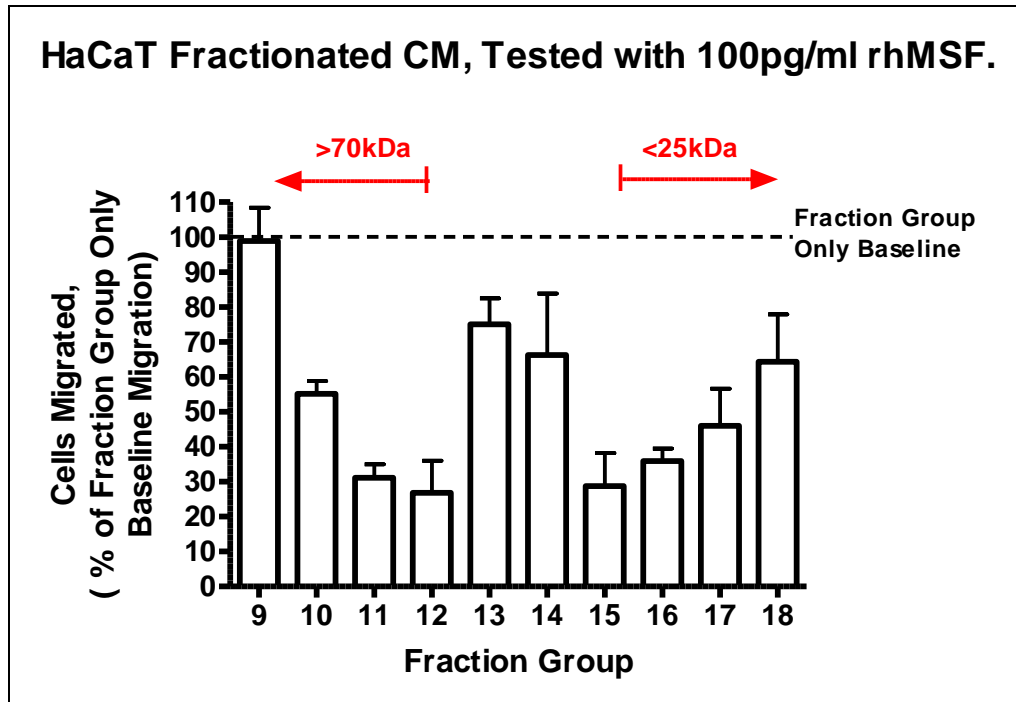


Figure 4.3: The motogenic activity of exogenous rhMSF in the presence of Superdex 75 fractionated conditioned medium from HaCaT keratinocytes. The fractionated conditioned medium (CM), fraction groups 9-18, from HaCaT cell line was tested in the 3D collagen gel fibroblast migration assay (final dilution 1/20), with and without the presence of 100pg/ml rhMSF. The number of cells migrated is expressed as a percentage of each individual fraction group only baseline migration i.e. Fraction group 9 = 100%, as represented by the hatched line. The results represent an average of 4 experiments (one of the four experiments was performed by Dr.I.Ellis).

4.5 THE IDENTIFICATION OF MSF EXPRESSION BY HACAT KERATINOCYTES

Total CM collected from cultured HaCaT keratinocytes showed no motogenic activity, however upon SEC fractionation stimulatory activity was discovered in the high molecular weight fractions (63-84kDa), equivalent to fraction groups 11 and 12. Due to the nature of the bioactivity and the molecular weight it was proposed that the HaCaT cells must be expressing MSF. In order to prove the hypothesis various biochemical, immunohistochemical and biological activity investigations were performed.

4.5.i Western Blot Identification of MSF

Using a specific anti-MSF antibody, RpVSI, attempts were made to identify MSF by immunoblotting of the total CM collected from HaCaT keratinocytes. CM was separated by 12% SDS PAGE under reducing conditions followed by immunoblotting with the RpVSI antibody. On each gel, 250pg rhMSF (25ng/ml) was loaded as a positive control; this resulted in a clear, strong main band of approximately 70-80kDa on the immunoblot. Unfortunately, no similar bands were ever observed for the HaCaT CM even when using CM concentrated by factor of up to 50 (Amicon method). Since, the same volume of the HaCaT samples as the rhMSF standard was loaded onto the gel one can conclude that if MSF is present in the HaCaT CM it is at a concentration below the limit of detection of this assay, which is less than 25ng/ml.

4.5.ii Colorimetric Sandwich ELISA for Total MSF

The development of a Colorimetric Sandwich ELISA assay for MSF had the potential to both identify and quantify MSF present within the HaCaT CM. The anti-IGD antibody, MAb PepQ 5.1, was employed for capture and the specific anti-MSF antibody, RPVSI, for identification (Materials & Methods chapter 2). A standard curve of rhMSF was included in every experiment; a maximum concentration of 200ng/ml serially diluted to 1.5625ng/ml. 100µl of each standard or sample was tested per well, with duplicate wells tested for each variable and an average reading calculated. SF MEM and coating buffer were used as negative controls. (Figure 4.4).

Unfortunately, whether using neat or 10x concentrated CM, OD readings consistently failed to be higher than the negative controls. Again, this would imply that either MSF

is not expressed by the HaCaT cells or it is present at concentrations below the assay's sensitivity, 12.5ng/ml. In addition the quality of the standard curve obtained in replicate experiments would suggest the assay is limited due to the suitability and quality of the antibodies used.

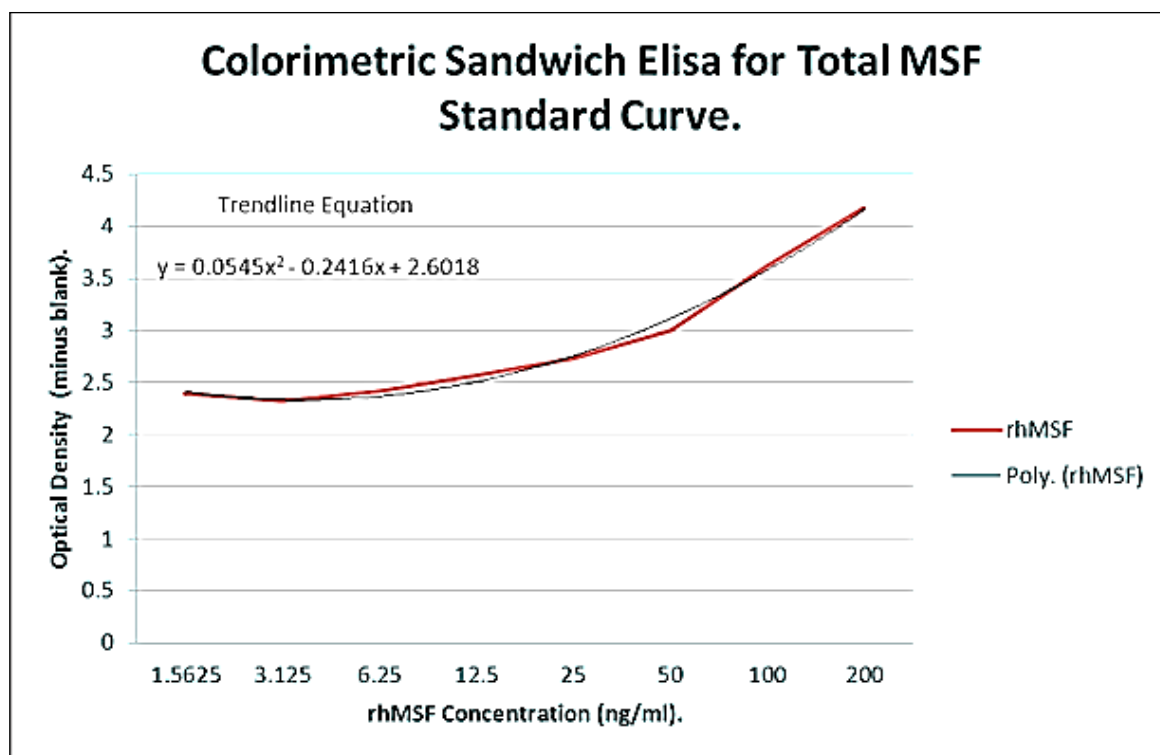


Figure 4.4: The standard curve of colorimetric Sandwich Elisa for Total MSF. An anti-IGD monoclonal antibody, MAb PepQ5.1 was employed for capture and a specific anti-MSF antibody, RpVSI, was used for the identification of a range of rhMSF standards (200-1.56ng/ml). OD readings were measured at 450nm. The results shown are an average of four individual experiments.

4.5.iii Immunolocalisation of MSF in HaCaT Keratinocytes.

By adopting an immunohistochemical method of detection, it was hoped any complications of MSF degradation in the HaCaT CM would be eliminated. Concerns were raised that the inability to detect MSF by the Western Blot and Sandwich ELISA techniques was a result of MSF having a short half-life in the CM; either due to the action of proteases present within the CM or as a consequence of storage (effect of freeze/ thaw cycles). It was also thought that the fixation step required in this technique could possibly assist in preserving any MSF present.

As described in Materials and Methods, Chapter 2, a rabbit polyclonal anti-VSI antibody (Rp2), raised against the MSF unique carboxyl terminal decapeptide, was used for the immunolocalisation of MSF in the HaCaT keratinocytes. A series of optimisation experiments were initially performed to select the optimum antibody concentration which ensured the best possible staining but also a consistent negative control at the same concentration (normal rabbit IgG) and no cross- reaction with the biotinylated secondary antibody (Goat Anti-Rabbit IgG). The known MSF negative cell line, FSF44, was also included in each experiment as additional control. In addition the primary keratinocyte cell line HEK 102-05a (ECACC No. 06091505) was also included in order to determine whether primary and transformed keratinocytes share a similar MSF expression.

Each cell line was plated onto plastic cell culture dishes and allowed to attach for 24-48 hours before fixation. Consistently the FS44 cells showed no MSF localisation, once again justifying their suitability in the 3D collagen gel migration. The HaCaT cells however repeatedly displayed a heterogeneously positive localisation of MSF. Whilst the HEK primary keratinocytes were also positive for MSF but displayed a more homogenous staining pattern; the staining also appeared to be stronger in intensity compared to the HaCaT cells. Staining with a normal rabbit IgG, at the same concentration as the anti-MSF antibody, was negative for all the cell lines assessed. This result therefore confirms that HaCaT cells express MSF and that MSF could possibly be responsible for the migration stimulating bioactivity detected in the fractionated HaCaT CM (Figure 4.5).

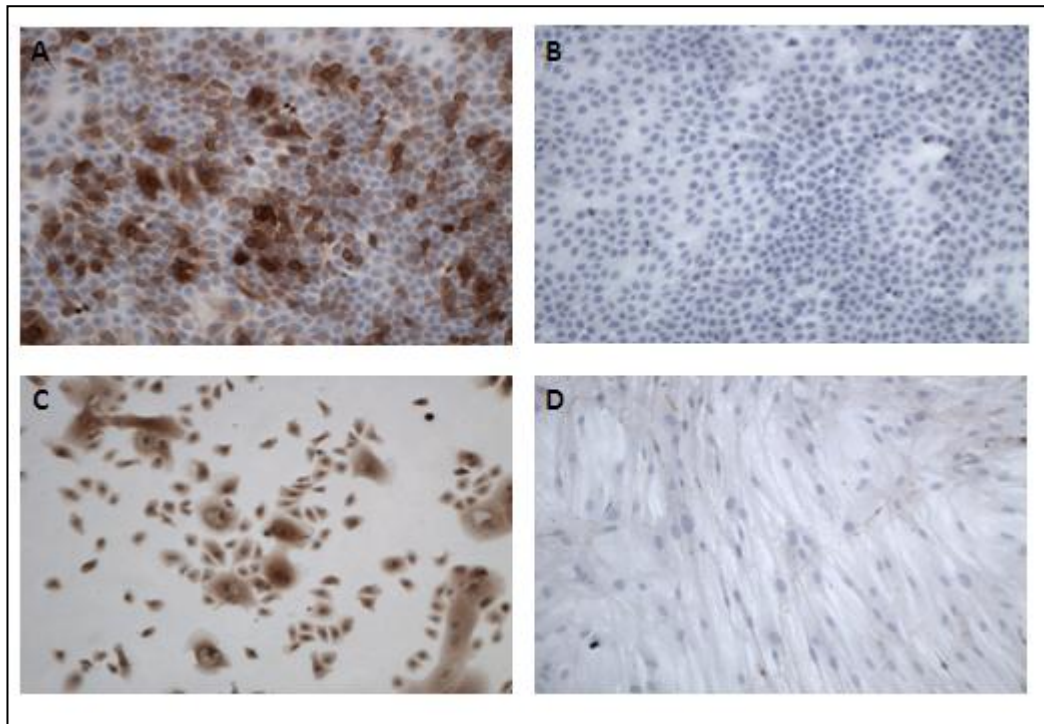


Figure 4.5: Immunolocalisation of MSF in human fibroblasts and keratinocytes.

Cells were plated onto plastic cell culture dishes and assessed for the presence of MSF by immunocytochemistry using the specific anti-MSF rabbit polyclonal Rp2 antibody (5 μ g/ml). MSF positive expression resulted in brown coloured staining. Control cultures were incubated with normal rabbit IgG at the same concentration as the MSF specific antibody (5 μ g/ml) (B). Images and observations were made at x20 magnification. Results showed that FSF44 fibroblasts (D) were negative for MSF, whilst both primary (C) and transformed keratinocytes (A) express MSF. However, there appears to be a difference in the intensity and distribution; primary keratinocytes displayed homogenous staining whereas HaCaT cultures showed a heterogeneous expression. Negative results were achieved with all cultures stained with the normal rabbit IgG.

A. HaCaT, Anti-MSF Rabbit polyclonal Rp2.

B. HaCaT, Normal Rabbit IgG

C. HEK, 102-5a primary keratinocytes, Anti-MSF Rabbit polyclonal Rp2.

D. FSF44. Anti-MSF Rabbit polyclonal Rp2.

4.5.iv The Characterisation of HaCaT Endogenous Motogenic Bioactivity.

The IGD function-neutralising monoclonal antibody, PEPQ 1.1, is a known inhibitor of MSF stimulated migration in the fibroblast collagen gel assay. It reliably inhibits the stimulatory activity of rhMSF back to SF MEM baseline levels, with maximal inhibition

of up to 1ng/ml rhMSF. By testing the motogenically active SEC fractions of HaCaT CM with the addition of PEPQ 1.1 antibody it is possible to determine whether the stimulatory activity detected is actually due to the presence of HaCaT expressed MSF. The motogenic SEC fraction groups 11 and 12 (63-84kDa) were pooled together (now referred to as F-msa; fractions displaying migration stimulating activity) and tested (final 1/20 dilution) in the presence of the PEPQ 1.1 antibody (50ng/ml). The criteria set for the inhibition of motogenic activity was a reduction in migration by at least 50% compared to the baseline level.

With SF MEM and 100pg/ml rhMSF acting as controls it was shown that the PEPQ 1.1 antibody had no effect on the SF MEM only baseline migration but was capable of completely inhibiting the rhMSF stimulated migration back to SF MEM only levels (approximately a 70% reduction in migration). A similar level of inhibition was seen in two separate experiments with the HaCaT F-msa sample. When tested alone F-msa stimulated migration by 3.7 fold more than SF MEM only baseline level, however upon addition of the PEPQ 1.1 antibody motogenic activity was inhibited on average by 60-70%. (Figure 4.6). These results suggest that the motogenic activity present in the HaCaT CM is due to the presence of an IGD motif, as found in MSF or other fibronectin- related molecules (i.e. fibronectin breakdown products).

4.5.v The Identification of MSF Expression in HaCaT Size Exclusion Fractionated Conditioned Medium.

As shown, the motogenic activity discovered in the SEC fractionated CM of HaCaT keratinocytes possesses characteristics similar to MSF. However, in order to provide definitive proof that HaCaT keratinocytes do express MSF immunoprecipitation (IP) with Protein G using the specific identification antibody, RpVSI, was performed. The rabbit polyclonal VSI antibody only recognises the MSF-unique carboxyl terminal decapeptide and consequently, under the appropriate conditions, any protein which binds to it must be MSF.

As described in Chapter 2, Materials & Methods, this technique involves the binding of any MSF present in the HaCaT SEC fraction groups 11 and 12 (F-msa) to the specific anti-MSF VSI antibody, and then capturing the complexes with immobilised protein G, thereby removing them from solution. After which the complexes are eluted and tested for bioactivity in the 3D collagen gel fibroblast migration assay. If the bound elution possesses the same motogenic activity as the original F-msa sample then the conclusion

would be that MSF is present in the HaCaT CM. In preparation, F-msa (MW 63-84kDa) from two separate SEC runs were pooled, dialysed against distilled water and then concentrated 100x by freeze drying. Immunoprecipitation was performed using 1ml of the resuspended F-msa sample. The resultant fractions were then tested for bioactivity in the collagen gel assay and where possible each was tested in duplicate at a range of dilutions; the 100x concentrated F-msa sample, unbound material and bound elutions 1 and 2. The same criteria as previously used to determine motogenic activity was adopted, namely an increase in migration of at least 50% as compared to SF MEM control baseline.

As expected, the 100x concentrated F-msa sample displayed the ability to stimulate fibroblast migration to a similar extent as 100pg/ml rhMSF control; a 3.-3.5 fold increase above SF MEM baseline levels. Following IP it would appear that all motogenic activity had been removed, as no stimulatory activity was detected in the unbound sample. However, the samples tested after the first elution (bound elution 1) demonstrated once again a level of motogenic activity similar to the rhMSF control; approximately a 2.8 fold increase above SF MEM baseline levels. Further elutions displayed no bioactivity. Figure 4.7.

As stated previously, the RpVSI antibody recognises the MSF-unique carboxyl terminal decapeptide. Therefore the discovery that the motogenic activity present in the high molecular weight SEC fractions of HaCaT CM could be removed upon binding to RpVSI would imply that the motogen responsible must possess the same unique VSI sequence. This result, coupled with the IHC and PEPQ1.1 antibody experiments, would validate the proposal that HaCaT keratinocytes express a bioactive form of MSF.

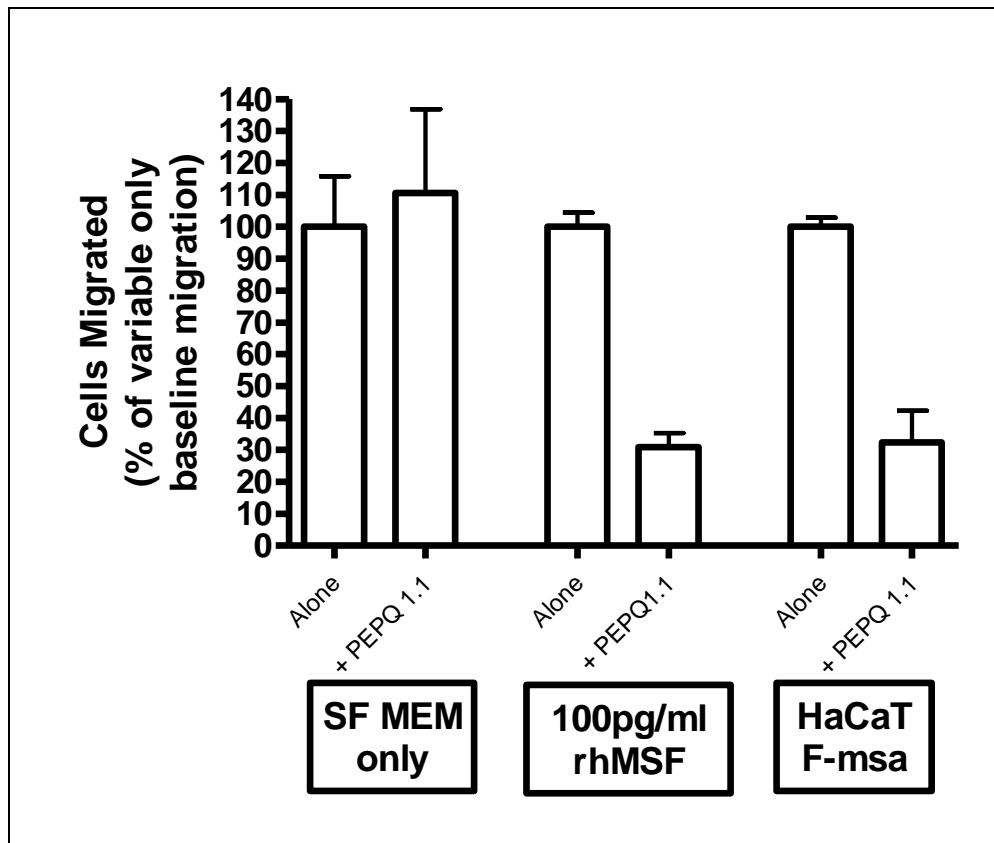


Figure 4.6: The effect of the MSF-Inhibitor, function neutralising antibody PEPQ 1.1, on the endogenous motogenic bioactivity of HaCaT Fractionated CM. The motogenic active Superdex 75 fraction groups 11 and 12 were pooled (referred to as F-msa) and tested (final dilution 1/20), with PEPQ1.1 (50ng/ml) antibody in the 3D collagen gel fibroblast migration assay. The number of cells migrated is expressed as a percentage of the variable only baseline migration i.e. HaCaT F-msa only = 100%. The effect of PEPQ 1.1 antibody on SF MEM and 100pg/ml rhMSF is shown for comparison. (SF MEM only migration is equivalent to 1.9 +/- 0.3 cells migrated, whereas 100pg/ml rhMSF is 6.8 +/- 0.3). The results represent an average of two experiments (one of the two experiments were performed by Dr.I.Ellis).

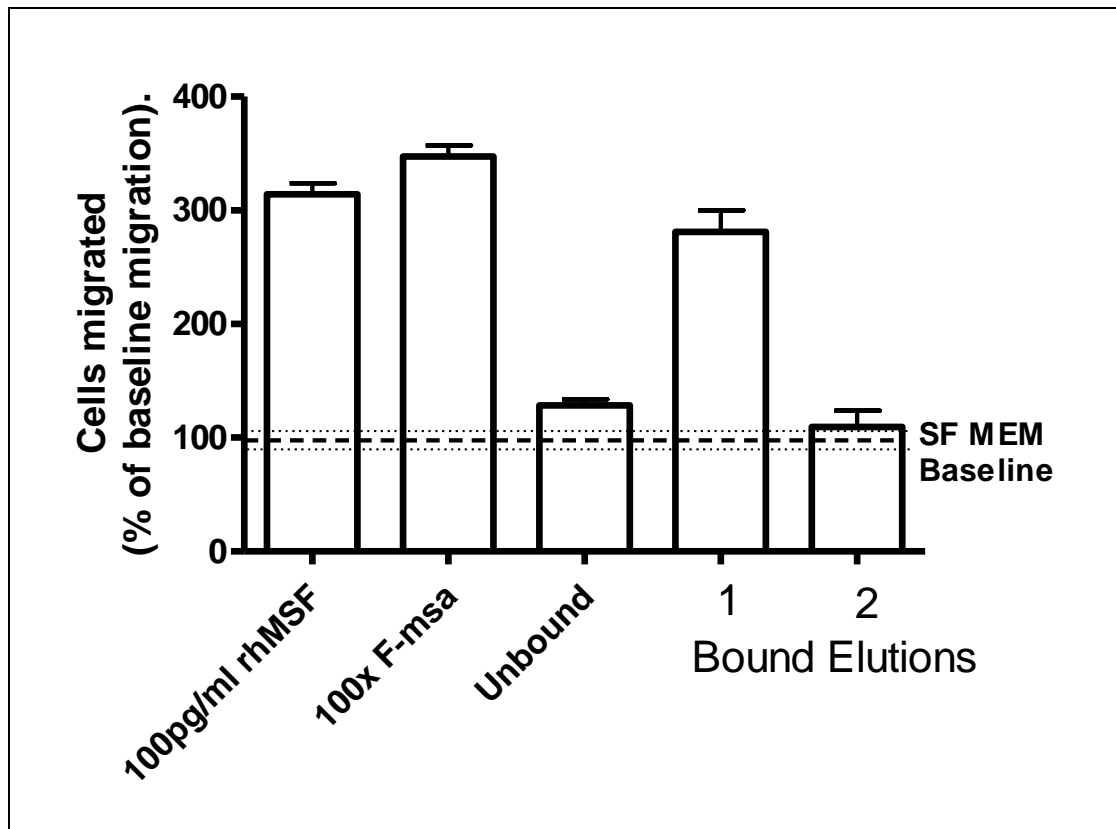


Figure 4.7: The motogenic activity of HaCaT SEC fractionated CM before and after immunoprecipitation with MSF-specific identification antibody RpVSI. The motogenic SEC fraction groups 11 and 12, equivalent to MW 63-84 kDa, were pooled (referred to as F-msa), dialysed and then concentrated 100x by freeze drying (100x F-msa). After which, immunoprecipitation with RpVSI MSF identification antibody was performed; unbound and two bound elutions were collected and tested. (The immunoprecipitation was performed by Dr S. Jones). All variables were tested alone in the 3D collagen gel fibroblast migration assay at a final dilution of 1/100. The number of cells migrated is expressed as a percentage of the SF MEM control baseline i.e. SF MEM Baseline = 100 +/- 9.52 represented by hatched and dotted lines (mean and SD respectively). This was equivalent to 2.1 +/-0.2 migrated cells. 100pg/ml rhMSF is shown for comparison (6.6 +/-0.2 migrated cells).

4.6 THE ISOLATION AND IDENTIFICATION OF MSF-I

It has been consistently shown that conditioned medium collected from cultured HaCaT keratinocytes contains a molecule with the ability to inhibit the motogenic activity of rhMSF. After SEC fractionation this MSF- inhibitory activity was located in the lower molecular weight fraction groups 15-17, equivalent to 16-27kDa. The next stage was to isolate and then, ultimately identify this MSF inhibitor (MSF-I).

4.6.i The Ion Exchange Fractionation of HaCaT Conditioned Medium.

SEC fractionation of HaCaT CM established that MSF-I must have a molecular weight below 30kDa but in order to identify the molecule responsible for the bioactivity further purification steps were required. By undertaking ion exchange chromatography the proteins present in the MSF-I active SEC fraction groups 15-17 would be separated further by the nature and degree of their ionic charge.

Initially optimisation experiments were performed, assessing the suitability of various anionic and cationic columns. The process of selection was determined by whether MSF-I bioactivity could be retained in the fraction containing the lowest percentage of total protein, thereby making subsequent purification steps easier. Before application to the columns, the MSF-I active SEC fraction groups 15-17 were pooled and dialysed against the appropriate buffer. Both bound and unbound fractions were then collected and tested in the 3D collagen gel fibroblast migration assay for the presence of MSF-I bioactivity; MSF-I activity determined by the ability to reduce 100pg/ml rhMSF motogenic activity by at least 50%, as compared to rhMSF control baseline. Where sample size permitted, each fraction was tested in duplicate and at a selection of dilutions.

Optimum results were achieved using the anion-exchange ANX column, where proteins with an overall negative charge bind to the column. As described in Chapter 2, Materials & Methods, the pooled SEC fractions were dialysed against 20mM Tris-HCl and then applied to the ANX column at a rate of 1ml/minute. Material unbound to the ANX column was collected and the bound material eluted as a single peak by washing the column with 20mM Tris-HCl pH 7.5 1M NaCl. Figure 4.8. Testing at a final dilution of 1/20 revealed that the MSF-I bioactivity was present in the unbound fraction, which represented 32% of the total protein applied to the column. On average the unbound material had the ability to inhibit rhMSF by 43.4% (+/- 7.01%). Figure 4.9. MSF-I, therefore, appears to have an overall positive charge at pH 7.5.

4.6.ii The SDS Electrophoresis Separation of HaCaT Anion Exchange Unbound Fractions.

Thus far, two chromatographic methods have been used, SEC and anion-exchange, to purify the MSF inhibitor present in the HaCaT CM. They have been successful in

separating MSF-I into a smaller and smaller subset of proteins. The final stage in MSF-I purification was to separate the components of the ANX unbound fraction by SDS electrophoresis under reducing conditions.

In preparation, the unbound material from several ANX runs were pooled together and concentrated by freeze drying, after dialysis against distilled water. The sample was redissolved in Laemmli loading buffer containing 5% (v/v) 2-mercaptoethanol and heated for 5 minutes at 95°C, prior to loading onto a pre-run 12% separating 5% stacking SDS polyacrylamide gel. (Chapter 2, Materials & Methods). Two lanes were run, one was stained with Coomassie for visualisation, and the other was cut into nine 0.5cm slices for protein elution. The protein present in each of the gel segments, S1-9 (from low to high molecular weights), was eluted during an overnight incubation in 1ml of elution buffer. Subsequently, the presence of MSF-I bioactivity in the gel elutes was determined in the 3D collagen gel fibroblast migration assay; that is the ability to reduce 100pg/ml rhMSF motogenic activity by at least 50%, as compared to rhMSF control baseline. Each elution tested at a final dilution of 1/1000.

The Coomassie stained lane displayed four distinct protein bands at 20-25kDa, 25kDa, 37kDa and 60kDa. Meanwhile, definitive MSF-I bioactivity was located in the gel elutions 3, 4 and 5; the elutions displaying the ability to inhibit 100pg/ml rhMSF by an average of 66%. Both elutions 4 and 5 corresponded to a protein band at 20-25kDa and 25kDa respectively (Figure 4.10 and 4.11A).

4.6.iii The Identification of MSF-I by Peptide Mass Fingerprinting.

The two protein bands, 4 and 5, possessing MSF-I bioactivity were sent to the University of Dundee's "Fingerprints" Proteomics Facility for protein identification. Each band underwent tryptic digest before analysis by mass spectrometry, MALDI-ToF-ToF (MS/MS) technique, using an Applied Biosystems 4700 Proteomic Analyser. Subsequently the "peak list" of protein masses was then compared to database data of known protein sequences, in order to find the best match.

The identity of the proteins in bands 4 and 5 were neutrophil gelatinase associated lipocalin (NGAL or lipocalin-2) and triosephosphate isomerase (TPI), respectively. A literature search on both proteins revealed that NGAL is a member of a large family of small secreted glycoproteins, which are characterised by a highly conserved tertiary structure, 8-stranded anti-parallel β -barrel, and their ability to bind and transport small lipophilic molecules (Flower 1996, 2000). NGAL was first isolated from neutrophils as

a heterodimer covalently linked to matrix metalloproteinase-9 (MMP-9) (Kjeldsen *et al.*, 1993). NGAL is a multifunctional protein having numerous roles attributed including bacteriostatic agent, acute-phase protein, inducer of mesenchymal-epithelial transition during development and the opposing roles of both tumour promoter and suppressor (Gwira 2005, Bratt 2000). TPI is a glycolytic enzyme present in all cells and is essential for efficient energy production. A deficiency of TPI in humans is a rare autosomal recessive multisystem disorder characterised by progressive neurological dysfunction and childhood death (Orosz *et al.*, 2006, Olah *et al.*, 2002).

The information gathered from the literature search indicated that NGAL would appear to be the most likely candidate responsible for the MSF-I activity present in HaCaT CM. The main reasons being firstly, that NGAL was located in band 4 which possessed the maximal MSF inhibitory activity. Also, since primarily experiments revealed that not all cell types possess the ability to inhibit MSF bioactivity, the knowledge that TPI is found in all cells in numerous organisms does not tally with our findings. It has also been reported that keratinocytes do express NGAL (Mallbris *et al.*, 2002, Seo *et al.*, 2004). Finally, of the numerous functions attributed to NGAL its association with MMP-9, where it acts in a protective manner preserving MMP-9 from degradation, suggested that it has the potential to bind to MSF (Yan *et al.*, 2001). MSF shares some structural similarity to MMP-9, with both molecules containing fibronectin type II domains and zinc binding motifs, with the conserved sequence HEXXH in MSF and AHXXGHXXGXXH in MMP-9 (Houard *et al.*, 2005, Van de Steen 2001). Consequently, the next stage was to prove definitively that NGAL is indeed responsible for the MSF inhibitory activity present in HaCaT CM.

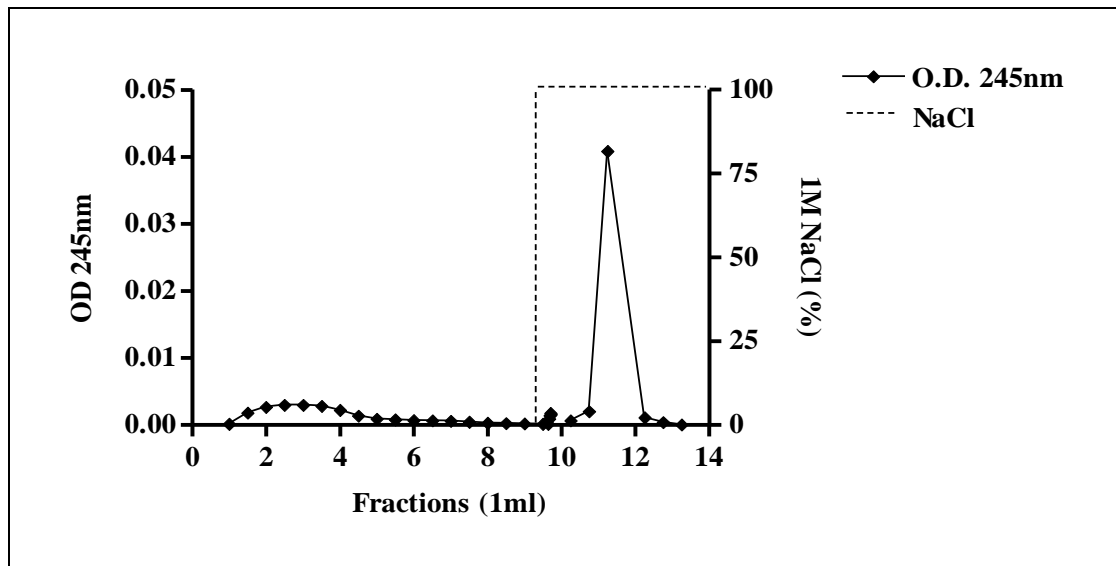


Figure 4.8: The purification of MSF-I active SEC fractions by Anion- Exchange Chromatography. After HaCaT conditioned medium was fractionated by size exclusion chromatography (SEC), the MSF-I bioactive fractions (MW16-27kDa) were applied to an ANX anion-exchange column (Hi trap FF), at a flow rate of 1ml/min, for further separation. Analysis of protein peaks (measured at 254nm) revealed that 68% of the total protein bound to the column, with 32% in the unbound fraction. Fractionation performed by Dr S. Jones.

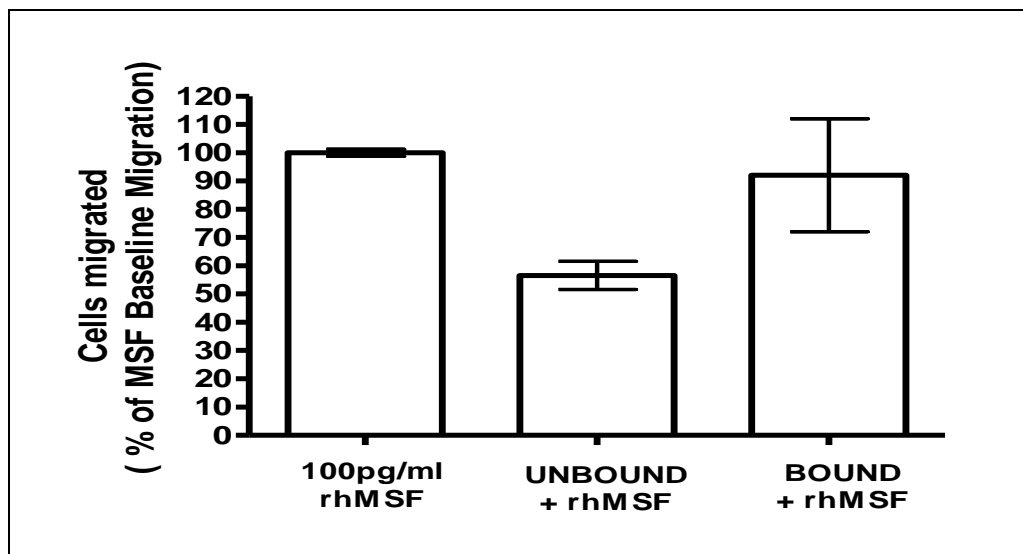


Figure 4.9: The bioactivity of Anion-Exchange, ANX, purified MSF-I bioactive HaCaT SEC fractions. After HaCaT conditioned medium was fractionated by size exclusion chromatography (SEC), the MSF-I bioactive fractions (MW16-27kDa) were applied to an ANX anion-exchange column (Hi trap FF), at a flow rate of 1ml/min, for further separation. The unbound and bound material was then tested in the 3D collagen gel fibroblast migration assay (final dilution 1/20), in presence of 100pg/ml rhMSF. The number of cells migrated is expressed as a percentage of the 100pg/ml rhMSF control baseline migration i.e. MSF Baseline = 100 +/- 1.24% (mean and SD). This is equivalent to 5.65 +/- 0.07 migrated cells.

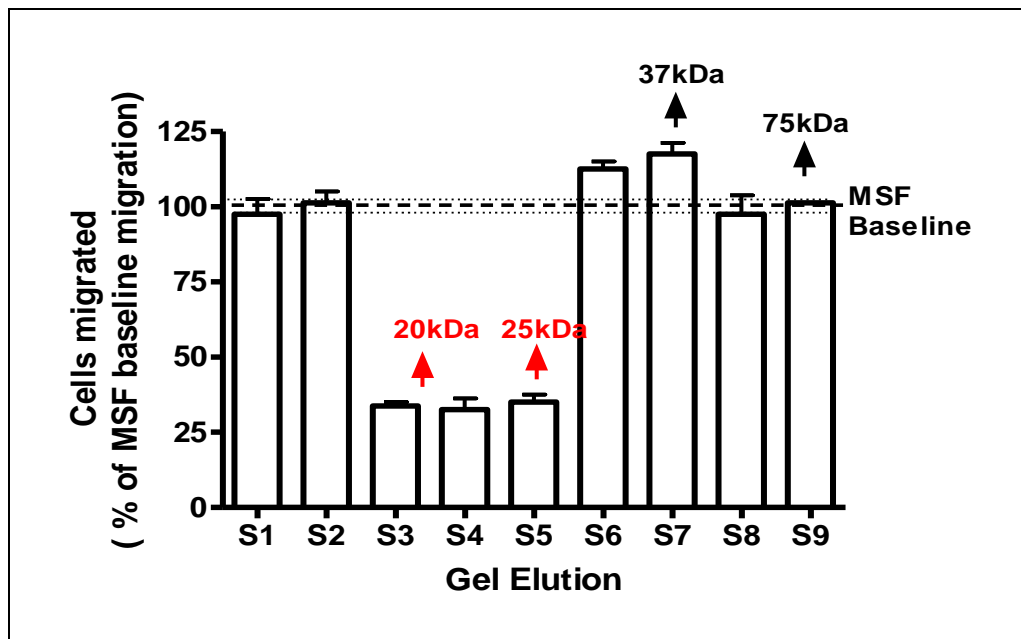


Figure 4.10: The MSF-Inhibitory activity of gel elutions from the SDS Electrophoresis fractionation of ANX purified MSF-I bioactive HaCaT SEC fractions. After the SDS electrophoresis of the HaCaT ANX sample and segmentation of the gel, the protein eluted from each segment (S1-9) was tested (final dilution 1/1000) in the 3D collagen gel fibroblast migration assay in the presence of 100pg/ml rhMSF. The number of cells migrated is expressed as a percentage of the 100pg/ml rhMSF control baseline migration i.e. MSF Baseline = 100 +/- 1.25, as represented by the hatched and dotted lines (mean and SD). This is equivalent to 8.0 +/- 0.1 migrated cells.

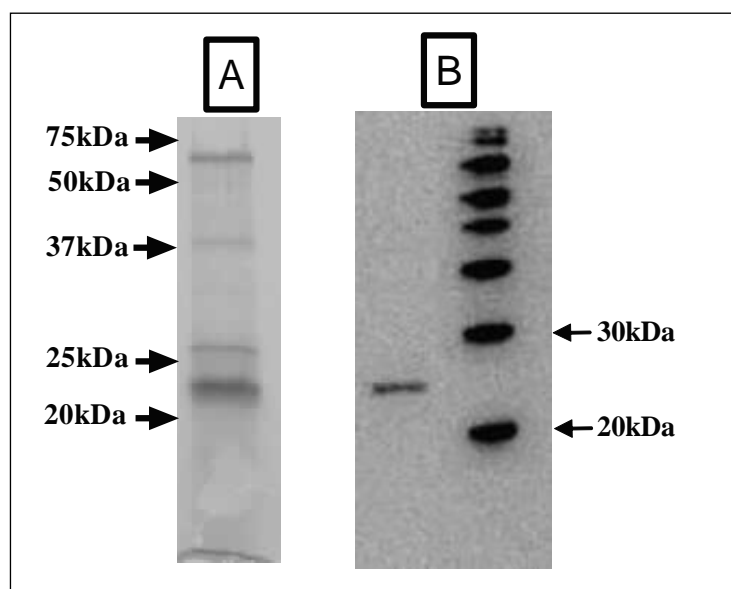


Figure 4.11:

A. The purification of MSF-I by SDS electrophoresis. The unbound material of the ANX fractionation of HaCaT SEC fractions, possessing MSF-I bioactivity was pooled, concentrated and then further separated by 12% SDS PAGE under reducing conditions. Two identical sample lanes were run, one for protein elution (see Figure 4.9) and the other, as shown, stained with Coomassie blue to visualise protein bands. The major protein band at 20-25kDa corresponded to maximal MSF-I bioactivity as detected in the fibroblast migration assay. The image shown was performed by Dr S. Jones.

B. The identification of NGAL in HaCaT un-fractionated CM by Immunoblotting. Immunoblot of the 12% SDS PAGE separation of HaCaT Series 5x concentrated CM, under reducing conditions, with specific anti-NGAL antibody, Mab1757. A distinct band was seen at approximately 25kDa, confirming the presence of NGAL. A lane of standards is shown as a molecular weight reference. The image shown was performed by Dr S. Jones.

4.7 THE VERIFICATION OF NGAL AS THE HACAT MSF-I

In order to purify MSF-I bioactivity and identify NGAL as the molecule responsible, the HaCaT CM underwent a series of fractionation and concentration steps.

It was therefore necessary to prove definitively that the HaCaT keratinocytes do express NGAL and that it is present within HaCaT CM, thereby silencing any suggestion that the discovery is either an artefact of the process or a contaminant. It is also necessary to confirm that NGAL alone is responsible for the MSF-I bioactivity of HaCaT CM and is not reliant on another, as yet, unidentified factor(s) in the HaCaT CM.

4.7.i Western Blot Identification of NGAL in Un-Fractionated HaCaT CM

The simplest method to prove that NGAL was present in the HaCaT CM was to perform an immunoblot using a specific anti-NGAL antibody, Mab1757. Total HaCaT CM was tested neat and concentrated 5x, using the Amicon method and then separated by 12% SDS PAGE under reducing conditions, followed by immunoblotting with the anti-NGAL antibody (Chapter 2, Materials & Methods). Visualisation by chemiluminescence identified a clear band at approximately 20-25kDa, in both neat and concentrated samples. Thereby, confirming that NGAL is present in the HaCaT CM (Figure 4.11B).

4.7.ii Colorimetric Indirect ELISA for NGAL in Un-Fractionated HaCaT CM.

The concentration of NGAL in HaCaT CM was determined by indirect ELISA using a specific anti-NGAL antibody (polyclonal antibody AF1757), as described in Materials & Methods Chapter 2. Included in each experiment was a standard curve for NGAL, performed using recombinant human NGAL (in house preparation) at a range of concentrations from 1.5625 to 300ng/ml (Figure 4.12). Each standard or sample of HaCaT CM was tested in duplicate, 100µl per well, and an average reading calculated. SF MEM and coating buffer were used as negative controls.

Initial experiments were performed using concentrated HaCaT CM but it soon became apparent that the concentration of NGAL present in the CM was higher than expected, since all OD readings were off the standard scale. However, by using neat CM and subsequently diluting it with coating buffer credible readings were achieved.

As shown in Table 4.1, it would appear that on average the NGAL concentration per ml of HaCaT CM is 1.77 +/- 0.05µg/ml. Taking into account the standard protocol for the collection of CM; whereby 7ml of SF MEM is used per 90mm dish of confluent HaCaT cells for a 48hr incubation period, and that on average each confluent dish would contain 5.4×10^6 cells (as measured with the Z1 Series Coulter Counter), which gives a total of 7.7×10^5 cells per ml of CM. Estimating therefore, that each HaCaT keratinocyte must be responsible for producing 2.3pg of NGAL per ml of CM, during a 48hr incubation period. This is of course an extremely approximate value as no accountability has been taken for the role which storage conditions and proteolysis may play in affecting the NGAL concentration.

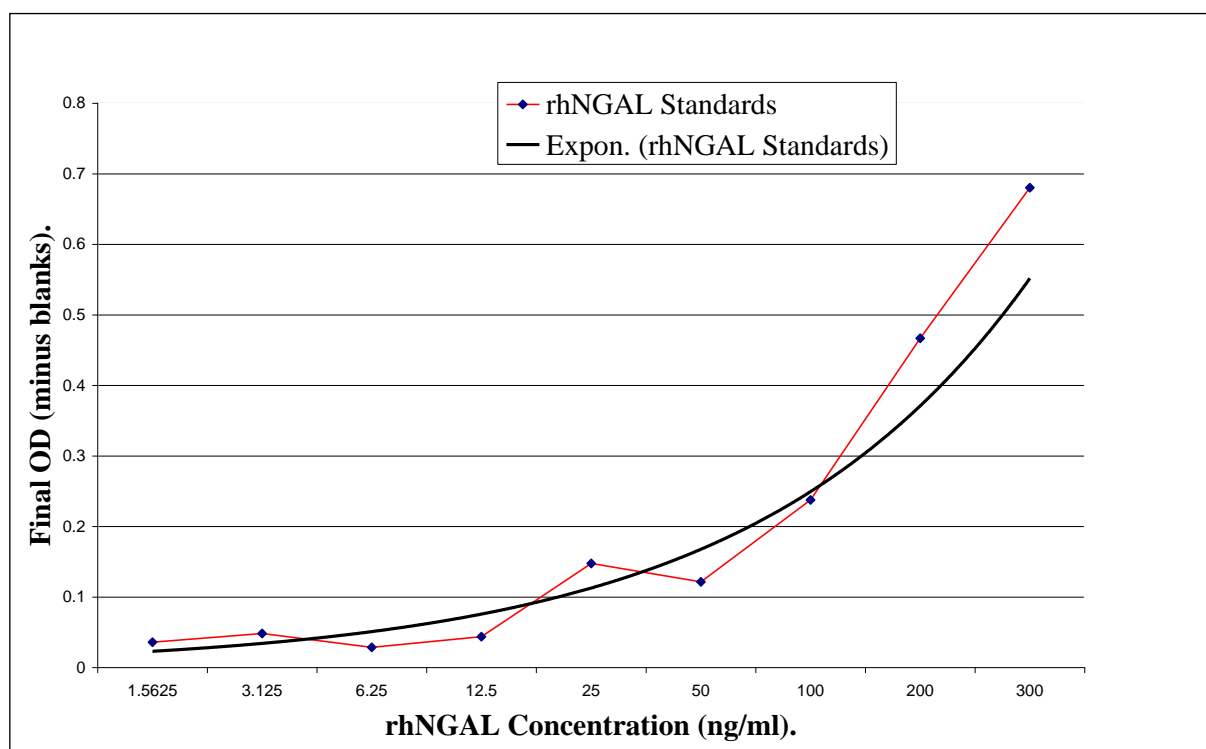


Figure 4.12: The standard curve of NGAL Indirect Elisa. Using a specific anti-NGAL antibody (polyclonal antibody AF1757) the OD readings for a range of rhNGAL concentrations (in –house preparation), were measured at 450nm. The results shown are an average of five individual experiments.

Table 4.1: The OD readings and calculated concentration of NGAL in HaCaT conditioned medium, as measured in the Indirect ELISA assay using a specific anti-NGAL antibody (polyclonal antibody, AF1757). OD readings measured at 450nm and all conditioned medium (CM) dilutions made using coating buffer. These results imply that the average concentration of NGAL per ml of HaCaT CM is 1.77 +/- 0.05 μ g/ml.

CM Dilution (Coating buffer diluent)	Final OD (450nm) Minus Blank.	NGAL Concentration (ng/ml)	NGAL Concentration- Adjusted for dilution (μ g/ml)
1:8	0.472	220.05	1.76
1:16	0.231	107.69	1.72
1:32	0.122	56.88	1.82

4.7.iii Immunolocalisation of NGAL in HaCaT Series

As previously discussed, a successful method of proving HaCaT cells expressed MSF was by immunolocalisation using the specific anti-MSF, rabbit polyclonal anti-VSI, antibody. Therefore immunolocalisation of NGAL in the cultured HaCaT keratinocytes was performed in order to determine whether there was any variation in the staining patterns of MSF and NGAL. As with the MSF identification, cells were plated onto plastic tissue culture dishes. Using a polyclonal antibody specific for NGAL, (AF1757), optimisation experiments were performed first. Thereby, enabling the selection of the most appropriate concentration of anti-NGAL antibody; that is optimum staining whilst ensuring the negative control (normal serum goat IgG) used at the same concentration was consistently negative. The secondary antibody, biotinylated polyclonal swine anti-goat IgG, was also optimised to ensure no cross-reactivity. In each experiment, the FSF44 fibroblast cell line acted as an internal negative control. In addition the primary keratinocyte cell line HEK102-05a (ECACC No. 06091505) was also included. Confirming the results of the immunoblotting and ELISA experiments, staining of HaCaT cells with a specific anti-NGAL antibody resulted in a positive result. NGAL and MSF appear to have a similar staining pattern; HaCaT cultures showing a heterogeneous expression whilst the primary keratinocytes displayed a homogenous expression with a slight increase in intensity too. As anticipated, the FSF44 fibroblasts did not express NGAL. A consistent negative result was also attained when using the normal goat IgG (Figure 4.13).

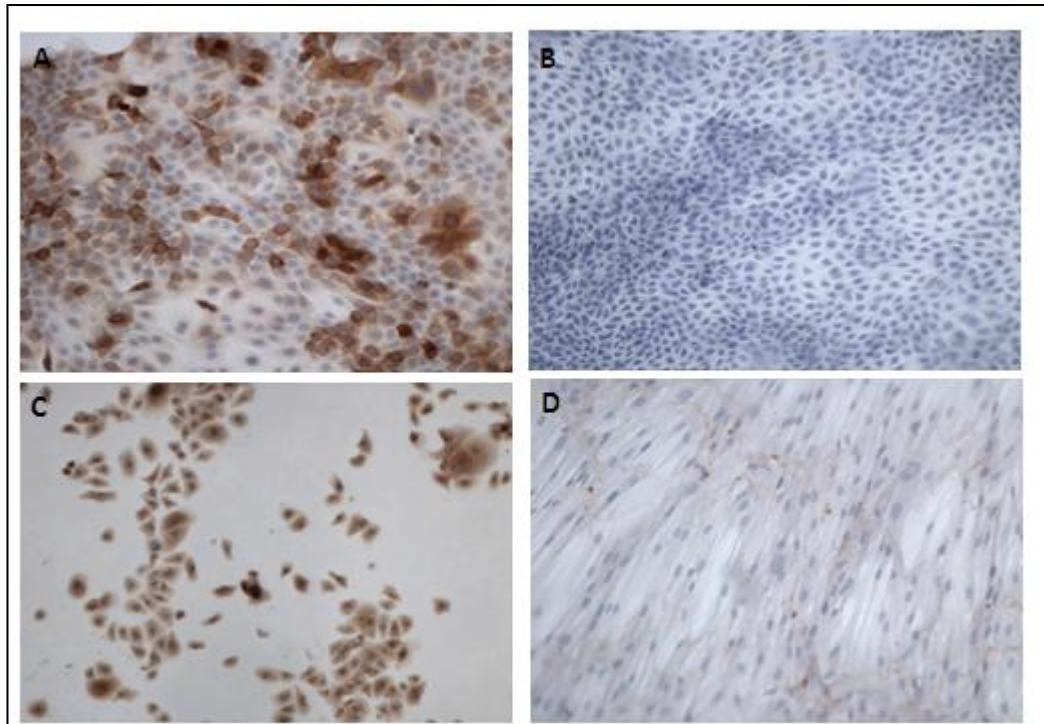


Figure 4.13: Immunolocalisation of NGAL in human fibroblasts and keratinocytes.

Cells were plated onto plastic cell culture dishes and assessed for the presence of MSF by immunocytochemistry using the specific anti-NGAL goat polyclonal AF1757 (0.5 μ g/ml). NGAL positive expression resulted in brown coloured staining. Control cultures were incubated with normal goat IgG at the same concentration as the NGAL specific antibody (0.5 μ g/ml) (B). Images and observations were made at x20 magnification. Results showed that FSF44 fibroblasts (D) were negative for NGAL, whilst both primary (C) and transformed keratinocytes (B) express NGAL. However, there appears to be a difference in the intensity and distribution; primary keratinocytes displayed homogenous staining, whereas HaCaT cultures showed a heterogeneous expression. Negative results were achieved with all cultures stained with the normal goat IgG.

A. HaCaT, anti-NGAL goat polyclonal AF1757.

B. HaCaT, Normal Goat IgG

C. HEK, 102-5a primary keratinocytes, anti-NGAL goat polyclonal AF1757.

D. FSF44, anti-NGAL goat polyclonal AF1757.

4.7.iv The MSF Inhibitory Activity of NGAL

NGAL isolated and purified from HaCaT CM has been shown to have the ability to inhibit the motogenic bioactivity of rhMSF in the 3D collagen fibroblast migration assay. Using the same assay, NGAL from three different sources was tested in order to validate the findings; NGAL isolated from a MMP-9/ NGAL complex isolated from activated neutrophils (complex purchased from Calbiochem), eukaryotic rhNGAL (purchased from R&D Systems) and prokaryotic rhNGAL (in-house preparation). As with the first isolation of NGAL by Kjeldsen *et al.*, 1993, from neutrophils as a heterodimer covalently linked to MMP-9, NGAL was isolated from a MMP-9 complex (Calbiochem) (performed by Dr S.J. Jones). The complex was fractionated into its separate components by electrophoresis under reducing conditions, using loading buffer containing 2-mercaptoethanol followed by separation on 12% SDS PAGE . Each lane was loaded with 1.5µg of the reduced complex. Using a lane for visualisation; staining with Coomassie blue revealed three distinct protein bands at the following molecular weights 15-20kDa, 20-25kDa and 75-100kDa. An immunoblot, using specific anti-NGAL antibody, Mab1757, was performed and the bands at 20-25kDa and 75-100kDa were identified. One could presume that the larger molecular weight band of 75-100kDa corresponded to non-reduced MMP-9/ NGAL complex (and free MMP-9), while the 20-25kDa band represented free NGAL. The 15-20kDa may correspond to the C-terminus fragment of MMP-9. A subsequent lane was used for protein elution; where upon each protein band was isolated and the proteins eluted overnight in elution buffer (Material & Methods, Chapter 2).

In order to determine which band contained the isolated NGAL each of the three elutions were tested in the 3D collagen gel fibroblast migration assay at a range of dilutions (1/1000 to 1/30,000). The majority of MSF inhibitory activity was discovered in the elutions of the lower molecular weight protein bands 15-20kDa and 20-25kDa; elutions 2 and 3 respectively (similar results in 3/3 experiments). Observations from the SDS PAGE gel formed the conclusion that elution 3, 20-25kDa, probably contained the majority of the free NGAL.

It was estimated that elution 3 diluted 1/20,000 with SF MEM, would contain an estimated NGAL concentration of 5-10ng/ml. This dilution was then subsequently tested in the 3D collagen gel fibroblast migration assay, against a range of rhMSF concentrations (1pg- 10ng/ml). When tested by itself, the NGAL elution had no effect on fibroblast migration, with levels similar to the SF MEM control. rhMSF tested by

itself displayed a typical bell-shaped dose response; migration stimulated by rhMSF concentrations 1pg/ml to 10ng/ml, with maximal motogenic activity at 500pg/ml, an average 3 fold increase above the SF MEM levels. The addition of the NGAL elution inhibited MSF activity, with MSF stimulated migration (10-500pg/ml) inhibited on average by 54% +/- 4.00. However, at the higher rhMSF concentration of 10ng/ml, the addition of the NGAL elution actually caused an increase in cell migration This is thought to be due to partial inhibition of MSF by NGAL, thereby shifting the dose response to levels where migration is actually stimulated (Figure 4.14 a and b).

This NGAL elution was also tested with the HaCaT sample referred to as Fmsa (fractions displaying migration stimulatory activity). As previously described Superdex fractionated HaCaT CM exhibited MSF- like bioactivity in fraction groups 11 and 12, equivalent to 63-84kDa. These MSF active fraction groups from numerous Superdex runs were pooled and subsequently concentrated by freeze drying; referred to now as F-msa. The 100x F-msa was tested at a range of dilutions (1/100 to 1/10,000) with the NGAL elution (1/20,000 dilution). As expected, from previous experiments the HaCaT F-msa exhibited the ability to stimulate fibroblast migration in a dose response manner similar to rhMSF; peak activity at 1/250 dilution. The addition of the NGAL elution inhibited this migratory activity; 1/250 dilution migration reduced by 60% (Figure 4.14c). This result and previous evidence supports our finding that the HaCaT cell line expresses both MSF and a MSF inhibitor (MSF-I), identified as NGAL (Figure 4.14 c). The other two types of NGAL which were tested was from both a eukaryotic (R&D, 1757-LC) and prokaryotic (in-house preparation) source. Each was tested in the 3D collagen gel fibroblast migration assay at a range of concentrations (100pg/ml to 1µg/ml) with a constant rhMSF concentration of 100pg/ml rhMSF. At the range of concentrations tested, both eukaryotic and prokaryotic NGAL had no effect on baseline migration. For example, in a comparison of three experiments using the prokaryotic NGAL, the average migration measured for all NGAL concentrations, when tested alone, was 2.16 +/-0.233 cells compared to 2.57 +/-0.551 for the SF MEM. A similar result was achieved for the eukaryotic NGAL; average NGAL only migration being 3.175 +/-0.222 as compared to 3.79 +/-0.293 for SF MEM baseline.

Consistently, migration is stimulated by approximately 50% upon addition of 100pg/ml rhMSF to SF MEM. Eukaryotic NGAL could inhibit this activity by an average of 44.4 +/-5.01% over a range of concentrations from 1ng/ml to 1µg/ml, with peak inhibitory activity of 51.53 +/- 3.50% at 1ng/ml (an average of three experiments). Prokaryotic NGAL had the same rhMSF inhibitory range of 1ng/ml to 1µg/ml with an average

inhibition of 59.6% +/- 9.13, peaking at 100ng/ml with migration reduced by 72.73 +/- 8.18% (an average of three experiments) (Figure 4.15).

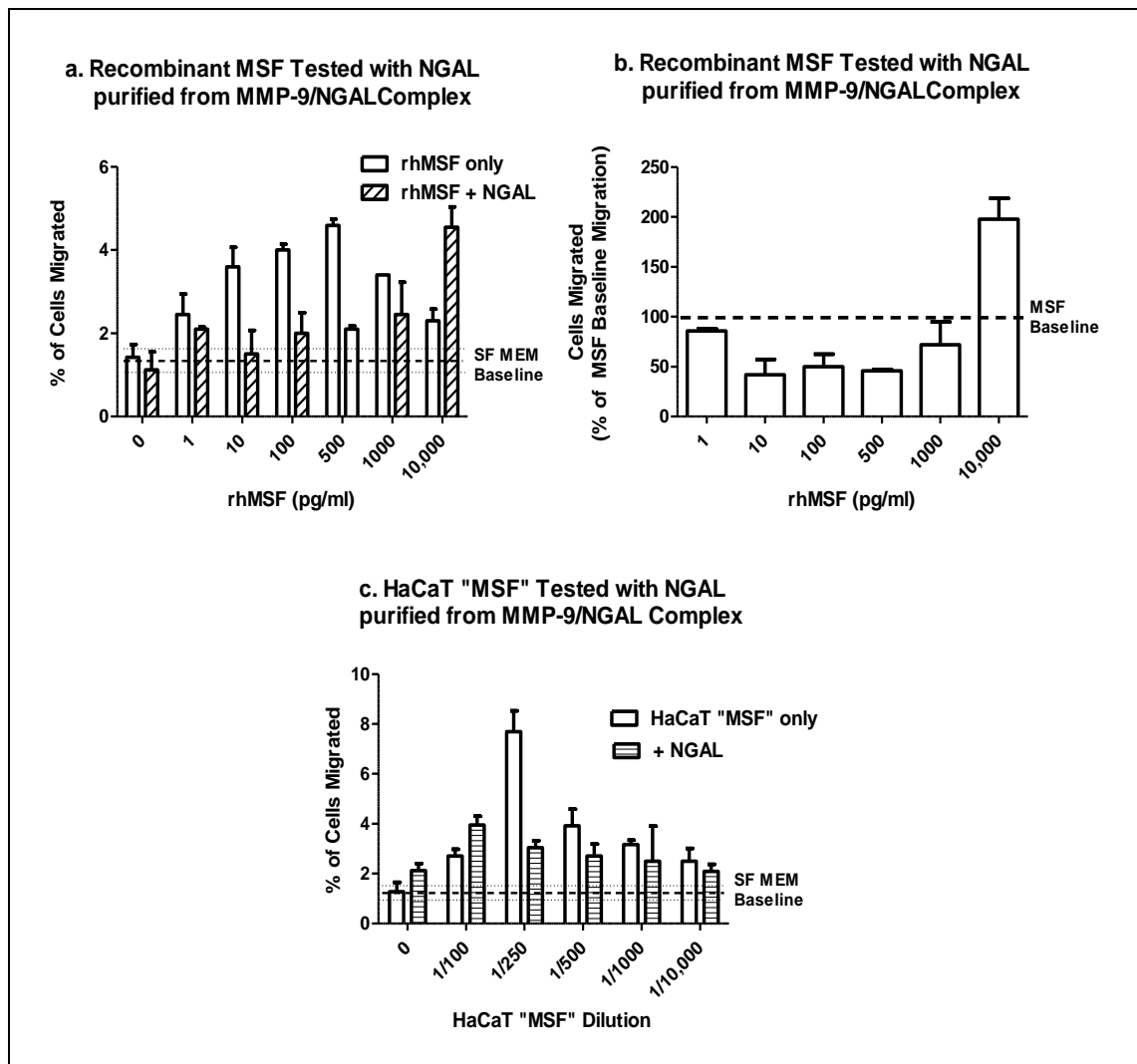


Figure 4.14. The MSF-Inhibitory activity of NGAL purified from MMP-9/NGAL

complex. NGAL was purified from the MMP-9/NGAL complex (Calbiochem) by SDS PAGE

separation followed by gel elution. The majority of free NGAL was found to be present in Gel Elution 3

(20-25kDa) at an estimated concentration of 5-10ng/ml when diluted 1/20,000 with SF MEM. This

dilution was tested against a range of concentrations of rhMSF (1pg/ml to 10ng/ml) and also a range of

dilutions of the HaCaT F-msa (Superdex fractions of HaCaT CM displaying migration stimulating

activity) in 3D collagen gel fibroblast migration assay. A representative experiment is shown. Graph a.

Effect of purified NGAL on a dose response of rhMSF, expressed as the percentage of cells migrated. SF

MEM baseline migration = 1.425 +/- 0.310, as represented by the hatched and dotted lines (mean and SD

respectively). Graph b. Effect of purified NGAL on a dose response of rhMSF. The number of cells

migrated expressed as a percentage of MSF baseline for each rhMSF concentration point i.e. 1pg/ml to

10ng/ml rhMSF baseline = 100%, as represented by hatched line. Graph c. Effect of purified NGAL on a

dose response of HaCaT Fmsa, expressed as the percentage of cells migrated. SF MEM Baseline = 1.28

+/- 0.250, as represented by the hatched and dotted lines (mean and SD respectively).

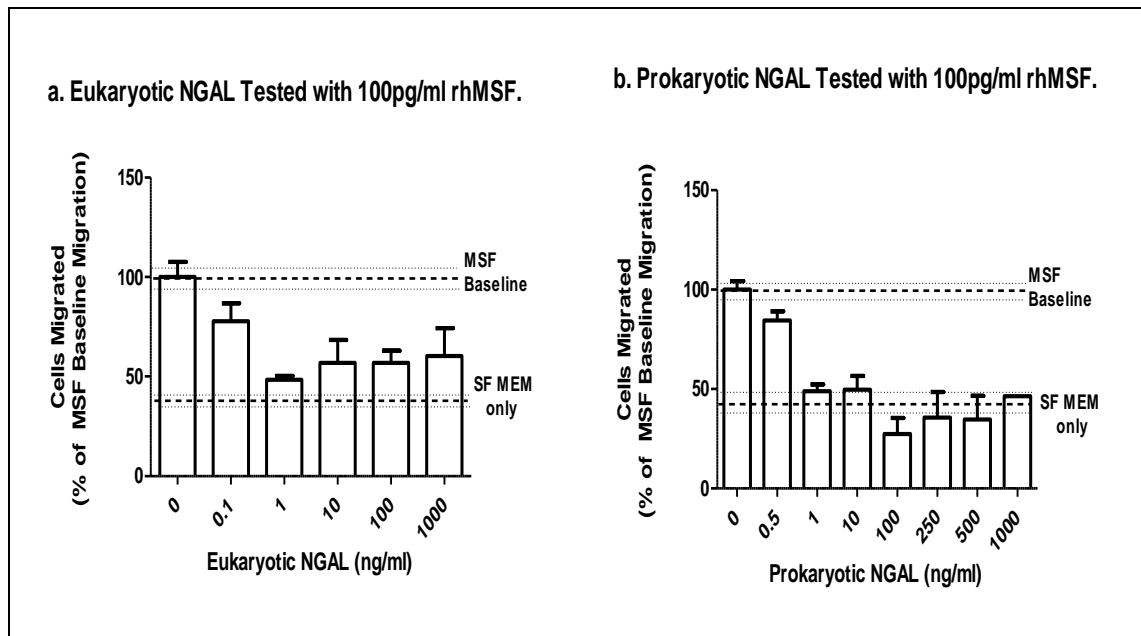


Figure 4.15 The MSF-Inhibitory activity of NGAL purified from a eukaryotic and prokaryotic source. A range of concentrations of both eukaryotic and prokaryotic expressed NGAL were tested in combination with a single concentration of 100pg/ml rhMSF in the 3D collagen gel fibroblast migration assay.

Graph a. The MSF-I activity of Eukaryotic NGAL. The number of cells migrated is expressed as a percentage of 100pg/ml rhMSF control baseline migration. i.e. MSF Baseline = 100 +/- 7.526, as represented by the hatched and dotted lines (mean and SD respectively). This is equivalent to 7.84 +/- 0.590 migrated cells. The results represent an average of three experiments (one of the three experiments performed by Dr I. Ellis).

Graph b. The MSF-I activity of Prokaryotic NGAL. The number of cells migrated is expressed as a percentage of 100pg/ml rhMSF control baseline migration. i.e. MSF Baseline = 100 +/- 4.17, as represented by the hatched and dotted lines (mean and SD respectively). This is equivalent to 6.05 +/- 0.252 migrated cells. The results represent an average of three experiments (one of the three experiments performed by Dr I. Ellis).

4.7.v The Effect of NGAL on Fibroblast Morphology, Viability and Proliferation.

No obvious toxicity problems had been observed when testing NGAL (all sources), alone or in combination with rhMSF, in the 3D collagen gel assay. Fibroblast morphology was normal and indistinguishable from the controls. However, as the assay requires the FSF44 fibroblasts to be plated at a high density (2×10^5 per gel) proliferation is limited; the number of cells on the collagen gel surface remains constant

over the four day period incubation period. Therefore, a simple growth curve experiment was performed in order to determine the effect NGAL had on fibroblast proliferation. Cells were plated at a low density (2×10^4 per 35mm dish) in the presence of 1% DCS MEM with and without the addition of various concentrations of prokaryotic expressed rhNGAL. Cell counts were measured successively over a 7 day period. The trypan blue assay was used to calculate cell viability (Chapter 2, Materials & Methods). In six experiments, prokaryotic rhNGAL tested at 0.01-1 μ g/ml had no effect on fibroblast morphology, viability and proliferation. Observations of the fibroblasts in the control (1% DCS MEM only) and those with the addition of NGAL showed no apparent differences and this were confirmed by comparable levels of cell viability and proliferation rates. The incubation period of the 3D collagen gel assay is 4 days and in a 4 day period in the growth curve assay cell numbers for all the variables tested was practically identical; a 3.525 \pm 0.096 fold increase in cell numbers whilst cell viability was a healthy 88.3 \pm 2.14% (Figure 4.16)

4.7.vi The MSF- Inhibitory Activity of NGAL can be Temporally Separated from MSF.

In all previous experiments the effect of NGAL on the MSF stimulated migration of fibroblasts in the collagen gel was performed with the co-incubation of rhNGAL and rhMSF. In order to understand the nature of NGAL's ability to inhibit MSF, it was investigated whether NGAL required direct contact with MSF for inhibition to occur. A variation of the 3D collagen gel fibroblast migration assay was performed; fibroblasts were plated onto the gels as normal but then pre-incubated with rhNGAL, after which media was removed and the gels washed with SF MEM, followed by a four day incubation with rhMSF. Three pre-incubation times were tested (1, 6 and 24 hours) with two concentrations of rhNGAL (prokaryotic source) in SF MEM; 10ng/ml and 50ng/ml having previously shown the ability to inhibit 100pg/ml rhMSF stimulated migration to baseline levels. The 100pg/ml rhMSF incubation was at a final serum concentration of 1% DCS MEM. Controls were performed to eliminate any possible artefacts occurring due the effect of washing the gels after NGAL pre-incubation.

It would appear from the results that pre-incubating the fibroblasts with NGAL for a minimum of 24 hours induces the same MSF inhibitory activity as seen with co-incubation of NGAL and MSF. The number of cells migrated into the gels in the controls were comparable to those under the standard protocol; 100pg/ml MSF

stimulating migration on average by 2 fold above SF MEM baseline levels. For rhNGAL to exert MSF inhibition to the same extent as measured during NGAL/MSF co-incubation the pre- incubation must be at least 24 hours; no effect was seen after a one hour incubation and partial MSF inhibition detected after six hours (Figure 4.17).

4.7.vii The MSF-Inhibitory activity of NGAL is Iron Independent.

The acquisition of iron is critical in development, cell growth and survival as iron contributes to enzyme activity in DNA synthesis, metabolism and oxygen response (Dunn *et al.*, 2007). Although, most cells acquire iron by capturing iron-loaded transferrin, another pathway is mediated by NGAL. NGAL is considered to play an important role in iron metabolism both during organogenesis and host defence (Iannetti *et al.*, 2008). The cellular uptake and delivery of NGAL-bound iron to epithelial cells is essential for epithelial cell differentiation in the developing kidney (Yang *et al.*, 2002). It has also been proposed that the expression of NGAL by numerous epithelial tumours bestows these cells with an iron retrieving mechanism that adds to the growth potential of the tumour (Hvidberg *et al.*, 2005). The pro-survival activity of NGAL in human thyroid cancer cells is mediated by its ability to bind iron and to transport it inside the cells, preventing apoptosis (Devireddy *et al.*, 2005, Iannetti *et al.*, 2008).

Therefore an investigation as to whether the MSF inhibitory activity of NGAL was dependent on its ability to sequester iron was performed. The iron chelator, deferoxamine mesylate (DFOM, Sigma-Aldrich) was selected as it had previously been shown to reverse the effects of NGAL on the phenotype of Ras- transformed breast cancer cells. DFOM removes both free iron and bound iron from hemosiderin; it has been shown to deplete iron from an intracellular pool as concentrations of 2-5 μ M in tissue culture (Hanai *et al.*, 2005).

A 3D collagen gel fibroblast migration assay was performed whereby the cells were incubated with DFOM alone or in combination with 100pg/ml rhMSF and 10ng/ml rhNGAL. The two concentrations of DFOM tested, 2 and 5 μ M, appeared to have no effect on the SF MEM baseline level of cell migration. Fibroblast morphology appeared unaffected by the presence of DFOM and cell numbers of fibroblasts present on the cell surface were comparable to the controls. A cell viability and proliferation assay confirmed that neither concentration of DFOM had any detrimental effect upon the cells (Table 4.2)

The motogenic bioactivity of rhMSF appears to be affected by incubation with DFOM. Increasing concentrations of DFOM having a greater ability to inhibit MSF stimulated fibroblast migration; compared to the 100pg/ml rhMSF control the addition of 2 and 5 μ M DFOM reduced migration by 43.5% and 69.4% respectively. This obviously limited the assessment of the effect iron chelation had on the MSF- inhibitory activity of NGAL. However, although 2 μ M DFOM reduced MSF stimulated migration it was still 1.8 fold more than the SF MEM baseline level. The addition of 10ng/ml rhNGAL reduced this increase back to the SF MEM levels. This effect was confirmed in two experiments. As MSF activity was completely diminished by 5 μ M DFOM, the addition of rhNGAL had no effect on migration levels (Figure 4.18).

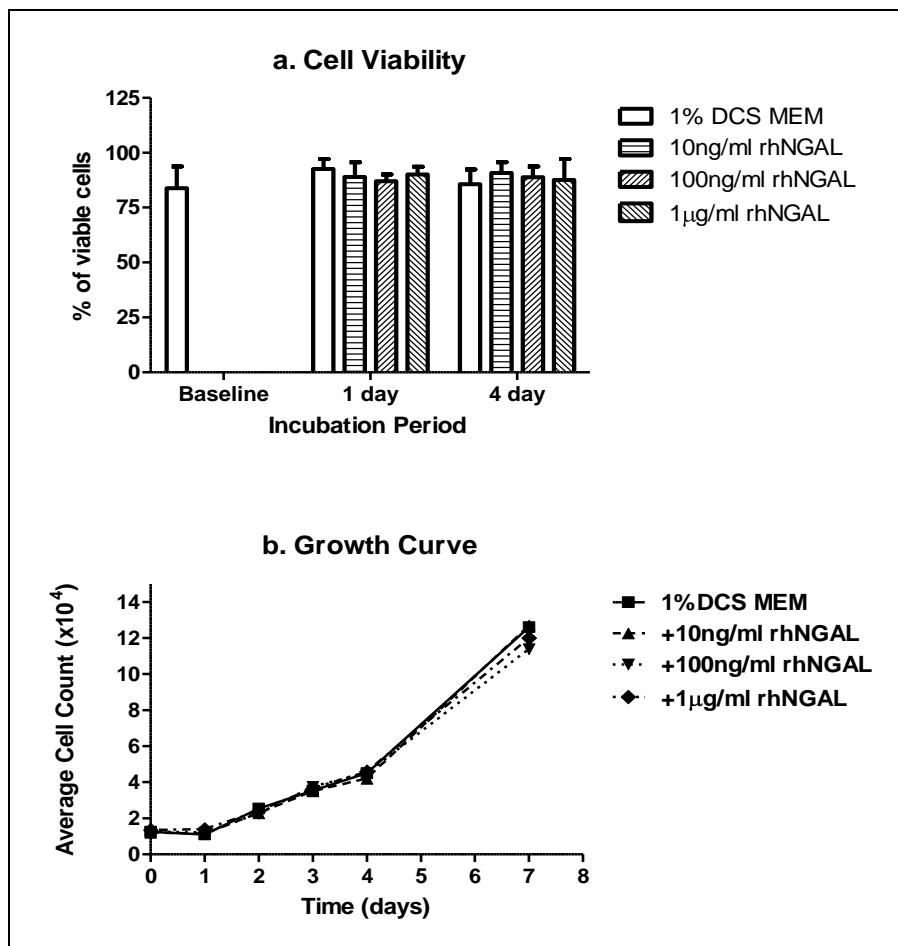


Figure 4.16. The effect of NGAL on fibroblast viability and proliferation.

Fibroblasts, FSF44, were plated at low density (2×10^4 per 35mm) in the presence of 1% DCS MEM with and without the addition of 0.1- 1 μ g/ml rhNGAL. Cell viability and cell counts were taken over a 4-7day incubation period. An average of six experiments is shown.

Graph a. The percentage of cell viability of each variable was measured by the trypan blue assay. Graph b. The average cell count at each time point, for each variable was measured with the Coulter Counter Z1 Series (Beckmann Coulter).

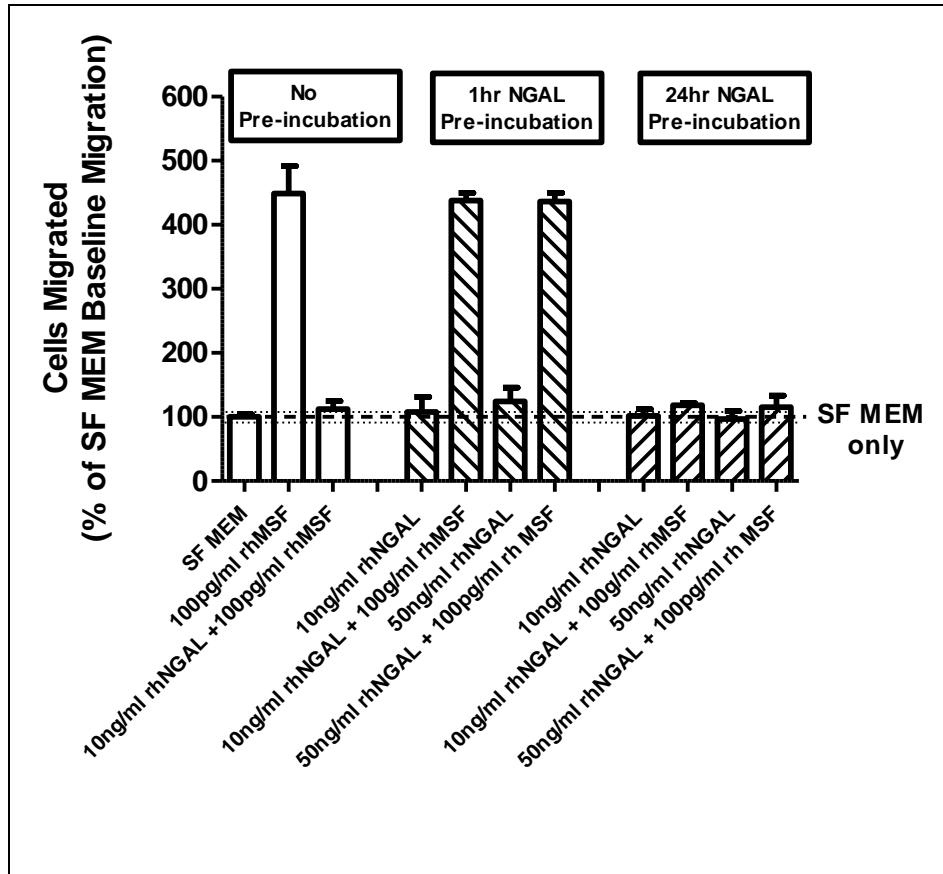


Figure 4.17. The effect of a NGAL pre-incubation on MSF bioactivity in the 3D collagen gel fibroblast migration assay. A variation of the standard 3D collagen gel fibroblast migration assay was performed; fibroblasts plated onto the surface of the collagen gel were pre-incubated (1 or 24 hours) with rhNGAL (10 or 50ng/ml), after which the gels were washed and then followed by the standard four day rhMSF incubation. The number of cells migrated is expressed as a percentage of SF MEM control baseline migration. i.e. MSF Baseline = 100 +/- 4.24, as represented by the hatched and dotted lines (mean and SD respectively). This is equivalent to 3.3 +/- 0.140 migrated cells. A representative experiment is shown.

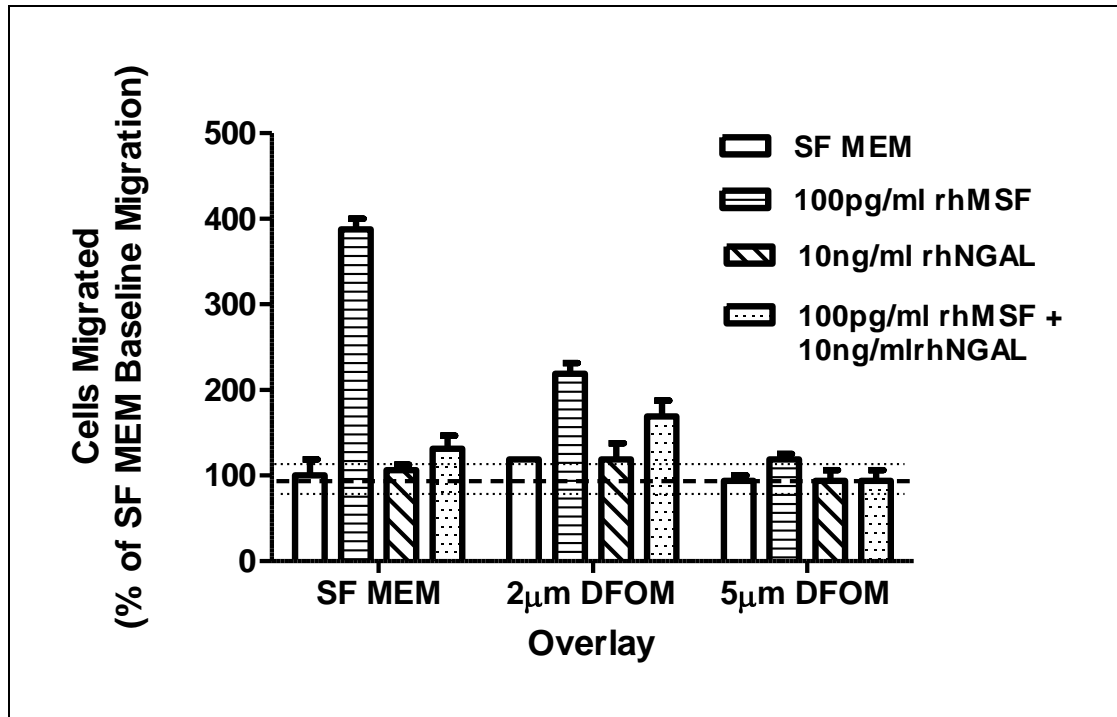


Figure 4.18. The effect of the iron chelator Deferoxamine mesylate (DFOM) on the MSF inhibitory activity of NGAL. A 3D collagen gel fibroblast migration assay was performed with and without the addition of DFOM (2 or 5µM), either alone or in the presence of 100pg/ml rhMSF and/ or 10ng/ml rh NGAL. The number of cells migrated is expressed as a percentage of SF MEM control baseline migration. i.e. SF MEM Baseline = 100 +/- 18.750, as represented by the hatched and dotted lines (mean and SD respectively). This is equivalent to 1.6 +/- 0.30 migrated cells. A representative experiment is shown.

	1% DCS MEM		2µM DFOM		5µM DFOM	
Time Line	Cell count	% Viability	Cell count	% Viability	Cell count	% Viability
Baseline	1.25 x 10 ⁴	83.9 +/- 9.78	-		-	
Post 1 day	1.8 x 10 ⁴	93.7 +/- 4.45	1.65 x 10 ⁴	94.0 +/- 3.75	1.75 x 10 ⁴	97.0 +/- 4.75
Post 4 days	6.63 x 10 ⁴	87.5 +/- 6.26	7.83 x 10 ⁴	97.0 +/- 4.75	6.05 x 10 ⁴	84.5 +/- 4.85

Table 4.2. The effect of the iron chelator Deferoxamine mesylate (DFOM) on fibroblast viability and proliferation. Fibroblasts, FSF44, were plated (2x10⁴ per 35mm) in the presence of 1%DCS MEM with and without the addition of 2-5µM DFOM. Cell viability (trypan blue test) and cell counts (measured on the Coulter counter Z1 series) were taken over a four day incubation period. An average of two experiments is shown.

4.8 **DISCUSSION**

Analysis of conditioned medium collected from the immortalised human keratinocyte cell line HaCaT showed that it possessed the ability to inhibit the motogenic activity of MSF in the 3D collagen gel fibroblast migration assay. A process of fractionation of the HaCaT CM, by both molecular weight and ionic charge, followed by sequence analysis led to the identification of the protein responsible for the MSF- inhibitory activity as Neutrophil Gelatinase Associated Lipocalin (NGAL). The fractionation process also unexpectedly revealed the presence of motogenic bioactivity, which is normally obscured within the HaCaT CM; which was subsequently identified as MSF. It therefore transpired that cultured HaCaT keratinocytes express MSF but its motogenic bioactivity appears to be inactivated by the co-expression of an inhibitor, NGAL. The identification of NGAL as accountable for the MSF-inhibitory activity detected in HaCaT CM followed a fractionation process involving separation by size exclusion and ion exchange chromatography followed by SDS electrophoresis (reducing conditions) (Figure 4.19). At each stage in the process the bioactivity of the resultant fractions were tested in 3D collagen gel fibroblast migration assay for their ability to inhibit MSF stimulated fibroblast migration. After, the initial molecular weight separation on the Superdex 75 HiLoad 26/60 column the unforeseen presence of the two opposing bioactivities were discovered in the HaCaT CM; molecular weight fractions 63-84kDa displayed the ability to stimulate fibroblast migration whilst 16-27kDa fractions possessed MSF-inhibitory activity.

This motogenic activity was shown to be inhibited by the IGD function neutralising monoclonal antibody, PEPQ1.1, thereby implying that the protein contained an IGD motif, similar to MSF. Subsequently, immunoprecipitation with Protein G showed that the motogenic fraction bound to the RpVSI antibody which recognises the MSF unique carboxyl terminal decapeptide. These findings, plus the nature of the motogenic bioactivity and molecular weight lead to the conclusion that the HaCaT keratinocytes express MSF. Immunolocalisation confirmed that both cultured HaCaT and primary keratinocytes express MSF. A summary of the experimental data that lead to the disclosing that HaCaT keratinocytes express MSF, is shown in Table 4.3.

The identification of NGAL as the protein isolated from HaCaT CM responsible for the MSF-inhibitory bioactivity was confirmed by the same activity being displayed by NGAL obtained from an additional three different sources; a eukaryotic and a prokaryotic sourced recombinant protein and NGAL isolated from MMP-9/NGAL

complex produced by activated neutrophils (Table 4.5). Similar levels of MSF-I activity was measured in all types of NGAL tested and toxicity issues were eliminated by morphology, viability and proliferation assays showing no adverse effects at NGAL concentrations displaying MSF-I activity. In addition, proof that HaCaT keratinocytes normally express NGAL was provided by Western Blot and indirect ELISA analysis of unfractionated HaCaT CM and confirmed by immunolocalisation of NGAL in the cultured cells (Table 4.4).

The inhibition of MSF by NGAL is a novel activity. NGAL is known by a variety of names including neutrophil glucosaminidase-associated lipocalin, 24p3, utercalin, siderocalin, lipocalin 2, p25, human neutrophil lipocalin (HNL) and α 1-microglobulin (Li and Cahn, 2011, Chakraborty *et al.*, 2012). It is a member of the Lipocalin family; a diverse family of small secreted proteins that act as carriers, transporting predominantly small lipophilic molecules although additional functions including cell regulation, differentiation, cell to cell adhesion and cell survival have recently been revealed (Chakraborty *et al.*, 2012). Members of the lipocalin family share little amino acid similarity but share a common secondary and tertiary structural feature called the “lipocalin fold”; an anti-parallel beta barrel structure comprising of 8 beta sheets that are hydrogen bonded to one another forming a calyx- or cup-shaped cavity (with a lid-like structure) that can bind specific ligands (Flower, 2000). The difference in sequence identity enables a wide variety of ligands to be bound by the lipocalin family. The lipocalin family has been further classified by the presence of structurally conserved regions, as either kernel or outer lipocalins. NGAL is a kernel lipocalin (Flower, 1996 and 2000, Kjeldsen *et al.*, 1993, Kjeldsen *et al.*, 2000).

NGAL is a 198 amino acid long secreted glycoprotein encoded by a gene located at the chromosome locus 9q34.11 (Chakraborty *et al.*, 2012). It was first purified from a culture of murine kidney cells infected with the simian virus (SV-40) or the polynoma virus (Hraba-Renevey *et al.*, 1989) and subsequently isolated as a 25kDa protein disulphide bonded to the monomeric inactive form of matrix metalloproteinase-9 (MMP-9) (Triebel *et al.*, 1992, Kjeldsen *et al.*, 1993, Yan *et al.*, 2001). MMP-9 is a gelatinase secreted by neutrophils that degrades basement membranes and ECM components (Triebel *et al.*, 1992). The binding of NGAL to MMP-9 does not affect the activity of the enzyme but enhances its stability by protecting it against inactivation by its natural inhibitor TIMP-1 (Yang *et al.*, 2001, Van der Steen *et al.*, 2006, Chakraborty *et al.*, 2012).

The knowledge that NGAL binds to MMP-9 initially suggested that its capacity to inhibit MSF was also due to a direct relationship since MSF shares some structural similarity to MMP-9; both molecules contain fibronectin type II domains and zinc binding motifs, with the conserved sequence HEXXH in MSF and AHEXGHXXGXXH in MMP-9 (Houard *et al.*, 2005, Van dee Steen 2001). However, pre-incubation experiments have shown that NGAL does not have to be in direct contact with MSF in order to exert an inhibitory effect; fibroblasts pre-incubated with NGAL for 24 hours become unresponsive to MSF. This would imply that NGAL inhibits MSF either by blocking an MSF-activated signal transduction pathway or indirectly via an intermediate molecule.

The first ligands to be identified for NGAL were bacterial catecholate-type ferric siderophores. NGAL has since been identified as a potent bacterostatic agent; inhibiting bacterial growth by sequestering the iron-binding bacterial siderophores and blocking bacterial access to iron (Strong *et al.*, 1998, Goetz *et al.*, 2002, Flo *et al.*, 2004). NGAL deficient mice showed increased susceptibility to bacterial infections (Cramer *et al.*, 2012). In healthy humans NGAL was found to be concentrated in tissues predisposed to contact with microorganisms (the trachea, lung and stomach) and also highly expressed at the sites of inflammation (an acute-phase protein) having a key role in the innate immune response (Lim *et al.*, 2007). NGAL is proposed to have a role in mammalian iron metabolism and thereby regulation of iron-responsive genes (Gwira *et al.*, 2005). During kidney development by delivering iron inside mesenchymal progenitor cells, NGAL induces their differentiation into epithelial tubules (Yang *et al.*, 2002 and 2009). NGAL also has the ability to induce apoptosis by affecting the intracellular iron content of cells (Devireddy *et al.*, 2005).

The MSF-inhibitory activity of NGAL does not appear reliant on its ability to transport iron. Identical MSF-I bioactivity was described for NGAL from three different sources (purified from HaCaT CM and recombinant NGAL from eukaryotic and prokaryotic sources) which would imply iron independence, as each source would have varying amounts of bound iron (Goetz *et al.*, 2002). Plus the addition of the iron chelator, DFOM, had no effect NGAL inhibition of MSF in the 3D collagen gel fibroblast migration assay. Finally, NGAL inhibition of MSF takes place at concentrations (1-10ng/ml) which are 5000 fold lower than those required for iron-dependent transcriptional effects (Hanai *et al.*, 2005, Yang *et al.*, 2002).

NGAL is a multifunctional protein but the exact pathophysiological roles of NGAL are not fully understood. In addition to suppression of bacterial growth and iron

transportation, several functions have been ascribed to NGAL; induction of apoptosis, modulation of inflammatory response, fatty acid transportation and protection of cells against thermal and oxidative stress conditions (Wang *et al.*, 2012). It has been attributed in playing an important role in a seemingly diverse range of conditions including infectious disease, renal and cardiac disease or injury, metabolic syndrome and thermal dysregulation, dermatitides and the inflammatory disease of lung and bone (Bando *et al.*, 2007, Saiga *et al.*, 2008, Martineau *et al.*, 2007, Eagan *et al.*, 2010, Li and Chan, 2011, Chakraborty *et al.*, 2012). Three major categories of cellular stress have been described as causing increased expression of NGAL; environmental (hypoxia, ischemia- reperfusion, pathogen- associated molecular pattern activated by infections or LPS), metabolic (hyperlipidemia, obesity, insulin resistance) and developmental (conceptus attachment and reproductive tissue involution, bone plate maturation, epithelial-mesenchymal transformation and malignancy) (Li and Chan, 2011). NGAL expression has been observed in many human solid and hematopoietic tumours including breast (Stoesz *et al.*, 1998), colon (Nielsen *et al.*, 1996), lung (Shi *et al.*, 2008), ovary (Bartsch and Tschesche, 1995), pancreas (Furuntani *et al.*, 1998), thyroid (Iannetti *et al.*, 2008) and chronic myelogenous leukaemia (Leng *et al.*, 2009). It has been suggested that NGAL influences cancer progression by affecting two critical processes; cell survival via apoptosis and cell migration preceding tumour invasion and metastasis (Yang and Moses, 2009, Chen and Chan, 2011). A literature review indicates that the functional role of NGAL, whether pro or anti- tumorigenic is neoplasia-specific and also varies with the different stages of cancer progression and degree of tumour differentiation. A pro- tumoural effect has been described in breast, stomach, oesophagus, kidney and thyroid cancer, whilst attributed to anti-tumoural activity in ovary and pancreatic cancer. Studies on colorectal cancer have reported conflicting results (Wenners *et al.*, 2012). (Table 4.6 is a review of the reported roles of NGAL in malignant disease). Due to its small size, secreted nature and the availability of robust quantitative assays NGAL has become an extremely attractive target both as a diagnostic and prognostic biomarker in solid organ malignancies (it is already used in clinical monitoring of tissue response to renal and cardiac injuries as well as several sepsis)(Haase *et al.*, 2009, Li and Chan, 2011).

The epithelial to mesenchymal transition (EMT) is one of the key mechanisms underlying tumour invasion and metastasis (Thiery *et al.*, 2006). EMT causes tumour cells to adopt a more mobile phenotype, thereby facilitating their invasion into the local extracellular matrix, intravasation and extravasation of blood vessels with the resultant

invasion and settlement in secondary organ sites (Yang and Moses, 2009). Conflicting reports have been published on the relationship between epithelial differentiation and NGAL expression levels. For example, in ovarian tissue increased NGAL levels were associated with well-differentiated epithelial ovarian tumours with expression reduced as the cancer progressed and the epithelial tumours became poorly differentiated (Cho and Kim, 2009). The opposite situation was described in a breast cancer study by Bauer and colleagues (2008).

Malbris and colleagues (2002) have also reported that HaCaT keratinocytes have a high expression level of NGAL as determined by RT-PCR analysis. They also described that in normal adult skin, NGAL expression was weak and limited to hair follicles.

However, in agreement with our results, they discovered that cultured normal keratinocytes from normal skin unlike their *in vivo* counterparts express NGAL. This highlights the difference in cell status between *in vitro* and *in vivo* situations which results in substantial changes in protein expression (Lee *et al.*, 2008). Due to the embryonic spatio-temporal expression pattern and increased expression in skin disorders characterised by dysregulated epithelial differentiation (psoriasis, pityriasis rubra and squamous cell carcinoma) they suggested that NGAL plays a role in epithelial differentiation. Foetal skin and adult skin undergoing de-differentiation have the same NGAL expression pattern. Interestingly, in the skin epithelium, MMP-9 was not co-expressed with NGAL mRNA.

MSF is an oncofetal protein, expressed during foetal development by keratinocytes, fibroblasts and endothelial cells with expression lost in the equivalent healthy adult cells. However, MSF is persistently re-expressed by both tumoral and stromal cells in various human cancers including breast, lung, colorectal, oral, prostate and oesophageal (Schor *et al.*, 2003, 2005, Jones *et al.*, 2007). The discovery that NGAL inhibits the motogenic activity of MSF proposes numerous questions about their relationship during cancer progression. The use of the *in vitro* model for human skin carcinogenesis developed by the Fusening and Boukamp group enabled the investigation of the expression levels of MSF and NGAL in relation to the different stages of carcinogenesis. The HaCaT-ras clones (BEN, MAL and MET) represent a shift in tumourigenic potential from the benign to malignant to metastatic. In addition, the bioactivity present within the conditioned medium of the HaCaT-ras clones was examined and related to the expression levels of NGAL and MSF. That is, with increasing degree of malignancy does NGAL continue to mask the motogenic activity of MSF?

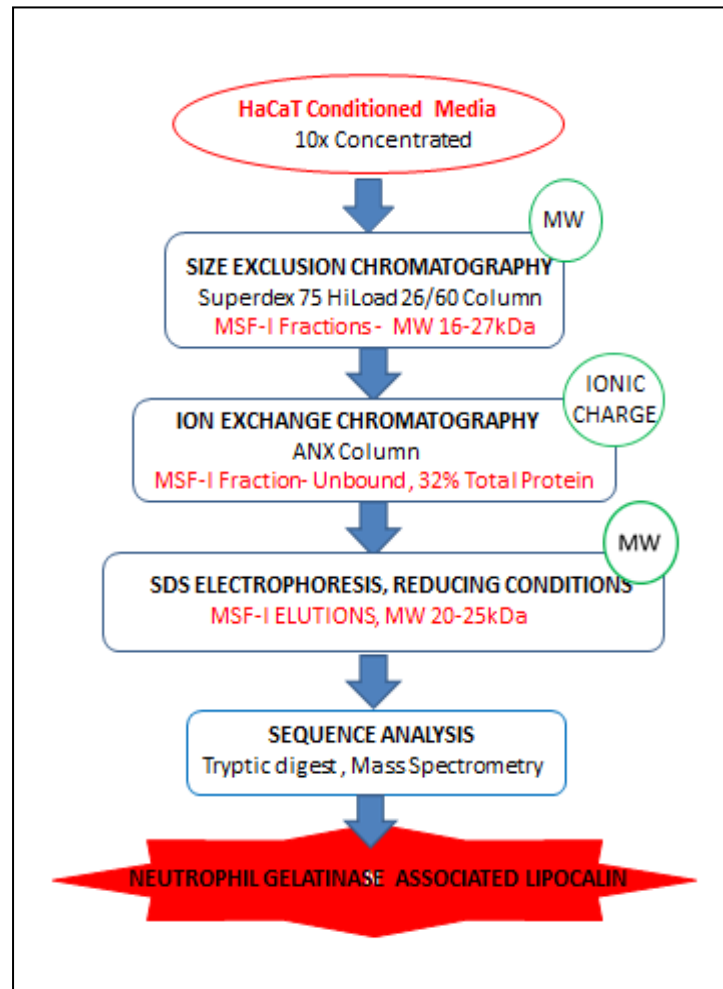


Figure 4.19. A systematic representation of the protocol employed for the isolation and subsequent identification of the protein responsible for the MSF inhibitory activity of total HaCaT conditioned medium- NGAL. The process involved separation by molecular weight and ionic charge (green circles). At each stage the subsequent fractions were analysed for the presence of MSF inhibitory activity by testing in the 3D collagen gel fibroblast migration assay.

Table 4.3. Summary of experimental data providing evidence of that cultured HaCaT keratinocytes express MSF.

Technique	Experimental Details.	Sample Tested	Results
1. Immunolocalisation of MSF.	Anti-MSF antibody, Rp2/98pFA2pFn1.	Cultured HaCaT keratinocytes.	Heterogeneous staining for MSF in HaCaT cells. Controls consistently negative.
2. IGD Function Neutralisation of Motogenic Activity.	Motogenic active HaCaT fractions tested in the 3D collagen gel fibroblast migration assay with addition of Pep Q 1.1- IGD function neutralising antibody.	SEC Fractionated HaCaT CM-motogenic fractions of MW 63-84kDa (F-msa).	HaCaT fractions alone stimulated fibroblast migration by 3.7 fold. Addition of PepQ1.1 inhibited this motogenic activity by 60-70%.
3. Immunoprecipitation for MSF.	Protein G coupled to RpVSI antibody which recognises MSF unique carboxyl terminal decapeptide. Unbound and bound elutions tested for motogenic activity in the 3D collagen gel fibroblast migration assay.	SEC Fractionated HaCaT CM-motogenic fractions of MW 63-84kDa (F-msa).	Motogenic activity of HaCaT F-msa immobilised on RpVSI coupled Protein G. No motogenic activity present in unbound sample. Motogenic activity present in elutions; 2.8 fold increase in fibroblast migration.
4. NGAL inhibition of motogenic activity.	Motogenic active HaCaT fractions tested in the 3D collagen gel fibroblast migration assay with addition of NGAL isolated from MMP-9/NGAL complex.	SEC Fractionated HaCaT CM-motogenic fractions of MW 63-84kDa (F-msa). Various dilutions tested.	Peak motogenic activity of HaCaT F-msa at 1/250 dilution inhibited by 60% by addition of NGAL.

Table 4.4: Summary of experimental data providing evidence of that cultured HaCaT keratinocytes express NGAL.

Technique	Experimental Details.	Sample Tested	Results
1. Immunolocalisation of NGAL.	Anti-NGAL antibody, AF1757 (R&D Systems).	Cultured HaCaT keratinocytes.	Heterogeneous staining for NGAL in HaCaT cells. Controls consistently negative
2. Immunoblot For NGAL.	Anti-NGAL antibody, MAB1757 (R&D Systems).	Total HaCaT conditioned medium (neat and 5x concentrated).	Clear band identified, MW 20-25kDa in both neat and concentrated HaCaT CM.
3. Colorimetric Indirect ELISA for NGAL.	Anti-NGAL antibody, AF1757 (R&D Systems),	Total HaCaT conditioned medium.	NGAL concentrated per ml of unstandardised CM measured as 1.77 +/-0.05µg/ml.

Table 4.5: The verification of NGAL as an inhibitor of MSF motogenic bioactivity.

NGAL from three different sources was tested in the 3D collagen gel fibroblast migration assay for its ability to inhibit the motogenic of rhMSF.

NGAL Source	Concentration Tested	Effects in 3D Collagen Gel Fibroblast Migration Assay		
		<u>Tested Alone</u> (as compared to SF MEM Baseline)	<u>Percentage Inhibition of 100pg/ml rhMSF</u> (as compared to rhMSF Baseline)	
		All Concentrations	Average / SD All concentrations	Peak Activity Concentration (Aver/ SD)
Isolated from NGAL/MMP-9 Complex (Calbiochem), 20-25kDa Gel elution 3	Diluted 1/20,000, est. 5-10ng/ml	None	54.4 +/- 4.00%	est. 5-10ng/ml 54.4 +/- 4.00%
Eukaryotic NGAL (R&D Systems)	1ng-1µg/ml	None	44.4 +/-5.01%	1ng/ml rhNGAL 51.5 +/- 3.50%
Prokaryotic NGAL (In-house Prep)	1ng-1µg/ml	None	59.6 +/- 9.13%	1ng/ml rhNGAL 72.7 +/- 8.18%

Table 4.6: The role of NGAL in malignant disease. Observations in animal models and human studies have reported NGAL expression in a number of cancers thereby making it an attractive target as both a biomarker and for pathophysiologic study. The conundrum is whether to assign NGAL a pro or anti-cancer role. The following table lists contradicting evidence of NGALs involvement in tumour development. In conclusion, the role of NGAL in promoting or suppressing tumour growth appears to be highly dependent on the tissue of origin and neoplasia-specific.

i. Evidence supporting NGAL as a tumour promoter.

<p>Tissue- GENERAL</p> <ul style="list-style-type: none"> • M. Coles <i>et al.</i>, 1999. L. Yan <i>et al.</i>, 2001 <p>NGAL enhances MMP-9 activity by protecting the enzyme from degradation. MMP-9 is implicated in cancer progression; promotes tumour invasion and metastasis by degrading basement membrane, also promotes tumour growth and proliferation via angiogenesis.</p>
<p>Tissue- BLOOD</p> <ul style="list-style-type: none"> • C. Villalava <i>et al.</i>, 2008. X. Leng <i>et al.</i>, 2008 <p>NGAL expression correlated with expression of BCR-ABL fusion oncogene which is found in the majority of chronic myeloid leukemia (CML) patients. Serum NGAL levels elevated in CML patients. Mechanistic studies indicated that NGAL may mediate BCR-ABL induced tumourgenesis; NGAL expression in tumour cells was induced by BCR-ABL resulting in apoptosis in normal hematopoietic cells thereby facilitating tumour cell expansion.</p>
<p>Tissue- BRAIN</p> <ul style="list-style-type: none"> • M-F Liu <i>et al.</i>, 2011. <p>NGAL and NGALR are overexpressed in gliomas and appear to correlate with tumour grade; associated with a poor prognosis as it represents a more malignant phenotype.</p>
<p>Tissue- BREAST</p> <ul style="list-style-type: none"> • S.P Stoesz <i>et al.</i>, 1998. <p>A significant association between NGAL expression and several other markers of poor breast cancer prognosis, including estrogen and progesterone receptor-negative status and high proliferation (confirmed in breast cancer cell lines MCF-7 and T47D). However, no significant relationship between NGAL expression and disease- free or overall survival observed.</p> <ul style="list-style-type: none"> • P. Seth <i>et al.</i>, 2002. <p>Addition of recombinant NGAL to MCF10, an immortalised normal breast epithelial cell line, resulted in a significant increase in the number of colonies. Suggesting that NGAL may stimulate proliferation in normal breast epithelial cells.</p>

- Fernandez *et al.*, 2005.

NGAL found to be over-expressed in breast cancer cells. Cells exhibit increased growth rates, angiogenesis and proliferation. Breast cancer patient urine samples shown to contain NGAL /MMP-9 complex.

- H. Shi *et al.*, 2008.

In vitro, overexpression of NGAL in 4T1 mouse mammary cancer cells increased migration and invasiveness. Whilst, *in vivo* overexpression promoted lung metastasis through inhibition of PI3/Akt pathway. However, NGAL did not affect cancer cell proliferation rate.

- M. Bauer *et al.*, 2008.

NGAL shown to be an independent prognostic marker for decreased survival in breast cancer. NGAL expression strongly correlated with characteristics associated with poor prognosis (poor histologic grade, lymph node metastasis, high proliferation). NGAL detection may have the potential to be used as a risk assessment to identify patients requiring more aggressive adjunct therapy. Suggested that NGAL probably contributes directly to cancer progression.

- J. Yang *et al.*, 2009. J. Jang and M.A. Moses, 2009.

NGAL expression elevated in Stage I-III breast cancer samples compared to normal breast tissues. Increased urine NGAL levels in metastatic breast cancer patients compared to healthy controls; urine levels increase with disease progression. NGAL shown to induce the epithelial to mesenchymal transition (EMT) in human breast cancer. Propose NGAL as a potential non-invasive biomarker for breast cancer.

- X. Leng *et al.*, 2009.

Used a spontaneous mouse breast cancer model to study the function of NGAL in breast tumourgenesis. Mice lacking NGAL displayed delayed tumour formation and metastasis, associated with reduced serum MMP-9 activity. NGAL expression appeared to enhance aggressive behaviour including lung metastasis, tumour cell migration and invasion and anchorage-dependent growth. Injection of an anti-NGAL antibody into mice bearing established breast tumours resulted in a significant inhibition of lung metastasis. Proposed that NGAL is a critical factor in enhancing breast tumour formation and progression, possibly via MMP-9 stabilisation. Inhibition of NGAL could have potential as a breast cancer treatment, especially aggressive forms.

Tissue- COLON

- L. Hu *et al.*, 2009.

Overexpression of NGAL in a stably transfected colon carcinoma cell line, KM12C, altered subcellular localisation of E-cadherin and catenins resulting in decreasing E-cadherin mediated cell-cell adhesion, enhanced matrix attachment, increased cell motility and *in vitro* invasion. The NGAL regulation of cell migration maybe mediated via an alteration in the subcellular localisation of Rac1.

- Y. Sun *et al.*, 2011.

Immunohistochemical analysis of colorectal tissue showed an overexpression of NGAL correlated with colorectal adenoma- carcinoma sequence. Animal model experiments indicated that NGAL overexpression increased tumourgenesis and liver metastasis of colorectal cancer cells. Plus

survival analysis showed NGAL expression was an independent predictor for colorectal cancer patient survival.

Tissue- ENDOMETRIUM

- T. Miyamoto *et al.*, 2011.

Ectopic expression of NGAL in endometrial cancer cells increases *in vitro* rate of proliferation. NGAL expressing cells showed increased invasiveness, suggesting possible role for NGAL in growth and metastasis of human endometrial cancer. NGAL expression (strong cytoplasmic and nuclear) was associated with a significant reduction in overall survival among endometrial carcinoma patients suggesting possible use of NGAL as prognostic marker.

Tissue- LIVER

- A.A. Zabron *et al.*, 2011.

NGAL levels in bile were significantly higher in patients with malignant compared to benign biliary obstruction. However, no difference observed in NGAL serum or urine levels. Suggestion that NGAL has potential to be a bile biomarker.

Tissue- LUNG

- Z. Tong *et al.*, 2005.

In vitro, NGAL expression is upregulated in A549 and human breast MCF-7 cancer cells in response to apoptosis inducing agents. NGAL acts as a survival factor in lung cancer A549 cells by reducing sensitivity to apoptosis inducing agent OSU03012.

- S.U.R Mir *et al.*, 2012.

Revealed that NGAL is required for tumour formation in lung cancer cells (A549). NGAL transcription and activation of NGAL/MMP-9 complex is directed by S2R^{Pgrmc1} (also elevated in lung cancer); S2R^{Pgrmc1} activates NF^κB via EGFR.

Tissue- OESOPHAGUS

- Li *et al.*, 2003

NGAL shown to promote tumour cell invasion of the oesophageal carcinoma cell line, SHEEC.

- H. Zhang *et al.*, 2007.

NGAL upregulated in a heterogeneous pattern in oesophageal squamous cell carcinoma tissue (ESCC); expression level correlating positively to cell differentiation. Enzymatic activity of NGAL/MMP-9 complex elevated in ESCC compared to normal mucosa.

- W.K. Fang *et al.*, 2007.

Identified a novel splice variant of NGAL receptor in oesophageal carcinoma cells; NgalR-3 exhibits co-localisation and interaction with NGAL protein *in vivo* implying it may play a role in NGAL-mediated iron transport in oesophageal carcinoma.

- L. Cui *et al.*, 2008.

Expression of NGAL receptor found to be higher in oesophageal squamous cell carcinoma (ESCC) than in normal oesophageal epithelium.

NGALR hypomethylation contributed to its expression in ESCC. NGALR overexpression may therefore play a role in pathogenesis.

- Z-P Du *et al.*, 2011.

High expression of NGAL and its receptor observed in ESCC compared to low expression in normal oesophageal tissue; NGAL/NGALR co-expression correlated to histological differentiation grade. Overexpression of NGAL was associated with poor prognosis. NGAL and NGALR appear to act independently; potential as prognostic factors.

Tissue- OVARY

- R. Lim *et al.*, 2007. H. Cho *et al.*, 2009.

NGAL associated with the progression of epithelial ovarian malignancies; expression in ovarian tumours changed with disease grade as reflected in serum NGAL concentration. NGAL has a negative expression in normal ovaries and weak in benign. Highest level displayed in borderline and Grade 1 tumours whilst decreased in Grade 2 and 3. NGAL expression is linked to the epithelial phenotype of the ovarian tumour, being lost as the cancer progresses and the tumours become poorly differentiated. NGAL expression downregulated in ovarian cancer cell lines undergoing EMT. NGAL may be involved in the progression of epithelial ovarian malignancies and could possibly be used as a marker to monitor changes of ovarian cancer progression from benign to malignant.

Tissue- STOMACH

- H.J.Wang *et al.*, 2010

NGAL is upregulated in the early stage of gastric carcinogenesis; may play an important role in the early development of gastric cancer. NGAL could serve as an early diagnostic marker as serum NGAL levels found to be higher in gastric cancer patients than healthy controls. A significant correlation was observed between serum NGAL level and NGAL expression in tumour cells, suggesting that the serum NGAL levels could tumour derived. The high expression of NGAL in gastric cancer tissues indicates tumour metastasis and poor prognosis.

Tissue- THYROID

- A. Iannetti *et al.*, 2008.

NGAL required for survival of thyroid cancer cells in serum deprived conditions *in vitro*. NGAL silencing leads to reduction in anchorage independent clonogenic growth *in vitro* and decreased tumorigenicity and tumour size in nude mice. NGAL expression elevated in papillary, follicular and anaplastic thyroid carcinoma.

Tissue- UTERUS

- T. Miyamoto *et al.*, 2011.

The ectopic expression of NGAL in endometrial cancer cells increases *in vitro* rate of proliferation. NGAL expressing cells showed increased invasiveness, suggesting possible role for NGAL in growth and metastasis of human endometrial cancer. NGAL expression (strong cytoplasmic and nuclear) was associated with a significant reduction in overall survival among endometrial carcinoma patients suggesting possible use of NGAL as prognostic marker.

ii. Evidence supporting a role NGAL as a tumour suppressor.

Tissue- GENERAL

- P. Bahmani *et al.*, 2010.

Protective role for NGAL against cell injury mediated by reactive oxygen species (ROS). NGAL inhibits the reduction of iron and generation of hydroxyl free radicals.

Tissue- BREAST

- J. Hanai *et al.*, 2005.

NGAL shown to be a suppressor of metastasis in Ras- transformed 4T1 mouse mammary tumour cells; stimulating epithelial phenotype, reversing metastatic potential and reducing tumour growth.

- S. Venkatesha *et al.*, 2006.

Ras- induced expression of VEGF in 4T1 mouse mammary tumour cells is inhibited by NGAL via down-regulation of MAPK and ras-PI3K signalling. Tumour angiogenesis, as demonstrated by the intradermal tumour angiogenesis assay, was suppressed by NGAL (mediated by caveolin-1). Tumours formed by 4T1-ras cells into which NGAL was stably introduced displayed an increased expression of the anti-angiogenic molecule thrombospondin-1.

- E.P. Cramer *et al.*, 2012.

MMTV-PyMT/FVB/N Mouse model for breast cancer showed that NGAL did not affect the aggressiveness of the breast cancers; despite being upregulated in breast cancer cells, no significant effect on tumour growth and metastasis was observed. In addition, demonstrated that unlike the human orthologue, mouse NGAL cannot bind directly to MMP-9 and therefore lacks the ability to mediate MMP-9 activation or inhibit degradation.

Tissue- COLON

- H.J. Lee *et al.*, 2006.

Ectopic NGAL expression suppressed the ability of human colon carcinoma cells, KM12SM, to invade Matrigel *in vitro* and substantially inhibited liver metastasis *in vivo*. NGAL may serve as a suppressor of colon cancer metastasis.

Tissue- KIDNEY

- Gwira *et al.*, 2005.

Study of mouse inner medullary collecting duct (mIMCD)-3 cells (kidney epithelial) showed that NGAL binds directly to Hepatocyte Growth Factor, inhibiting HGF-stimulated c-Met receptor phosphorylation and downstream signalling. Resulting in an inhibition of HGF –stimulated cell migration and single-cell morphogenesis.

Tissue- LIVER

- E.K Lee *et al.*, 2011.

NGAL may play a protective role against the progression of human hepatocellular carcinoma (HCC) by suppressing cell proliferation and invasion. NGAL expression level increased in HCC compared to normal liver tissue. Ectopic expression of NGAL in HCC cell line, *in vivo* and *in vitro*, inhibited the growth of the cells, reduced HCC cell invasive potential and inhibited MMP-2 expression. Actions thought to be due to NGAL inhibition of C-Jun N-terminal kinase and PI3K/Akt signalling pathways.

Tissue- PANCREAS

- M. Furutani *et al.*, 1998. H. Han *et al.*, 2002.

Microarray analysis revealed that NGAL is up regulated by nearly 27 fold in pancreatic cancer cells compared to normal ductal cells.

- N. Moniaux *et al.*, 2008.

A specific and differential expression pattern of NGAL observed in pancreatic adenocarcinoma compared to normal controls. NGAL expression found to be low in normal pancreas and in pancreatitis but very high in early dysplastic lesions (PanINs); suggests that NGAL could be a marker of early dysplasia in the pancreas. In adenocarcinomas, NGAL expression correlated positively with the grade of differentiation; moderate levels for highly differentiated whilst negative for poorly differentiated cancer. Hypothesise that loss of NGAL expression promotes the progression of pancreatic ductal carcinoma from well to poorly differentiated tumour. In addition serum NGAL levels elevated in both pancreatic inflammation and malignancy but no defining difference between pancreatitis and cancer.

- Z. Tong *et al.*, 2008.

NGAL overexpression resulted in reduction of pancreatic cancer cell adhesion, invasion and angiogenesis, *in vitro*. Reduction in cellular invasion attributed to NGAL inhibition of FAK phosphorylation whilst anti-angiogenic effect due to inhibition of VEGF expression. In addition, NGAL overexpression in an orthotopic Nude mouse pancreatic cancer model displayed inhibited local/distant metastasis and reduced tumour microvessel density. Proposed that loss of NGAL expression is a biomarker for pancreatic cancer progression and possibly means of controlling angiogenesis and metastasis by altering NGAL expression.

- S.Chakraborty *et al.*, 2012

Plasma NGAL levels (and pancreatic juice) shown to be highly specific (88%) in differentiating pancreatic cancer and chronic pancreatitis patients from healthy controls. Potential as a novel diagnostic biomarker, although NGAL levels not able to discriminate between pancreatic cancer and chronic pancreatitis.

Tissue- UTERUS

- C-J. Liao *et al.*, 2012.

NGAL expression was significantly increased in endometrial hyperplasia compared to adenomyosis and correlated positively with the COX-2 and E-cadherin expression. Liao *et al.*, propose that NGAL may assists in preventing the transition of epithelial cells to mesenchymal cells; acting as

protective factor against cell stress. High NGAL expression in tissues may imply imminent tumorigenesis, thereby altering NGAL expression in endometrial hyperplasia may control carcinoma development.

Chapter 5: Results

THE EXPRESSION OF MSF AND NGAL IN RELATION TO TUMOUR PROGRESSION.

5.1 AIMS

The fractionation of HaCaT conditioned medium has shown that the non-tumourigenic transformed human keratinocyte cell line expresses both MSF and NGAL. However, upon analysis of the HaCaT total CM in the 3D collagen gel fibroblast migration assay, the motogenic bioactivity of the endogenous MSF is masked due to inactivation by the co-secreted NGAL (Jones *et al.*, 2007).

The HaCaT cell line is the founding member of the HaCaT/ HaCaT-*ras in vitro* human skin carcinogenesis model. The three subsequent HaCaT -*ras* clones (BEN, MAL and MET) display a shift tumourigenic potential (Fusenig and Boukamp, 1998).

The dysregulated expression of both MSF and NGAL has been implicated in various benign and malignant diseases (Schor *et al.*, 2003 and 2005, Hu *et al.*, 2009, Chakraborty *et al.*, 2012). The aim was therefore to establish whether MSF and NGAL are expressed by the tumorigenic keratinocytes cell lines (BEN, MAL and MET) in order to determine whether expression levels can be related to the tumorigenic potential of each clone.

For ease of discussion the cell lines of the HaCaT/ HaCaT-*ras in vitro* human skin carcinogenesis will be referred to as the HaCaT series. The presence of MSF and NGAL in the HaCaT series conditioned medium was explored by Western Blot analysis and ELISA techniques, whilst immunolocalisation was employed for direct visualisation of expression.

5.2 BACKGROUND

The HaCaT cells were developed from normal adult human skin keratinocytes during prolonged cultivation at a reduced calcium concentration and elevated temperature. The cell line is considered by many researchers to be a close approximation to normal keratinocytes in both growth and differentiation potential and is frequently used as a model system to study keratinocyte biology and transformation (Boukamp *et al.*, 1988).

The cells remain non-tumourigenic through extended culture passages and maintain a stable chromosome content. Because of their genetic stability and primarily maintained phenotypic normality, these immortalised keratinocytes are considered to represent a very early stage in skin tumorigenesis (Fusenig and Boukamp, 1998).

Using the HaCaT cell line Fusenig and colleagues developed an *in vitro* model to study process of human skin carcinogenesis, characterising the different stages of tumour development and progression, similar to the Fearon and Vogelstein's model for colon cancer (Fearon and Vogelstein, 1990). The tumourigenic conversion of HaCaT cells was achieved by introducing additional genetic alterations via transfection with the mutated val-12 Harvey-*ras* oncogene (Boukamp *et al.*, 1990). Mutant *ras* genes are present in various human tumours and activated *ras* has been detected in squamous and basal cell carcinoma (Ananthaswamy and Pierceall, 1992). The transfected cells attained a selective growth advantage and altered phenotype.

Numerous HaCaT-*ras* clones were produced, which after subcutaneous injection into nude mice grew into tumours. The tumours were classified by their growth behaviour and histological phenotype. Clones which grew slowly eventually forming epidermoid cysts were designated as benign, while those forming well- differentiated squamous cell carcinomas as malignant. The malignant clones were associated with the loss of copies of chromosome 15 (Boukamp *et al.*, 1990 and 1997). A metastatic phenotype was only achieved by the *in vivo* passaging of a benign HaCaT-*ras* clone; resulting in a very fast growing clone which, after subcutaneous injection into nude mice spontaneously metastasised to the lung and lymph nodes (Mueller *et al.*, 2001).

The HaCaT-*ras* clones, each displaying shifting tumourigenic potential, were established as the cell lines BEN (benign), MAL (malignant, non-metastatic) and MET (metastatic). Each clone, originating from the same parental line, represented a distinct stage in tumour progression, thereby creating an *in vitro* carcinogenesis model for human skin keratinocytes. The model is comparable to the known stages of human epithelial skin carcinomas *in vivo* as well as of derived carcinoma cell lines and has enabled the identification of genetic alterations and phenotypic characteristics associated with the different stages of transformation (Fusenig and Boukamp, 1998).

5.3 THE IDENTIFICATION OF MSF EXPRESSION IN THE HACAT SERIES CELL LINES.

5.3.i Western Blot Identification of MSF

The unfractionated CM from each cell line was separated by 12% SDS PAGE under reducing conditions followed by immunoblotting with a specific anti-MSF antibody, RpVSI. A control sample of rhMSF (250pg) was always included as a positive control and an appropriate main band of approximately 77kDa was consistently observed as a clear strong band on the immunoblot.

Numerous attempts were made to identify MSF in the CM of the HaCaT series keratinocytes, but none proved successful. Various concentrations of the CM were tested; the maximum being a 1000x concentrated sample prepared by Amicon concentration followed by dialysis and subsequent freeze drying. However, the problem with concentrating the CM to such an extent is that some of the protein tends to come out of solution and cannot be efficiently resuspended again. This has been observed even with 10x concentrated CM. One must conclude that if MSF is present in the HaCaT series CM it is at such a concentration that it cannot be detected by Western blot analysis; that is less than 25ng/ml.

5.3.ii Colorimetric Sandwich ELISA for Total MSF

Identification and quantification of MSF in the HaCaT series CM was also attempted by the colorimetric sandwich ELISA assay for total MSF. An anti-IGD antibody, MAb PEPQ 5.1, was used for capture and a specific anti-MSF antibody, RpVSI, for identification (Chapter 2, Materials & Methods). For each ELISA experiment a standard curve for MSF was performed using recombinant MSF; a maximum concentration of 200ng/ml serially diluted to 1.5625ng/ml. 100µl of each standard or sample was tested per well, duplicate wells were tested for each variable and an average reading calculated. SF MEM and Coating buffer were used as negative controls.

Initially neat CM from each cell line was tested but this proved unsuccessful in identifying MSF in the CM. 10x concentrated CM was then trialled but this was also negative, failing to give final OD readings above those of the negative controls. Once again, it would appear that either MSF is not expressed by the cells or that if MSF is present in the HaCaT series CM, it is present at concentrations below this assay's

sensitivity, 12.5ng/ml. As discussed previously in regards to the HaCaT CM (4.5.ii, Chapter 4) the poor standard curve that was achieved using rhMSF standards questions the reliability and suitability of the antibodies used.

5.3.iii Immunolocalisation of MSF in HaCaT Series Keratinocytes.

The two previous methods adopted to detect MSF expression were based on its identification in the CM collected from the cultured cells. The inability to detect MSF in the CM by Western Blot and Sandwich ELISA techniques may be due to sensitivity. Another explanation could be that any MSF present in the CM has become unrecognisable to the specific anti-MSF antibodies. MSF may have a short half-life in the CM, being degraded by the actions of proteases present within the CM or due to a consequence of storage (freeze/thaw cycles). Therefore, a method was chosen that would identify MSF directly within the cell i.e. immunohistochemistry. As this technique includes a fixation step it may assist in preserving any MSF present.

A rabbit polyclonal anti-VSI antibody (Rp2), raised against the MSF unique carboxyl terminal decapeptide, was used for the immunolocalisation of MSF in the HaCaT series cell lines. Optimisation experiments allowed the selection of the most appropriate concentration of anti-MSF antibody which gave the best possible staining whilst ensuring a consistent negative control (normal rabbit IgG) and no cross- reaction with the biotinylated secondary antibody (Goat Anti-Rabbit IgG). The cell line FSF44, previously identified as not expressing MSF (Chapter 4.5 iii) was included in each experiment, as a negative control.

Since all CM tested was from confluent cultures grown directly on plastic dishes it was appropriate to perform MSF immunolocalisation under these same conditions.

However, the significance of the matrix has become increasingly apparent to researchers regarding cellular activity and the affect upon protein expression (Merne and Syranen, 2003). Consequently, the cells when cultured on other 2D matrices (native collagen and gelatin coated dishes) and when plated within a 3D type I collagen gel were tested. For each of the different matrices IHC experiments were repeated a minimum of twice, with cells at different passages, to confirm reproducibility. Observations were performed in ten fields per experiment for each variable and categorised by the overall percentage of positive cells, the level of staining intensity and background staining. Assessment was made by myself and Dr. Ana Schor.

The keratinocyte cell lines BEN, MAL and MET were all shown to express MSF. The staining for MSF was heterogeneous on all four matrices and the overall intensity was highest when the cells were plated within the 3D type I collagen gel. There appeared to be little variation in the pattern of staining between the three 2D matrices tested. The cell line which consistently displayed the most intensely stained cells was the MET, which also infrequently exhibited negative cells. When compared to the MET, the MAL and BEN cells had fewer of the highest intensity but more of the moderate and weaker stained cells. (Figure 5.1, Table 5.1).

When the cells were plated on the 2D matrices it became apparent that cells in certain areas were expressing MSF at a greater extent than others. This heterogeneous expression was most obvious with the MET cell line, where the maximum staining intensity for MSF was located in compact areas dense with multiple layers of cells. Morphologically these dense areas look like separate colonies, but when isolated and subsequently grown to confluence under standard culture conditions they display exactly the same MET morphology as their original culture. Also, MET cells plated at a lower cell density and stained when subconfluent display a homogenous staining intensity in all cells. Therefore one could conclude that cell density and cell to cell contact appears to have an impact on MSF expression.

On observing the staining of the type I collagen gel pellets it was obvious that the background was consistently scoring at the highest level. It appeared that the collagen gel was being stained, especially in the vicinity of cells. It was hypothesised that the high background could actually be due to the cells secreting MSF into the collagen matrix. A number of experiments were carried out to prove whether this was the case using the protein transport inhibitor Brefeldin A (BFA). BFA is a fungal lactone antibiotic which inhibits the Arflp GTPase, thus interfering with protein transport from the ER to the Golgi apparatus resulting in the accumulation of protein within the ER. (Fishman and Curran 1992, Klausner, 1992).

Firstly, in order to eliminate concerns about BFA toxicity the cells (FSF44 and HaCaT series) were initially plated on plastic dishes and incubated at a range of BFA concentrations (maximum concentration 5µg/ml); thereby allowing any adverse effects to be observed. Subsequently, cells were plated within type I collagen gels and incubated with BFA at 2.5 and 5µg/ml, after which the gels were fixed and processed into paraffin blocks. Immunolocalisation of MSF on the BFA treated keratinocytes showed very little difference in the level of collagen gel staining although the staining intensity of the actual cells did appear overall to be stronger. No difference was

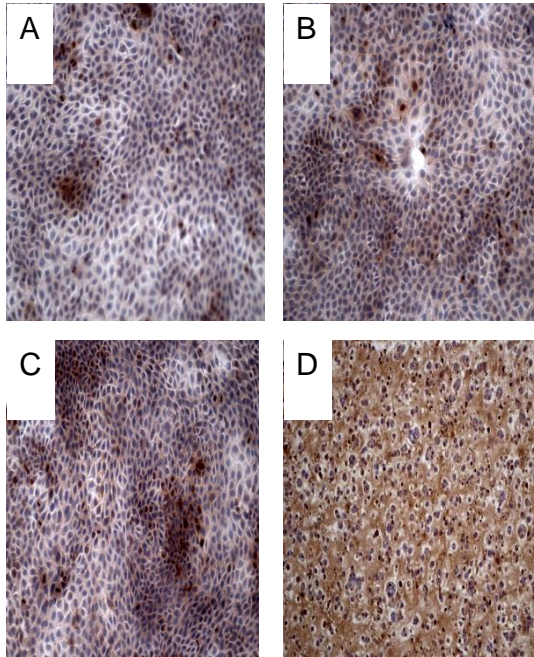
observed between BFA treated and untreated FSF44 cells. As an additional control, the cells (FSF44 and the keratinocytes) were also plated onto plastic and treated in the same manner with the BFA followed by fixation and immunolocalisation for MSF. As with the cells in the collagen gels, the stain intensity was slightly increased but overall there were no major differences to the untreated cells.

Figure 5.1: Immunolocalisation of MSF in human fibroblasts and keratinocytes.

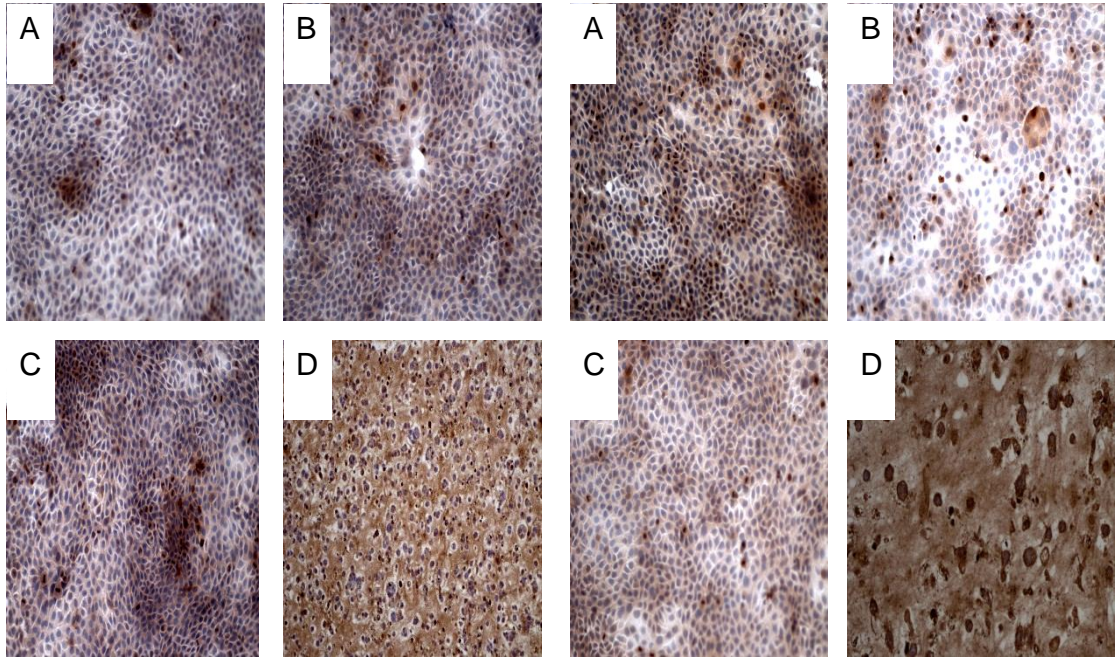
Cells were plated onto or within four different matrices: A. Plastic cell culture dishes, B. Native collagen coated dishes, C. Gelatin coated dishes, D. Type I collagen gel pellet.

A specific anti-MSF antibody, Rp2, was used at the following concentrations: Matrices A, B and C- 5µg/ml. Matrix D- 33µg/ml. Positive staining resulted in a brown colour. Control cultures incubated with normal rabbit IgG were all negative when tested at both antibody concentrations (pictures not shown). Images and observations were made at x20 magnification. Results showed that the human FSF44 fibroblasts were negative for MSF. BEN, MAL and MET keratinocytes all express MSF heterogeneously. The level of MSF expression does appear to be dependent on the plating matrix.

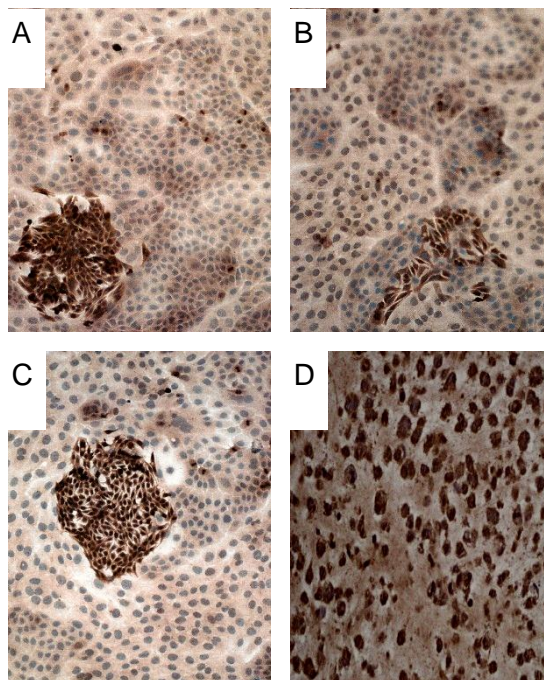
BEN Keratinocytes



MAL Keratinocytes



MET Keratinocytes



FSF44 Fibroblasts

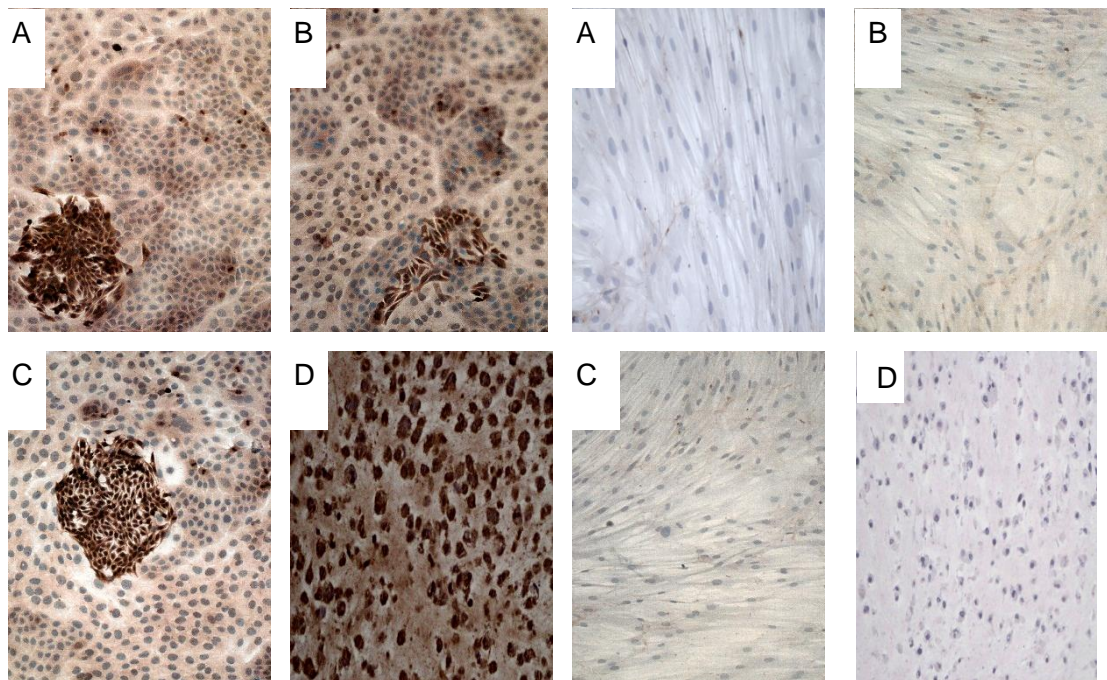


Table 5.1: Immunolocalisation of MSF in human fibroblasts and keratinocytes.

Cells were plated onto or within four different matrices: A. Plastic cell culture dishes, B. Native collagen coated dishes, C. Gelatin coated dishes, D. Type I collagen gel pellet.

A specific anti-MSF antibody, Rp2, was used at the following concentrations: Matrices A, B and C- 5µg/ml. Matrix D- 33µg/ml. Observations were made at x20 magnification.

Observations from multiple experiments were categorised as follows:

1. Overall % of cells stained positive.
2. % of cells stained at each level of staining intensity: high (3), medium (2), weak (1) and negative (0).
3. Overall score of staining intensity, calculated as (% of cells at high intensity x 3) + (% of cells at medium intensity x 2) + (% of cells at weak intensity x 1) + (% of cells negative x 0).
4. Level of background staining: negative, low, medium, high.

Matrix A. Plastic cell culture dishes

Cell Line	% of Cells Stained Positive	% of Cells at each Level of Stain Intensity				% Overall Score	Background Level
		High (3)	Medium (2)	Weak (1)	Negative (0)		
FSF44	0	0	0	0	100	0	Negative
BEN	90-100	5	10-20	70-80	0-10	105- 135	Negative
MAL	90-100	10	60-70	20-30	0-5	170- 200	Negative
MET	100	20	5-10	60-70	0	130- 150	Negative

Matrix B. Native Collagen coated dishes.

Cell Line	% of Cells Stained Positive	% of Cells at each Level of Stain Intensity				% Overall Score	Background Level
		High (3)	Medium (2)	Weak (1)	Negative (0)		
FSF44	0	0	0	0	100	0	Negative
BEN	90-100	5	40-50	40-50	10	135- 165	Negative
MAL	90-100	5	20-30	60-70	0-10	115- 145	Negative
MET	100	10-20	5	65-75	0	105- 145	Negative

Matrix C. Gelatin coated dishes.

Cell Line	% of Cells Stained Positive	% of Cells at each Level of Stain Intensity				% Overall Score	Background Level
		High (3)	Medium (2)	Weak (1)	Negative (0)		
FSF44	0	0	0	0	100	0	Negative
BEN	90-100	10	40-50	40-50	0-10	150- 180	Negative
MAL	90-100	5	40-50	40-50	0-10	135- 215	Negative
MET	100	20	5-10	65-75	0	135- 155	Negative

Matrix D. 3D Type I Collagen gel pellet

Cell Line	% of Cells Stained Positive	% of Cells at each Level of Stain Intensity				% Overall Score	Background Level
		High (3)	Medium (2)	Weak (1)	Negative (0)		
FSF44	0	0	0	0	100	0	Low-Med
BEN	70-80	20-30	10-20	10-20	20-30	90- 150	High
MAL	90-100	60-70	10-20	10-20	0-10	210- 270	High
MET	100	80-90	0-10	0-10	0	240- 300	Med- High

5.4 THE IDENTIFICATION OF NGAL EXPRESSION IN THE HACAT SERIES CELL LINES.

5.4.i Western Blot Identification of NGAL

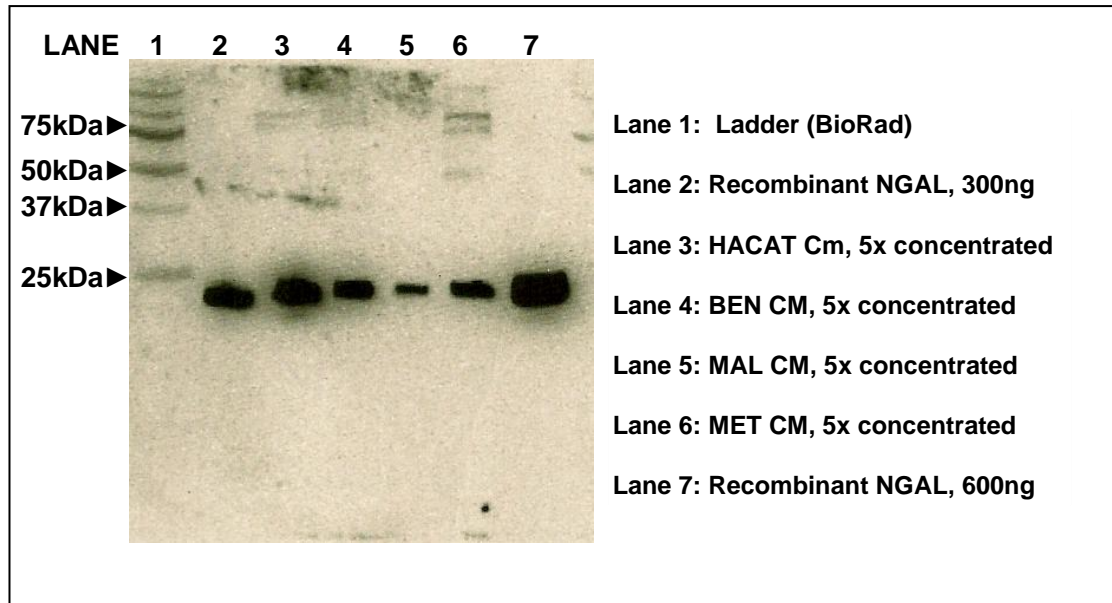
Unfractionated CM from each cell line was separated by 12% SDS PAGE under reducing conditions followed by immunoblotting with a specific anti-NGAL antibody Mab1757. The method was optimised using different concentrations of CM with the best results achieved using the 5x Amicon concentrated CM (Materials and Methods, Chapter 2).

For all the HaCaT cell lines a clear, strong band was visualised by chemiluminescence at approximately 20-25kDa, confirming NGAL was present in the CM. (Figure 5.2). Two other, but very much weaker, bands were observed in the BEN and MET lanes at higher molecular weights. These bands were located to 37-50 kDa and 100-150kDa ranges and probably correspond to other known forms of NGAL; the 46kDa disulfide linked homodimer and the 135kDa disulfide linked heterodimer with neutrophil gelatinase. A further even weaker band was also seen at approximately 50kDa in the BEN and MET lanes.

Immunoblotting for NGAL was adopted as an initial assessment of the CM for the presence of NGAL. The CM screened was not standardised and therefore no conclusion can be made over the relative NGAL expression levels of each cell line. Also, as the CM tested was concentrated approximately 5x, one must not discount the likelihood that some protein may come out of solution during the concentration process and therefore making comparisons problematic.

Figure 5.2. The identification of NGAL in HaCaT Series CM by immunoblotting.

Immunoblot of 12% SDS PAGE separation of HaCaT Series 5x concentrated CM, under reducing conditions, with specific anti-NGAL antibody, Mab1757. A distinct band was seen at approximately 25kDa, confirming the presence of NGAL.



5.4.ii Colorimetric Indirect ELISA for NGAL.

NGAL concentration was determined by indirect ELISA using a specific anti-NGAL antibody (polyclonal antibody AF1757), as described in Chapter 2, Materials & Methods. For each ELISA experiment, a standard curve for NGAL was performed using recombinant human NGAL (in house preparation) at a range of concentrations from 1.5625 to 300ng/ml (Figure 5.3). 100µl of each standard or sample were tested per well, duplicate wells were tested in each experiment and an average reading calculated. SF MEM and coating buffer were used as negative controls.

Initial experiments confirmed that all members of the HaCaT series secreted NGAL which could be measured by the indirect ELISA method.

The CM was then standardised by cell number to enable a direct comparison of NGAL concentration between the different cell lines. Although, all CM was collected using the same protocol (7ml SF MEM per 90mm) variation existed between the cell lines regarding the total number of cells present per 90mm when at confluence. (Table 5.2). Therefore, the CM for each cell line was adjusted/ diluted to the equivalent cell numbers i.e. 5.0×10^5 cells per ml of CM (dilutions made with SF MEM). These CM

preparations were then tested in the indirect ELISA both neat and at a range of dilutions (dilutions made with coating buffer).

Using the standardised CM, NGAL was detected in the CM of the all members of the HaCaT series except the MET cells (Table5.3). NGAL had been measured in the CM of the MET, however when it was standardised to equal 5.0×10^5 cells per ml, the amount of NGAL present was too low to be detected by the indirect ELISA method.

According to the results from the analysis of HaCaT CM by indirect ELISA for NGAL, NGAL expression in un-concentrated CM is from highest to lowest; MAL, BEN, HaCaT, MET.

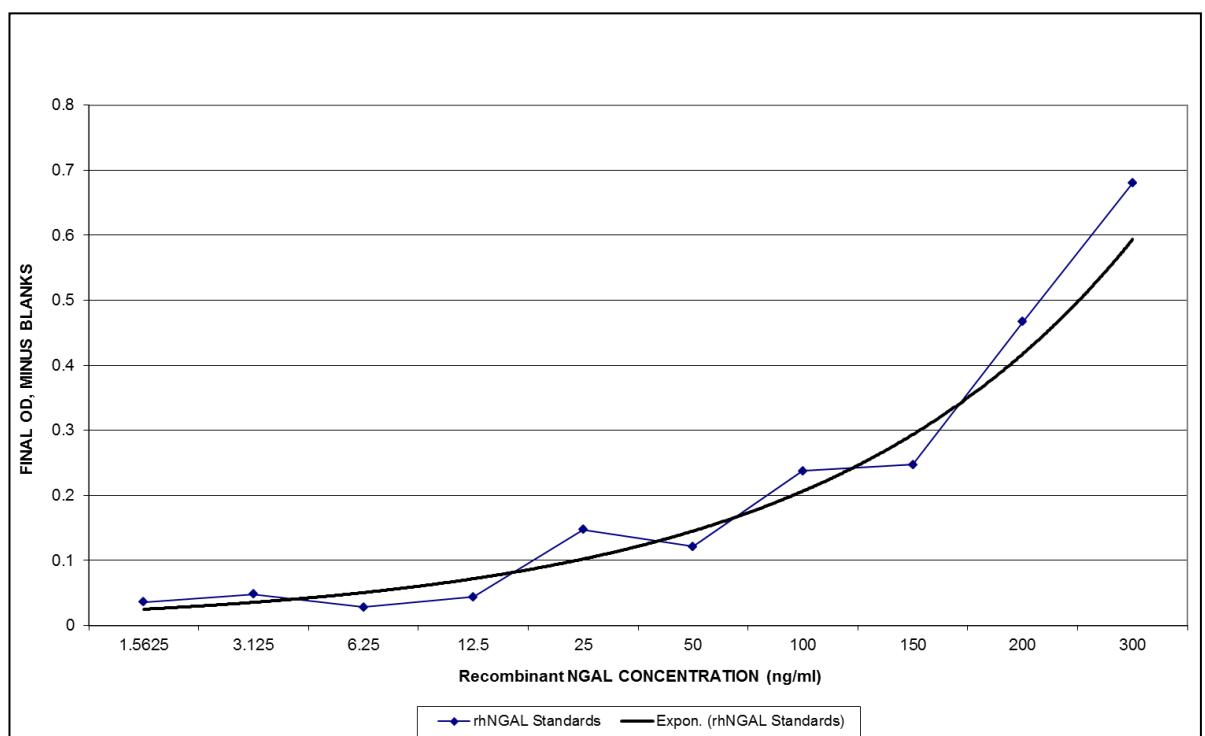


Figure 5.3. The standard curve of Colorimetric Indirect ELISA for NGAL. A specific anti-NGAL antibody, polyclonal AF1757 (R&D Systems) was used for the identification of a range of rhNGAL standards (300 to 1.5625ng/ml). OD readings were measured at 450nm. The results shown are an average of three individual experiments.

Table 5.2. The average cell counts per 90mm dish for the HaCaT series keratinocytes.

Cells from each keratinocyte cell line were plated onto 90mm plastic culture dishes and grown to confluence. After trypsinisation, cell counts were measured for each cell line from 5 separate dishes, with average cell count calculated. Cell counts measured by the Coulter Counter Z1series cell counter. Conditioned medium was collected by incubating confluent 90mm dishes with 7ml of SF MEM, therefore the average number of cells per ml of CM was calculated.

Cell Line	Confluent 90mm Average Number of Cells present.	Confluent 90mm Number of cells per ml of CM
HaCaT	5.4×10^6	7.7×10^5
BEN	5.8×10^6	8.3×10^5
MAL	5.4×10^6	7.7×10^5
MET	4.1×10^6	5.9×10^5

Table 5.3: The concentration of NGAL in HaCaT Series conditioned medium, as measured by the Colorimetric Indirect Elisa for NGAL.

Cell Line	NGAL Concentration (ng/ml)	
	Unstandardised CM	Standardised CM (5×10^5 cells per ml)
HaCaT	1059.1	370.6
BEN	1775.1	692.7
MAL	1569.05	808.7
MET	863.0	undetected

5.4.iii Immunolocalisation of NGAL in HaCaT Series

Although NGAL had been identified in the CM of the HaCaT series by immunoblotting and indirect ELISA (unlike MSF) immunolocalisation of NGAL was also performed. IHC was used to determine if there was any variation in the staining patterns of MSF and NGAL. Cells were plated onto the four different matrices, as for the MSF identification. As discussed previously, unlike cultured keratinocytes normally NGAL expression in skin is very restricted and the process of culturing keratinocytes is thought to be responsible for changes in their protein expression. As cell-matrix interactions have been shown to influence epithelial structure, growth and differentiation, the

HaCaT series was cultured on different 2D and 3D matrices in order to determine whether the matrix type would affect NGAL expression (Merne and Syranen, 2003). An antibody specific for NGAL, anti-NGAL goat polyclonal AF1757, was used for the immunolocalisation of NGAL in the cells. Optimisation experiments were performed first, to enable the selection of the most appropriate concentration of anti-NGAL antibody that gave the best staining whilst ensuring that the negative control, normal serum goat IgG, used at the same concentration was consistently negative. The secondary antibody, biotinylated polyclonal swine anti-goat IgG, was also optimised to ensure no cross-reactivity. The FSF44 fibroblast cell line was included in each experiment as an internal negative control, as had previously been showed not to express NGAL (Chapter 4.7iii).

As expected, the cells of the different members of the HACAT series all expressed NGAL while the FSF44 fibroblasts were negative. The BEN, MAL and MET cells stained heterogeneously for NGAL on all the matrices tested. For each cell line, the proportion of positive to negative cells did not vary significantly with the different matrix types; NGAL expression was independent of the plating matrix. However, variations were noted when comparing between each keratinocyte cell line. In confirming the ELISA results, overall, NGAL expression was highest in the BEN and MAL, and lowest in the MET (Figure 5.4, Table 5.4).

Figure 5.4: Immunolocalisation of NGAL in human fibroblasts and keratinocytes.

Cells were plated onto or within four different matrices: A. Plastic cell culture dishes, B. Native collagen coated dishes, C. Gelatin coated dishes, D. Type I collagen gel pellet.

A specific antibody, anti-NGAL goat polyclonal AF1757, was used at the following concentrations: Matrices A, B and C- 0.5 μ g/ml. Matrix D- 2 μ g/ml. Positive staining resulted in a brown colour. Control cultures incubated with normal goat IgG were all negative when tested at both antibody concentrations (pictures not shown). Images and observations were made at x20 magnification.

Results showed that the human FSF44 fibroblasts are negative for NGAL. BEN, MAL and MET keratinocytes all express NGAL heterogeneously. NGAL expression appears to be independent of the matrix.

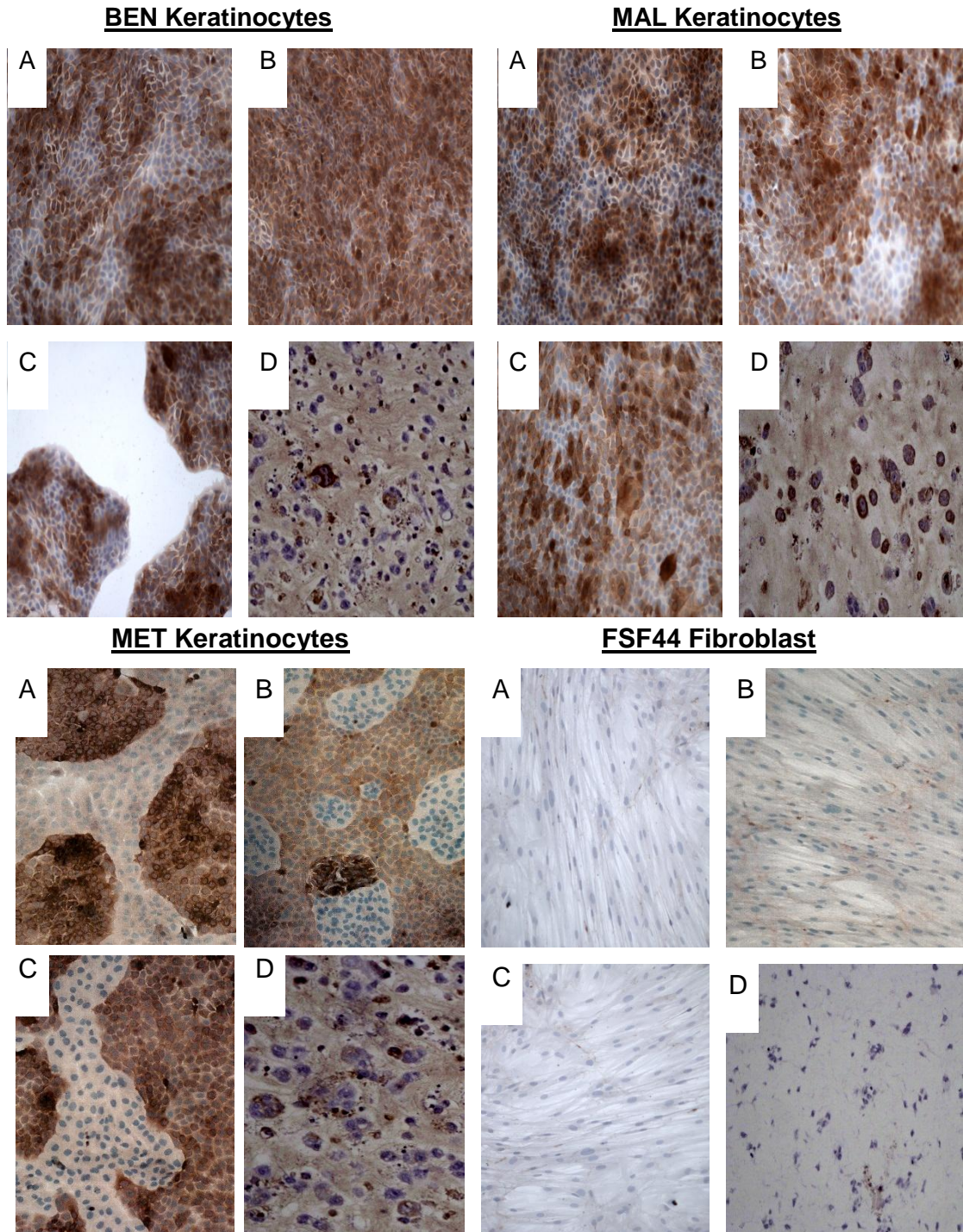


Table 5.4: Immunolocalisation of NGAL in human fibroblasts and keratinocytes.

Cells were plated onto or within four different matrices: A. Plastic cell culture dishes, B. Native collagen coated dishes, C. Gelatin coated dishes, D. Type I collagen gel pellet.

A specific antibody, anti-NGAL goat polyclonal AF1757, was used at the following concentrations: Matrices A, B and C- 0.5µg/ml. Matrix D- 2µg/ml. Observations made at x20 magnification.

Observations from multiple experiments was categorised as follows:

1. Overall % of cells stained positive.
2. % of cells stained at each level of stain intensity: high (3), medium (2), weak (1) and negative (0).
3. Overall score of stain intensity, calculated as (% of cells at high intensity x 3) + (% of cells at medium intensity x 2) + (% of cells at weak intensity x 1) + (% of cells negative x 0).
4. Level of background stain: negative, low, medium, high.

Matrix A. Plastic cell culture dishes.

Cell Line	% of Cells Stained Positive	% of Cells at each Level of Stain Intensity				% Overall Score	Background Level
		High (3)	Medium (2)	Weak (1)	Negative (0)		
FSF44	0	0	0	0	100	0	Negative
BEN	90-100	40-50	40	10	0-10	210- 240	Negative
MAL	80-90	10-20	70	10	10-20	180- 210	Negative
MET	60-70	5-10	10	40-50	30-40	75- 100	Negative

Matrix B. Native collagen coated dishes.

Cell Line	% of Cells Stained Positive	% of Cells at each Level of Stain Intensity				% Overall Score	Background Level
		High (3)	Medium (2)	Weak (1)	Negative (0)		
FSF44	0	0	0	0	100	0	Negative
BEN	90-100	30-40	40	10-20	0-10	180- 220	Negative
MAL	80-90	10-20	70	10	0-10	180- 210	Negative
MET	60-70	5-10	40-50	5-10	30-40	100- 140	Negative

Matrix C. Gelatin coated dishes.

Cell Line	% of Cells Stained Positive	% of Cells at each Level of Stain Intensity				% Overall Score	Background Level
		High (3)	Medium (2)	Weak (1)	Negative (0)		
FSF44	0	0	0	0	100	0	Negative
BEN	90-100	40-50	40	10	0-10	210- 240	Negative
MAL	80-90	10-20	40	40	0-10	150- 180	Negative
MET	60-70	5-10	40-50	5-10	30-40	100- 140	Negative

Matrix D. 3D Type I collagen gel pellet.

Cell Line	% of Cells Stained Positive	% of Cells at each Level of Stain Intensity				% Overall Score	Background Level
		High (3)	Medium (2)	Weak (1)	Negative (0)		
FSF44	0	0	0	0	100	0	Low-Med
BEN	80-90	30-40	30-40	10-20	10-20	160-240	Med- High
MAL	80-90	30-40	30-40	10-20	10-20	160-240	Med- High
MET	70-80	20-30	10-20	10-20	10-20	90-170	Med- High

5.5 DISCUSSION

Cancer development is a multistep process whereby, due to the accumulation of genetic alterations, a cell gradually progresses from a normal to malignant phenotype.

The mechanism for malignancy development it is still uncertain; as to whether a required amount of genetic alterations must occur or if there is a defined sequence of genetic events. Various experimental procedures have been adopted to study the conversion to malignancy including the use of rodent models, carcinoma derived cell lines or non-malignant cells treated with potent oncogenic stimuli.

Experimental animal model systems and cultured rodent cells traditionally formed the basis of many studies however major differences to humans exist. Inter- species discrepancies in sensitivity to carcinogenic agents and subsequent transformation are reflected in the frequency of immortalisation. Human cells, unlike rodent, possess a notable resistance to transformation by oncogenes and chemical or physical carcinogens. Species- related factors such as natural life span, degree of rodent inbreeding and the higher genetic stability of human genome have been attributed for the disparity (Sager, 1984, Fusenig and Boukamp, 1998).

Cell lines derived from primary tumours, especially from epithelial tissues, are often difficult to culture. Established lines are often considered to represent an elite subset of tumour cells which have the capacity to survive and adapt to the cell culture environment. The intensity of the selection pressures imposed on them during extensive cell culture may result in a genetic or phenotypic drift. This may explain the often contradictory data arising from studies using cancer cell lines, where results reflect a distinctive characteristic of a specific cell line (Marques *et al.*, 2006).

Successful immortalisation of human cells is rare when using chemical and physical agents but can be reproducibly induced by DNA viruses such as simian virus 40, adenovirus types 5 and 12, human papilloma virus types 16, 18 and 33(Rhim *et al.*, 1990). However, subsequent changes to the cell(s) may be virus- related rather than a result of transformation. For example, the immortalisation of human keratinocytes with SV40 was accompanied by dramatic changes in differentiation potential (Steinberg and Defendi, 1983). Unlike the spontaneously immortalised HaCaT cell line, which exhibit practically a normal amount of morphologic differentiation with the ability to form a well structured epidermis after transplantation *in vivo* (Boukamp *et al.*, 1988). The development of permanent and stable *in vitro* cultures, like the HaCaT keratinocytes, has offered unlimited sample amount and more flexibility.

Researchers also noted that many of the models studied lacked the capacity to investigate the intermediate stages of cancer progression. However, the introduction of additional genetic alterations in the *in vitro* cultures offered the potential to develop models characterising the different stages of tumour development and progression. *In vitro* model systems similar to the HaCaT series have been established for other tissue types including breast (MCF10A and HMT-3522) and prostate (PC346) (Soule *et al.*, 1990, Dawson *et al.*, 1996, Rizki *et al.*, 2008, Marques *et al.*, 2006).

The HaCaT series model of human skin carcinogenesis has revealed that both MSF and NGAL are expressed by keratinocytes representing the different stages of tumour development. All members of the HaCaT series; BEN, MAL and MET express both MSF and NGAL, although at varying degrees. Overall, the results show that during tumour progression the expression level of NGAL decreases whilst that of MSF increases.

NGAL was easily identified in the conditioned medium collected from each cell line of the HaCaT series by using the techniques of immunoblotting and indirect ELISA and subsequently confirmed by immunolocalisation using a specific anti-NGAL antibody. By standardising the conditioned medium, taking into account the variation in cell numbers from which the CM was collected, analysis by indirect ELISA revealed that MET cells expressed the lowest amount of NGAL while BEN and MAL express the most. This result was confirmed by the semi-quantitative assessment of the stained keratinocytes cultured on plastic dishes; the greatest percentage of high intensity staining was consistently detected in the BEN as opposed to the MET cultures which possessed the highest percentage of negatively stained cells.

Testing of the standardised HaCaT series CM for NGAL by indirect ELISA identified a pattern of expression from highest to lowest as being- BEN/ MAL > HaCaT > MET. That is compared to normal HaCaT keratinocyte levels, NGAL expression increases during the benign and low –grade malignancy phases of tumour progression but is then drastically reduced at the advanced metastatic stage. A similar situation has been described in studies on ovarian, pancreatic and colon carcinoma with many believing NGAL could potentially be an early stage biomarker for a variety of cancers (Lim *et al.*, 2007, Tong *et al.*, 2008, Lee *et al.*, 2006, Yang and Moses 2009). In these carcinomas, NGAL seems to have an anti-metastatic action. For example, in ovarian cancer NGAL expression blocked the epithelial to mesenchymal transition (EMT), which is crucial for invasive neoplasia (Lim *et al.*, 2007). Cho and Kim (2009) showed NGAL immunoreactivity in ovarian cancers was significantly associated with tumour

differentiation; well-differentiated tumours having the highest expression values compared with moderately and poorly differentiated tumours. A grade specific pattern of NGAL expression has also been described for pancreatic tumours and oral squamous cell carcinoma (Hana *et al.*, 2005, Moniaux *et al.*, 2008, Lin *et al.*, 2012).

Mallbris *et al* (2002) also proposed a role linking NGAL to keratinocyte differentiation pathway.

However, the opposite situation has been described in breast cancer studies where elevated NGAL expression is associated with a poor prognosis; suggested NGAL promotes breast cancer progression by regulating EMT due to its ability to stabilise MMP-9 (Yang *et al.*, 2009, Leng *et al.*, 2009). Increased NGAL levels are also considered a poor prognostic indicator in gastric, oesophageal squamous cell and anaplastic thyroid carcinoma (Kubben *et al.*, 2007, Zhang *et al.*, 2007, Iannetti *et al.*, 2008, Wang *et al.*, 2010). Overexpression of NGAL has been ascribed an important role in the malignant transformation of human immortalised oesophageal epithelial cells and shown to enhance the differentiation and invasion of oesophageal squamous cell carcinoma cells (Du *et al.*, 2011). The effects of NGAL therefore appear to be neoplasia- specific; a description that is often used when reviewing NGAL research (Bolognani *et al.*, 2010, Chakraborty *et al.*, 2012). See Table 4.6 for literature review. The identification of MSF expression proved to be more elusive. Analysis of MSF by immunoblotting and the sandwich ELISA failed to give a positive result. However, immunolocalisation of MSF in the cultured cells proved both successful and reproducible. Consequently, the conclusion was that the HaCaT series keratinocytes do express MSF but it must be present in the CM at concentrations below the limits of sensitivity of the assays (25ng/ml limit of the Western Blot and 12.5ng/ml limit of the Sandwich ELISA). Semi-quantitative evaluation of the MSF stained keratinocytes suggested an opposite expression pattern to NGAL. MET cells displayed the highest intensity of MSF localisation and had the fewest number of negative cells. The BEN cultures had the most MSF-negative cells.

MSF is an oncofetal protein; expressed during foetal development but diminished in healthy adult cells. Expression is transiently switched on during acute wound healing and persistently expressed by both tumour and stromal cells in various human cancers (Schor *et al.*, 2003, 2005, Jones *et al.*, 2007). The discovery that the highest intensity of MSF expression is greatest in the keratinocyte cell line representing the metastatic stage of carcinogenesis concurs with the observation that an elevated expression of MSF in breast tumours is associated with a poorer prognosis (Aljorani *et al.*, 2011).

Predominantly, when cultured within the 3D type I collagen matrix the HaCaT series model of human skin carcinogenesis displayed an increased MSF expression with increasing tumour progression.

The inability to identify MSF in the HaCaT series CM may lead to the presumption that if the conditioned medium was tested in the fibroblast migration assay any MSF bioactivity would be masked by the NGAL present. A situation similar to that described for the HaCaT keratinocytes. However, MSF possesses a potent motogenic bioactivity, with half-maximal response exhibited at femtomolar concentrations, 0.1-1pg/ml. This is clearly below the limits of the assays adopted to identify MSF in the CM. Another consideration is that the antibodies used in the identification assays only recognise the unique decapeptide sequence of MSF. It maybe that this is no longer recognisable when MSF is secreted into the CM either due to change in conformation, the vulnerability of the VSI sequence to the action of proteolytic enzymes due to its C-terminus location or masking due association with an accessory protein. However, the motogenic activity of MSF located in the GBD domain and retains its bioactivity after cleavage. (Schor *et al.*, 1996 and 2003).

Ambiguous results were achieved in the assessment of the effect different culture matrix compositions had on keratinocyte NGAL and MSF expression. Each of the HaCaT series was cultured on a selection of 2D matrices (plastic, gelatin and native collagen coated dishes) and within a 3D type I collagen gel. NGAL staining appeared to follow a similar if not an identical pattern irrespective of the matrix, that is BEN and MET having the highest and lowest overall scores respectively. MSF staining patterns were similar for the plastic and 3D collagen matrix, but at odds with those for gelatin and native collagen. It was also clear that MSF staining intensity was maximal when the keratinocytes were cultured within the type I collagen. These results support the concept that matrix composition can influence keratinocyte protein expression. Although the cells are plated as monolayers on all the 2D surfaces different cell-matrix interactions will occur, indeed the inert and uniform nature of the plastic surface immediately set it apart. Plating the keratinocytes within the 3D collagen matrix results in differences in cell-matrix and cell-cell interactions which ultimately effect both morphology and protein expression. Although the results are less informative than expected, they do highlight and agree with Merne and Syrjanen (2003) on the importance of using a standardised matrix to avoid the confounding effects on keratinocyte protein expression. In conclusion, the analysis of MSF and NGAL expression in the HaCaT series model of human skin carcinogenesis has shown that during tumour progression NGAL

expression decreases while MSF increases. Each of the HaCaT-*ras* clones (BEN, MAL and MET) represents a shift in tumourigenic potential from the benign situation, malignancy and finally to metastasis. The next step was to assess the bioactivity of CM collected from the HaCaT series cell lines in the 3D collagen gel fibroblast migration assay. The presence of both pro- and anti- motogenic activity was evaluated in order to determine whether the expression levels of NGAL and MSF can be related to the bioactivity present in the conditioned medium of the HaCaT-*ras* clones? The analysis of the HaCaT total CM in the 3D collagen gel fibroblast migration assay showed that the motogenic bioactivity of the endogenous MSF is masked due to inactivation by the co-secreted NGAL (Jones *et al.*, 2007). Consequently, the proposed question is- will the stoichiometric relationship between NGAL and MSF alter with the increasing degree of malignancy of the HaCaT-*ras* clones?

Chapter 6: Results

THE EXPRESSION OF PRO- AND ANTI- MOTOGENIC BIOACTIVITY BY THE HACAT-RAS CLONES.

6.1 AIMS

To assess the bioactivity of CM collected from the HaCaT *-ras* clones (HaCaT series cell lines) in the 3D collagen gel fibroblast migration assay. To ascertain the presence of both pro- and anti- motogenic activity, in order to identify the possible contribution made by MSF and NGAL during tumour progression.

6.2 BACKGROUND

It has already been established that both MSF and NGAL are expressed by cultured non-tumourigenic HaCaT and tumorigenic BEN, MAL and MET keratinocyte cell lines. However, expression levels are not uniform; as the tumourigenic potential increases there is a relative elevation in MSF and a decline in NGAL expression.

Previous experiments, analysing the bioactivity of conditioned medium (CM) collected from the HaCaT line demonstrated that the motogenic activity of the HaCaT MSF is undetected due to inactivation by the co-secreted NGAL. With the discovery that the HaCaT series lines also express MSF and NGAL, one could conclude that the endogenous NGAL would also have the potential to suppress any endogenous MSF bioactivity in the CM too. However, ELISA analysis of the HaCaT series CM for NGAL has shown that while BEN and MAL express more NGAL than the HaCaT cells the opposite is true for the MET. Plus semi-quantitative evaluation of MSF immunolocalisation in the keratinocytes revealed that the highest staining intensity was consistently located in the MET cells. In addition, compared to the BEN and MAL cultures the MET cells were consistently MSF positive, that is no MSF-negative cells were identified. Therefore, this altered balance of MSF and NGAL compared to the HaCaT has led to the postulation that of all the tumorigenic keratinocytes, the MET would differ from the HaCaT CM and actually display motogenic activity attributable to MSF. This prediction, of course, does not take into consideration other motogenic

factors which may also be present in the CM, with the potential to affect the CM bioactivity of each cell line.

6.3 THE ASSESSMENT OF THE BIOACTIVITY OF HACAT SERIES CONDITIONED MEDIUM

6.3i The Motogenic Activity of HaCaT Series Conditioned Medium

Serum free (SF) conditioned medium was collected from each HaCaT series cell line and tested for motogenic activity in a minimum of five separate 3D collagen gel fibroblast migration experiments. The CM was tested alone, at a range of dilutions from 1/4 to 1/40,000 (all dilutions made with SF MEM). Bioactivity was classified as motogenic when fibroblast migration was stimulated to increase by a minimum of 50%, as compared to SF MEM control baseline level.

As discussed previously, when recombinant MSF is tested in the migration assay its motogenic activity is characterised by a bell-shaped dose response. Maximal MSF stimulation migration occurs at concentrations of 100-500pg/ml, with migration 2-3 times that of the SF MEM baseline, (Figure 6.1a). When tested, both BEN and MAL CM displayed a pattern of motogenic activity similar to rhMSF; a bell shaped dose response with peak stimulation at the 1/1000 dilution point, 2-2.5 times that of SF MEM baseline level (Figure 6.1b-c).

MET CM also possessed stimulatory bioactivity, but this activity was not characterised by the same response pattern. Every dilution point from 1/40,000 to 1/100 demonstrated a similar level in motogenic activity; 2-2.5 times more than SF MEM baseline level. (Fig6.1d). Since MET bioactivity did not diminish at the higher dilutions as occurred with BEN and MAL, one can conclude that the MET CM possessed the most motogenic activity and therefore the motogen responsible must be present at a higher concentration in the MET CM. As stated previously, when MET cells are grown on a 90mm culture dish fewer cells are present at confluence, when CM is collected, than compared to the BEN and MAL lines, (Table 5.2). Hence, a fewer number of MET cells are required to condition medium for maximal bioactivity; the motogen expression and secretion must consequently be higher.

The highest dilutions of MET CM tested (1/40,000 and 1/20,000) still displayed motogenic activity. The same dilutions of BEN CM showed no activity, whereas MAL

CM appeared to show borderline activity (i.e. MAL CM was motogenic at 1/40,000 in 2/4 experiments and showed no activity in the rest). Within the range of dilutions tested, maximal motogenic activity was obtained at 1/40,000 for the MET CM and 1/4,000 - 1/1,000 for the BEN and MAL CM. These results indicate that the concentration of a putative motogenic factor(s) in the MET CM may be at least 10 fold higher than in the BEN CM, with the MAL somewhere in between. Although, at this stage it cannot be presumed that the motogenic activity is due to a single factor, the presence and activity of other factors cannot be dismissed.

If the presumption is that MSF is the only motogen responsible for the HaCaT series stimulatory bioactivity, then these results are in accord with those gained from MSF immunolocalisation experiments; the most tumorigenic cell line, the metastatic MET keratinocytes, expresses the most MSF while the MAL and BEN have similar expression levels. That is, for the HaCaT series increasing MSF expression levels corresponds to increasing motogenic bioactivity present within the CM, which equates to the tumourigenic potential of the cell line.

6.3ii The MSF-Inhibitory Activity of HaCaT Series Conditioned Medium

To assess whether the HaCaT series CM possessed MSF-I bioactivity, CM was tested in the 3D collagen gel fibroblast migration assay in the presence of 100pg/ml rhMSF. A minimum of three experiments were performed for each cell line, with the CM tested at a range of dilutions from 1/4 to 1/40,000 (all dilutions made with SF MEM). 100pg/ml of rhMSF reproducibly increases fibroblast migration by at least two fold by comparison to the control, SF MEM baseline. Therefore, a dilution was categorised as having MSF inhibitory activity if upon addition of 100pg/ml rhMSF it reduced migration by at least 50% when compared to the control 100pg/ml rhMSF baseline. Experiments with recombinant NGAL have demonstrated its ability to inhibit the bioactivity of 100pg/ml rhMSF back to SF MEM baseline levels. NGAL concentrations of 1ng/ml and below do not inhibit MSF stimulated migration, while concentrations of 10ng/ml and above do, returning migration levels back to the SF MEM baseline. NGAL does not have the ability to reduce migration to below the SF MEM baseline (maximum concentration tested 1µg/ml). (Figure 6.2a).

In comparison to the effect NGAL has on rhMSF, the HaCaT series BEN and MAL cell lines CM also reduces MSF motogenic activity. Overall, as the concentration of BEN and MAL CM increased so did their MSF-I bioactivity and similar to rhNGAL,

migration was not inhibited below SF MEM baseline. BEN and MAL displayed a similar level of MSF-I activity meeting the set criteria of a 50% reduction in migration at dilution points 1/1000 to 1/4, (Figure 6.2b and c). These results are in accordance to the data gained from the assessment of NGAL in CM by ELISA, where BEN and MAL have similar NGAL concentration in un-standardised CM (Table 5.3).

However, MET CM displayed no MSF-I activity. All dilution points tested failed to reduce migration by the set criteria, (Figure 6.2d). NGAL quantification by ELISA indicated that MET secreted the least NGAL (or lowest amount).

6.3iii The Motogenic Activity of Recombinant MSF in the Presence of HaCaT Series Conditioned Medium.

Each of the HaCaT series cell lines (BEN, MAL and MET) demonstrated the ability to stimulate fibroblast migration in the 3D collagen gel assay, possessing an endogenous motogenic activity. Therefore, an additional method of analysis was required to eliminate the possibility that this activity may mask the effect of any MSF- inhibitor(s) present in the CM. Instead of determining an increase or decrease in migration by comparison to the positive (rhMSF) or negative (SF MEM) controls, the CM when tested alone, at each individual dilution, was considered as the baseline migration. That is, MSF-inhibitory bioactivity was defined, upon addition of 100pg/ml rhMSF, as the inability to increase CM baseline migration by a minimum of 50%.

If MSF is responsible for the motogenic activity detected in the CM, the nature of MSF's bioactivity, a bell shaped dose response, may cause misinterpretation of the results. For example, if the MSF present in the CM is at a low concentration i.e. below 10pg/ml, the addition of 100pg/ml rhMSF would result in an increase in migration due to "tipping" over of the bell-shaped response to MSF concentrations which give maximal migration. Whereas, if the MSF present in the CM is at a concentration above 500pg/ml, in theory, the addition of 100pg/ml could result in a reduction in migration. However, results from the ELISA and immunoblot experiments, to detect MSF, imply that the MSF concentrations present in the HaCaT series CM are low and therefore any reduction in migration is probably due to the action of a MSF- inhibitor. Finally, if there appeared to be no effect upon addition of rhMSF the conclusion was either that it was the actions of an inhibitor or that MSF within the CM must be at the concentration of peak bioactivity (100-500pg/ml) and therefore the addition of a further 100pg/ml would make little or no difference to cell migration.

As shown previously, BEN and MAL CM display both endogenous motogenic bioactivity, when tested alone, and MSF- inhibitory activity upon addition of rhMSF. Now that the baseline migration is taken into account this shows that BEN and MAL CM possess a distinct MSF-inhibitory activity, (Figure 6.3 a and b). The addition of 100pg/ml rhMSF appeared to have no effect on the baseline migration at the majority of dilution points tested. A limited increase in migration was noted in the MAL CM at the maximal dilutions but this did not reach the set criteria for MSF stimulation. High standard deviations at these dilutions demonstrate the effects such high dilutions have on experimental variability and reproducibility. The BEN CM also increased migration, which met the set criteria of MSF bioactivity, at 1/20,000 dilution; when previously tested alone this dilution point displayed no motogenic activity, (Figure 6.1.b). Previously, MET CM displayed motogenic activity (Figure 6.1.d) whilst having no ability to inhibit MSF bioactivity, (Figure 6.2.d). However, this analysis has shown the addition of rhMSF actually had no effect on increasing cell migration above the baseline level at the various dilutions tested, (Figure 6.3.c) suggesting possible MSF inhibitory activity. Presuming the motogenic activity of the MET CM is due to the expression of endogenous MSF then this “inhibitory activity” could actually be due to the addition of excess MSF causing a “tipping” over of the bell shaped dose response, where the higher MSF concentration (>500pg/ml) results in a reduction in migration, (Figure 6.3c).

6.4 THE CHARACTERISATION OF HACAT SERIES ENDOGENOUS MOTOGENIC BIOACTIVITY.

The CM from each HaCaT series cell lines has consistently displayed the ability to stimulate the migration of fibroblasts in the migration assay in a similar way to the bioactivity of MSF. Testing the CM in the presence of NGAL and the MSF function neutralising antibody, PEPQ1.1, should determine whether this endogenous motogenic activity could be attributed to the secretion of MSF. Both NGAL and the PEPQ antibody inhibit MSF bioactivity back to baseline levels; however they have different levels of potency. The maximum MSF concentration that 10ng/ml of NGAL can inhibit is 500pg/ml, whereas a 50ng/ml of PEPQ 1.1 can inhibit up to 1ng/ml of MSF. The set criteria for NGAL and PEPQ1.1 inhibition was a reduction in CM baseline migration by at least 50% and each cell line was tested a minimum of three times.

NGAL appeared to have a minimal effect on reducing the motogenic activity of the HaCaT series CM. CM only baseline migration was decreased upon addition of NGAL at a few dilution points, but for all the cell lines it failed to reach the set criteria of a 50% reduction. Maximal inhibition by rhNGAL was 38%, 40% and 31% at dilutions 1/10, 1/4000 and 1/10 for BEN, MAL and MET respectively, (Figure 6.4a-d).

The PEPQ1.1, MSF function neutralising antibody, appeared to have more of an effect in limiting the motogenic activity of the HaCaT series CM. However, in the majority of cases, any inhibition which did occur, failed to meet the set criteria of a 50% reduction. The maximum level of inhibition by PEPQ 1.1 antibody was 68% at 1/10 dilution of BEN CM and 51% for MET CM 1/1000 dilution; other dilution points had borderline results, (Figure 6.5a-d). Overall, the level of inhibition by PEPQ 1.1 was greater than that of NGAL in both the number of motogenic dilutions with reduced migration and the level of inhibition achieved- a foreseeable result knowing the different intensities of MSF-I activity displayed by each inhibitor, as discussed earlier. (Table 6.1)

The inability to achieve the set criteria of a 50% reduction in motogenic bioactivity could be due to numerous factors. The most obvious being that too little NGAL and PEPQ1.1 were added to the CM which resulted in incomplete inhibition due to the discrepancy between inhibitor potency and actual amount of MSF present in the CM. However, the level of motogenic activity detected in the HaCaT series CM appeared to be below that measured for 100pg/ml rhMSF, which would imply that ample concentrations of inhibitors were used since 10ng/ml NGAL and 50ng/ml of PEPQ1.1 can inhibit the activity of 500pg/ml and 1ng/ml rhMSF respectively. (100pg/ml rhMSF = 300% of cells migrated compared to SF MEM baseline, maximal migration achieved by HaCaT series CM = 250%).

The consequences of the nature of MSF bioactivity should be also be considered. By adding an inhibitor to the CM was excess MSF being “removed” allowing the bell-shaped dose response to tip back over into concentrations where upon migration was actually stimulated? However, only the addition of NGAL resulted in an increase in migration compared to baseline levels and only at a few random dilution points; no pattern emerged to support this theory.

Another reason could be the presence of another motogen(s) in the CM, which would be unaffected by the MSF-inhibitors. Therefore, the criteria to determine whether inhibition was achieved by NGAL and PEPQ1.1 was maybe set too high and did not take this into account. However, since the exact concentration of MSF present within the CM was unknown the setting of the criteria was arbitrary and understandably high

in order to eliminate false positive results. Nonetheless, from these experiments the overall conclusion was that at least a proportion of the motogenic bioactivity present within the CM of the HaCaT series could be attributed to MSF.

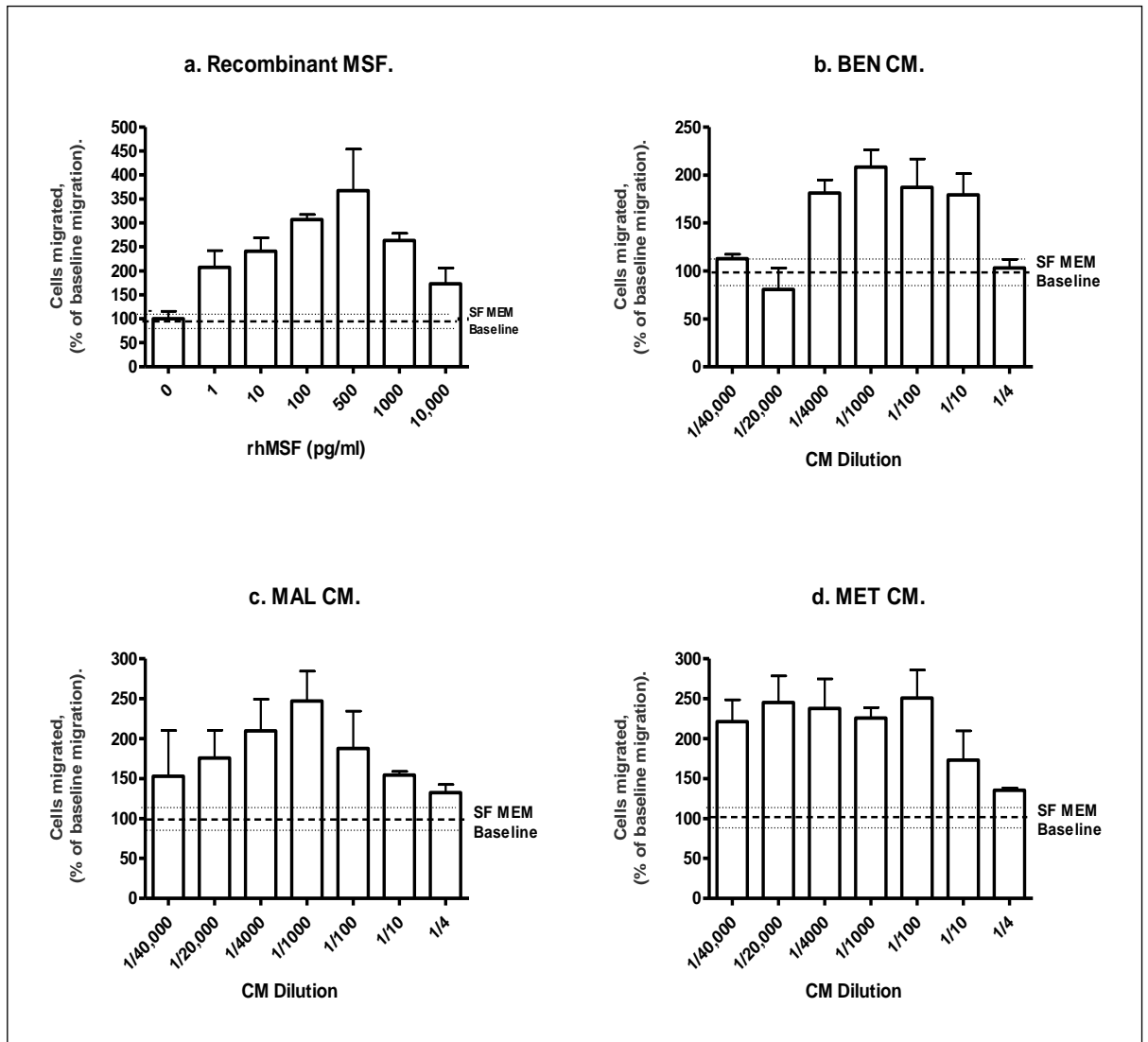


Figure 6.1: The motogenic activity of conditioned medium from HaCaT Series cells, comparison with rhMSF. Conditioned medium (CM) from each cell line (BEN, MAL and MET) was tested, on its own, at various dilutions in the 3D Collagen gel fibroblast migration assay. The number of cells migrated is expressed as a percentage of the SF MEM control baseline migration i.e. SF MEM Baseline = 100 +/- 16.07%, as represented by hatched and dotted lines (mean and SD respectively). This was equivalent to 2.8 +/- 0.45 migrated cells. (100pg/ml rhMSF only = 8.6 +/- 0.28 migrated cells). The results represent an average of three experiments. Dose response to rhMSF is shown for comparison.

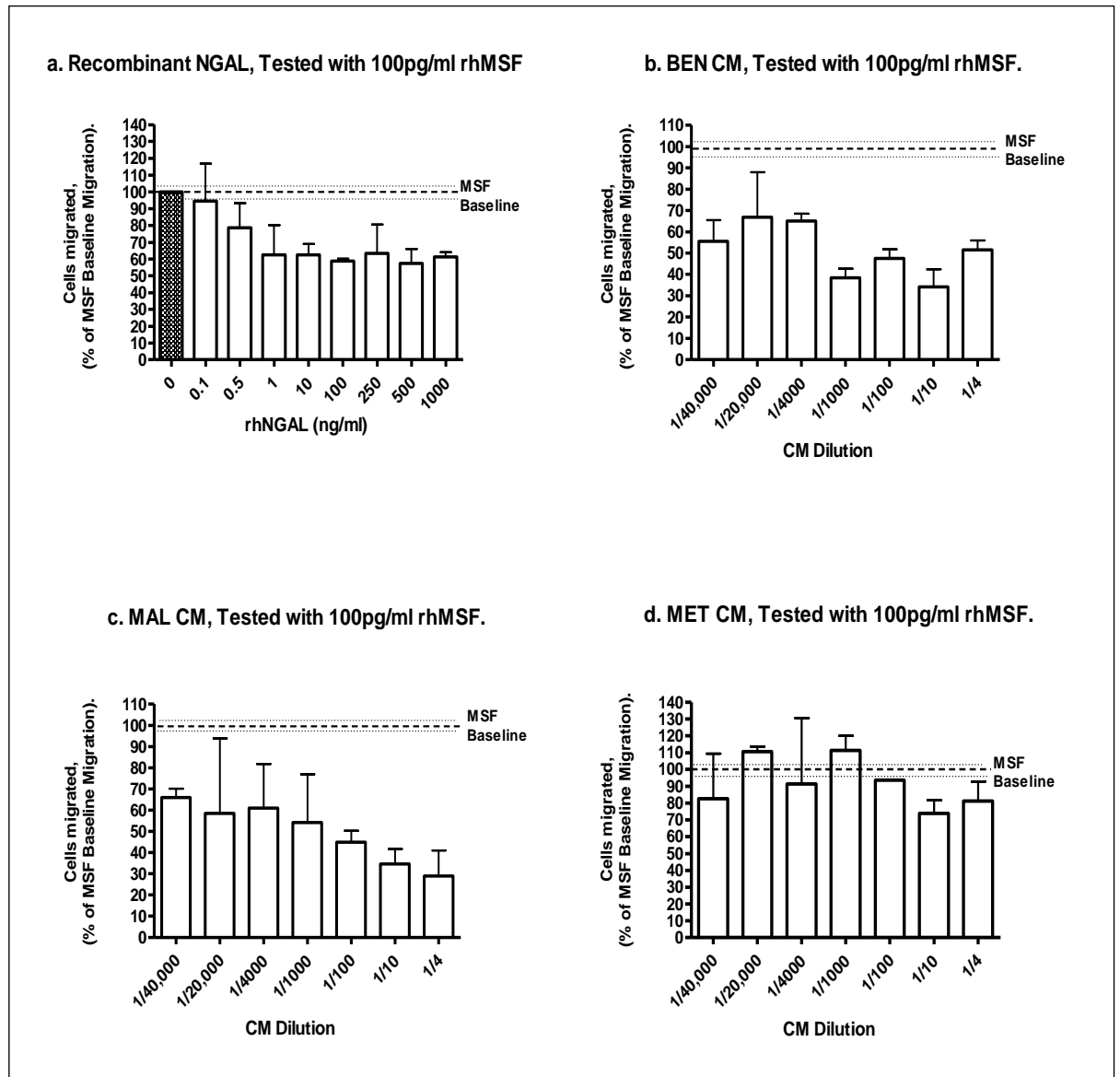


Figure 6.2: The MSF-inhibitory activity of conditioned medium from HaCaT

Series cells, comparison with rhNGAL. Conditioned medium (CM) from each cell line

(BEN, MAL and MET) was tested at various dilutions in the 3D collagen gel fibroblast

migration assay in the presence of 100pg/ml rhMSF. The number of cells migrated is expressed

as a percentage of the 100pg/ml rhMSF control baseline migration i.e. MSF Baseline = 100 +/-

3.26%, as represented by hatched and dotted lines (mean and SD respectively). This was

equivalent to 8.6 +/- 0.28 migrated cells. The results represent an average of three experiments.

Dose response to rhNGAL is shown for comparison.

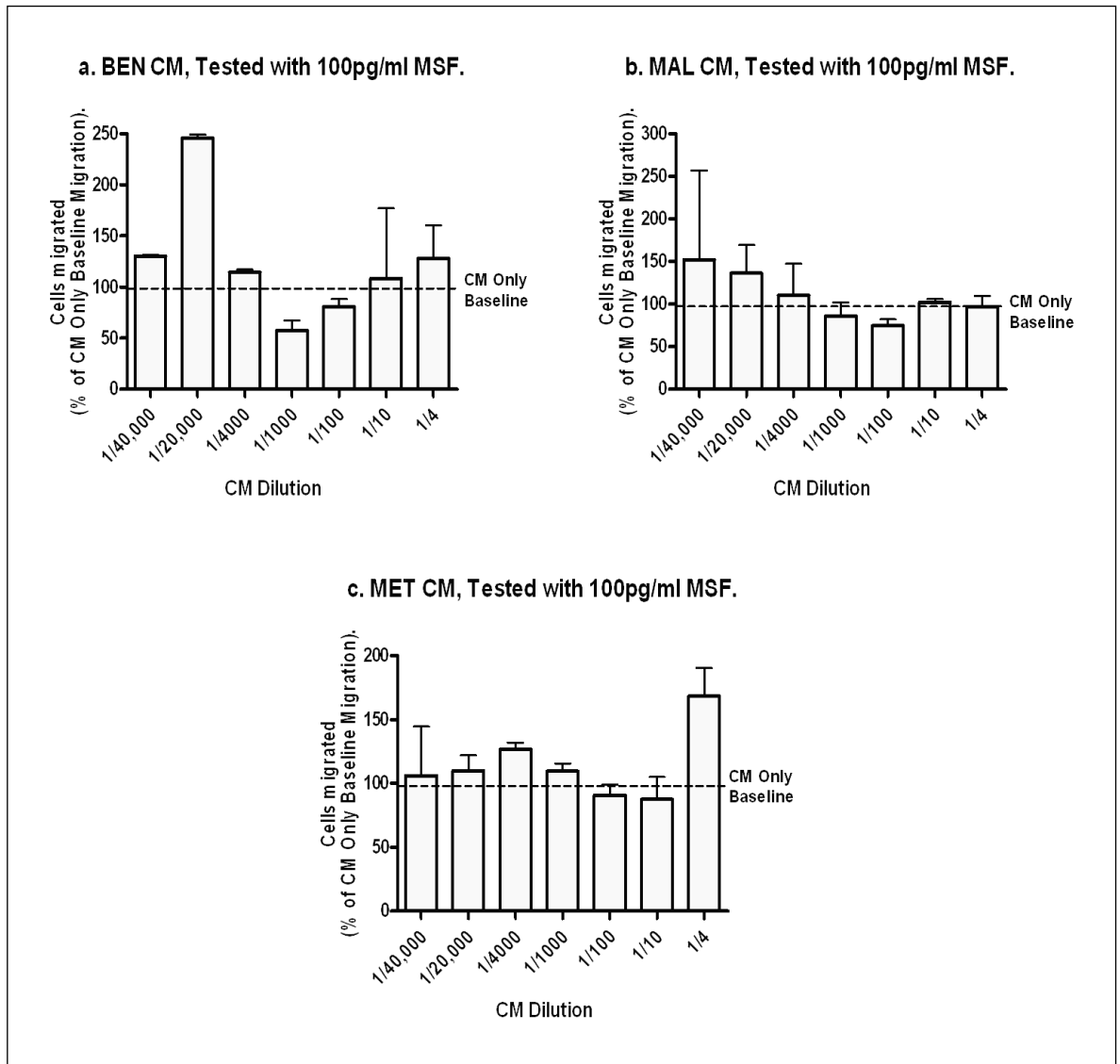


Figure 6.3. The motogenic activity of exogenous rhMSF in the presence of conditioned medium. Conditioned medium (CM) from each cell line (BEN, MAL and MET) was tested, at various dilutions, in the 3D collagen gel fibroblast migration assay with and without the presence of 100pg/ml rhMSF. The number of cells migrated is expressed as a percentage of the CM only baseline migration at each individual dilution point. i.e. 1/4 dilution CM only = 100%, as represented by hatched line. The results represent an average of three experiments.

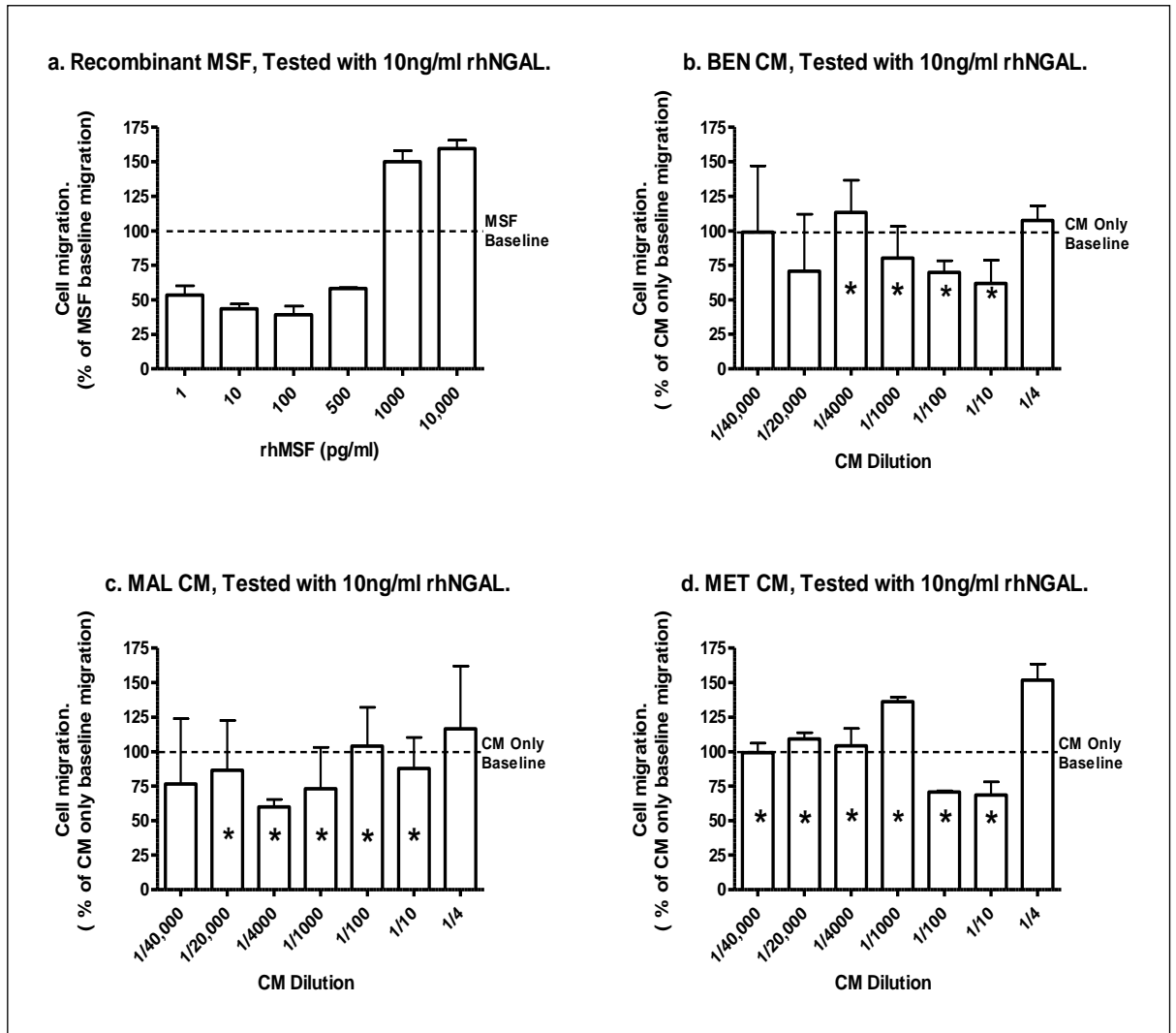


Figure 6.4: The effect of NGAL on the endogenous motogenic bioactivity of HaCaT Series CM, comparison with rhMSF. Conditioned medium (CM) from each cell line (BEN, MAL and MET), at various dilutions, in the 3D collagen gel fibroblast migration assay in the presence of 10ng/ml rhNGAL. The number of cells migrated is expressed as a percentage of the CM only baseline migration at each individual dilution point. i.e. 1/4 dilution CM only = 100%, as represented by hatched line. CM dilutions which display motogenic activity, when tested alone, are identified by a star (*). The results represent an average of three experiments. Effect of rhNGAL on the dose response of rhMSF is shown for comparison.

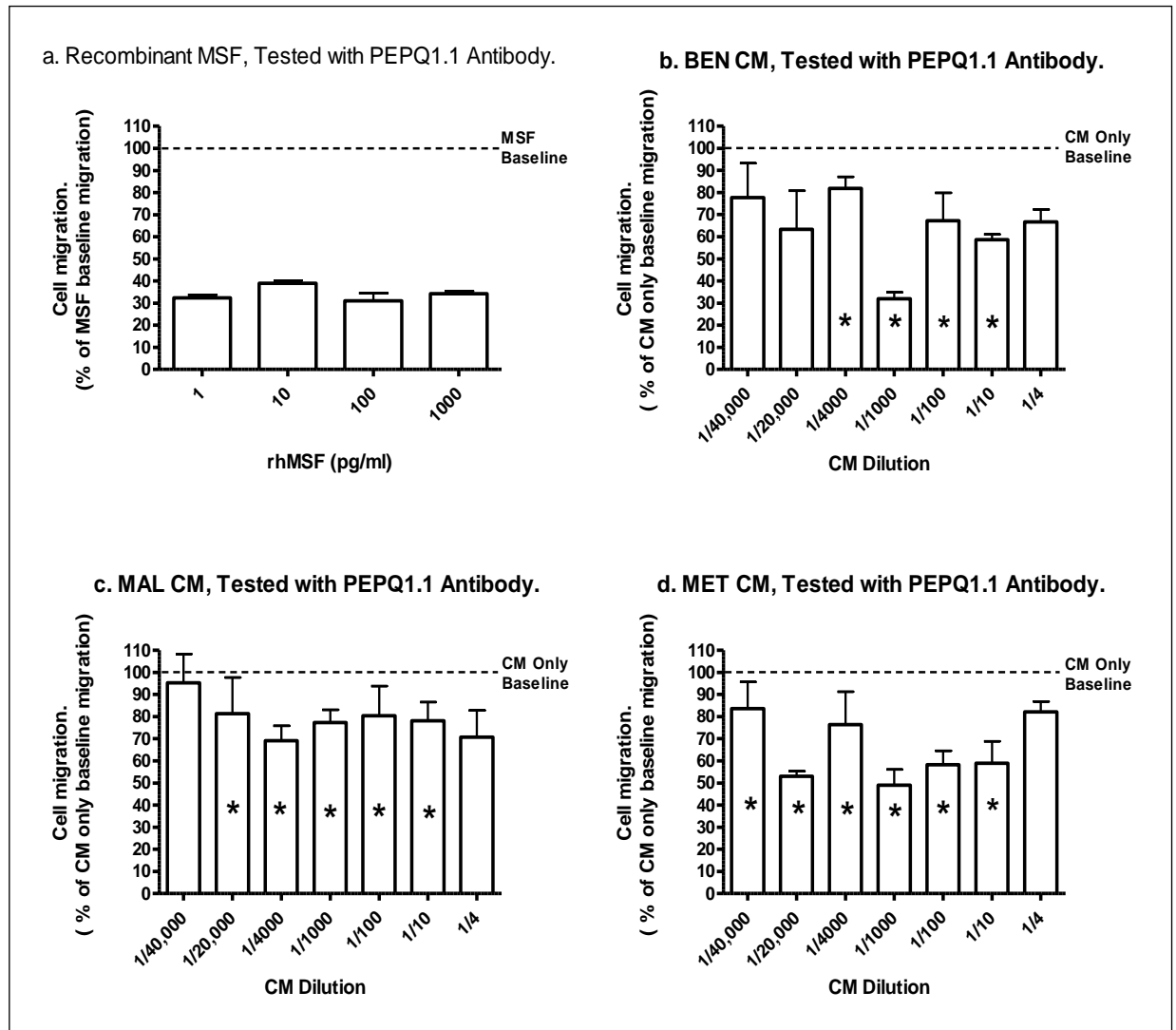


Figure 6.5: The effect of MSF-neutralising antibody, PEPQ1.1, on the endogenous motogenic bioactivity of HaCaT Series CM, comparison with rhMSF. Conditioned medium (CM) from each cell line (BEN, MAL and MET), at various dilutions, in the 3D collagen gel fibroblast migration assay in the presence of 50ng/ml PEPQ1.1. The number of cells migrated is expressed as a percentage of the CM only baseline migration at each individual dilution point. i.e. 1/4 dilution CM only = 100%, as represented by hatched line. CM dilutions which display motogenic activity, when tested alone, are identified by a star (*). The results represent an average of three experiments. Effect of PEPQ1.1 on the dose response of rhMSF is shown for comparison.

Table 6.1. The Characterisation of HaCaT Series Endogenous Motogenic Bioactivity.

Conditioned medium (CM) from each cell line (BEN, MAL and MET) tested at various dilutions, in the 3D collagen gel fibroblast migration assay in the presence of either 10ng/ml rhNGAL or 1/180 dilution of PEPQ1.1 antibody.

a. The Effect of NGAL on the Endogenous Motogenic Bioactivity of HaCaT Series Conditioned Medium.

	BEN	MAL	MET
Motogenic Dilutions (50% increased migration compared to SF MEM baseline)	1/4000 -1/10	1/20,000 – 1/10	1/40,000 – 1/10
Dilutions with reduced migration upon addition of 10ng/ml rhNGAL.	1/10, 1/100	1/4000	1/10, 1/100
Maximal inhibition of migration by 10ng/ml rhNGAL	38% @ 1/10	40% @ 1/4000	31% @ 1/10
NGAL inhibition which met set criteria (50% reduction compared to CM only baseline).	None	None	None

b. The Effect of MSF- Neutralising Antibody, PEPQ 1.1, on the Endogenous Motogenic Bioactivity of HaCaT Series Conditioned Medium.

	BEN	MAL	MET
Motogenic Dilutions (50% increased migration compared to SF MEM baseline)	1/4000 -1/10	1/20,000 – 1/10	1/40,000 – 1/10
Dilutions with reduced migration upon addition of PEPQ1.1 antibody.	ALL	1/20,000 – 1/4	ALL
Maximal inhibition of migration by PEPQ 1.1 antibody	68% @ 1/1000	31% @ 1/4000	51% @ 1/1000
PEPQ 1.1 inhibition which met set criteria (50% reduction compared to CM only baseline).	1/1000	None	1/1000

Table 6.2. Result Summary 1. The Bioactivity of HaCaT Series CM.

Conditioned medium collected from the HaCaT series cell lines BEN, MAL and MET, were tested at various dilutions in the 3D collagen gel fibroblast migration assay with and without the presence of 100pg/ml rhMSF. By comparison to SF MEM or rhMSF baseline controls the nature of each cell line's bioactivity, at each dilution point, was determined.

Cell line	Bioactivity in CM Compared to SF MEM Baseline		Response to rhMSF Compared to MSF Baseline			Response to rhMSF Compared to CM Baseline		
	None	Motogenic	None	Stimulation	Inhibition	None	Stimulation	Inhibition
BEN	1/4 1/40,000	1/10 1/100 1/1000 1/4000	1/4000 1/20,000	-	1/4 1/10 1/100 1/1000 1/40,000	-	1/20,000	1/4 1/10 1/100 1/1000 1/4000 1/40,000
MAL	1/4 1/40,000	1/10 1/100 1/1000 1/4000 1/20,000	1/1000 1/4000 1/20,000 1/40,000	-	1/4 1/10 1/100	-	1/20,000 1/40,000	1/4 1/10 1/100 1/1000 1/4000 1/20,000
MET	1/4	1/10 1/100 1/1000 1/4000 1/20,000 1/40,000	1/4 1/10 1/100 1/1000 1/4000 1/20,000 1/40,000	-	-	-	1/4	1/10 1/100 1/1000 1/4000 1/20,000 1/40,000

Table 6.3. Result Summary 2. The Bioactivity of HaCaT Series CM.

Conditioned medium collected from the HaCaT series cell lines BEN, MAL and MET, was tested at various dilutions in the 3D collagen gel fibroblast migration assay with and without the presence of 100pg/ml rhMSF. By comparison to SF MEM or rhMSF baseline controls the nature of each cell line's bioactivity, at each dilution point, was determined.

Cell Line	Motogenic Activity Compared to SF MEM Baseline (CM tested alone)	MSF-I Activity Compared to MSF Baseline (CM + 100pg/ml rhMSF)	MSF-I Activity Only No endogenous motogenic activity.
BEN	1/10 1/100 1/1000 1/4000	1/4 1/10 1/100 1/1000 1/40,000	1/4 1/40,000
MAL	1/10 1/100 1/1000 1/4000 1/20,000	1/4 1/10 1/100	1/4
MET	1/10 1/100 1/1000 1/4000 1/20,000 1/40,000	none	none

6.5 THE SUPERDEX FRACTIONATION OF HACAT SERIES CONDITIONED MEDIUM

The analysis of total CM collected from the HaCaT series cell lines revealed the presence of both motogenic and MSF-inhibitory bioactivity, the proportion of which varied between the cell lines. The next phase was to determine the nature of these bioactivities; that is can each bioactivity be separated into a distinct entity? Size exclusion chromatography (SEC), as used previously to fractionate the HaCaT keratinocyte CM, was selected to separate the proteins by molecular weight.

The Superdex 75 HiLoad 26/60 (GE Healthcare) column, which has a fractionation range of 3-70kDa, was used to fractionate 4ml of ten times Amicon concentrated CM (Materials & Methods, Chapter 2). Multiple runs were completed in order to provide sufficient material for downstream analysis. For each individual run 100 x 3ml fractions were collected (2ml/min) and numbered 1 to 100; the corresponding fractions from the duplicate runs were then pooled together, (Figure 6.6). Subsequently the fractions were pooled into groups of three; Groups 1 to 33. For each cell line Groups 13 to 23 (fractions 37-69), equivalent to the main absorbance peak with a molecular weight range of approximately >70kDa to 20kDa, were tested at a final dilution of 1/20 for bioactivity in the 3D collagen gel fibroblast migration assay, (Figure 6.7, Table 6.4).

Table 6.4. The Estimated Molecular Weight of the Size Exclusion

Chromatography Fractions. The Superdex 75 HiLoad 26/60n column was calibrated prior to sample loading with known molecular mass markers (albumin, ovalbumin and chymotrypsinogen) thereby permitting an estimated molecular weight for each fraction and subsequently each fraction group. The table shows the selected fractions, 37-69, equivalent to the main absorbance peak which were pooled into groups of three (fraction groups 13-23) and tested for bioactivity in the 3D collagen gel fibroblast migration assay.

Fraction Number	Equivalent Fraction Group	Location of Calibration Markers	Estimated Molecular Weight
37, 38, 39	13		>70kDa
40, 41, 42	14		
43, 44, 45	15		
46, 47, 48	16		
49, 50, 51	17	Albumin MWt = 66kDa	>60kDa
52, 53, 54	18		Approx 50kDa
55, 56, 57	19	Ovalbumin MWt = 45kDa	>40kDa
58, 59, 60	20		Approx 30-40kDa
61, 62, 63	21	Chymotrypsinogen MWt = 25kDa	>=25kDa
64, 65, 66	22		
67, 68, 69	23		Approx 20kDa

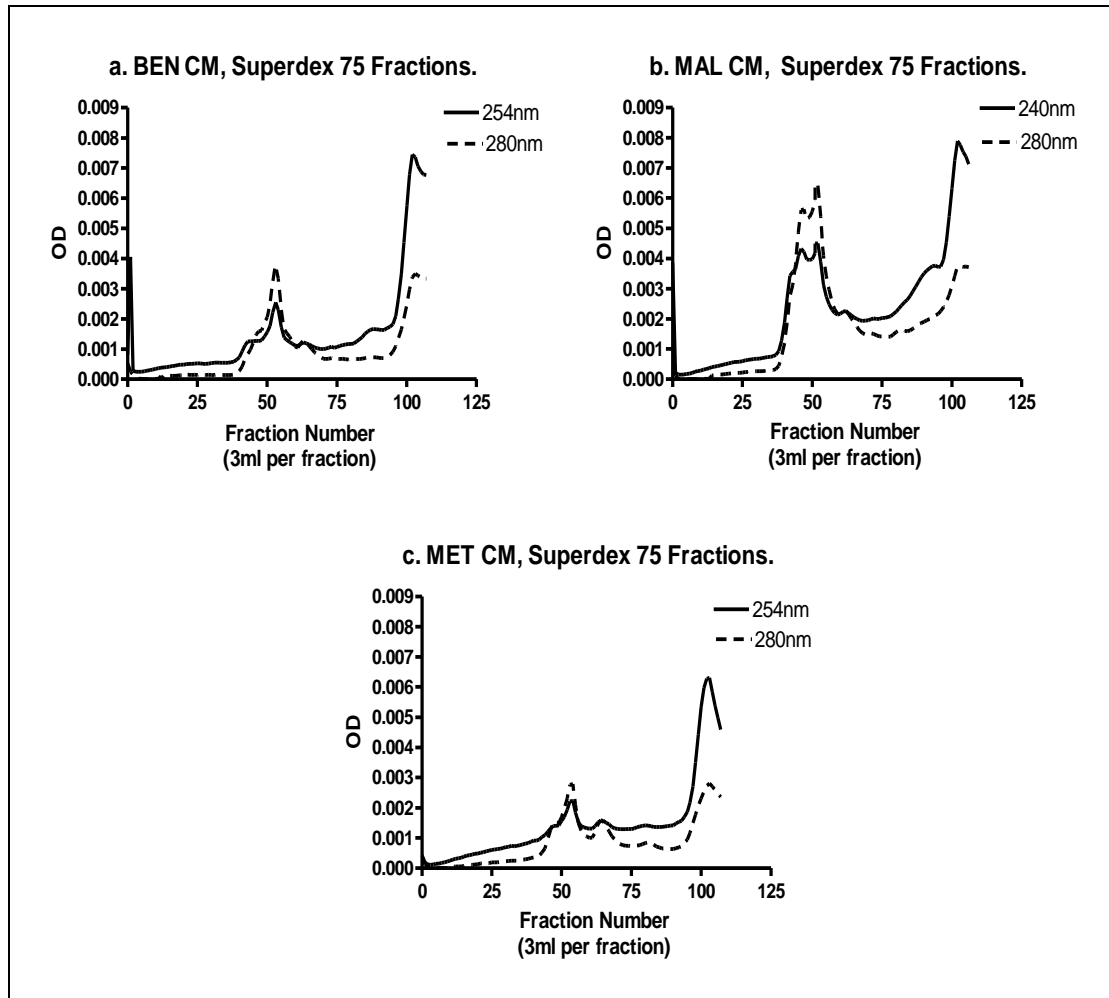


Figure 6.6. The Fractionation of HaCaT Series Conditioned Medium by Size-Exclusion Chromatography. 4ml of 10x concentrated CM from each HaCaT Series cell line (BEN, MAL, MET) was applied to a Superdex 75 HiLoad 26/60n column. 100 x 3ml fractions were collected (2ml/min). The eluant was monitored for absorbance at 254nm and 280nm.

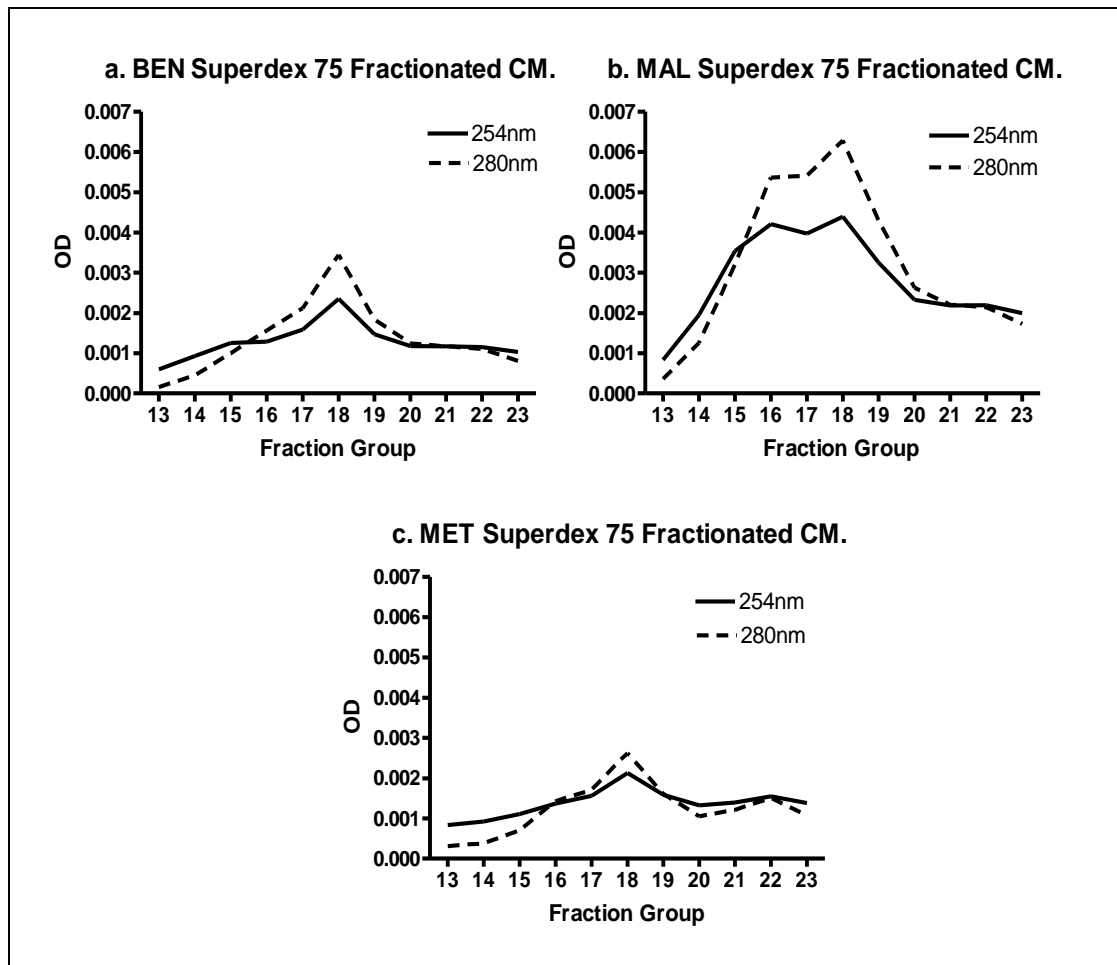


Figure 6.7. The Fractionation of HaCaT Series Conditioned Medium by Size-Exclusion Chromatography. 4ml of 10x concentrated CM from each cell line (BEN, MAL, MET) was applied to a Superdex 75 HiLoad 26/60n column. The eluant was monitored for absorbance at 254nm and 280nm. 100 x 3ml fractions were collected (2ml/min). The collected fractions were pooled together into groups of three. Fraction groups 13 to 23, equivalent to the main absorbance peak, were assayed for biological activity in the 3D collagen fibroblast migration assay.

6.9 THE ASSESSMENT OF THE BIOACTIVITY OF SEC FRACTIONATED HACAT SERIES CONDITIONED MEDIUM

6.6i The Motogenic Activity of Size- Exclusion Fractionated HaCaT Series Conditioned Medium.

As previously performed with the unfractionated HaCaT Series CM, the SEC fractionated CM was tested alone in the 3D collagen gel fibroblast migration assay in order to determine the presence of motogenic activity. Fraction groups 13 to 23 were tested at a final dilution of 1/20 (all dilutions made with SF MEM). Each fraction group was considered as motogenic if fibroblast migration was stimulated by at least 50% when compared to SF MEM control baseline levels.

As expected, each cell line exhibited motogenic activity, with bioactivity commonly present in the higher molecular weight fraction groups (13-16) (Figure 6.8). The majority of stimulatory activity was detected in the MAL fractions; groups 13 to 21 all met the set criteria for motogenic activity (approx. >70kDa to 25kDa). Also, compared to the BEN and MET results the highest levels of fibroblast migration were measured in the MAL experiments; on average twice the SF MEM baseline level. However, as the fractions were not standardised by protein concentration and only tested at a single dilution, the level of bioactivity of the MAL fractions may merely be a result of a greater protein concentration compared to the others as displayed by the absorbance readings monitored during fractionation, (Figure 6.7).

In the BEN experiments, the lowest molecular weight group, 23 (approx. 20kDa), displayed motogenic activity twice that of the SF MEM baseline. Suggesting that either breakdown products of MSF, namely IGD containing fragments, were responsible for this bioactivity or it is due to the presence of another motogen.

6.6ii The MSF-Inhibitory Activity of Size- Exclusion Fractionated HaCaT Series Conditioned Medium.

SEC fraction groups for each cell line were tested in the 3D collagen gel fibroblast migration assay in the presence of 100pg/ml rhMSF in order to determine the presence of MSF-inhibitor(s) within the fractionated CM. Each group was tested at a final dilution of 1/20 and the criteria set for MSF inhibition was the ability to limit fibroblast

migration by at least 50% upon addition of 100pg/ml rhMSF, as compared to the MSF baseline.

The addition of 100pg/ml rhMSF should result in a minimal two fold increase in fibroblast migration, overall this failed to be achieved when tested with the fraction groups of the HaCaT series fractionated CM. For each cell line, inhibitory activity was detected at varying degrees; the majority of fraction groups displaying MSF- inhibition although not necessarily reaching the set criteria of 50%. All BEN fraction groups failed to have an increase in migration upon addition of MSF but only groups 13, 16, 18, 21, 23 met the strict criteria. MAL and MET inhibitory groups were 13, 15, 21, 22, 23 and 17, 18, 19 respectively. (Figure 6.9). This does appear to suggest that if NGAL is solely responsible for the MSF inhibitory activity of the CM then it must be present within all the fractions implying that either the fractionation process has failed to separate the proteins or that NGAL has formed higher molecular weight complexes with other molecules. As previously stated NGAL has been described as having a molecular weight of 20-25kDa but is also known to form a 46kDa homodimer and a 135kDa disulfide linked heterodimer with neutrophil gelatinase. If NGAL has made these associations then the results would imply that NGAL still retains its ability to inhibit MSF when complexed. Another possibility is that NGAL has formed non-specific protein interactions as a consequence of storage conditions, pH and/ or salt concentration.

Unlike the stimulatory activity detected when tested alone, there failed to be a common zone of similar molecular weight fractions possessing inhibitory activity. If the nature of the MSF bell shaped dose response bioactivity is taken into account and presume that the inhibition displayed by fraction groups which previously displayed motogenic activity when tested alone is actually due to the addition of 100pg/ml rhMSF causing a shift in bell- shaped response. Then, it does become apparent that “true” MSF- inhibitory activity may reside in the lower molecular weight fractions (<25kDa), with MAL and BEN having similar activity in fraction groups 21-23. However, BEN fraction group 23 had also displayed motogenic activity when tested alone.

6.6iii The Motogenic Activity of Recombinant MSF in the Presence of HaCaT Series Size- Exclusion Fractionated Conditioned Medium.

This analysis enables the existence of any motogenic activity within the HaCaT series CM, which may mask the effect of any MSF-inhibitors also present, to be taken into

account. The baseline is set for each individual fraction group when it is tested alone in the assay and MSF –inhibition is determined by a failure of migration to increase by 50% upon addition of 100pg/ml rhMSF. However, to interpret this analysis the nature of MSF's motogenic activity, which functions in a bell shaped dose-response, must be taken into account. That is, any inhibitory activity detected needed to be established as genuine and not accumulative effect of endogenous MSF and additional rhMSF causing the overall MSF concentration to shift to the level where it has an inhibitory effect. By comparison to the baseline levels, a number of the BEN fraction groups appeared to possess MSF-I activity; 13, 14, 16, 18, 23. However, when tested alone, stimulatory activity had previously been discovered in groups 13, 14, 16 and 23. Only fraction group 18 (MW approx. 50kDa) appeared to display a true inhibition of the rhMSF, as no stimulatory activity had previously been detected. Similarly, numerous MAL fraction groups displayed the ability to inhibit rhMSF (13-17, 21- 23) but once those groups that had previous stimulatory activity (13-21) were precluded only two appeared to have indisputable MSF-I activity- groups 22 and 23, with MW equivalent to approximately 25kDa or less. The majority of the MET fraction groups (13-19) also exhibited varying levels MSF-I activity. After excluding the higher molecular weight fraction groups 13-15 because stimulatory activity was detected previously, only the MSF-I activity of groups 17-19 could be considered as genuine (MW approximately >60- 40kDa) (Figure 6.10).

In conclusion, these results appear to be ambiguous, as the MSF-I activity of the HaCaT series CM does not appear to be located in identical fraction group(s). The inability of the cell lines to share similar activities may of course be due to a concentration issue as the CM tested was not standardised and only one dilution was tested. However, overall there does appear to be a separation between the detected stimulatory and MSF-I activity by molecular weight, as the motogenic activity was detected predominantly in the higher molecular weight fraction groups (13-16), greater than 70kDa. While MSF-I bioactivity appeared to be located in the lower molecular weight fraction groups, but over a greater range (groups 17-23).

Presuming that the two bioactivities detected in the HaCaT series total CM, motogenic and MSF-inhibition, were due to MSF and NGAL respectively then one would expect to locate them in the fractionated CM in two distinct molecular weight locations of approximately 70kDa and 25kDa. A possible explanation why this did not occur would be that the Superdex 75 column was overloaded with the 10x concentrated CM resulting in an inadequate separation. However, when the OD traces of the fractionated CM were

examined, it would appear that the protein concentrations were actually very low. (Figure 6.7). Another possibility would be that the NGAL present in the HaCaT series CM has formed higher molecular weight associations. Moreover, it may be a consequence of concentrating the CM to such a high degree (10 times) that non-specific associations have formed, possibly to the point of proteins precipitating out of solution. Plus, although repeated freeze/ thaw cycles were kept to a minimum, the impact that storage had on the integrity of the CM proteins cannot be overlooked.

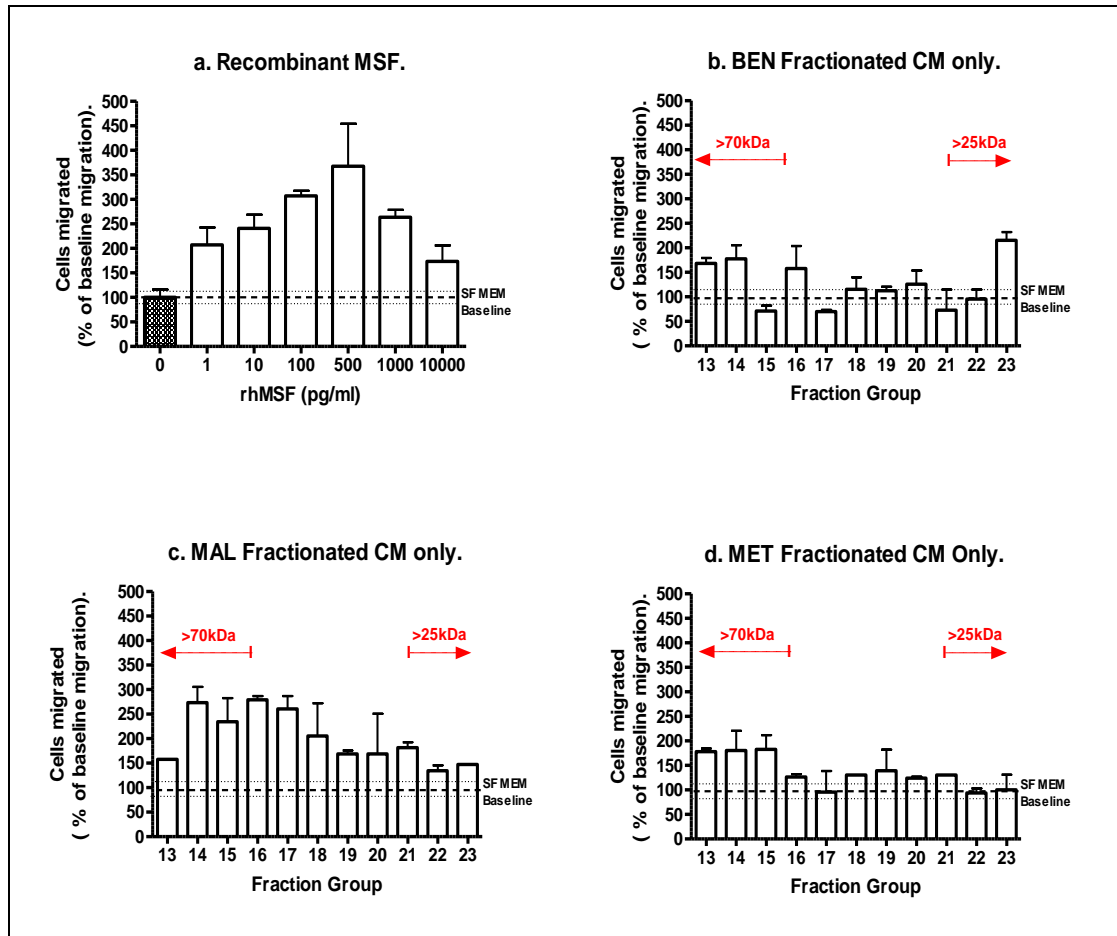


Figure 6.8: The motogenic activity of Superdex 75 fractionated conditioned medium from HaCaT Series cells, comparison with rhMSF. The fractionated conditioned medium (CM), fraction groups 13-23, from each cell line (BEN, MAL and MET) was tested, alone in the 3D collagen gel fibroblast migration assay. The number of cells migrated is expressed as a percentage of the SF MEM control baseline migration i.e. SF MEM Baseline = 100 +/- 16.07%, as represented by hatched and dotted lines (mean and SD respectively). This was equivalent to 2.8 +/- 0.45 migrated cells. (100pg/ml rhMSF only = 8.6 +/- 0.28 migrated cells). Dose response to rhMSF is shown for comparison. The results represent an average of two experiments.

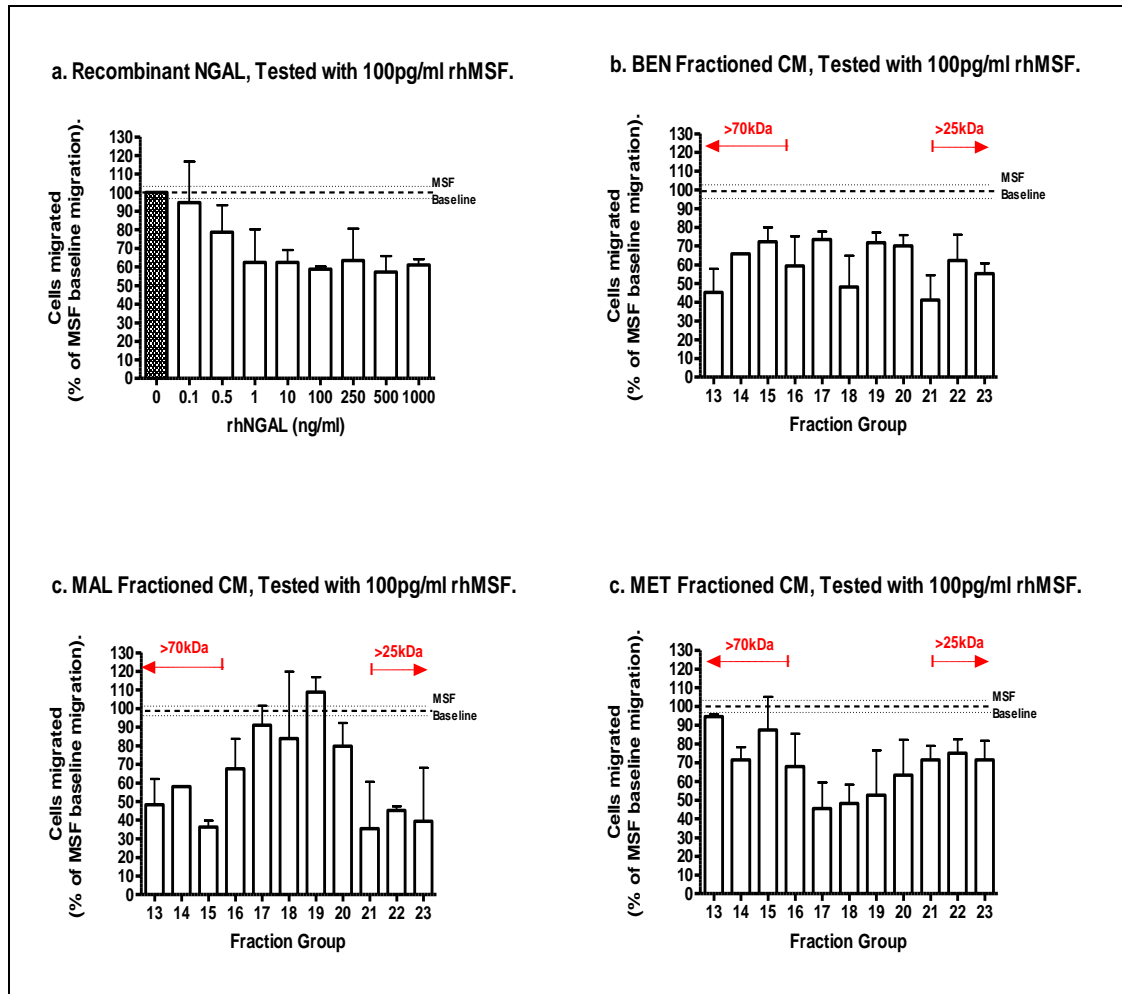


Figure 6.9: The MSF-inhibitory activity of Superdex 75 fractionated conditioned medium from HaCaT Series cells, comparison with rhNGAL. The fractionated conditioned medium (CM), fraction groups 13-23, from each cell line (BEN, MAL and MET), was tested in the fibroblast migration assay in the presence of 100pg/ml rhMSF. The number of cells migrated is expressed as a percentage of the 100pg/ml rhMSF control baseline migration i.e. MSF Baseline = 100 +/- 3.26%, as represented by hatched and dotted lines (mean and SD respectively). This was equivalent to 8.6 +/- 0.28 migrated cells. Dose response to rhNGAL is shown for comparison. The results represent an average of two experiments.

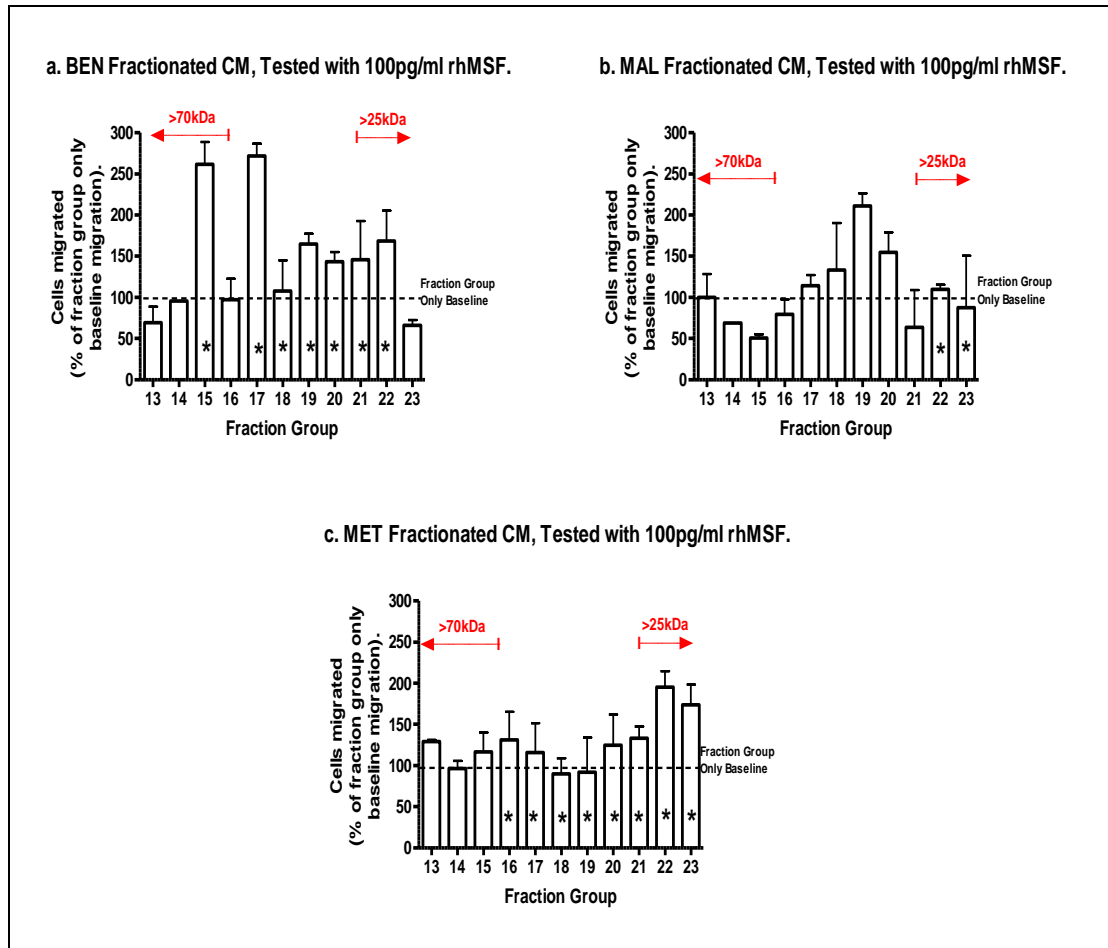


Figure 6.10. The motogenic activity of exogenous rhMSF in the presence of Superdex 75 fractionated conditioned medium. Fractionated conditioned medium (CM), fraction groups 13-23, from each cell line (BEN, MAL and MET) was tested in the fibroblast migration assay with and without the presence of 100pg/ml rhMSF. The number of cells migrated is expressed as a percentage of the CM only baseline migration at each individual dilution point. i.e. $\frac{1}{4}$ dilution CM only = 100%, as represented by hatched line. Fraction groups which lacked motogenic activity when previously tested alone are identified by a star (*). The results represent an average of two experiments.

6.7 THE IDENTIFICATION OF NGAL IN THE HACAT SERIES SIZE- EXCLUSION FRACTIONATED CONDITIONED MEDIUM.

A colorimetric indirect ELISA with specific anti-NGAL antibody was performed in order to detect the presence of NGAL in the fractionated HaCaT series CM. Adopting the method as previously described in Materials & Methods, Chapter 2. For each cell line 100 μ l of every fraction group, 13-23, were tested neat in duplicate wells; two

separate Superdex 75 runs were analysed. SF MEM and coating buffer were used as negative controls.

The results were assessed in a qualitative manner, to give a yes or no answer as to whether NGAL was present in each fraction group, as it was unfeasible to directly compare the ELISA results for each cell line. A quantitative analysis was not appropriate as firstly, the CM which was fractioned was un-standardised either by protein concentration or per cell number. Secondly, the effects of storage and concentrating the CM before fractionation, as discussed previously, must be taken in account as protein may have been lost due to precipitation and this would not be reflected in the ELISA results. Also, there was a very limited amount of sample available to test and unfortunately dilutions of the positive fraction groups were unable to be performed in order to bring them in line with the range of the rhNGAL standard curve.

A fraction was considered to be positive for the presence of NGAL if the final OD reading (minus blanks) was 0.1 or above; comparing to a standard curve of rhNGAL this is equivalent to 25ng/ml (Figure 5.3). For BEN and MAL all fraction groups were positive for NGAL, with all final ODs well above the cut-off point. For the MET line all fraction groups were positive except the higher molecular weight (>70kDa) fraction groups 13-14. This result substantiated the reasoning why a clear zone of NGAL inhibitory activity was not detected in the 3D collagen gel migration assays; that is NGAL was present at a bioactive concentration in the majority of the fraction groups. (Figure 6.11).

Observation of the OD readings measured in the MET fraction groups noted that NGAL is present predominately at the lower molecular weight (<25kDa) range. This is also true for BEN CM too. However, a similar OD reading was measured for all MAL fraction groups. As previously discussed, this was a qualitative assessment so limited conclusions can be drawn from these observations.

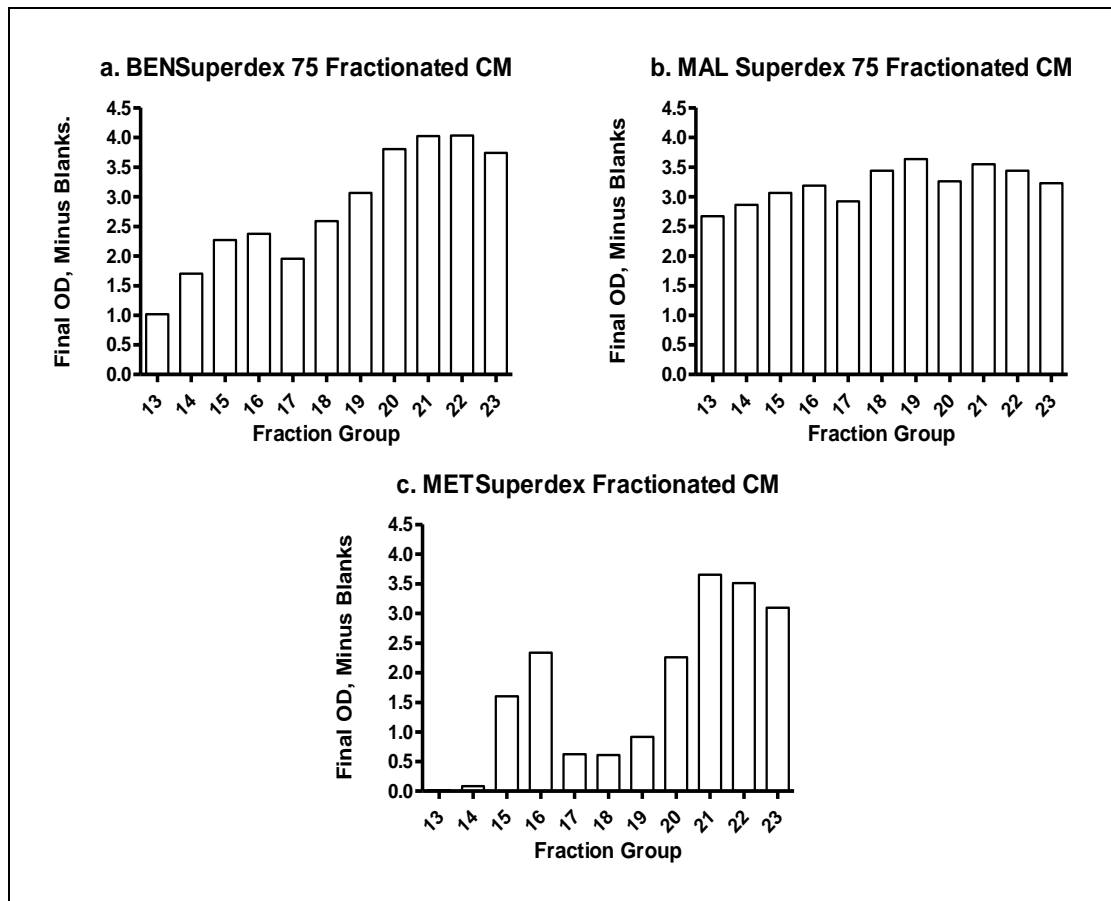


Figure 6.11: The NGAL Indirect ELISA analysis of Superdex 75 fractionated conditioned medium. Non- standardised fractionated conditioned medium (CM), fraction groups 13-23, from each cell line (BEN, MAL and MET) was analysed for the presence of NGAL by the indirect ELISA method. The average final OD (minus blanks), from two individual Superdex runs, is displayed for each fraction group. A fraction group was defined as positive for NGAL if final OD equalled 0.1 or above.

6.8 THE IDENTIFICATION OF MSF IN THE HaCaT SERIES **SIZE-EXCLUSION FRACTIONATED CONDITIONED MEDIUM.**

Numerous bioactivity experiments have shown that CM collected from each cell line of the HaCaT series possesses a degree of motogenic activity. The ability to stimulate fibroblast migration in the 3D collagen gel assay was first noted in dilutions of total CM and subsequently in the high molecular weight fractions of the SEC fractionated CM. Immunolocalisation experiments using specific anti-MSF antibodies revealed that the HaCaT series cell lines all express MSF, at varying extents. However, difficulty arises when trying to prove that endogenous MSF is responsible for the stimulatory activity

detected in the CM, as both ELISA and immunoblot analysis of total CM (including concentrated CM) using specific anti-MSF antibodies failed to give a positive result. Since any MSF present in the total CM is below the detection limits of the ELISA and immunoblot assays it would be futile to try to analyse the fractionated CM by these methods. Instead, the technique of immunoprecipitation with Protein G using MSF-specific identification antibody, RpVSI, was selected in order to prove that endogenous MSF was responsible for the motogenic bioactivity detected in HaCaT series CM. The process involves the binding of MSF, present in the fractionated CM, to a specific anti-MSF antibody, thereby removing it from solution, after which it could be eluted and tested for bioactivity in the 3D collagen gel assay. If the bound elutions possess stimulatory bioactivity then it was concluded that MSF is responsible as the rabbit polyclonal VSI antibody only recognises the MSF-unique carboxyl terminal decapeptide and then consequently the HaCaT series cell lines secrete bioactive MSF into their CM.

Analysis of size exclusion fractionated CM consistently located motogenic bioactivity to similarly high molecular weight fractions (F37-48 for BEN, F37-63 for MAL and F37-45 for MET). Hence, for each cell line fractions 30-50, equivalent to molecular weight of 60kDa and greater, were selected and pooled from two separate SEC runs. Following dialysis against distilled water the pooled fractions were concentrated 100 times by freeze drying (sample now referred to as F-msa; fractions displaying migration stimulating activity). 1ml of F-msa, from each cell line, was then incubated with the rabbit polyclonal RpVSI antibody followed by immunoprecipitation as described in Materials & Methods, Chapter 2. The original pooled fractions, 100x concentrated F-msa sample, unbound material and the elutions of bound material were tested for migration stimulating activity in the 3D collagen gel assay. Where possible each test sample was analysed in duplicate at a range of dilutions. The same criteria used in previous bioactivity experiments to detect motogenic activity was adopted; stimulatory activity was defined as an increase in migration of at least 50% when compared to the SF control baseline.

Testing of the pooled fractions 30-50, the original sample, showed as expected, for each cell line, the ability to stimulate fibroblast migration, although at different potencies. (Figure 6.12). The MET appear to have maximal activity at the highest dilution whilst the MAL had a borderline stimulation as poor replicates gave a high standard deviation. After dialysis and 100x concentration, sample F-msa, each cell line retains stimulatory activity although peak activity was located in the BEN sample. After concentration the

MET appeared to lose bioactivity, maybe as a consequence of the concentration process whereby protein fails to return to solution or possibly MSF has been concentrated to such an extent that it was present at the levels which does not stimulate migration.

It would appear that any MSF present in the F-msa sample for the BEN and MET bound to the RpVSI antibody and allowing it to be eluted from the solution; since the unbound elution demonstrated a complete lack of motogenic activity. The MAL unbound elution, however, did exhibit a borderline stimulatory activity which may mean the presence of a motogen other than MSF or that the F-msa sample had too high a concentration of MSF for it all to be successfully bound and removed from solution.

For each cell line the bound material was eluted five times and each was tested for motogenic activity. For BEN the first two elutions caused an increase in migration of nearly 3 and 4 times that of the SF baseline levels, although high standard deviations highlighted poor reproducibility. All five MET elutions displayed a distinct motogenic activity, peaking in elution 3, with 4 times the baseline level of migration. The first MAL elute failed to stimulate migration however the four subsequent elutions did, peaking with elution 5.

These results are palpable evidence that each member of the HaCaT series cell lines, BEN, MAL and MET, express MSF and that it is responsible for the motogenic activity detected in their CM. As the RpVSI antibody used for the immunoprecipitation only recognises the MSF-unique carboxyl terminal decapeptide. However, in order to further substantiate that MSF was responsible for the motogenic activity detected in the bound elutions they were tested with NGAL and PEPQ1.1 antibody in the 3D collagen gel assay. As previously discussed, both NGAL and the IGD function neutralising antibody, PEPQ1.1, are potent inhibitors of MSF bioactivity. 10ng/ml rhNGAL can inhibit up to 500pg/ml rhMSF, while 1/80 dilution of PEP1.1 antibody has the potential to reduce the bioactivity of up to 1ng/ml rhMSF back to SF baseline levels. As the MSF concentration within the samples was unknown, the inhibitors were added in excess in order to try and completely eliminate any bioactivity. The criteria set for the inhibition of motogenic activity was a reduction in migration by at least 50% compared to the baseline level. (Bound elutions were pooled in some instances due a shortage material). The findings verified that the migration stimulating activity detected in the CM of the keratinocyte cell lines BEN, MAL and MET was due to MSF. (Figure 6.13) In all cases the motogenic activity of the bound elutions was inhibited by the addition of MSF inhibitors NGAL and PEPQ1.1 antibody. It is of interest to note that the level of

inhibition by NGAL and PEPQ 1.1 antibody sometimes varied. For example, 100pg/ml rhMSF was inhibited to a similar extent by the NGAL and PEPQ1.1, by 70.5% and 67.2% respectively. However, the inhibition of BEN F-msa bound elutions 1+2 was 59.6% by NGAL but 75.1% by PEPQ1.1 a difference of 15.5%. While MET F-msa Bound elute 5 had its stimulatory activity inhibited by 85.2% by NGAL but only 68.5% by PEPQ, a difference of 16.7%. This variation is difficult to explain as all samples were treated in the same manner, plus both NGAL and PEPQ1.1 were used at excess to try and eliminate all motogenic activity. There is also no consistency in either NGAL or PEPQ having a greater inhibitory effect on the samples. This may imply the presence of another motogen but this seems highly unlikely since the samples are the result of immunoprecipitation for MSF using a specific anti-MSF antibody, which only recognises MSF's unique carboxyl-terminal decapeptide.

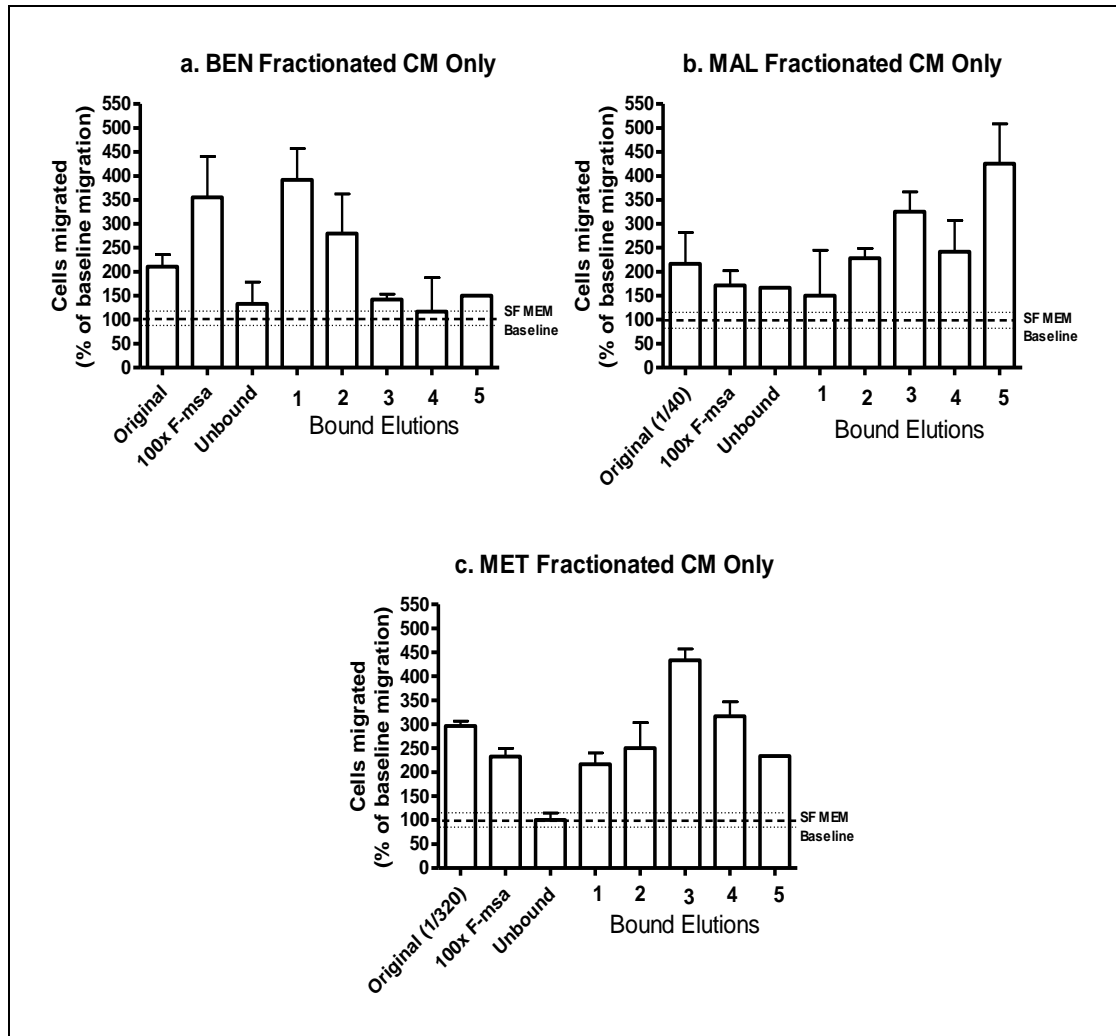


Figure 6.12: The motogenic activity of the HaCaT Series SEC Fractionated CM before and after Immunoprecipitation with MSF-specific identification antibody RpVSI. For each cell line the motogenic SEC fractions F30-50, molecular weight equivalent to greater than 60kDa, were pooled (original) and then concentrated 100x by freeze drying (100x F-msa). After which, immunoprecipitation with the RpVSI MSF identification antibody was performed; unbound and five bound elutions were collected. All variables were tested alone in the 3D collagen gel fibroblast migration assay at a final dilution of 1/80 (unless otherwise stated). The number of cells migrated is expressed as a percentage of the SF MEM control baseline migration i.e. SF MEM Baseline = 100 +/- 17.50 represented by hatched and dotted lines (mean and SD respectively). This was equivalent to 2.0 +/- 0.35 migrated cells. (100pg/ml rhMSF only = 8.2 +/- 0.78 migrated cells).

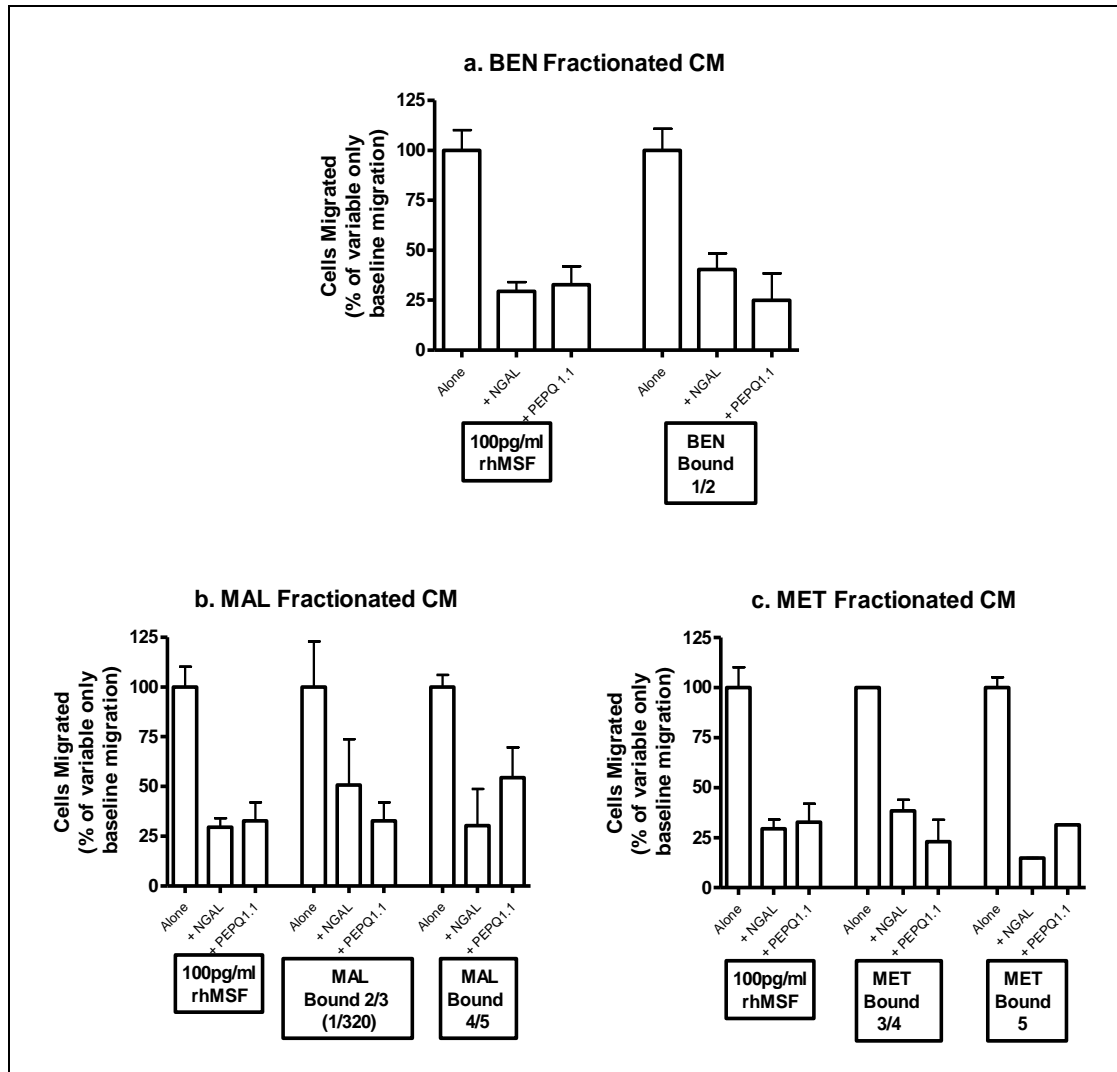


Figure 6.13: The effect of MSF-Inhibitors, NGAL and function neutralising antibody PEPQ1.1, on the endogenous motogenic bioactivity of HaCaT series Fractionated CM post Immunoprecipitation. For each cell line immunoprecipitation for MSF, using the MSF specific identification antibody RpVSI, was performed on the SEC fractionated CM, F30-50. The motogenic active bound elutions were then tested with both 10ng/ml rhNGAL and 50ng/ml PEPQ1.1 antibody in the 3D collagen gel fibroblast migration assay, at a final dilution of 1/80 (unless otherwise stated). The number of cells migrated is expressed as a percentage of the variable only baseline migration i.e. Bound Elution 2 only = 100%. The effect of rhNGAL and PEPQ1.1 antibody on 100pg/ml rhMSF is shown for comparison. (100pg/ml rhMSF only = 8.4 +/- 0.85).

6.9 THE SDS POLYACRYLAMIDE GEL ELECTROPHORESIS OF HaCaT SERIES CONDITIONED MEDIUM.

As SEC fractionation failed to conclusively show that the two bioactivities, of motogenicity and MSF-inhibition, detected in the total CM of the HaCaT series could be separated into two distinct entities another approach was required. Complications had arisen with SEC fractionation with NGAL detected in the majority of fractions, possibly due to the formation of high molecular weight associations. By choosing to fractionate the CM by SDS PAGE electrophoresis under reducing conditions it was hoped that this artefact could be eliminated. By heating the CM briefly with the reducing agent 2 β -mercaptoethanol the proteins present were denatured by reducing disulfide linkages and then subsequently separated by their electrophoretic mobility, which due to the binding of SDS causes an identical charge per unit mass; therefore ultimately separating the proteins by their size.

Equal volumes of Laemmli loading buffer and 10x Amicon concentrated CM were loaded onto a pre-run 12% separating 5% stacking SDS polyacrylamide gel. Following electrophoresis each lane was cut into 12 segments, from high to low molecular weight (S1-12), and the proteins were eluted from the gel by an overnight incubation in 1ml of elution buffer. (Materials & Methods, Chapter 2). After which the bioactivity of each gel elution was determined by testing, at a final dilution of 1/1000, in the 3D collagen gel assay with and without the presence of 100pg/ml rhMSF.

6.10 THE ASSESSMENT OF THE BIOACTIVITY OF SDS ELECTROPHORESIS FRACTIONATED HACAT SERIES CONDITIONED MEDIUM

6.10i The Motogenic Activity of SDS Electrophoresis Fractionated HaCaT Series Conditioned Medium

For each cell line, in order to determine the presence of motogenic activity the proteins eluted from each gel segment were tested alone in the 3D collagen gel fibroblast migration assay. A gel elution was considered motogenic if it caused fibroblast migration to increase by 50% above the baseline level set by the SF MEM control.

A similar pattern of activity was detected in the BEN and MAL experiments with a peak of motogenic activity in the higher molecular weight segments (BEN S1-2 and MAL S1-3) equivalent to 100kDa and above. Activity was also located in lowest molecular weight gel elutions; BEN S10 and MAL S10 and 12. However, motogenic activity was discovered in practically all the MET elutions, with only S11 not showing any stimulatory activity. Also, the level of activity of the MET elutions were considerably greater than the BEN and MAL with peak levels being equivalent to or more than that measured for 500pg/ml of rhMSF. The peak areas of activity appear to be located at the higher and lower molecular weight segments. (Figure 6.14).

6.10ii The MSF- Inhibitory Activity of SDS Electrophoresis Fractionated HaCaT Series Conditioned Medium

In order to determine which gel elutions contained proteins with the ability to inhibit MSF bioactivity, the eluted proteins were tested in the 3D collagen gel assay in the presence of 100pg/ml rhMSF. The addition of 100pg/ml rhMSF should cause migration to be stimulated by a minimum of 50% therefore a gel elution was determined as possessing inhibitory activity if migration failed to increase by this amount. For BEN and MAL, a clear result was obtained with peak inhibitory activity of 60% and 67% respectively, located in S6 which corresponds to a molecular weight of 20-25kDa. Immunoblotting of HaCaT series CM with a specific antibody for NGAL identifies a positive band at this molecular weight, suggesting that NGAL is responsible for the inhibitory bioactivity. Other BEN segments showed potential inhibitory activity but failed to reach the set criteria; namely S7-9 with approximately 42% inhibition. For the MAL the only other area displaying inhibitory activity was S1, molecular weight >100kDa; inhibiting the motogenic activity of 100pg/ml MSF by 62%. This gel elution had previously shown borderline stimulatory activity when tested alone. Meanwhile, all gel segments of the MET CM failed to reach the criteria for MSF-inhibitory activity with maximal inhibition peaking at only 12% (S7). (Figure 6.15).

6.10iii The Motogenic Activity of Recombinant MSF in the Presence of HaCaT Series SDS Electrophoresis Fractionated Conditioned Medium

Comparison of the effect of the addition of 100pg/ml MSF to the baseline activity of each gel elution allows any endogenous stimulatory activity to be taken into account. As

inhibitory activity may actually be a consequence of the MSF bell shaped dose response bioactivity. Therefore, inhibitory activity was defined as the inability of baseline migration to be stimulated by 50%, upon addition of 100pg/ml rhMSF.

When tested alone proteins eluted from BEN gel segments S1, S2 and S10 all displayed stimulatory activity. However, upon addition of exogenous rhMSF all these elutions exhibited inhibitory activity. A similar situation occurred with MET and MAL gel elutions which possess endogenous stimulatory activity but upon addition of rhMSF demonstrate MSF-inhibitory bioactivity. The dilemma is whether this MSF-inhibitory activity is actually due to the presence of an inhibitor or is it merely an effect of the MSF dose response, whereby the additional MSF has caused a shift into the higher concentrations (>500pg/ml) resulting in a reduction in migration.

However, if the gel elutions with endogenous stimulatory activity are eliminated a clearer picture emerges. For the BEN and MAL CM a distinct MSF-inhibitory activity is located in S5 and S6 respectively, equivalent to molecular weight of 37-20kDa.

Applying the same principles to the MET, then all gel elutions, except S11, would have to be removed from the analysis as all displayed endogenous stimulatory activity. While the MET S11, upon addition of rhMSF showed no MSF-inhibitory activity as migration increased by 2.8 fold. Subsequently, the conclusion would be that no MSF-inhibitory activity was detected in MET fractionated CM.

But, by eliminating all gel elutions with endogenous stimulatory activity the presumption is that MSF is responsible for all the motogenic activity detected in the fractionated CM. This does seem somewhat unrealistic considering the array of proteins each cell line expresses, plus the stimulatory activity was detected in a whole range of molecular weights (>100 to <20kDa). It could also suggest that the amount of protein added to the gel was too great resulting in the inefficient separation. However, clear distinct bands were detected when duplicate gels were stained with Coomassie Blue and not just a streak of protein as would be expected with an overloaded lane. Biochemical characterisation of MSF has shown that it is a 70kDa protein, and that the potent motogenic activity of MSF is indistinguishable from its proteolytically generated 43kDa Gel-BD functional domain and 21kDa IGD tripeptide. This may explain why the motogenic activity is spread over such an array of molecular weights since no protease inhibitors were added to the CM.

Also, if the nature of MSF's bioactivity is taken into account; a bell shaped dose response whereby a threshold concentration is required to initiate cell migration and negative feedback mechanism at the higher concentration results in an inhibition of

migration. It can be seen that the addition of rhMSF to the MET gel segments which possessed maximal stimulatory activity of 3 to 5 times the SF baseline (S1, S2, S6, S7, S8 and S10) resulted in maximum inhibition back to the SF MEM control baseline level. Thereby suggesting the additional rhMSF had caused a major shift of the bell shaped dose response to the higher concentrations of MSF which result in a complete inhibition of cell migration. However, those gel elutions that displayed motogenic activity on a similar scale to the 100pg/ml rhMSF control (S3, S4 and S5) did exhibit inhibition upon addition of exogenous rhMSF but to a far lesser extent. The additional rhMSF must have resulted in just a “tipping” over of the bell shaped dose response. Finally those segments which displayed borderline or no stimulatory activity (S11, S12) were not inhibited by the exogenous rhMSF but migration was actually stimulated to the 100pg/ml rhMSF control level, (Figure 6.16).

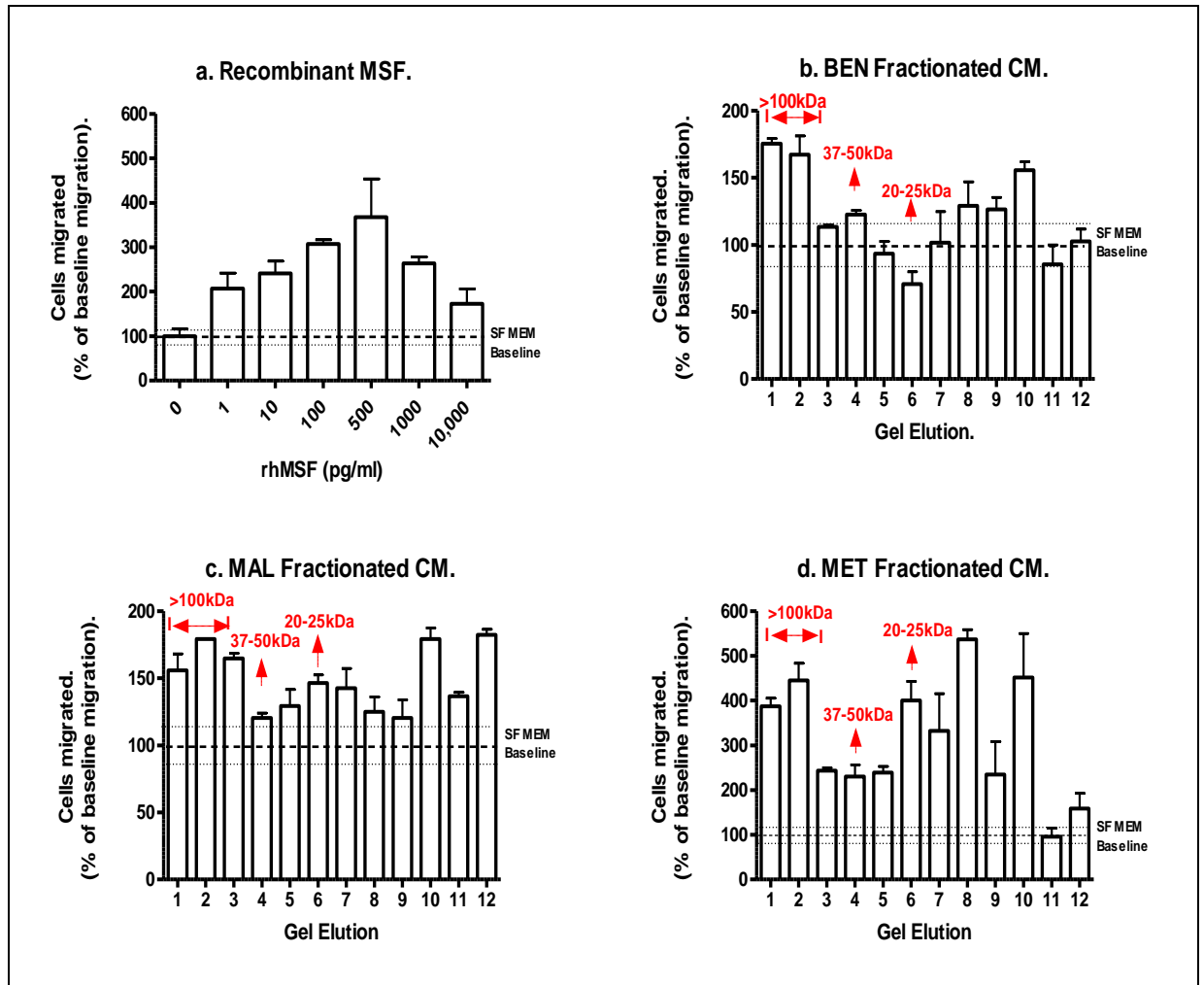


Figure 6.14: The motogenic activity of the gel elutions from the SDS

Electrophoresis fractionation of HaCaT Series conditioned medium, comparison with rhMSF. After the SDS electrophoresis of CM and segmentation of the gel, the protein eluted from each segment (1-12) was tested alone in the 3D collagen gel fibroblast migration assay. The number of cells migrated is expressed as a percentage of the SF MEM control baseline migration i.e. SF MEM Baseline = 100 +/- 16.07%, as represented by hatched and dotted lines (mean and SD respectively). This was equivalent to 2.8 +/- 0.45 migrated cells. (100pg/ml rhMSF only = 8.6 +/- 0.28 migrated cells). Dose response to rhMSF is shown for comparison. The results represent an average of two experiments.

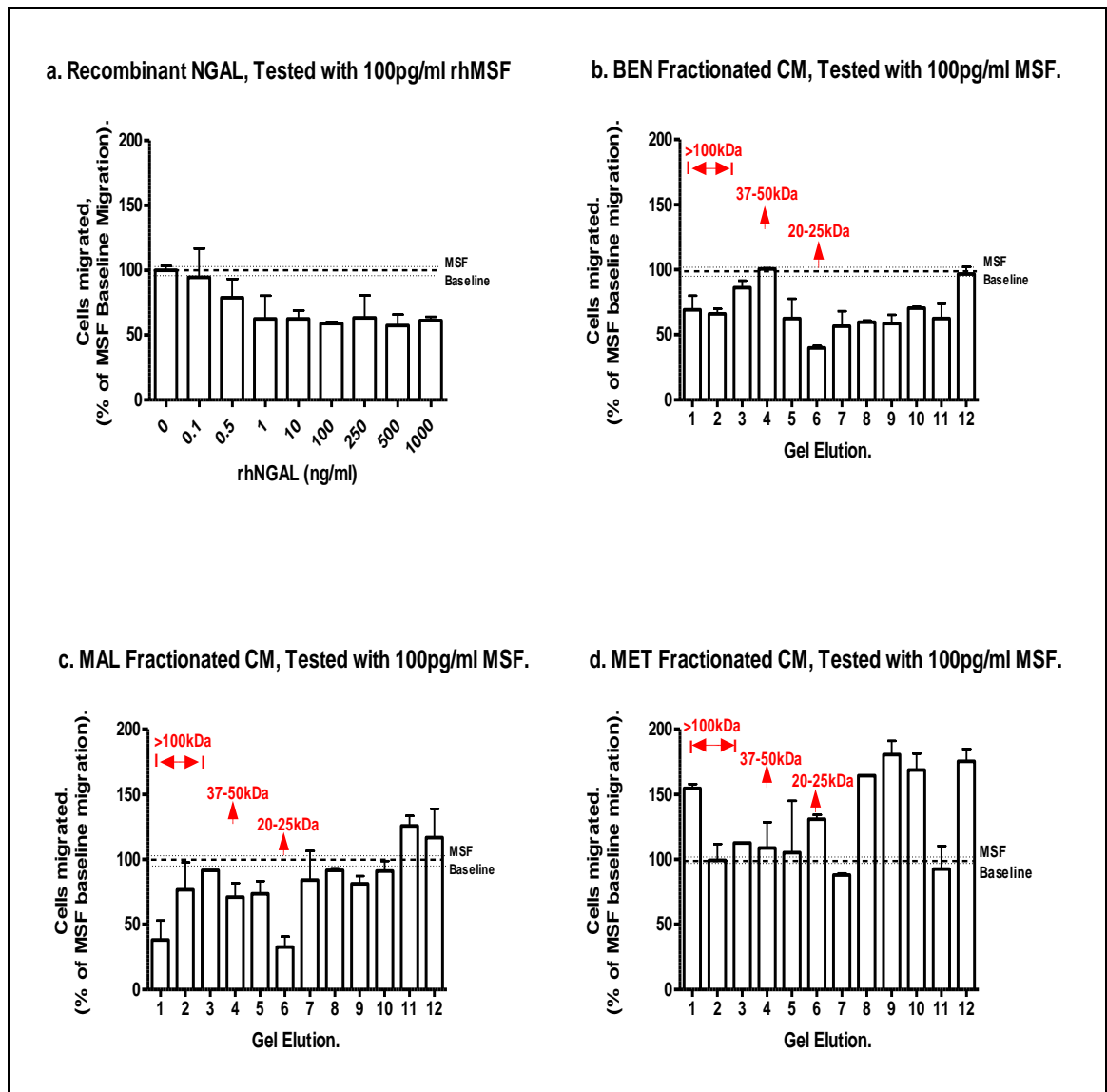


Figure 6.15: The MSF-inhibitory activity of gel elutions from the SDS

Electrophoresis fractionation of HaCaT Series conditioned medium, comparison

with rhNGAL. After the SDS electrophoresis of CM and segmentation of the gel, the protein eluted from each segment (1-12) was tested in the 3D collagen gel fibroblast migration assay in the presence of 100pg/ml rhMSF. The number of cells migrated is expressed as a percentage of the 100pg/ml rhMSF control baseline migration i.e. MSF Baseline = 100 +/- 3.26%, as represented by hatched and dotted lines (mean and SD respectively). This was equivalent to 8.6 +/- 0.28 migrated cells. Dose response to rhNGAL is shown for comparison. The results represent an average of two experiments.

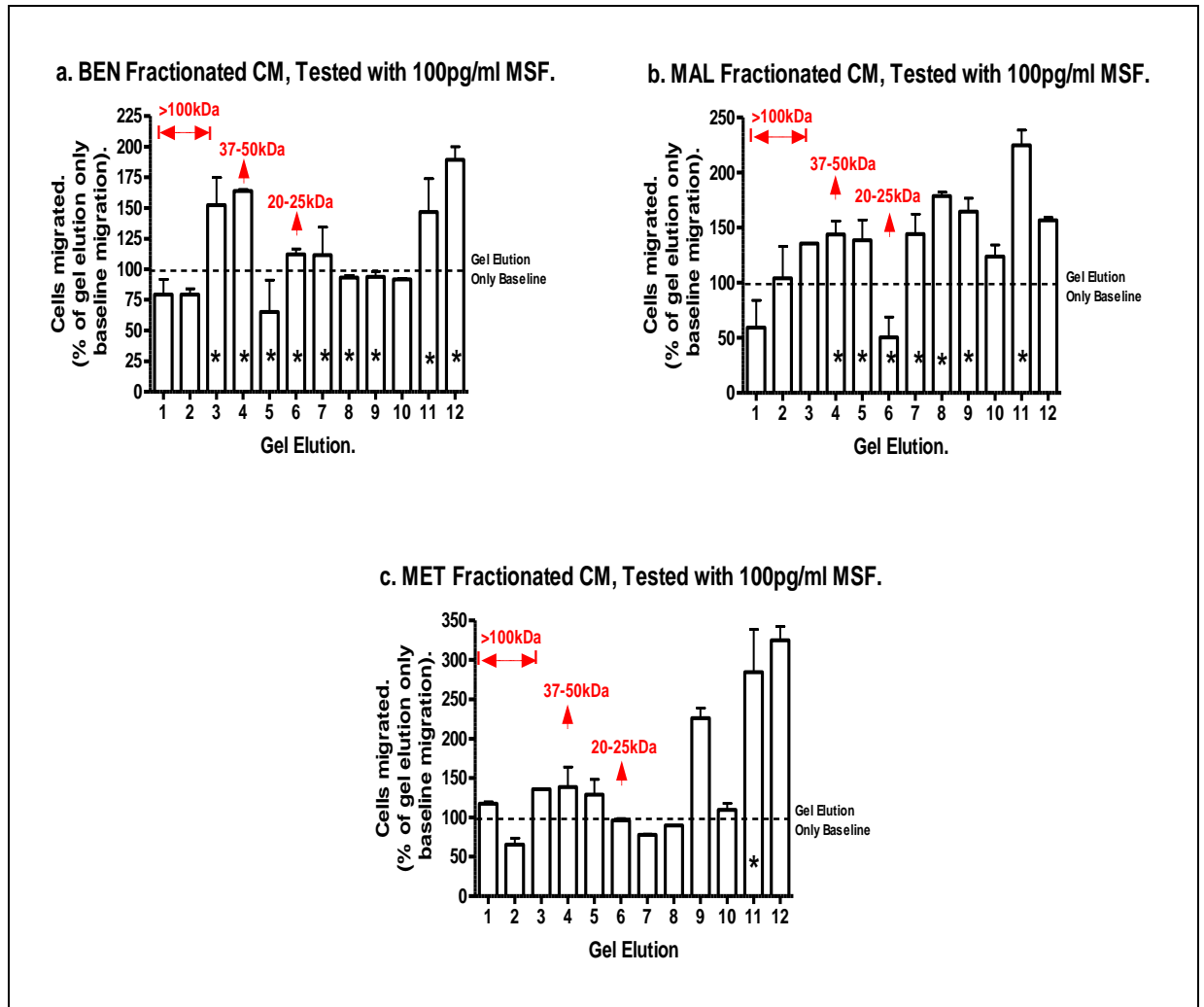


Figure 6.16. The motogenic activity of exogenous rhMSF in the presence of gel elutions from the SDS Electrophoresis fractionation of HaCaT Series conditioned medium. After the SDS electrophoresis of CM and segmentation of the gel, the protein eluted from each segment (1-12) was tested in the 3D collagen gel fibroblast migration assay with and without the presence of 100pg/ml rhMSF. The number of cells migrated is expressed as a percentage of the CM only baseline migration at each individual dilution point. i.e. $\frac{1}{4}$ dilution CM only = 100%, as represented by hatched line. Elutions which lacked motogenic activity when previously tested alone are identified by a star (*). The results represent an average of two experiments.

Table 6.5. Result Summary. The Bioactivity of Fractionated HaCaT Series Conditioned Medium.

Conditioned medium (CM) collected from the HaCaT series cell lines BEN, MAL and MET, was fractionated by two methods of size exclusion chromatography (SEC) and SDS PAGE electrophoresis with subsequent fractions/ elutions tested in the fibroblast migration assay with and without the presence of 100pg/ml rhMSF. Using 10x Amicon concentrated CM the fractionation conditions were as follows:

1. SEC performed using Superdex 75 Hiload 26/60 column (GE Healthcare), multiple runs performed with fractions pooled together into groups of three (13-23) equivalent to MW >70kDa to 20kDa, and tested at final dilution of 1/20.
2. Electrophoresis (12% separating, 5% stack SDS polyacrylamide gel) performed under reducing conditions; gel divided into 12 segments (>100kDa to >20kDa) and proteins eluted during an overnight incubation in 1ml elution buffer; elutions subsequently tested at a final dilution of 1/1000. By comparison to SF MEM or rhMSF baseline controls the nature of each cell line's bioactivity was determined.

Cell Line	Fractionation Method	Motogenic Activity Compared to SF MEM Baseline (Tested alone)		MSF-I Activity Compared to MSF Baseline (Tested with 100pg/ml rhMSF)		MSF-I Activity Only No endogenous motogenic activity.	
		Fraction Group/ Elution	Equivalent MW	Fraction Group/ Elution	Equivalent MW	Fraction Group/ Elution	Equivalent MW
BEN	SEC	13, 14, 16 23	>70kDa Approx 20kDa	13 18 21	>70kDa Approx 50kDa >=25kDa	18 21	Approx 50kDa >=25kDa
	SDS	1, 2, 10	>=100kDa <20kDa	6	25-20kDa	6	25-20kDa
MAL	SEC	13-21	>70-25kDa	13,15 21, 22, 23	>70kDa 25-20kDa	22, 23	25-20kDa
	SDS	1, 2, 3 10, 12	>=100kDa <20kDa	1 6	>100kDa 25-20kDa	6	25-20kDa
MET	SEC	13, 14, 15	>70kDa	17, 18, 19	60-40kDa	17, 18, 19	60-40kDa
	SDS	1-10, 12	>100kDa- <20kDa	none	-----	none	-----

6.11 DISCUSSION

The *in vitro* model system of the HaCaT series keratinocyte cell lines offers the potential to investigate the different stages of tumour development and progression. The previous chapter described that, during tumour progression from the benign condition, malignancy and ultimately metastasis the relative expression of NGAL decreases whilst MSF increases. The next stage therefore, was to ascertain the effect an alteration in the co-expression levels of MSF and NGAL had on the bioactivity of the CM, when tested in the 3D collagen gel fibroblast migration assay. As shown with the CM of the normal HaCaT keratinocytes, the prospective motogenic bioactivity of the endogenous MSF is rendered functionally inactive by the co-secreted MSF inhibitor, NGAL. It could therefore be postulated that any modification to the balance of stimulator and inhibitor would be reflected in the bioactivity. Consequently it was of interest to discover whether the tumourigenic potential of the HaCaT series keratinocytes was mirrored by a reduction in the NGAL inhibition of MSF thereby resulting in increased motogenic activity.

On testing the HaCaT series CM in the migration assay it was soon apparent that the bioactivity was indeed different to that of the normal HaCaT keratinocytes. Overall, the autogenous bioactivity of BEN, MAL and MET keratinocytes was motogenic; each possessing the ability to stimulate fibroblast migration by a minimum of 50% above baseline levels. For BEN and MAL the bioactivity exhibited a bell-shaped dose response similar to that of rhMSF; maximal stimulation of 2-2.5 times that SF MEM baseline at the 1/1000 dilution point, while the highest and lowest dilution points tested displayed none or minimal activity. However, MET motogenic activity was the most prevalent with maximal stimulation measured at the majority of dilution points tested (5/7). (Figure 6.1, Table 6.2) These results correlated with the immunolocalisation data whereby the highest intensity of MSF expression was identified in the MET, as compared to MAL and BEN. Indeed it would appear that if MSF was solely responsible for the increased motogenic activity of MET then, taking into account cell numbers per ml of CM, the MSF concentration in its CM must be ten times higher than BEN or MAL.

By using known MSF inhibitors (NGAL and IGD function neutralising PEPQ1.1 antibody) it was attempted to prove whether this motogenic bioactivity could be attributed to the presence of MSF within the CM. Certainly, a proportion of motogenic activity could be accredited to MSF, as there was a reduction in the level of CM

stimulated migration upon addition of the inhibitors, however it would appear that other active motogen(s) must be present in the CM (Figure 6.4 and 6.5, Table 6.1). Both inhibitors were added in excess compared to the expected MSF concentration, as estimated from the level of cell migration, but still failed to eliminate all activity (generally a 2-2.5 times increase in migration requires 100pg/ml rhMSF, while 10ng/ml NGAL and 1/80 dilution of PEPQ 1.1 antibody inhibits up to 500pg/ml and 1ng/ml of rhMSF respectively). Indeed, it could be suggested that the criteria to determine an inhibition in bioactivity was set too high, at 50% reduction compared to CM only baseline level, and did not take into account the effect of other motogens present within the CM. But, even raising the criteria to requiring only a 30-40% reduction in migration would still not have resolved the issue that NGAL and PEPQ1.1 appear to have different inhibitory properties, with PEPQ1.1 being a more potent inhibitor than NGAL. The exact mechanism of action of NGAL inhibition of MSF is unknown, but there is evidence that direct binding of NGAL to MSF is not required. Pre-incubation experiments of fibroblasts with NGAL still resulted in the inhibition of rhMSF stimulated migration, suggesting that NGAL may act by blocking an MSF-activated signal transduction pathway or indirectly by inducing expression of an intermediate inhibitory molecule. (Jones *et al.*, 2007). However, the PEPQ1.1 antibody was raised against the 21mer peptide containing the IGDQ sequence present in module 1-7 and has the ability to recognise both MSF and the proteolytically generated GBD. Hence, the increased inhibitory efficiency maybe due to the ability of PEPQ1.1 to inhibit both MSF and the GBD, the bioactivity of which is indistinguishable. Since biological assays were being performed with the CM, no protease inhibitors were added and subsequently any MSF present would be subject to proteolysis.

Another point of consideration is the bioactivity characteristics of MSF, whereby a threshold concentration (1pg/ml) is required to initiate migration, while a negative feedback mechanism operates at high concentrations, above 500pg/ml, to inhibit migration. This complicates the issue when estimating the concentration of MSF present in CM, because if MSF was solely responsible for the peak motogenic activity (2-2.5 fold increase compared to SF MEM baseline) this would mean that the concentration was either approximately 100pg/ml or 1ng/ml, when compared to similar levels of migration for the rhMSF dose response. While PEPQ1.1 can still inhibit 1ng/ml rhMSF, 10ng/ml NGAL fails, instead causing an increase in migration (Figure 6.4a and 6.5a). A similar situation occurs with the 1/4 dilution of MET CM; unlike the other MET dilutions no motogenic activity is detected when tested alone, however the addition of

10ng/ml NGAL resulted in approximately 50% increased migration compared to the baseline whereas PEPQ1.1 antibody caused a slight decrease (Figure 6.1d, 6.4d and 6.5d). This would imply that NGAL somehow “removes/ deactivates” the inhibitory effect of excess MSF into the realms of a concentration which stimulates migration. Since it appears that NGAL does not bind directly to MSF the mechanism of how NGAL achieves the “removal/ deactivation” of MSF remains a mystery.

In order to determine whether MSF-I activity was present in the HaCaT series CM, each was tested in the migration assay with 100pg/ml rhMSF; which is known to stimulate baseline migration by a minimum of 50%. To assess the capacity of the CM to inhibit the rhMSF the level of migration was compared to both the rhMSF and CM baseline migration. BEN CM was the most effective MSF inhibitor with the majority of dilution points preventing any rhMSF stimulated migration. MAL CM followed with the MET having the least MSF-I activity (Table 6.2). Considering the ELISA data for the assessment of NGAL concentration in total CM these results confirm what was expected; NGAL concentration was discovered to be highest in the BEN and MAL CM, while MET CM had the lowest. However, it does not explain how the HaCaT series CM can stimulate migration but at the same time inhibit the bioactivity of exogenous MSF. Although there is proof that the cells express MSF and NGAL, a direct link of these proteins to CM bioactivity is required.

In order to determine the origins of the motogenic and MSF-I bioactivity within the HaCaT series CM the route previously described for the HaCaT keratinocytes was followed; by fractionating the CM by molecular weight selection using both size exclusion chromatography (SEC) and SDS polyacrylamide gel electrophoresis under reducing conditions.

Difficulties arose in trying to separate the two bioactivities into distinct entities. The process of concentrating the CM appeared to cause non-specific binding of proteins making SEC separation inefficient and some protein was lost due to precipitation, making any quantitative assessment meaningless. Also the inability to halt proteolysis of proteins within the CM, by the addition protease inhibitors, due to the biological assessment of bioactivity resulted in the production of bioactive breakdown products which made it difficult to identify a specific location/ molecular weight of protein responsible for each bioactivity.

MSF-I bioactivity was discovered in a number of different SEC fractions with various molecular weights (Table 6.5). Subsequent ELISA analysis using NGAL- specific antibodies identified a bioactive level of NGAL in all BEN and MAL fractions, and the

majority of MET too. Although, the maximal concentrations of NGAL was predominantly localised to the lower MW fractions (<25kDa); especially seen in BEN and MET CM (Figure 6.11). NGAL can bind to itself and other proteins, it has been previously described as having a molecular weight of 20-25kDa, forming a 46kDa homodimer and a 135kDa disulfide linked heterodimer with neutrophil gelatinase. Therefore, when SDS polyacrylamide gel electrophoresis of the CM was performed under reducing conditions a clearer picture emerged with BEN and MAL MSF-I activity being localised to 20-25kDa, which was equivalent to a positive band when immunoblotting of the CM was performed using a specific anti-NGAL antibody. For the MET CM, the presence of NGAL was detected both by ELISA and immunoblotting at this MW, although MSF-I bioactivity was the lowest measured of all the cell lines. The localisation of motogenic activity in fractionated CM also proved challenging. If MSF was indeed responsible it would be bioactive at a molecular weight of approximately 70kDa and also in the form of its proteolytically generated breakdown products; 43kDa GBD and 21kDa IGD-containing peptide. SDS PAGE separation of the CM identified MET CM as possessing the greatest motogenic activity but like BEN and MAL it could not be localised to a specific MW, although the majority of bioactivity was focused in the highest and lowest molecular weight segments. SEC separation confirmed that the higher molecular weight fractions possessed the most bioactivity, although MAL appeared to have the largest amount.

As previously revealed, the sensitivity limits of the ELISA and immunoblot to identify MSF are too low to give a positive result for HaCaT series CM. Consequently, using the higher molecular weight SEC fractions (>60kDa), immunoprecipitation (IP) with immobilised Protein G was performed, using the specific MSF identification antibody, RpVSI, followed by confirmation of MSF bioactivity in the 3D collagen gel fibroblast migration assay. Motogenic activity was present in the bound fractions of BEN, MAL and MET, confirming that MSF is indeed present in the HaCaT series CM. It would be erroneous to comment on which cell line gave the highest motogenic activity since it would be impossible to estimate how much protein was lost due to precipitation during the concentration process required for sample preparation and the scarcity of sample did not allow for a total protein measurement. The presence of MSF was further substantiated, by testing the bound elutions with the known MSF inhibitors, NGAL and the IGD function neutralising PEPQ1.1 antibody. Using the inhibitors in excess, the motogenic activity of the IP bound samples of each cell line was inhibited confirming MSF was responsible for the bioactivity.

In conclusion, it has been verified that the HaCaT series keratinocytes (BEN, MAL and MET) secrete bioactive forms of both MSF and NGAL. However, unlike the normal HaCaT cell line, an alteration in the balance of these pro and anti- motogenic factors manifests itself by the CM having an inherent motogenic activity, although with BEN and MAL still retaining the capability to inhibit rhMSF. Considering the data from the ELISA analysis for NGAL (presented in Chapter 5), where NGAL is present at a higher concentration in BEN and MAL CM than in the normal HaCaT, this was an unexpected outcome.

Comparing the bioactivity of BEN, MAL and MET CM with the parental HaCaT, where the production of NGAL appeared to obstruct the activity of endogenous MSF, there are two possible explanations as to why HaCaT series CM displays an inherent motogenic bioactivity. Firstly, the concentration of MSF must be far greater in the HaCaT series CM than in normal HaCaT CM to enable motogenic activity to prevail over NGAL MSF-I activity. This would be particularly relevant for the BEN and MAL as they had the highest levels of NGAL. However, the semi-quantitative evaluation of MSF immunolocalisation in the HaCaT series keratinocytes showed that MET had the highest intensity of MSF expression, borne out in also possessing the greatest motogenic bioactivity in their total CM. BEN cells cultured on plastic dishes, however had the least amount of MSF staining and highest NGAL concentration in the ELISA analysis but still exhibited an inherent motogenic activity similar to rhMSF, whilst retaining the capacity to inhibit rhMSF. Unfortunately the limit of detection of the MSF ELISA prevents a direct measurement of MSF concentration in the CM, making the migration assay as the only means of detecting the presence of MSF in the CM. As discussed earlier the characteristics of MSF bioactivity lead to complications in relating the level of migration to MSF concentration. It can also not be discounted that the CM contains other motogens, which are unaffected by the inhibitory actions of NGAL, and therefore contribute to the motogenic potential of the CM. Since the addition of MSF inhibitors, NGAL and PEPQ1.1 antibody, to the total CM failed to eliminate all motogenic activity. Possibly by performing MSF immunoprecipitation on total CM instead of fractionated, MSF contribution to the motogenic activity of HaCaT series CM could be conclusively be determined.

The second possible explanation is that the NGAL produced by the cells is only capable of inhibiting rhMSF but not the endogenously produced MSF. This suggests that the HaCaT series MSF is somehow different to the normal HaCaT keratinocyte produced MSF, making it NGAL resistant. Indeed, when recombinant NGAL was used in attempt

to knock-out the motogenic activity in the total CM, it proved to be less effective than the PEPQ1.1 antibody. However, MSF semi-purified from the HaCaT series CM (RpVSI immunoprecipitation of motogenic SEC fractions) did appear to be similarly inhibited by NGAL and PEPQ1.1. This implies that other factors in the CM are affecting NGAL efficiency in inhibiting endogenous MSF thereby contributing to the HaCaT series motogenic activity.

NGAL is known to have a protective role of MMP-9, safeguarding it from proteolytic degradation and is therefore involved in the remodelling of the extracellular matrix a precursor to neoplastic diffusion and metastatisation (Yan *et al.*, 2001). Therefore, it is possible that the higher concentrations of NGAL expressed by BEN and MAL lead to increased migration because of its indirect influence on ECM degradation. NGAL's association with MMP-9 has been linked to promoting breast, gastric and esophageal cancer tumourigenesis (Leng *et al.*, 2009, Fernandez *et al.*, 2005, Kubben *et al.*, 2007, Zhang *et al.*, 2007). However, many other studies (ovarian, pancreatic and colon) have described high levels of NGAL present in well-differentiated neoplasias but then almost negative in the high grade ones (Lim *et al.*, 2007, Tong *et al.*, 2008, Lee *et al.*, 2006). Lim *et al.*, described increased NGAL expression in benign ovarian tumours compared to normal tissue, but was then reduced in invasive high-grade carcinomas. This reflects the situation of the HaCaT series, with BEN and MAL having higher levels of NGAL compared to the normal HaCaT while the metastatic line, MET, has lowest NGAL levels with very limited MSF-I activity, therefore resulting in the highest motogenic activity. This would be in agreement with the Lee *et al.*, (2006) study involving the KM12SM colon cancer cell line, where an inverse correlation between NGAL expression and metastatic potential was described.

Each cell line of the HaCaT series expresses different amounts of MSF and NGAL and it has been shown that an alteration in balance of stimulator and inhibitor appears to directly influence the bioactivity of their CM. The results show that as the metastatic potential of the keratinocytes increased there was a relative increase in intensity of MSF immunolocalisation and motogenic bioactivity. While the expression level of NGAL was the lowest in the metastatic cells, peaking in the benign and malignant keratinocytes although exhibiting a restricted capacity to inhibit the motogenic bioactivity of endogenous MSF. Many questions still require answering and considerable further investigation is required to understand the relationship between the two proteins and their mechanism of interaction however, it has emerged that NGAL and MSF do indeed play a role in tumour growth and metastasis. Ultimately, the genetic

modification of NGAL and MSF expression levels and the subsequent use of experimental animal models would lead to a greater understanding of their importance in tumorigenesis and possible clinical relevance.

Chapter 7: Results

THE IDENTIFICATION OF MSF-I PRODUCED BY ENDOTHELIAL CELLS

7.1 AIMS

The initial aim was to ascertain whether endothelial cells express MSF and NGAL. This was the first step in a process to determine whether endothelial MSF was the source of the motogenic bioactivity present in the conditioned medium collected from sprouting endothelial cells and whether an endothelial NGAL was responsible for the MSF-I activity present in the conditioned medium of endothelial cells expressing the cobblestone phenotype. Consequently, these findings should help to establish if the phenotype of an endothelial cell can be defined by the expression of either MSF or a MSF-inhibitor. However, the situation may be similar to the keratinocyte HaCaT series where both MSF and the MSF-inhibitor NGAL are expressed, but at varying levels. An additional aim was to ascertain what effect NGAL and MSF have on the morphology of endothelial cells, specifically focusing on the consequence MSF inhibition has on endothelial sprouting cells.

7.2 BACKGROUND

Previous investigations revealed that the bioactivity of conditioned medium (CM) collected from endothelial cells *in vitro* was determined by endothelial phenotype. *In vitro*, endothelial cells retain the phenotypic plasticity observed *in vivo*. A reversible phenotypic conversion enables expression of two distinctive cell morphologies, described as cobblestone and sprouting, which are considered to be comparable to the resting and angiogenic endothelial cells observed *in vivo* (Schor *et al.*, 1983). The CM collected from the sprouting endothelial cells exhibited an endogenous motogenic activity. Conversely, CM from the cobblestone phenotype had the ability to inhibit the motogenic activity of rhMSF in the 3D collagen gel fibroblast migration assay. A similar MSF- inhibitory bioactivity was discovered in the CM of the immortalised human keratinocyte cell line, HaCaT, and subsequently identified as Neutrophil Gelatinase Associated Lipocalin (NGAL). In addition, upon fractionation of the HaCaT

CM the existence of a previously obscured motogenic activity was discovered, which was identified as MSF. It therefore transpired that the HaCaT keratinocytes express MSF but its motogenic activity was inactivated by the co-expression of NGAL. Subsequent investigation of the HaCaT series cell lines, which represent the progressive stages of tumour development from benign, malignant to metastatic, showed that each cell line expressed a differing amount of MSF and NGAL and that the alteration in the balance of stimulator and inhibitor had a direct influence on the bioactivity of their CM. In both *in vitro* and *in vivo* models MSF and NGAL are reported to have opposing effects on angiogenesis. An *in vitro* application of rhMSF to an endothelial cobblestone monolayer, under serum free culture conditions, will induce a greater number of sprouting cells compared to a serum free only control (Schor and Schor, 2010). MSF also stimulates angiogenesis *in vivo* in the chicken yolk-sac membrane assay (Schor and Schor, 2010, unpublished observations). Meanwhile, NGAL significantly reduces the tube formation of HUVEC endothelial cells and over-expression of NGAL has been shown to mediate a reduction in angiogenesis in an orthotopic mouse model of pancreatic cancer and an intradermal tumour angiogenesis assay (Venekatesha *et al.*, 2006, Tong *et al.*, 2008).

The first line of investigation was therefore to determine whether MSF and NGAL were expressed by the cultured endothelial cells and whether there were phenotypic differences in expression. Since endothelial cell morphology appears to determine CM bioactivity, it will be interesting to discover if both factors are expressed together and whether the relative expression levels determine bioactivity and possibly morphology.

7.3 THE IDENTIFICATION OF NGAL EXPRESSION IN ENDOTHELIAL CELL LINES

7.3.i Western Blot Identification of NGAL

To determine whether NGAL was present in endothelial cell conditioned medium (CM) the immunoblot method previously optimised for the HaCaT series study was performed using a specific anti-NGAL antibody, Mab1757 (Materials & Methods, Chapter 2). A variety of endothelial cell lines, of both human and bovine origin were cultured on a 2D surface of 0.1% (w/v) gelatin coated plastic cell cultures dishes and CM was collected when cells had reached confluence and displayed the cobblestone phenotype. In addition, CM was collected from ENDO 742 and BAEC cells plated

either on or within a 3D type I collagen matrix; the cells displaying a cobblestone and sprouting phenotype respectively. CM collected from a blank type I collagen gel (no cells) acted as a control. The CM was tested both neat and at various concentrations (Amicon method). A control sample of rhNGAL (300ng) was always included as a positive control.

The unfractionated CM was separated by 12% SDS PAGE under reducing conditions, followed by immunoblotting with the anti-NGAL antibody (Chapter2, Materials & Methods). Visualisation by chemiluminescence identified a clear band of approximately 20-25kDa in the rhNGAL control lane, however no positive bands was observed in the any of endothelial CM lanes. Irrespective of endothelial cell origin (human or bovine), cell phenotype (cobblestone or sprouting) or CM concentration (tested neat and maximum concentration x50) the result was consistently negative for the presence of NGAL. (Figure 7.1).

The immunoblot experiments were repeated using a different anti-NGAL antibody, polyclonal AF1757. The results confirmed that either NGAL was not present in the endothelial CM or if present it was at a concentration below the sensitivity of the assay.

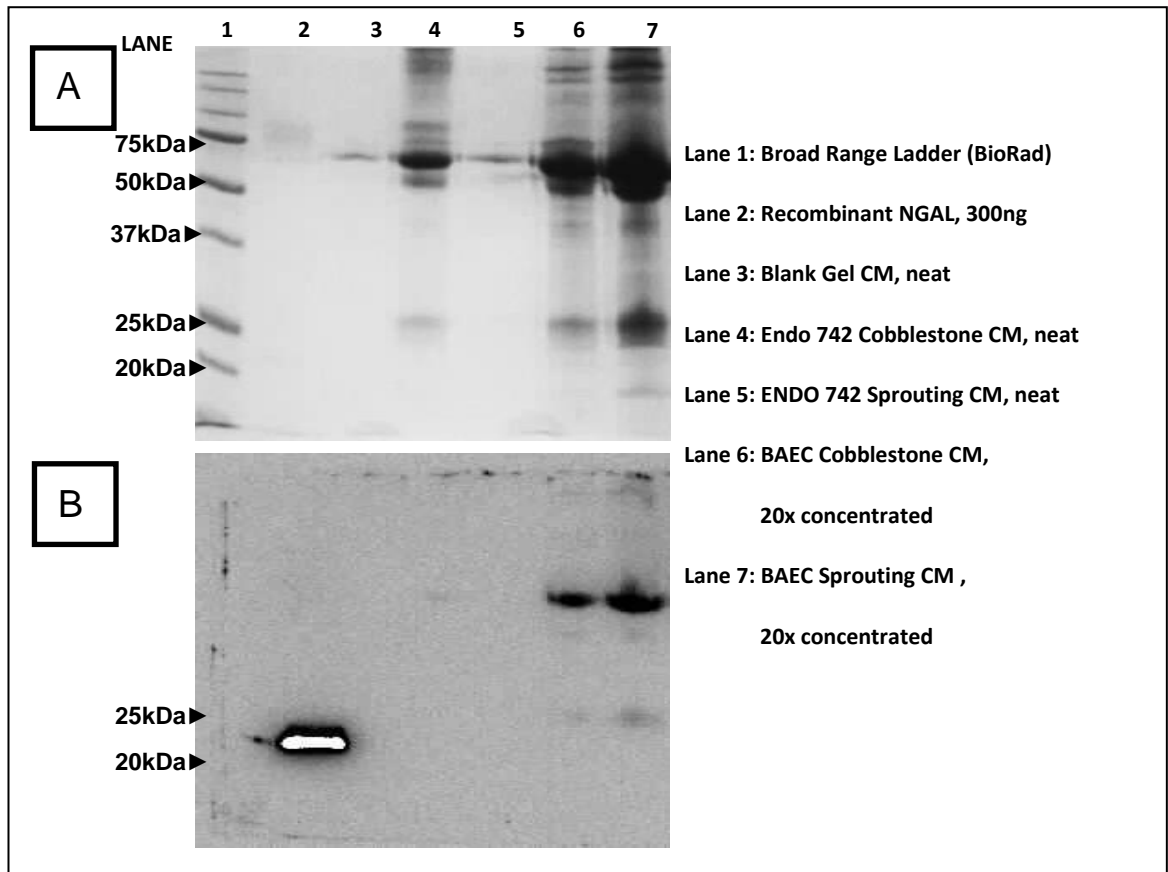


Figure 7.1.

A. The Separation of endothelial conditioned medium by SDS PAGE.

Endothelial CM collected from cultures displaying either cobblestone or sprouting phenotype was separated by 12% SDS PAGE under reducing conditions. Protein bands were visualised by Coomassie Blue.

B. The identification of NGAL in endothelial cell lines by immunoblotting.

Immunoblot of 12% SDS PAGE separation of endothelial cell CM, under reducing conditions, with specific anti-NGAL antibody, Mab1757. A distinct band was seen at 20-25kDa in the rhNGAL lane. No correspondingly sized bands were located in any of the endothelial CM. Diffuse bands were observed in Lanes 6 and 7 but were located at the wrong molecular weight and considered an artefact due to the high concentration of protein present in the sample; especially, since no bands were ever detected in un-concentrated or less concentrated CM. In conclusion, by this method, the endothelial CM of both bovine and human origin, whether displaying the cobblestone and sprouting phenotype were negative for NGAL.

7.3.ii Immunolocalisation of NGAL in Endothelial Cell Lines

In order to confirm the results achieved by the immunoblot experiments, immunolocalisation of NGAL in cultured endothelial cell lines was performed. Endothelial cell lines of both human and bovine origin were plated on either the surface

of a 2D 0.1% (w/v) gelatin coated plastic cell cultures dish or a 3D type I collagen matrix and also within a 3D type I collagen matrix; thereby insuring both endothelial phenotypes, cobblestone and sprouting, were screened.

The method optimised for HaCaT experiments using the NGAL specific antibody, anti-NGAL goat polyclonal AF1757, was adopted (Materials & Methods, Chapter 2). Each immunolocalisation experiment included an internal control of normal serum goat IgG, (used at same concentration as anti-NGAL antibody) and secondary antibody only (biotinylated polyclonal swine anti-goat IgG). In addition, known NGAL positive and negative cell lines HaCaT and FSF44, respectively, were included as an additional check.

The results obtained corroborated those gained by immunoblot with all endothelial cell lines negative for the presence of NGAL, irrespective of species type, phenotype and plating matrix (Figure 7.2).

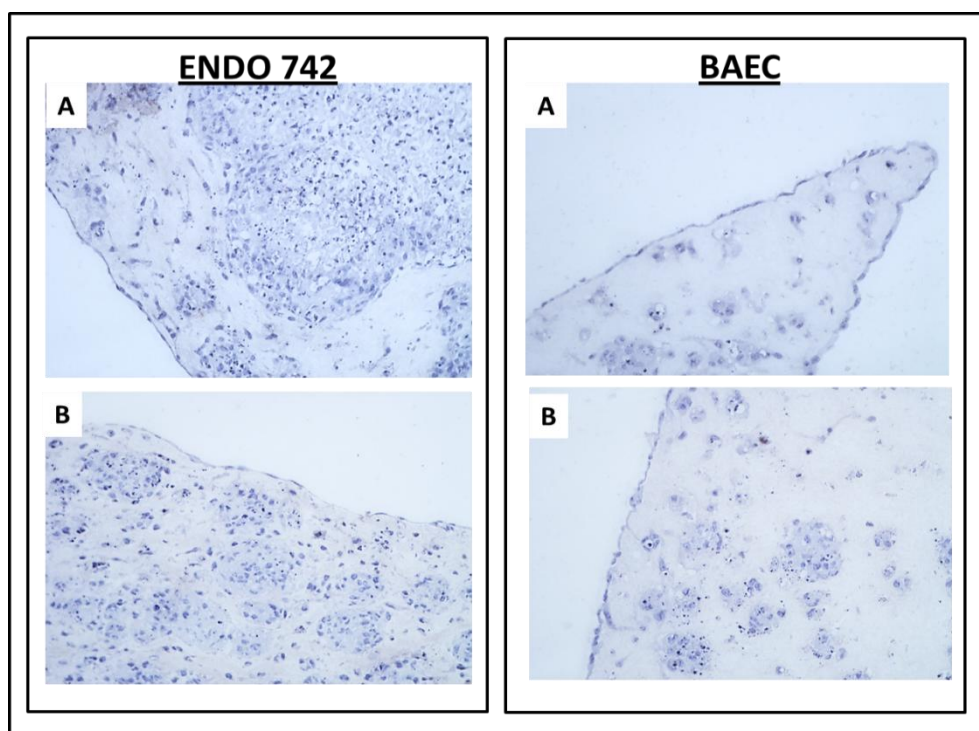


Figure 7.2: Immunolocalisation of NGAL in endothelial cells. Endothelial cells of both human and bovine origin, ENDO 742 and BAEC respectively, were plated on and within a 3D collagen type I matrix. Thereby, insuring both endothelial phenotypes, cobblestone and sprouting, were exhibited. The presence of NGAL was assessed by immunocytochemistry using the specific anti-NGAL goat polyclonal AF1757 (0.5 μ g/ml); Image A. NGAL positive expression resulted in a brown colour staining. Control cultures were incubated with normal goat IgG at the same concentration as the NGAL specific antibody (0.5 μ g/ml); Image B. Images and observations were made at x20 magnification.

7.4 THE IDENTIFICATION OF MSF EXPRESSION IN ENDOTHELIAL CELL LINES

7.4.i Western Blot Identification of MSF

In a repeat of the immunoblot performed to determine endothelial expression of NGAL, a variety of CM collected from various human and bovine endothelial cells were tested for the presence of MSF. As previously described, CM was collected from endothelial cells expressing either the cobblestone and sprouting endothelial cells, when cultured on a 2D (0.1% (w/v) gelatin coated plastic) and on or within a 3D matrix (type I collagen gel).

The un-fractionated CM was separated by 12% SDS PAGE under reducing conditions followed by immunoblotting with a specific anti-MSF antibody, RpVSI (Materials & Methods, Chapter 2). A control sample of rhMSF (250pg) consistently resulted in a main band of approximately 77kDa on the immunoblot. However, no bands were observed in any of the lanes containing the variety of endothelial CM tested. A selection of concentrated endothelial CM (maximum concentration x50) was tested but all yielded a negative result. (Figure 7.3).

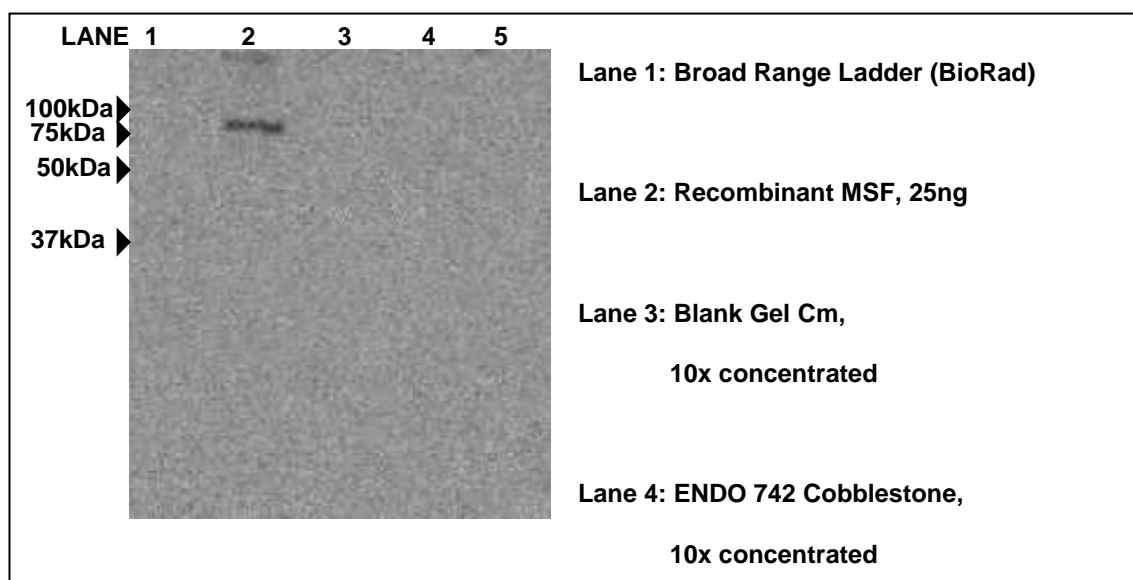


Figure 7.3. The identification of MSF in endothelial cell lines by immunoblotting.

Immunoblot of 12% SDS PAGE separation of endothelial cell CM, under reducing conditions, with specific anti-MSF antibody, RpVSI. A distinct band was seen at approximately 75-80kDa in the rhMSF lane, however all endothelial CM tested was negative.

7.4.ii Immunolocalisation of MSF in Endothelial Cell Lines

In a direct repeat of experiments performed for the NGAL immunolocalisation in endothelial cell lines the same set of samples were screened for the presence of MSF. A rabbit polyclonal anti-VSI antibody (Rp2), raised against the MSF unique carboxyl terminal decapeptide was employed for MSF identification. Two negative controls were included in every experiment; the secondary antibody (biotinylated goat anti-rabbit IgG) tested alone and normal rabbit IgG used at the same concentration as the anti-VSI antibody (Materials & Methods, Chapter 2). In addition the FSF44 and HaCaT cell lines were included as internal controls since they had previously been shown to be MSF negative and positive, respectively.

In contrast to the MSF immunoblot results, both bovine (BAEC Clone 2 and Clone 2-2 U7) and human (ENDO 742, HUVEC) cell lines were shown to express MSF.

However, MSF expression appeared to be dependent upon the endothelial phenotype. In the majority of experiments (4/5), endothelial cells (BAEC, HUVEC and ENDO 742) plated on a 2D surface (0.1% (w/v) gelatin coated plastic) and displaying the cobblestone phenotype were negative for MSF. Yet, when the same cells were cultured to post-confluence, forming sprouting networks, the highest intensity of MSF positive staining appeared to be specifically localised to the sprouting cells whilst areas of cobblestone remained negative or very weak positive.

The phenotypic-specific expression of MSF was also seen when the endothelial cells (BAEC, ENDO 742, HUVEC) were plated either on the surface of or within a 3D collagen type I matrix. Endothelial cells plated within a 3D matrix spontaneously adopt a sprouting phenotype which, in time, develop into sprouting networks however when endothelial cells are plated on a gel surface they form a typical cobblestone appearance. Again, the sprouts consistently stained positive with intensity ranging from weak to strong, whereas the cobblestone endothelial cells were either completely negative or very weakly positive. However, in a minority of cases (2/7 experiments) a few strong positive cells were noted on the gel surface. From the observations of these MSF positive cells it would appear that they did not have a free apical surface but were in fact plated underneath other endothelial cells. As seen in the HaCaT series study, the background staining of the type I collagen gel pellet was itself scoring (weakly) positive. (Figure 7.4).

These results seem to imply that MSF expression in endothelial cells is dependent on the loss of apical-basal polarity, irrespective of whether that is achieved by plating the cells within a 3D environment or cells growing beneath a cobblestone monolayer. However, the discovery of positive MSF expression is at odds with the immunoblot results where both cobblestone and sprouting CM were MSF negative. As previously discussed for the HaCaT CM immunoblot experiments to identify MSF; the conclusion was that endothelial cells do express MSF but that it must be present in the CM at concentrations below the limits of sensitivity of the immunoblot assay (25ng/ml).

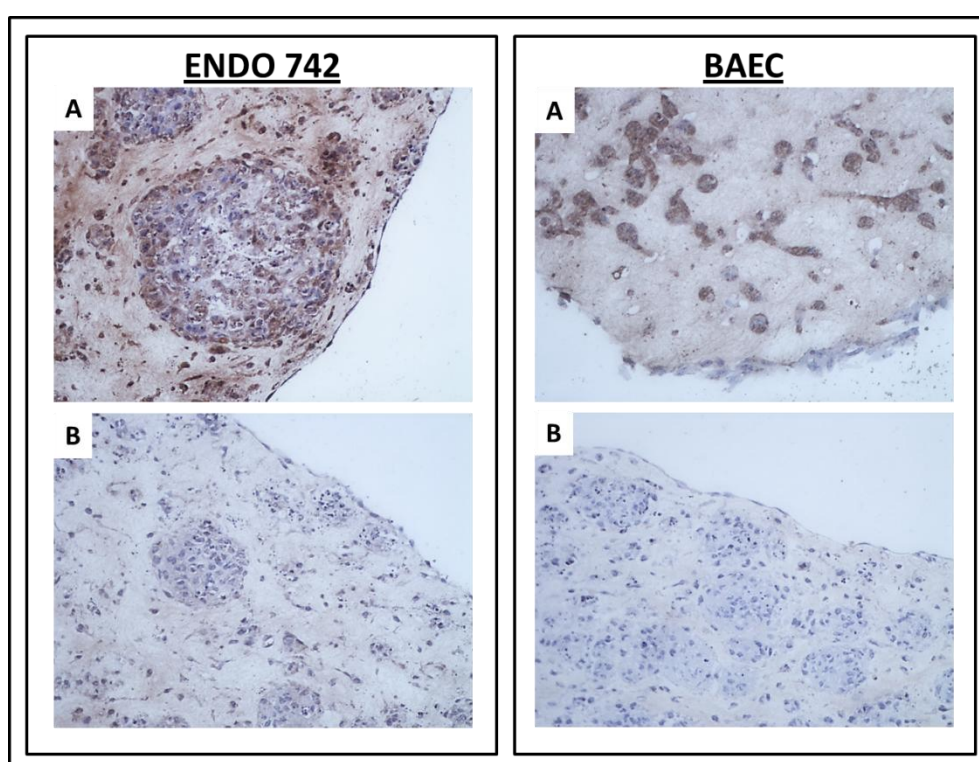


Figure 7.4: Immunolocalisation of MSF in endothelial cells. Endothelial cells of both human and bovine origin, ENDO 742 and BAEC respectively, were plated on and within a 3D collagen type I matrix. Thereby, ensuring both endothelial phenotypes, cobblestone and sprouting, were exhibited. The presence of MSF was assessed by immunocytochemistry using the specific anti-MSF antibody, Rp2 (5 μ g/ml); Image A. MSF positive expression resulted in a brown colour staining. Control cultures were incubated with normal rabbit IgG at the same concentration as the MSF specific antibody (5 μ g/ml); Image B. Images and observations were made at x20 magnification.

7.5 THE CHARACTERISATION OF ENDOTHELIAL ENDOGENOUS MOTOGENIC BIOACTIVITY.

During the initial screening, the bioactivity of endothelial conditioned medium was assessed by testing in the 3D collagen gel fibroblast migration assay. Bioactivity was discovered to be phenotype dependent; cobblestone CM possessed the ability to inhibit rhMSF stimulated fibroblast migration whilst it emerged that the sprouting CM had endogenous motogenic activity. Immunolocalisation experiments have detected MSF in sprouting endothelial cells, however immunoblot analysis of endothelial CM failed to identify any MSF present. Consequentially by characterising the endothelial CM motogenic bioactivity it should be possible to determine whether an endothelial expressed MSF is indeed responsible for this motogenic bioactivity.

Taking direction from the HaCaT study, endothelial CM was fractionated and the subsequent fractions tested for bioactivity in the 3D collagen gel fibroblast migration assay. The motogenic active fractions were then characterised by testing with known MSF inhibitors, NGAL and PEPQ 1.1. If endothelial MSF was present then all motogenic activity would be neutralised by addition of the MSF-inhibitors. Two methods of fractionation were adopted, size exclusion chromatography and SDS electrophoresis. Although both methods separate proteins according to their molecular weight by performing the SDS PAGE under reducing conditions some higher molecular weight associations between proteins would be eliminated. Thereby, diminishing the possibility of concealment of bioactivity due to associations between proteins; a possible result of an artefact of the CM collection and concentration process.

In order to ensure that the CM was collected from a specific phenotype of endothelial cells CM was collected from ENDO 742 cells plated either within or upon a type I collagen gel; sprouting and cobblestone phenotype respectively. Although motogenic activity was only detected in the sprouting CM, the cobblestone CM was also fractionated since, as seen with the HaCaT study, motogenic activity may be undetected in the total CM due to inactivation by a co-secreted inhibitor. CM collected from a blank collagen gel was used as a control. For ease of discussion, the CM was classified as Blank (gel only no cells), Sprouting (ENDO 742 plated within gel exhibiting spontaneous sprout phenotype) and Cobblestone (ENDO 742 plated upon a gel exhibiting cobblestone phenotype).

7.5i The Motogenic Activity of Size- Exclusion Fractionated ENDO 742 Conditioned Medium.

As previously used for the HaCaT study, the Superdex 75 HiLoad 26/60 (GE Healthcare) column, which has a fractionation range of 3-70kDa, was used to fractionate 4ml of ten times Amicon concentrated CM (Materials & Methods, Chapter 2). Multiple runs were completed in order to provide sufficient material for downstream analysis. For each individual run 100 x 3ml fractions were collected (2ml/min) and numbered 1 to 100; the corresponding fractions from the duplicate runs were then pooled together. Subsequently the fractions were pooled into groups of three; Groups 1 to 33. Groups 11 to 23 (fractions 31-69), equivalent to the main absorbance peak with a molecular weight range of approximately >70kDa to 20kDa were selected for analysis. The SEC fractionated CM of each variable (sprout, cobblestone and blank) was tested alone in the 3D collagen gel fibroblast migration assay in order to determine the presence of motogenic activity. Fraction groups 11 to 23 were tested at a final dilution of 1/20 (all dilutions made with SF MEM). Each fraction group was considered as motogenic if fibroblast migration was stimulated by at least 50% when compared to SF MEM control baseline levels (100 +/- 12.22%).

As expected, the Blank CM displayed a complete absence of motogenic activity in all fraction groups tested (11-23) with migration levels comparable to the SF MEM baseline. For both Cobblestone and Sprout CM motogenic activity was located within the higher molecular weight fraction groups (>70kDa). (Figure 7.5b).

The fraction groups 11-14 of the Cobblestone CM had an average migration of 183.0 +/- 32.16% compared to the SF MEM baseline migration. Maximum migration of twice baseline level was achieved by fraction groups 13 and 14. Group 15 displayed motogenic activity but results were inconsistent between experiments resulting in a high standard deviation. Lower molecular weight fraction groups exhibited no motogenic activity which met the criteria of 50% above SF MEM baseline. (Figure 7.5c). The discovery of motogenic activity is at odds with the result achieved from the unfractionated CM collected from cobblestone endothelial cells where no motogenic activity was measured. However, it is similar to the masked motogenic activity, attributed to MSF, present in total HaCaT CM.

The motogenic activity of the Sprout CM was located in fraction groups 11-15 with an average migration of 212.7 +/- 24.59% compared to SF MEM baseline. Overall, the

level of migration was greater than that of the Cobblestone CM, peaking at 2.4 times SF MEM baseline in Fraction group 12. No motogenic activity was detected in the lower molecular weight fraction groups. (Figure 7.5d).

7.5ii The Effect of MSF-Inhibitors on the ENDO742 Motogenic SEC Fractionated Conditioned Medium.

The motogenic active SEC fractions of each ENDO 742 CM type were pooled together (Cobblestone CM fraction groups 11-14 and Sprout CM fraction groups 11-15).

Dilutions 1/20 to 1/1000 were made with SF MEM and then tested alone in the 3D collagen gel fibroblast migration assay.

A similar level of motogenic activity was measured in pooled samples as compared to those previously found in the individual fraction groups for both the Cobblestone and Sprout CM. For both CM types, maximum motogenic activity was present in the 1/200 dilution; 213.9 +/- 39.17 and 210.0 +/-31.43 for Cobblestone and Sprout CM respectively. The dilutions 1/400 and 1/1000, for both CM types, failed to increase migration by 50% above the SF MEM baseline. Overall, the motogenic activity appeared to adopt a bell-shaped dose response with the lowest and highest dilutions displaying less activity than the mid-range dilution which possessed maximal activity (Figure 7.6b and c). However, the activity is certainly not as distinct as compared to the dose response of rhMSF (Figure 7.6a).

In order to determine whether this endogenous motogenic activity of the endothelial CM could be attributed to the expression of MSF, the pooled SEC fractions were tested in the presence of NGAL and the MSF function neutralising antibody, PEPQ 1.1. Both NGAL and the PEPQ 1.1 antibody possess the ability to inhibit MSF bioactivity back to baseline levels; but at different levels of potency. The maximum MSF concentration that 10ng/ml of NGAL can inhibit is 500pg/ml while a 50ng/ml of PEPQ 1.1 can inhibit up to 1ng/ml of MSF. The set criterion for NGAL and PEPQ1.1 inhibition was a reduction in baseline migration by at least 50%. The SEC fractions were again tested at a range of dilutions, 1/20 to 1/1000.

In the two experiments performed, the effect of the MSF inhibitors on the endothelial SEC motogenic fractions was ambiguous. For the Cobblestone SEC motogenic fractions, the criteria for inhibition by NGAL was only achieved in dilutions 1/20 and 1/40 (average 64.4 +/- 6.65% inhibition) and by PEPQ 1.1 in dilution 1/40 (53.5%

inhibition). The motogenic activity of the Sprout SEC fractions was only inhibited by PEPQ1.1 at the 1/20 dilution (51.4% inhibition) (Figure 7.7).

However, if the dilution 1/200 which achieved maximal motogenic activity was analysed in isolation, the effect of the addition of NGAL and PEPQ 1.1 was similar for both Sprout and Cobblestone SEC fractions. Although the level of inhibition failed to reach the set criteria it was apparent that PEPQ 1.1 had nearly twice the inhibitory ability than NGAL: with an average $46.0 \pm 4.24\%$ inhibition compared to $26.0 \pm 2.83\%$, respectively. Overall, PEPQ 1.1 showed the greater ability to inhibit the motogenic activity than NGAL; particularly for the Sprout SEC fractions.

From the analysis of the level of motogenic activity measured for both Cobblestone and Sprout CM, compared to a rhMSF dose response curve, both NGAL and PEPQ 1.1 were added in excess and should have neutralised all migration if MSF-induced migration. Since motogenic activity was inhibited to some degree, a plausible conclusion would be that MSF was present in both ENDO 742 Cobblestone and Sprout CM in addition to another motogen. However, the indeterminate results may also have arisen because the MSF inhibitors were not functioning efficiently possibly due to the formation of non-specific protein associations; as an artefact of the sample preparation process.

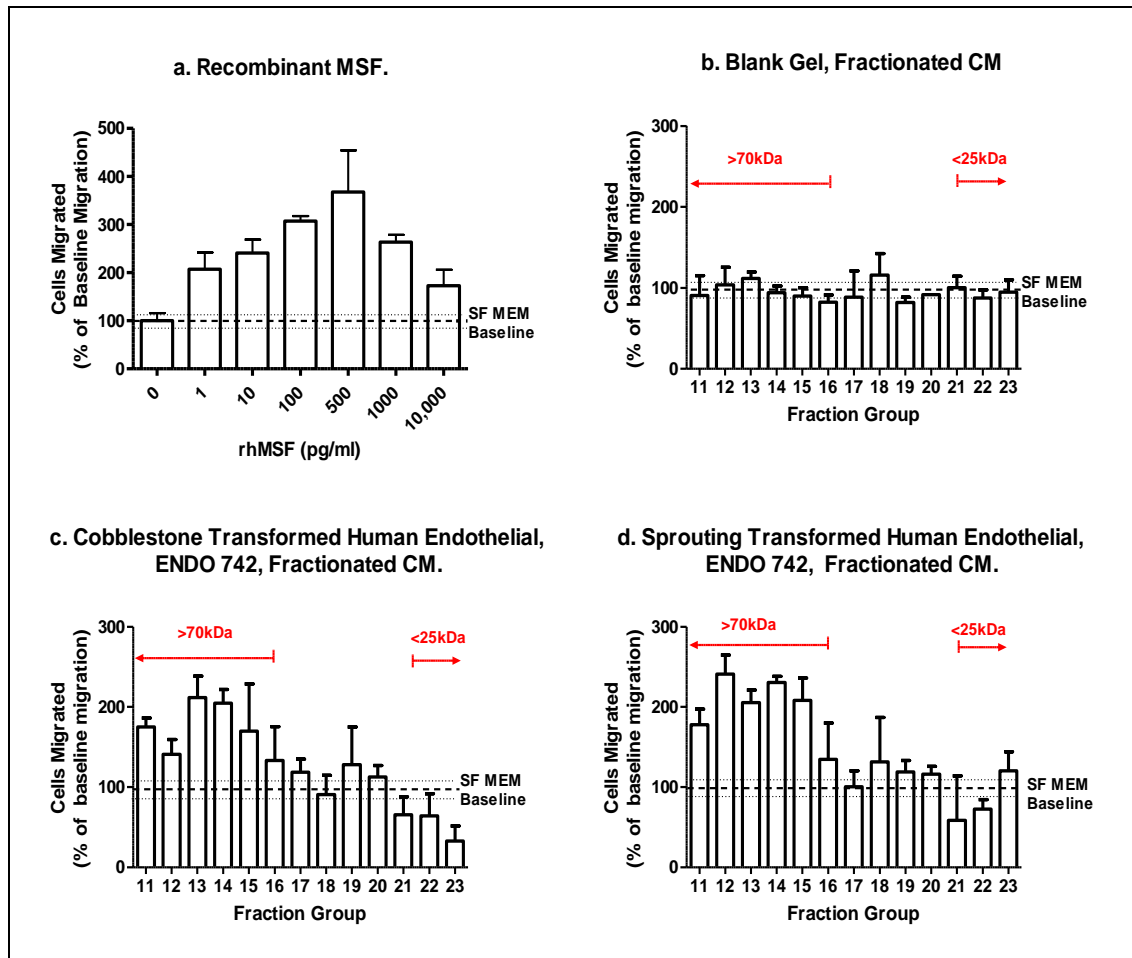


Figure 7.5: The motogenic activity of Superdex 75 fractionated conditioned medium from ENDO 742 cells. Comparison with rhMSF. Conditioned medium was collected from ENDO 742 cells grown either on or within a collagen gel matrix; thereby displaying either a cobblestone or sprouting phenotype respectively. As a control, conditioned medium was also collected from a blank collagen gel (no cells). The Superdex 75 fractionated conditioned medium (CM), fraction groups 11-23, was tested, alone in 3D collagen gel fibroblast migration assay. The number of cells migrated is expressed as a percentage of SF MEM control baseline migration i.e. SF MEM Baseline = 100 +/- 12.22%, as represented by the hatched and dotted lines (mean and SD respectively). This was equivalent to 2.7 +/- 0.33 migrated cells. (100pg/ml rhMSF only = 7.8 +/- 0.32 migrated cells). Dose response to rhMSF is shown for comparison. The results represent an average of two experiments.

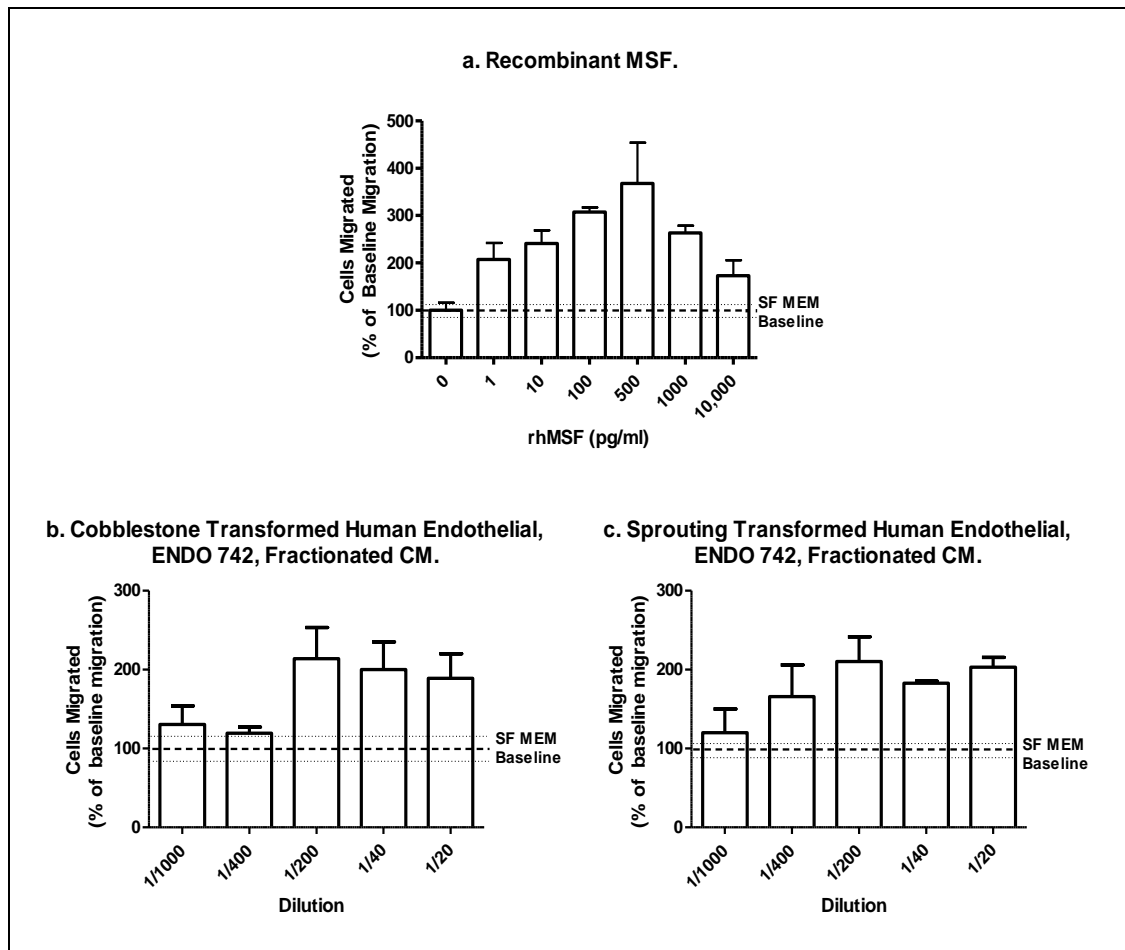


Figure 7.6: The motogenic bioactivity of Superdex 75 fractionated ENDO 742

conditioned medium. Comparison with rhMSF.

Conditioned medium was collected from ENDO 742 cells grown either on or within a collagen gel matrix; thereby displaying either a cobblestone or sprouting phenotype respectively. The Superdex 75 fractionated conditioned medium (CM), fraction groups 11-23, was previously tested, alone in 3D collagen gel fibroblast migration assay. For cobblestone and sprouting CM fraction groups 11-14 and 11-15, respectively were shown to possess motogenic activity. Following pooling, the motogenic fraction groups were then tested alone in the 3D collagen gel fibroblast migration assay, at a range of dilutions. The number of cells migrated is expressed as a percentage of SF MEM control baseline migration i.e. SF MEM Baseline = 100 +/- 8.28%, as represented by the hatched and dotted lines (mean and SD respectively). This was equivalent to 3.5 +/- 0.29 migrated cells. (100pg/ml rhMSF only = 8.2 +/- 0.63 migrated cells). Dose response to rhMSF is shown for comparison. The results represent an average of two experiments.

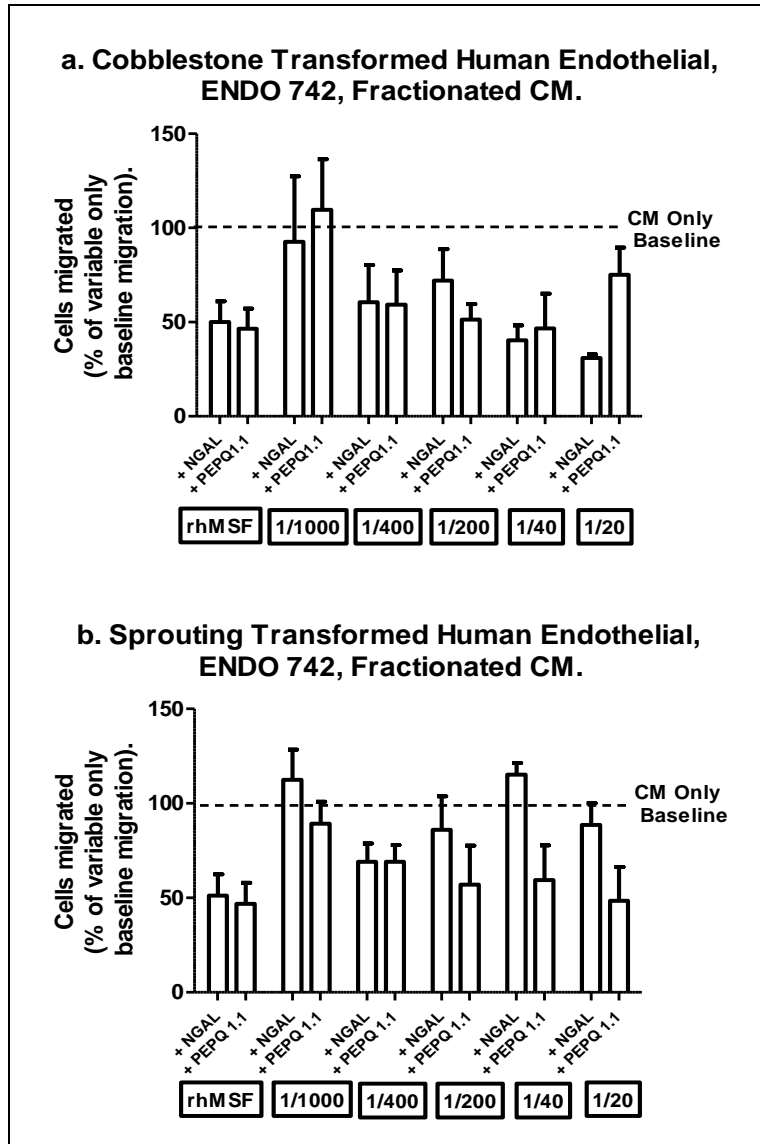


Figure 7.7: The effect of MSF-Inhibitors, NGAL and function neutralising antibody PEPQ1.1, on the endogenous motogenic bioactivity of Superdex 75 fractionated ENDO 742 conditioned medium. Conditioned medium was collected from ENDO 742 cells grown either on or within a collagen gel matrix; thereby displaying either a cobblestone or sprouting phenotype respectively. The Superdex 75 fractionated conditioned medium (CM), fraction groups 11-23, was tested, alone in the 3D collagen gel fibroblast migration assay. For cobblestone and sprouting CM fraction groups 11-14 and 11-15, respectively were shown to possess motogenic activity. Following pooling the motogenic fraction groups were then tested with both 10ng/ml rhNGAL and 50ng/ml PEPQ1.1 antibody in the 3D collagen gel fibroblast migration assay, at a range of dilutions. The number of cells migrated is expressed as a percentage of the variable only baseline migration i.e. Cobblestone ENDO 742 groups 11-14 diluted 1/20 only = 100 +/- 16.47. The effect of rhNGAL and PEPQ1.1 antibody on 100pg/ml rhMSF is shown for comparison (100pg/ml rhMSF only = 8.4 +/- 0.49).

7.5iii The Motogenic Activity of SDS PAGE Fractionated ENDO 742 Conditioned Medium

The same ten times concentrated CM used for the SEC fractionation (ENDO 742 Cobblestone and Sprout plus Blank CM) was fractionated by SDS PAGE under reducing conditions. Equal volumes of the 10x Amicon concentrated CM and Laemmli loading buffer, containing the reducing agent 2 β -mercaptoethanol, was heated for five minutes thereby denaturing the proteins present by reducing the disulfide linkages. The samples were then loaded onto a pre-run 12% separating 5% stacking SDS polyacrylamide gel. Following electrophoresis each lane was cut into 12 segments, from high to low molecular weight (1-12), and the proteins were eluted from the gel segments by an overnight incubation in 1ml of elution buffer. (Materials & Methods, Chapter 2). To determine the presence of motogenic activity, the proteins eluted from each gel segment were tested alone, at a final dilution of 1/1000, in the 3D collagen gel fibroblast migration assay. A protein elution was considered motogenic if it caused fibroblast migration to increase by 50% above the baseline level set by the SF MEM control. Once again, the Blank CM showed no bioactivity in any of the protein elutions with migration equivalent to the SF MEM baseline level (Figure 7.8a). Comparable to the results from the SEC fractionated endothelial CM, the higher molecular weight protein elutions of both cobblestone and sprout CM exhibited maximal motogenic activity. Motogenic activity was restricted to elutions 3 and 4 of the Cobblestone CM (37-100kDa) with an average migration of 169.7 +/- 4.17% compared to the SF MEM baseline (Figure 7.8b). Sprout CM elutions 2 and 3, corresponding to 75-100kDa, exhibited an average migration of 161.95 +/- 14.21 (Figure 7.8c). For both Cobblestone and Sprout no other protein elution displayed the ability to stimulate migration above 50% of the SF MEM baseline.

7.5iv The Effect of MSF-Inhibitors on the ENDO742 Motogenic SDS PAGE Fractionated Conditioned Medium.

The next stage was to pool the migration stimulatory gel elutions and to test then with NGAL and PEPQ1.1 antibody in the 3D collagen gel assay. In order to ensure the complete neutralisation of any MSF-induced motogenic activity the inhibitors were added in excess. The criteria set for the inhibition of motogenic activity was a reduction

in migration by at least 50% compared to the baseline level. The pooled elutions were only tested at a final dilution of 1/1000.

In an average of two experiments, the pooled elutions 3-4 of the Cobblestone CM showed increased migration by 1.7 times that of SF MEM baseline. The addition of NGAL and PEPQ 1.1 inhibited this activity by 40.8 +/- 7.24% and 46.9 +/- 9.63% respectively. Sprout CM pooled elutions 2-3 stimulated migration by a similar level, which was reduced by 34.0 +/- 5.96% with addition of NGAL and 40.4 +/- 4.47% by PEPQ 1.1. (Figure 7.9). Although inhibition of motogenic activity was achieved it failed to reach the set criteria of at least 50% compared to the baseline level.

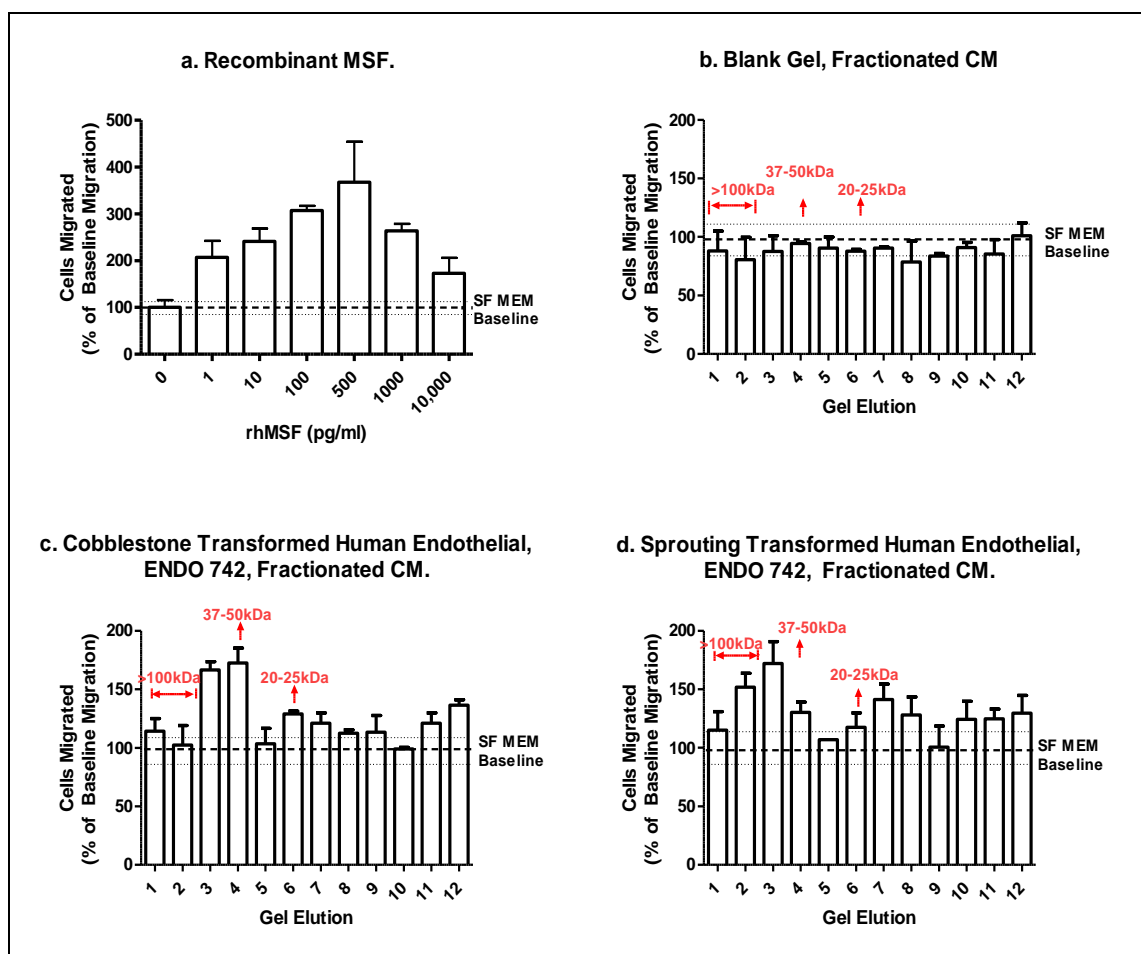


Figure 7.8: The motogenic activity of the gel elutions from the SDS electrophoresis fractionation of ENDO 742 conditioned medium. Comparison with rhMSF.

Conditioned medium was collected from ENDO 742 cells grown either on or within a collagen gel matrix; thereby displaying either a cobblestone or sprouting phenotype respectively. As a control conditioned media was also collected from a blank collagen gel (no cells). After electrophoresis of the CM and segmentation of the gel, the protein eluted from each segment (1-12) was tested alone in the 3D collagen gel fibroblast migration assay (final concentration 1/1000). The number of cells migrated is expressed as a percentage of the SF MEM control

baseline migration i.e. SF MEM Baseline = 100 +/- 15.64%, as represented by the hatched and dotted lines (mean and SD respectively). This was equivalent to 3.9 +/- 0.61 migrated cells. (100pg/ml rhMSF only = 11.7 +/- 0.40 migrated cells). Dose response to rhMSF is shown for comparison. The results represent an average of two experiments.

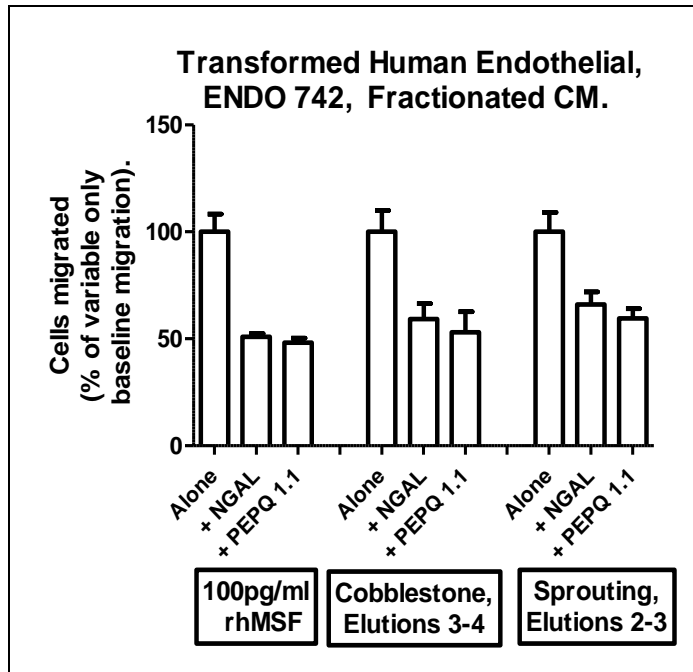


Figure 7.9: The effect of MSF-Inhibitors, NGAL and function neutralising antibody PEPQ1.1, on the endogenous motogenic bioactivity of the gel elutions from the SDS electrophoresis fractionation of ENDO 742 conditioned medium.

Conditioned medium was collected from ENDO 742 cells grown either on or within a collagen gel matrix; thereby displaying either a cobblestone or sprouting phenotype respectively. After electrophoresis of the CM and segmentation of the gel, the protein eluted from each segment (1-12) was tested alone in the 3D collagen gel fibroblast migration assay. The following gel elutions were shown to possess motogenic activity; ENDO 742 On Gel elutions 3-4 and ENDO 742 In Gel elutions 2-3. The motogenic active gel elutions were pooled and then tested with both 10ng/ml rhNGAL and 50ng/ml PEPQ1.1 antibody in the 3D collagen gel fibroblast migration assay, at a final dilution of 1/1000. The number of cells migrated is expressed as a percentage of the variable only baseline migration i.e ENDO 742 gel elutions 9-10 only = 100 +/- 10.00. The effect of rhNGAL and PEPQ1.1 antibody on 100pg/ml rhMSF is shown for comparison (100pg/ml rhMSF only = 11.4 +/- 0.95).

7.6 THE CHARACTERISATION OF ENDOTHELIAL MSF-INHIBITORY BIOACTIVITY.

The preliminary experiments where conditioned medium (CM) from various cell lines was assessed for bioactivity in the 3D collagen gel fibroblast migration assay, revealed that endothelial cells exhibiting the cobblestone phenotype expressed a factor that had the ability to inhibit rhMSF. That is, endothelial cobblestone CM impeded rhMSF from stimulating fibroblast migration. A similar ability to inhibit rhMSF was detected in HaCaT keratinocyte CM and after a purification process NGAL was subsequently identified as the protein responsible. Immunolocalisation and immunoblot experiments disclosed that endothelial cells, *in vitro*, do not express NGAL and therefore it cannot be accountable for the endothelial MSF- inhibitory bioactivity. Consequently, the next stage was to characterise the endothelial MSF inhibitory bioactivity.

As described previously, for the characterisation of endogenous endothelial motogenic bioactivity, the endothelial CM underwent a process of fractionation by two methods; size exclusion chromatography and SDS PAGE. Then, in order to determine the presence of endothelial MSF-inhibitory activity the fractionated CM was again tested in the 3D collagen gel fibroblast migration assay but this time in the presence of 100pg/ml rhMSF. Both cobblestone and sprouting fractionated ENDO 742 CM were tested, plus the Blank gel CM was included as a control.

Two means of analysis were employed to determine whether MSF inhibition had occurred. Firstly, the criteria set for MSF inhibition was the ability to limit fibroblast migration by at least 50% upon addition of 100pg/ml rhMSF, as compared to the rhMSF baseline. Secondly, since motogenic activity had been identified in both sprouting and cobblestone fractionated CM, this activity was taken into account during analysis of the results in order to reduce any masking effect of MSF-inhibitory activity present by the endogenous motogenic bioactivity. Therefore, baseline migration was set for each individual fraction group (or elution) when tested alone in the assay and MSF inhibition was determined by a failure of migration to increase by 50% upon addition of 100pg/ml rhMSF. In addition, since an endothelial expressed MSF had been attributed for at least a portion of this endogenous motogenic activity then the nature of MSF motogenic activity, which displays a bell-shaped dose-response, needed to be reflected in the interpretation of the results. That is, to define the MSF-inhibitory activity as either genuine or simply due to the accumulative effect of the endogenous MSF and additional

rhMSF causing the overall MSF concentration to shift to the level where upon it has an inhibitory effect.

7.6i The MSF-Inhibitory Activity of Size- Exclusion Fractionated ENDO 742 Conditioned Medium.

The pooled SEC fraction groups 11 to 23 which had been previously generated for the characterisation of motogenic activity (Chapter 7.5i) and corresponding to a molecular weight range of approximately >70kDa to 20kDa, were selected for analysis. Each group was tested in the 3D collagen gel fibroblast migration assay, at a final dilution of 1/20 in the presence of 100pg/ml rhMSF and the level of fibroblast migration was assessed. Normally, the addition of 100pg/ml rhMSF should result in a minimal two fold increase in fibroblast migration. The fibroblast migration measured in presence of the SEC fraction groups was therefore labelled as MSF-inhibitory when migration was restricted by at least 50% upon addition of 100pg/ml rhMSF, as compared to the rhMSF baseline.

As expected the control CM, from a Blank gel, displayed no ability to inhibit rhMSF bioactivity. The average migration level for all the fraction groups was 96.1 +/- 9.40% as compared to the 100pg/ml rhMSF only baseline migration of 100 +/- 14.13%. (Figure 7.10b).

The fractionated Cobblestone CM had the greatest number of fraction groups which meet the criteria for MSF-inhibitory activity; groups 16, 17, 21 and 22. Maximal inhibition could be categorised as either having a molecular weight (MW) of approximately 70kDa, groups 16 and 17, or a MW of <25kDa, groups 21 and 22. Compared to the MSF baseline (100% migration) groups 16 and 17 reduced rhMSF stimulated fibroblast migration by 49.4 +/- 7.44% and 60.5 +/- 8.26% respectively; an average of 54.95 +/- 7.85%. Migration was reduced by the lower MW fraction groups 21 and 22 by 63.9 +/- 0.00% and 59.8 +/- 10.83% respectively; an average of 61.85 +/- 2.90%. (Figure 7.10c).

When the un-fractionated Sprout CM was analysed the only bioactivity observed was motogenic; that is when tested alone the CM stimulated fibroblast migration. However, upon fractionation the Sprout CM also exhibited MSF-inhibitory activity; fraction groups 19, 20 and 23 all met the set criteria. Akin to the Cobblestone fractionated CM, maximal activity was found in the lower MW fraction groups of 25kDa and less. Fraction groups 19, 20 and 23 reduced rhMSF stimulated migration by 56.3 +/- 0.00%,

64.9 +/- 6.62% and 57.6 +/- 2.48% respectively. (Figure 7.10d). It was noted that although the Cobblestone CM MSF-inhibitory activity was present in a larger range of fraction groups compared to the Sprouting CM, the actual level of inhibition achieved was similar.

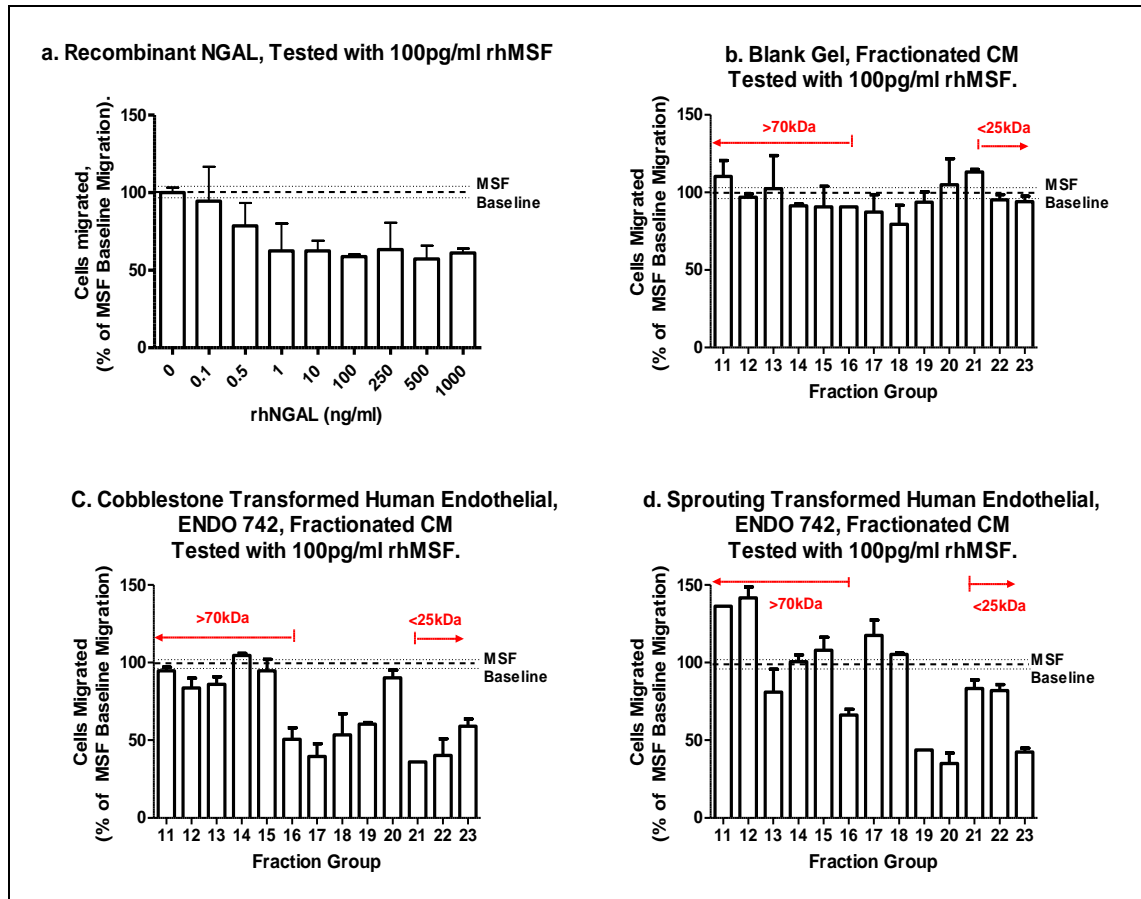


Figure 7.10 : The MSF-inhibitory activity of Superdex 75 fractionated conditioned medium from ENDO 742 cells. Comparison with rhNGAL. Conditioned medium (CM) was collected from ENDO 742 cells grown either on or within a collagen gel matrix; thereby displaying either a cobblestone or sprouting phenotype respectively. As a control conditioned medium was also collected from a blank collagen gels (no cells). The Superdex 75 fractionated conditioned medium, fraction groups 11-23, was tested in the 3D collagen gel fibroblast migration assay with 100pg/ml rhMSF. The number of cells migrated is expressed as a percentage of the 100pg/ml rhMSF control baseline migration i.e. MSF Baseline = 100 +/- 4.10%, as represented by hatched and dotted lines (mean and SD respectively). This was equivalent to 7.8 +/- 0.32 migrated cells. Dose response to rhNGAL, a known MSF-inhibitor, is shown for comparison. The results represent an average of two experiments.

7.6ii The Motogenic Activity of Recombinant MSF in the Presence of ENDO 742 Size- Exclusion Fractionated Conditioned Medium.

The motogenic activity of the fractionated Cobblestone and Sprout CM was detected in the higher MW fraction groups. Subsequent analysis with known MSF inhibitors, NGAL and PEPQ 1.1 antibody, partly attributed this motogenic bioactivity to an endothelial expressed MSF. Therefore this method of analysis enabled the existence of the endogenous motogenic activity present in the endothelial CM, which may mask the effect of any MSF-inhibitors also present, to be taken into account. The baseline was set for each individual fraction group when it was tested alone in the assay and the inhibition of rhMSF was determined by a failure of migration to increase by 50% upon addition of 100pg/ml rhMSF.

When tested alone the fraction groups of the control, Blank gel fractionated CM, displayed no motogenic activity and subsequently when tested with the addition of 100pg/ml rhMSF no MSF-inhibitory was detected either. On average, the addition of 100pg/ml rhMSF increased migration by 2.6 +/-0.31 fold (Figure 7.11a).

Compared to the baseline level of migration for each of the Cobblestone CM fraction groups rhMSF appeared to be inhibited by the majority of fraction groups; 11-17, 19, 21, 22 and 24 all displayed MSF-inhibitory activity (Figure 7.11b). A similar situation occurred for the Sprout CM; 12-16, 19, 20, 23 fraction groups all inhibited rhMSF stimulated migration (Figure 7.11c). However, since these higher MW fraction groups (Cobblestone CM groups 11-14 and Sprout CM groups 11-15) have been shown to contain MSF then the MSF-inhibitory displayed could potentially be due to the accumulation effect of endogenous MSF and additional rhMSF causing a shift to MSF concentrations that cause inhibition of fibroblast migration instead of stimulation. The lower MW (25kDa and lower) fraction groups had shown no endogenous motogenic activity and were therefore considered to contain a genuine inhibitor(s) of MSF.

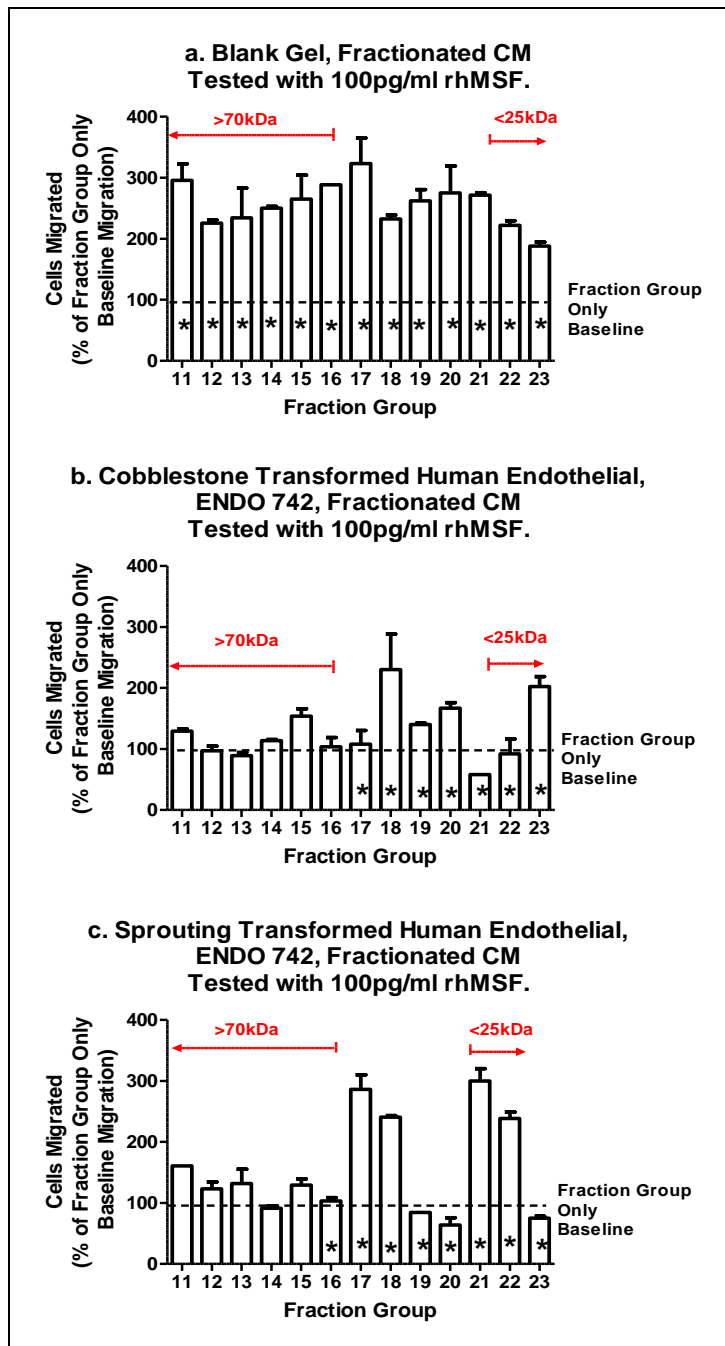


Figure 7.11. The motogenic activity of exogenous rhMSF in the presence of Superdex 75 fractionated ENDO 742 conditioned medium. Conditioned medium (CM) was collected from ENDO 742 cells grown either on or within a collagen gel matrix; thereby displaying either a cobblestone or sprouting phenotype respectively. As a control, conditioned medium was also collected from a blank collagen gels (no cells). The Superdex 75 fractionated conditioned medium, fraction groups 11-23, was tested in the 3D collagen gel fibroblast migration assay (final dilution 1/20), with and without the presence of 100pg/ml rhMSF. The number of cells migrated is expressed as a percentage of each individual fraction group only baseline migration i.e. Fraction group 11 = 100%, as represented by the hatched line. Fraction groups which lacked motogenic activity when previously tested alone are identified by a star (*). The results represent an average of two experiments.

7.6iii The MSF- Inhibitory Activity of SDS PAGE Fractionated ENDO 742 Conditioned Medium

The protein elutions of SDS PAGE fractionated ENDO 742 CM previously tested for motogenic activity were also analysed for the presence MSF-inhibitory activity. The protein elutions (1-12) of SDS PAGE fractionated cobblestone and sprout ENDO 742 CM plus the control CM (collected from a blank gel) were tested at a final dilution of 1/1000 in the 3D collagen gel fibroblast migration assay with the addition of 100pg/ml rhMSF. The level of migration achieved was analysed by the same techniques as described for the SEC fractionated CM. Firstly, the level of migration attained for each elution when in the presence of 100pg/ml rhMSF was compared to the rhMSF baseline level. An elution was considered to be displaying MSF- inhibitory activity if migration was restricted by at least 50% upon addition of 100pg/ml rhMSF, as compared to the rhMSF baseline.

No MSF inhibitory activity was detected in any of the protein elutions of the control CM. The average migration of the elutions 1-12 was 93.0 +/- 6.80%, whilst the rhMSF baseline migration was 100+/- 9.08%. These results were analogous to the results gained from the SEC fractionated control CM.

Although not reaching the set criteria of a 50% reduction in rhMSF stimulated migration, two elutions of cobblestone CM did show a distinct MSF-inhibitory activity. Elution 3 (MW approximately 75kDa) and Elution 8 (MW approximately 20kDa) were able to reduce rhMSF stimulated migration by 49.05 +/- 8.93% and 46.5 +/- 1.77%, respectively. It should be noted that Elution 3 had previously displayed motogenic activity when tested alone in the assay. Elutions 6 and 9 (MW 25kDa and less) also displayed an ability to inhibit rhMSF activity but level was far below the set criteria; 39.2 +/-10.44% and 33.05 +/-10.10% reduction in migration, respectively.

As seen with the SEC fractionated CM, the MSF-inhibitory activity of the sprout CM elutions could be classified as having either a high or low molecular weight. Of the higher MW protein elutions, the maximum reduction in migration was achieved by elution 4 (50-75kDa); rhMSF motogenic activity was restricted by 70.5 +/- 3.75%. Meanwhile elution 5 (25-50kDa) limited migration by 54.2 +/- 11.07%. The lower MW elutions (<20kDa) 8 and 10 displayed an ability to reduce MSF bioactivity by 49.8 +/- 5.98% and 56.0 +/- 8.57% respectively. Borderline MSF-inhibitory activity was noted in elutions 2 and 11.

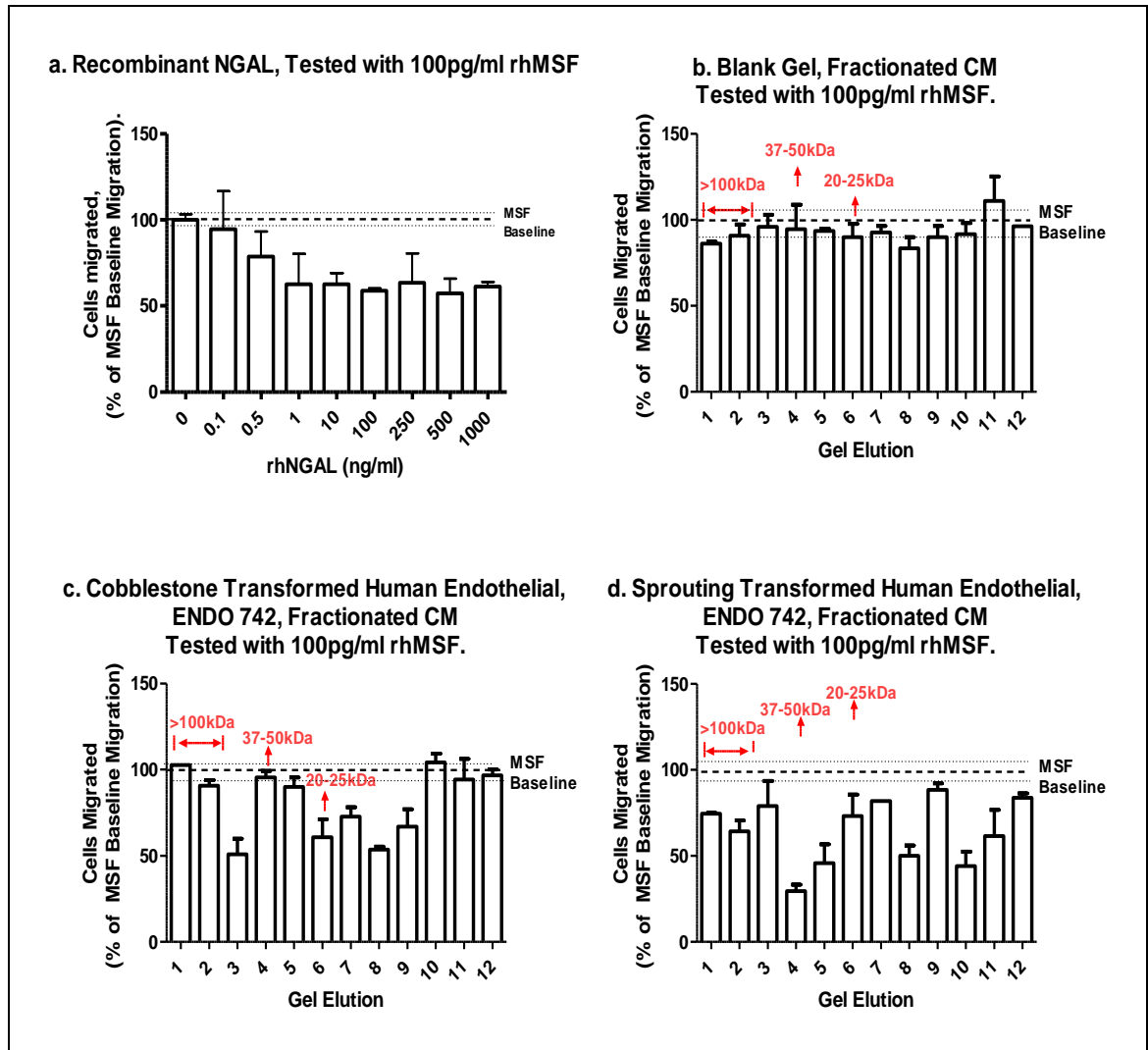


Figure 7.12: The MSF-inhibitory activity of gel elutions from the SDS PAGE fractionation of ENDO 742 conditioned medium. Comparison with rhNGAL.

Conditioned medium (CM) was collected from ENDO 742 cells grown either on or within a collagen gel matrix; thereby displaying either a cobblestone or sprouting phenotype respectively. As a control conditioned medium was also collected from a blank collagen gels (no cells). After SDS PAGE of the CM and segmentation of the gel, the protein eluted from each segment (1-12) was tested in the 3D collagen gel fibroblast migration assay in the presence of 100pg/ml rhMSF. The number of cells migrated is expressed as a percentage of the 100pg/ml rhMSF control baseline migration i.e. MSF Baseline = 100 +/- 9.08%, as represented by hatched and dotted lines (mean and SD respectively). This was equivalent to 10.9 +/- 0.99 migrated cells. Dose response to rhNGAL, a known MSF-inhibitor, is shown for comparison. The results represent an average of two experiments.

7.6 iv The Motogenic Activity of Recombinant MSF in the Presence of ENDO 742 SDS PAGE Fractionated Conditioned Medium

The second method of data analysis enabled the presence of endogenous motogenic activity within the protein elutions of the fractionated CM to be taken into account. As discussed previously, the protein elutions of fractionated control CM from a blank gel (no cells) showed no motogenic activity. Compared to the baseline level of migration achieved for each elution the addition of 100pg/ml rhMSF increased migration by a minimum of 51.9 +/- 6.32% (elution 7) and a maximum of 90.6 +/-14.87% (elution 8). For all the elutions migration was on average increased by 63.0 +/- 13.14% with addition of rhMSF (Figure 7.13a).

For the cobblestone CM, by comparison to the 'elution only' baseline migration the addition of 100pg/ml rhMSF failed to increase migration by at least 50% in a total of 8 elutions (2, 3, 4, 6, 7, 8, 9 and 12). Elutions 3 and 4 had previously shown a distinct motogenic activity; when pooled together migration was stimulated by factor of 1.7 compared to the SF MEM baseline. In addition this stimulatory activity could be markedly inhibited by MSF inhibitors NGAL and PEPQ 1.1 antibody, thereby prompting the supposition that an endothelial MSF was present in these elutions. Therefore the inhibition of migration seen with the addition of exogenous rhMSF was probably an effect of the nature of the MSF bell-shaped dose-response bioactivity. However, the other elutions had not shown any motogenic activity when tested alone so the inhibitory activity was considered to be due to the presence of an MSF-inhibitor(s). Of these, protein elutions 6 and 8 (MW 20-25kDa) showed maximal inhibitory activity (Figure 7.13b).

The sprout CM also had a number of elutions which prevented the level of migration increasing by 50% upon addition of 100pg/ml rhMSF (2, 3, 4, 5, 8, 10 and 11). Motogenic activity, presumed to be endothelial MSF had been previously detected in elutions 2 and 3. However, none of the other elutions had displayed the ability to meet the criteria for the presence of motogenic activity; the ability to increase migration by at least 50% compared to the SF MEM baseline. As described before, the MSF inhibitory activity could be categorised by the elutions having a high or low MW; elutions 4 and 5 have a molecular weight of 50-25kDa and elutions 8, 10 and 11 have a MW of 20kDa and less (Figure 7.13c). The maximal level of rhMSF inhibition achieved was by elution 4. The effect of the rhMSF upon elution 9 should also be noted; compared to when elution 9 was tested alone migration increased by 2.75 fold upon addition of 100pg/ml

rhMSF. This increase in migration was far greater than the rhMSF control, which had increased migration by 1.9 fold compared to the SF MEM baseline.

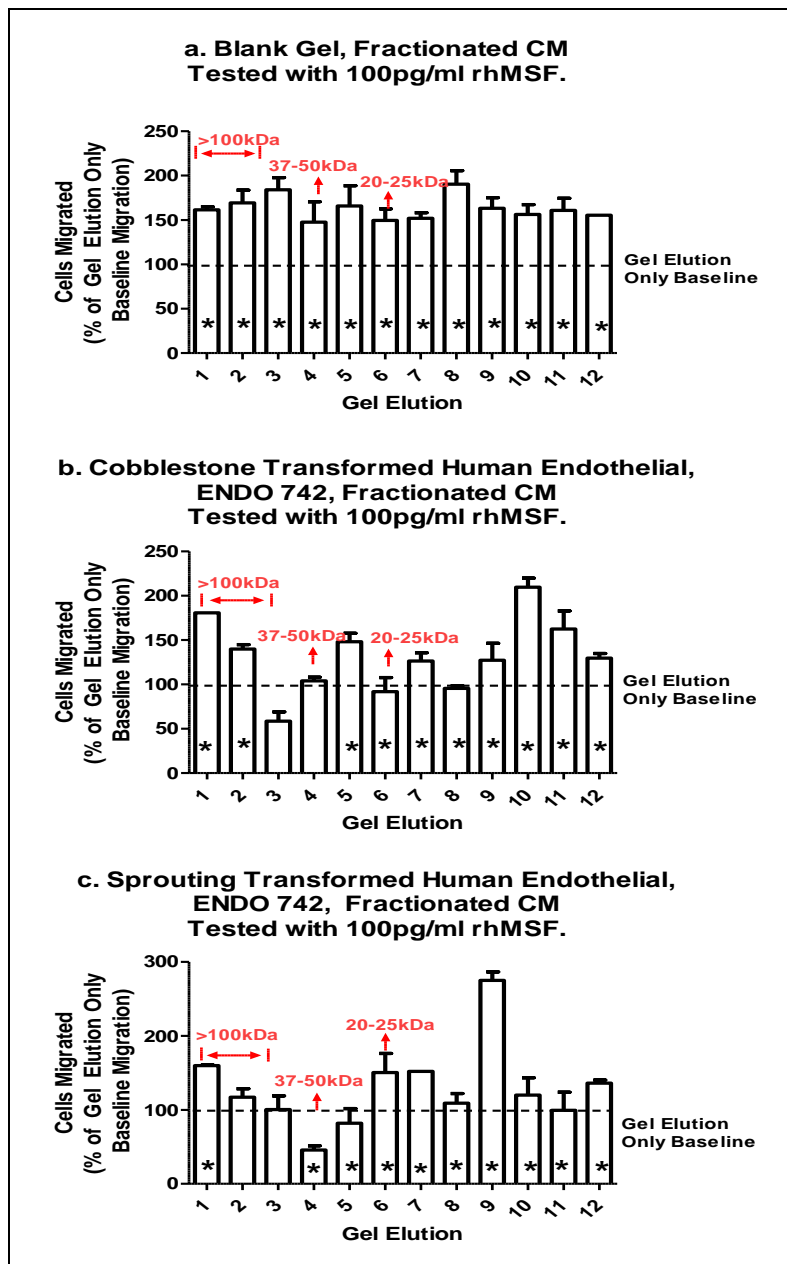


Figure 7.13: The motogenic activity of exogenous rhMSF in the presence of gel elutions from the SDS PAGE fractionation of ENDO 742 conditioned medium.

Conditioned medium (CM) was collected from ENDO 742 cells grown either on or within a collagen gel matrix; thereby displaying either a cobblestone or sprouting phenotype respectively. As a control, conditioned medium was also collected from a blank collagen gels (no cells). After SDS PAGE of the CM and segmentation of the gel, the protein eluted from each segment (1-12) was tested in the 3D collagen gel fibroblast migration assay in the presence of 100pg/ml rhMSF. The number of cells migrated is expressed as a percentage of each individual gel elution only baseline migration i.e. gel elution 1 = 100%, as represented by hatched line. Elutions which lacked motogenic activity when previously tested alone are identified by a star (*). The results represent an average of two experiments.

7.7 **THE EFFECT OF MSF ON ENDOTHELIAL MORPHOLOGY.**

As discussed previously, MSF has been shown to induce angiogenesis in both *in vivo* and *in vitro* models. *In vivo* examples include the stimulation of angiogenesis when MSF was applied to chicken yolk-sac membranes and when included in subcutaneous implants placed in rat and pig models (Schor 2010, unpublished data). *In vitro* angiogenesis assays have also shown that the addition of MSF to a monolayer of resting cobblestone endothelial cells causes a dramatic induction of the endothelial cells to exhibit the sprouting phenotype; sprouts which progressively form an interconnected sprout network.

Endothelial cells plated on a 2D surface (plastic, gelatin, collagen) typically form a cobblestone monolayer which is stable under serum free conditions. Sprouting is only induced either by culture in high serum concentrations or by the addition of specific angiogenic factors (for example MSF, FGF, VEGF). However, endothelial cells spontaneously form sprouts when plated within a 3D type I collagen gel suggesting that the cells must produce an endogenous angiogenic factor(s). Analysis of un-fractionated endothelial conditioned medium has indeed shown that an endogenous motogenic activity is present in the sprouting endothelial CM but is absent from cobblestone endothelial CM. Plus, the addition of MSF-inhibitors reduced this motogenic activity thereby implying the expression of an endothelial MSF.

In order to determine whether endothelial morphology can be altered by MSF a series of sprouting assays were performed. Aims were firstly, to corroborate the reported findings and secondly to investigate what effect known MSF-inhibitors, PEPQ 1.1 antibody and NGAL, have on endothelial morphology; specifically to determine whether MSF is accountable for the spontaneously sprouting morphology of endothelial cells plated in a 3D matrix.

7.7i **The Induction of Endothelial Sprouting Phenotype by rhMSF.**

A variety of *in vitro* angiogenesis assays were performed to show the effect rhMSF has on endothelial morphology. The common denominator was that the endothelial cells were plated onto a 2D surface and cultured in high serum conditions (15% DCS) until they achieved confluence, forming a cobblestone monolayer. Conditions were then changed to low serum with and without the addition of rhMSF; range tested 0.1-100ng/ml. All test variables were performed in either duplicate or triplicate. The

cultures were then observed microscopically over the subsequent days to determine any changes in endothelial morphology.

Differences between assays included the 2D plating surface, the serum concentration of the test conditions and the method adopted to determine the level of sprouting activity.

The 2D surfaces tested, included the untreated plastic surfaces of cell cultures dishes and the same dishes coated with either 0.1% (w/v) gelatin or native type I collagen. The serum concentration of the test conditions ranged from zero to a maximum of 5% DCS.

Whilst the degree of sprouting activity was determined by observations over an incubation period ranging from one to five days by either simply determining whether sprouts were present, counting the number of sprouts present whether as single cells or in groups/ associations or by performing a 40 point count. Irrespective of the method used, data was collected from ten fields of view per dish.

Of the various experiments performed, the data collected led to the same conclusion and verified previous findings that rhMSF stimulated cobblestone endothelial cells to exhibit a sprouting morphology (Figure 7.14). Dissimilarity to the control cultures was seen within 24 hours of incubation with MSF and the effect was identical irrespective of the 2D plating surface.

The angiogenic effect of MSF was shown to increase with increasing concentration. In comparison to the control cultures, 0.1-1ng/ml rhMSF displayed no effect. 10ng/ml rhMSF was the minimal rhMSF concentration that could induce the sprouting phenotype. The maximum concentration of rhMSF tested, 100ng/ml, on average increased the number of sprouts present by at least three fold. Two representative experiments are shown in Tables 7.1 and 7.2. In addition, to showing the angiogenic effect of rhMSF, the results also reveal that rhMSF appears to stimulate the sprouts to gather together to form groups/ associations which eventually establish an interconnecting sprout network over the entire surface of the dish.

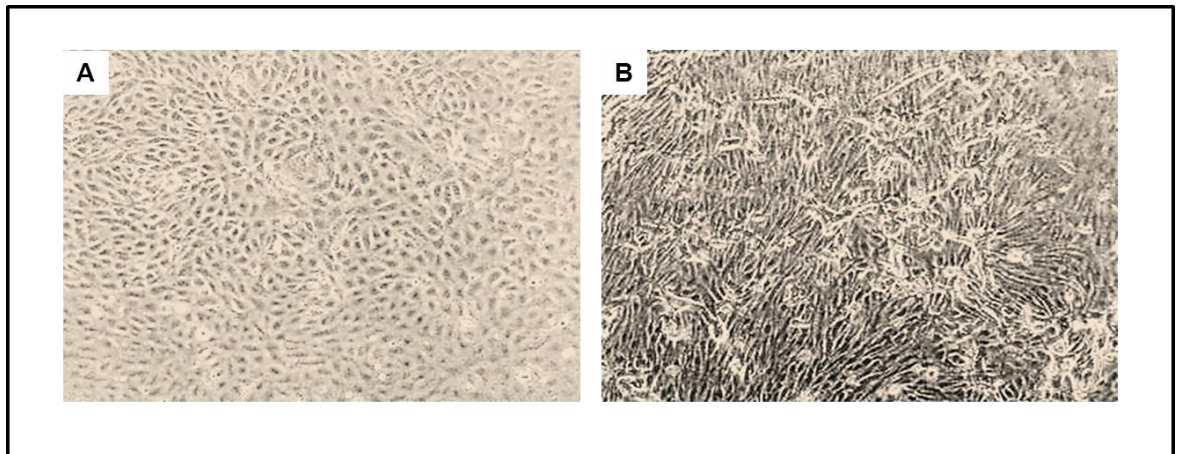


Figure 7.14: The effect of MSF on endothelial morphology. Bovine aortic endothelial cells (BAEC) were plated on to a 2D surface of 0.1% (w/v) gelatin coated plastic cell culture 35mm dish and cultured in the presence of 15% DCS MEM until confluence was achieved and a cobblestone monolayer was formed (A). Conditions were then changed to 1%DCS with addition of 100ng/ml rhMSF. After a three day incubation the endothelial cells had been induced to change morphology, to the sprouting phenotype, forming a network underneath the cobblestone monolayer (B). Observations made at 10x magnification.

Variable	Average number of Sprouts per Field (Aver/Stdev)	% of Fields Containing (Aver/Stdev)			
		No Sprouts	Single Sprouts	Sprouts Associations 2-3cells	Sprout Associations 3+ cells
5% DCS MEM	1.6 +/- 0.17	36.25 +/- 9.57	48.75 +/- 19.45	15.0 +/- 9.57	-
0.1ng/ml rhMSF	1.625 +/- 0.11	30.0 +/- 14.14	50.0 +/- 14.14	15.0 +/- 7.07	5.0 +/- 1.15
1ng/ml rhMSF	1.42 +/- 0.16	16.7 +/- 7.07	60.2 +/- 5.13	18.3 +/- 7.64	4.8 +/- 7.07
10ng/ml rhMSF	3.4 +/- 0.70	12.8 +/- 12.51	47.2 +/- 16.07	27.7 +/- 2.51	12.3 +/- 2.52
100ng/ml rhMSF	4.6 +/- 0.20	8.7 +/- 2.89	35.0 +/- 3.61	28.0 +/- 5.29	28.3 +/- 7.51

Table 7.1: The effects of rhMSF on endothelial morphology. Bovine aortic endothelial cells (BAEC) cultured on a 2D surface of 0.1% (w/v) gelatin coated plastic cell culture 35mm dishes, in the presence of 15% DCS MEM were grown to confluence and displayed a typical cobblestone morphology. The conditions were then changed to 5% DCS MEM with and without the addition of rhMSF (0.1- 100ng/ml); each variable tested in triplicate. Changes in the endothelial morphology were observed, especially the emergence of sprouting endothelial cells. After three days in the test conditions the following observations were noted in ten separate fields of view per dish- the number of fields with exhibiting sprouting endothelial cells, if present the total number of sprouts and whether these sprouts were present as either single or integrated to form groups of sprouts of either 2-3 cells and 3+ cells (termed sprout associations). The data shown is an average of three experiments.

<u>Variable</u>	<u>DAY ONE</u>			<u>DAY THREE</u>		
	ALL AREAS		AREAS OF HIGH SPROUTING DENSITY	ALL AREAS		AREAS OF HIGH SPROUTING DENSITY
	No. of Fields with Sprouts Present	Average Point Count	Average Point Count	No. of Fields with Sprouts Present	Average Point Count	Average Point Count
2.5% DCS	6/30	0.4 +/- 0.83	5.0 +/- 2.0	18/30	1.1 +/- 1.10	1.7 +/- 0.58
1ng/ml rhMSF	6/30	0.3 +/-0.68	3.0 +/- 1.0	15/30	0.4 +/- 0.70	4.0 +/- 1.52
10ng/ml rhMSF	18/30	0.9 +/- 1.29	6.3 +/- 0.58	30/30	3.4 +/- 2.32	9.3 +/- 1.16
100ng/ml rhMSF	27/30	2.8 +/- 0.99	15.7 +/- 3.06	30/30	15.7 +/- 6.18	22.3 +/- 1.53

Table 7.2: The effects of rhMSF on endothelial morphology. Bovine aortic endothelial cells (BAEC) cultured on a 2D surface of native collagen coated plastic cell culture 35mm dishes, in the presence of 15% DCS MEM were grown to confluence and displayed a typical cobblestone morphology. Conditions were then changed to 2.5% DCS MEM with and without the addition of rhMSF (1- 100ng/ml); each variable tested in triplicate. Observations were made after one and three day exposure to the test conditions. In ten random fields of view per dish the presence of sprouts was noted followed by a 40 point count (the number of points were sprouts present). In addition, where possible, a 40 point count was performed in the areas where sprouts were present in the highest density. The data shown is a representative example of the three experiments performed

7.7ii The Effect of MSF Inhibitor, PEPQ 1.1 Antibody, on Spontaneous Endothelial Sprouts

In order to achieve a homologous spontaneous sprouting phenotype, bovine aortic endothelial cells (BAEC) were cultured within a 0.5ml type I collagen gel (plating density 6.5×10^5 per ml). The gels were plated into 24 well tissue culture plates to set and then over-laid with 0.5ml 20% DCS. After a three day incubation, only the healthy cultures displaying a typical sprout morphology, with single sprouts and small associations present, were selected. The media was then changed to 1% DCS MEM with and without the addition of the PEPQ 1.1 antibody. The antibody was tested at the range 10-30 μ g/ml. To rule out a potential dilution effect of the final serum concentration by the addition of the antibody, a series of controls were included, whereby for each antibody concentration the equivalent volume of serum free MEM was added instead. Each control and test overlay was performed in triplicate. Analysis of the effect of PEPQ 1.1 antibody consisted of performing a 40 point count in ten fields per gel after a 24 hour and 48 hour incubation period. The total number of sprouts counted was then calculated for each variable.

Three experiments were performed with similar results. Initially, when the total number of sprouts counted after a 24 and 48 hour incubation were compared, it appeared that the number of sprouts was decreasing in 1% DCS MEM control. However, the counts were not reflecting the true situation within the gel. Although the number of individual sprouts did decrease, the reason was not due to the loss of sprouts but due to the formation of sprout associations. Owing to the density and complexity of these associations, which eventually form a whole network of interconnecting sprouts within the gel, it was incredibly difficult to count the number of individual sprouts present. This however, did not explain the dramatic decrease in the number of sprouts counted in the wells exposed to the PEPQ 1.1 antibody. The effects of PEPQ 1.1 antibody increased with increasing concentration, with sprouting cells practically annihilated on addition of 30 μ g/ml. A 24 hour exposure to 30 μ g/ml resulted in an average 67.9 +/- 19.31% reduction in the number of sprouts as compared to the 1%DCS MEM control. By 48 hours the vast majority of endothelial sprouts were dead; only 2.1 +/- 1.80% remained (as compared to control). Whilst 24 and 48 hour incubation with 20 μ g/ml PEPQ 1.1 caused 42.6 +/-23.99% and 80.5 +/- 5.99% reductions in sprouts, respectively, as compared to the control. The lowest PEPQ 1.1 antibody concentration tested, 10 μ g/ml, displayed the greatest similarity to the 1% DCS MEM control. (Figure

7.15, Table 7.3). Any dilution effect on final serum concentration due to the antibody volume was dismissed as the addition of the equivalent volume of SF MEM showed no adverse effect on sprout numbers; comparable to the 1% DCS MEM control. The results therefore show that MSF must be expressed by the spontaneous sprouts. Plus, as well as influencing endothelial morphology, MSF must also act as an endothelial survival factor since neutralisation of MSF compromises the viability of sprouts. However, the role of MSF as a survival factor appears to be specific to endothelial sprouts, as previously reported results on the effect of MSF neutralising antibodies on a mixed population of sprouting and cobblestone endothelial cells showed that apoptotic death was only induced in sprouting cells whilst the co-cultured cobblestone cells was unaffected (Schor 2010, Schor *et al.*, 2003).

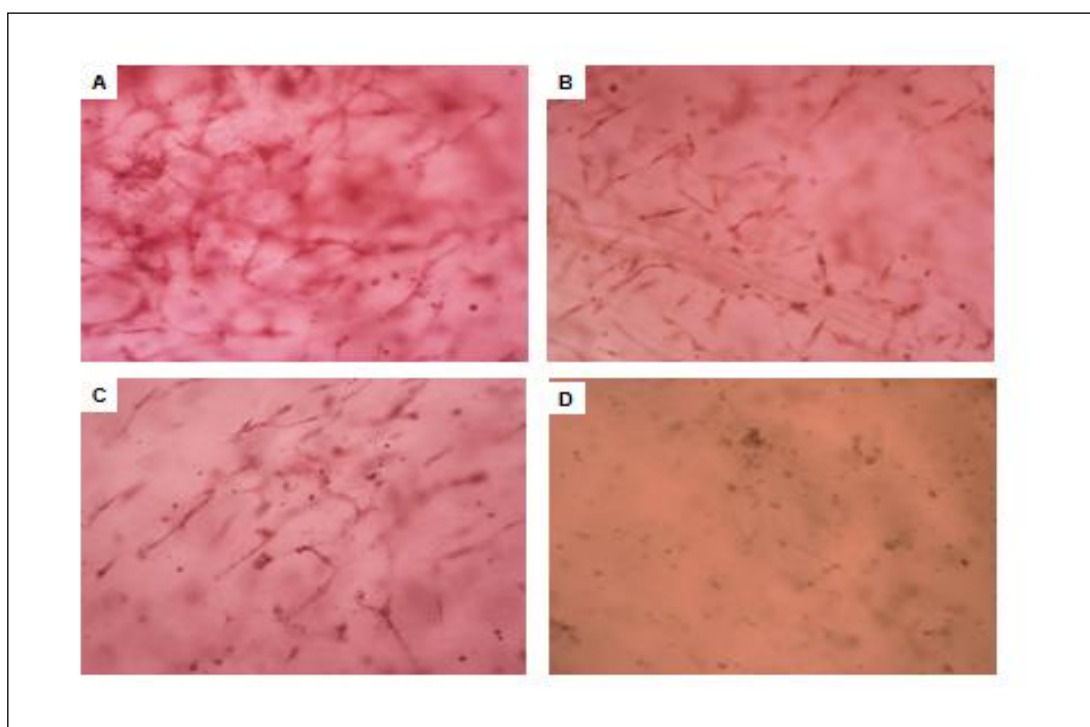


Figure 7.15. The effect of MSF-Inhibitor PEPQ1.1 antibody on endothelial cells exhibiting the spontaneous sprouting phenotype. Endothelial cells (BAEC) were plated within a 0.5ml type I collagen gel at a plating density of 6.5×10^5 per ml. After a three day incubation in the presence of 20% DCS MEM the endothelial cells spontaneously formed sprouts within the gel. Conditions were then changed to the 1% DCS MEM with and without the addition of PEPQ 1.1 antibody (10-30 μ g/ml).The images display the effect seen on the endothelial sprouts after a 48hour incubation with either:

A. 1% DCS MEM

B. 10 μ g/ml PEPQ 1.1 Antibody

C. 20 μ g/ml PEPQ 1.1 Antibody

D. 30 μ g/ml PEPQ 1.1 Antibody

Images were taken at 10x magnification.

Variable	Average Number of Sprouts	
	Post 24hr	Post 48hr
CONTROLS:		
1. 1% DCS MEM	124.5 +/- 19.62	118.0 +/- 15.03
2. SF MEM equivalent to 10µg/ml PEPQ 1.1	133.5 +/- 13.43	122 +/- 15.56
3. SF MEM equivalent to 20µg/ml PEPQ 1.1	143.0 +/- 12.73	117.0 +/- 14.14
4. SF MEM equivalent to 30µg/ml PEPQ 1.1	142.5 +/- 14.85	115.5 +/- 17.68
PEPQ 1.1 Antibody:		
1. 10µg/ml	134.0 +/-22.63	81.5 +/- 10.61
2. 20µg/ml	71.5 +/-28.99	23.0 +/- 7.07
3. 30µg/ml	40.0 +/-24.04	2.5 +/-2.12

Table 7.3: The effect of MSF inhibitor PEPQ1.1 on the number of spontaneous endothelial sprouts present in a Type I collagen gel. Endothelial cells (BAEC) were plated within a 0.5ml type I collagen gel at a plating density of 6.5×10^5 . After a three day incubation in the presence of 20% DCS MEM the endothelial cells spontaneously formed sprouts within the gel. Conditions were then changed to the 1% DCS MEM with and without the addition of PEPQ 1.1 antibody (10-30µg/ml) or the equivalent volume of serum free MEM. Each variable was tested in duplicate. A 40 point count was performed in 10 fields per variable and the total number of sprouts was calculated. The results shown are an average of two experiments.

7.7iii The Effect of MSF Inhibitor, NGAL, on Spontaneous Endothelial Sprouts

The spontaneous sprouting experiments performed to investigate the effect of MSF-inhibitor PEPQ 1.1 antibody were repeated in order to determine the effect of the other known MSF inhibitor, NGAL. Three different sources of NGAL were tested; NGAL isolated from a MMP-9/ NGAL complex isolated from activated neutrophils (complex purchased from Calbiochem), free NGAL purified from the complex by SDS PAGE separation followed by gel elution (Chapter 4, Results), eukaryotic rhNGAL

(purchased from R&D Systems, 1757-LC) and prokaryotic rhNGAL (in-house preparation).

Preliminary experiments were performed using the NGAL purified from MMP-9/NGAL complex at a range of dilutions (1/100,000 to 1/5000) equivalent to an estimated NGAL concentration range of 1- 40ng/ml (15%DCS MEM diluent). Over a 3 day observation period no obvious differences to the 15% DCS MEM only control was noted. However on day 4, in 2/3 experiments, a transient effect was seen with a minority of sprouts developing vacuoles but by day 5 they had recovered and were akin to the controls.

The prokaryotic NGAL was tested at a concentration range of 1ng/ml-1 μ g/ml. A lower serum concentration was used in order to minimise any antagonistic effect by factors present with the serum. A total of four experiments were performed, two using 1%DCS MEM and the other two with 5%DCS MEM. As seen previously with NGAL gel elution, the sprouts appeared to be unaffected by the lower concentrations 1-100ng/ml of prokaryotic NGAL; typically displaying healthy sprouts which formed associations of 10+ cells by day 6. However, adverse effects of 500ng/ml and 1 μ g/ml NGAL were initially noted on day 2 (Figure 7.16). Compared to the controls the sprouts were less numerous, of poor quality and smaller; there was also an increase the amount of debris present. By day 5 this had progressed severely, with the majority of sprouts having died and those which did remain were in a poor condition with vacuoles present and surrounded by debris. The serum concentration did not appear to affect the outcome with the same results achieved at 1% and 5%DCS.

The eukaryotic NGAL was tested at a more limited range of concentrations, 100ng/ml to 1 μ g/ml and a similar effect was observed. 100ng/ml was indistinguishable from the 1% DCS MEM control. Whilst by day 2 the majority of sprouts had rounded up when exposed to 500ng/ml and 1 μ g/ml NGAL, progressing to cell death by day 3. Very few sprouts remained by day 4 and those that did were of poor quality.

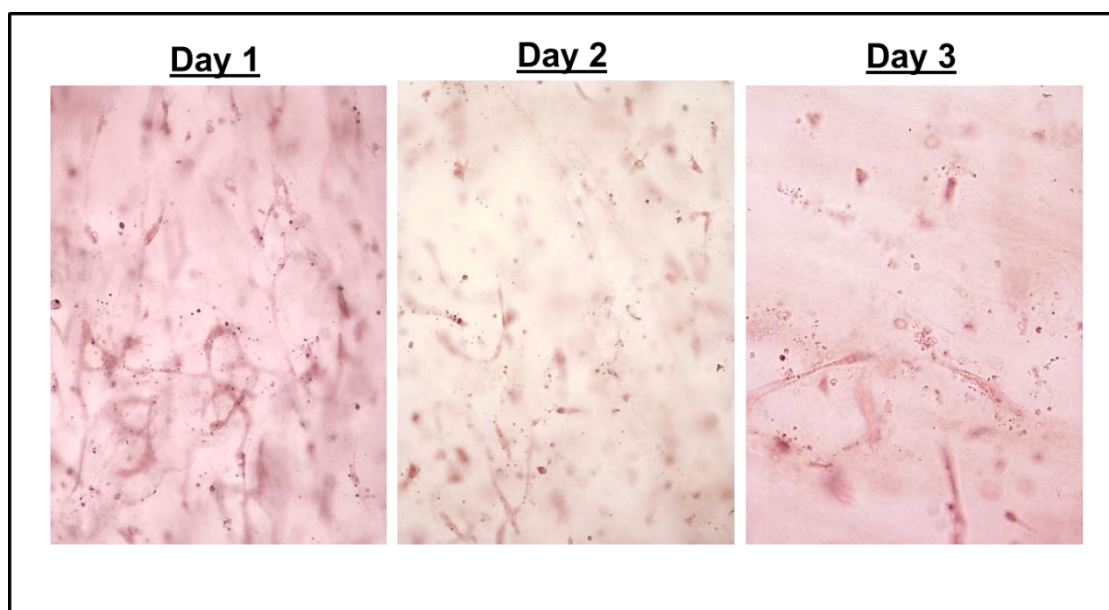


Figure 7.16: The effect of MSF-Inhibitor, NGAL on endothelial cells exhibiting the spontaneous sprouting phenotype. Endothelial cells (BAEC) were plated within a 0.5ml Type I collagen gel at a plating density of 6.5×10^5 per ml. After a three day incubation in the presence of 20% DCS MEM the endothelial cells spontaneously formed sprouts within the gel. Conditions were then changed to the 1% DCS MEM with and without the addition of 500ng/ml prokaryotic rhNGAL (in-house preparation). The images display the effect seen of incubating the endothelial sprouts with 500ng/ml prokaryotic rhNGAL over three day incubation period. Images were taken at 10x (A and B) and x20 magnification (C).

7.7iv The Effect of MSF Inhibitor, NGAL, on Post- Confluent Endothelial Sprouts

The effect of rhNGAL on spontaneous endothelial sprouts was similar to that of the PEPQ 1.1 antibody. The next stage was to determine what effect NGAL had on a mixed population of endothelial cells, expressing both the cobblestone and sprouting phenotype.

Endothelial cells (BAEC) were plated onto the 2D surface of a 0.5ml type I collagen gel in the presence of 15%DCS MEM. Once a confluent cobblestone monolayer had formed across the entire surface of the gel (typically after a 3 day incubation period) the overlays were changed to the test conditions. In order to induce sprouting, a high serum dilution of 15%DCS was used. Initially experiments were performed with NGAL isolated from a MMP-9/ NGAL complex isolated from activated neutrophils (NGAL gel elution) and repeated with prokaryotic rhNGAL. Observations were made regarding the

health and appearance of the cobblestone monolayer, the development of sprouts and the migration of sprouts into the underlying collagen gel.

Four separate experiments were performed using the NGAL gel elution, tested (in triplicate) at a dilution range of 1/100,000 to 1/500, equivalent to approximately 1-400ng/ml. In the controls, 15%DCS MEM only, sprouting was not observed until around day 2-3. By day 5 single sprouts had formed small associations of 5+ cells beneath the cobblestone monolayer and a few had started to migrate into the collagen gel. By day 8 sprouting networks had formed over the surface of the gel and within the gel the numerous single sprouts had started to form associations. Meanwhile, throughout the incubation period, the cobblestone monolayer kept intact and healthy. In the higher dilutions of the NGAL gel elution tested, 1/100,000 to 1/20,000 (est.1-10ng/ml), cultures were indistinguishable from the controls. The mid-range dilutions 1/10,000 to 1/500 (est.10-40ng/ml) showed slightly reduced sprouting activity compared to the controls; with surface sprouting activity confined until day 4 and sprouts only appearing in the gel by day 7-8. Eventually a sprouting network did form underneath the cobblestone by day 9-10, although in the majority of cases it failed to extend across the entire gel surface.

No sprouts were observed within the collagen gels that were exposed to the highest dilutions of the NGAL gel elution, 1/1000 and 1/500 (est. 200-400ng/ml). Only a limited number of sprouts were seen on the surface by day 5, which eventually progressed to form restricted areas of sprout associations (10-15 cells). The cobblestone monolayer also appeared to be have been affected; although still intact over the gel surface the endothelial cells were less healthy and the cobblestone looked disorganised plus there was distinctly more debris than the controls.

Using the same protocol, prokaryotic rhNGAL was tested at a concentration range of 1ng/ml -1 μ g/ml (2 experiments) and similar observations to the NGAL gel elution were noted. The lower concentrations 1-100ng/ml showed no difference to the 15% DCS MEM control. No sprouts were observed in cultures exposed to the higher concentrations of 500ng and 1 μ g/ml. The higher concentrations of rhNGAL had a very apparent adverse effect on the cobblestone monolayer; vacuoles developed within the cells by day 4 and by day 5, 1 μ g/ml rhNGAL induced the complete disruption of the cobblestone monolayer with loss of typical morphology, increased cell death and debris.

7.7v The Effect of NGAL on Endothelial Proliferation and Viability.

It has been reported that when PEPQ 1.1 antibody was tested in a mixed endothelial cell population it had the selective ability to eliminate cells exhibiting the sprouting phenotype whilst appearing to leave the underlying cobblestone monolayer unaffected (Schor *et al.*, 2010). However, in a mixed culture rhNGAL displayed an adverse effect on both endothelial phenotypes, especially when tested at the higher concentrations (500ng- 1µg/ml). In order to eliminate the possibility that the effect of rhNGAL was due to toxicity, viability and proliferation assays were performed with both prokaryotic and eukaryotic rhNGAL.

The bovine endothelial cells (BAEC) were plated on a 2D surface of a 0.1% (w/v) gelatin coated 35mm plastic cell culture dish at a concentration of 1×10^5 per dish in 15% DCS and incubated overnight to allow the cells to attach. The next day a baseline count and viability was measured. Before changing to the test conditions, all dishes were washed twice with Hanks solution. Both source of rhNGAL were tested at 10ng/ml, 100ng/ml and 1µg/ml in a final serum concentration of 5% DCS. The control (5%DCS MEM only) and variables were tested in duplicate in two separate experiments. Over a 5 day period cell counts and viability were measured by the Coulter Counter Z1 Series (Beckmann Coulter) and the trypan blue assay, respectively (Chapter 2, Materials & Methods).

Both prokaryotic and eukaryotic rhNGAL affected the endothelial cells in the same manner. As expected from the sprout assay(s) observations, the lower rhNGAL concentrations of 10ng/ml and 100ng/ml had no adverse effects on endothelial cell proliferation or viability. However, 1µg/ml rhNGAL over the 5 day course of the experiment when compared to the 5%DCS control decreased endothelial proliferation on average by 20.5 +/-5.14% and 23.2 +/- 5.49%, prokaryotic and eukaryotic respectively. Yet, it had no effect on endothelial cell viability. 5% DCS MEM had an average cell viability of 94.4 +/-3.19%, whilst 1µg/ml prokaryotic and eukaryotic rhNGAL had an average cell viability of 91.6 +/- 2.76% and 90.85 +/- 3.16%, respectively.

It should be noted that the same sources of rhNGAL, at a range of concentrations 0.01- 1µg/ml, had been extensively tested on fibroblasts (FSF44) in the 3D collagen migration assay and no toxic effects were ever observed. Indeed, fibroblast viability and proliferation assays performed with prokaryotic rhNGAL, 0.01-1µg/ml, showed

rhNGAL had no effect on fibroblast morphology, viability and proliferation when compared to the control.

Table 7.4: The effect of NGAL on endothelial viability and proliferation.

Endothelial cells, BAEC, were plated at a density of 1×10^5 per 35mm dish, in the presence of 15%DCS MEM. After a 24 hour attachment period, conditions were changed to 5% DCS MEM with and without the addition of rhNGAL. Both prokaryotic and eukaryotic sources of rhNGAL were tested, in duplicate, at a range of concentrations (1ng/ml, 100ng/ml and 1 μ g/ml). Cell viability and cell counts were taken over a 1-5 day incubation period. The percentage of cell viability for each variable was measured by the trypan blue assay. The average cell count at each time point, for each variable was measured with the Coulter Counter Z1 Series (Beckmann Coulter). The results shown are an average of two experiments.

7.8 DISCUSSION

The ability to inhibit the motogenic activity of MSF has been discovered in the conditioned medium of both the keratinocyte HaCaT cell line and endothelial cell lines specifically displaying a cobblestone phenotype. Neutrophil gelatinase associated lipocalin (NGAL) has subsequently been identified as the keratinocyte expressed MSF-inhibitor. By performing immunoblot and IHC experiments, using specific anti-NGAL antibodies, it has emerged that endothelial cells *in vitro* do not express NGAL. CM from various endothelial cell lines, of both bovine and human origin, were tested in the immunoblot assays at a range of concentrations (neat to 50x concentrated) using both monoclonal and polyclonal specific anti-NGAL antibodies. Despite all the experimental variations performed no band(s) of the appropriate molecular weight for NGAL were identified. Negative results were also achieved in the immunohistochemistry experiments, irrespective of whether the cells displayed a cobblestone or sprouting morphology and regardless of the plating matrix. The conclusion was drawn that the cultured endothelial cells were not expressing NGAL, although it could be suggested that NGAL may have been present but at concentrations below the detection limits of the assays.

A literature search of the reported expression of NGAL by endothelial cells is limited and generally endothelial expression of NGAL is associated with disease states. Furthermore, an analysis of NGAL expression by endothelial cells *in vitro* has not previously been performed. Limited expression of NGAL has been identified in endothelial cells present within atherosclerotic plaques (Boekhorst *et al.*, 2011). A study of human and experimental rat heart failure, where immunostaining for NGAL was performed on the myocardium, revealed some immunoreactivity in endothelial cells; especially those endothelial cells within the microvascular at the border zone between ischaemic and non-ischaemic regions in post-myocardial infarction rats (Yndestad *et al.*, 2009, Ding *et al* 2010). Induction of NGAL expression was also reported to be associated with an inflammatory response in endothelial cells of mice, eight hours after a sublethal intra-peritoneal infection with *E.coli* H9049 (Flo *et al.*, 2004).

In actuality the discovery of an absence of NGAL expression by cultured endothelial cells may not reflect the *in vivo* situation. The isolation of endothelial cells from their natural tissue microenvironment has been reported to generate alterations in endothelial gene expression and can result in a phenotypic drift (Lacorre *et al.*, 2004). Because

endothelial cells sense and react to their environment, changes occur in their messenger RNA and protein expression when they become separated from crucial extracellular signals (Aird *et al.*, 2013). Yet, the endothelial cells analysed for NGAL expression were plated on and within various different matrices (plastic, gelatin, type I collagen) and all were consistently negative. However, the limitations of *in vitro* studies should always be considered.

In addition to CM from cobblestone endothelial cells possessing MSF-inhibitory activity, the other bioactivity detected in endothelial CM appeared to be specific to the sprouting phenotype. Endothelial cells exhibiting the sprouting phenotype were shown to possess a motogenic bioactivity which resulted in the increased migration of fibroblasts in the 3D collagen gel assay. Due to the nature of this stimulatory activity it was proposed that an endothelial MSF was responsible. Initial investigations adopting immunoblot and immunohistochemistry analysis produced conflicting results. Conditioned medium collected from a variety of endothelial lines, expressing cobblestone and/ or sprouting phenotypes, on/ within numerous different matrices when tested by immunoblot, using anti-MSF RpVSI antibody, constantly resulted in no bands being identified as MSF. Immunostaining experiments however, identified a MSF expression located within the endothelial cells specifically displaying the sprouting phenotype. The cobblestone phenotype was negative for MSF in the majority of experiments (9/12). It was suggested that the disparity in results between the immunoblot and IHC methods for the sprouting endothelial was due to MSF being present in the CM at concentrations below the sensitivity limits of the immunoblot assay, namely 25ng/ml.

In order to further characterise the motogenic activity of the endothelial sprouting CM, direction was taken from the HaCaT series study. Conditioned medium was collected from homogenous cultures of sprouting endothelial cells, ENDO 742, plated within a type I collagen gel. To provide a comparison and a relevant control, CM was also collected from cobblestone endothelial cells (plated on the surface of the collagen gels) and from a blank gel (no cells), respectively. Firstly, CM was fractionated by both size exclusion chromatography and SDS electrophoresis, and then the subsequent fractions/elutions tested for bioactivity in the 3D collagen gel fibroblast migration assay. The motogenic active fractions were then tested with known MSF inhibitors, NGAL and PEPQ 1.1.

From analysis of un-fractionated endothelial CM, bioactivity was considered to be phenotype specific yet upon fractionation previously masked activities were revealed.

As opposed to possessing either motogenic or MSF- inhibitory bioactivity it appears that the cobblestone and sprouting endothelial cells simultaneously express both. This is similar to the discovery for the HaCaT series keratinocytes whereby both MSF and its inhibitor, NGAL, are expressed; although at varying rates which then determines the overall bioactivity exhibited by the unfractionated CM.

Unfortunately, the results are inconclusive as to whether an endothelial expressed MSF is solely responsible for the migration stimulatory activity detected in the sprout and cobblestone CM. Yet, there is evidence to support the presence of an endothelial MSF (Table 7.5). Firstly, the motogenic active fractions of both SEC and SDS PAGE fractionated endothelial CM was within the molecular weight range for MSF. Secondly, although the addition of MSF inhibitors did not completely neutralise the motogenic activity migration was reduced by a significant degree. Finally, immunolocalisation experiments also identified MSF expression by endothelial cells.

However, an anomaly arises when comparing MSF immunolocalisation results with fractionated CM bioactivity experiments. In the majority of immunolocalisation experiments (5/7) cobblestone endothelial cells were negative for MSF. Whilst in the 3D collagen gel assay the ability of the fractionated cobblestone CM (SEC and SDS PAGE) to stimulate fibroblasts migration was measured at a similar level to the activity of the fractionated sprout CM, suggesting the motogen present was at a comparable concentration. The NGAL and PEPQ 1.1 inhibition experiments also imply that MSF was present in similar quantities in both cobblestone and sprout CM.

If MSF is responsible for the motogenic activity detected in fractionated Cobblestone CM then MSF present in cobblestone endothelial cells must be associated with another protein(s) which not only inhibits its bioactivity in the total CM but also masks it from identification by the anti-MSF Rp2 antibody. Therefore, both the MSF unique carboxyl terminal decapeptide, which the Rp2 antibody has been raised against, and the IGD motif, which is responsible for MSF bioactivity, would have to be concealed. Yet, this interaction with another protein(s) must be weak since fractionation of the cobblestone CM by SEC appears to be enough to unmask the motogenic activity previously hidden in the total cobblestone CM.

However, the method used to collect CM may be somewhat accountable for the anomaly in the levels of bioactivity of the cobblestone and sprout CM. In order to insure a single population of sprouting cells the ENDO 742 cells were plated within a type I collagen gel matrix, whilst the cobblestone CM was collected from the cells plated on the surface of the gel. Obviously, any proteins expressed and released by the endothelial

cells on the gel surface will enter the overlying media more efficiently than those secreted by the cells within the gel. As already discussed in MSF immunolocalisation experiments, when cells are plated within a collagen gel matrix (keratinocytes, foetal fibroblasts and endothelial cells) a high background staining of collagen gel occurs. Therefore, it could be possible that the MSF expressed by the sprouting endothelial cells is becoming trapped within the collagen matrix resulting in only a small percentage ever reaching the overlaying media. In retrospect, total protein levels of the cobblestone and sprout CM should have been measured to insure an accurate comparison of motogen concentration and bioactivity.

Since the evidence from immunoblot and immunostaining experiments implied NGAL was not the source of MSF-inhibitory bioactivity present in cobblestone CM further characterisation of the inhibitory bioactivity was required. The fractions/elutions of the fractionated CM (cobblestone, sprouting and blank) were tested for the ability to inhibit the bioactivity of rhMSF in the 3D collagen gel fibroblast migration assay. This testing process confirmed the presence of an endothelial MSF-I in the cobblestone CM but also revealed a previously hidden MSF-inhibitory activity present within the sprouting CM (Table 7.6).

The MSF-I activity in both the cobblestone and sprouting CM appears to share a similar molecular weight and unexpectedly a comparable level of activity (Table 7.7). The bioactivity was located to three molecular weight zones of approximately 70kDa, 40kDa and ≤ 25 kDa. As seen previously with the HaCaT series experiments the fractionation process, by both SEC and SDS PAGE, failed to pin-point the MSF-I activity to a specific molecular weight region.

Since the MSF-I bioactivity of the sprout CM is normally masked in un-fractionated CM it was surprising to discover that it shared a similar capability to inhibit rhMSF as the cobblestone CM did (Table 7.7). However, any comparisons should be restrained due to the lack of total protein concentrations of the two CM types. Nevertheless, although the endothelial cells were expressing different phenotypes the CM was collected from cultures of the same number of cells and then subsequently underwent the same concentration and fractionation processes.

Obviously, this analysis was the first stage in a process to identify the protein responsible for endothelial MSF-I bioactivity, however from these initial results the presumption was that the same protein would be accountable in both the cobblestone and sprouting endothelial cell cultures. However, a difference between cobblestone and sprouting CM was noted by a variation in activity levels of fractions/elutions at an

approximate molecular weight of 40kDa; more MSF-inhibitory was present in the sprout fractionated CM than the cobblestone.

As seen with the discovery of motogenic activity in the cobblestone CM the concealment of the MSF-I in the sprouting CM is highly efficient, although any association must be weak as it is easily separated by SEC fractionation. Possibly, the method of inhibition is via a method other than direct interaction. Further investigation is required to identify the protein responsible for endothelial MSF-I activity.

It has previously been reported that MSF has pro-angiogenic bioactivities *in vitro* due to its capacity to induce endothelial cells to undertake a phenotypic change from the cobblestone to the sprouting phenotype. It was also suggested that MSF is accountable for the spontaneous sprouting morphology endothelial cells adopt when plated in a 3D matrix (Schor, 2010). Although, it was discovered that NGAL was not expressed by the endothelial cells an investigation was undertaken to determine its effect on endothelial cells; specifically to ascertain whether NGAL can inhibit MSF pro-angiogenic bioactivity in addition to inhibiting MSF ability to stimulate fibroblast migration. MSF ability to induce a sprouting phenotype in homogenous cobblestone endothelial cell culture was easily reproduced in *in vitro* angiogenesis assays. The effect of stimulating phenotypic change by MSF was identical irrespective of the 2D plating surface (plastic, 0.1% w/v gelatin, native type I collagen) or endothelial cell line (BAEC, HUVEC, ENDO 742). The minimum concentration of rhMSF to initiate sprouting was 10ng/ml; whilst 48 hour incubation with 100ng/ml rhMSF increased sprout numbers three fold compared to the control (1% DCS MEM).

It has previously been reported that treatment of heterogeneous cultures displaying both cobblestone and sprouting endothelial cells with the IGD function neutralising monoclonal antibody, PEPQ 1.1, resulted in the apoptotic death of the sprouting cells whilst the cobblestone cells remained unaffected (Schor, 2010). Unsurprisingly, the exposure of a homogenous culture of spontaneous endothelial sprouts (cells plated within a 3D collagen gel) to the PEPQ1.1 also resulted in programmed cell death. A minimal PEPQ 1.1 concentration of 20µg/ml caused a significant reduction in sprout numbers within 24 hours: average decrease of 42.6± 28.99% compared to control cultures. The death of practically all sprouts was observed after a 48 hour incubation with 30µg/ml PEPQ 1.1.

As MSF has been proven to induce the sprouting phenotype, it was conceivable to predict that treatment with MSF-inhibitors may have caused a reversal of phenotype from sprout to the cobblestone. However, the apoptotic cell death that was evoked

implies that in addition to stimulating angiogenesis, MSF must also play the role as a survival factor for the sprouting cells. The predominant bioactivity of the total CM of sprouting and cobblestone cells is motogenic or MSF-inhibitory, respectively. These initial investigations insinuated that sprouting cells expressed MSF while the cobblestone cells expressed a MSF-inhibitor. However, upon fractionation of the CM it was discovered that both endothelial phenotypes expressed both MSF and a MSF-inhibitor. Therefore, MSF role as a survival factor is unique to the sprout phenotype as the cobblestone endothelium appears to remain unaffected by exposure to PEPQ 1.1 antibody. It will be interesting to discover what role the masking of cobblestone MSF bioactivity has on its ability to be resistant to the PEPQ 1.1. Since PEPQ 1.1 neutralises the function of the IGD motif it would imply that this motif is implicated in MSF role as a sprout survival factor.

NGAL has been proven to be an inhibitor of MSF stimulation of fibroblast migration in the 3D collagen gel assay. Although NGAL was shown not to be responsible for the endothelial expressed MSF-inhibitory activity its effect on endothelial morphology was investigated. Initially, NGAL was shown to have a similar effect on spontaneous sprouts as the PEPQ 1.1 antibody; 500ng-1 μ g/ml reduced sprout numbers by day 2, with the majority of sprouts undergoing apoptosis by day 5 (lower concentrations 1-100ng/ml had no effect). However, as opposed to PEPQ 1.1 selective effect on only sprouts in a heterogeneous culture of cobblestone and sprouts cells, NGAL was found to target both. Although 1-100ng/ml rhNGAL had no effect on either the cobblestone or the formation of sprouts in post-confluent cultures the higher concentrations of 400ng-1 μ g/ml inhibited all sprout development plus adversely affected the cobblestone. Initially NGAL caused disorganisation of the uniform cobblestone monolayer, but with longer incubation cell death started to occur. Irrespective of the source of NGAL tested (prokaryotic and eukaryotic) the effect was the same.

Growth and viability studies revealed that the NGAL had the ability to reduce proliferation of endothelial cells, although did not affect cell viability. As expected the lower NGAL concentrations, 10-100ng/ml, had no effect. Yet 1 μ g/ml which induced sprout and cobblestone apoptosis in the sprout assays caused a significant reduction in endothelial proliferation; decreased by 20.5 +/- 5.14% and 23.2 +/- 5.49% with 1 μ g/ml prokaryotic and eukaryotic rhNGAL respectively. Yet the same rhNGAL concentrations used in growth and viability assays performed with fibroblasts had no effect. It would appear therefore the effect of NGAL is cell type dependent.

It is questionable whether the effect of NGAL on endothelial cells is solely due to inhibition of endothelial expressed MSF since NGAL is known to induce apoptosis, mainly through its ability to chelate iron from cells; cellular iron deprivation triggers programmed cell death (Devireddy *et al.*, 2005, Virzi *et al.*, 2013). Therefore future sprout assays should include analysing the effect of the iron chelator DFOM. Yet, NGAL from both prokaryotic and eukaryotic sources, which will have varying amounts of bound iron, both display the same effect on endothelial cells. Plus, in the spontaneous sprout assays both PEPQ 1.1 and NGAL display the same effect on the sprouts; the actions of PEPQ 1.1 antibody is achieved by neutralising the function of the IGD motif of MSF. Finally, the capability of NGAL to transport iron has been shown not to be relevant to its ability to inhibit MSF stimulated fibroblast migration.

A role for NGAL as an angiogenesis inhibitor has been previously reported in breast and pancreatic cancer studies; its effects have been implicated with VEGF expression. Ras-induced tumour angiogenesis in 4T1 mouse breast cancer model was shown to be inhibited by NGAL via down-regulation of VEGF expression and an up-regulation of TSP-1 expression (Venkatesha *et al.*, 2006). Later Tong *et al.*, 2008, reported NGAL could inhibit angiogenesis in *in vitro* and *in vivo* models of pancreatic cancer. The formation of endothelial tubes by sprouting HUVEC cells was shown to be inhibited by NGAL possibly through decreased VEGF production or a blockade of the VEGF receptor. NGAL induced reduction in endothelial tube formation was also suggested to occur through perturbations of FAK-integrin mediated signalling events (Tong *et al.*, 2008).

It would therefore be interesting to investigate whether MSF stimulation of sprout formation entails an up-regulation of VEGF expression.

It should be noted that different concentrations of both of the MSF-inhibitors, NGAL and PEPQ1.1 are required to generate an effect in the fibroblast and endothelial assays. In the 3D fibroblast migration assays, MSF- inhibition is achieved by minimal concentrations of 1-10ng/ml and 50ng/ml of rhNGAL and PEPQ 1.1 antibody, respectively. However, minimum concentrations of 400ng/ml rhNGAL and 20µg/ml PEPQ 1.1 are required to induce an effect in the endothelial sprout assays. Another, main difference in assays is the source of MSF to be inhibited; exogenous or endogenous. In the 3D collagen gel assay, an exogenous source of MSF (rhMSF, total CM, fractionated CM) is applied to the fibroblasts and the actions of the inhibitors observed. Whilst in the sprouting assays it is endogenous endothelial expressed MSF which is attempted to be inhibited by the addition of rhNGAL and PEPQ 1.1.

These initial experiments have revealed some interesting starting points for future work. Obviously, further purification of the endothelial CM is required to identify the protein responsible for endothelial MSF-I activity. The identification of the endothelial MSF inhibitor will therefore initiate a whole plethora of experiments to determine its relationship with MSF and its involvement in regulating endothelial cell morphology and bioactivity. In addition, further work is required to understand the nature of MSF angiogenic capabilities and the ability of NGAL to inhibit angiogenesis.

Table 7.5: Summary of experimental data providing evidence that cultured ENDO 742 endothelial cells displaying both the cobblestone and sprouting phenotype express MSF.

<u>TECHNIQUE</u>	<u>EXPERIMENTAL DETAILS</u>	<u>ENDOTHELIAL CELLS, ENDO 742</u>			
		<u>COBBLESTONE</u>		<u>SPROUTING</u>	
Western Blot Identification of MSF	Anti-MSF Antibody, RpVSI. 10x Amicon concentrated CM tested.	negative		negative	
Immunolocalisation of MSF.	Anti-MSF antibody, Rp2/98pFA2pFn1. Cells plated on 2D surface; tested at confluence (cobblestone) and post-confluence (sprouting). Cells plated on (cobblestone) and within 3D collagen gel (sprouting).	<u>2D surface:</u> 4/5 expts- negative 1/5 expts -strong positive	<u>3D surface:</u> 5/7 expts- negative 2/7 expts- strong positive	<u>2D surface post-confluence:</u> 5/5 expts- positive	<u>Within 3D gel:</u> 7/7 expts- weak to strong positive
Motogenic Activity of Fractionated CM	10x concentrated CM fractionated by 2 methods; SEC and SDS electrophoresis. Subsequent fractions/elutions tested in 3D collagen gel fibroblast migration assay for motogenic activity. Level of migration compared to SF MEM baseline.	<u>SEC</u> Fractions 11-14 (> 70kDa) 1/200 dilution - 2 fold increase in migration	<u>SDS PAGE</u> Elutions 3-4 (37-100kDa) 1/1000 dilution -1.7 fold increase in migration	<u>SEC</u> Fractions 11-15 (>70kDa) 1/200 dilution -2 fold increase in migration	<u>SDS PAGE</u> Elutions 2-3 (75-100kDa) 1/1000 dilution -1.6 fold increase in migration
IGD Function Neutralisation of Motogenic Activity.	Motogenic active ENDO 742 cobblestone and sprouting CM fractions/elutions pooled and tested in the 3D collagen gel fibroblast migration assay with addition of 50ng/ml Pep Q 1.1- IGD function neutralising antibody. Effect on migration compared to baseline levels.	<u>SEC</u> Migration decreased by 48.7 +/- 8.31%	<u>SDS PAGE</u> Migration decreased by 40.8 +/- 7.24%	<u>SEC</u> Migration decreased by 42.9 +/- 20.54%	<u>SDS PAGE</u> Migration decreased by 34.0 +/- 5.96%
NGAL inhibition of Motogenic activity.	Motogenic active ENDO 742 cobblestone and sprouting CM fractions/elutions pooled and tested in the 3D collagen gel fibroblast migration assay with addition of 10ng/ml rhNGAL. Effect on migration compared to baseline levels.	<u>SEC</u> Migration decreased by 27.9 +/- 16.62%	<u>SDS PAGE</u> Migration decreased by 46.9 +/- 9.63%	<u>SEC</u> Migration decreased by 13.9 +/-17.69%	<u>SDS PAGE</u> Migration decreased by 40.4 +/- 4.47%

Table 7.6: Result Summary. The bioactivity of fractionated ENDO 742 conditioned medium. Conditioned medium (CM) was collected from ENDO 742 cells grown either on or within a collagen gel matrix; thereby displaying either a cobblestone or sprouting phenotype respectively. As a control, conditioned medium was also collected from a blank collagen gels (no cells). After concentration each type of CM was fractionated by two methods, size exclusion chromatography (SEC) and SDS electrophoresis. The subsequent fractions/ elutions were tested in the 3D collagen gel fibroblast migration assay; with and without the presence of 100pg/ml rhMSF. By comparison to SF MEM or rhMSF baseline controls the nature of each cell line's bioactivity was determined. The conditions for fractionation of the 10x Amicon concentrated CM was as follows:

1. SEC performed using Superdex 75 Hiload 26/60 column (GE Healthcare), multiple runs performed with fractions pooled together into groups of three (13-23) equivalent to MW >70kDa to 20kDa, and tested at final dilution of 1/20.
2. Electrophoresis (12% separating, 5% stack SDS polyacrylamide gel) performed under reducing conditions; gel divided into 12 segments (>100kDa to >20kDa) and proteins eluted during an overnight incubation in 1ml elution buffer; elutions subsequently tested at a final dilution of 1/1000.

Cell Line	Fractionation Method	Motogenic Activity Compared to SF MEM Baseline (Tested alone)		MSF-I Activity Compared to MSF Baseline (Tested with 100pg/ml rhMSF)		MSF-I Activity Only No endogenous motogenic activity.	
		Fraction Group/ Elution	Equivalent MW	Fraction Group/ Elution	Equivalent MW	Fraction Group/ Elution	Equivalent MW
BLANK GEL	SEC	none	-	none	-	-	-
	SDS	none	-	none	-	-	-
COBBLESTONE ENDO 742	SEC	11-14	≥70kDa	16,17 21, 22	70-60kDa ≤25kDa	15-17 19 21, 22	70-60kDa >40kDa ≤25kDa
	SDS	3-4	100-37kDa	3 8	approx. 75kDa approx. 20kDa	6, 7, 8, 9, 12 (maximum activity 6 + 8)	≤25kDa
SPROUTING ENDO 742	SEC	11-15	≥70kDa	19, 20, 23	≤25kDa	16, 19 20, 23	>70kDa >40kDa ≤25kDa
	SDS	2-3	75-100kDa	4 5	50-75kDa 25-50kDa	5, 4 8, 10, 11 (maximum activity 4)	25-75kDa ≤ 20kDa

Table 7.7: A comparison of MSF-Inhibitory bioactivity present detected in the fractionated conditioned medium of endothelial cells exhibiting either the cobblestone or sprouting phenotype.

Conditioned medium (CM) was collected from ENDO 742 cells grown either on or within a type I collagen gel matrix; thereby displaying either a cobblestone or sprouting phenotype respectively. After concentration each type of CM was fractionated by two methods, size exclusion chromatography (SEC) and SDS electrophoresis. The subsequent fractions/ elutions were tested in the 3D collagen gel fibroblast migration assay with addition of 100pg/ml rhMSF. The level of inhibition of MSF motogenic activity was calculated by comparison to MSF baseline levels and elution/fraction only baseline levels.

The conditions for fractionation of the 10x Amicon concentrated CM was as follows:

1. SEC performed using Superdex 75 Hiload 26/60 column (GE Healthcare), multiple runs performed with fractions pooled together into groups of three (13-23) equivalent to MW >70kDa to 20kDa, and tested at final dilution of 1/20.
2. Electrophoresis (12% separating, 5% stack SDS polyacrylamide gel) performed under reducing conditions; gel divided into 12 segments (>100kDa to >20kDa) and proteins eluted during an overnight incubation in 1ml elution buffer; elutions subsequently tested at a final dilution of 1/1000.

1. Fractionation by Size Exclusion Chromatography.

Cobblestone Phenotype		Sprouting Phenotype	
Molecular Weight	% of MSF Inhibition	Molecular Weight	% of MSF Inhibition
70-60kDa	41.6 +/- 18.92	>70kDa	46.9 +/- 5.77
>40kDa	9.7 +/- 2.26	>40kDa	65.4 +/- 0.00
≤25kDa	38.15 +/- 2.90	≤25kDa	45.1 +/- 20.51

2. Fractionation by SDS Electrophoresis.

Cobblestone Phenotype		Sprouting Phenotype	
Molecular Weight	% of MSF Inhibition	Molecular Weight	% of MSF Inhibition
75kDa	49.05 +/- 8.93	50-75kDa	87.4 +/- 23.83
-	-	25-50kDa	61.1 +/- 9.76
≤25kDa	41.19 +/- 7.51	≤20kDa	40.5 +/- 10.40

Chapter 8

CONCLUDING DISCUSSION

Migration Stimulating Factor is a potent oncofetal protein which has numerous bioactivities pertinent to cancer progression including stimulating motogenesis and angiogenesis (Schor *et al.*, 2003, Schor, 2010). Only femtomolar concentrations of MSF are required to produce half-maximal motogenic activity. Plus the proteolytic degradation of MSF results in the release of bioactive IGD domains. Consequently, there appears to be a necessary requirement to limit unrestricted MSF bioactivity. A mRNA cleavage event within the nucleus is known to control MSF expression but it is unknown whether there is a mechanism to regulate the bioactivity of the actual MSF protein (Schor *et al.*, 2003). It was the primary objective of this project to discover a source and then ultimately identify potential MSF inhibitor(s). However, as the project progressed and novel discoveries were made, further aims were subsequently proposed (Table 8.1).

Motogenesis, matrix remodelling via proteolytic activity, hyaluronan biosynthesis and angiogenesis are all bioactivities exhibited by MSF (Schor *et al.*, 1988, 1989, 1990, Kay *et al.*, 2005, Ellis *et al.*, 1992, Houvard *et al.*, 2005). It is the ability of MSF to stimulate the migration of various cell types (fibroblast, epithelial and endothelial cells) which appears to be pivotal to its contribution to carcinogenesis (Schor *et al.*, 2003).

Therefore, the sensitive *in vitro* bioassay for assessing the motogenic bioactivity of MSF, the 3D type I collagen gel fibroblast migration assay, was selected to be the principal assay for the identification of potential MSF-I activity.

After a rudimentary screening process of the conditioned medium (CM) from various cell lines, two sources of MSF- inhibitory activity were discovered; keratinocytes and endothelial cells specifically those exhibiting the cobblestone phenotype. Due to ease of culture and subsequent collection of CM, the keratinocyte MSF-I activity was investigated first. The CM from the HaCaT cell line, a spontaneously immortalised human keratinocyte line, underwent a process of fractionation, by both molecular weight and ionic charge, followed by sequence analysis to ultimately identify the protein responsible for the MSF-I bioactivity as Neutrophil Gelatinase Associated Lipocalin (Figure 4.19, Table 8.1).

Unexpectedly, the fractionation process of HaCaT CM also revealed the presence of motogenic bioactivity, which was normally obscured within the total HaCaT CM. The

protein responsible for this motogenic bioactivity was subsequently identified as MSF (Table 4.3, 8.1). It therefore transpired that cultured HaCaT keratinocytes express MSF but its motogenic bioactivity appears to be inactivated (or masked) by the co-expression of an inhibitor, NGAL.

The inhibition of MSF by NGAL is a novel discovery. A member of the lipocalin family, NGAL is a multifunctional protein although its exact pathophysiological roles are not entirely understood. Numerous functions have been ascribed to NGAL; bacteriostatic agent, iron transportation, induction of apoptosis, modulation of inflammatory response, fatty acid transportation and protecting cells against thermal and oxidative stress conditions (Strong *et al.*, 1998, Goetz *et al.*, 2002, Flo *et al.*, 2004, Weng *et al.*, 2012).

NGAL has the ability to bind to the matrix metalloproteinase MMP-9, protecting it from proteolytic degradation. As MSF and MMP-9 share some structural similarity, with both molecules containing fibronectin type II domains and zinc-binding motifs, it was initially supposed that NGAL would also bind directly to MSF in order to exert its effect. Yet, pre-incubation experiments revealed that NGAL does not require direct contact with MSF in order to exert an inhibitory effect; fibroblasts pre-incubated with NGAL for 24 hours were shown to become unresponsive to MSF. This result inferred that NGAL inhibits MSF either by blocking an MSF-activated signal transduction pathway or indirectly via an intermediate molecule.

Further investigation into the nature of NGAL ability to inhibit MSF revealed that it is not dependent upon its iron transportation capability. Testing NGAL in the presence of the iron chelator DFOM had no effect its MSF-I activity. Plus, three sources of NGAL (purified from HaCaT CM, prokaryotic and eukaryotic rhNGAL) possessing varying amounts of bound iron were found to exhibit an identical MSF-I activity.

NGAL has been implicated in cancer progression due to its capacity to affect two critical processes; cell survival via apoptosis and cell migration preceding tumour invasion and metastasis (Yang and Moses, 2009, Chen and Chan, 2011). However, the conclusion from a literature review of NGAL was that a pro or anti- tumourigenic role for NGAL is neoplasia-specific and also varies with the different stages of cancer progression and degree of tumour differentiation. In addition, NGAL is considered to play a role in epithelial differentiation due to its embryonic-spatial expression pattern and increased expression in skin disorders characterised by dysregulated epithelial differentiation (psoriasis, pityriasis rubra and squamous cell carcinoma) (Malbris *et al.*, 2002). Therefore, in common with MSF, NGAL has been implicated in various benign

and malignant diseases (Schor *et al.*, 2003 and 2005, Hu *et al.*, 2009, Charkraborty *et al.*, 2012).

Consequently, the relationship of these pro- and anti-motogenic factors, MSF and NGAL respectively, during cancer progression was investigated using the *in vitro* model for human skin carcinogenesis developed by Fusenig and Boukamp. Developed from the non- tumourigenic transformed HaCaT keratinocyte cell line, the HaCaT-*ras* clones (BEN, MAL and MET- the HaCaT series) represent a shift in tumourigenic potential from the benign to malignant to metastatic (Fusenig and Boukamp, 1998). For ease of the discussion the BEN, MAL and MET keratinocytes were referred to as the HaCaT series cell lines.

Various techniques (IHC, immunoblotting, ELISA) were employed to determine the expression levels of MSF and NGAL by each of the HaCaT-*ras* clones. Similar to the HaCaT keratinocytes all members of the HaCaT series expressed both MSF and NGAL, but as the tumourigenic potential of the cell lines increased there was a distinctive variation in the expression level of each protein. NGAL expression, from lowest to highest, was discovered to be MET, MAL, BEN. The reverse situation was found for MSF (BEN, MAL, MET); the highest intensity of MSF immunolocalisation was detected in MET cultures, especially when grown within a 3D type I collagen matrix. Overall, during tumour progression the expression level of NGAL decreases whilst that of MSF increases.

These findings correlated with reported data. A grade specific pattern of NGAL expression has been described in pancreatic tumours and oral squamous cell carcinoma (Hana *et al.*, 2005, Moniaux *et al.*, 2008, Lin *et al.*, 2012). Furthermore, NGAL expression has been shown to increase during the benign and low-grade malignancy phases of tumour progression but then drastically reduced at the advanced metastatic stage in ovarian, pancreatic and colon carcinoma. These findings have led to NGAL being currently considered as a potential early stage biomarker for a variety of cancers (Lim *et al.*, 2007, Tong *et al.*, 2008, Lee *et al.*, 2006, Yang and Moses, 2009). Whereas, MSF expression is habitually low in normal breast tissue but becomes elevated in breast tumours; a poor prognosis associated with an increased expression of MSF. Over-expression of MSF is also a characteristic of both epithelial and stromal cells of malignant salivary gland tumours (Aljorani *et al.*, 2011)

The presence of MSF in the HaCaT CM was not revealed in the initial analysis of the total CM, as the co-expressed NGAL inactivated any motogenic bioactivity. Therefore, the objective was set to ascertain what effect the altering co-expression levels of MSF

and NGAL exhibited by the HaCaT series cell lines had on the bioactivity present in CM. It was subsequently discovered that unlike the HaCaT keratinocytes the autogenous bioactivity of BEN, MAL and MET was motogenic. For BEN and MAL CM, the motogenic bioactivity adopted a bell-shaped dose response similar to that of rhMSF. Maximal motogenic bioactivity was detected in MET CM, which correlated with the MET cells having the highest MSF expression levels. However, fractionation of the HaCaT series CM revealed that BEN and MAL CM still retained the ability to inhibit rhMSF. This implied that the HaCaT series keratinocytes did secrete bioactive forms of both MSF and NGAL, and it was the balance of these pro and anti-motogenic factors which determined the inherent bioactivity present in the CM.

Yet, the ELISA analysis for NGAL in the HaCaT series CM revealed that NGAL was present in a higher concentration in BEN and MAL CM than in the normal HaCaT CM. This data therefore inferred that BEN and MAL unfractionated CM should be exhibiting MSF inhibitory bioactivity rather than motogenic bioactivity. Thus it was concluded that the MSF concentration must be far greater in the HaCaT series CM than in the normal HaCaT CM to enable motogenic activity to prevail over NGAL MSF-I activity. Unfortunately, due to limitations of the MSF ELISA assay, only a semi-quantitative immunohistochemical analysis of MSF expression levels was available. Consequently, there was inadequate proof to determine the relative concentration of MSF compared to NGAL.

In addition, the failure of MSF inhibitors, NGAL and IGD function neutralising PEPQ 1.1 antibody, when added in excess to achieve complete inhibition of the motogenic bioactivity also insinuated the presence of another motogen in the HaCaT series CM. Yet, when MSF was semi-purified from the fractionated HaCaT series CM (RpVSI immunoprecipitation of motogenic SEC fractions) its motogenic activity was inhibited by NGAL and PEPQ1.1 antibody. Perhaps, more information regarding the presence of other motogen(s) could have been achieved if MSF immunoprecipitation had been performed on total HaCaT series CM rather than selected motogenic SEC fractions. Another obstacle encountered was the failure of the fractionation process to achieve a good separation of the two opposing factors. This was considered to be a result of concentrating the CM excessively which caused the formation of non-specific associations between proteins. Also, due to the biological assessment of bioactivity, protease inhibitors could not be added to the CM to halt proteolysis. It was supposed that the production of bioactive breakdown products contributed to the difficulty

encountered when trying to localise each bioactivity to fractions of a specific molecular weight.

Furthermore, the nature of MSF bioactivity contributed to difficulties in isolating the presence of genuine MSF-I bioactivity. MSF acts in a bell-shaped dose response manner, whereby motogenic activity increases steadily with increasing concentration peaking at a maximum (500pg/ml) followed by a mirror-image decrease in activity towards the baseline level as the concentration increases further. That is, the addition of 100pg/ml rhMSF, used to determine the MSF-I activity, could combine with MSF and its IGD bioactive breakdown products present in the CM, to give a final concentration that would actually result in a reduction in motogenic activity. Biochemical characterisation of MSF has revealed that the potent motogenic activity of the MSF protein is indistinguishable from its proteolytically generated Gel-BD functional domain and IGD tripeptide, therefore motogenic activity could be present in fractions of MW 70kDa, 43kDa and 21kDa, respectively.

Once NGAL was identified as the source of MSF inhibitory activity in the HaCaT keratinocyte CM, the next stage was to determine whether NGAL was also responsible for the MSF-I activity detected in the CM collected from endothelial cells specifically exhibiting a cobblestone phenotype. By performing immunoblot and IHC experiments, using specific anti-NGAL antibodies, it emerged that endothelial cells, *in vitro*, do not express NGAL. This finding was irrespective of the endothelial cell line, phenotype, and species of origin. However, the possibility that NGAL was present but at levels below the detection limits of the assays cannot be discounted.

In the initial analysis of conditioned medium for the presence of MSF-I activity the bioactivity of endothelial CM appeared to be determined by the phenotype exhibited by the cells. Conditioned medium collected from a homogenous population of cobblestone endothelial cells specifically displayed the ability to inhibit MSF bioactivity, while the CM from a homogenous population of sprouting endothelial cells distinctly exhibited a motogenic activity. Having established a protocol for the identification of the source of MSF-I activity in HaCaT CM the same procedure of fractionating the CM (SEC and SDS PAGE) was followed with the purpose of localising the bioactivity to a specific MW. Both cobblestone and sprouting ENDO 742 CM was analysed for the presence of MSF-I and motogenic bioactivity.

Comparable to the analysis of HaCaT fractionated CM, the fractionation of endothelial ENDO 742 CM revealed previously masked bioactivities. Previously, the bioactivity of endothelial CM was considered to be the phenotypic specific however it would appear

that both phenotypes secrete bioactive forms of both motogenic and MSF-I bioactivity. Although not conclusive, evidence was gained to suggest that an endothelial MSF was at least partially responsible for the motogenic activity detected in both sprouting and cobblestone CM. That is, the fractions displaying motogenic bioactivity were within the MW range for MSF and although the addition of MSF-inhibitors, NGAL and PEPQ 1.1 antibody, didn't completely abolished all activity it was diminished by significant degree.

However, it transpired that an anomaly existed when comparing the results from immunohistochemical analysis of MSF expression by the two endothelial phenotypes and the level of motogenic bioactivity in the fractionated CM. In 5/7 IHC experiments the endothelial cells exhibiting the cobblestone phenotype on the surface of a 3D type I collagen gel were negative for MSF whereas in 7/7 IHC experiments the sprouting endothelial cells were MSF positive. Yet the motogenic fractions of cobblestone CM share a similar MW and level of bioactivity as the sprouting CM, which would imply that the motogen responsible was present at a comparable concentration. The NGAL and PEPQ 1.1 inhibition experiments also suggested that MSF was present in similar quantities in both cobblestone and sprout CM.

A possible explanation for this anomaly was the CM collection method. In order to collect CM from a homogenous population of sprouting endothelial cells the ENDO742 cells were plated within a 3D type I collagen gel whereas the cobblestone CM was collected from cells plated on the surface of a gel. Obviously, any proteins secreted by the cells would enter the overlaying media more efficiently from the cobblestone cells than the sprouting cells. Due to the high background staining of the collagen gel in the IHC experiments it was suggested that MSF expressed by the sprouting cells was becoming entrapped within the collagen gel, thereby resulting in only a small percentage reaching the overlying media.

An alternative explanation was that MSF present within the cobblestone cells was associated with another protein which has the ability to inhibit its bioactivity in the total CM but also masks it from identification by the anti-MSF Rp2 antibody. This would therefore require concealment of both the unique MSF carboxyl terminal decapeptide, which is the epitope of the Rp2 antibody, and the IGD motif, which is responsible for the MSF bioactivity. However, this interaction must be weak since SEC fractionation of the cobblestone CM appears to be enough to unmask the motogenic activity previously hidden in the total cobblestone CM.

As well as, having similar motogenic activity the fractionated cobblestone and sprouting endothelial CM also had comparable levels of MSF inhibitory activity. The MSF-I activity of both phenotypes could be located in fractions of MW 70kDa, 40kDa and ≤ 25 kDa which implied that the protein responsible could possibly be forming complexes with itself or with other protein(s); a situation similar to that of NGAL.

Alternatively, maybe more than one MSF inhibitor is present. It is still presumptuous at this stage, to suggest that the same protein is responsible for the MSF-I activity in both cobblestone and sprout CM. Future work will clearly require further purification of the CM to enable the subsequent identification of the protein responsible for the endothelial MSF-I activity. Since there was an obvious difficulty in pinpointing the MSF-I activity to a specific MW it may be more efficient to choose another fractionation method. Ion exchange chromatography, for example where proteins are separated according to their net charge, may prove more efficient. Also, using less extensively concentrated CM should help to reduce the formation of non-specific protein associations.

Although it was concluded that NGAL was not responsible for endothelial MSF-I activity, it was relevant to determine what effect NGAL would have on the endothelial phenotype especially since MSF was known to induce the development of sprouting endothelial cells when applied to a cobblestone monolayer (Schor *et al.*, 2003, Schor, 2010). Comparing previously reported data, in both *in vitro* and *in vivo* models, it emerged that NGAL and MSF exhibit opposing effects on angiogenesis. Over-expression of NGAL has been shown to facilitate a reduction in angiogenesis in an orthotopic mouse model of pancreatic cancer plus it significantly reduces the tube formation of HUVEC endothelial cells (Venekatesha *et al.*, 2006, Tong *et al.*, 2008). Whereas MSF stimulates angiogenesis *in vivo* in the chicken yolk sac membrane assay and *in vitro* sprouting assays (Schor 2010).

In addition to pro-angiogenic role, it has been suggested that MSF also plays a role in promoting the survival of sprouting endothelial cells. The foundation of the spontaneous sprouting assay is the capability of endothelial cells, when cultured within a 3D type I collagen matrix, to automatically establish a homogenous population exhibiting the sprouting phenotype. Exposure of these sprouts to the IGD function neutralising antibody, PEPQ 1.1, resulted in all of the sprouts undergoing apoptosis. Yet when a cobblestone monolayer is exposed, at the same concentration, to the PEPQ 1.1 antibody no adverse effects on the monolayer are observed. In addition, the antibody exhibits a selective ability to restrict the development of post-confluent sprouts on the endothelial

monolayer (Schor 2010). These results therefore propose that MSF, specifically the IGD motif, is implicated in the process of endothelial sprout formation and survival.

The effect of rhNGAL on the endothelial morphology was also tested in the *in vitro* post-confluent and spontaneous sprouting assays. Comparable to the PEPQ 1.1 antibody, incubation with rhNGAL in the spontaneous sprouting assay resulted in apoptotic death of the homogenous sprout population. In the post-confluent sprouting assay, NGAL initially inhibited the development of any sprouting activity but also initiated disruption to the normally uniform cobblestone monolayer. The continued incubation with rhNGAL resulted in the induction of apoptotic cell death in all the endothelial cells. This result was irrespective of the source of NGAL tested (prokaryotic and eukaryotic). It therefore emerges, that unlike PEPQ 1.1, the effect NGAL has on endothelial cells is not phenotype specific. Subsequent growth assays revealed that NGAL also acts to reduce the rate of endothelial cell proliferation; at the same concentrations previously shown to have no effect on fibroblast growth.

As discussed, analysis of the fractionated endothelial CM revealed that both cobblestone and sprouting endothelial cells express a bioactive motogen that shares many characteristics to MSF. Therefore, if the effect on endothelial cells by NGAL was due to it inhibiting endogenous MSF then it is not too unexpected that NGAL would have a similar effect on both phenotypes. Yet, the phenotype selective effect of the PEPQ 1.1 antibody would concur with previous statements suggesting that MSF, specifically its IGD motif, expressed by cobblestone endothelial cells is somehow masked; possibly by the protein responsible for endothelial MSF-I activity. Since this “masking” does occur with sprouting MSF it is vulnerable to the actions of the PEPQ 1.1 antibody. Thus the proposition is that a similar situation occurs in cobblestone endothelial cells as was discovered in the HaCaT keratinocytes; that is MSF is expressed by the cobblestone endothelial cells but its bioactivity is inactivated by the co-expression of an inhibitor. However, NGAL is known to induce apoptosis, mainly through its ability to chelate iron from cells: this cellular iron deprivation triggers programmed cell death (Devireddy *et al.*, 2005, Virzi *et al.*, 2013). Therefore, further investigation is required before any definitive statements can be made.

In conclusion, both keratinocytes and endothelial cells *in vitro* express MSF, the bioactivity of which is regulated by the co-expression of an inhibitor. The protein responsible for the MSF inhibitory activity is cell- type specific. Neutrophil gelatinase associated lipocalin, NGAL, was identified as the source of keratinocyte MSF-I activity. Using an *in vitro* model for human skin carcinogenesis, the HaCaT *-ras* clones, the

relative expression levels of the pro and anti-motogenic factors, MSF and NGAL respectively, have been implicated in playing a role during tumour progression.

Table 8.1: Summary of project aims and results.**CHAPTER 3: ASSESSMENT OF THE BIOACTIVITY OF CONDITIONED MEDIUM.**

Aims	Assay	Result
1. Primary screen of total CM collected from various cell lines for the presence of motogenic activity.	<ul style="list-style-type: none"> • 3D collagen gel fibroblast migration assay 	Motogenic detected in the CM of: <ul style="list-style-type: none"> • Human foetal fibroblast (FFD4, F110a) • Human and bovine endothelial cell lines, specifically expressing sprouting phenotype (BAEC, ENDO742, HAEC, HOEC, HUVEC).
2. Primary screen of total CM collected from various cell lines for the presence of MSF-inhibitory bioactivity.	<ul style="list-style-type: none"> • 3D collagen gel fibroblast migration assay 	MSF-inhibitory activity detected in the CM of: <ul style="list-style-type: none"> • HaCaT, transformed human keratinocyte • Human and bovine endothelial cell lines, specifically expressing cobblestone phenotype (BAEC, ENDO742, HAEC, HOEC, HUVEC).

CHAPTER 4: THE IDENTIFICATION OF MSF-I PRODUCED BY KERATINOCYTES.

Aims	Assay	Result
1. To isolate the factor responsible for MSF-inhibitory activity detected in HaCaT CM.	<ul style="list-style-type: none"> • Size exclusion chromatography (Superdex) of HaCaT total CM. * • Ion exchange chromatography (ANX) of SEC fractions MW 16-27kDa.* • SDS Electrophoresis of ANX unbound fraction. * 	<ul style="list-style-type: none"> • MSF-I activity detected in fractions of MW 16-27kDa. (Motogenic activity detected, fractions of MW 63-84kDa). • MSF-I activity detected in unbound fraction, equivalent to 32% of total protein. • MSF-I activity detected in gel elutions of MW 20-25kDa.

<p>2. To identify the factor responsible for MSF-inhibitory activity detected in HaCaT CM.</p>	<ul style="list-style-type: none"> • Sequence analysis (tryptic digest, mass spectrometry) of SDS electrophoresis elution of MW 20-25kDa. • Immunolocalisation of NGAL (Anti-NGAL antibody, AF1757). • Immunoblot for NGAL (Anti-NGAL antibody, MAB1757). • Colorimetric Indirect ELISA for NGAL (Anti-NGAL antibody, AF1757) 	<ul style="list-style-type: none"> • Neutrophil Gelatinase Associated Lipocalin (NGAL) identified. • Heterogeneous staining for NGAL in HaCaT cells. • Clear band identified at MW 20-25kDa in both neat and concentrated HaCaT CM. • NGAL concentrated per ml of unstandardised NGAL CM measured as 1.77 +/-0.05µg/ml.
<p>3. To verify the ability of NGAL to inhibit the motogenic bioactivity of MSF.</p>	<p>NGAL from three sources tested for MSF-I activity:</p> <ul style="list-style-type: none"> • NGAL isolated from NGAL/MMP-9 Complex (Calbiochem), 20-25kDa Gel elution 3. * • Eukaryotic NGAL (R&D Systems). * • Prokaryotic NGAL (In-house Prep). * 	<ul style="list-style-type: none"> • Peak MSF-I activity at est. 5-10ng/ml. • Peak MSF-I activity at 1ng/ml. • Peak MSF-I activity at 1ng/ml.
<p>4. To characterise the nature the MSF-inhibitory activity of NGAL.</p>	<ul style="list-style-type: none"> • NGAL from three sources tested for MSF-I activity.* 	<ul style="list-style-type: none"> • Implies MSF-I activity of NGAL is independent of ability to transport iron, as all three sources have different amounts of bound iron but share identical MSF-

	<ul style="list-style-type: none"> • Effect of iron chelator, DFOM, on NGAL ability to inhibit rhMSF. * • NGAL pre-incubation 3D Type I collagen gel fibroblast migration experiments. 	<p>I activity.</p> <ul style="list-style-type: none"> • Addition of DFOM had no effect on NGAL inhibition of MSF. • Fibroblast pre-incubated with NGAL for 24 hours become unresponsive to MSF. Imply direct interaction with MSF not required for NGAL to exert an inhibitory effect.
<p>5. To verify MSF as the factor responsible for the motogenic bioactivity detected in fractionated HaCaT CM.</p>	<ul style="list-style-type: none"> • Immunoblot for MSF (Anti-MSF antibody, RpVSI). • Immunolocalisation of MSF (Anti-MSF antibody, Rp2/98pFA2pFn1). • IGD Function Neutralisation of Motogenic Activity (Pep Q 1.1 antibody). * • Immunoprecipitation for MSF (Protein G coupled to RpVSI antibody).* • NGAL inhibition of motogenic activity. * 	<ul style="list-style-type: none"> • No bands identified in HaCaT CM, irrespective of CM concentration (neat to 50x concentrated tested). If MSF present in HaCaT CM, is at concentration below limits of the assay, <25ng/ml. • Heterogeneous staining for MSF in HaCaT cells. • Motogenic SEC fractions, MW 63-84kDa, alone stimulated fibroblast migration by 3.7 fold. Addition of PepQ1.1 inhibited motogenic activity by 60-70%. • Motogenic SEC fractions, MW 63-84kDa, immobilised on RpVSI coupled Protein G. No motogenic activity present in unbound sample. Motogenic activity present in elutions; 2.8 fold increase in fibroblast migration. • Peak motogenic activity of motogenic SEC fractions, MW 63-84kDa, at 1/250 dilution inhibited by 60% by

	addition of NGAL.
--	-------------------

*bioactivity confirmed by testing in the 3D collagen gel fibroblast migration assay.

CHAPTER 5: THE EXPRESSION OF MSF AND NGAL IN RELATION TO TUMOUR PROGRESSION.

Aims	Assay	Result
1. To establish whether MSF was expressed by the other cell lines of the HaCaT series (BEN, MAL and MET), which displayed an increasing tumorigenic potential.	<ul style="list-style-type: none"> Immunoblot for MSF (Anti-MSF antibody, RpVSI). Immunolocalisation of MSF (Anti-MSF antibody, Rp2/98pFA2pFn1). 	<ul style="list-style-type: none"> No bands identified in CM of either BEN, MAL and MET, irrespective of CM concentration (neat to 1000x concentrated tested). If MSF present in HaCaT series CM, it is at concentration below the limits of the assay, >25ng/ml. Heterogeneous staining for MSF in BEN, MAL and MET keratinocytes. Staining intensity highest in MET, decreasing in MAL, and lowest in BEN.
2. To establish whether NGAL was expressed by the other cell lines of the HaCaT series (BEN, MAL and MET), which displayed an increasing tumorigenic potential.	<ul style="list-style-type: none"> Immunoblot for NGAL (Anti-NGAL antibody, MAB1757). Immunolocalisation of NGAL (Anti-NGAL antibody, AF1757). Colorimetric Indirect ELISA for NGAL (Anti-NGAL antibody, AF1757). 	<ul style="list-style-type: none"> Clear band identified at MW 20-25kDa in both neat and concentrated BEN, MAL and MET CM. Heterogeneous staining for NGAL in BEN, MAL and MET keratinocytes. Staining intensity highest in BEN, decreasing in MAL, and lowest in MET. NGAL detected in CM (neat and concentrated) of BEN, MAL and MET. NGAL concentration highest in BEN, decreasing in MAL and lowest in MET.
3. To determine whether NGAL and MSF expression levels could be	<ul style="list-style-type: none"> Assays as above. 	<ul style="list-style-type: none"> As the tumorigenic potential of the HaCaT series keratinocytes increases then expression level of

related to tumorigenic potential.		<p>NGAL decreases whilst expression level of MSF increases.</p> <ul style="list-style-type: none"> • The NGAL pattern of expression from highest to lowest is BEN/MAL > HaCaT > MET. • The MSF pattern of expression from highest intensity to lowest is MET > MAL > BEN.
-----------------------------------	--	---

CHAPTER 6: THE EXPRESSION OF PRO- AND ANTI- MOTOGENIC BIOACTIVITY BY THE HACAT-RAS CLONES.

Aims	Assay	Result
1. To ascertain bioactivity of total CM of the HaCaT series cell lines.	<ul style="list-style-type: none"> • 3D collagen gel fibroblast migration assay 	<ul style="list-style-type: none"> • Motogenic bioactivity detected in BEN, MAL and MET CM. BEN and MAL display bell shaped dose response; peak stimulation of 2-2.5 fold increase in migration at 1/1000 dilution point. Maximal motogenic activity displayed by MET CM; majority of dilution points (1/40,000- 1/10) stimulated a 2-2.5 fold increase in migration. • MSF-inhibitory activity detected in BEN and MAL CM at dilution points 1/1000- 1/4. No MSF-I activity detected in MET CM.
2. To ascertain whether the fractionated CM of the HaCaT series cell lines exhibited motogenic activity.	<ul style="list-style-type: none"> • Size exclusion chromatography (Superdex) of HaCaT series total CM.* • SDS Electrophoresis of HaCaT series total CM.* 	<ul style="list-style-type: none"> • Majority of motogenic activity located in higher molecular weight fractions, ≥ 60kDa; F37-48 for BEN, F37-63 for MAL and F37-45 for MET. • Motogenic activity located in either higher or lower MW gel elutions. BEN- elutions 1-2 and 10. MAL- elutions 1-3 and 10-12. MET- elutions 1-10 and 12. Equivalent to

		MW \geq 100kDa and <20kDa.
3. To ascertain whether MSF was responsible for the motogenic activity of HaCaT series CM.	<ul style="list-style-type: none"> • Immunoprecipitation for MSF (Protein G coupled to RpVSI antibody).* • IGD Function Neutralisation of Motogenic Activity (Pep Q 1.1 antibody). * • NGAL inhibition of motogenic activity.* 	<ul style="list-style-type: none"> • Motogenic fractions F30-50, equivalent to MW \geq60kDa, for BEN, MAL and MET, immobilised on RpVSI coupled Protein G. Motogenic activity present in bound elutions: BEN elutions 1-2, MAL elutions 2-5, MET elutions 1-5. • BEN, MAL and MET motogenic active IP bound elutions inhibited by addition of PEPQ1.1 • BEN, MAL and MET motogenic active IP bound elutions inhibited by addition of NGAL.
4. To ascertain whether the fractionated CM of the HaCaT series cell lines exhibited MSF-inhibitory activity.	<ul style="list-style-type: none"> • Size exclusion chromatography (Superdex) of HaCaT series total CM.* • SDS Electrophoresis of HaCaT series total CM.* 	<ul style="list-style-type: none"> • MSF-inhibitory exhibited by BEN, MAL and MET but unable to locate activity to any specific area, activity distributed in a variety of fractions/ MW. • MSF-inhibitory activity specifically located to elution 6, MW 20-25kDa, for BEN and MAL. No MSF-I activity detected in MET elutions.
5. To ascertain whether NGAL was responsible for the MSF-I inhibitory activity of HaCaT series CM.	<ul style="list-style-type: none"> • Colorimetric Indirect ELISA for NGAL (Anti-NGAL antibody, AF1757). • Immunoblot for NGAL (Anti NGAL antibody, MAB1757). 	<ul style="list-style-type: none"> • NGAL detected in every SEC fraction group of BEN and MAL CM, and in the majority of MET too. Fractionated CM un-standardised therefore limited analysis possible. • Clear band identified at MW 20-25kDa in both neat and concentrated BEN, MAL and MET CM.

CHAPTER 7: THE IDENTIFICATION OF MSF-I PRODUCED BY ENDOTHELIAL CELLS

Aims	Assay	Result
1. To determine whether endothelial cells express NGAL.	<ul style="list-style-type: none"> • Immunoblot for NGAL (Anti-NGAL antibody, MAB1757). • Immunolocalisation of NGAL (Anti-NGAL antibody, AF1757). 	<ul style="list-style-type: none"> • Consistently negative for NGAL, irrespective of endothelial cell line (human and bovine), phenotype exhibited by the endothelial cells (cobblestone or sprouting) or concentration of the CM tested. • Consistently negative for NGAL, irrespective of endothelial cell line (human and bovine), phenotype exhibited by the endothelial cells (cobblestone or sprouting) or plating matrix (3D collagen gel, 2D surface coated with 1% (w/v) gelatin).
2. To determine whether endothelial cells express MSF.	<ul style="list-style-type: none"> • Immunolocalisation of MSF (Anti-MSF antibody, Rp2/98pFA2pFn1). 	<ul style="list-style-type: none"> • Cobblestone endothelial cells negative for MSF in 4/5 experiments when plated on 2D surface and 5/7 experiments when plated on 3D surface. Sprouting endothelial cells consistently positive for MSF irrespective of plating matrix (within a 3D collagen gel or post-confluent sprouting on 2D surface coated with 0.1% (w/v) gelatin).
3. To characterise the bioactivity of endothelial cells expressing a sprouting phenotype.	<ul style="list-style-type: none"> • Size exclusion chromatography (Superdex).* • SDS Electrophoresis.* 	<ul style="list-style-type: none"> • Motogenic bioactivity detected in fraction groups 11-15, equivalent to a MW >70kDa. MSF- inhibitory activity detected in fraction groups 19, 20, and 23, equivalent to a MW ≤ 25kDa. • Motogenic bioactivity detected in gel elutions 2-3, equivalent to a MW 75-100kDa. MSF- inhibitory activity detected in gel elutions 4-5 equivalent to a MW 25-75kDa.

<p>4. To characterise the bioactivity of endothelial cells expressing a cobblestone phenotype.</p>	<ul style="list-style-type: none"> • Size exclusion chromatography (Superdex).* • SDS Electrophoresis.* 	<ul style="list-style-type: none"> • Motogenic bioactivity detected in fraction groups 11-14, equivalent to a MW >70kDa. MSF- inhibitory activity detected in fraction groups 19, 21, 22-24, equivalent to a MW ≤ 25kDa. • Motogenic bioactivity detected in gel elutions 3-4, equivalent to a MW 37-100kDa. MSF- inhibitory activity detected in gel elution 8 equivalent to a MW approximately 20kDa.
<p>5. To determine whether MSF was responsible for the motogenic activity detected in fractionated endothelial CM.</p>	<ul style="list-style-type: none"> • IGD Function Neutralisation of Motogenic Activity (Pep Q 1.1 antibody). * • NGAL inhibition of motogenic activity.* 	<ul style="list-style-type: none"> • Motogenic active fractionated sprout and cobblestone CM (SEC and SDS PAGE) showed only partial inhibition, failing to reach set criteria of 50% inhibition. • Motogenic active fractionated sprout and cobblestone CM (SEC and SDS PAGE) showed only partial inhibition, failing to reach set criteria of 50% inhibition.
<p>6. To determine what effect MSF had on endothelial morphology.</p>	<ul style="list-style-type: none"> • 2D Post-confluent endothelial sprouting assay. 	<ul style="list-style-type: none"> • rhMSF stimulated cobblestone endothelial cells to exhibit a sprouting morphology. 100ng/ml rhMSF increased number of sprouts 3 fold compared to control. rhMSF appears to stimulate formation of sprout associations.
<p>7. To determine the effect IGD Function Neutralisation, PEPQ 1.1 antibody had on endothelial morphology.</p>	<ul style="list-style-type: none"> • 3D Spontaneous endothelial sprouting assay. 	<ul style="list-style-type: none"> • 24 hour exposure to 20-30µg/ml PEPQ 1.1 antibody decreased sprout numbers. By 48hours majority of sprouts underwent apoptosis.
<p>8. To determine the effect MSF inhibitor, NGAL had on endothelial morphology.</p>	<ul style="list-style-type: none"> • 2D Post-confluent endothelial sprouting assay. 	<ul style="list-style-type: none"> • NGAL from three sources tested with similar results. 1-100ng/ml rhNGAL, no effect. 500ng-1µg/ml rhNGAL inhibited sprout development and disruption of cobblestone monolayer (vacuole formation and cell death).

	<ul style="list-style-type: none"> • 3D Spontaneous endothelial sprouting assay. • Endothelial proliferation and viability assay. 	<ul style="list-style-type: none"> • NGAL from three sources tested with similar results. 1-100ng/ml rhNGAL, no effect. 500ng-1µg/ml rhNGAL decreased sprout numbers within 48 hours, majority of sprout undergoing apoptosis by Day 5. • Prokaryotic and eukaryotic rhNGAL tested with similar results. 10-100ng/ml rhNGAL, no effect. 1µg/ml rhNGAL decreased proliferation by 20.5 +/- 5.14% and 23.2 +/- 5.49% with prokaryotic and eukaryotic rhNGAL, respectively. rhNGAL had no effect on endothelial cell viability.
--	---	--

***bioactivity confirmed by testing in the 3D collagen gel fibroblast migration assay.**

CHAPTER 9

FUTURE WORK

Although this project has achieved its original aim and identified an inhibitor of MSF, new discoveries have unleashed a plethora of questions and potential routes of investigation. Prospective future studies could include the following:

- A major obstacle encountered during this project was the inability to identify and quantify MSF in CM by immunoblot and ELISA techniques, respectively. The antibodies used in the identification assays recognised the unique decapeptide sequence of MSF which may no longer be recognisable when MSF is secreted into CM either due to conformational change, masking due to association with an accessory protein(s) or degradation by proteolytic enzymes (the VSI sequence is vulnerable to proteolysis due to its C-terminus location). The addition of protease inhibitors to the CM upon collection would have reduced proteolysis but this may have limited any subsequent *in vitro* analysis of bioactivity.
The suitability of the Rp VSI antibody for use in the immunoblot and ELISA assay was also questioned. A frequent obstacle was poor reproducibility and an inadequate rhMSF standard curve in the ELISA assay. However, the same antibody was successfully used in both immunohistochemical and immunoprecipitation assays; implying its use is limited to specific applications. Therefore, the development of improved specific anti-MSF antibodies is required. Yet, as MSF is a truncated form of fibronectin, identical to the N-terminus of fibronectin, the choice of a specific epitope will be restricted to the unique decapeptide sequence.
- It was the original observations of the disparity in migratory potential between adult and foetal fibroblasts (Schor *et al.*, 1985) that eventually led to the discovery of MSF. MSF was subsequently shown to be responsible for the greater migratory activity of the foetal fibroblasts. It will, therefore be of interest to determine whether NGAL can directly affect the migratory activity of the foetal fibroblasts; that is, can NGAL inhibit endogenous MSF activity as well as the activity of exogenous MSF?

Pre-incubating adult fibroblasts with NGAL resulted in the cells becoming unresponsive to MSF, implying that NGAL does not require direct association with MSF in order to exert its inhibitory effect. Consequently, what is the effect on the migratory activity of foetal fibroblasts if they are pre-exposed to NGAL before assessment in a migratory assay? The 3D type I collagen gel assay will be invaluable in this investigation, although it would be interesting to determine whether the same result is achieved in the Boyden chamber migration assay too.

- The mechanism NGAL uses to inhibit MSF clearly requires further exploration. Preliminary experiments revealed that direct association between NGAL and MSF is not required and that MSF-I activity of NGAL is not reliant upon its ability to transport iron. Numerous functions have been attributed to NGAL; of particular interest is the ability to preserve the enzymatic activity of MMP-9 by protecting it from proteolytic degradation (Yan *et al.*, 2001). Matrix metalloproteinases are capable of degrading all of the molecular components of the ECM, including fibronectin (Fn). A study of monocytes has revealed a feedback loop exists between MMP-9 and fibronectin; as MMP-9 degrades Fn and binding of Fn upregulates the expression of MMP-9 (Marom *et al.*, 2007). It will therefore be of interest to determine whether MMP-9 is implicated in the process of NGAL inhibition of MSF. That is, is the MSF-I activity of NGAL actually a consequence of its protective role of MMP-9? Knowing the characteristic bell-shaped dose- response behaviour of MSF bioactivity is the reduction in MSF bioactivity actually a consequence of the production of Fn breakdown fragments containing the GBD sequence which contribute to a shift in concentration levels to those which actually inhibit cell migration. Or does MSF inhibition by NGAL actually result from NGAL protecting MSF from degradation, therefore leading to an accumulation of MSF to concentrations where cell migration is inhibited rather than stimulated?
- Through a series of bioactivity and identification techniques the variation in the expression of NGAL and MSF by the HaCaT series cell lines was revealed. However, this data could be further validated by measuring MSF and NGAL gene expression levels by reverse transcription polymerase chain reaction (RT-PCR).

- The HaCaT series of cell lines were originally classified by their growth behaviour and histological phenotype when subcutaneously injected into nude mice. That is, the HaCaT keratinocytes were non-tumourigenic, the BEN keratinocytes formed epidermoid cysts, MAL formed well-differentiated squamous cell carcinomas and MET exhibited a metastatic phenotype spreading to the lung and lymph nodes (Mueller *et al.*, 2001). By genetically modifying the expression levels of NGAL and MSF in the HaCaT series cell lines the effect on the tumourigenic potential could be investigated; to determine whether an alteration in the ratio of NGAL and MSF expression would result in a change in the cell lines ability to form tumours in nude mice. This could lead to a greater understanding of the roles NGAL and MSF play during epithelial- mesenchymal transition and possible clinical relevance of NGAL and MSF as biomarkers of EMT. For this investigation the technique of gene silencing using small interfering RNAs (siRNA) could be employed to reduce and potentially eliminate NGAL and MSF protein production.
- Although MSF-I activity was detected in endothelial CM, further work is still required to identify the factor responsible. Preliminary experiments to fractionate the endothelial CM by size-exclusion chromatography and SDS electrophoresis failed to pinpoint a specific MW where MSF-I activity could be located. In addition, the HaCaT series experiments also revealed that the CM concentration process may result in non-specific binding of proteins and proteins precipitating out of solution. Therefore, a more efficient approach to identify endothelial MSF-I should adopt a different fractionation process, for example ion-exchange chromatography and use less concentrated CM. Once the source of endothelial MSF-I activity has been identified it will be of interest to determine the relationship it has with the co- expressed MSF and whether it plays a role in regulating endothelial phenotype. In addition, do endothelial MSF-I and the keratinocyte MSF-I, NGAL, act in a similar manner to inhibit MSF and are they substitutable?
- *In vitro* endothelial sprouting assays testing the effect of NGAL on both sprout and cobblestone phenotypes, revealed its ability to induce programmed cell death. NGAL is known to induce apoptosis due to its ability to chelate iron triggering cellular iron deprivation (Tong *et al.*, 2008). Therefore, future

sprouting assays should include the iron chelator, DFOM, in order to determine whether NGAL anti-angiogenic activity is due to its ability to transport iron.

However, since different sources of NGAL (prokaryotic and eukaryotic) achieved similar results it would imply that iron transportation is not involved, as each source would possess varying amounts of bound iron.

Other studies have reported the anti-angiogenic activity of NGAL is associated with either a decrease in VEGF production or a blockade of VEGF receptor (Tong *et al.*, 2008). Consequently, the relationship between NGAL and VEGF is also another avenue for investigation. In addition, the *in vivo* anti-angiogenic activity of NGAL should be investigated.

- Further investigation is required to understand the role MSF plays during angiogenesis. This project has shown that MSF pro-angiogenic bioactivities include its ability to induce endothelial cells, *in vitro*, to undertake a phenotypic change from the cobblestone to the sprouting phenotype and its role as a survival factor for sprouting endothelial cells. The ability of the IGD function neutralising monoclonal antibody, PEPQ 1.1 to specifically induce apoptosis of endothelial sprouts implies that the IGD motif must be implicated in the role of MSF as a sprout survival factor. The development of mutant forms of MSF, by site- directed mutagenesis and their subsequent testing in *in vitro* and *in vivo* angiogenic assays should reveal which MSF domains are responsible for its pro-angiogenic bioactivities.

Chapter 10**REFERENCES****A**

Abdollahi A., Hlatky L., Huber P.E. Endostatin: the logic of antiangiogenic therapy. *Drug Resistance Update*, 2005, 8, 59-74.

Adams R.H., Alitalo K. Molecular regulation of angiogenesis and lymphangiogenesis. *Nature Review, Molecular Cell Biology*, 2007, 8, 464-478.

Aird W.C. Endothelial cell heterogeneity. *Cold Spring Harbor Perspectives in Medicine*, 2012, 2, a006429.

Aird W.C. Phenotypic heterogeneity of the endothelium. *Circulation Research*, 2007, 100, 158-173.

Aljorani L.E., A.Bankfalvi et al., Migration-stimulating factor as a novel biomarker in salivary gland tumours. *Journal of Oral Pathology and Medicine*, 2011, 40 (10), 747-754.

Allen T.D, Schor S.L., Schor A.M. Ultrastructural review of collagen gels, a model system for cell-matrix cell- basement membrane and cell- cell interactions. *Scanning Electron Microscopy*, 1984, V, 375-390.

Alonso S.R., et al. A high-throughput study in melanoma identifies epithelial-mesenchymal transition as a major determinant of metastasis. *Cancer Research*, 2007, 67, 3450-3460.

Alpini G., et al. Regulation of placental growth factor by microRNA-125b in hepatocellular cancer. *Journal of Hepatology*, 2011, 55 (6), 1339-1345.

Ananthaswamy H N, Pierceall W E. Molecular alterations in human skin tumours. *Progress in Clinical Biological Research*, 1992, 376, 61-84.

Ansieau S., et al. Induction of EMT by twist proteins as a collateral effect of tumour-promoting inactivation of premature senescence. *Cancer Cell*, 2008, 14 (1), 79-89.

Auerbach R., et al. A simple procedure for the long-term cultivation of chicken embryos. *Developmental Biology*, 1974, 41, 391-394.

Auerbach W., Auerbach R. Angiogenesis inhibition: a review. *Pharmacology & Therapeutics*, 1994, 63, 265-311.

B

- Bahmani P., et al.**, Neutrophil gelatinase –associated lipocalin induces the expression of heme oxygenase-1 and superoxide dismutase 1, 2. *Cell Stress Chaperones*, 2010, 15, 395-403.
- Bando M., et al.** Interleukin-1alpha regulates antimicrobial peptide expression in human keratinocytes. *Immunology and Cell Biology*, 2007, 532-537.
- Bardeesy N., et al.** Smad4 is dispensable for normal pancreas development yet critical in progression and tumour biology of pancreas cancer. *Genes Development*, 2006, 20, 3130-3146.
- Bartsch S. Tschesche H.** Cloning and expression of human neutrophil lipocalin cDNA derived from bone marrow and ovarian cancer cells. *FEBBS Letters*, 1995, 357, 255-259.
- Bastid J.** EMT in carcinoma progression and dissemination: facts, unanswered questions, and clinical considerations. *Cancer Metastasis Review*, 2012, 31, 277-283.
- Battle E., et al.** The transcription factor Snail is a repressor of E-cadherin gene expression in epithelial tumour cells. *Nature Cell Biology*, 2000, 2 (2), 84-89.
- Bauer M., et al.** Neutrophil gelatinase-associated lipocalin is a predictor of poor prognosis in human primary breast cancer. *Breast Cancer Research Treatment*, 2008, 108, 389-397.
- Belalcazar A et al.** Targeting the Met pathway in lung cancer. *Expert Review of Anticancer Therapy*, 2012, 12 (4), 519-528.
- Bergers G., Hanahan D., Coussens L.M.** Angiogenesis and apoptosis are cellular parameters of neoplastic progression in transgenic mouse models of tumorigenesis. *International Journal of Developmental Biology*, 1998, 42, 995-1002.
- Bergers G., et al.** Benefits of targeting both pericytes and endothelial cells in tumour vasculature with kinase inhibitors. *Journal of Clinical Investigation*, 2003, 111, 1287-1295.
- Bergers G, Hanahan D.** Modes of resistance to anti-angiogenic therapy. *Nature Reviews Cancer*, 2008, 8, 592-603.
- Bergsland E.K.** Update on clinical trials targeting vascular endothelial growth factor in cancer. *American Journal of Health-System Pharmacy*, 2004, 61, 12-20.
- Bernier S.G., et al.** Fumagillin class inhibitors of methionine aminopeptidase-2. *Drugs of the Future*, 2005, 30 (5), 497-508.
- Bingle L., Brown N.J., Lewis C.E.** The role of tumour-associated macrophages in tumour progression: implications for new anticancer therapies. *Journal of Pathology*, 2002, 196, 254-265.
- Bissell M.J., et al.** The organising principle: microenvironment influences in the normal and malignant breast. *Differentiation*, 2002, 70, 537-546.
- Blehschmidt K., et al.** The E-cadherin repressor Snail is associated with lower overall survival of ovarian cancer patients. *British Journal of Cancer*, 2008, 98, 489-495.
- Boehm T., et al.** Anti-angiogenic therapy of experimental cancer does not induce acquired drug resistance. *Nature*, 1997, 390, 404-407.

- Boekhorst B.C., et al.** Molecular MRI of murine atherosclerotic plaque targeting NGAL: a protein associated with unstable human plaque characteristics. *Cardiovascular Research*, 2011, 89, 680-688.
- Bolignano G., et al.** From kidney to cardiovascular diseases: NGAL as a biomarker beyond the confines of nephrology. *European Journal of Clinical Investigation*, 2010, 40, 273-276.
- Bolignano G., et al.** Neutrophil Gelatinase –associated lipocalin (NGAL) in human neoplasias: a new protein enters the scene. *Cancer Letters*, 2010, 288, 10-16.
- Bonnomet A., et al.** A dynamic *in vivo* model of epithelial to mesenchymal transitions in circulating tumour cells and metastases of breast cancer. *Oncogene*, 2012, 31, 3741-3753.
- Boukamp P. et al.** Normal keratinization in a spontaneously immortalised aneuploid human keratinocyte cell line. *The Journal of Cell Biology*, 1988, 106, 761-771.
- Boukamp P, Stanbridge Ej, Foo DY, Cerutti PA, Fusenig NE.** c-Ha-ras oncogene expression in immortalised human keratinocytes (HaCaT) alters growth potential *in vivo*, but lacks correlation with malignancy. *Cancer Research* 1990, 50, 2840-2847.
- Boukamp P., et al.** Sustained nontumorigenic phenotype correlates with a largely stable chromosome content during long-term culture of the human keratinocyte line HaCaT. *Genes, Chromosomes and Cancer*, 1997, 19, 201-214.
- Boukamp P., et al.** Functional evidence for tumour-suppressor activity on chromosome 15 in human skin carcinoma cells and thrombospondin-1 as the potential suppressor. *Journal of Cell Physiology*, 1997, 173, 256-260.
- Brabletz T., et al.** Variable β -catenin expression in colorectal cancers indicates tumour progression driven by the tumour environment. *Proceedings of National Academy of Science, America*, 2001, 98, 10356-10361.
- Brash D.E., et al.** Role of sunlight in skin cancer: UV induced p53 mutations in squamous cell carcinoma. *Proceedings National Academy of Sciences, America*, 1991, 88, 10124-10128.
- Bratt T.** Lipocalins and cancer. *Biochimica Biophys Acta*, 2000, 1482, 318-326.
- Breitkreutz D et al.** Epidermal differentiation and basement membrane formation by HaCaT cells in surface transplants. *European Journal of Cell Biology*, 1998, 75, 273-286.
- Brekken R.A., et al.** Selective inhibition of vascular endothelial growth factor (VEGF) receptor 2 activity by a monoclonal anti-VEGF antibody blocks tumour growth in mice. *Cancer Research*, 2000, 60, 5117-5124.
- Brenner M., Hearing V.J.** The protective role of melanin against UV damage in human skin. *Photochemistry and Photobiology*, 2008, 84 (3), 539-549.
- Brooks P.C., et al.** Requirement of vascular integrin α v β 3 for angiogenesis. *Science*, 1994, 264, 569-571.
- Browder T., et al.** Antiangiogenic scheduling of chemotherapy improves efficacy against experimental drug-resistant cancer. *Cancer Research*, 2000, 60, 1878-1886.

Bruns C.J., et al. Vasucular endothelial growth factor is an *in vivo* survival factor for tumour endothelium in a murine model of colorectal carcinoma liver metastases. *Cancer*, 2000, 89, 488-499.

Burk U., et al. A reciprocal repression between ZEB1 and members of the miR-200 family promotes EMT and invasion in cancer cells. *EMBO Reproduction*, 2008, 9, 582-589.

Burri P.H., Hlushchuk R., Djonov V. Intussusceptive angiogenesis; its emergence, its characteristics, and its significance. *Developmental Dynamics*, 2004, 1654, 13-22.

C

Canefield A.E., Schor A.M., Schor S.L., Grant M.E. The biosynthesis of extracellular- matrix components by bovine retinal endothelial cells displaying distinctive morphological phenotypes. *Journal of Biochemistry*, 1986, 235, 375-383.

Canefield A.E., Boot-Handford R.P., Schor A.M. Thrombospondin gene expression by endothelial cells in culture is modulated by cell proliferation, cell shape and the substratum. *Journal of Biochemistry*, 1990, 268, 225-230.

Canefield A.E., et al. Aortic endothelial cell heterogeneity in vitro. Lack of association between morphological phenotype and collagen biosynthesis. *Journal of Science*, 1992, 102, 807-814.

Canefield A.E., Schor A.M. Evidence that tenascin and thrombospondin-1 modulate sprouting of endothelial cells. *Journal of Cell Science*, 1995, 108, 797-809.

Cano A., et al. The transcription factor snail controls epithelial-mesenchymal transition by repressing E-cadherin expression. *Nature Cell Biology*, 2000, 2 (2), 76-83.

Cao Y., et al. Elevated levels of urine angiostatin and plasminogen/ plasmin in cancer patients. *International Journal of Molecular Medicine*, 2000, 5, 547-551.

Cao Y., et al. Improvements of antiangiogenic cancer therapy by understanding the mechanisms of angiogenic factor interplay and drug resistance. *Seminars in Cancer Biology*, 2009, 19, 338-343.

Carito V., et al. Metabolic remodelling of the tumour microenvironment. Migration stimulating factor (MSF) reprograms myofibroblasts toward lactate production, fueling anabolic tumour growth. *Cell Cycle*, 2012, 11 (18), 3403-3414.

Carmeliet P., et al. Abnormal blood vessel development and lethality in embryos lacking a single VEGF allele. *Nature*, 1996, 380, 435-439.

Carmeliet P. Angiogenesis in health and disease. *Nature Medicine*, 2003, 9, 653-660.

Carmeliet P. Angiogenesis in life, disease and medicine. *Nature*, 2005, 438 (15), 932-936.

Carmeliet P., Tesser-Lavigne M. Common mechanisms of nerve and blood vessel wiring. *Nature*, 2005, 436, 193-200.

- Carmeliet P., Jain R. K.** Molecular mechanisms and clinical applications of angiogenesis. *Nature*, 2011, 473, 298-307.
- Casanovas O., et al.** Drug resistance by evasion of antiangiogenic targeting of VEGF signalling in late-stage pancreatic islet tumours. *Cancer Cell*, 2005 8, 299-309.
- Chaffer C.L., et al.** Mesenchymal-to-epithelial transition facilitates bladder cancer metastasis: Role of fibroblast growth factor receptor-2. *Cancer Research*, 2006, 66 (23), 11271-11278.
- Chakraborty S., et al.,** The multifaceted roles of neutrophil gelatinase associated lipocalin (NGAL) in inflammation and cancer. *Biochimica et Biophysica Acta*, 2012, 1826, 129-169.
- Chang C.J., et al.** p53 regulates epithelial-mesenchymal transition and stem cell properties through modulating miRNAs. *Nature Cell Biology*, 2011, 13 (3), 317-323.
- Chen C.N., et al.** Identification of calreticulin as a prognosis marker and angiogenic regulator in human gastric cancer. *Annals of Surgical Oncology*, 2009, 16, 524-533.
- Chen J., Imanaka N., Griffin J.D.** Hypoxia potentiates Notch signalling in breast cancer leading to decreased E-cadherin expression and increased cell migration and invasion. *British Journal of Cancer*, 2010, 102, 351-360.
- Chen L., Chan Y.R.** Lipocalin 2 regulation and its complex role in inflammation and cancer. *Cytokine*, 2011, 56, 435-441.
- Cheng G.Z., et al.** Twist transcriptionally up-regulates AKT2 in breast cancer cells leading to increased migration, invasion, and resistance to paclitaxel. *Cancer Research*, 2007, 67, 1979-1987.
- Cho H., Kim J.** Lipocalin2 expressions correlate significantly with tumour differentiation in epithelial ovarian cancer. *Journal of Histochemistry and Cytochemistry*, 2009, 57 (5), 513-52.
- Chua, K.N., Ma J., Theiry J.P.** Targeted therapies in control of EMT in carcinoma and fibrosis. *Drug Discovery Today*, 2008, 4, 261-267.
- Chung A.S., Lee J., Ferrara N.** Targeting the tumour vasculature: insights from physiological angiogenesis. *Nature Reviews Cancer*, 2010, 10, 505-514.
- Chung A.S., Ferrara N.** Developmental and pathological angiogenesis. *Annual Review Cellular Developmental Biology*, 2011, 27, 563-584.
- Chung C.H., et al.** Molecular classification of head and neck squamous cell carcinomas using patterns of gene expression. *Cancer Cell*, 2004, 5, 489-500.
- Chung C.H., et al.** Gene expression profiles identify epithelial-to-mesenchymal transition and activation of nuclear factor κ B signalling as characteristics of a high risk head and neck squamous cell carcinoma. *Cancer Research*, 2006, 66, 8210-8218.
- Citron M.L., et al.** Randomised trial of dose-dense versus conventionally scheduled and sequential versus concurrent combination chemotherapy as postoperative adjuvant treatment of node-positive primary breast cancer: first report of Intergroup Trial C9741/Cancer and Leukaemia Group B Trial 9741. *Journal of Clinical Oncology*, 2003, 21, 1431-1439.

- Claesson-Welsh L.** Blood vessels as targets in tumour therapy. *Upsala Journal of Medical Sciences*, 2012, 117, 178-186.
- Cochrane D.R., et al.** MicroRNA-200c mitigates invasiveness and restores sensitivity to microtubule-targeting chemotherapeutic agents. *Molecular Cancer Therapeutics*, 2009, 8, 1055-1066.
- Coles M., et al.** The solution, structure and dynamics of human neutrophil gelatinase-associated lipocalin. *Journal of Molecular Biology* 1999, 289, 139-157.
- Cooper A.C., et al.** A novel methionone aminopeptidase-2 inhibitor, PPI-2458, inhibits non-Hodgkin's lymphoma cell proliferation in vitro and in vivo. *Clinical Cancer Research*, 2006, 12, 2583-2590.
- Cotta-Pereira G., et al.** Studies of morphologically atypical (sprouting) cultures of bovine aortic endothelial cells. Growth characteristics and connective tissue protein synthesis. *Journal of Cell Physiology*, 1980, 102, 183-191.
- Coultas L., Chawengsaksophak K., Rossant J.** Endothelial cells and VEGF in vascular development. *Nature* 2005, 438, 937-945.
- Cui L., et al.** NAGLR is overexpressed and regulated by hypomethylation in oesophageal squamous cell carcinoma. *Clinical Cancer Research*, 2008, 14, 7674-7681.
- Current protocols in Protein Science** 1990. Supp.8.4, John Wiley & Sons, Inc.
- Coussens L.M., et al.** MMP-9 supplied by bone marrow-derived cells contributes to skin carcinogenesis. *Cell*, 2000, 103, 481-490.
- Coussens L. M., Werb Z.** Inflammation and cancer. *Nature*, 2002, 420, 860-867.
- Cramer E.P., et al.** No effect of NGAL/Lipocalin-2 on aggressiveness of cancer in the *MMTV-PyMT/FVB/N* mouse model for breast cancer. *PLoS ONE*, 2012, 7 (6), e39646.

D

- Dawson P.J., et al.** MCF1-10AT: A model for the evolution of cancer from proliferative breast disease. *American Journal of Pathology*, 1996, 148 (1), 313-319.
- Dayan F., et al.** A dialogue between the hypoxia-inducible factor and the tumour microenvironment. *Cancer Microenvironment* 2008, 1, 53-68.
- DeBock K., et al.** Vessel abnormalisation: another hallmark of cancer? Molecular mechanisms and therapeutic implications. *Current Opinion in Genetics and Development*, 2011, 21, 73-79.
- Deckers M., et al.** The tumour suppressor Smad4 is required for transforming growth factor β induced epithelial to mesenchymal transition and bone metastasis of breast cancer cells. *Cancer Research*, 2006, 66, 2202-2209.

- De Craene B., Berx G.** Regulatory networks defining EMT during cancer initiation and progression. *Nature Reviews Cancer*, 2013, 13, 97-110.
- Dell'Eva R., et al.** Inhibition of tumour angiogenesis by angiostatin: from recombinant protein to gene therapy. *Endothelium*, 2002, 9 (1), 3-10.
- Deng X., et al.** Migration-stimulating factor (MSF) is over-expressed in non-small cell lung cancer and promotes cell migration and invasion in A549 cells overexpressing MSF. *Experimental Cell Research*, 2013, 319, 2545-2553.
- Derynck R., Akhurst R.J., Balmain A.** TGF β signalling in tumour suppression and cancer progression. *Nature Genetics*, 2001, 29, 117-129.
- Devireddy L.R., et al.** A cell- surface receptor for lipocalin 24p3 selectively mediates apoptosis and iron uptake. *Cell*, 2005, 123, 1293-1305.
- Ding L., et al.** Lipocalin-2/Neutrophil gelatinase-B associated lipocalin is strongly induced in hearts of rats with autoimmune myocarditis and in human myocarditis. *Circulation Journal*, 2010, 74, 523-530.
- Dinney C.P., et al.** Inhibition of basic fibroblast growth factor expression, angiogenesis, and growth of human bladder carcinoma in mice by systemic interferon- α administration. *Cancer Research* 1998, 58, 808-814.
- DiMasi J.A., et al.** The price of innovation: new estimates of drug development costs. *Journal of Health Economics*, 2003, 22, 151-185.
- DiPalo J.A.** Relative difficulties in transforming human and animal cell in vitro. *Journal of National Cancer Institute*, 1983, 70, 3-8.
- DiPersio J.F. et al.** Phase III prospective randomised double-blind placebo-controlled trial of plerixfor plus G-CSF compared with placebo plus G-CSF for autologous stem-cell mobilisation and transplantation for patients with non-Hodgkin's lymphoma. *Journal of Clinical Oncology*, 2009, 27, 4767-4773.
- Doane K.J., Birk D.E.** Fibroblasts retain their tissue phenotype when grown in three-dimensional collagen gels. *Experimental Cell Research*, 1991, 195, 432-442.
- Dorland W.A.** *Dorland's illustrated medical dictionary*. 1965, 24th Edition. Philadelphia (PA), Saunders Co.
- Dufraine J., et al.** Notch signalling regulates tumour angiogenesis by diverse mechanisms. *Oncogene*, 2008, 27, 5124-5131.
- Dunehoo A.L., et al.** Cell adhesion molecules for targeted drug delivery. *Journal of Pharmacological Science*, 2006, 95, 1856-1872.
- Dunn L.L., et al.** Iron uptake and metabolism in the new millennium. *Trends in Cell Biology*, 2007, 17, 93-100.

E

Eagan T.M., et al. Neutrophil gelatinase-associated lipocalin: a biomarker for COPD. *Chest*, 2010, 888-895.

Eberhard A., et al. Heterogeneity of angiogenesis and blood vessel maturation in human tumours; implications for antiangiogenic tumour therapies. *Cancer Research*, 2000, 60, 1388-1393.

Ebos J.M.L., et al. Accelerated metastasis after short-term treatment with a potent inhibitor of tumour angiogenesis. *Cancer Cell*, 2009, 15, 232-239.

Ebos J.M., et al. Tumour and host-mediated pathways of resistance and disease progression in response to antiangiogenic therapy. *Clinical Cancer Research*, 2009, 15, 5020-5025.

Ellis I., Grey A-M., et al. Antagonistic effects of transforming growth factor β and MSF on fibroblast migration and hyaluronic acid synthesis: possible implications for wound healing. *Journal of Cell Science*, 1992, 102,447-456.

Ellis I., Jones S.J. et al. Multi-factorial modulation of IGD motogenic potential in MSF (Migration Stimulating Factor). *Experimental Cell Research*, 2010, 316 (15), 2465-2476.

Ellis I., et al. Migration stimulating factor (MSF) promotes fibroblast migration by inhibiting AKT. *Cellular Signalling*, 2010, 22, 1655-1659.

Erdreich-Epstein A, et al. Integrins alpha v beta 3 and alpha v beta 5 are expressed by endothelium of high-risk neuroblastoma and their inhibition is associated with increased endogenous ceramide. *Cancer Research*, 2000, 60, 712-721.

Eremina V., Baelde H.J., Quaggin S.E. Role of the VEGF-A signalling pathway in the glomerulus: Evidence for crosstalk between components of the glomerular filtration barrier. *Nephron Physiology*, 2007, 106, 32-37.

F

Faivre S., et al. Safety, pharmacokinetic, and antitumour activity of SU11248, a novel oral multi-target tyrosine kinase inhibitor, in patients with cancer. *Journal of Clinical Oncology*, 2006, 24, 25-35.

Fakhrejehani E., Toi M. Tumour angiogenesis: pericytes and maturation are not to be ignored. *Journal of Oncology*, 2012, 261750.

Fang W.K., et al. A novel alternative spliced variant of neutrophil gelatinase-associated lipocalin receptor in oesophageal carcinoma cells. *Biochemistry Journal*, 2007, 403, 297-303.

Fearon ER, Volgestein B. A genetic model for colorectal carcinogenesis. *Cell*, 1990, 61, 759-767.

- Fernandez M., et al.** The matrix metalloproteinase e-9/neutrophil gelatinase associated lipocalin complex plays role in breast tumour growth and is present in the urine of breast cancer patients. *Clinical Cancer Research*, 2005, 11, 5390-5395.
- Ferrantini M., et al.** Interferon-alpha and cancer: mechanisms of action and new perspectives of clinical use. *Biochimie*, 2007, 89 (6-7), 884-893.
- Ferrara N., Henzel W.J.** Pituitary follicular cells secrete a novel heparin-binding growth factor specific for vascular endothelial cells. *Biochemical & Biophysical Research Communication*, 1989, 161, 851-858.
- Ferrara N.** Vascular endothelial growth factor: basic science and clinical progress. *Endocrinology Review*, 2004, 25, 581-611.
- Ferrara N., et al.** Discovery and development of bevacizumab, an anti-VEGF antibody for treating cancer. *Nature Review Drug Discovery*, 2004, 3, 391-400.
- Ferrara N.** Role of myeloid cells in vascular endothelial growth factor- independent tumour angiogenesis. *Current Opinion in Hematology*, 2010, 17, 219-224.
- Fett J.W., et al.** Isolation and characterisation of angiogenin, an angiogenic protein from human carcinoma cells. *Biochemistry*, 1985, 24, 5480-5486.
- Fidler I.J.** The pathogenesis of cancer metastasis: the 'seed and soil' hypothesis revisited. *Nature Reviews Cancer*, 2003, 3, 453-458.
- Fishman P.H., Curran P.K.** Brefeldin A inhibits protein synthesis in cultured cells. *FEBS Letters*, 1992, 314 (3), 371-374.
- Flaherty K.T.** Sorafenib: Delivering a targeted drug to the right targets. *Expert Review Anticancer Therapy*, 2007, 7, 617-626.
- Flo T.H., et al.** Lipocalin 2 mediates an innate immune response to bacterial infection by sequestering iron. *Nature*, 2004, 432, 917-921.
- Flower D.R.** The lipocalin protein family: structure and function. *Biochemical Journal*, 1996, 318, 1-14.
- Flower D.R.** The lipocalin protein family: structural and sequence overview. *Biochimica Biophys Acta*, 2000, 1482, 9-24.
- Folkman J.** Tumour angiogenesis: therapeutic implications. *New England Journal of Medicine*, 1971, 285, 1182-1186.
- Folkman J., Haudenschild C.C., Zetter B.R.** Long-term culture of capillary endothelial cells. *Proceeding of National Academy of Sciences, America*, 1979, 76, 10, 5217-5221.
- Folkman J., Haudenschild C.C.** Angiogenesis *in vitro*. *Nature*, 1980, 288, 551-556.
- Folkman J., Haudenschild C.C.** Angiogenesis by capillary endothelial cells in culture. *Transactions of the Ophthalmological Societies of the United Kingdom*, 1980, 100 (3), 346-353.
- Folkman J.** What is the evidence that tumours are angiogenesis dependent? *Journal of the National Cancer Institute*, 1990, 82, 4-6.

- Folkmann J.** Antiangiogenesis in cancer therapy- endostatin and its mechanisms of action. *Experimental Cell Research*, 2006, 312, 594-607.
- Foulds L.** The experimental study of tumour progression. 1954, Volumes I-III, Academic Press, London.
- Franco M., et al.** Targeted anti-vascular endothelial growth factor receptor-2 therapy leads to short-term and long-term impairment of vascular function and increase in tumour hypoxia. *Cancer Research*, 2006, 66, 3639- 3648.
- Fredriksson L., Li H., Eriksson U.** The PDGF family; four gene products form five dimeric isoforms. *Cytokine Growth Factor Review*, 2004, 15, 197-204.
- Friedl P., Brocker E-B.** The biology of cell locomotion within three-dimensional extracellular matrix. *Cellular and Molecular Life Sciences*, 2000, 57, 41-64.
- Friedl P., Wolf K.** Tube travel: the role of proteases in individual and collective cancer cell invasion. *Cancer Research*, 2008, 68, 7247-7249.
- Friedl P., Wolf K.** Plasticity of cell migration: a multiscale tuning model. *Journal of Cell Biology*, 2010, 188, 11-19.
- Furutani M., et al.** Identification of neutrophil gelatinase-associated lipocalin mRNA in human pancreatic cancers using a modified signal sequence trap method. *Cancer Letters*, 1998, 122, 209-214.
- Fuchs B.C., et al.** Epithelial-to –mesenchymal transition and integrin-linked kinase mediate sensitivity to epidermal growth factor receptor inhibition in human hepatoma cells. *Cancer Research*, 2008, 68, 2391-2399.
- Fuchs E.** Epidermal Differentiation: The Bare Essentials. *Journal of Cell Biology* 1990, 111, 2807-2814.
- Fusenig N.E., Boukamp P.** Multiple stages and genetic alterations in immortalisation, malignant transformation and tumour progression of human skin keratinocytes. *Molecular Carcinogenesis*, 1998, 23, 144-158.

G

- Gal A., et al.** Sustained TGF β exposure suppresses Smad and non-Smad signalling in mammary epithelial cells, leading to EMT and inhibition of growth arrest and apoptosis. *Oncogene*, 2008, 27, 1218-1230.
- Galvez B.G., et al.** Membrane type 1-matrix metalloproteinase is activated during migration of human endothelial cells and modulates endothelial cells and modulates endothelial motility and matrix remodelling. *Journal of Biological Chemistry*, 2001, 276, 37941-37950.
- Gasparini G.** The rationale and future potential of angiogenesis inhibitors in neoplasia. *Drugs*, 1999, 58, 17-38.

- Gasparrini G.** Metronomic scheduling: The future of chemotherapy? *Lancet Oncology*, 2001, 2, 733-740.
- Gerber H.P., et al.** VEGF couples hypertrophic cartilage remodelling, ossification and angiogenesis during endochondral bone formation. *Nature Medicine*, 1999, 5, 623-628.
- Gerber H.P., et al.** VEGF is required for growth and survival of neonatal mice. *Development*, 1999, 126, 1149-1159.
- Gay R, Swiderek M., Nelson D., Ernesti A.** The living skin equivalent as a model *in vitro* for ranking the toxic potential of dermal irritation. *Toxic In Vitro*. 1992, 6, 303-315.
- Gimbrone Jr. M.A., et al.** Tumour angiogenesis: iris neovascularisation at a distance from experimental intraocular tumours. *Journal of National Cancer Institute*, 1973, 50 (1), 219-228.
- Goetz D.H., et al.** The neutrophil lipocalin NGAL is a bacteriostatic agent that interferes with siderophore- mediated iron acquisition. *Molecular Cell*, 2002, 10, 1033-1043.
- Gordon M.S. et al.** A phase I study of sonopizumab (S), a humanised monoclonal antibody to sphingosine-1-phosphate, in patients with advanced solid tumours. *Journal of Clinical Oncology*, 2010, 28 (15s): 219s.
- Graham T.R., et al.** Insulin-like growth factor -1-dependent upregulation of ZEB1 drives epithelial-to-mesenchymal transition in human prostate cancer cells. *Cancer Research*, 2008, 68, 2479-2488.
- Gravdal K., Halvorsen O.J., Haukaas S.A., Akslen L.A.** A switch from E-cadherin to N-cadherin expression indicates epithelial to mesenchymal transition and is of strong and independent importance for the progress of prostate cancer. *Clinical Cancer Research*, 13, 7003-7011.
- Green, F. J., ed.** The Sigma- Aldrich Handbook of Stains, Dyes and Indicators, Aldrich Chemical Co., Milwaukee, WI:1990.
- Greenburg G., Hay E.D.** Epithelia suspended in collagen gels can lose polarity and express characteristics of migrating mesenchymal cells. *The Journal of Cell Biology*, 1982, 95 (1), 333-339.
- Greenberger L.M. et al.** A RNA antagonist of hypoxia-inducible factor-1 alpha, EZN-2968, inhibits tumour cell growth. *Molecular Cancer Therapy*, 2008, 7, 3598-3608.
- Grepin R., Pages G.** Molecular mechanisms of resistance to tumour anti-angiogenic strategies. *Journal of Oncology*, 2010, 835680.
- Grey A-M., Schor A.M., Rushton G., Ellis I., Schor S.L.** Purification of the migration stimulating factor produced by fetal and breast cancer patient fibroblasts. *Proceedings of the National Academy of Sciences of the United States of America*, 1989, 86 (7), 2438-2442.
- Guo X., et al.** Stromal fibroblasts activated by tumour cells promote angiogenesis in mouse gastric cancer. *Journal of Biological Chemistry*, 2008, 283 (28), 19864-19871.

Gutheil J.C. et al. Targeted antiangiogenic therapy for cancer using Vitaxin: a humanised monoclonal antibody to the integrin $\alpha v \beta 3$. *Clinical Cancer Research*, 2000, 6, 3056-3061.

Gwira J.A., et al. Expression of neutrophils gelatinase- associated lipocalin regulates epithelial morphogenesis in vitro. *Journal Biological Chemistry*, 2005, 280, 7875-7882.

H

Haase M., et al. Accuracy of neutrophil gelatinase-associated lipocalin (NGAL) in diagnosis and prognosis in acute kidney injury; asystematic review and meta-analysis.

American Journal of Kidney Disease, 2009, 1012-1024.

Hagemann T., et al. Molecular profiling of cervical cancer progression. *British Journal of Cancer*, 2007, 96, 321-328.

Han H., et al. Identification of differentially expressed genes in pancreatic cancer cells using cDNA microarray. *Cancer Research*, 2002, 62, 2890-2896.

Hanahan D, Folkman J. Patterns and emerging mechanisms of the angiogenic switch during tumorigenesis. *Cell*, 1996, 86, 353-364.

Hanahan D., Weinberg R.A. The hallmarks of cancer. *Cell*, 2000, 100, 57-70.

Hanahan D., et al. Less is more regularly; metronomic dosing of cytotoxic drugs can target tumour angiogenesis in mice. *Journal Clinical Investigation*, 2000, 105, 1045-1047.

Hanahan D., Weinberg R.A. Hallmarks of Cancer: the next generation. *Cell*, 2011, 144, 646-674.

Hanai J., et al. Lipocalin 2 diminishes invasiveness and metastasis of Ras-transformed cells. *Journal of Biological Chemistry*, 2005, 280, 13641- 13647.

Hapani S., Chu D., Wu S. Risk of gastrointestinal perforation in patients with cancer treated bevacizumab: A meta-analysis. *Lancet Oncology*, 2009, 10, 559-568.

Hardy B., et al. Snail family transcription factors are implicated in thyroid carcinogenesis. *The American Journal of Pathology*, 2007, 171, 1037-1046.

Hay E.D. Organisation and fine structure of epithelium and mesenchyme in the developing chick embryo. *Epithelial-mesenchymal Interactions*, 1968, Editors- Fleischmajer R., Billingham R.E., Williams &Williams Co, 31-55.

Hedlund E.M. et al. malignant cell-derived PIGF promotes normalisation and remodelling of the tumour vasculature. *Proceedings of National Academy of Science, America*, 2009, 106, 17505-17510.

Helfrich I., et al. Angiopoietin-2 levels are associated with disease progression in metastatic malignant melanoma. *Clinical Cancer Research*, 2009, 15, 1384-1392.

Hendrix M.J., et al. Vascular mimicry and tumour-cell plasticity: lessons from melanoma. *Nature Reviews Cancer*, 2003, 3, 411-421.

- Herbert S.P., Stainer D.Y.R.** Molecular control of endothelial cell behaviour during blood vessel morphogenesis. *Nature Reviews, Molecular Cell Biology*, 2011, 12, 551-564.
- Herbst R.S. et al.** Safety, pharmacokinetics and antitumour activity of AMG-386, a selective angiopoietin inhibitor, in adult patients with advanced solid tumours. *Journal of Clinical Oncology*, 2009, 27, 3557-3565.
- Hida K., Hida Y., Shindoh M.** Understanding tumour endothelial cell abnormalities to develop ideal anti-angiogenic therapies. *Cancer Science*, 2008, 99, 459-466.
- Hidalgo M., Eckhardt G.** Development of matrix metalloproteinase inhibitors in cancer therapy. *Journal of National Cancer Institute*, 2001, 93, 178-193.
- Hlubek F., et al.** Heterogenous expression of Wnt/ β -catenin target genes within colorectal cancer. *International Journal of Cancer*, 2007, 121, 1941-1948.
- Hofmann U.B., et al.** Expression and activation of matrix metalloproteinase-2 (MMP-2) and its co-localisation with membrane- type 1 matrix metalloproteinase (MT1-MMP) correlate with melanoma progression. *Journal of Pathology*, 2000, 191, 245-256.
- Hood J.D. et al.** VEGF upregulates eNOS message, protein and NO production in human endothelial cells. *American Journal of Physiology*, 1998, 274, 1054-1058.
- Holash J., et al.** VEGF-Trap: a VEGF blocker with potent antitumour effects. *Proceedings of National Academy of Science, America*, 2002, 99, 11393-11398.
- Hotz B., et al.** Epithelial to mesenchymal transition: expression of the regulators snail, slug and twist in pancreatic cancer. *Clinical Cancer Research*, 2007, 13, 4769-4776.
- Houvrad X., Germain S., et al.** Migration-stimulating factor displays HEXXH-dependent catalytic activity important for promoting tumour cell migration. *International Journal of Cancer*, 2005, 116, 378-384
- Hrada-Renevey S., et al.** SV40-induced expression of mouse gene 24p3 involves a post-transcriptional mechanism. *Oncogene*, 1989, 4, 601-608.
- Hsu Y.M., et al.** KCl co-transporter-3 downregulates E-cadherin/ β -catenin complex to promote epithelial-to-mesenchymal transition. *Cancer Research*, 2007, 67, 11064-11073.
- Hu H., Ran Y., et al.** Antibody library –based tumour endothelial cells surface proteomic functional screen reveals migration-stimulating factor as an anti- angiogenic target. *Molecular and Cellular Proteomics*, 2009, 8, 816-826.
- Hu L., et al.** NGAL decreases E-cadherin mediated cell- cell adhesion and increase cell motility and invasion through Rac1 In colon carcinoma cells. *Laboratory Investigation*, 2009, 89(5), 531-548.
- Hugo H., et al.** Epithelial-mesenchymal and mesenchymal-epithelial transitions in carcinoma progression. *Journal of Cell Physiology*, 2007, 213, 374-383.
- Hurwitz H, et al.** Bevacizumab plus irinotecan, fluorouracil, and leucovorin for metastatic colorectal cancer. *New England Journal of Medicine*, 2004, 350, 2335-2342.

Hvidberg V., et al. The endocytic receptor megalin binds the iron transporting neutrophil-gelatinase-associated lipocalin with high affinity and mediates its cellular uptake. *FEBS Letters*, 2005, 579 (3), 773-777.

Hynes R. Fibronectins. New York, Springer-Verlag, 1990.

I

Iannetti A., et al. The neutrophil gelatinase-associated lipocalin, a NF- κ B- regulated gene, is a survival factor for thyroid neoplastic cells. *Proceedings of National Academy of Sciences, America*, 2008 105 (37), 14058-14063.

Inai T., et al. Inhibition of vascular endothelial growth factor signalling in cancer causes loss of endothelial fenestrations, regressions of tumour vessels, and appearance of basement membrane ghosts. *American Journal of Pathology*, 2004, 165, 35-52.

Inoue A., et al. Slug, a highly conserved zinc finger transcriptional repressor, protects hematopoietic progenitor cells from radiation-induced apoptosis *in vivo*. *Cancer Cell*, 2002, 2 (4), 279-288.

Iwatsuki M., et al. Epithelial-mesenchymal transition in cancer development and its clinical significance. *Cancer Science*, 2010, 101 (2), 293-299.

J

Jain R.K. Normalisation of tumour vasculature: an emerging concept in antiangiogenic therapy. *Science*, 2005, 307 (5706).

Jakoby W.B. Crystallisation as a purification technique. *Enzyme Purification and Related Techniques, Methods in Enzymology*, 1971, 22, Academic Press.

Jiang Y., Goldberg I.D., Shi Y.E. Complex roles of tissue inhibitors of metalloproteinases in cancer. *Oncogene*, 2002, 21, 2245-2252.

Jones S.F. et al. Safety, tolerability and pharmacokinetics of TAK-701, a humanized anti-hepatocyte growth factor (HGF) monoclonal antibody, in patients with advanced nonhematologic malignancies: first-in-human phase I dose-escalation study. *Journal Clinical Oncology*. 2010, 28s.

Jones S.J., Florence M.M. et al. Co-expression by keratinocytes of migration stimulating factor (MSF) and a functional inhibitor of its bioactivity (MSFI). *Experimental Cell Research*, 2007, 313 (20), 4145-4157.

Jungert K., et al. Sp1 is required for TGF β - induced mesenchymal transition and migration in pancreatic cancer cells. *Cancer Research*, 67, 1563-1570.

K

- Kadler K.E., Hill A., Canty-Laird E.G.** Collagen fibrillogenesis: fibronectin, integrins and minor collagens as organizers and nucleators. *Current Opinion in Cell Biology*, 2008, 20, 495-501.
- Kajita M., McClinic K.N., Wade P.A.** Aberrant expression of the transcription factors snail and slug alters the response to genotoxic stress. *Molecular and Cellular Biology*, 2004, 24 (17), 7559-7566.
- Kajiyama H., et al.** Chemoresistance to paclitaxel induces epithelial-to-mesenchymal transition and enhances metastatic potential for epithelial ovarian carcinoma cells. *International Journal of Oncology*, 2007, 31, 277-283.
- Takeji Y., Teicher B.A.** Preclinical studies of the combination of angiogenic inhibitors with cytotoxic agents. *Investigational New Drugs* 1997, 15, 39-48.
- Kalluri R.** EMT: when epithelial cells decide to become mesenchymal-like cells. *The Journal of Clinical Investigation*, 2009, 119 (6), 1417-1419.
- Kalluri R., Weinberg R.A.** The basics of epithelial-mesenchymal transition. *The Journal of Clinical Investigation*, 2009, 119 (6), 1420-1428.
- Karlan B.Y. et al.** Randomised double blind, placebo- controlled phase II study of AMG-386 combined with weekly paclitaxel in patients with recurrent ovarian cancer. *Journal of Clinical Oncology*, 2012, 30 (4), 362-371.
- Kay R.A., Ellis I., et al.** The expression of migration-stimulating factor, a potent oncofetal cytokine, is uniquely controlled by 3'-untranslated region-dependent nuclear sequestration of its precursor messenger RNA. *Cancer Research*, 2005, 65 (23), 10742-10749.
- Kerbel R.S.** Tumour angiogenesis. *New England Journal of Medicine*, 2008, 358, 2309-2049.
- Kesisis G., Broxterman H., Giaccone G.** Angiogenesis inhibitors. Drug selectivity and target specificity. *Current Pharmaceutical Design*, 2007, 13, 2795-2809.
- Khakoo A.Y., et al.** Does the renin-angiotensin system participate in regulation of human vasculogenesis and angiogenesis? *Cancer Research*, 2008, 68, 9112-9115.
- Kieran M.W., et al.** A feasibility trial of antiangiogenic (metronomic) chemotherapy in paediatric patients with recurrent or progressive cancer. *Journal of Paediatric Hematology/Oncology*, 2005, 27 (11), 573-581.
- Kim K. J. et al.** Inhibition of vascular endothelial growth factor induced angiogenesis suppresses tumour growth *in vivo*. *Nature*, 1993, 362, 841-844.
- Kim S., et al.** Regulation of angiogenesis *in vivo* by ligation of integrin alpha5beta1 with the central cell-binding domain of fibronectin. *American Journal of Pathology*, 2000, 156, 1345-1362.
- Kioi M., et al.** Inhibition of vasculogenesis, but not angiogenesis, prevents the recurrence of glioblastoma after irradiation in mice. *Journal of Clinical Investigation*, 2010, 1-12.

- Kitajima Y., Ide T., Ohtsuka T., Miyazaki K.** Induction of hepatocyte growth factor activator gene expression under hypoxia activates the hepatocyte growth factor/ c-Met system via hypoxia inducible factor-1 in pancreatic cancer. *Cancer Science*, 2008, 99, 1341-1347.
- Kjeldsen L., et al.** Isolation and primary structure of NGAL, a novel protein associated with human neutrophils gelatinase. *Journal of Biological Chemistry*, 1993, 268, 10425-10432.
- Kjeldsen L., et al.** Human neutrophil gelatinase-associated lipocalin and homologous proteins in rat and mouse. *Biochim Biophys Acta*, 2000, 1482, 272-283.
- Klausner R.D., et al.** A brefeldin-A like phenotype is induced by the overexpression of a human ERD-2-like protein, ELP-1. *Cell*, 1992, 69 (4), 625-635.
- Klement G., et al.** Continuous low-dose therapy with vinblastine and VEGF receptor 2 antibody induces sustained tumour regression without over toxicity. *Journal of Clinical Investigation*, 2000, 105, 15-24.
- Knutson K.L., et al.** Immunoediting of cancers may lead to epithelial to mesenchymal transition. *Journal of Immunology*, 2006, 177 (3), 1526-1533.
- Koh Y.J., et al.** Double antiangiogenic protein, DAAP, targeting VEGF-A and angiopoietins in tumour angiogenesis, metastasis, and vascular leakage. *Cancer Cell*, 2010, 18, 171-184.
- Konner J., Dupont J.** use of the soluble recombinant decoy receptor vascular endothelial growth factor trap (VEGF Trap) to inhibit vascular endothelial growth factor activity. *Clinical Colorectal Cancer*, 2004, 4 (Suppl 2), S81-S85.
- Kornblihtt A.R., Pesce C.G., et al.** The fibronectin gene as a model for splicing and transcription studies. *The FASEB Journal*, 1996, 10, 248-257.
- Kubben F.J., et al.** Clinical evidence for a protective role of lipocalin-2 against MMP-9 autodegradation and the impact for gastric cancer. *European Journal of Cancer*, 2007, 43, 1869-1876.
- Kubota T., et al.** NK4, an HGF antagonist, prevents haematogenous pulmonary metastasis by inhibiting adhesion of CT26 cells to endothelial cells. *Clinical & Experimental Metastasis* 2009, 26, 447-456.
- Kuhnert F., et al.** Dll4- Notch signalling as a therapeutic target in tumour angiogenesis. *Vascular Cell*, 2011, 3, 20-28.
- Kuo C.J., et al.** Comparative evaluation of the antitumour activity of antiangiogenic proteins delivered by gene transfer. *Proceedings of the National Academy of Sciences*, 2001, 98, 4605-4610.
- Kurein B.T., Scofield R.H.** Extraction of proteins from gels: a brief review. *Methods in Molecular Biology*, 2012, 869, 403-405.
- Kuso-Saito C., et al.** Cancer metastasis is accelerated through immunosuppression during Snail-induced EMT of cancer cells. *Cancer Cell*, 2009, 15, 195-206.

Kut C., Mac Gabhann F., Popel A.S. Where is VEGF in the body? A meta-analysis of VEGF distribution in cancer. *British Journal of Cancer*, 2007, 97, 978-985.

L

Lacorre D-A., et al. Plasticity of endothelial cells: rapid dedifferentiation of freshly isolated high endothelial venule endothelial cells outside the lymphoid tissue microenvironment. *Blood*, 2004, 103 (11), 4161-4172.

Laemmli U.K. Cleavage of structural proteins during the assembly of the head of bacteriophage T4. *Nature*, 1970, 227 (5259), 680-685.

Lee E.K., et al. Inhibition of the proliferation and invasion of hepatocellular carcinoma cells by lipocalin 2 through blockade of JNK and PI3K/Akt signalling. *International Journal of Oncology*, 2011, 38, 325-333.

Lee H.J., et al. Ectopic expression of neutrophil gelatinase-associated lipocalin suppresses the invasion and liver metastasis of colon cancer cells. *International Journal of Cancer*, 2006, 118, 2490-2497.

Lee K.H., Kim J.R. Hepatocyte growth factor induced up-regulation of VEGF through Egr-1 in hepatocellular carcinoma cells. *Clinical & Experimental Metastasis*, 2009, 10, 709-717.

Lee J-H., et al. Expression of neutrophil gelatinase-associated lipocalin in calcium-induced keratinocyte differentiation. *Journal of Korean Medical Science*, 2008, 23, 302-306.

Lee M.Y., Chou C.Y., Tang M.J., Shen M.R. Epithelial-mesenchymal transition in cervical cancer: correlation with tumour progression, epidermal growth factor receptor overexpression and snail up-regulation. *Clinical Cancer Research*, 2008, 14, 4743-4750.

Lee S.H. Taniburumab (TTAC-0001): a fully human monoclonal antibody targets vascular endothelial growth factor receptor 2. *Archives of Pharmacological Research*, 2011, 34 (8), 1223-1226.

Lefkore B., et al. Fumagillin Review. *Expert Review Anti-Infection Therapy*, 2007, 5 (4), 573-579.

Lehmann T.A., et al. p53 mutations in human immortalised epithelial cell lines. *Carcinogenesis*, 1993, 14, 833-839.

Leng X., et al. Lipocalin 2 is required for BCR-ABL-induced tumorigenesis. *Oncogene*, 2008, 27, 6110-6119.

Leng X., et al. Lipocalin 2 is required for BCR-ABL-induced tumorigenesis in oesophageal carcinoma cells. *Biochemistry Journal*, 2007, 403, 297-303.

Leng X., et al. Inhibition of lipocalin 2 impairs breast tumorigenesis and metastasis. *Cancer Research*, 2009, 69 (22), 8579-8584.

Leng X., et al. Requirement of lipocalin 2 for hematopoietic and solid tumour malignancies. *Advanced Enzyme Regulation*, 2009, 49, 142-146.

Li J.L., et al. Expression of delta-like ligand 4 and markers of hypoxia in colon cancer. *British Journal of Cancer*, 2007, 67 (23), 11244-11253.

- Li J.L., et al.** Functions of neutrophil gelatinase associated lipocalin in the esophageal carcinoma cell line SHEZ-P Du et al., Neutrophil gelatinase-associated lipocalin and its receptor: independent prognostic factors of oesophageal squamous cell carcinoma. *Journal of Clinical Pathology*, 2011, 64, 69-74.
- Li Q.Q., et al.** Twist1-mediated Adriamycin-induced epithelial-mesenchymal transition relates to multidrug resistance and invasive potential in breast cancer cells, *Clinical Cancer Research*, 2009, 15, 2657-2665.
- Li X., Wu J-F.** Recent developments in patient anti-cancer agents targeting the matrix metalloproteinases. *Recent Patents on Anti-Cancer Drug Discovery*, 2010, 5 (2), 109-141.
- Li Y., et al.** Up-regulation of miR-200 and let-7 by natural agents leads to the reversal of epithelial-to-mesenchymal transition in gemcitabine-resistant pancreatic cancer cells. *Cancer Research*, 2009, 69, 6704-6712.
- Liao D., Johnson R.S.** Hypoxia: a key regulator of angiogenesis in cancer. *Cancer Metastasis Review*, 2007, 26, 281-290.
- Liao C-J., et al.** The cancer marker neutrophil gelatinase-associated lipocalin is highly expressed in human endometrial hyperplasia. *Molecular Biology Reports*, 2012, 39, 1029-1036.
- Lien W.H., et al.** Participation of cyclin D1 deregulation in TNP-470-mediated cytostatic effect: Involvement of senescence. *Biochemical Pharmacology*, 2004, 68, 729-738.
- Lim R., et al.** Neutrophil gelatinase-associated lipocalin (NGAL) an early-screening biomarker for ovarian cancer: NGAL is associated with epidermal growth factor-induced epithelial-mesenchymal transition. *International Journal of Cancer*, 2007, 120, 2426-2434.
- Ling Y., et al.** Endostar, a novel recombinant human endostatin, exerts antiangiogenic effect via blocking VEGF-induced tyrosine phosphorylation of KDR/Flk-1 of endothelial cells. *Biochemical and Biophysical Research Communication*, 2007, 361, 79-84.
- Liu M-F., et al.** NGAL and NGALR are frequently overexpressed in human gliomas and are associated with clinical prognosis. *Journal of Neurooncology*, 2011, 104, 119-127.
- Liu Y., et al.** Zeb1 links epithelial-mesenchymal transition and cellular senescence. *Development*, 2008, 135, 579-588.
- Longo R., et al.** Anti-angiogenic therapy: Rationale, challenges and clinical studies. *Angiogenesis*, 2002, 5, 237-256.
- Louis K.S., Siegel A.C.** Mammalian cell viability: methods and protocols. *Methods in Molecular Biology*, 2011, 740, 7-12.
- Lunt S.J., et al.** The tumour microenvironment and metastatic disease. *Clinical and Experimental Metastasis*, 2009, 26, 19-34.
- Luo Y., et al.** Over-expression of hypoxia-inducible factor-1 alpha increases the invasive potency of LNCaP cells in vitro. *British Journal of Cancer*, 2006, 98, 1315-1319.

M

McMahon G. VEGF receptor signalling in tumour angiogenesis. *Oncologist*, 200, 5, 3-10.

Ma L., Teruya-Feldstein J., Weinberg R.A. Tumour invasion and metastasis initiated by micro-RNA-10b in breast cancer. *Nature*, 2007, 449, 682-688.

Madsen C.D., Sahai E. Cancer dissemination- lessons from leukocytes. *Developmental Cell*, 2010, 19, 13-26.

Maharaji A.S., et al. Vascular endothelial growth factor localisation in the adult. *American Journal of Pathology*, 2006, 168, 639-648.

Maharaji A.S., D'Amore P.A. Roles for VEGF in the adult. *Microvascular Research*, 2007, 74, 100-113.

Maharaj A.S., et al. VEGF and TGF- β are required for the maintenance of the choroid plexus and ependymal. *Journal of Experimental Medicine*, 2008, 205, 491-501.

Makarski J.S. Evidence for reversible morphologic phenotypes (sprouts) of cultured endothelial cells. *Cell Biology International Reports*, 1982, 6, 225-233.

Mallibris L., et al. Neutrophil gelatinase-associated lipocalin is a marker for dysregulated keratinocyte differentiation in human skin. *Experimental Dermatology*, 2002, 11, 584-591.

Mani S.A., et al. The epithelial-mesenchymal transition generates cells with properties of stem cells. *Cells*, 2008, 133 (4), 704-715.

Marshall E. Cancer therapy. Setbacks for endostatin. *Science*, 2002, 295, 2198-2199.

Martineau A.R., et al. Neutrophil- mediated innate immune resistance to mycobacteria. *Journal of Clinical Investigation*, 2007, 117, 1988-1994.

Martinsson- Niskanen T., et al. Monoclonal antibody TB-403: A first –in-human, phase I, double blind, dose escalation study directed against placental growth factor in healthy male subjects. *Clinical Therapeutics*, 2011, 33 (9), 1142-1149.

Maestro R., et al. Twist is a potential oncogene that inhibits apoptosis. *Genes & Development*, 1999, 13 (17), 2207-2217.

Mather, J.P., Roberts P.E. *Introduction to Cell and Tissue Culture: Theory and Technique.* Plenum Press. New York and London, 1998.

Mauriz J.L., et al. Antiangiogenic treatment of cancer. *Cirugia Espanola* 2005, 78, 3-11.

Mauriz J.L., et al. Cell-cycle inhibition by TNP-470 in an in vivo model of hepatocarcinoma is mediated by a p53 and p21MAF1/CIP1 mechanism. *Translational Research*, 2007, 149, 46-53.

Mauriz J., Gonzalez-Gallego J. Antiangiogenic drugs: current knowledge and new approaches to cancer therapy. *Journal of Pharmaceutical Sciences*, 2008, 97 (10), 4129-4152.

Merne M., Syrjanen S. The mesenchymal substrate influences the epithelial phenotype in a three –dimensional cell culture. *Archives of Dermatological Research*, 2003, 295 (5), 190-198.

- Micalizzi D.S., Farabaugh S.M., Ford H.L.** Epithelial-mesenchymal transition in cancer: parallels between normal development and tumour progression. *Journal of Mammary Gland Biology Neoplasia*, 2010, 18, 117-134.
- Mir S.U.R., et al.** Neutrophil gelatinase-associated lipocalin expression is dependent on the tumour-associated sigma-2 receptor S2R Pgrmc1. *Journal of Biological Chemistry*, 2012, 287 (18), 14494-14501.
- Miriam L., et al.** Angiostatin and anti-angiogenic therapy in human disease. *Endocrine Journal*, 2004, 73-104.
- Mita A.C., et al.** Phase I study of AMG-386, a selective angiopoietin 1/2 - neutralising pepti-body, in combination with chemotherapy in adults with advance solid tumours. *Clinical Cancer Research*, 2010, 16, 3044-3056.
- Mitchell D.C., Bryan B.A.** Anti-angiogenic therapy: adapting strategies to overcome resistant tumours. *Journal of Cellular Biochemistry*, 2010, 111, 543-553.
- Mitchell D., et al.** ALK1-Fc inhibits multiple mediators of angiogenesis and suppresses tumour growth. *Molecular Cancer Therapy*, 2010, 9, 379-388.
- Miyamoto T., et al.** Laser-captured microdissection-microarray analysis of the genes involved in endometrial carcinogenesis: stepwise up-regulation of lipocalin2 expression in normal and neoplastic endometria and its functional relevance. *Human Pathology*, 2011, 42, 1265-1274.
- Miyoshi A., et al.** Snail and SIP1 increase cancer invasion by upregulating MMP family in hepatocellular carcinoma cells. *British Journal of Cancer*, 2004, 90, 1265-1273.
- Moniaux N., et al.** Early diagnosis of pancreatic cancer: neutrophil gelatinase-associated lipocalin as a marker of pancreatic intraepithelial neoplasia. *British Journal of Cancer*, 2008, 98, 1540-1547.
- Morel A.P., et al.** Generation of breast cancer stem cells through epithelial-mesenchymal transition. *PLoS One*, 2008, 3 (8), e2888.
- Mosmann, T.** Rapid Colorimetric assay for cellular growth and survival: application to proliferation and cytotoxicity assaays. *Journal of Immunology Methods*, 1983, 65, 55-63
- Motegi K., Harada K., Ohe G., et al.** Differential involvement of TGF- β 1 in mediating the motogenic effects of TSP-1 on endothelial cells, fibroblasts and oral tumour cells. *Experimental Cell Research*, 2008, 314, 2323-2333.
- Mueller M.M., et al.** Tumour progression of skin carcinoma cells in vivo promoted by clonal selection, mutagenesis and autocrine growth regulation by granulocyte colony- stimulated factor and granuolocyte- macrophage colony- stimulating factor. *American Journal of Pathology*, 2001, 159 (4), 1567-1579.
- Myers S.R., Leigh I.M., Navsaria H.** Epidermal repair results from activation of follicular and epidermal progenitor keratinocytes mediated by a growth factor cascade. *Wound Repair and Regeneration*, 2007, 15 (5), 693-701.

N

Nagy J.A., et al. VEGF-A and the induction of pathological angiogenesis. *Annual Review Pathology*, 2007, 2, 251-275.

Nervi B., et al. Chemosensitization of acute myeloid leukemia (AML) following mobilisation by the CXCR4 antagonist AMD3100. *Blood*, 2009, 113, 6206-6214.

Nicosia R.F., Nicosia S.V., Smith M. Vascular endothelial growth factor, platelet-derived growth factor, and insulin-like growth factor-1 promote rat aortic angiogenesis *in vitro*. *American Journal of Pathology*, 1994, 145, 1023-1029.

Nicosia R.F., Tusynski G.P. Matrix-bound thrombospondin promotes angiogenesis *in vitro*. *Journal of Cell Biology*, 1994, 124, 183-193.

Nieves B.J., D'Amore P.A., Bryan B.A. The function of vascular endothelial growth factor. *Biofactors*, 2009, 35, 332-337.

Nielsen B.S., et al. Induction of NGAL synthesis in epithelial cells of human colorectal neoplasia and inflammatory bowel disease. *Gut*, 1996, 38, 414-420.

Nielsen D.L., Sengelov L. Inhibition of placenta growth factor with TB-403: a novel antiangiogenic cancer therapy. *Expert Opinion on Biological Therapy*, 2012, 12 (6), 795-804.

Nolan D.J., et al. Bone marrow-derived endothelial progenitor cells are a major determinant of nascent tumour neovascularisation. *Genes & Development*, 2007, 21, 1546-1558.

Norden A.D., et al. Bevacizumab for recurrent malignant gliomas: Efficacy, toxicity, and patterns of recurrence. *Neurology*, 2008, 70, 779-787.

Nowell P.C. The clonal evolution of tumour cell populations. *Science*, 1976, 194, 23-28.

O

O'Hare M.J., Bond J., et al. Conditional immortalisation of freshly isolated human mammary fibroblasts and endothelial cells. *Proceedings of National Academy of Science, America*, 2001, 98, 646-651.

O'Reilly M.S., et al. Angiostatin: A novel angiogenesis inhibitor that mediates the suppression of metastases by a Lewis lung carcinoma. *Cell*, 1994, 79, 315-328.

O'Reilly M.S. Angiostatin: an endogenous inhibitor of angiogenesis and of tumour growth. *EXS*, 1997, 79, 273-294.

O'Reilly M.S., et al. Endostatin: An endogenous inhibitor of angiogenesis and tumour growth. *Cell*, 1997, 88, 277-285.

Olah J., et al. Triosephosphate isomerase deficiency: a neurodegenerative misfolding disease. *Biochemical Society Transactions*, 2002, 3 (2), 30-38.

Olmeda D., et al. Snail silencing effectively suppresses tumour growth and invasiveness. *Oncogene*, 2007, 26 (13), 1862-1874.

Orimo A., et al. Stromal fibroblasts present in invasive human breast carcinomas promote tumour growth and angiogenesis through elevated SDF-1/CXCL12 secretion. *Cell*, 2005, 121 (3), 335-348.

Orosz F., et al. Triosephosphate isomerase deficiency: facts and doubts. *IUBMB Life*, 2006, 58 (12), 703-715.

Ostman A. PDGF receptors- mediators of autocrine tumour growth and regulators of tumour vasculature and stroma. *Cytokine Growth Factor Review*, 2004, 15, 275-286.

Ostman A., Heldin C.H. PDGF receptors as targets in tumour treatment. *Advanced Cancer Research*, 2007, 97, 247-274.

P

Paetz-Ribes M., et al. Antiangiogenic therapy elicits malignant progression of tumours to increased local invasion and distant metastasis. *Cancer Cell*, 2009, 15, 220-231.

Pahler J.C., et al. Plasticity in tumour- promoting inflammation; impairment of macrophage recruitment evokes a compensatory neutrophil response. *Neoplasia*, 2008, 10, 329-340.

Palomaki P. Simultaneous use of poly- and monoclonal antibodies as enzyme tracers in a one-step enzyme immunoassay for the detection of Hepatitis B surface antigen. *Journal of Immunology Methods*, 1992, 145, 55-63

Patnaik A., et al. Phase I study of SCH900105 (SC), an anti-hepatocyte growth factor (HGF) monoclonal antibody (MAb), as a single agent and in combination with erlotinib (E) in patients with advanced tumours. *Journal of Clinical Oncology*, 2010, 28s.

Patel N.S., et al. Up-regulation of endothelial delta-like 4 expression correlates with vessel maturation in bladder cancer. *Clinical Cancer Research*, 2006, 12, 4836-4844.

Patiar S., Harris H.L. Role of hypoxia-inducible factor-1 alpha as a cancer therapy target. *Endocrine- Related Cancer*, 2006, 13 (suppl), S61-S75.

Peinado H., et al. Snail and E47 repressors of E-cadherin induce distinct invasive and angiogenic properties *in vivo*. *Journal of Cell Science*, 2004, 117, 2827-2839.

Peinado H., Olmeda D., Cano A. Snail, Zeb and bHLH factors in tumour progression: an alliance against the epithelial phenotype? *Nature Reviews Cancer*, 2007, 7 (6), 415-428.

Pfeifer A., et al. Suppression of angiogenesis by lentiviral delivery of PEX, a noncatalytic fragment of matrix metalloproteinase 2. *Proceedings of National Academy of Science, USA* 2000, 97, 12227-12232.

Phng L.K., Gerhardt H. Angiogenesis: a team effort coordinated by notch. *Developmental Cell* 2009, 16, 196-208

Picardo M., Schor S.L., et al. Migration stimulating activity in serum of breast cancer patients. *Lancet* 1991, 337, 130-133.

Plate K.H., et al. Up-regulation of vascular endothelial growth factor and its cognate receptors in a rat glioma model of tumour angiogenesis. *Cancer Research*, 1993, 53, 5822-5827.

Plate K.H., et al. Vascular endothelial growth factor and glioma angiogenesis: coordinate induction of VEGF receptors, distribution of VEGF protein and possible in vivo regulatory mechanisms. *International Journal of Cancer* 1994, 59 (4), 520-529.

Porta C., et al. Predictive value of baseline serum vascular endothelial growth factor and neutrophil growth factor and neutrophil gelatinase-associated lipocalin in advanced kidney cancer patients receiving sunitinib. *Kidney International*, 2010, 77, 809-815.

Prall F. Tumour budding in colorectal carcinoma. *Histopathology*, 2007, 50 (1), 151-162.

Prall F., Ostwald C. High-degree tumour budding and podia-formation in sporadic colorectal carcinomas with K-ras gene mutations. *Human Pathology*, 2007, 38 (11), 1696-1702.

Proksch E., Brandner J., Jensen J.M. The skin: an indispensable barrier. *Experimental Dermatology*, 2008, 17 (12), 1063-1072.

Pugh C.W., Ratcliffe P.J. The von Hippel- Lindau tumour suppressor, hypoxia- inducible factor-1 (HIF-1) degradation, and cancer pathogenesis. *Seminars Cancer Biology*, 2003, 13, 83-89.

Puisieux A., Valsesia-Wittmann S., Ansieau S. A twist for survival and cancer progression. *British Journal of Cancer*, 2006, 94, 13-17.

Q

R

Radisky D.C., et al. Rac1b and reactive oxygen species mediate MMP-3-induced EMT and genomic instability. *Nature*, 2005, 436, 123-127.

Rak J., Kerbel R.S. Treating cancer by inhibiting angiogenesis. New hopes and potential pitfalls. *Cancer Metastasis Review*, 1996, 15, 231-236.

Ranpura V., et al. increased risk of high-grade hypertension with bevacizumab in cancer patients: A meta-analysis. *American Journal of Hypertension*, 2010, 23, 460-468.

Rapisardia A., Melillo G. Role of hypoxic tumour microenvironment in the resistance to anti-angiogenic therapies. *Drug Resistance Update*, 2009, 12, 74-80.

Recamier J.C. Recherches sur le traitement du cancer sur la compression methodique simple ou comibinee et sur l'histoire generale de la meme maladie. 2nd Edition, 1829.

Rim J.S., et al. Evidence for the multistep nature of *in vitro* human epithelial cell carcinogenesis. *Cancer Research*, 1990, 50 (17), 5653s-5657s.

Rizki A., et al. A human breast cell model of preinvasive to invasive transition. *Cancer Research*, 2008, 68 (5), 1378-1387.

Rolony C., et al. HRG inhibits tumour growth and metastasis by skewing macrophage polarization and vessel normalisation through downregulation of PIGF. *Cancer Cell*, 2011, 19 (1), 31-44.

Rubin D.B. The radiation biology of vascular endothelium. CRC Press 1998.

Rundhaug J.E. Matrix metalloproteinases and angiogenesis. *Journal of Cellular and Molecular Medicine*, 2005, 9, 267-285.

Ryle C.M., et al. Density dependent modulation of synthesis of keratin 1 and 10 in the human keratinocyte line HaCaT and in ras-transfected tumorigenic clones. *Differentiation*, 1989, 40, 42-54.

S

Sabbadini R.A. Sphingosine-1-phosphate antibodies as potential agents in treatment of cancer and age-related macular degeneration. *British Journal of Pharmacology*, 2011, 162 (6), 1225-1238.

Sabeh F., Shimizu-Hirota R., Weiss S.J. Protease-dependent versus –independent cancer cell invasion programs: three-dimensional amoeboid movement revisited. *Journal of Cell Biology*, 2009, 185, 11-19.

Sager R.K., et al. Resistance of human cells to tumourigenesis induced by cloned transforming genes. *Proceedings of National Academy of Sciences, America*, 1983, 80, 7601-7605.

Saiga H., et al. Lipocalin 2-dependent inhibition of mycobacterial growth in alveolar epithelium. *Journal of Immunology*, 2008, 8521-8527.

Sane D.C., Anton L., Brosnihan K.B. Angiogenic growth factors and hypertension. *Angiogenesis*, 2004, 7, 193-201.

Santisteban M., et al. Immune-induced epithelila to mesenchymal transition *in vivo* generates breast cancer stem cells. *Cancer Research*, 2009, 69 (7), 2887-2895.

Scappaticci F.A., et al. Surgical wound healing complications in metastatic colorectal cancer patients treated with bevacizumab. *Journal of Surgical Oncology*, 2005, 91, 173-180.

Scharorsky O.G. Metronomic chemotherapy: changing the paradigm that more is better, *Current Oncology*, 2009, 16 (2), 7-15.

Schoop V.M, Stark H-J., Fusenig N.E. Growth and differentiation of immortalised human skin keratinocytes (HACAT) in organotypic culture. *Biochemical Society Transactions*, 1996, 24 (4), 552S.

- Schoop V.M., Mircancea N., Fusenig N.E.** Epidermal organisation and differentiation of HaCaT keratinocytes in organotypic coculture with human dermal fibroblasts. *The Journal of Investigate Dermatology*. 1999, 112, 343-353.
- Schor A.M., Schor S.L., Allen T.D.** Effects of culture conditions on the proliferation, morphology and migration of bovine aortic endothelial cells. *Journal of Cell Science*, 1983, 62, 267-285.
- Schor A.M., Schor S.L.** Tumour angiogenesis. *Journal of Experimental Pathology*, 1983, 141, 385-413.
- Schor A.M., Rushton G., Ferguson J.E, et al.** Phenotypic heterogeneity in breast fibroblasts - functional anomaly in fibroblasts from histologically normal tissue adjacent to carcinoma. *International Journal of Cancer*, 1994, 59, 25-32.
- Schor A.M., Schor S.L.** Angiogenesis and tumour progression: migration-stimulating factor as a novel target for clinical intervention. *Eye*, 2010, 24, 450-458.
- Schor S.L.** Cell-proliferation and migration on collagen substrata *in vitro*. *Journal of Cell Science*, 1980, 41, 159-175.
- Schor S.L., Schor A.M., Winn B., Rushton G.** The use of three-dimensional collagen gels for the study of tumour cell invasion in vitro. Experimental parameters influencing cell migration into the gel matrix. *International Journal of Cancer* 1982, 29 (1), 57-62.
- Schor S.L., Schor A.M., Rushton G., Smith L.** Adult, foetal and transformed fibroblasts display different migratory phenotypes on collagen gels - evidence for an isoformic transition during foetal development. *Journal of Cell Science*, 1985, 73, 221-234.
- Schor S.L., Schor A.M., Grey A-M., Rushton G.** Foetal and cancer patient fibroblasts produce an autocrine Migration-Stimulating Factor not made by normal adult cells. *Journal of Cell Science*, 1988, 90, 391-399.
- Schor S.L., Schor A.M., Grey A.M., Chen J., Rushton G., Grant M.E., Ellis I.** Mechanism of action of the migration-stimulating factor produced by fetal and cancer patient fibroblast: effect on hyaluronic acid synthesis. *In Vitro Cellular and Developmental Biology*, 1989, 25, 737-746
- Schor S.L., Schor A.M.** Characterization of migration stimulating activity (MSF): evidence for its role in cancer pathogenesis. *Cancer Investigation* 1990, 8, 665-667.
- Schor S.L., et al.** Migration Stimulating Factor: its structure, mode of action and possible function in health and disease. *Symposia of the Society of Experimental Biology*, 1993, 47, 235-251.
- Schor S.L.** Cytokine control of cell motility: modulation and mediation by the extracellular matrix. *Progress in Growth Factor Research*, 1994, 5, 223-248.

- Schor S.L., Ellis I., Grey A-M., et al.** Substratum-dependent stimulation of fibroblast migration by the gelatin-binding domain of fibronectin. *Journal of Cell Science*, 1996, 109, 2581-2590.
- Schor S.L., Grey A-M., et al.** Migration stimulating factor: its structural homology to the gelatine-binding domain of fibronectin, mode of action and possible function in health and disease. *Cell Behaviour: Adhesion and Motility*. Eds G.Evans, C.Wigley,
- Schor S.L., Ellis I., Banyard J., Schor A.M.** Motogenic activity of IGD-containing synthetic peptides. *Journal of Cell Science* 1999, 112, 3879-3888.
- Schor S.L., Schor A.M.** Phenotypic and genetic alterations in mammary stroma: implications for tumour progression. *Breast Cancer Research*, 2001, 3 (6), 373-379.
- Schor S.L., Ellis I.R., Jones S.J., et al.** Migration-stimulating factor: a genetically truncated onco-fetal fibronectin isoform expressed by carcinoma and tumour-associated stromal cells. *Cancer Research*, 2003, 63, 8827-8836.
- Schor S.L., Schor A.M., Keach R.P., Belch J.J.F.** Role of matrix macromolecules in the aetiology and treatment of chronic ulcers. *The Wound Healing Management Manual* (Bok Y Lee), 2005, Chapter 10, 109-121.
- Seo E-Y., et al.** Identification of calcium- inducible genes in primary keratinocytes using suppression-subtractive hybridization. *Experimental Dermatology*, 2004, 13, 163-169.
- Seo S.J., et al.** Expression of neutrophil gelatinase-associated lipocalin in skin epidermis. *Journal of Investigative Dermatology*, 2006, 126, 510-512.
- Seth P., et al.** Cellular and molecular targets of estrogen in normal human breast tissue. *Cancer Research*, 2002, 62, 4540-4544.
- Shi H., et al.** Lipocalin 2 promotes lung metastasis of murine breast cancer cells. *Journal of Experimental and Clinical Cancer Research*, 2008, 83.
- Shojaei F., et al.** HGF/c-Met as an alternative angiogenic pathway in sunitinib-resistant tumours. *Cancer Research*, 2010, 70 (24), 10090-10100.
- Shord S.S., et al.** Understanding and managing the possible adverse effects associated with bevacizumab. *American Journal of Health System Pharmacy*, 2009, 66, 999-1013.
- Singh S., et al.** Small- molecule antagonists for CXCR2 and CXCR1 inhibit human melanoma growth by decreasing tumour cell proliferation, survival and angiogenesis. *Clinical Cancer Research*, 2009, 15, 2380-2386.
- Solinas G., et al.** Tumour-conditioned macrophages secrete migration-stimulating factor: a new marker for M2-polarisation, influencing tumour cell motility. *The Journal of Immunology*, 2010, 185, 642-652.
- Song S., et al.** PDGFR β + perivascular progenitor cells in tumours regulate pericyte differentiation and vascular survival. *Nature Cell Biology*, 2005, 7, 870-879.

- Sottile J.** Regulation of angiogenesis by extracellular matrix. *Biochim Biophys Acta*, 2004, 1654, 13-22.
- Soule H.D., et al.** Isolation and characterisation of a spontaneously immortalised human breast epithelial cell line, MCF-10. *Cancer Research*, 1990, 50 (18), 6075-6086.
- Spaderna S., et al.** A transient, EMT-linked loss of basement membranes indicates metastasis and poor survival in colorectal cancer. *Gastroenterology*, 2006, 131 (3), 830-840.
- Spoelstra N.S., et al.** The transcription factor ZEB1 is aberrantly expressed in aggressive uterine cancers. *Cancer Research*, 2006, 66 (7), 3893-3902.
- Spratlin J.** Ramucirumab (IMC-1121B): monoclonal antibody inhibition of vascular endothelial growth factor receptor-2. *Current Oncology Reports*, 2011, 13, 97-102.
- Steinberg M.L., Defendi V.** Transformation and immortalisation of human keratinocytes by SV40. *Journal of Investigative Dermatology*, 1983, 81 (Suppl), 131s-136s.
- Stewart M.W., et al.** Aflibercept. *Nature Reviews Drug Discovery*, 2012, 11, 269-270.
- Stoesz S.P., et al.** Heterogeneous expression of the lipocalin NGAL in primary breast cancers. *International Journal of Cancer*, 1998, 79, 565-572.
- Stoker M., Perryman M.** An epithelial scatter factor released by embryo fibroblasts. *Journal of Cell Science*, 1985, 77, 209-223.
- Stoker M., et al.** Scatter factor is a fibroblast-derived modulator of epithelial cell mobility. *Nature*, 1987, 327 (6119), 239-242.
- Sumpio B.E., Riley J.T., Dardik A.** Cells in focus: endothelial cell. *Journal of Biochemistry and Cell Biology*, 2002, 34, 1508-1512.
- Sun Y., et al.** NGAL expression is elevated in both colorectal adenoma-carcinoma sequence and cancer progression and enhances tumorigenesis in xenograft mouse models. *Clinical Cancer Research*, 2011, 17, 4331-4340.
- Sutton A.B., et al.** The response of endothelial cells to TGF- β 1 is dependent upon cell shape, proliferative state and the nature of the substratum. *Journal of Cell Science*, 1991, 99, 777-787.

T

- Takakura N., et al.** A role for hematopoietic stem cells in promoting angiogenesis. *Cell*, 2000, 102, 199-209.
- Talmadge J.E., Fidler I.J.** AACR centennial series: the biology of cancer metastasis: historical perspective. *Cancer Research*, 2010, 70, 5649-5669.
- Tarin D., et al.** The fallacy of epithelial mesenchymal transition in neoplasia. *Cancer Research*, 2005, 65 (14), 5996-6000.
- Tazzyman S., Lewis C.E., Murdoch C.** Neutrophils: key mediators of tumour angiogenesis. *International Journal of Experimental Pathology*, 2009, 90, 222-231.

- Teicher B.A., Fricker S.P.** CXCL12 (SDF-1)/ CXCR4 pathway in cancer. *Clinical Cancer Research*, 2010, 16, 2924-2931.
- Teicher B.A.** Antiangiogenic agents and targets; A perspective. *Biochemical Pharmacology*, 2011, 81, 6-12.
- Teschendorff A.E., et al.** Elucidating the altered transcriptional programs in breast cancer using independent component analysis. *PloS Comput Biol*, 2007, 3, e161.
- Thiery J.P.** Epithelial-mesenchymal transitions in tumour progression. *Nature Reviews Cancer*, 2002, 2 (6), 442-454.
- Thiery J.P., et al.** Epithelial-mesenchymal transitions in development and disease. *Cell*, 2009, 139 (5), 871-890.
- Thompson C, Leong S., Messersmith W.** Promising targets and drugs in development of colorectal cancer. *Seminars in Oncology*, 2011, 38 (4), 588-597.
- Tiwari N., Gheldof A., Tatari M., Christofori G.** EMT as the ultimate survival mechanism of cancer cells. *Seminars in Cancer Biology*, 2012, 22, 194-207.
- To K.K., Koshiji M., Hammer S., Humang L.E.** Genetic instability: The dark side of the hypoxic response. *Cell Cycle*, 2005, 4, 881-882.
- Tong Z., et al.** Neutrophil gelatinase-associated lipocalin as a survival factor. *Biochemical Journal*, 2005, 391, 441-448.
- Tong z., et al.** Neutrophil gelatinase –associated lipocalin: A novel suppressor of invasion and angiogenesis in pancreatic cancer. *Cancer Research*, 2008, 68 (15), 6100-6108.
- Towbin H., Staehelin T., Gordon J.** Electrophoretic transfer of proteins from polyacrylamide gels to nitrocellulose sheets - procedure and some applications. *Proceedings of National Academy of Sciences, America*, 1979, 76, 4350-4354.
- Treibel S., et al.** A 25kDa α 2- macroglobulin related protein is a component of the 125kDa form of human gelatinase. *FEBS Letters*, 1992, 314, 386-388.
- Trimboli A.J., et al.** Direct evidence for epithelial-mesenchymal transitions in breast cancer. *Cancer Research*, 68 (3), 937-945.

U

V

- Van Roy F., Bex G.** The cell-cell adhesion molecule E-cadherin. *Cell Molecular Life Science*, 2008, 65, 3756-3788.
- Van der Steen P.E., et al.** Matrix remodelling enzymes, the protease cascade and glycosylation. *Biochimica et Biophysica Acta- General Subjects*, 2001, 1528, 61-73.

- Van den Steen P.E., et al.** The hemopexin and O-glycosylated domains tune gelatinase B/MMP-9 bioavailability via inhibition and binding cargo receptors. *Journal of Biological Chemistry*, 2006, 281, 18626-18637.
- Van der Veire S., et al.** Further pharmacological and genetic evidence for the efficacy of PIGF inhibition in cancer and eye disease. *Cell*, 2010, 141, 178-190.
- Vasko V., et al.** Gene expression and functional evidence of epithelial-to-mesenchymal transition in papillary thyroid carcinoma invasion. *Proceedings of National Academy of Science, America*, 2007, 104, 2803-2808.
- Venkatesha S. et al.** Lipocalin 2 antagonises the proangiogenic action of *ras* in transformed cells. *Molecular Cancer Research*, 2006, 4, 821-829.
- Villalva et al.** Neutrophil gelatinase-associated lipocalin expression in chronic myeloid leukaemia. *Leukemia Lymphoma*, 2008, 49, 984-988.
- Virzi G.M., et al.** Genomics and biological activity of neutrophil gelatinase-associated lipocalin in several clinical settings. *Blood Purification*, 2013, 35, 139-143.

W

- Wahl M.L., et al.** Angiostatin and anti-angiogenic therapy in human disease. *The Endocrine Society*, 2004, 73-104.
- Wang H.J., et al.** Expressions of neutrophil gelatinase-associated lipocalin in gastric cancer; a potential biomarker for prognosis and an ancillary diagnostic test. *The Anatomical Record*, 2010, 293, 1855-1863.
- Wang L-H., et al.** Neutrophil gelatinase-associated lipocalin regulates intracellular accumulation of Rh123 in cancer cells. *Genes to Cells*, 2012, 17, 205-217.
- Warn R.** Cytoskeletal changes associated with cell motility. *S.E.B Symposium Cambridge: Society of Experimental Biology*, 1993,47, 325-338.
- Weller T.H., Coons A.H.** Fluorescent antibody studies with agents of varicella and herpes zoster propagated *in vitro*. *Proceedings of Society of Experimental Biology*, 1954, 96, 789-794.
- Weis S.M., Cheresh D.A.** Tumour angiogenesis: molecular pathways and therapeutic targets. *Nature Medicine*, 2011, 17 (11), 1359-1370.
- Weng D.E., Usman N.** Angiozyme: A novel angiogenesis inhibitor. *Current Oncology Report*, 2001, 3, 141-146.
- Wenners A.S., et al.** Neutrophil gelatinase-associated lipocalin (NGAL) predicts response to neoadjuvant chemotherapy and clinical outcome in primary human breast cancer. *PLOS One*, 2012, 7(10) 45826.
- Willet C.G., et al.** Direct evidence that the VEGF-specific antibody bevacizumab has antivasular effects in human rectal cancer. *Nature Medicine*, 2004, 10, 145-147.

Wilson, A.P. Cytotoxicity and Viability Assays in animal Cell Culture: A Practical Approach. 3Rd Ed, Oxford University Press, Oxford 2000, Vol1

Winkler F., et al. Kinetics of vascular normalisation by VEGFR2 blockade governs brain tumour response to radiation: role of oxygenation, angiopoietin-1 and matrix metalloproteinases. *Cancer Cell*, 2004, 6, 553-563.

Wu H-C., Li P-C. Proteins expressed on tumour endothelial cells as potential targets for anti-angiogenic therapy. *Journal of Cancer Molecules*, 2008, 4 (1), 17-22.

Wu, W.S., et al. Slug antagonises p53-mediated apoptosis of hematopoietic progenitors by repressing puma. *Cell*, 2005, 123 (4), 641-653.

Wyckoff J.B., et al. Direct visualisation of macrophage-assisted tumour cell intravasation in mammary tumours. *Cancer Research*, 2007, 67, 2649-2656.

X

Xie B., et al. Blockade of sphingosine-1-phosphate reduces macrophage influx and retinal and chorial neovascularisation. *Journal of Cell Physiology*, 2009, 218, 192-198.

Y

Yan L., et al. The high molecular weight urinary matrix metalloproteinase (MMP) activity is a complex of gelatinase B/MMP-9 And neutrophil gelatinase- associated lipocalin (NGAL)-modulation of MMP-9 activity by NGAL. *Journal of Biological Chemistry*, 2001, 276 (40), 37528- 37265.

Yan M. Therapeutic promise and challenges of targeting DLL4/ Notch 1. *Vascular Cell*, 2011, 3 (17).

Yang A.D., et al. Chronic oxaliplatin resistance induces epithelial-to-mesenchymal transition in colorectal cancer cell lines. *Clinical Cancer Research*, 2006, 12, 4147-4153.

Yang M-H., et al. Direct regulation of TWIST by HIF-1alpha promotes metastasis. *Nature Cell Biology*, 2008, 10 (3), 295-305.

Yang M-H., et al. Comprehensive analysis of the independent effect of Twist and Snail in promoting metastasis of hepatocellular carcinoma. *Hepatology*, 2009, 50, 1-11.

Yang J., et al. An iron delivery pathway mediated by a lipocalin. *Molecular Cell*, 2002, 10, 1045-1056.

Yang J., et al. Twist, a master regulator of morphogenesis, plays an essential role in tumour metastasis. *Cell*, 2004, 117 (7), 927-939.

Yang J., Weinberg R.A. Epithelial-mesenchymal transition: at the crossroads of development and tumour metastasis. *Developmental Cell*, 2008, 14, 818-829.

- Yang J., et al.** Lipocalin 2 promotes breast cancer progression. *Proceeding of National Academy of Science, America*, 2009, 106, 3913-3918.
- Yang J., Moses M.A.** Lipocalin 2. A multifaceted modulator of human cancer. *Cell Cycle*, 2009, 8 (15), 2347-2352.
- Yazici S., et al.** Dual inhibition of the epidermal growth factor and vascular endothelial growth factor phosphorylation for antivascular therapy of human prostate cancer in the prostate of nude mice. *Prostate*, 2005, 65, 203-215.
- Yndestad A., et al.** Increased systemic and myocardial expression of neutrophil gelatinase-associated lipocalin in clinical and experimental heart failure. *European Heart Journal*, 2009, 30, 1229-1236.
- Yokota J.** Tumour progression and metastasis. *Carcinogenesis*, 2000, 21 (3), 497-503.
- Yokoyama Y., et al.** Synergy between angiostatin and endostatin; inhibition of ovarian cancer growth. *Cancer Research*, 2000, 60, 2190-2196.
- Yoshino I., et al.** Induction of epithelial- mesenchymal transition related genes by benzo(a)pyrene in lung cancer cells. *Cancer*, 2007, 110, 369-374.
- You W.K., MacDonald D.M.** The hepatocyte growth factor/ c-Met signalling pathway as a therapeutic target to inhibit angiogenesis. *BMB Reports*, 2008, 41, 833-839.

Z

- Zabron A.A., et al.** Elevated levels of neutrophil gelatinase-associated lipocalin in bile from patients with malignant pancreatobiliary disease. *American Journal of Gastroenterology*, 2011, 106 (9), 1711-1717.
- Zangari M., et al.** Survival effect of venous thromboembolism in patients with multiple myeloma treated with lenalidomide and high-dose dexamethasone. *Journal of Clinical Oncology* 2009, 28, 132-135.
- Zeisberg M., Shah A.A., Kalluri R.** Bone morphogenetic protein-7 induces mesenchymal to epithelial transition in adult renal fibroblasts and facilitates regeneration of injured kidney. *Journal of Biological Chemistry*, 2005, 280, 8094-8100.
- Zeisberg M., Neilson E.G.** Biomarkers for epithelial-mesenchymal transitions. *Journal of Clinical Investigations*, 2009, 119, 1429-1437.
- Zhang H., et al.** Upregulation of neutrophil gelatinase-associated lipocalin in oesophageal squamous cell carcinoma: significant correlation with cell differentiation and tumour invasion. *Journal of Clinical Pathology*, 2007, 60 (5), 555-561.
- Zhang S., Zhang D., Sun B.** Vasculogenic mimicry: Current status and future prospects. *Cancer Letters*, 2007, 254, 157-164.

Zhao Q., Liu X., Collodi P. Identification and characterization of a novel fibronectin in zebrafish. *Experimental Cell Research*, 2001, 268, 211-219.

Zhu X., et al. Risks of proteinuria and hypertension with bevacizumab, an antibody against vascular endothelial growth factor: Systemic review and meta-analysis. *American Journal of Kidney Disease*, 2007, 49, 186-193.

Chapter 11

APPENDICES

Appendix 2.1a: The Preparation Methods of Cell Culture Reagents

Hanks Solution

3x 500ml 10x HBSS without Calcium and Magnesium

13.5ltr. Distilled water

5.25g Sodium Bicarbonate

0.2µm filter sterilised before aliquoting (30 x 500ml). Stored at room temperature.

MEM

3x 500ml 10x Minimum Medium Eagle

150ml Penicillin-Streptomycin Stabilised

150ml 100x MEM Non-Essential Amino Acid Solution

150ml 100Mm Sodium Pyruvate

33g Sodium Bicarbonate

13ltr Distilled water

0.2µm filter sterilised before aliquoting (30 x 500ml). Stored at 4°C.

Heat – Inactivation Treatment of Donor Calf Serum (HIDCS)

Donor calf serum was slowly defrosted on the benchtop or overnight at 4°C and then placed in 60°C waterbath for 30-40 minutes, to heat treat.

The serum was then decanted into 75ml aliquots and stored at -20°C.

Trypsin Solution (ET)

980ml Distilled water

5x PBS Tablets

0.76g EGTA

20ml 10x Trypsin Solution

The PBS tablets were dissolved in the distilled water and then the solution was decanted into 2x 500ml bottles and autoclaved. After the solution was allowed to cool 10ml

Trypsin 10x solution was added to each bottle. After mixing, the solution was decanted into 100ml aliquots and stored at -20°C.

Freeze Mix

170ml 15%DCS, 1% l-Glutamine, MEM

20ml HIDCS

10ml Dimethyl Sulfoxide

Reagents mixed together and then aliquoted into 20ml universals. Stored at -20°C.

Appendix 2.1b: Supplier details for the cell culture reagents.

Abbreviation	Full Name	Company	Prod. No.
AA	L-Ascorbic Acid	GIBCO BRL/ Invitrogen	15240-096
DCS	Donor calf serum	SLS/ Euroclone Thermo-Fisher, Perbio, Hyclone	EC 50040L Lot No: EUS003855, EUS005475 SH30072.03 Lot No: APD21173, ANH19288
DMEM	Dublbecco's MEM With glutamax-1, Na pyruvate, 100mg/ml glucose, pyridoxine	GIBCO BRL/ Invitrogen	21885-025
DMSO	Dimethyl sulfoxide	Sigma-Aldrich	D-5879
COLLAGEN		In house Prep	-----
EGTA	Ethylene Glycol-bis (b-aminomethyl ether)- N,N,N',N'-Tetreacetic Acid	Sigma-Aldrich	E-4378
FCS	Fetal Bovine Serum	Sigma-Aldrich	F-2442
FUNGI'ZONE	Antibiotic- Antimycotic 100X	Invitrogen	15240-096
GELATIN	Gelatine Powder	Merck/ BDH/ VWR	44045
GLUT	L-Glutamine 200mM	Sigma-Aldrich	G-7513
HBSS	Hanks Balanced Salt Solution w/o calcium and magnesium	Sigma-Aldrich	H-4641
MEM	Minimum Essential Medium Eagle 10x	Sigma-Aldrich	M-0275
MEM w/o phenol red	Minimum Essential Medium 1x with Earle's salts w/o L-glutamine w/o phenol red	GIBCO/ Invitrogen	51200-038
MTT		Sigma-Aldrich	
MYCOPLASM A REMOVAL AGENT	50ug/ml	ICN/ Invitrogen	30-500-44
NEAA	MEM Non-Essential Amino Acid Solution 100X	Sigma-Aldrich	M-7145

PEN/ STREP	Penicillin- Streptomycin Stabilised	Sigma-Aldrich	P-4333
PBS	Phosphate Buffered Saline	Sigma-Aldrich	P-4417
PFHM11 (1X)	Protein Free Hybridoma Medium	GIBCO BRL/ Invitrogen	12040-051
NaHCO₃	Sodium Bicarbonate	Merck/ BDH/ VWR	301515V
Na BIC SOLUTION	Sodium Bicarbonate Solution	Sigma-Aldrich	S-8761
Na PYRUVATE	Sodium Pyruvate 100Mm Solution	Sigma-Aldrich	S-8636
TRYPSIN	Trypsin 10x Solution	Sigma-Aldrich	T-4549